

NASA CR 114 600  
AVAILABLE TO THE PUBLIC

## V/STOL TILT ROTOR AIRCRAFT STUDY

### VOLUME VII

## TILT ROTOR FLIGHT CONTROL PROGRAM FEEDBACK STUDIES

H. R. Alexander

W. Eason

K. Gillmore

J. Morris

R. Spittle

MARCH 1973

Prepared Under Contract No. NAS2-6598 Phase 3 (Task C)

For

National Aeronautics and Space Administration

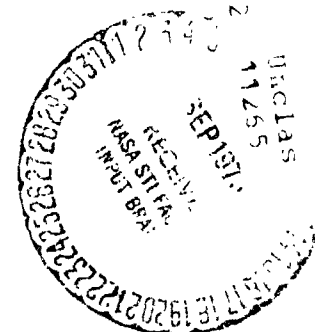
Ames Research Center

By

BOEING VERTOL COMPANY

Philadelphia, Pennsylvania 19142

(NASA-CR-114600) V/STOL TILT ROTOR  
AIRCRAFT STUDY. VOLUME VII: TILT ROTOR  
FLIGHT CONTROL PROGRAM FEEDBACK STUDIES  
(Boeing Vertol Co., Phila, Del.)  
364 p HC \$20.25



N73-30011

D222-10060-3

**V/STOL TILT ROTOR AIRCRAFT STUDY**

**VOLUME VII**

**TILT ROTOR FLIGHT CONTROL PROGRAM FEEDBACK STUDIES**

H. R. Alexander

W. Eason

K. Gillmore

J. Morris

R. Spittle

MARCH 1973

Prepared Under Contract No. NAS2-6598 Phase 3 (Task C)

For

National Aeronautics and Space Administration

Ames Research Center

By

BOEING VERTOL COMPANY

Philadelphia, Pennsylvania 19142

D222-10060-3

THE **BOEING** COMPANY

VERTOL DIVISION · PHILADELPHIA, PENNSYLVANIA

CODE IDENT. NO. 77272

NUMBER D222-10060-3

TITLE V/STOL TILT ROTOR AIRCRAFT STUDY -  
TILT ROTOR FEEDBACK CONTROL TECHNOLOGY

ORIGINAL RELEASE DATE \_\_\_\_\_ . FOR THE RELEASE DATE OF  
SUBSEQUENT REVISIONS, SEE THE REVISION SHEET. FOR LIMITATIONS  
IMPOSED ON THE DISTRIBUTION AND USE OF INFORMATION CONTAINED  
IN THIS DOCUMENT, SEE THE LIMITATIONS SHEET.

MODEL NA CONTRACT NAS2-6598 Phase III Task C

ISSUE NO. \_\_\_\_\_ ISSUED TO: \_\_\_\_\_

PREPARED BY	<u>H. Alexander</u>	DATE	<u>3/26/73</u>
APPROVED BY	<u>K. Gillmore</u>	DATE	<u>4/3/73</u>
APPROVED BY	<u>D. Richardson</u>	DATE	<u>4/4/73</u>
APPROVED BY	<u>W. Peck</u>	DATE	<u>4/3/73</u>

LIMITATIONS

This document is controlled by TILT ROTOR PROJECT - ORG. 7810

All revisions to this document shall be approved by the  
above noted organization prior to release.



ACTIVE SHEET RECORD											
SHEET NUMBER	REV LTR	ADDED SHEETS				SHEET NUMBER	REV LTR	ADDED SHEETS			
		SHEET NUMBER	REV LTR	SHEET NUMBER	REV LTR			SHEET NUMBER	REV LTR	SHEET NUMBER	REV LTR
I	A					1	A				
II						2					
III						3					
IV						4					
V						5					
VI						6					
VII						7					
VIII						8					
IX						9					
X						10					
XI						11					
XII						12					
XIII						13					
XIV						14					
XV						15					
XVI						16					
XVII						17					
XVIII						18					
XIX						19					
XX						20					
XXI						21					
XXII						22					
XXIII						23					
XXIV						24					
XXV						25					
XXVI						26					
XXVII						27					
XXVIII						28					
XXIX						29					
XXX						30					
XXXI						31					
XXXII						32					
XXXIII						33					
						34					
						35					
						36					
						37					
						38					
						39					

## ACTIVE SHEET RECORD

SHEET NUMBER	REV LTR	ADDED SHEETS				SHEET NUMBER	REV LTR	ADDED SHEETS			
		SHEET NUMBER	REV LTR	SHEET NUMBER	REV LTR			SHEET NUMBER	REV LTR	SHEET NUMBER	REV LTR
40						79					
41						80					
42						81					
43						82					
44						83					
45						84					
46						85					
47						86					
48						87					
49						88					
50						89					
51						90					
52						91					
53						92					
54						93					
55						94					
56						95					
57						96					
58						97					
59						98					
60						99					
61						100					
62						101					
63						102					
64						103					
65						104					
66						105					
67						106					
68						107					
69						108					
70						109					
71						110					
72						111					
73						112					
74						113					
75						114					
76						115					
77						116					
78						117					
						118					

FORM 48289 (7/67)

**ACTIVE SHEET RECORD**

SHEET NUMBER	REV LTR	ADDED SHEETS				SHEET NUMBER	REV LTR	ADDED SHEETS			
		SHEET NUMBER	REV LTR	SHEET NUMBER	REV LTR			SHEET NUMBER	REV LTR	SHEET NUMBER	REV LTR
119						159					
120						160					
121						161					
122						162	A				
123						163	A				
124						164	A				
125						165	A				
126						166					
127						167					
128						168					
129						169	A				
130						170					
131						171					
132						172					
133						173					
134						174					
135						175					
136						176					
137						177	A				
138						178					
139						179					
140						180					
141						181					
142						182					
143						183	A				
144						184					
145						185					
146						186	A				
147						187					
148						188	A				
149						189	A				
150						190					
151						191					
152						192					
153						193					
154						194					
155						195					
156						196					
157						197					
158						198					

FORM 48288 (7/67)

## ACTIVE SHEET RECORD

SHEET NUMBER	REV LTR	ADDED SHEETS				SHEET NUMBER	REV LTR	ADDED SHEETS			
		SHEET NUMBER	REV LTR	SHEET NUMBER	REV LTR			SHEET NUMBER	REV LTR	SHEET NUMBER	REV LTR
199	A					239	A				
200						240					
201						241					
202						242					
203						243					
204						244					
205						245					
206						246					
207						247					
208						248					
209						249					
210						250					
211						251					
212						252					
213						253					
214						254					
215						255					
216						256					
217						257					
218						258					
219						259					
220						260					
221						261					
222						262					
223						263					
224						264					
225						265	A				
226						266					
227						267	A				
228						268					
229						269	A				
230						270					
231						271	A				
232						272					
233						273					
234						274					
235						275					
236						276					
237						277					
238						278					

FORM 46803 (7/67)

## ACTIVE SHEET RECORD

SHEET NUMBER	REV LTR	ADDED SHEETS				SHEET NUMBER	REV LTR	ADDED SHEETS			
		SHEET NUMBER	REV LTR	SHEET NUMBER	REV LTR			SHEET NUMBER	REV LTR	SHEET NUMBER	REV LTR
279	A					318					
280						319					
281						320					
282						321					
283						322	A				
284						323					
285						324					
286	A					325					
287						326					
288						327					
289						328					
290	A					329					
291											
292											
293											
294											
295											
296											
297											
298											
299											
300											
301											
302											
303	A										
304											
305											
306											
307											
308											
309											
310	A										
311											
312											
313											
314											
315											
316											
317											

REVISIONS			
LTR	DESCRIPTION	DATE	APPROVAL
A	Issued to incorporate comments of the customer, National Aeronautics and Space Administration, Moffett Field, California	7-11-73	<i>Hru</i>

This report is one of a series prepared by The Boeing Vertol Company, Philadelphia, Pennsylvania for the National Aeronautics and Space Administration, Ames Research Center, Moffett Field, California under contract NAS2-6598. The studies reported under Volumes I through IV and VIII through X were jointly funded by NASA and the U. S. Army Air Mobility Research and Development Laboratory, Air Force Directorate. Volumes V through VII were funded by the Air Force Flight Dynamics Laboratory, Wright Patterson Air Force Base, Ohio.

This contract was administered by the National Aeronautics and Space Administration. Mr. Richard J. Abbott was the Contract Administrator, Mr. Gary B. Churchill, Tilt Rotor Research Aircraft Project Office, was the Technical Monitor, and coordination and liaison with the U. S. Air Force Flight Dynamics Laboratory was through Mr. D. Fraga. The Boeing-Vertol Project Engineer for the work reported in Volume VII was Mr. H. R. Alexander.

The complete list of reports published under this contract is as follows:

- Volume I -- Conceptual Design of Useful Military and/or Commercial Aircraft, NASA CR-114437
- Volume II -- Preliminary Design of Research Aircraft, NASA CR-114438
- Volume III -- Overall Research Aircraft Project Plan, Schedules, and Estimated Cost, NASA CR-114439
- Volume IV -- Wind Tunnel Investigation Plan for a Full Scale Tilt Rotor Research Aircraft, CR-114440
- Volume V -- Definition of Stowed Rotor Research Aircraft, NASA CR-114598
- Volume VI -- Preliminary Design of a Composite Wing for Tilt Rotor Aircraft, NASA CR-114599
- Volume VII -- Tilt Rotor Flight Control Program Feedback Studies, NASA CR-114600
- Volume VIII -- Mathematical Model for a Real Time Simulation of a Tilt Rotor Aircraft (Boeing Vertol Model 222), NASA CR-114601
- Volume IX -- Piloted Simulator Evaluation of the Boeing Vertol Model 222 Tilt Rotor Aircraft, NASA CR-114602
- Volume X -- Performance and Stability Test of a 1/4.622 Froude Scaled Boeing Vertol Model 222 Tilt Rotor Aircraft (Phase 1), NASA CR-114603

ABSTRACT

An exploratory study has been made of the use of feedback control in tilt rotor aircraft. This has included the use of swashplate cyclic and collective controls and direct lift control.

Various sensor and feedback systems are evaluated in relation to blade loads alleviation, improvement in flying qualities, and modal suppression.

Recommendations are made regarding additional analytical and wind tunnel investigations and development of feedback systems in the full scale flight vehicle. Estimated costs and schedules are given.



TABLE OF CONTENTS

<u>SECTION</u>	<u>TITLE</u>	<u>PAGE</u>
1.0	SUMMARY . . . . .	1
2.0	PROP/ROTOR HUB FORCE AND MOMENT DERIVATIVES . . .	6
2.1	Background . . . . .	6
2.2	Variation of Derivatives with Lead-Lag Frequency Ratio . . . . .	8
2.3	Variation of Lead-Lag and Flap Frequency Ratio over a Limited Range . . . . .	8
2.4	Effects of Altitude and Speed on Prop/Rotor Derivatives . . . . .	17
2.5	Correlation with Test Data . . . . .	17
2.5.1	Model 213 Four Blade Hingeless Rotor Correlation . . . . .	26
2.5.2	Correlation with Model 222 26-foot Diameter Rotor Test in NASA-Ames 40x80 Foot Tunnel . . . . .	26
2.5.3	Correlation with Model 222 1/4.522 Scale Model Data . . . . .	32
2.6	Conclusions from Derivative Study . . . . .	35
3.0	BLADE LOAD ALLEVIATION AND STABILITY AUGMENTATION SYSTEM . . . . .	37
3.1	Background and Objectives of Study . . . . .	37
3.2	Technical Basis for Use of Cyclic Pitch Feedback in Load Alleviation . . . . .	38
3.3	Test Demonstrations of Swashplate Feedback Systems . . . . .	40
3.4	Candidate Systems: Choice of Sensors . . . . .	41
3.5	System Characteristics . . . . .	44
3.6	Design of a System Effective for Quasi Steady Conditions . . . . .	44
3.6.1	System Designed to Null Rotor Hub Moments in Cruise . . . . .	44
3.6.2	System Authority Considerations . . . . .	51
3.7	Alternative System Definitions . . . . .	60

TABLE OF CONTENTS

<u>SECTION</u>	<u>TITLE</u>	<u>PAGE</u>
3.8	Dynamic Response Consideration . . . . .	69
3.8.1	Method of Investigation and Results. Cruise. . . . .	71
3.8.2	Results at Transition Velocities . . . . .	81
3.9	Conclusions and Direction for Development . . . . .	82
4.0	DIRECT LIFT FEEDBACK CONTROL . . . . .	93
4.1	Background and Objectives . . . . .	93
4.2	Gust Alleviation System Approach . . . . .	95
4.3	Evaluation of DLC Gust Alleviation System . . . . .	97
4.4	Conclusions . . . . .	112
5.0	MODAL SUPPRESSION AND AEROELASTIC STABILITY AUGMENTATION . . . . .	113
5.1	Background and Objectives . . . . .	113
5.2	Rational of Current Study . . . . .	114
5.3	Mathematical Model for Modal Suppression Studies . . . . .	119
5.4	Initial Explorative Studies . . . . .	128
5.4.1	Discussion of Results of Initial Studies . . . . .	131
5.4.2	Ideal System with First Order Time Lag . . . . .	138
5.4.3	Variations with RPM . . . . .	138
5.5	Synthesis of an Optimized System Accounting for Hardware Component Dynamics . . . . .	154
5.5.1	Acceleration Feedback . . . . .	162
5.5.2	Rate Feedback . . . . .	169
5.5.3	Position or Deflection Feedback . . . . .	169
5.6	Direction for Further Development . . . . .	177
5.6.1	Phased Swashplate Feedback . . . . .	183
5.6.2	Advantages of Phased or Wobbling Swashplate Control . . . . .	186

TABLE OF CONTENTS

<u>SECTION</u>	<u>TITLE</u>	<u>PAGE</u>
5.7	Conclusions . . . . .	186
6.0	BLADE TRANSIENT LOADS IN HOVER . . . . .	188
6.1	Background and Objective . . . . .	188
6.2	Mathematical Model . . . . .	189
6.3	Evaluation of System Sensing Ideal Signal . . . . .	190
6.4	Evaluation of System Sensing Hub In-Plane Velocity . . . . .	195
6.5	Conclusions . . . . .	196
7.0	THRUST MANAGEMENT AND ROTOR GOVERNING FEEDBACK SYSTEMS . . . . .	203
7.1	Background . . . . .	203
7.2	Study Approach . . . . .	205
7.3	Design Criteria . . . . .	206
7.4	Evaluation of Collective Pitch Governor Configurations . . . . .	210
	7.4.1 Single Governor with One Sensor . . . . .	211
	7.4.2 Dual Independent Governors . . . . .	211
	7.4.3 Single Governor with Two Sensors . . . . .	222
7.5	Effect of Governor on Flying Qualities . . . . .	239
7.6	Gust Response . . . . .	245
7.7	Conclusions . . . . .	258
8.0	FOLDING TILT ROTOR APPLICATIONS . . . . .	265
9.0	CONCLUSIONS AND RECOMMENDATIONS . . . . .	267
10.0	HARDWARE CONSIDERATIONS . . . . .	271
10.1	Introduction . . . . .	271
10.2	Stability Augmentation System (SAS). . . . .	271

TABLE OF CONTENTS

<u>SECTION</u>	<u>TITLE</u>	<u>PAGE</u>
10.2.1	Redundancy . . . . .	272
10.2.2	Hardware . . . . .	273
	10.2.2.1 Sensors . . . . .	273
	10.2.2.2 Signal Processing . . . . .	274
	10.2.2.3 Actuators . . . . .	274
10.3	Governor Systems . . . . .	275
	10.3.1 Dual Electro-Mechanical Governor System . . . . .	275
	10.3.2 Triple Electrohydraulic Governor System with Model Channel . . . . .	276
	10.3.3 Quadruple Electro-Mechanical Governor System . . . . .	277
10.4	Modification of Flight Controls . . . . .	278
	10.4.1 Tilt Rotor Modified Flight Control System . . . . .	278
10.5	Hardware Modifications . . . . .	279
	10.5.1 Load Alleviation . . . . .	279
	10.5.2 Lift Gust Alleviation . . . . .	279
	10.5.3 Modal Suppression . . . . .	280
11.0	RECOMMENDED PROGRAMS . . . . .	286
11.1	Recommended Analytical Studies . . . . .	286
11.2	Proposed Wind Tunnel Programs . . . . .	291
11.3	Programs Planned and Additional Recommended Programs: Full Scale Flight Test . . . . .	294
	11.3.1 Blade Load Alleviation System and Stability Augmentation on the NASA Tilt Rotor Research Vehicle . . . . .	294
	11.3.2 Direct Lift Flight Path Control and Gust Alleviation . . . . .	294
	11.3.3 Modal Suppression Systems Based on Rotor/Swashplate Feedback . . . . .	296

TABLE OF CONTENTS

<u>SECTION</u>	<u>TITLE</u>	<u>PAGE</u>
11.4	Planning Costs and Schedules.....	298
11.4.1	Analytical Studies.....	298
11.4.2	Design and Hardware Modification and Installation.....	298
11.4.3	Model Wind Tunnel Testing.....	299
11.4.4	Ground Aircraft Tests.....	299
11.4.5	Flight Tests.....	300
REFERENCES.....		303
APPENDIX A -	Description of the Math Model.....	304
APPENDIX B -	Single Governor With Two Sensors - Bode Analysis.....	309
APPENDIX C -	"Fly By Wire": Conversion of M222 Control System to Electrical Signaling.....	327

LIST OF FIGURES

<u>FIGURE</u>		<u>PAGE</u>
2.1	Mathematical Model for Rotor Derivative Parametric Trend Studies . . . . .	7
2.2	Effect of Variation of Blade Frequency Ratios on Cyclic Force Derivatives 250 Knots . . . . .	9
2.3	Effect of Variation of Blade Frequency Ratios on Cyclic Moment Derivatives 250 Knots . . . . .	10
2.4	Variation of Prop/Rotor Normal and Side Force Alpha Derivatives with Respect to Blade Lead- Lag Frequency . . . . .	11
2.5	Variation of Prop/ROTOR Pitching and Yawing Moment Alpha Derivatives with Respect to Blade Lead-Lag Frequency . . . . .	12
2.6	Sensitivity of M222 26 Ft Hingeless Rotor Alpha Derivatives for Normal and Side Force to Variations in Blade Lead-Lag and Flap Natural Frequencies . . . . .	13
2.7	Sensitivity of M222 26 Ft Hingeless Rotor Alpha Derivatives for Yawing Moment and Pitching Moment Variations in Blade Lead-Lag and Flap Natural Frequencies . . . . .	14
2.8	Sensitivity of M222 26 Ft Diameter Hingeless Rotor Cyclic Derivatives for Normal and Side Force to Variations in Blade Lead-Lag and Flap Natural Frequencies. . . . .	15
2.9	Sensitivity of M222 26 Ft Hingeless Rotor Cyclic Derivatives for Yawing and Pitching Moment, to Variations in Blade Lead-Lag and Flap Natural Frequencies . . . . .	16
2.10	Sensitivity of M222 26 Ft Diameter Hingeless Rotor Normal and Side Force Alpha Derivatives to Blade Lead-Lag and Flap Natural Frequencies . . . . .	18
2.11	Sensitivity of M222 26 Ft Diameter Hingeless Rotor Yawing and Pitching Alpha Derivatives with Respect to Blade Lead-Lag and Flap Natural Frequencies . . . . .	19
2.12	Sensitivity of M222 26 Ft. Diameter Hingeless Rotor Normal and Side Force Cyclic Derivatives with Respect to Blade Lead-Lag and Flap Natural Frequencies . . . . .	20

LIST OF FIGURES

<u>FIGURE</u>		<u>PAGE</u>
2.13	Sensitivity of M222 26 Ft Diameter Hingeless Rotor Yawing and Pitching Moment Cyclic Derivatives with Respect to Blade Lead-Lag and Flap Natural Frequencies . . . . .	21
2.14	Sensitivity of M222 26 Ft Diameter Hingeless Rotor Normal and Side Force Alpha Derivatives with Respect to Altitude and Velocity . . . . .	22
2.15	Sensitivity of M222 26 Ft Diameter Hingeless Rotor Yawing and Pitching Moment Alpha Derivatives with Respect to Altitude and Velocity . . . . .	23
2.16	Sensitivity of M222 26 Ft Diameter Rotor Normal Force Cyclic Derivatives to Altitude and Airspeed . . . . .	24
2.17	Sensitivity of M222 26 Ft Diameter Rotor Yawing and Pitching Moment Cyclic Derivatives to Altitude and Airspeed . . . . .	25
2.18	Model 213 1/9-Scale Conversion Mode - 85 FT/SEC Derivative Variation with RPM . . . . .	27
2.19	26 Ft Rotor Test Stand in NASA's 40x80 Tunnel . . . . .	28
2.20	Correlation of 26 Ft Rotor Test Data with Various Rotor Derivative Programs - $\alpha$ Derivatives . . . . .	29
2.21	Correlation of 26 Ft Rotor Test Data with Various Rotor Derivative Programs - Cyclic Moment Derivatives . . . . .	30
2.22	Correlation of 26 Ft Rotor Test Data with Various Rotor Derivative Programs - Cyclic Force Derivatives . . . . .	31
2.23	Rotor Moment and Azimuth Angle due to Angle of Attack - Correlation with 26-Ft Rotor Data (Abstracted from M222 - Proposal - Boeing D222-10050-2 . . . . .	33
2.24	Comparison of Calculated and Test Rotor Hub Force and Moment Derivatives for M222 1/4.622 Scale Model (Yaw Sweep) $\Omega=386$ RPM . . . . .	34
2.25	Comparison of Calculated and Test Rotor Hub Force and Moment Derivatives for M222 1/4.622 Scale Model (Pitch Sweep) $\Omega=386$ RPM . . . . .	36

LIST OF FIGURES

<u>Figure</u>	<u>Title</u>	<u>Page</u>
3.1	Blade Load Alleviation System Schematic of Feedback Loop	43
3.2	Gain Requirement As Function of Dynamic Pressure and Altitude for System Designed to Zero-Out Hub Moments	46
3.3	Azimuth Angle Requirement As Function of Dynamic Pressure and Altitude for Systems Designed to Zero-Out Hub Moments	47
3.4	Normal Force Derivative Without Feedback With Unrestricted Gain and With Arbitrary Limit of $1.5^\circ$ of $A_1$ and $B_1$	49
3.5	Side Force Derivative Without Feedback With Unrestricted Gain and With Arbitrary $1.5^\circ$ Limit on $A_1$ and $B_1$	50
3.6	Hub Yawing Moment Derivative Without Feedback and With Gain Restricted for Arbitrary Limit of $1.5^\circ$ $A_1$ and $B_1$	52
3.7	Hub Pitching Moment Derivative Without Feedback and With Gain Restricted for Arbitrary Limit of $1.5^\circ$ $A_1$ and $B_1$	53
3.8	Pitching Moment About Nacelle Pivot With and Without Feedback	55
3.9	Bode Diagram for System Designed to Reduce Hub Moments	57
3.10	Bode Diagram for System Designed to Reduce Hub Moments	58
3.11	Bode Diagram for System Designed to Reduce Hub Moments	59
3.12	Forces and Moments Vs Gain/Azimuth at 100 Knots, 386 RPM and Sea Level	61



LIST OF FIGURES

<u>Figure</u>	<u>Title</u>	<u>Page</u>
3.13	Forces and Moments Vs Gain/Azimuth at 250 Knots, 386 RPM and Sea Level	62
3.14	Gain/Azimuth for Zero Forces and Moments at 100 Knots	63
3.15	Gain/Azimuth for Zero Forces and Moments at 250 Knots	64
3.16	Reference Open Loop Frequency Response for Unit Gain in Feedback Loop	65
3.17	Reference Open Loop Frequency Response for Unit Gain in Feedback Loop	66
3.18	Effect of Feedback on the Dynamic Response of Rotor Hub Moments, at 250 Knots, 386 RPM	72
3.19	Effect of Feedback on the Dynamic Response of Rotor Hub Forces, at 250 Knots, 386 RPM	73
3.20	Variation of Peak Hub Normal Force With Gain and Azimuth of Feedback	74
3.21	Variation of Peak Hub Side Force With Gain and Azimuth of Feedback	75
3.22	Variation of Peak Hub Yawing Moment With Gain and Azimuth of Feedback	76
3.23	Variation of Peak Hub Pitching Moment With Gain and Azimuth of Feedback	77
3.24	Effect of Feedback on the Dynamic Response of Rotor Hub Forces at 250 Knots, 386 RPM	79
3.25	Effect of Feedback on the Dynamic Response of Rotor Hub Moments at 250 Knots, 386 RPM	80
3.26	Variation of Hub Normal Force With Azimuth and Feedback Gain at 80 Knots and 551 RPM	83

LIST OF FIGURES

<u>FIGURE</u>	<u>TITLE</u>	<u>PAGE</u>
3.27	Variation of Hub Side Force With Azimuth and Feedback Gain at 80 Knots and 551 RPM . . .	84
3.28	Variation of Hub Yawing Moment With Azimuth and Feedback Gain at 80 Knots and 551 RPM . . . . .	85
3.29	Variation of Hub Pitching Moment With Azimuth and Feedback Gain at 80 Knots and 551 RPM . . . . .	86
3.30	Effect of Feedback on the Dynamic Response of Rotor Hub Forces at 80 Knots and 551 RPM . . .	87
3.31	Effect of Feedback on the Dynamic Response of Rotor Hub Moments at 80 Knots and 551 RPM . . .	88
3.32	Variation of Short Period Mode Frequency With Azimuth and Feedback Gain at 80 Knots and 551 RPM . . . . .	89
3.33	Variation of Short Period Mode Damping With Azimuth and Feedback Gain at 80 Knots and 551 RPM . . . . .	90
4.1	Schematic of Direct Lift Control Gust Alleviation System . . . . .	96
4.2	Effect of Gust Alleviation System Gain on Normal Acceleration Response 250 Knots . . .	98
4.3	Aircraft Pitch Rate Response to Ramp Gust with and without DLC Gust Alleviation System . . .	99
4.4	Aircraft Cabin Normal Acceleration Response to Ramp Gust with and without DLC Gust Alleviation System . . . . .	101
4.5	Aircraft Response to Random Turbulence 250 Knots, No Feedback . . . . .	102
4.6	Aircraft Response to Random Turbulence 250 Knots, $\delta_F/\alpha=2.47, \delta_g/\alpha$ . . . . .	103

LIST OF FIGURES

<u>FIGURE</u>	<u>TITLE</u>	<u>PAGE</u>
4.7	Aircraft Response to Random Turbulence 250 Knots, $\delta_F/\alpha=4.95$ , $\delta_S/\alpha=9.75$ . . . . .	104
4.8	Aircraft Response to Random Turbulence 250 Knots, $\delta_F/\alpha=7.43$ , $\delta_S/\alpha=14.61$ . . . . .	105
4.9	Aircraft Response to Random Turbulence 100 Knots, No Feedback . . . . .	107
4.10	Aircraft Response to Random Turbulence 100 Knots, $\delta_F/\alpha=1.24$ , $\delta_S/\alpha=2.44$ . . . . .	108
4.11	Aircraft Response to Random Turbulence 100 Knots, $\delta_F/\alpha=2.47$ , $\delta_S/\alpha=4.78$ . . . . .	109
4.12	Aircraft Response to Random Turbulence 100 Knots, $\delta_F/\alpha=4.95$ , $\delta_S/\alpha=9.75$ . . . . .	110
4.13	Aircraft Response to Random Turbulence 100 Knots, $\delta_F/\alpha=7.43$ , $\delta_S/\alpha=14.61$ . . . . .	111
5.1	Schematic of Simplified Aeroelastic Stability Augmentation System . . . . .	116
5.2	Schematic of Aeroelastic Stability Augmenta- tion System for Air Resonance Mode . . . . .	118
5.3	Effect of Velocity on Tilt Rotor Modal Frequency . . . . .	120
5.4	Effect of Velocity on Tilt Rotor Modal Damping . . . . .	121
5.5	26 Ft Rotor - Full Stiffness Wing Modal Frequencies at V=100 Knots . . . . .	122
5.6	Correlation of Predicted Air Resonance Mode and Measured Damping of this Mode during Test. V=100 Knots . . . . .	123
5.7	26 Ft Rotor - Full Stiffness Wing - Modal Frequencies at V=150 Knots . . . . .	124
5.8	Correlation of Predicted Air Resonance Mode Damping and Measured Damping of this Mode during Test. V=140 Knots and 150 Knots . . . . .	125

LIST OF FIGURES

<u>FIGURE</u>	<u>TITLE</u>	<u>PAGE</u>
5.9	26 Ft Rotor - Full Stiffness Wing - Modal Frequencies at V=200 Knots . . . . .	126
5.10	Correlation of Predicted Air Resonance Mode Damping and Measured Damping of this Mode during this Test V=192 Knots and 200 Knots . . . . .	127
5.11	Sign Convention for Aeroelastic Stability Investigations . . . . .	130
5.12	Feedback Effect on Modal Damping of M-222 Wing Vertical Bending Mode . . . . .	132
5.13	Feedback Effect on Modal Damping of M-222 Wing Torsion Mode . . . . .	133
5.14	Feedback Effect on Modal Damping of M-222 Wing Vertical Bending Mode . . . . .	134
5.15	Feedback Effect on Modal Damping of M-222 Wing Torsion Mode . . . . .	135
5.16	Feedback Effect on Modal Damping of M-222 Stability for Feedback Combinations . . . . .	136
5.17	Feedback Effect on Modal Damping of M-222 Stability for Feedback Combinations . . . . .	137
5.18	Feedback Effect on Modal Damping of M-222 Wing Vertical Bending Mode with Time Constant. . . . .	139
5.19	Feedback Effect on Modal Damping of M-222 Wing Vertical Bending Mode with Time Constant. . . . .	140
5.20	Feedback Effect on Modal Damping of M-222 Wing Torsion Mode with Time Constant . . . . .	141
5.21	Feedback Effect on Modal Damping of M-222 Wing Torsion Mode with Time Constant . . . . .	142
5.22	Feedback Effect on Modal Damping of M-222 Wing Vertical Bending Mode with Time Constant. . . . .	143
5.23	Feedback Effect on Modal Damping of M-222 Wing Torsion Mode with Time Constant . . . . .	144
5.24	Feedback Effect on Modal Damping of M-222 Wing Vertical Beinding Mode . . . . .	145

LIST OF FIGURES

<u>FIGURE</u>	<u>TITLE</u>	<u>PAGE</u>
5.25	Feedback Effect on Modal Damping of M-222 Wing Torsion Mode . . . . .	. 146
5.26	Feedback Effect on Modal Damping of M-222 Stability for Feedback Combinations . . .	. 147
5.27	Feedback Effect on Modal Damping of M-222 Wing Vertical Bending . . . . .	. 148
5.28	Feedback Effect on Modal Damping of M-222 Wing Torsion Mode . . . . .	. 149
5.29	Feedback Effect on Modal Damping of M-222 Stability for Feedback Combinations . . .	. 150
5.30	Feedback Effect on Modal Damping of M-222 Wing Vertical Bending . . . . .	. 151
5.31	Feedback Effect on Modal Damping of M-222 Wing Torsion Mode . . . . .	. 152
5.32	Feedback Effect on Modal Damping of Aircraft Stability for Feedback Combinations . . .	. 153
5.33	Composite Feedback Gain Envelope for Various Flight Conditions . . . . .	. 155
5.34	Math Model Sign Conventions and Vector Orientation for HI-Rate System . . . . .	. 158
5.35	Aeroelastic Stability Augmentation System Open Loop Frequency Response - Acceleration Feedback - 100 Knot Cruise . . . . .	. 159
5.36	Aeroelastic Stability Augmentation System Open Loop Frequency Response - Acceleration Feedback - 150 Knot Cruise . . . . .	. 160
5.37	Aeroelastic Stability Augmentation System Open Loop Frequency Response - Acceleration Feedback - 200 Knot Cruise . . . . .	. 161
5.38	Aeroelastic Stability Augmentation System - Open Loop Frequency Response Filtered Acce- leration Feedback - 100 Knots . . . . .	. 163
5.39	Aeroelastic Stability Augmentation System Open Loop Frequency Response - Filtered Acceleration Feedback - 150 Knots . . . . .	. 164

LIST OF FIGURES

<u>FIGURE</u>		<u>PAGE</u>
5.40	Aeroelastic Stability Augmentation System Open Loop Frequency Response - Filtered Acceleration Feedback - 200 Knots . . . . .	165
5.41	Effect of Gain on Modal Stability Roots for Filtered Acceleration Feedback - 100 Knots . . . . .	166
5.42	Effect of Gain on Modal Stability Roots for Filtered Acceleration Feedback - 150 Knots . . . . .	167
5.43	Effect of Gain on Modal Stability Roots for Filtered Acceleration Feedback - 200 Knots . . . . .	168
5.44	HI-Rate Open Loop Frequency Response . . . . .	170
5.45	26 Ft Rotor Test Data - Damping vs High Rate System Gain at 192 Knots, 386 RPM, with Low Rate System Active . . . . .	171
5.46	Aeroelastic Stability Augmentation System Open Loop Frequency Response - Rate Feedback - 100 Knots . . . . .	172
5.47	Aeroelastic Stability Augmentation System Open Loop Frequency Response - Rate Feedback - 150 Knots . . . . .	173
5.48	Aeroelastic Stability Augmentation System Open Loop Frequency Response - Rate Feedback - 200 Knots . . . . .	174
5.49	Effect of Rate Feedback on Wing Vertical Bending Roots - 100 Knots . . . . .	175
5.50	Effect of Rate Feedback on Wing-Vertical Bending Roots - 200 Knots . . . . .	176
5.51	Aeroelastic Stability Augmentation System Open Loop Frequency Response - Position Feedback - 100 knots . . . . .	178
5.52	Aeroelastic Stability Augmentation System - Open Loop Frequency Response - Position Feedback - 150 Knots . . . . .	179

LIST OF FIGURES

<u>FIGURE</u>	<u>TITLE</u>	<u>PAGE</u>
5.53	Aeroelastic Stability Augmentation System Open Loop Frequency Response - Position Feedback - 200 Knots . . . . .	180
5.54	Effect of Gain on Wing Vertical Bending Stability Roots - Position Feedback - 100 Knots . . . . .	181
5.55	Effect of Gain on Wing Vertical Bending Stability Roots - Position Feedback - 200 Knots . . . . .	182
6.1	Lead-Lag Feedback Block Diagram . . . . .	191
6.2	Feedback Effect on the Lower Lead-Lag Mode . . . . .	192
6.3	Root Locus of the Lower Lead-Lag Mode . . . . .	193
6.4	Feedback Effect on Pitch Attitude . . . . .	194
6.5	Feedback Effect on the Lower Lead-Lag Mode . . . . .	197
6.6	Feedback Effect on Pitch Attitude . . . . .	198
6.7	Root Locus of Coupled Vertical Bending/ Lead-Lag Mode . . . . .	199
6.8	Feedback Effect on the Lower Lead-Lag Mode . . . . .	200
6.9	Feedback Effect on Pitch Attitude . . . . .	201
6.10	Root Locus of Coupled Vertical Bending/ Lead-Lag Mode . . . . .	202
7.1	Candidate Governor Schematic-Single Governor with One Sensor . . . . .	207
7.2	Candidate Governor Schematic-Dual Independent Governors . . . . .	208
7.3	Candidate Governor Schematic-Single Governor with Two Sensors . . . . .	209
7.4	Single Governor with One Sensor-Stability Root Variation . . . . .	212
7.5	Inner Loop Stability Variation for Dual Independent Governors without Cross Shaft . . . . .	214

LIST OF FIGURES

<u>FIGURE</u>	<u>TITLE</u>	<u>PAGE</u>
7.6	Inner Loop Stability Variation for Dual Independent Governors without Cross Shaft . . . .	215
7.7	Inner Loop Stability Variation for Dual Independent Governors without Cross Shaft . . . .	216
7.8	Inner Loop Stability Variation for Dual Independent Governors without Cross Shaft . . . .	217
7.9	Inner Loop Stability Variation for Dual Independent Governors without Cross Shaft . . . .	218
7.10	Dual Independent Governors - Inner and Outer Loop Stability Response . . . . .	220
7.11	Dual Independent Governors - Inner and Outer Loop Stability Response . . . . .	221
7.12	Dual Independent Governors - Inner and Outer Loop Stability Response . . . . .	223
7.13	Dual Independent Governors - Inner and Outer Loop Stability Response . . . . .	224
7.14	Single Governor with Two Sensors - Governor Gain Limits for RPM Feedback Inner Loop Stability . . . . .	226
7.15	Single Governor with Two Sensors Rotor Rotation Migration with RPM Feedback . . . . .	228
7.16a	Single Governor with Two Sensor Rotor Rotation Root Migration with RPM Feedback . . . . .	229
7.16b	Rotor Rotation Root Migration with RPM Feedback . . . . .	230
7.17	Single Governor with Two Sensors Rotor Rotation Root Migration with + RPM Feedback . . . . .	231
7.18	Single Governor with Two Sensors Rotor Rotation Root Migration with + RPM Feedback . . . . .	232
7.19a	Single Governor with Two Sensors Rotor Rotation Root Migration with + RPM Feedback . . . . .	233



LIST OF FIGURES

<u>FIGURE</u>		<u>PAGE</u>
7.19b	Single Governor with Two Sensors Rotor Rotation Root Migration with + RPM Feedback . . . . .	234
7.20	Single Governor with Two Sensors Rotor Rotation Root Migration with RPM Feedback . .	235
7.21	Single Governor with Two Sensors Rotor Rotation Root Migration with RPM Feedback . .	236
7.22	Single Governor with Two Sensors Rotor Rotation Root Migration with Integral Feedback . . . . .	237
7.23	Single Governor with Two Sensors Rotor Rotation Root Migration with RPM Feedback .	238
7.24	Single Governor with Two Sensors Rotor Rotation Root Migration with Velocity . . .	240
7.25	Effect of Governor on Roll and Vertical Translation Modes . . . . .	242
7.26	Criteria for Acceptable Hover Control . . .	243
7.27	Effect of Governor on Dutch Roll Mode . . .	244
7.28	Effect of Governor System Configuration on Power System Parameters . . . . .	246
7.29a	Aircraft Response to 1-cos Axial Gust 100 Knot Cruise . . . . .	250
7.29b	Aircraft Response to 1-cos Axial Gust 100 Knot Cruise . . . . .	251
7.30a	Aircraft Response to 1-cos Axial Gust 200 Knot Cruise . . . . .	252
7.30b	Aircraft Response to 1-cos Axial Gust 200 Knot Cruise . . . . .	253
7.31a	Aircraft Response to 1-cos Axial Gust 300 Knot Cruise . . . . .	254
7.31b	Aircraft Response to 1-cos Axial Gust 300 Knot Cruise . . . . .	255

LIST OF FIGURES

<u>FIGURE</u>	<u>TITLE</u>	<u>PAGE</u>
7.32	Aircraft Response to Axial Random Turbulence 300 Knots - Collective Pitch Governor . . .	255
7.33a	Aircraft Response to 1-cos Axial Gust Steady Hover . . . . .	259
7.33b	Aircraft Response to 1-cos Axial Gust Steady Hover . . . . .	260
7.34a	Aircraft Response to 1-cos Axial Gust Hover - 20 fps Climb . . . . .	261
7.34b	Aircraft Response to 1-cos Axial Gust Hover - 20 fps Climb . . . . .	262
7.35a	Aircraft Response to 1-cos Axial Gust Hover - 20 fps Descent . . . . .	263
7.35b	Aircraft Response to 1-cos Axial Gust Hover - 20 fps Descent . . . . .	264
10.1	Stability Augmentation System - Functional Block Diagram . . . . .	281
10.2	Governor - Dual Electro-Mechanical System .	282
10.3	Governor - Triple Electrohydraulic Sistem .	283
10.4	Model 222 Dual Foil Functional Governor System . . . . .	284
10.5	Flight Controls Schematic . . . . .	285
11.1	Schedules - Recommended Programs	302
 <b>APPENDICES</b>		
A-1	Model 222 - Rotor Blade Properties . . . .	305
A-2	Model 222 Rotor Blade Variation of 2nd Bending Natural Frequency with Rotor Speed and Collective Pitch . . . . .	306
A-3	Model 222 Rotor Blade Variation of 1st Bending Natural Frequency with Rotor Speed and Collective Pitch . . . . .	307
A-4	Wing Uncoupled Frequencies (Blades Off) Cruise Configuration . . . . .	308

## APPENDICES

		<u>PAGE</u>
B-1	Rotor Rotation Frequency Response with Actuator Dynamics . . . . .	311
B-2	Rotor Rotation Frequency Response with Actuator Dynamics . . . . .	312
B-3	Rotor Rotation Frequency Response with Actuator Dynamics . . . . .	313
B-4	Rotor Rotation Frequency Response with Actuator Dynamics . . . . .	314
B-5	Rotor Rotation Frequency Response with Actuator Dynamics . . . . .	315
B-6	Rotor Rotation Frequency Response with Actuator Dynamics . . . . .	316
B-7	Rotor Rotation Frequency Response with Actuator Dynamics . . . . .	317
B-8	Rotor Rotation Frequency Response with Actuator Dynamics . . . . .	318
B-9	Rotor Rotation Frequency Response with Actuator Dynamics . . . . .	319
B-10	Rotor Rotation Frequency Response with Actuator Dynamics . . . . .	320
B-11	Rotor Rotation Frequency Response with Actuator Dynamics . . . . .	321
B-12	Rotor Rotation Frequency Response with Actuator Dynamics . . . . .	322
B-13	Rotor Rotation Frequency Response with Actuator Dynamics . . . . .	323
B-14	Rotor Rotation Frequency Response with Actuator Dynamics . . . . .	324
B-15	Rotor Rotation Frequency Response with Actuator Dynamics . . . . .	325
B-16	Rotor Rotation Frequency Response with Actuator Dynamics . . . . .	326
C-1	Tilt Rotor Fly-By-Wire Control System (FBW).	328

LIST OF TABLES

<u>Table</u>	<u>Title</u>	<u>Page</u>
3.1	Candidate Signals and Sensors for Load Alleviation System . . . . .	42
3.2	Summary of Freedoms and Interactions with Blade Freedoms . . . . .	70
11.1	Recommended Analytical Studies . . . . .	287
11.2	Proposed Wind Tunnel Program . . . . .	292
11.3	Recommended Programs on Full Scale Aircraft with Supporting Model Test Programs . . . .	295

SYMBOLS

$A_1$	Cyclic pitch coefficient of cos term
$a_1, a$	Gain in $A_1$ cyclic channel
$B_1$	Cyclic pitch coefficient of sin term
$b_1, b$	Gain in $B_1$ cyclic channel
$C_{m_\alpha}$	Rotor pitching moment coefficient due to angle of attack
$C_{N_\alpha}$	Rotor normal force coefficient due to angle of attack
$C_{x_\alpha}$	Rotor yawing moment coefficient due to angle of attack
$C_{Y_\alpha}$	Rotor side force coefficient due to angle of attack
DLC	Direct lift control
$F_{xA_1}$	Normal force due to $A_1$ cyclic
$F_{x_\alpha}$	Rotor normal force due to angle of attack
$F_{yA_1}$	Rotor side force due to $A_1$ cyclic
$F_{Y_\alpha}$	Rotor side force due to angle of attack
$G_{GOV}$	Governor gain, governor proportional gain
$G_p$	Gain in lo-rate pitch channel - 26 ft rotor test
$G_y$	Gain in lo-rate yaw channel - 26 ft rotor test
$K_\beta$	Flapping stiffness in simplified rotor math model
$K_\zeta$	Lagging stiffness in simplified rotor math model
$K$	Gain, governor integral gain
$M_{xA_1}$	Rotor yawing moment due to $A_1$ cyclic
$M_{yA_1}$	Rotor pitching moment due to $A_1$ cyclic
$M_{Y_\alpha}$	Rotor pitching moment due to angle of attack

SYMBOLS

$M_{x_a}$	Rotor yawing moment due to angle of attack
$M_u$	Variation in aircraft pitching moment with velocity
NR1	Lagging frequency ratio for rotor blade $\omega_l/\Omega$
NR2	Flapping frequency ratio for rotor blade $\omega_f/\Omega$
1P	One per rev
S	Laplace operator
$T_u$	Variation in thrust with velocity
V	Aircraft velocity
W	Aircraft weight
$\omega$	Frequency RAD/SEC
$\omega_\beta$	Flap frequency
$\omega_c$	Wing chord frequency
$\omega_L$	Lag frequency
$\omega_N$	Natural frequency
$\omega_\alpha$	Wing torsion frequency
$\omega_v$	Wing vertical bending frequency
$\dot{z}_{VB}$	Vertical velocity of wing tip
$\ddot{z}_{VB}$	Vertical acceleration of wing tip
$z_{VB}$	Vertical translation of wing tip

SYMBOLS

$\alpha$	Angle of attack
$\gamma$	Locke number
$\delta_E$	Elevator deflection, positive down
$\delta_F$	Flap deflection, positive down
$\delta_S$	Spoiler deflection, positive up
$\zeta$	Damping ratio
$\theta_0$	Rotor blade collective pitch angle
$\lambda$	Inflow ratio
$\tau$	Control system time constant
$\psi$	Azimuthal location

1. SUMMARY

D222-10060-3

This work was carried out under Task C of NASA-Army Contract NAS2-6598.

The subject of this research contract was the application of feedback control in tilt rotor aircraft to accomplish the following objectives:

- . Improve handling qualities
- . Reduce blade loads
- . Alleviate gust response
- . Modal suppression and augmentation of  
aeroelastic stability

The feedback systems are primarily concerned with the application of swashplate cyclic and collective feedback, although a study has also been made of the use of flaps, spoilers and elevators for direct lift control. This work is preceded by the results of a parametric study of rotor derivatives in which special attention is given to the influence of blade frequencies. Load correlation with test data is demonstrated. Important differences are noted in the derivatives with respect to shaft angle of attack ( $\alpha$ ) and cyclic pitch ( $A_1$ ). The low in-plane stiffness blade is seen to have a negative hub pitching moment under normal flight conditions so that the net destabilizing effect of the rotor is less than would be the case for a high stiffness blade and this is confirmed by test data. This has beneficial effects on the horizontal and vertical



tail area requirements.

The blade load alleviation and stability augmentation studies show that various alternative objectives may be met using cyclic feedback. Alternative systems designed to minimize flapping and net pitching moment are examined. The requirements for cyclic pitch gain and azimuth in dynamic gust response situations are compared with those suitable for steady state alleviation and are shown to have differences. Methods or reading these differences are identified and recommended for further study. No stability problems were encountered up to optimal values of gain in any of the systems examined, although additional shaping is recommended in one case to increase the phase margin.

Direct lift control of normal acceleration response in turbulent air using flaps and spoilers feedback is examined. Reductions in normal acceleration demonstrated are approximately 45% in cruise and 15% in transition. This is considered highly encouraging since they are obtained without special effort at optimization or the use of elevator feedback to trim pitching moments due to flap and spoiler application.

In a low disk loading tilt rotor configuration, the combined

requirements of rotor governing and gust alleviation are shown to determine the selection of a governing system. A governing system, which senses the RPM variation of each rotor and feeds back to collective pitch an averaged signal, is shown to be optimal. A system design is discussed which meets selected error criteria in the presence of (1-cosine) and random axial gusts. The system is shown to be compatible with the flying quality characteristics of the aircraft. There is no significant degradation in basic flying qualities and at the same time a very substantial attenuation in responsiveness to axial gusts is noted.

The use of high rate swashplate feedback for modal suppression is shown to provide very substantial amounts of additional damping in the selected modes. Predicted results are compared with those obtained during full-scale tests. Attempts to introduce additional damping in blade modes showed promise but an extensive investigation was not made since this topic is currently of academic interest only. General conclusions and suggestions for additional study are made in each section. One general conclusion is that the full potential of some systems depends on the complementary effects from associated systems. These relationships are summarized in Table 9.1. For example, the effectiveness of a blade load alleviation

system will be augmented if aircraft vertical and pitching response to gusts is reduced by direct lift feedback control. Conversely, the effectiveness of a direct lift system in reducing cabin acceleration will be improved when working in parallel with a high rate swashplate modal suppression system. Thus, there is a strong case for eventually implementing all the systems discussed, although priority should be given to conventional SAS, rotor governing and load alleviation systems.

The implications of these proposals on hardware is discussed in Section 10. This section also considers the implications of fail-safe and fail-functional requirements and provides schematics for the various systems discussed. The changes necessary to the currently proposed M222 system in order to implement each of these systems are noted. The impact of converting to a fly-by-wire system is discussed.

Section 11 presents a number of recommended programs which are classified under the heading of additional analytical studies, wind tunnel program and implementation in a full-scale flight program.

Tentative costs and schedules for each of the proposed programs are given in Section 12.

## 2. PROP/ROTOR HUB FORCE AND MOMENT DERIVATIVES

### 2.1 BACKGROUND

Of fundamental importance to any feedback system using cyclic pitch is the manner in which hub forces and moments respond to changes in angle of attack and increments of pitch and yaw cyclic. It is known from previous work that rotor derivatives are sensitive to a number of parameters, in particular, blade frequency. In the case of soft in-plane prop/rotors the derivatives with respect to shaft angle of attack (alpha derivatives) have been shown to be particularly sensitive to variations in lead-lag frequency ratios near 1 per rev. An investigation of prop/rotor alpha derivative sensitivity to blade frequency and lock number is reported in Reference 2.1. The results reported here add to this body of knowledge by providing information on the behavior of hub forces and moments with respect to cyclic pitch ( $A_1$  derivatives). The mathematical model used for this study is shown in Figure 2.1. This model was chosen because it permits independent variation of flap and lag frequency without restriction. The mass and airfoil properties used are those of the Model 222 26-foot diameter prop rotor. Results for the same rotor with its actual root restraints are given for smaller variations in blade flap and lag per rev frequency and over a range of altitude and velocity. Since there are currently in use a number of different approaches toward non-dimensionalizing rotor derivatives, the results given in this report are quoted

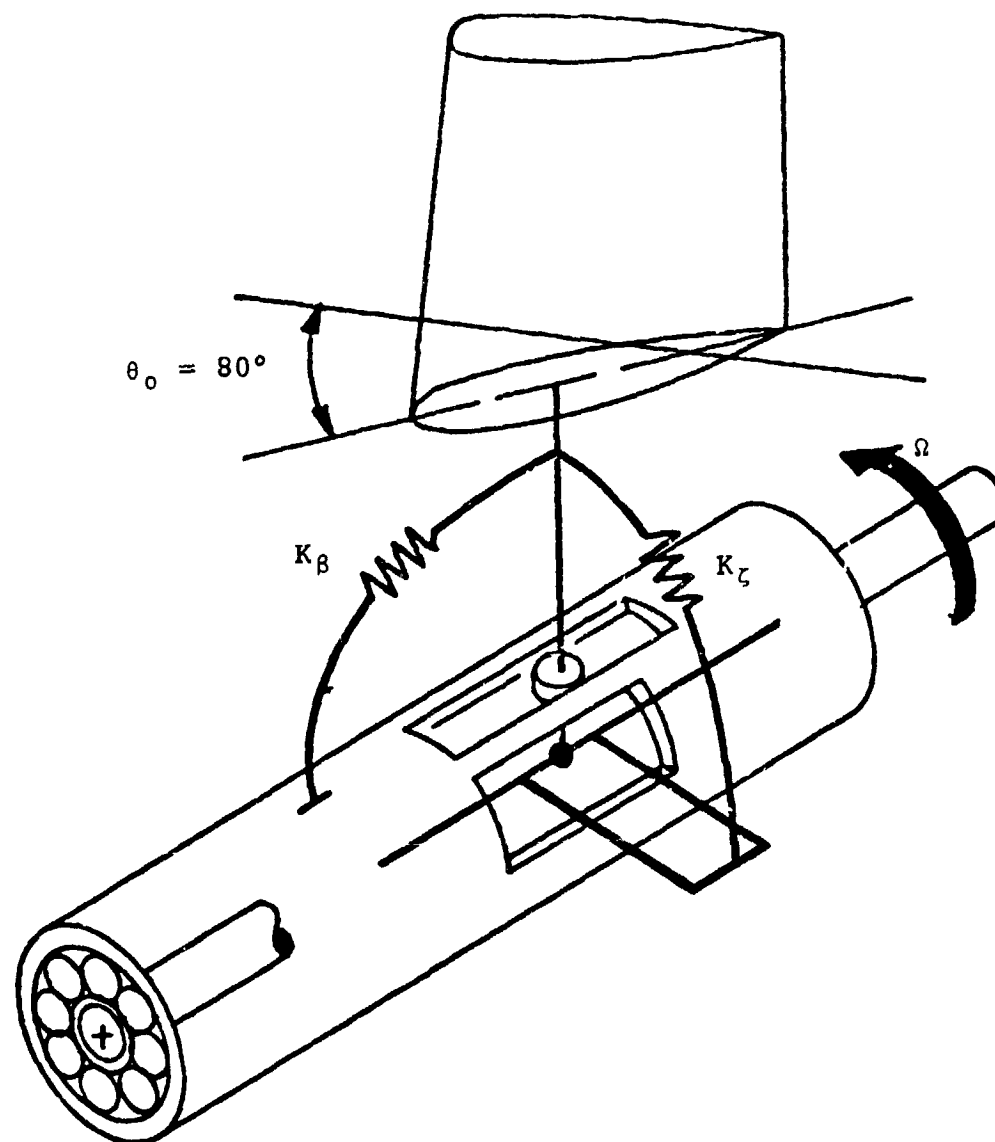


Figure 2.1 Mathematical Model for Rotor Derivative  
Parametric Trend Studies

in dimensional units to avoid ambiguity. Physical properties of the rotor are given in Appendix A.

## 2.2 VARIATION OF DERIVATIVES WITH LEAD-LAG FREQUENCY RATIO

The behavior of force and moment derivatives over the range of 0.6 to 2.0 per rev in lead-lag and 1.0, 1.3 and 1.5 for flap is given in Figures 2.2 through 2.5. It is noted that the alpha and cyclic derivatives share the high degree of sensitivity to lead-lag frequency ratio particularly values of  $N_{R_1}$  just below 1.0.

In both sets of derivatives normal force and yawing moment attain a minimum at  $N_{R_1} = 1$ , and that side force and pitching moment change sign when  $N_{R_1}$  drops below a value of unity.

This result for the alpha derivatives is the same as for the earlier study published in Reference 2.1; the present study confirms that similar behavior is encountered in the  $A_1$  derivatives.

## 2.3 VARIATION OF LEAD-LAG AND FLAP FREQUENCY RATIO OVER A LIMITED RANGE

Figures 2.6 through 2.9 present carpets of alpha and cyclic derivatives for the Model 222 26-foot diameter rotor at 100 knots and 385 RPM. Since in the sign convention used positive  $A_1$  means that the blade angle is maximum at azimuth zero (top center), and shaft angle of attack implies maximum excursion in blade angle of attack at 90-degrees, some correspondence is expected between  $F_{X_\alpha}$  and  $F_{Y_{A_1}}$ ,  $M_{Y_\alpha}$  and  $M_{X_{A_1}}$ , etc. It is

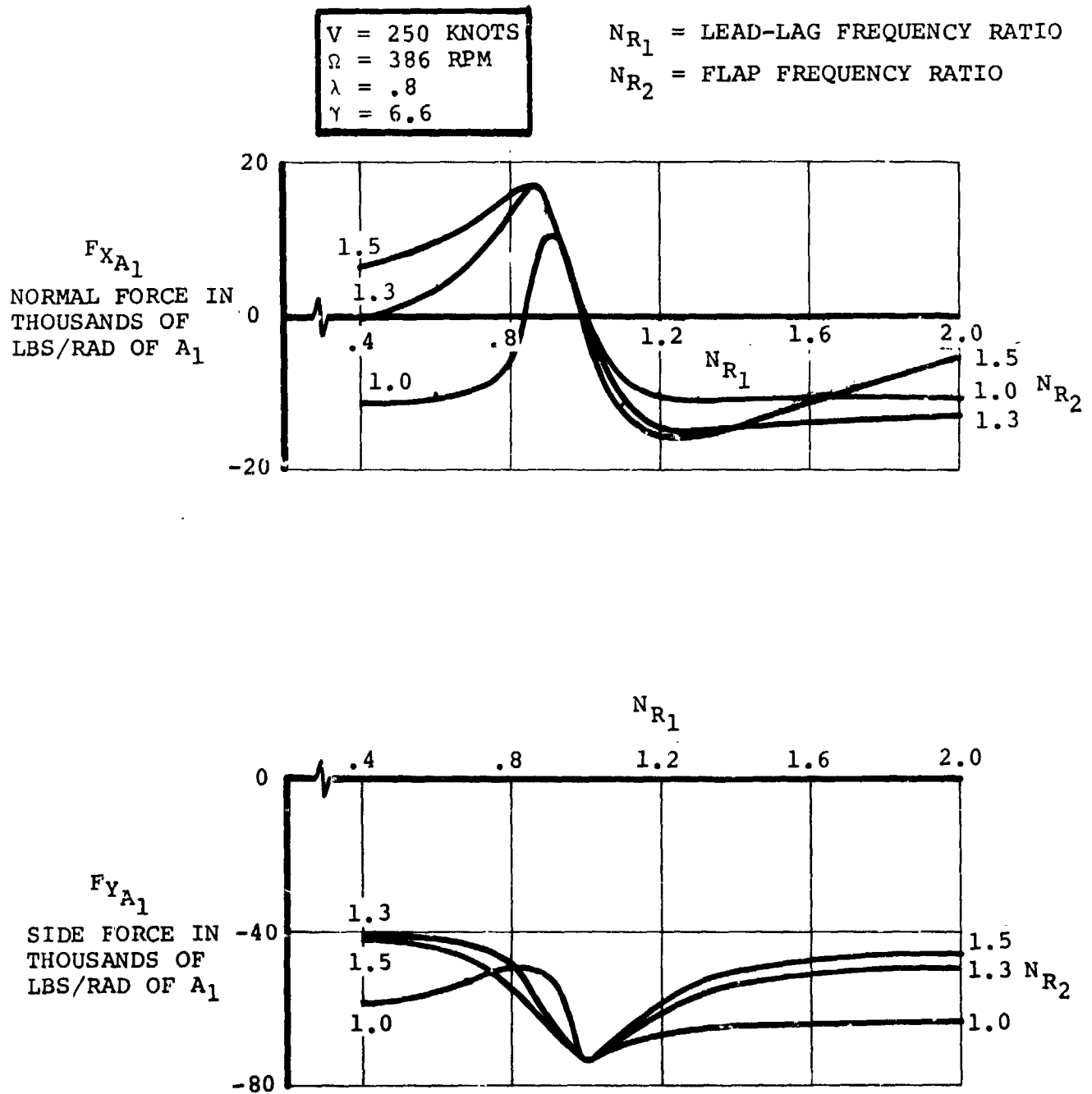


FIGURE 2.2. EFFECT OF VARIATION OF BLADE FREQUENCY RATIOS ON CYCLIC FORCE DERIVATIVES - 250 KNOTS



$V = 250$  KNOTS  
 $\Omega = 386$  RPM  
 $\lambda = .8$   
 $\gamma = 6.6$

$N_{R1} =$  LEAD-LAG FREQUENCY RATIO

$N_{R2} =$  FLAP FREQUENCY RATIO

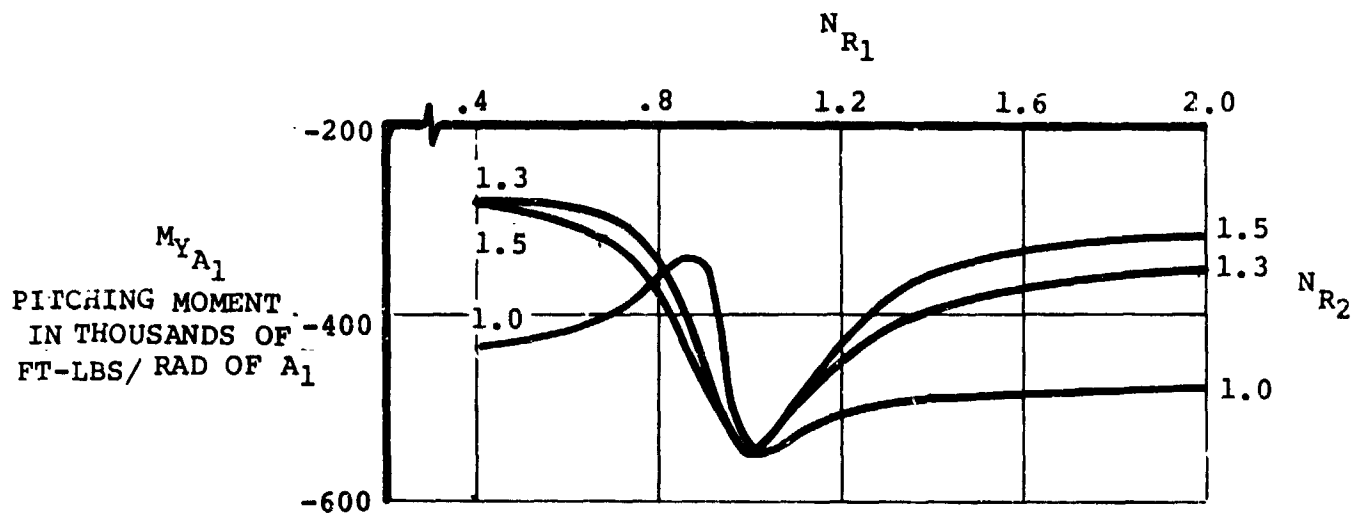
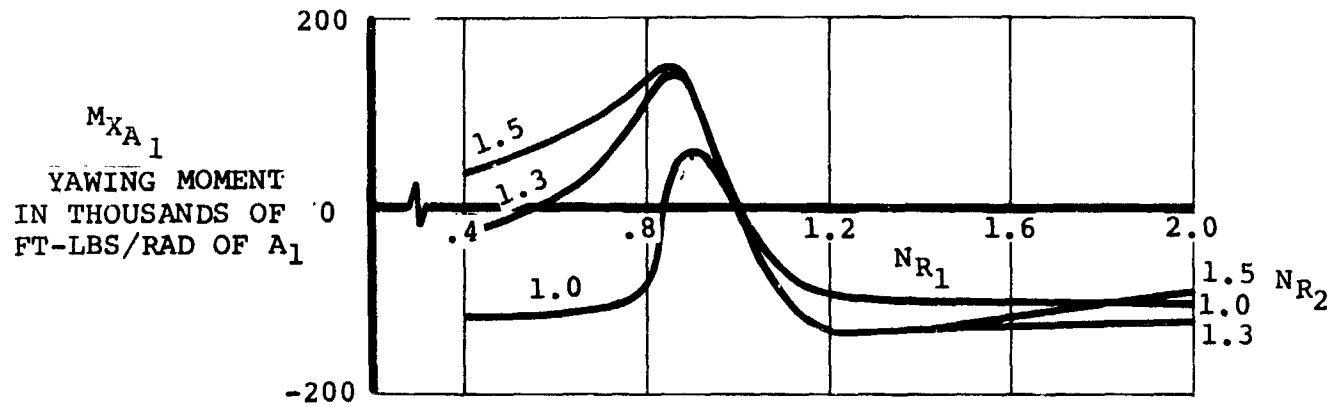


FIGURE 2.3. EFFECT OF VARIATION OF BLADE FREQUENCY RATIOS  
ON CYCLIC MOMENT DERIVATIVES - 250 KNOTS

$V = 250$  KNOTS  
 $\Omega = 386$  RPM  
 $\lambda = .8$   
 $\gamma = 6.6$

$NR_1$  = LEAD-LAG FREQUENCY RATIO

$NR_2$  = FLAP FREQUENCY RATIO

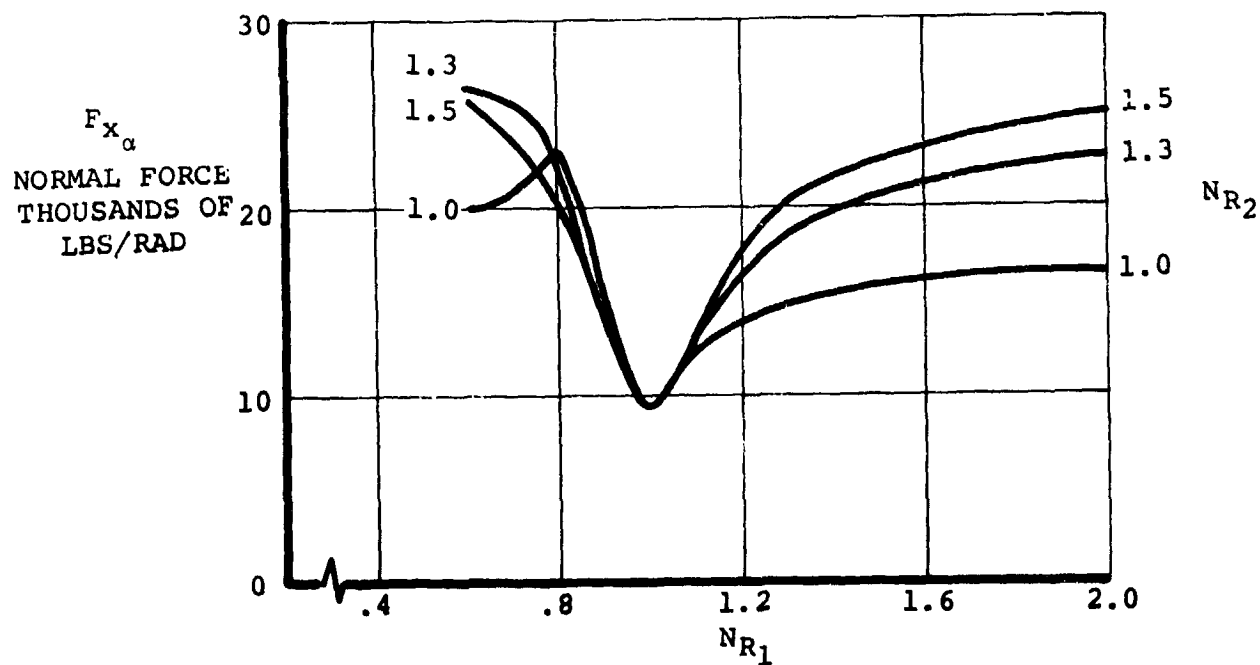
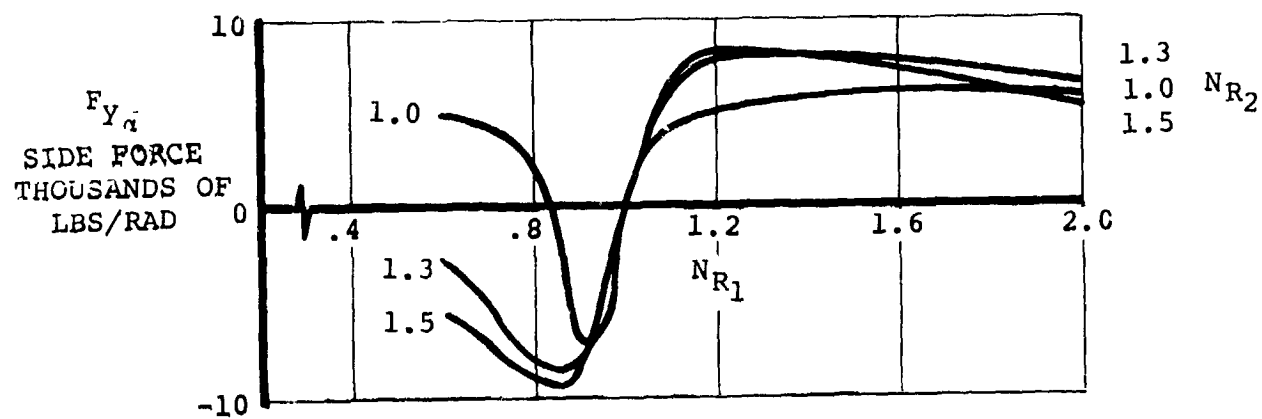


FIGURE 2.4. VARIATION OF PROP/ROTOR NORMAL AND SIDE FORCE ALPHA DERIVATIVES WITH RESPECT TO BLADE LEAD-LAG FREQUENCY.

$V = 250$  KNOTS  
 $\Omega = 386$  RPM  
 $\lambda = .8$   
 $\gamma = 6.6$

$N_{R1}$  = LEAD-LAG FREQUENCY RATIO

$N_{R2}$  = FLAP FREQUENCY RATIO

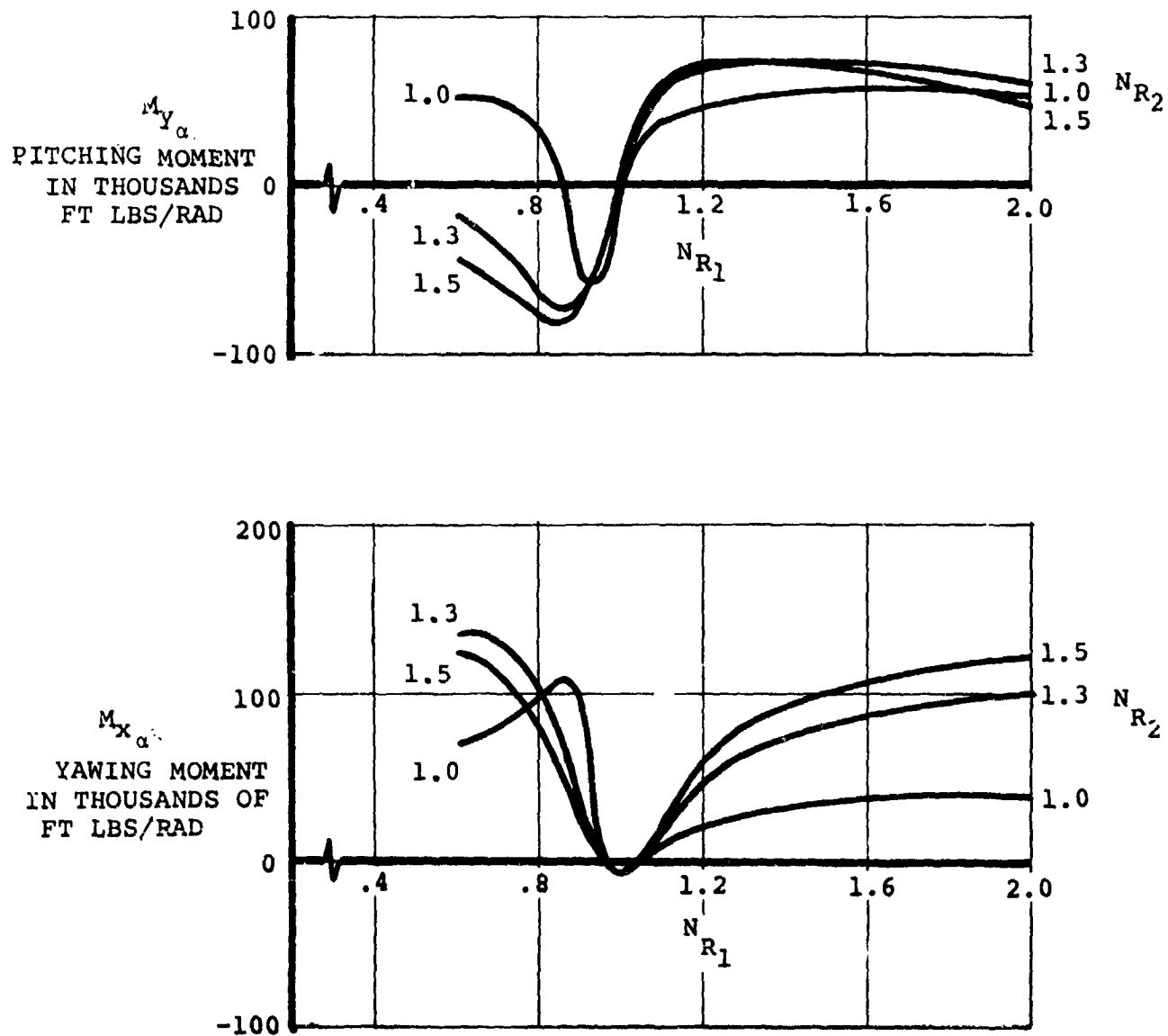
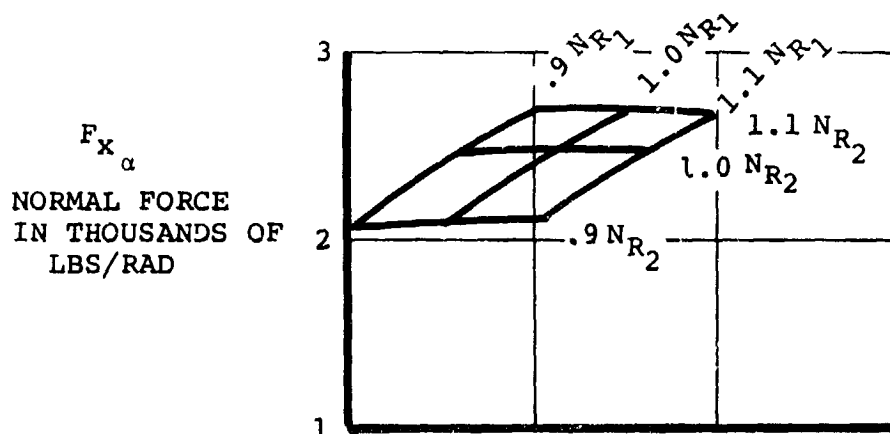


FIGURE 2.5. VARIATION OF PROP/ROTOR PITCHING AND YAWING MOMENT ALPHA DERIVATIVES WITH RESPECT TO BLADE LEAD-LAG FREQUENCY.



BASIC DATA  
 $\Omega = 386 \text{ RPM}$   
 $V = 100 \text{ KNOTS}$   
 $NR_1 = 0.74$   
 $NR_2 = 1.33$

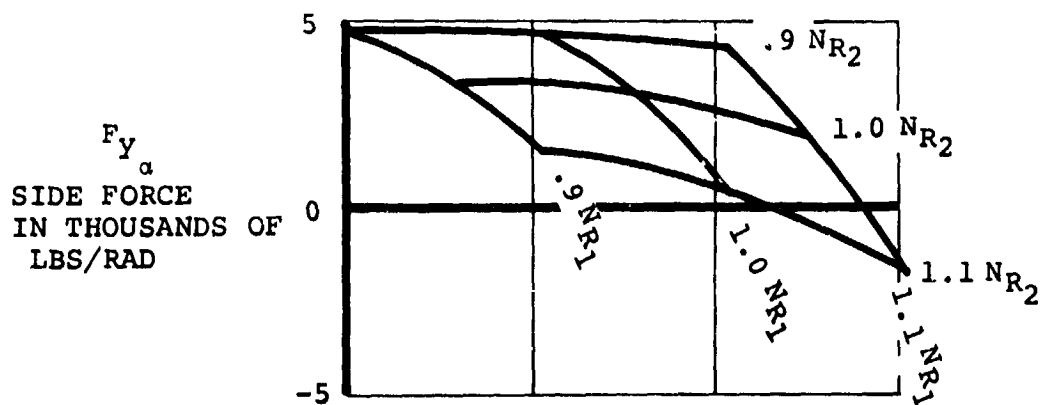


FIGURE 2.6 SENSITIVITY OF M222 26FT HINGELESS ROTOR ALPHA DERIVATIVES FOR NORMAL AND SIDE FORCE TO VARIATIONS IN BLADE LEAD-LAG AND FLAP NATURAL FREQUENCIES

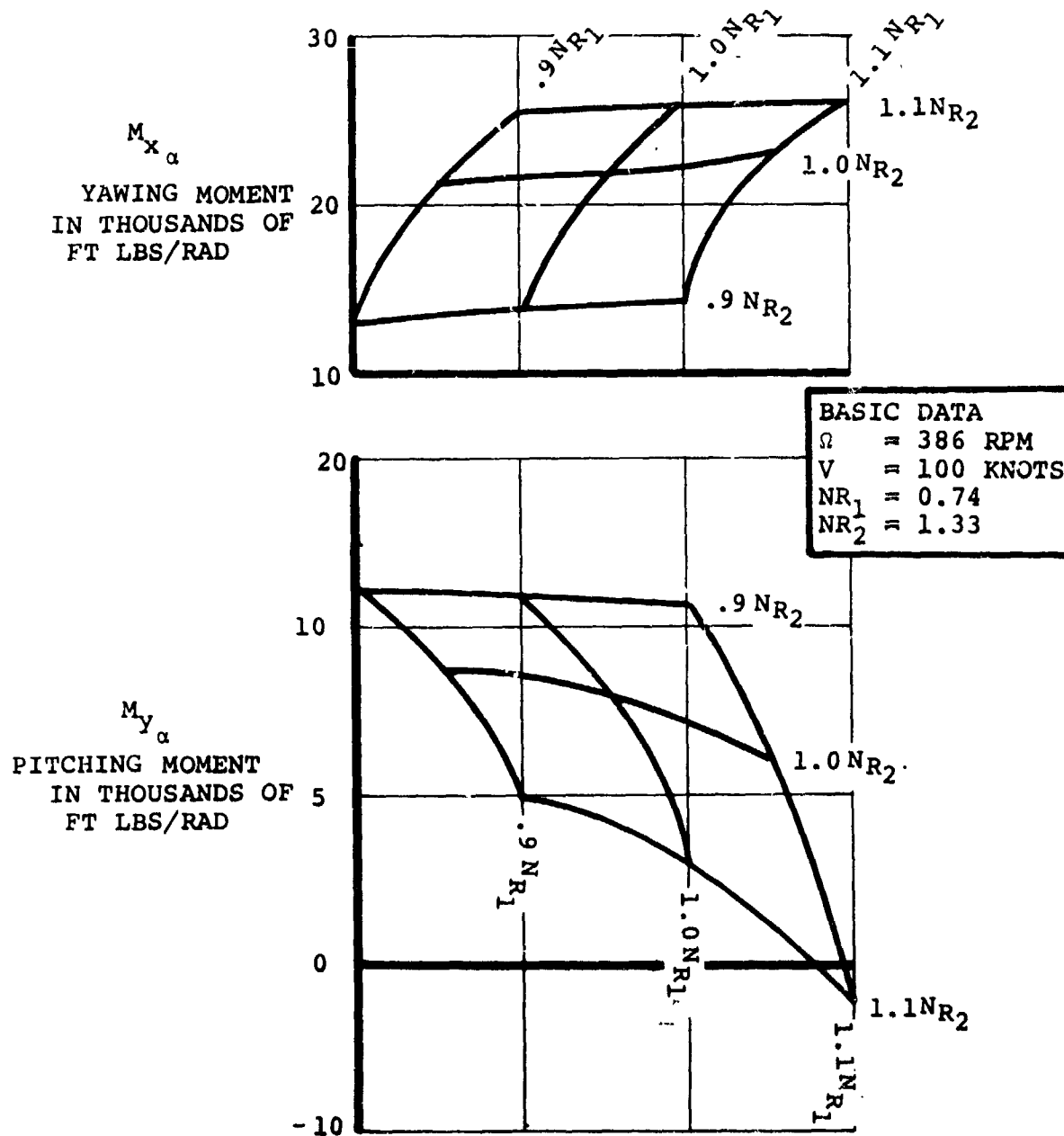


FIGURE 2.7 SENSITIVITY OF M222 26FT HINGELESS ROTOR ALPHA DERIVATIVES FOR YAWING MOMENT AND PITCHING MOMENT VARIATIONS IN BLADE LEAD-LAG AND FLAP NATURAL FREQUENCIES

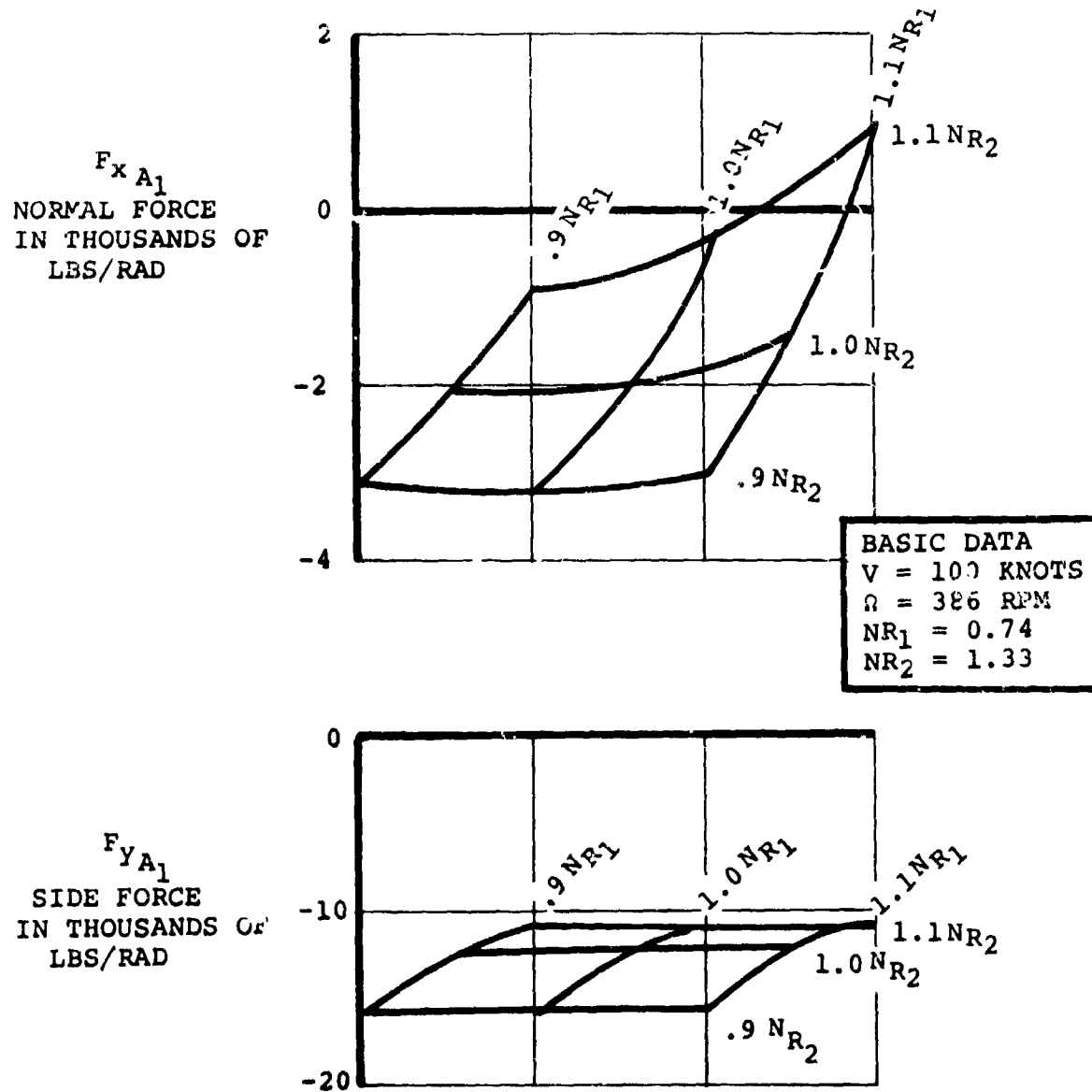
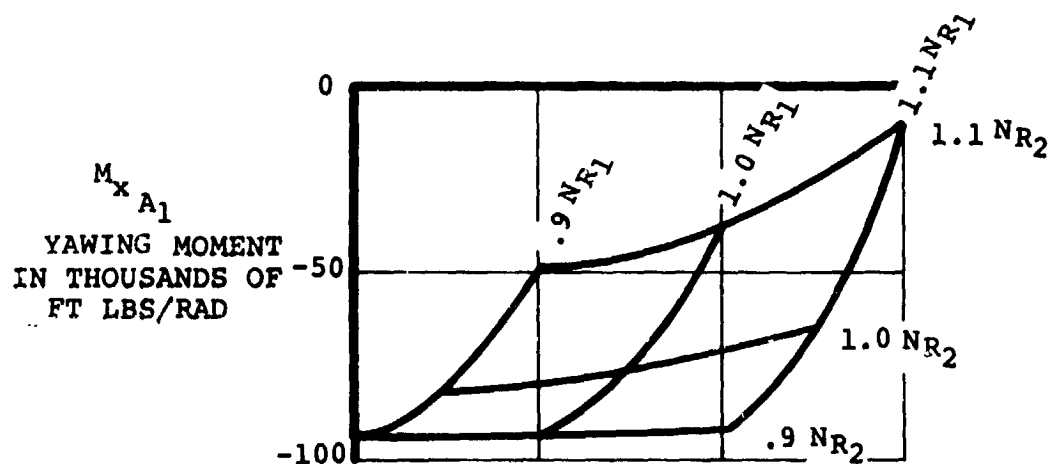


FIGURE 2 8 SENSITIVITY OF M222 26FT DIAMETER HINGELESS ROTOR  
CYCLIC DERIVATIVES FOR NORMAL AND SIDE FORCE TO  
VARITIONS IN BLADE LEAD-LAG AND FLAP NATURAL  
FREQUENCIES



BASIC DATA	
V	= 100 KNOTS
$\Omega$	= 386 RPM
$NR_1$	= 0.74
$NR_2$	= 1.33

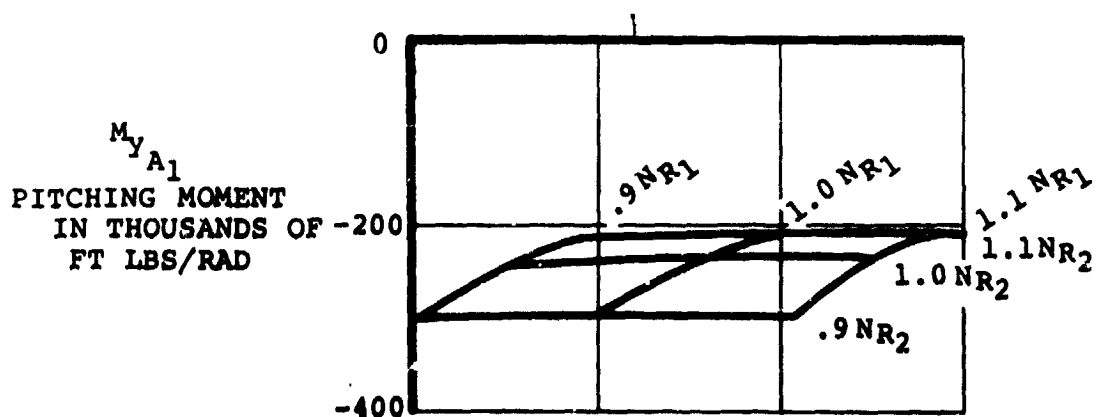


FIGURE 2.9 SENSITIVITY OF M222 26FT HINGELESS ROTOR CYCLIC DERIVATIVES FOR YAWING AND PITCHING MOMENT, TO VARIATIONS IN BLADE LEAD-LAG AND FLAP NATURAL FREQUENCIES

significant, however, that when such a correspondence is observed there are differences in magnitude. In particular the side force due to  $A_1$  is approximately four times larger than the normal force due to  $\alpha$ . Figures 2.10 through 2.13 present the equivalent data for 200 knots and a similar pattern is noted.

These comparisons of  $\alpha$  and cyclic derivatives are of considerable importance since they indicate that in some cases there are substantial differences which may be reflected as difficulties in selecting combinations of cyclic to zero out the hub forces and moments due to  $\alpha$ . That is to say, even under the simplest static conditions there will be limits to the effectiveness of swashplate feedback load alleviation system.

#### 2.4 EFFECTS OF ALTITUDE AND SPEED ON PROP/ROTOR DERIVATIVES

Figures 2.14 through 2.17 present carpets of  $\alpha$  and  $A_1$  derivatives for altitudes of 0, 10,000 and 20,000 feet and velocities of 100 through 300 knots. These plots display anticipated trends of increasing force and moment with velocity and reduction with altitude or density.

#### 2.5 CORRELATION WITH TEST DATA

The derivative studies in the preceding paragraphs were performed using the Boeing Vertol C-41 prop/rotor derivative program. This program has been used extensively in predicting and correlating with rotor derivatives and associated data obtained on test. In general prediction of trends is excellent



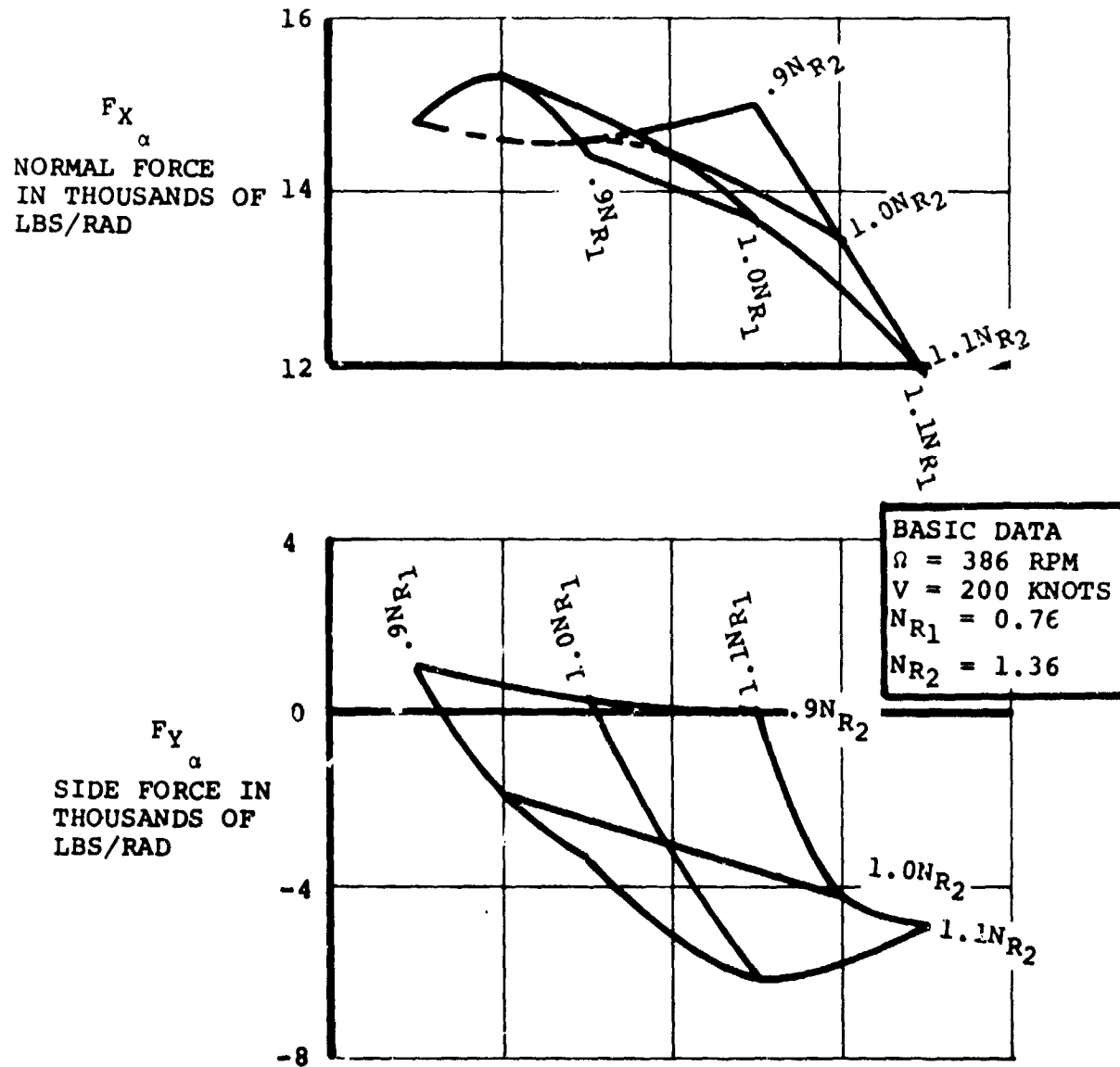


FIGURE 2.10. SENSITIVITY OF M222 26-FT DIAMETER HINGE-LESS ROTOR NORMAL AND SIDE FORCE ALPHA DERIVATIVES TO BLADE LEAD-LAG AND FLAP NATURAL FREQUENCIES.

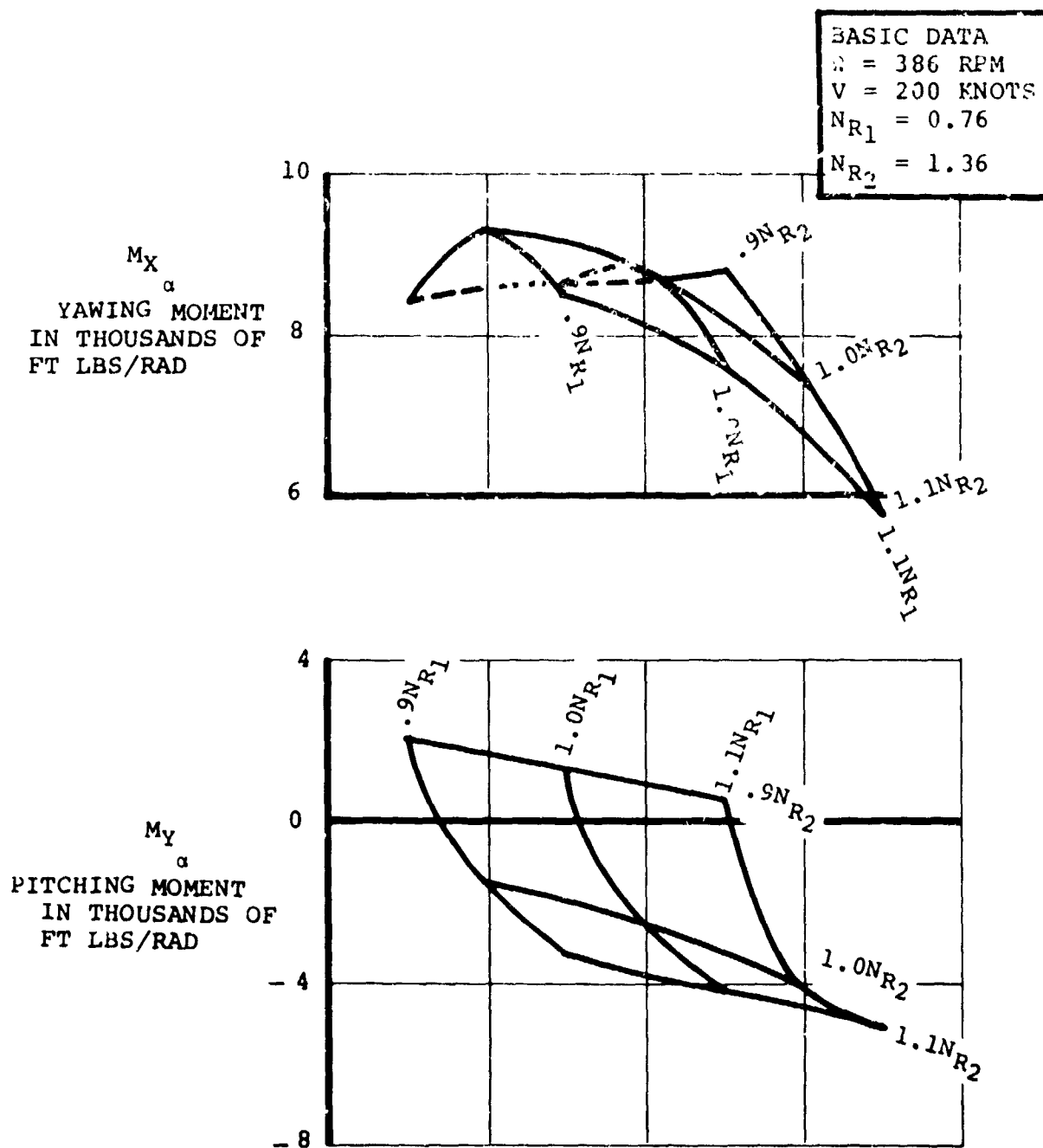


FIGURE 2.11. SENSITIVITY OF M222 26-FT DIAMETER HINGE-LESS ROTOR YAWING AND PITCHING MOMENT ALPHA DERIVATIVES WITH RESPECT TO BLADE LEAD-LAG AND FLAP NATURAL FREQUENCIES.

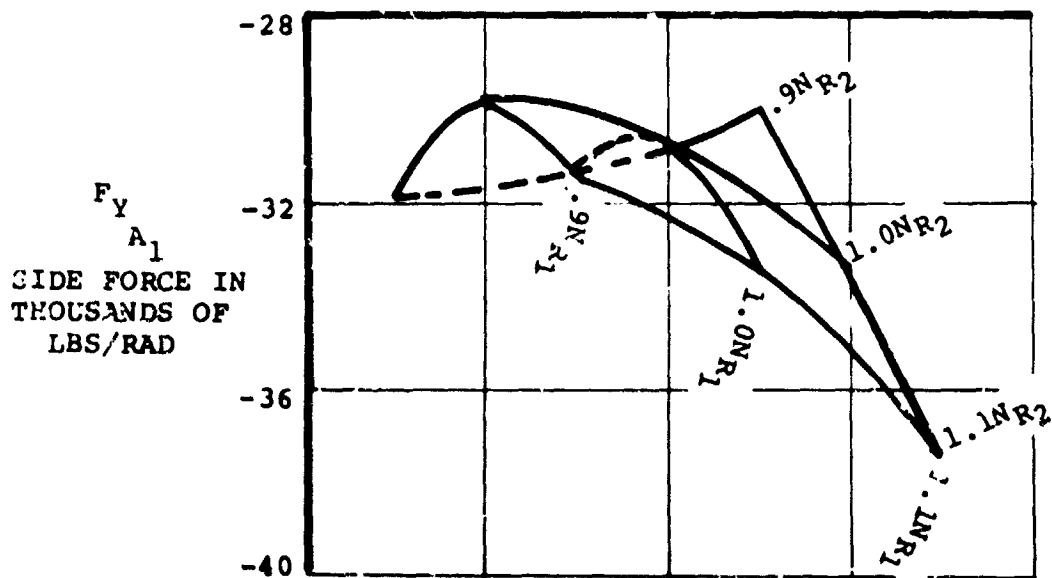
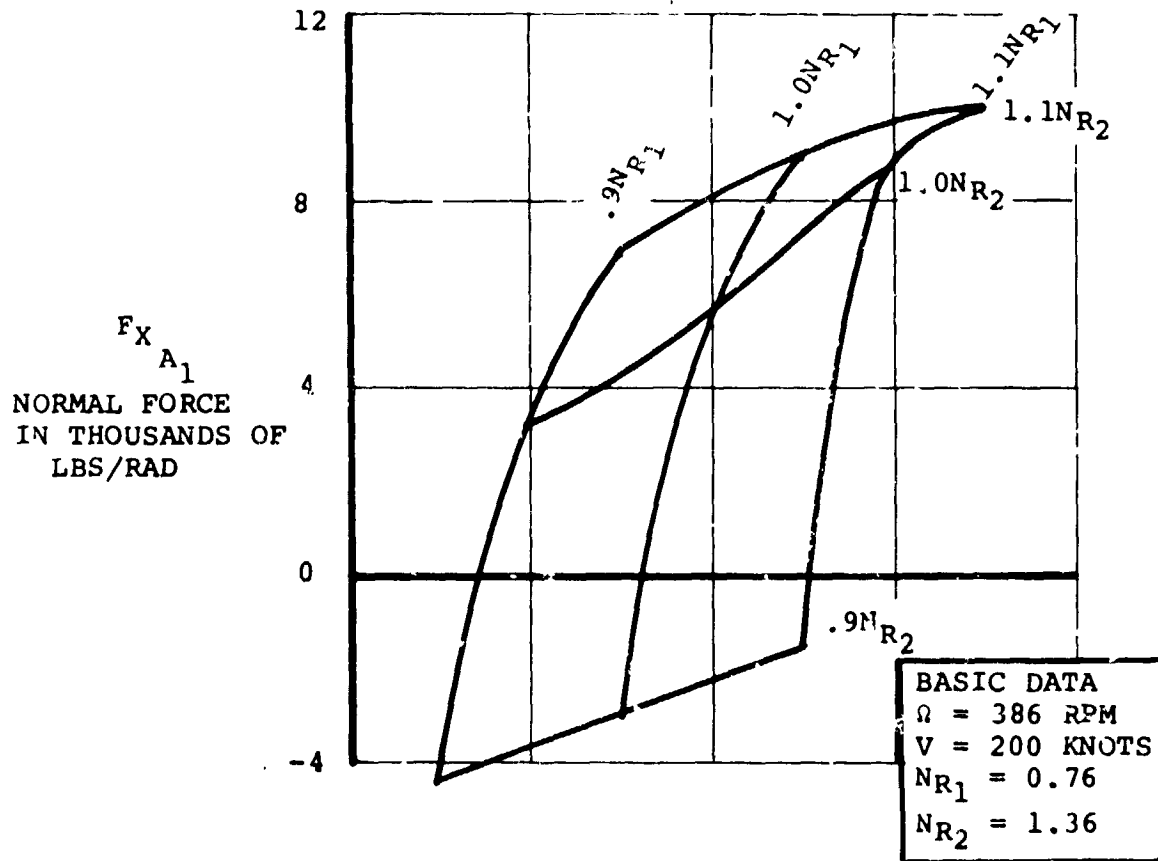


FIGURE 2.12. SENSITIVITY OF M222 26-FT DIAMETER HINGE-LESS ROTOR NORMAL AND SIDE FORCE CYCLIC DERIVATIVES WITH RESPECT TO BLADE LEAD-LAG AND FLAP NATURAL FREQUENCIES.

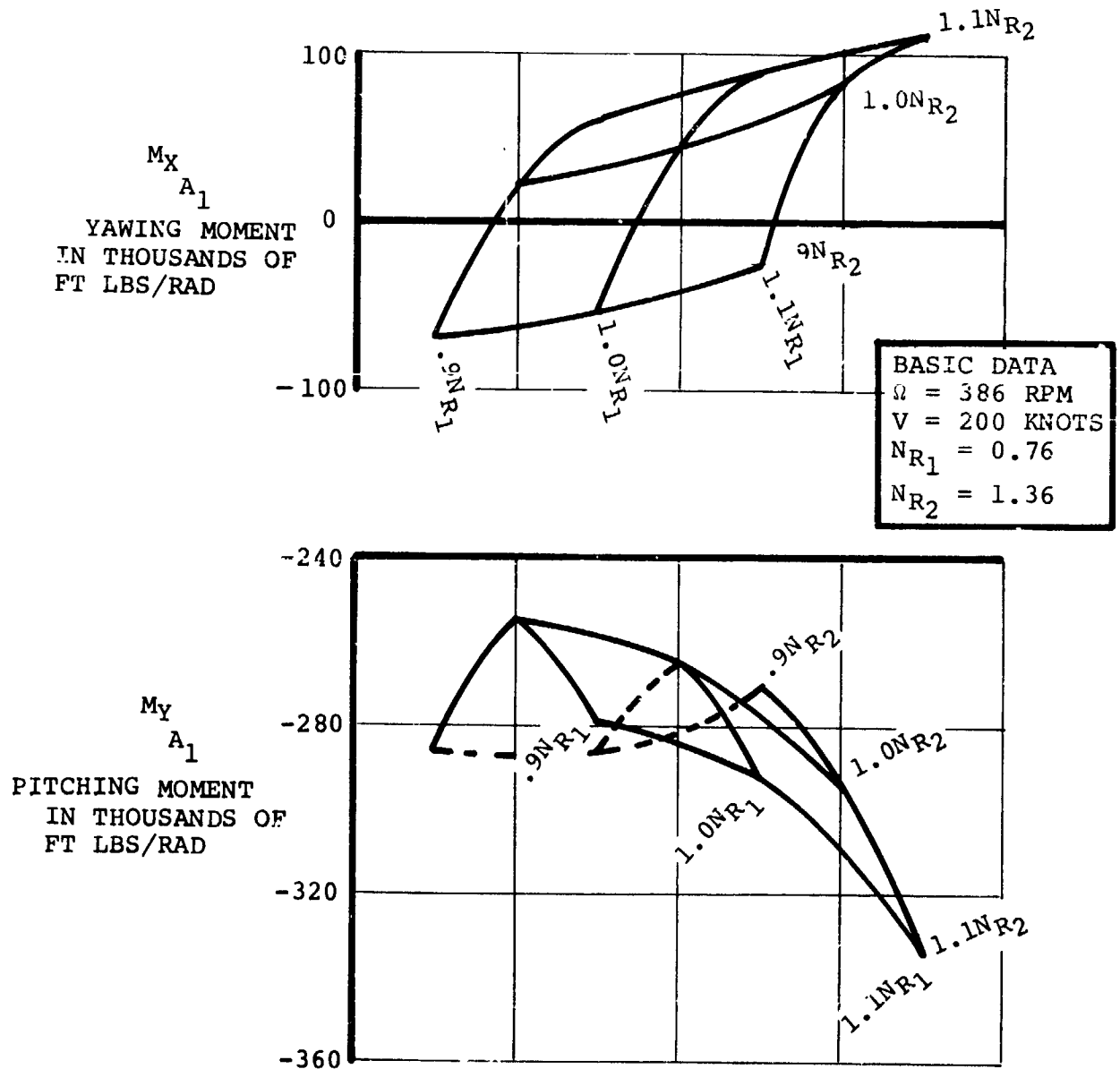
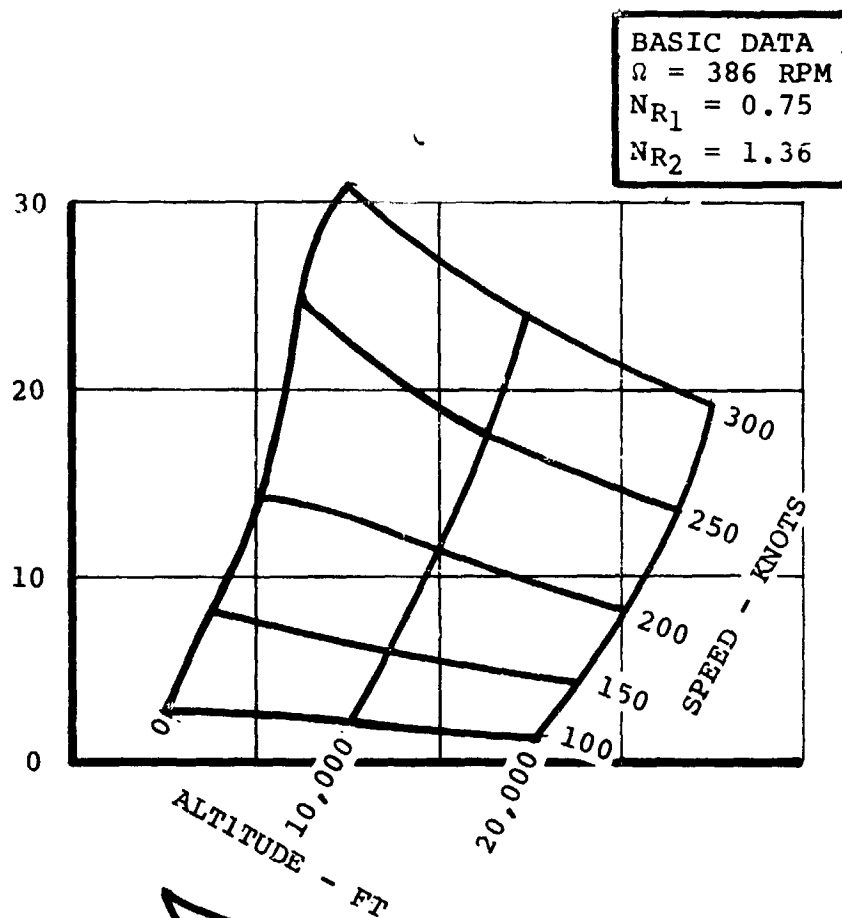


FIGURE 2.13. SENSITIVITY OF M222 26-FT DIAMETER HINGE-LESS ROTOR YAWING AND PITCHING MOMENT CYCLIC DERIVATIVES WITH RESPECT TO BLADE LEAD-LAG AND FLAP NATURAL FREQUENCIES.

$F_{X_\alpha}$   
NORMAL FORCE  
IN THOUSANDS OF  
LBS/RAD



$F_{Y_\alpha}$   
SIDE FORCE  
IN THOUSANDS  
OF LBS/RAD

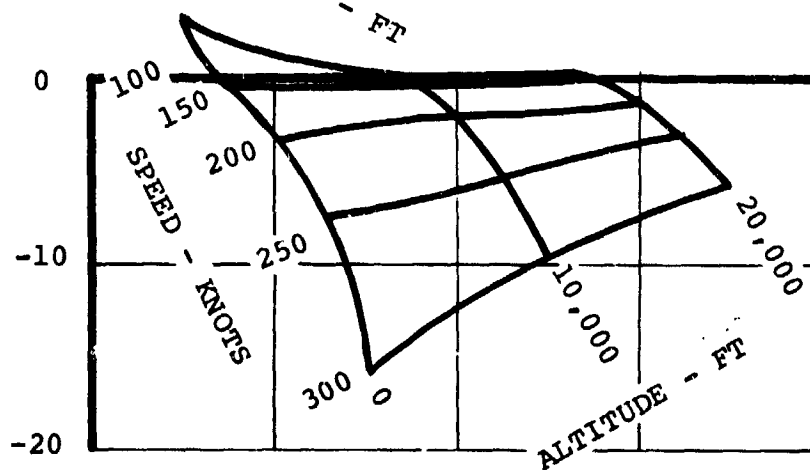


FIGURE 2.14. SENSITIVITY OF M222 26-FT DIAMETER HINGE-LESS ROTOR NORMAL AND SIDE FORCE ALPHA DERIVATIVES WITH RESPECT TO ALTITUDE AND VELOCITY.

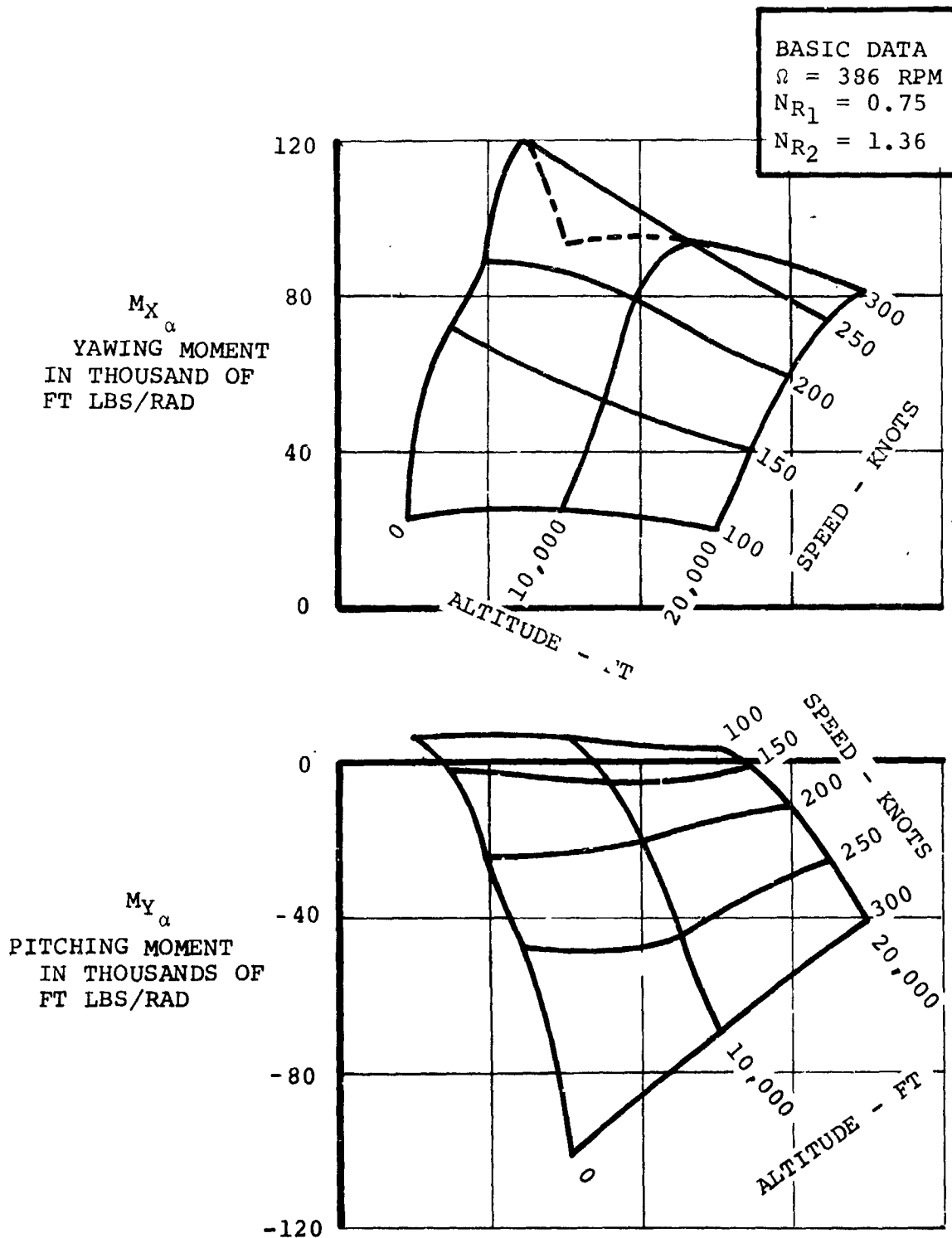
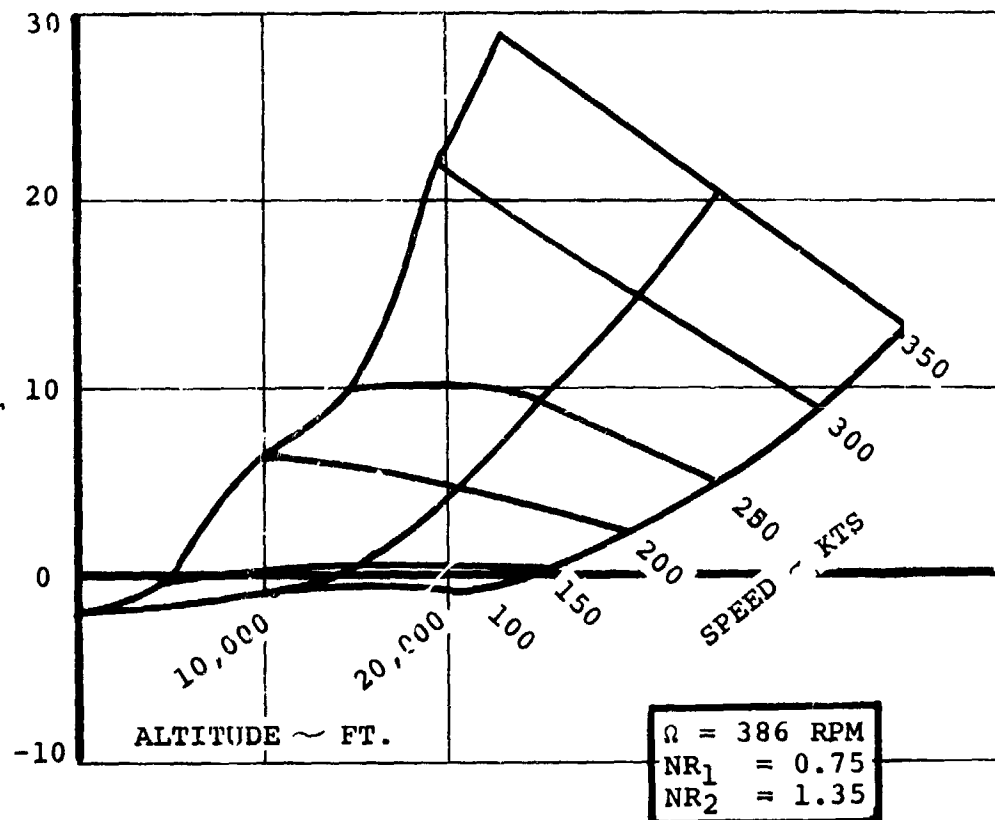


FIGURE 2.15. SENSITIVITY OF M222 26-FT DIAMETER HINGE-LESS ROTOR YAWING AND PITCHING MOMENT ALPHA DERIVATIVES WITH RESPECT TO ALTITUDE AND VELOCITY.

$F_{x A_1}$   
NORMAL FORCE  
IN THOUSANDS OF  
LBS/RAD



$F_{y A_1}$   
SIDE FORCE  
IN THOUSANDS OF  
LBS/RAD

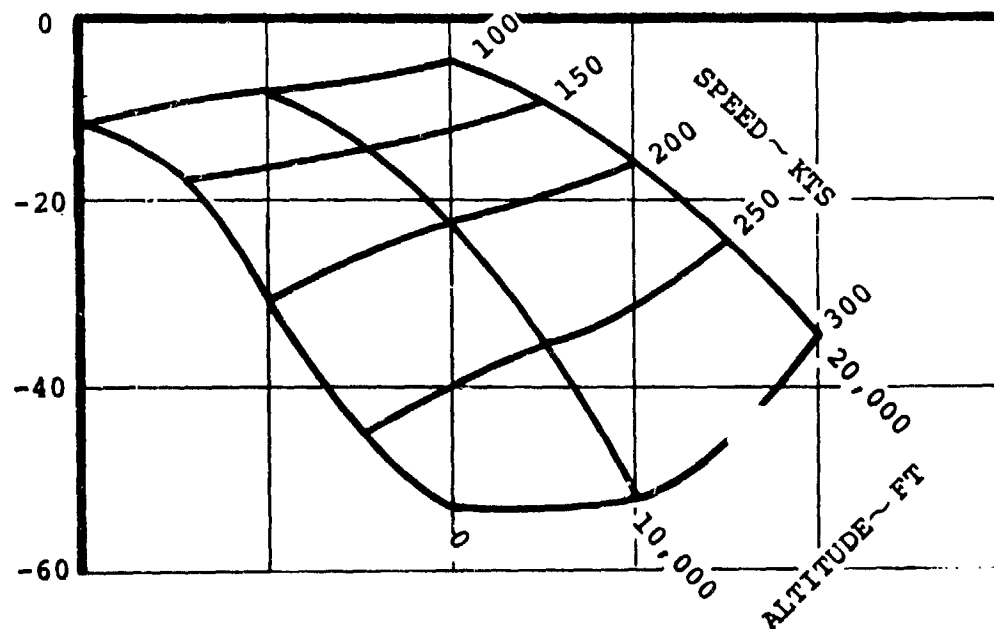


FIGURE 2.16 SENSITIVITY OF M222 26FT DIAMETER ROTOR  
NORMAL FORCE AND SIDE FORCE CYCLIC  
DERIVATIVES TO ALTITUDE AND AIRSPEED

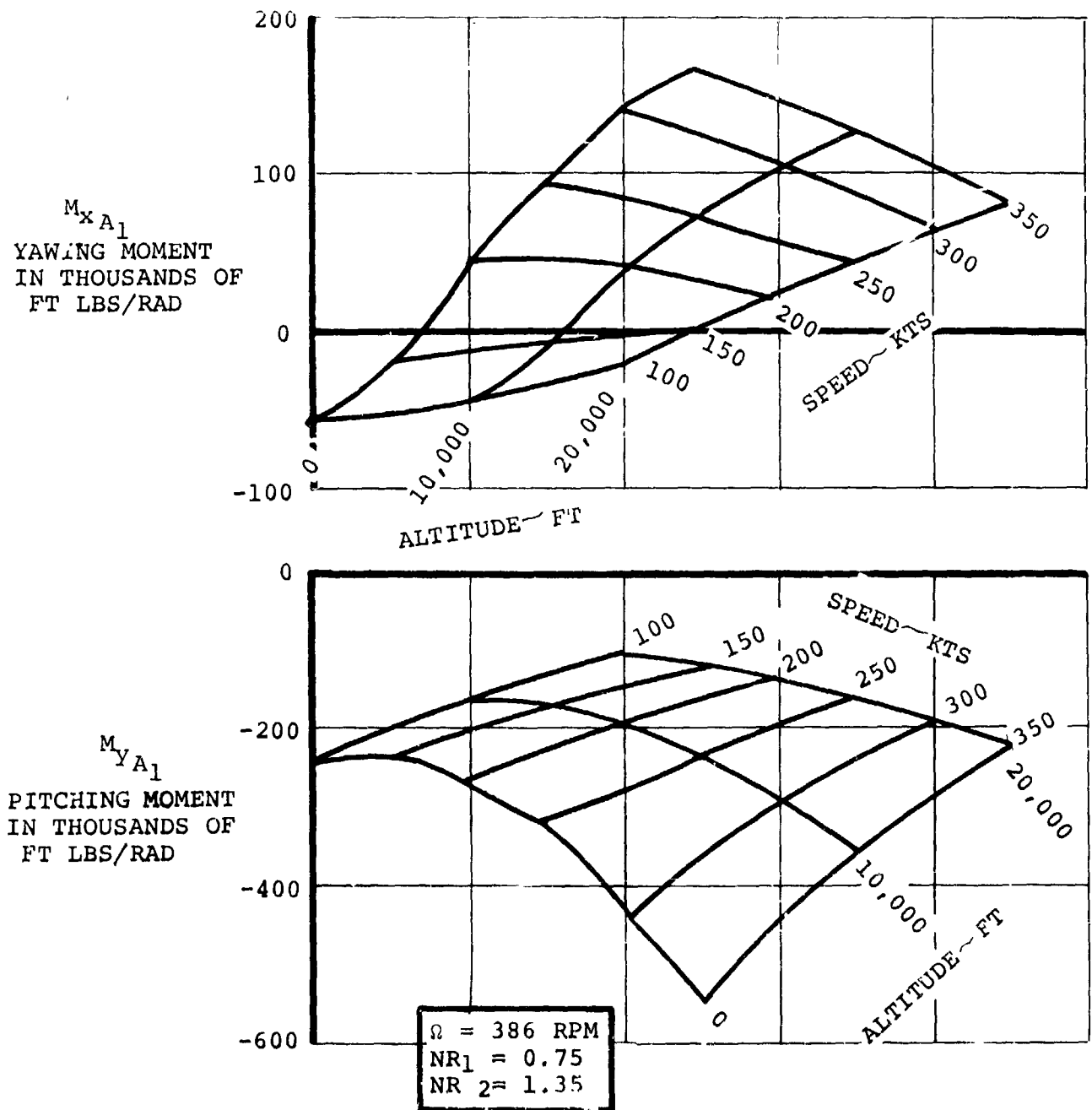


FIGURE 2.17. SENSITIVITY OF M222 26FT DIAMETER ROTOR YAWING AND PITCHING MOMENT CYCLIC DERIVATIVES TO ALTITUDE AND AIRSPEED



with quite good agreement in absolute magnitudes.

#### 2.5.1 Model 213 Four Blade Hingeless Rotor Correlation

Figure 2.18 presents correlation with rotor derivatives measured on a 1/9 scale dynamically similar model of a tilt/stowed rotor conversion model. In this test the rotor hub forces and moments were carefully measured over a range of RPM in which the lead-lag modal frequency progressed from less than 1 per rev at 900 RPM to values significantly greater than 1 per rev as the rotor was feathered. The measured values confirm the predicted behavior trend and the quantitative correlation is also excellent.

#### 2.5.2 Correlation With Model 222 26-Foot Diameter Rotor Test in NASA-Ames 40 X 80-Foot Tunnel

Figure 2.19 shows the schematic of the windmilling test stand and its instrumentation. Test data were obtained from strain gages mounted on the outer portion of the wing as shown, and calibrated to measure normal force, pitching moment and yawing moment. Comparison with test data was made by calculating the moments about the wing strain gage locations using forces and moments predicted by the C-41 program. The results of this comparison for alpha derivatives are given in Figure 2.20 and for cyclic pitch derivatives in Figures 2.21 and 2.22. The analysis did not attempt to account for force and moment contributions from nacelle and wing aerodynamic interference. Nevertheless, quite good correlation is observed. These plots also show the values of derivatives

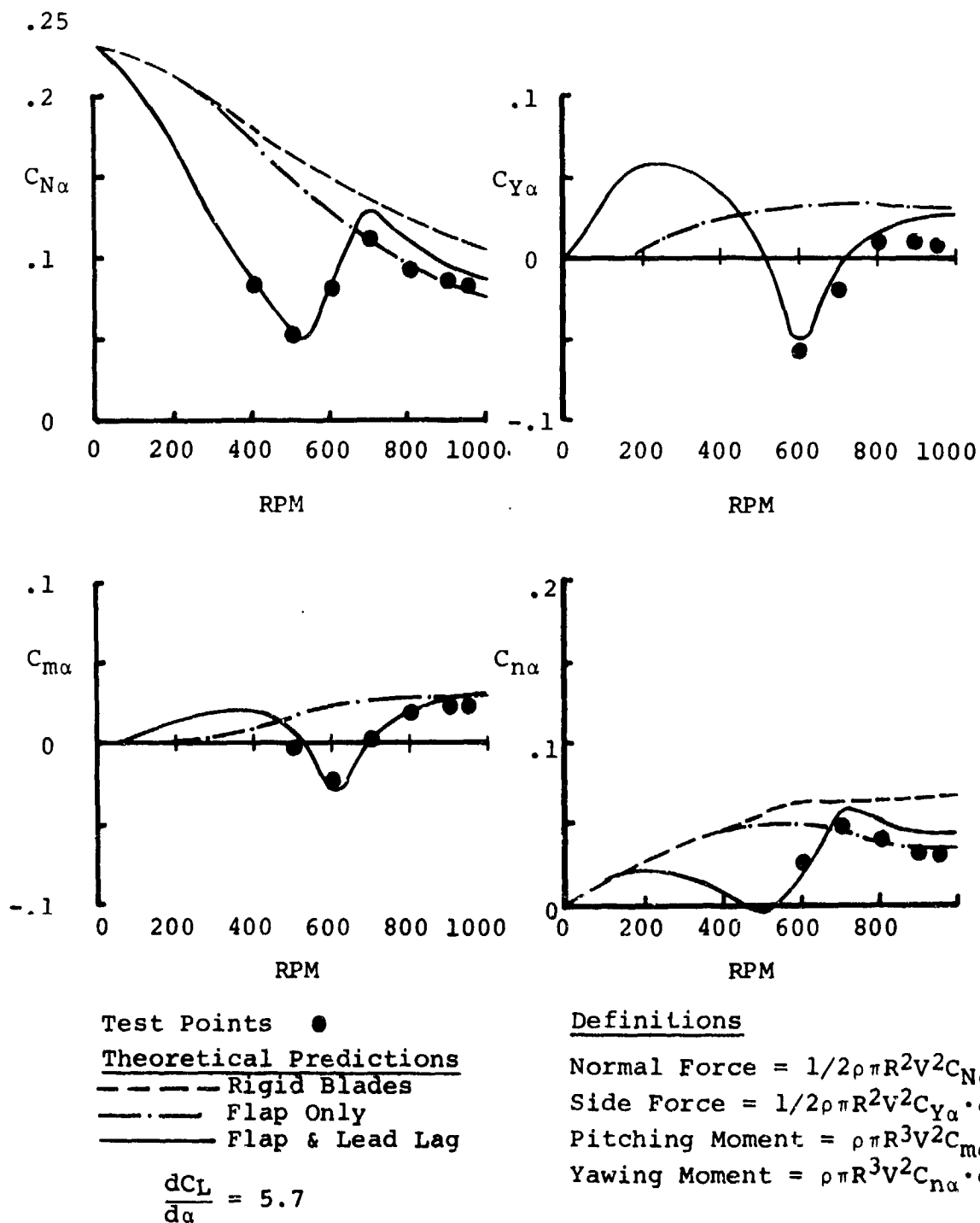


Figure 2.18. Model 213 1/9-Scale Conversion Model - 85 Ft/Sec  
Derivative Variation with RPM

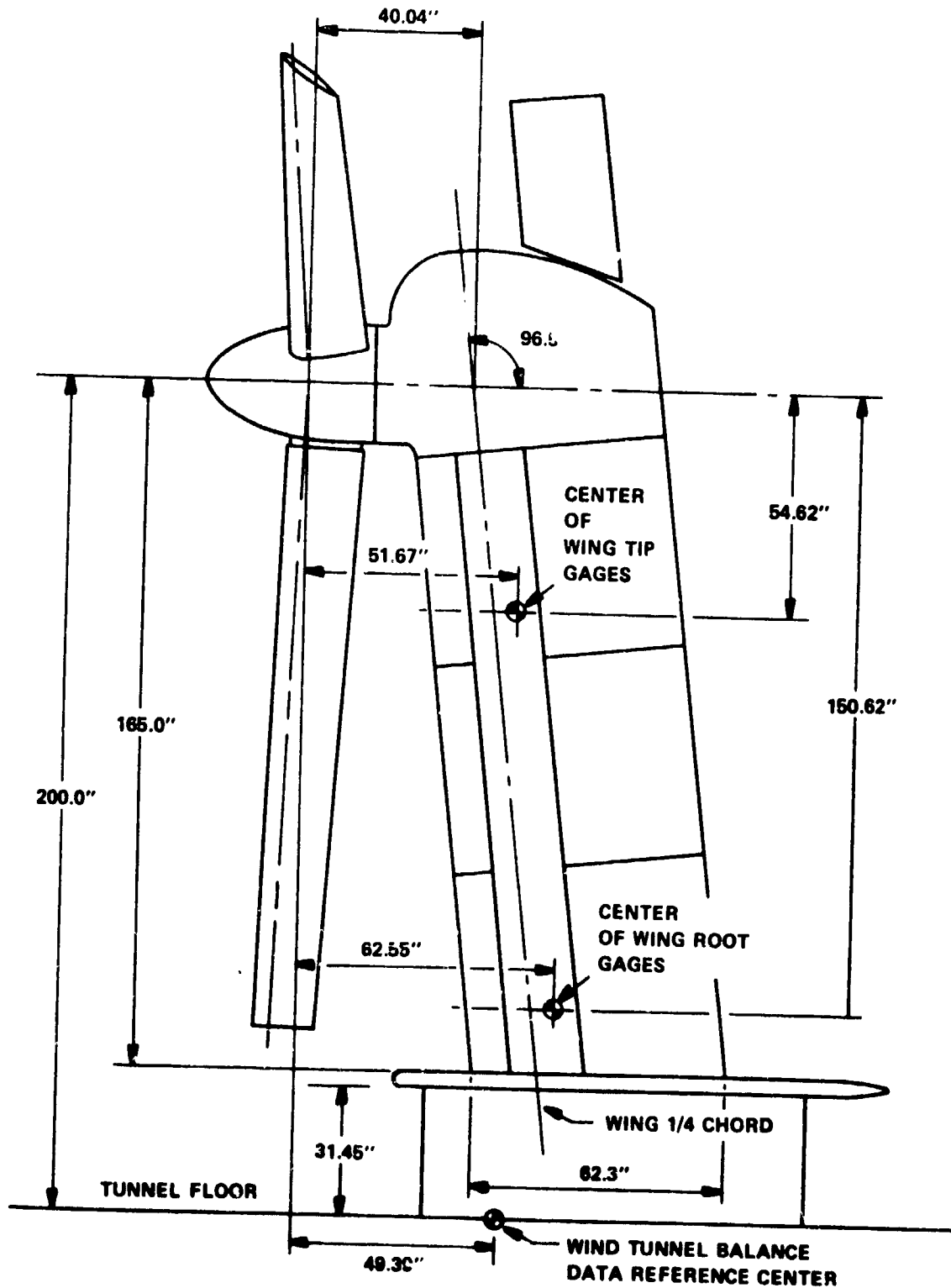


FIGURE 2.19. 26 FT. ROTOR TEST STAND IN NASA'S 40' X 80' TUNNEL

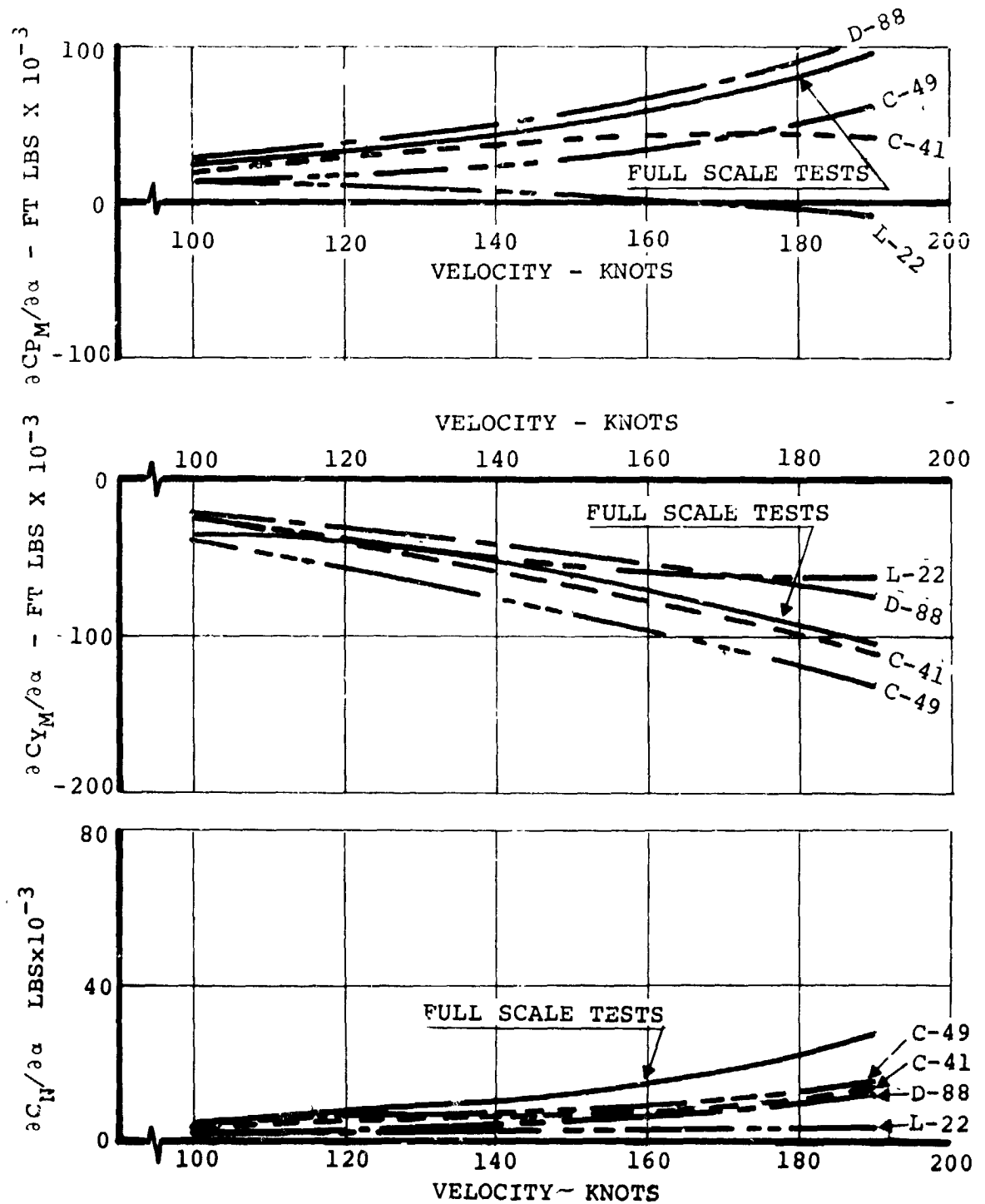


FIGURE 2.20. CORRELATION OF 26 FT. ROTOR TEST DATA WITH VARIOUS ROTOR DERIVATIVE PROGRAMS -  $\alpha$  DERIVATIVES

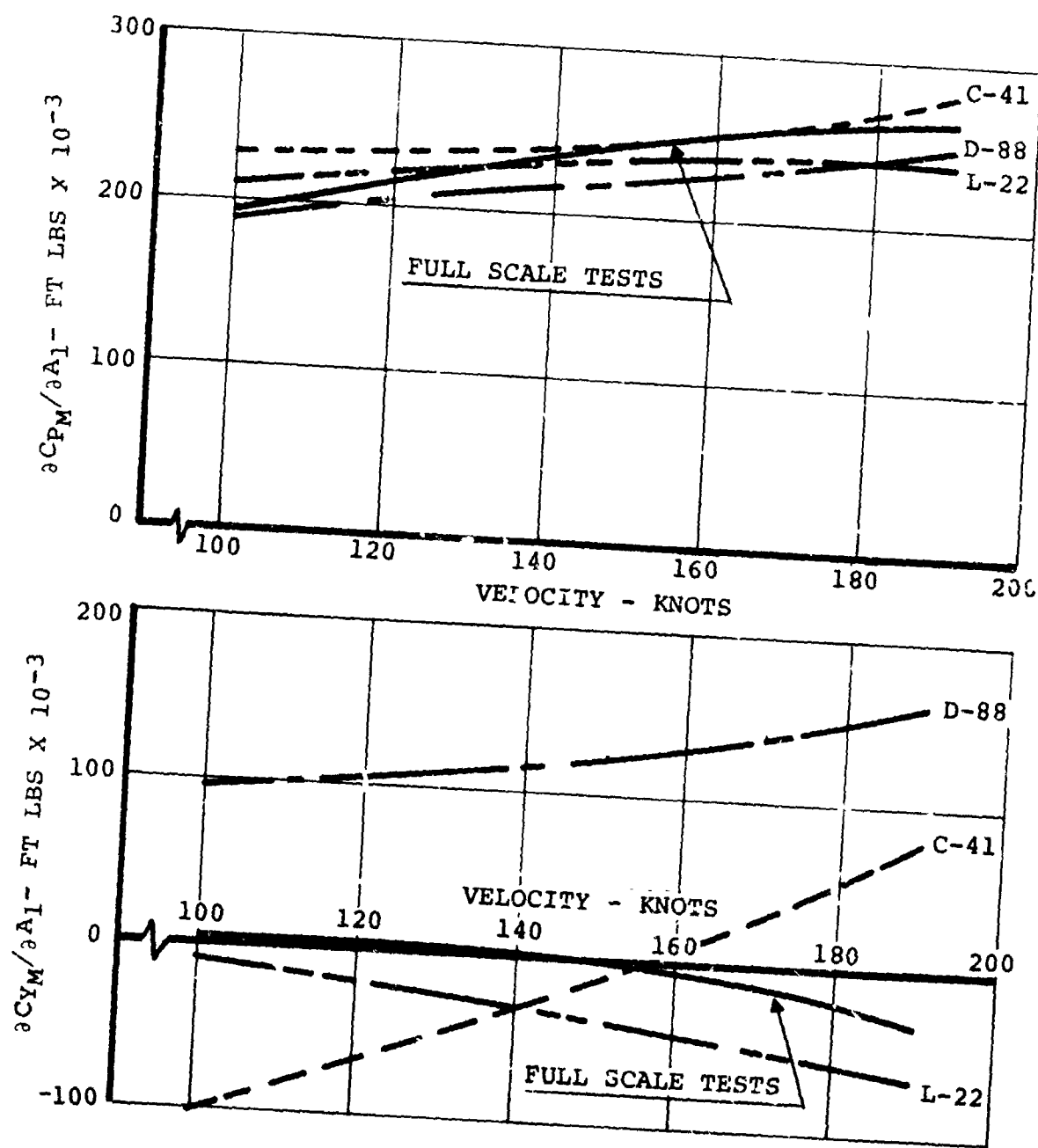


FIGURE 2.21. CORRELATION OF 26 FT. ROTOR TEST DATA WITH VARIOUS ROTOR DERIVATIVE PROGRAMS - CYCLIC MOMENT DERIVATIVES

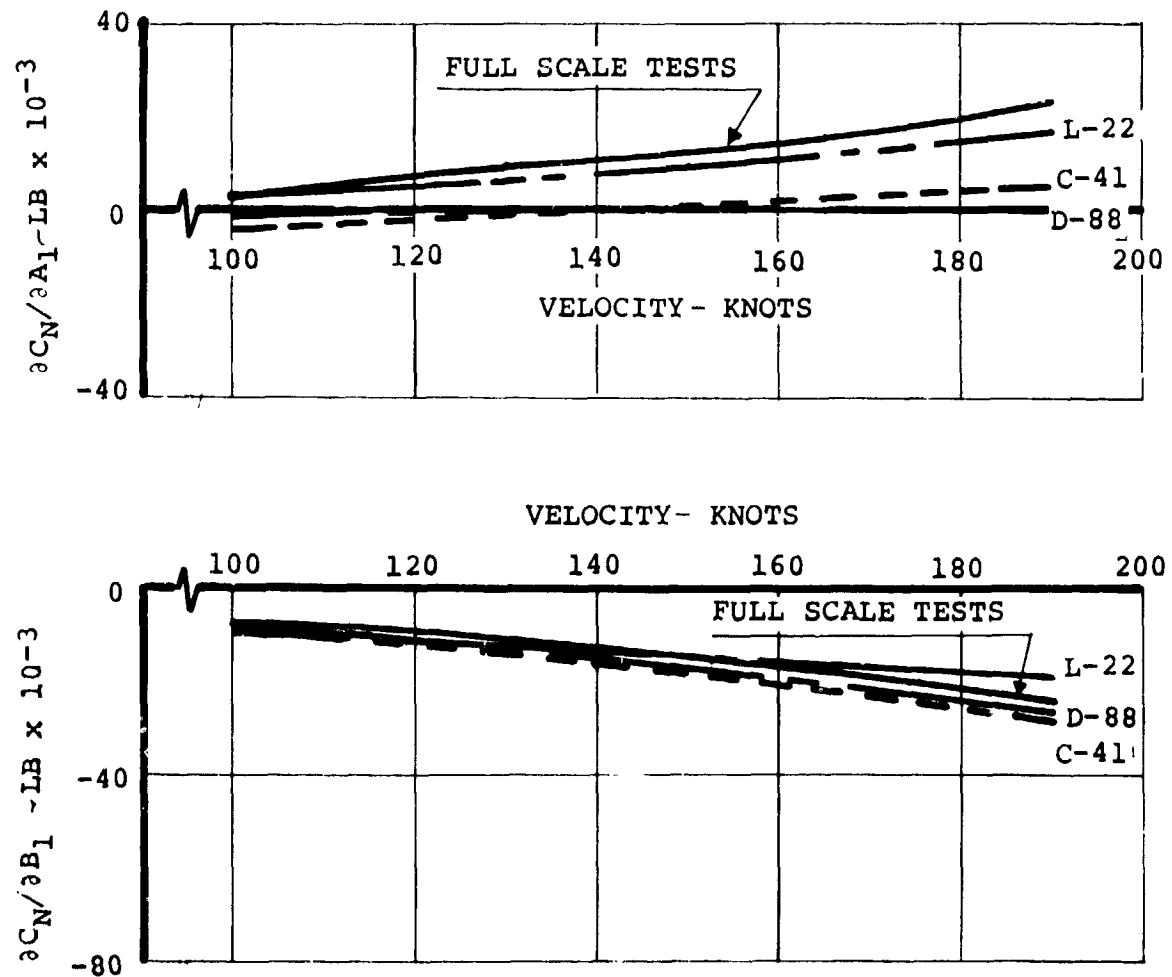


FIGURE 2.22. CORRELATION OF 26 FT. ROTOR TEST DATA WITH VARIOUS ROTOR DERIVATIVE PROGRAMS - CYCLIC FORCE DERIVATIVES

predicted by several other programs. These include D-88 which is a blade loads program which accounts for compressible non-linear downwash and L-22 which uses linear airfoil theory and uncoupled flap-lag freedoms. C-49 accounts for unsteady aerodynamics while C-41 uses a linear representation. C-41 and C-49 use a modal representation of blade freedoms (2 coupled flap-lag modes) while D-88 and L-22 make use of a finite element discrete mass representation.

The rotor derivative data was also compared with C-41 using a total unresolved moment approach. Total moments about the center of the wing tip gages and the reference azimuth position (orientation of the moment vector in the rotor disc plane) were calculated from the C-41 hub forces and moments and compared with test results (Figure 2.23). The interesting conclusion which is not apparent from the resolved forces and moments is that the total moment is predicted well but there are slight differences in the reference azimuth position.

### 2.5.3 Correlation with Model 222 1/4.622 Scale Model Data

The subject model is a dynamically similar version of the M222. The test data presented in Figures 2.24 and 2.25 were taken with the model mounted on a pedestal in the tunnel. The rotors were given angles of attack to the free stream by pitching the complete model with zero sideslip angle and yawing the model at zero angle of attack. The yawing data contains minimal wing induced flow effects and comparison with the pitch data

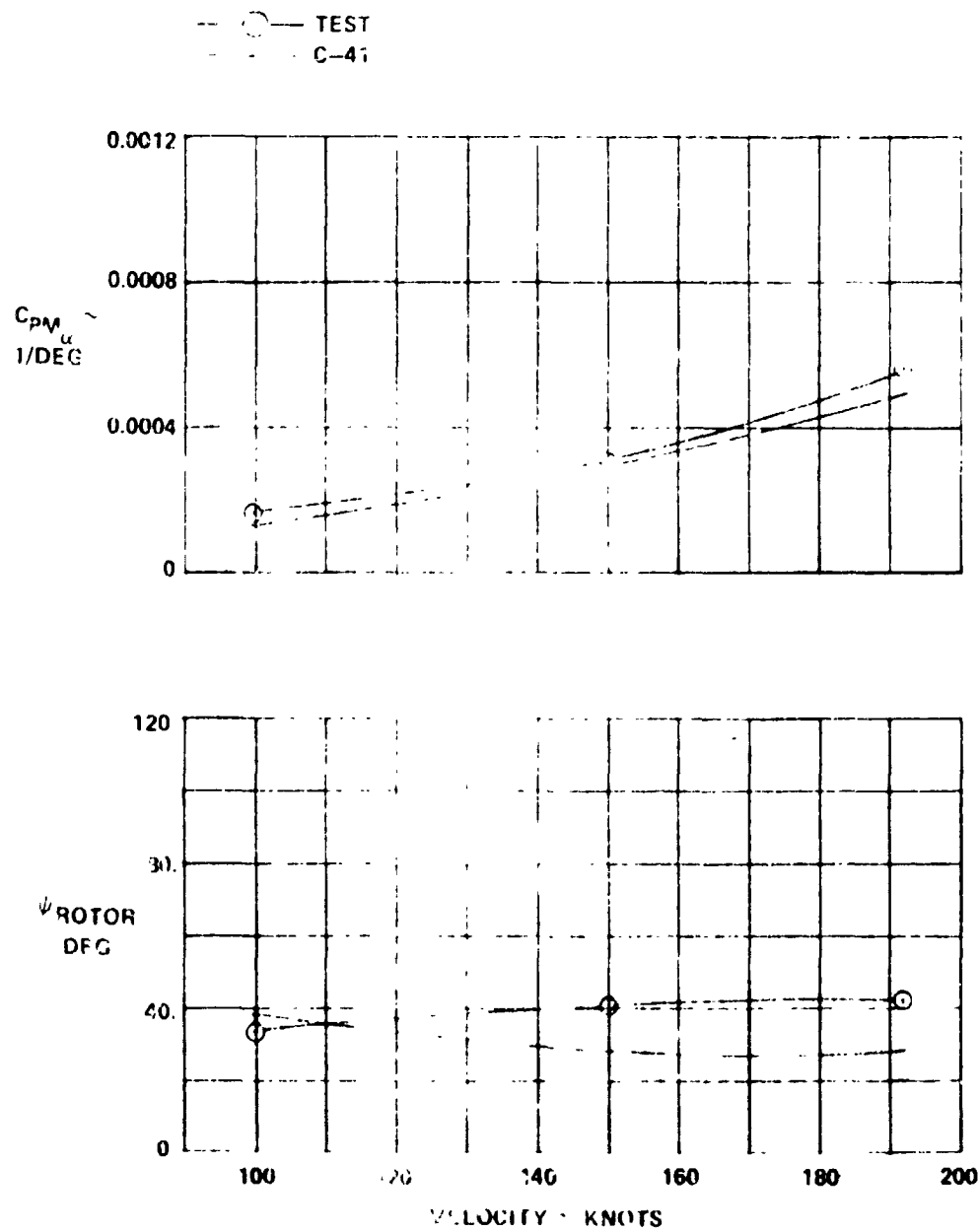


FIGURE 2.23. ROTOR MOMENT AND AZIMUTH ANGLE DUE TO ANGLE OF ATTACK - CORRELATION WITH 26-FT ROTOR DATA (ABSTRACTED FROM M222 PROPOSAL-BOEING D222-10050-2)



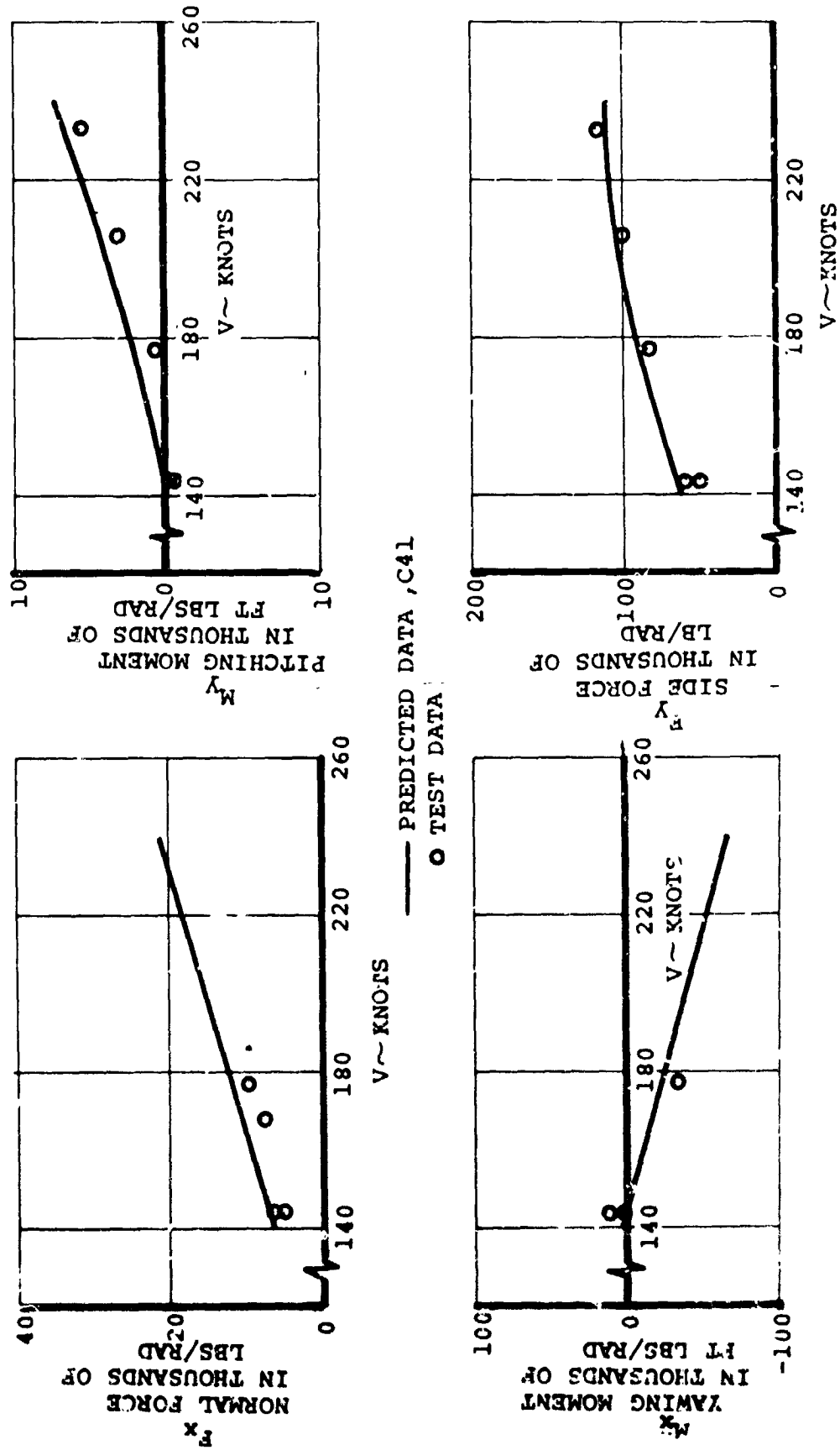


FIGURE 2.24. COMPARISON OF CALCULATED AND TEST ROTOR HUB FORCE AND MOMENT DERIVATIVES FOR M-222 1/4.622 SCALE

MODEL (YAW SWEEP) : 386 RPM

indicates the importance of induced flow on the rotor forces and moments. Forces and moments were computed for the isolated rotor and it is seen from Figure 2.24 that correlation with test data is excellent when wing induced effects are small; in Figure 2.25 wing effects introduce perceptible shifts which increase with dynamic pressure.

## 2.6 CONCLUSIONS FROM DERIVATIVE STUDY

It is seen that there is a strong similarity between the derivatives for angle of attack and cyclic; however, the differences are such that it is probably impossible using cyclic to completely null out simultaneously all hub forces and moments due to angle of attack. The variation of cyclic derivatives as a function of lag frequency is similar to that for angle of attack. Comparison of analytical data from isolated rotor with test shows that correlation is good when isolated rotor assumptions are effectively met, but that induced flow effects are important when this is not the case.

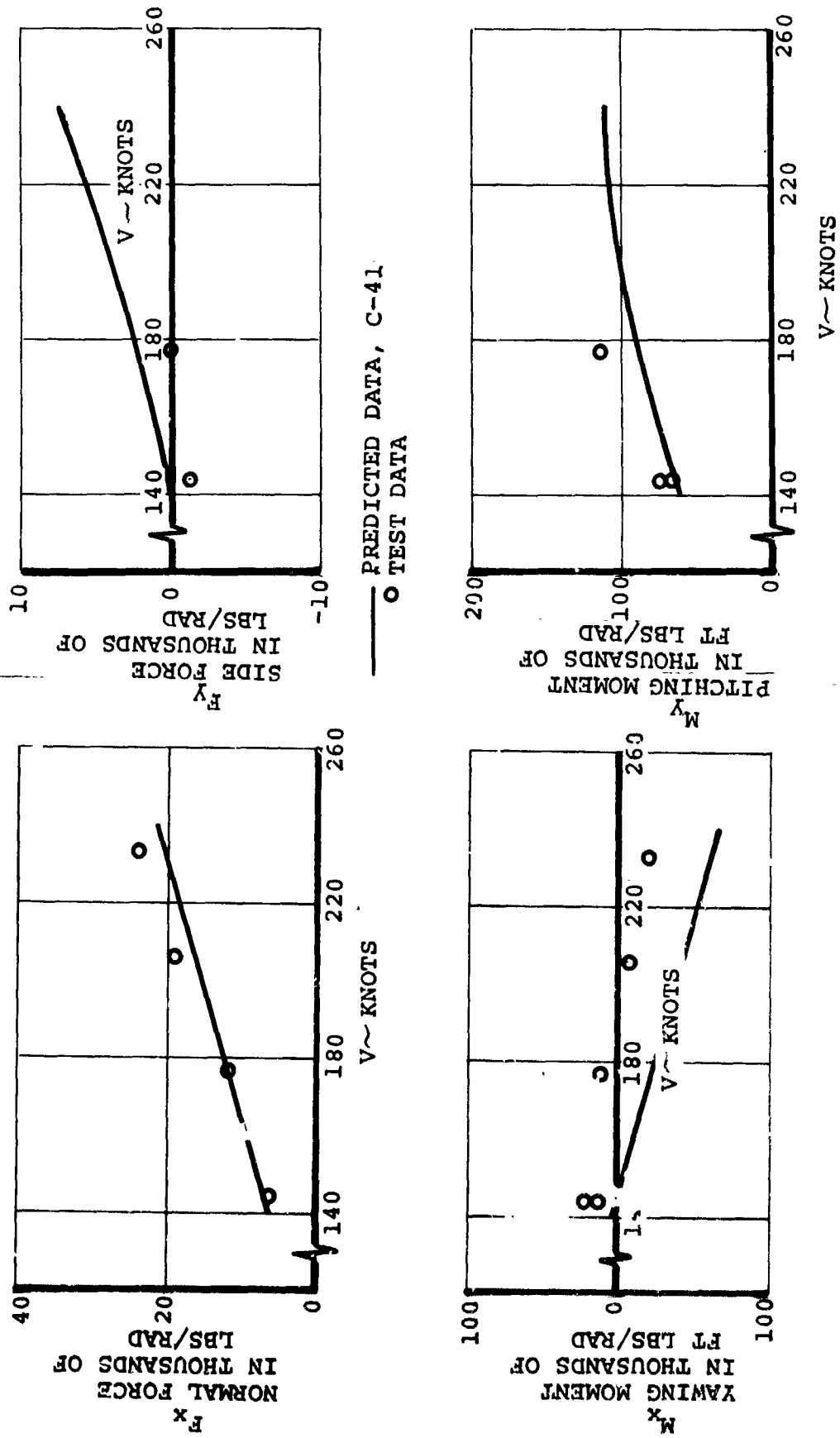


FIGURE 2.2.5. COMPARISON OF CALCULATED AND TEST ROTOR HUB FORCE AND  
MOMENT DERIVATIVES FOR M-222 1/4.622 SCALF MODEL  
(PITCH SWEEP)  $\Omega=386$  RPM

### 3. BLADE LOAD ALLEVIATION AND STABILITY AUGMENTATION SYSTEMS

#### 3.1 BACKGROUND AND OBJECTIVES OF STUDY

Tilting prop/rotor type aircraft experience significant blade loads as a result of non-axial flow in transition from hover to the cruise configuration, and in transient conditions such as maneuvers, gusts, sideslip, etc. However, since cyclic pitch is a basic feature of most tilt rotor control systems, it provides a means to significantly reduce the severity of loading conditions associated with skewed flow. This is accomplished in two ways. The first is to schedule the application of controlled amounts of longitudinal and lateral cyclic as a function of flight condition. The second, which is the primary topic of this report, is the automatic application of cyclic to reduce loads in amounts proportional to the deviations from the scheduled flight program, or to some equivalent loading in the structure caused by the deviation. Such a system will not only reduce blade loads, but will at the same time reduce the associated hub force and moment derivatives, thus increasing the static stability margin of the aircraft.

The objective of this study is to explore the use of load alleviation systems in a typical tilt rotor design, taking

into account those factors which might adversely affect performance in a practical situation. These include hardware characteristics, sensors and actuators, and the impact of dynamic transient effects as well as idealized steady state alleviation. System authority is also discussed for its impact on effectiveness at different flight conditions. The ability of a feedback control system working through the swashplate to influence the following will be analyzed:

- O Reduction of blade loads and hub forces and moments under steady maneuvers and gust encounters
- O Improvement of flying qualities by reducing destabilizing forces and moments from the rotors; improvement of short period response and pilot workload
- O Alleviation of airframe structural loads
- O Improve ride qualities by reduction of gust response accelerations

### 3.2 TECHNICAL BASIS FOR USE OF CYCLIC PITCH FEEDBACK IN LOAD ALLEVIATION

The predominant cause of vibratory loading in prop/rotors is blade dynamic response to cyclical angle of attack changes associated with non-axial flow caused by shaft tilt to the free stream or with cyclic pitch of the blade due to tilt of the swashplate. That is to say, in a propeller or rotor

whose shaft is inclined at an angle  $\alpha$  to the free stream each blade experiences a sinusoidal increment of incidence of amount  $\alpha \sin \Omega t$ . It also experiences a sinusoidal variation in relative velocity over the blade, and both these effects combine to give a variation in dynamic pressure and in angle of attack. The net effect is to produce cyclical perturbation in the blade loads and blade dynamic response. Associated with blade response are corresponding shears, bending moments and strains. Cyclic pitch imposes a 1 per rev variation in incidence and has accordingly much the same effect as shaft incidence except that the angle of attack increment is uniform across the blade and there is no directly associated variation in blade dynamic pressure. Cyclic pitch in appropriate amounts is, therefore, used to trim out the angle of attack variations caused by shaft tilt to the relative wind. The use of cyclic pitch to trim out blade loads and for stability augmentation is established practice in the helicopter field, and the extension to tilt rotor applications is clearly indicated. There is, however, minimal discussion of such topics as scheduling of cyclic to minimize blade loads for normal flight conditions. The emphasis is on the use of automatic feedback cyclic control to counteract loads occurring due to off-schedule conditions.

Such conditions occur during maneuvers and turbulence when the rotor experiences temporary departures from the trimmed unaccelerated flight condition.

### 3.3 TEST DEMONSTRATION OF SWASHPLATE FEEDBACK SYSTEMS

Two test programs were conducted in 1972 in which the use of swashplate feedback for load alleviation was demonstrated. The first, in May, was performed using a 1/9.622 scale model of the Model 222 rotor mounted on NASA wing in the Princeton Tunnel. The sensor system used consisted of strain gages measuring pitching moment and yawing moment in the wing. The system was demonstrated for static situations (i.e., steady wing angle of attack) and also for simulated long period gust conditions using the gust generating capability of the Princeton Tunnel. The results of this test indicated that substantial reductions in blade response were available with the correct selection of azimuth and gain. The results of this test are reported in Boeing Document D222-10047-1 (Reference 3.1). In September of the same year, the full scale version of the above model was tested in the NASA Ames 40 X 80-foot tunnel with a similar feedback system operative. This test also showed that substantial reductions in blade loads could be achieved using a swashplate feedback system. The results of this test are given in Boeing Document D222-10059-1 dated March 1973, (Reference 3.2). The results of both these tests tend to confirm the results presented in this report.

### 3.4 CANDIDATE SYSTEMS: CHOICE OF SENSORS

The principal feature differentiating one load alleviation system from another is the signal sensed and fed back through the swashplate. A number of potentially viable signals and sensors are tabulated in Table 3.1 along with the advantages and disadvantages of each system.

Of the sensors listed, the Aq or Bq sensor seems to offer the most advantage. The other sensors and signals would be acceptable in principle, but the issue of reliability makes strain gage systems undesirable. The Aq sensor has the additional advantage of minimum overall system lag, since each of the other signals results to a greater or lesser degree from dynamic response to the forces produced by Aq. This is not important for quasi-static cases such as steady maneuvers or long period gusts, but it could become important in dynamic situations.

A system based on Aq or Bq sensors has, therefore, been chosen for study.



TABLE 3.1. CANDIDATE SIGNALS AND SENSORS FOR LOAD ALLEVIATION SYSTEM

Signal	Sensor	For	Against
Blade Bending Moment	Strain Gage	Senses variable to be controlled	<ul style="list-style-type: none"> <li>•Questionable reliability</li> <li>•Signal in rotating system</li> <li>•No phase lead</li> </ul>
Hub Bending Moment	Strain Gage	Senses variable to be controlled	<ul style="list-style-type: none"> <li>•Questionable reliability</li> <li>•Signal in rotating system</li> <li>•No phase lead</li> </ul>
Aq, Bq Dynamic Pressure Delta Angle of Attack or Side-slip	Pressure Head	<ul style="list-style-type: none"> <li>•Senses variable which is primary cause of loading</li> <li>•Good reliability</li> <li>•Previous flight experience</li> </ul>	
Aircraft Normal, Side Acceleration	Accelerometer	Signal almost in phase with Aq	No use for unaccelerated cases such as unscheduled weight
Wing Bending Moments Torsion, Yaw	Strain Gage	<ul style="list-style-type: none"> <li>•Sensor in fixed system</li> <li>•Direct measure of variable affecting flying qualities</li> </ul>	<ul style="list-style-type: none"> <li>•Questionable reliability</li> <li>•Lags introduced by wing response</li> <li>•Needs additional sensing to subtract nacelle moment due to "g"</li> </ul>

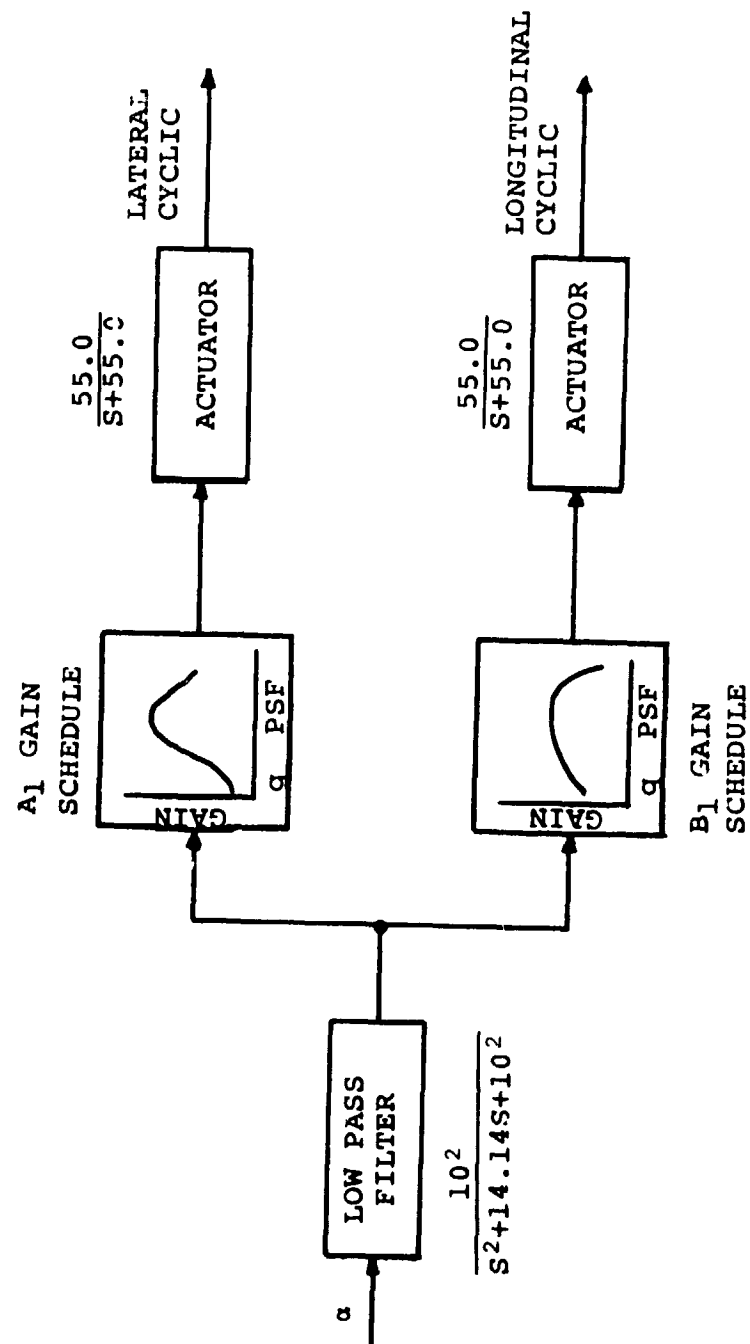


FIGURE 3.1. BLADE LOAD ALLEVIATION SYSTEM SCHEMATIC  
OF FEEDBACK LOOP

### 3.5 SYSTEM CHARACTERISTICS

Figure 3.1 is a schematic of the load alleviation system chosen for study.

The signal sensed is the net increment in angle of attack produced by a gust and the aircraft response. Transfer functions for filters are based on stability considerations and actuator transfer functions are typical of actual hardware. The filter has a cut-off frequency of 10 rad/sec and a damping factor of 0.707. The actuator transfer function is of first order with break frequency 55.0 rad/sec.

### 3.6 DESIGN OF A SYSTEM EFFECTIVE FOR QUASI-STEADY CONDITIONS

When quasi-steady conditions are considered the decision on system characteristics becomes a matter of:

- Selection of which forces or moments to control; since all hub forces and moments cannot be simultaneously brought to zero, a selection is required.
- How gain and azimuth requirements vary with flight conditions
- What signal shaping (filtering) is required to avoid destabilizing dynamic modes

#### 3.6.1 System Designed to Null Rotor Hub Moments in Cruise

The characteristics of gain and azimuth for a system designed

to work on hub pitching and yawing moments were evaluated. Since only steady state effects are considered, the required  $A_1$  and  $B_1$  gain settings are solvable exactly over a range of flight conditions from knowledge of the rotor hub moment alpha and cyclic derivatives. The results are expressed in terms of azimuth and resultant gain. The azimuth angle is defined as

$$\psi = \tan^{-1} \left\{ \frac{B_1 \text{ GAIN}}{A_1 \text{ GAIN}} \right\}$$

and is a direction perpendicular to the axis about which the swashplate tilts.

Questions to be addressed in this study were:

- Does system gain and azimuth require scheduling as a function of flight conditions?
- What is the impact of the system on the hub normal force and moments?
- What is the impact on aircraft static stability?

The values of  $A_1$  and  $B_1$  gain required were evaluated at different speeds and altitudes from the equations for hub pitch and yaw moments:

$$M_{Y \text{ TOTAL}} = M_{Y\alpha} \alpha + M_{YA_1} A_1 + M_{YB_1} B_1 = 0$$

$$M_{X \text{ TOTAL}} = M_{X\alpha} \alpha + M_{XA_1} A_1 + M_{XB_1} B_1 = 0$$

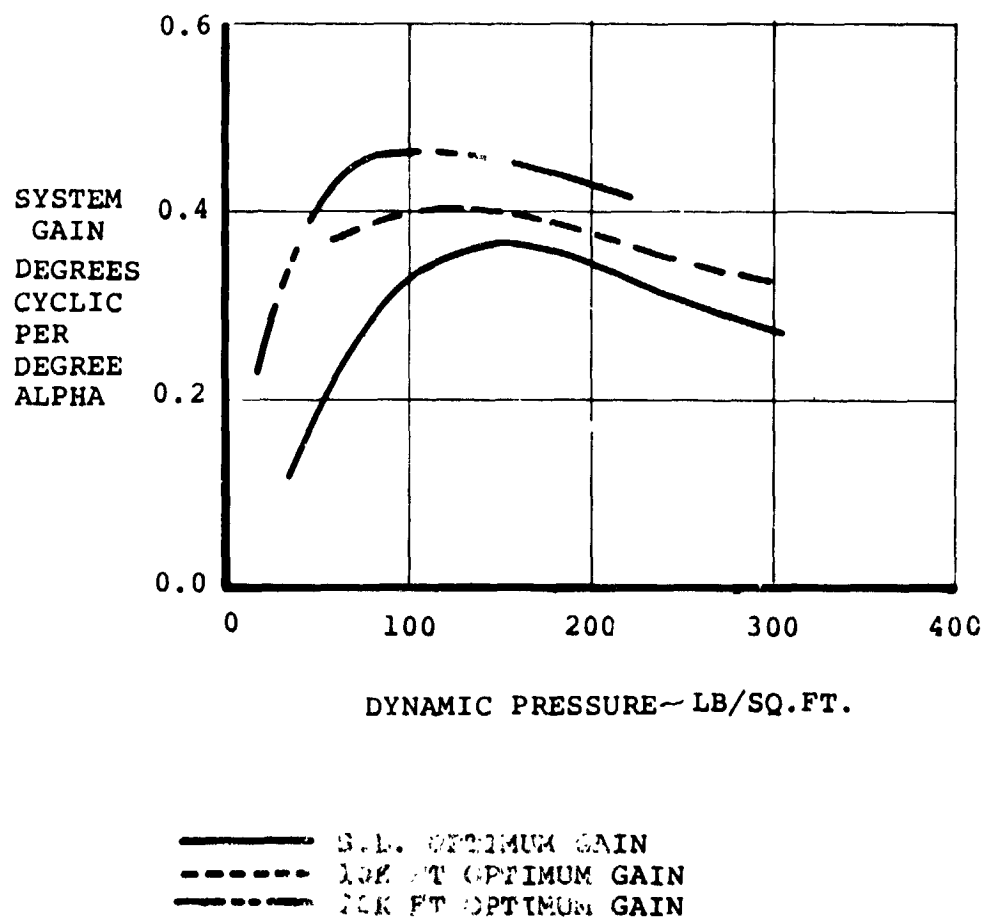


FIGURE 3.2. GAIN REQUIREMENT AS FUNCTION OF DYNAMIC PRESSURE AND ALTITUDE FOR SYSTEM DESIGNED TO ZERO-OUT HUB MOMENTS

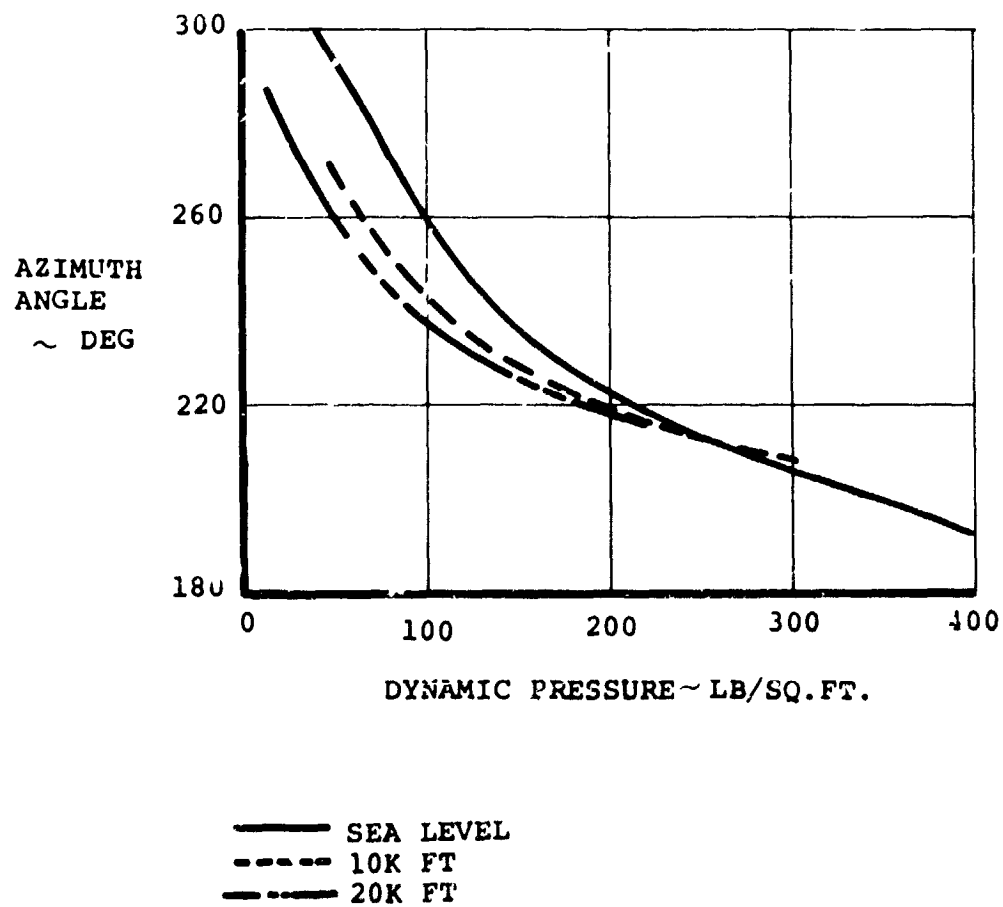


FIGURE 3.3. AZIMUTH ANGLE REQUIREMENT AS FUNCTION OF DYNAMIC PRESSURE AND ALTITUDE FOR SYSTEMS DESIGNED TO ZERO-OUT HUB MOMENTS

These equations are solved for the ratio of  $A_1$  and  $B_1$  to  $\alpha$  and to each other and the answers presented in terms of net swashplate cyclic gain and azimuth. Filtering requirements were determined using Bode Diagram Techniques and system stability was confirmed by examination of root locus. The analytical methodology used is incorporated in the C-48 Flying Qualities and Aeroelastic Stability Program. Transient dynamic response was not evaluated for this system.

Figure 3.2 shows the gain required in degrees of cyclic per angle of attack, over a speed range of 100 to 300 knots at altitudes of sea level, 10,000 ft. and 20,000 ft. The associated azimuth angles required are shown in Figure 3.3 and indicate that the angle required drops from around  $120^\circ$  at 100 knots to  $30^\circ$  at 300 knots. The conclusion to be drawn from these curves is that gain and azimuth scheduling as a function of speed is required if the system objectives are to be met at all speeds. The variation with altitude is not so striking so that scheduling of gain and azimuth with altitude is probably not required. The impact of these gain and azimuth settings at sea level on the hub normal and side forces are shown in Figures 3.4 and 3.5. It is seen that normal force and side force derivatives are also reduced by

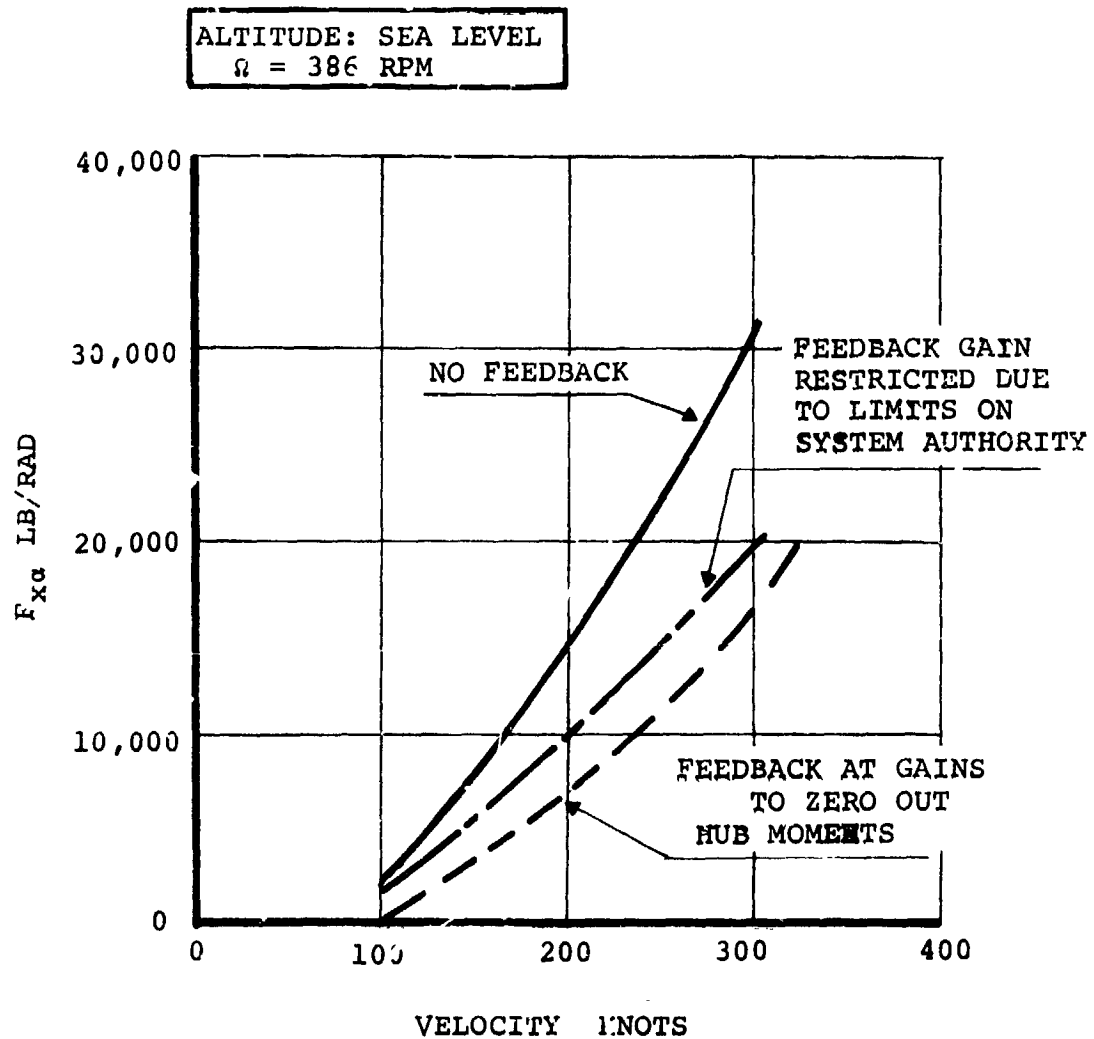


FIGURE 3.4. NORMAL FORCE DERIVATIVE WITHOUT FEEDBACK WITH UNRESTRICTED GAIN AND WITH ARBITRARY LIMIT OF  $1.5^\circ$  of  $A_1$  and  $B_1$



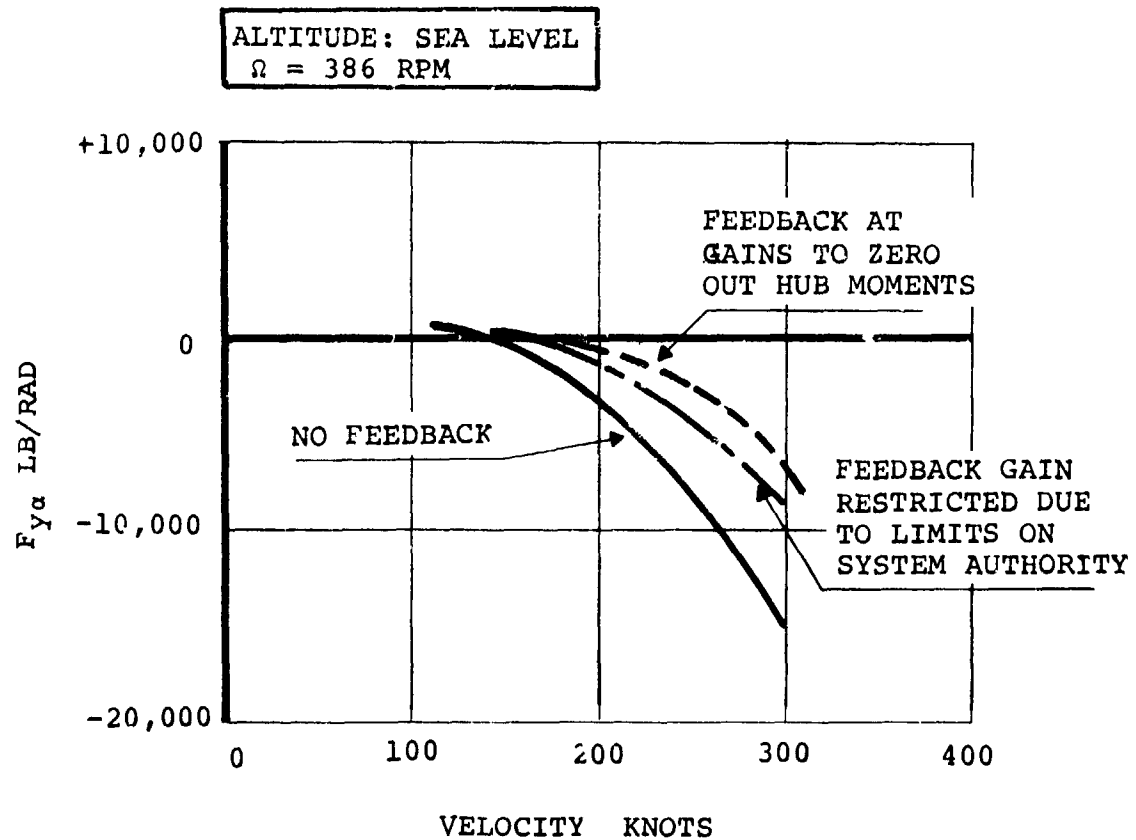


FIGURE 3.5. SIDE FORCE DERIVATIVE WITHOUT FEEDBACK, WITH UNRESTRICTED GAIN AND WITH ARBITRARY  $1.5^\circ$  LIMIT ON  $A_1$  and  $B_1$

approximately 50% at the higher speeds.

It is concluded from this study that a system can be defined which will reduce the blade flap bending moments and hub moments to zero, and that the hub normal and side forces will be reduced by the same system. This is a beneficial arrangement for blade loads but may be less acceptable from the point of view of aircraft static stability. The rotor hub pitching moment due to angle of attack is negative, i.e., nose down for low-in-plane stiffness rotors at cruise advance ratios. A reduction of hub pitching moment to zero without a similar reduction in normal force may lead to a net reduction in static margin. That is to say the objective of reduction of blade loads is not necessarily compatible with flying qualities objectives.

### 3.6.2 System Authority Considerations

Limits may be imposed on the authority of a feedback system because of runaway considerations. That is, unless the system is fail safe which implies triple redundancy, its authority must be less than that available to the pilot or from other control systems at each condition of flight. The stability characteristics of the aircraft will have a discontinuity when the system commands exceed the authority of the feedback

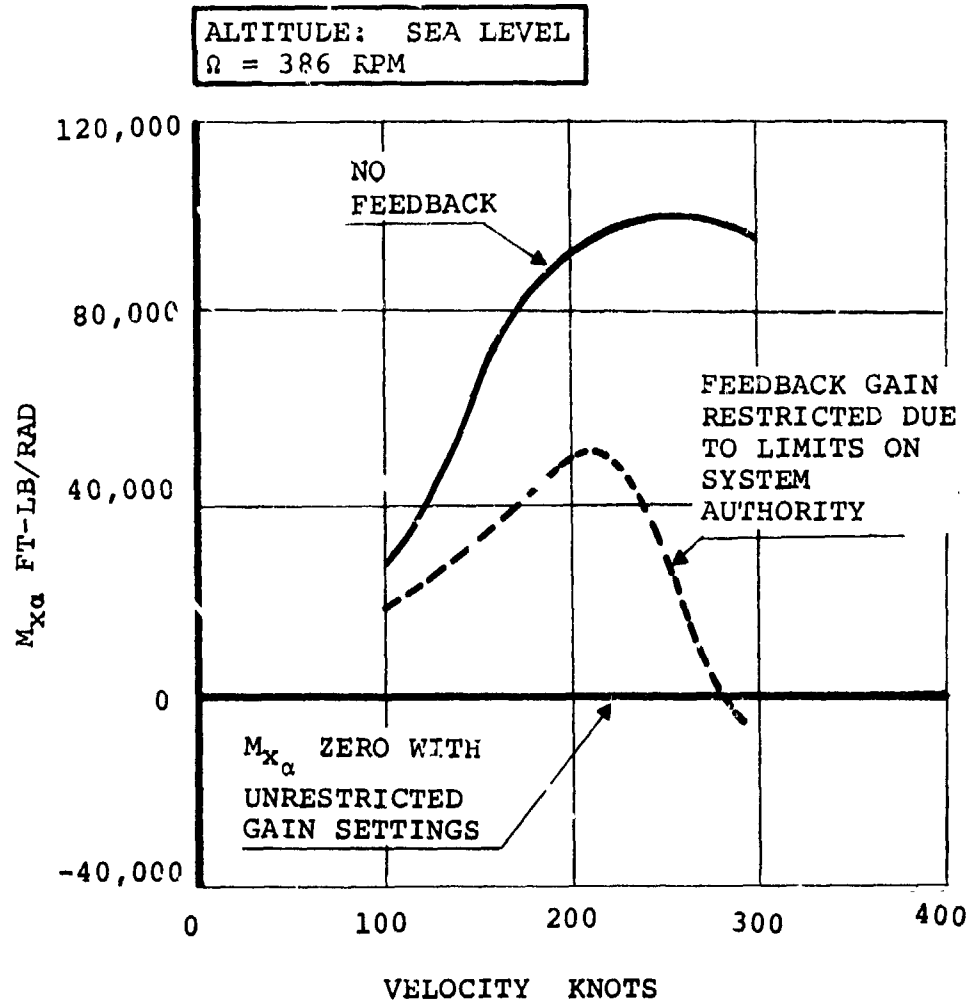


FIGURE 3.6. HUB YAWING MOMENT DERIVATIVE WITHOUT FEEDBACK AND WITH GAIN RESTRICTED FOR ARBITRARY LIMIT OF  $1.5^\circ A_1$  and  $B_1$

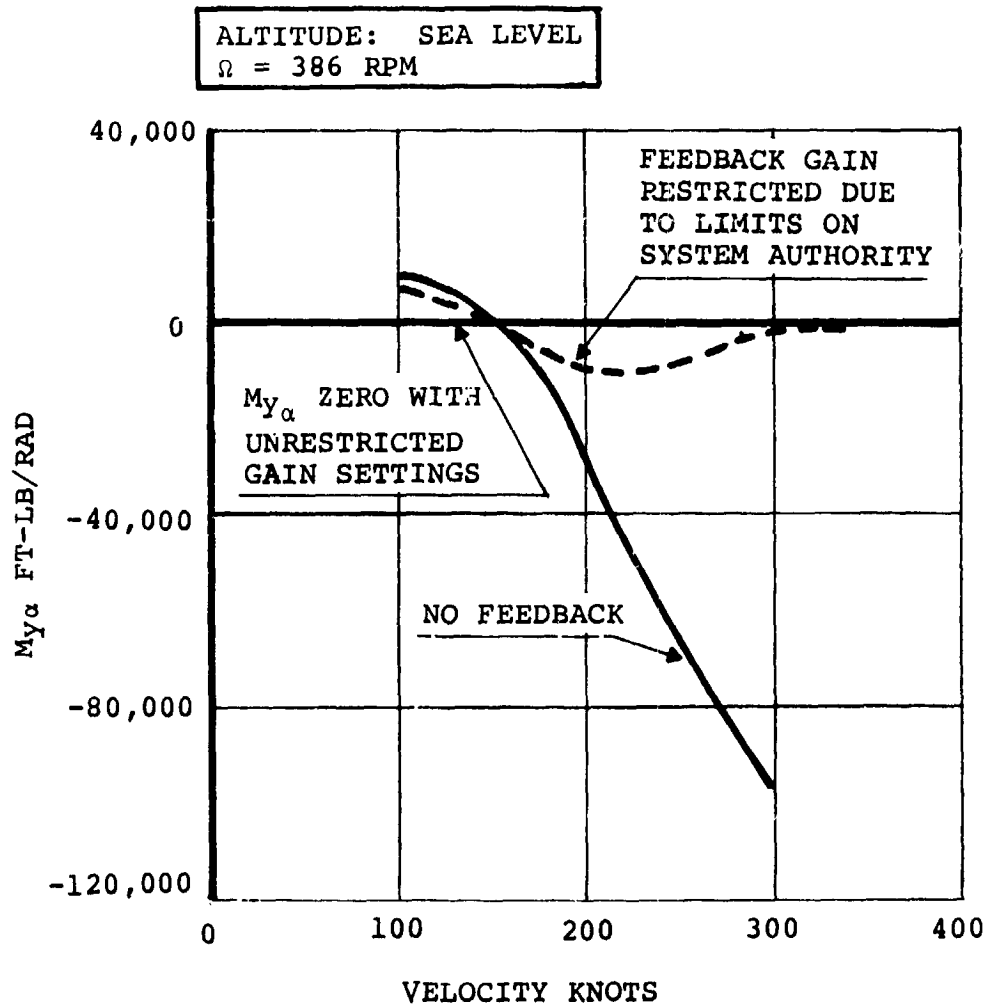


FIGURE 3.7. HUB PITCHING MOMENT DERIVATIVE WITHOUT FEEDBACK AND WITH GAIN RESTRICTED FOR ARBITRARY LIMIT OF  $1.5^\circ$   $A_1$  and  $B_1$

system and since this would be considered unacceptable within the flight envelope the system gain will be limited so that flight envelope  $A_1$  conditions will not generate demands which exceed system authority. This places constraint on gain scheduling which is a function of speed. Figures 3.4 through 3.7 show the impact of gain restrictions set so that an arbitrary system authority of  $1.5^\circ$  in the  $A_1$  and  $B_1$  channels is not exceeded by feedback signal demands associated with maximum flight envelope conditions. It is noted that even with restrictions on gain settings there is still a significant reduction in all the hub forces and moments, reflecting a similar reduction in blade bending moments and shears. The net effect on pitching moment about the nacelle pivot is important in relation to static stability. Figure 3.8 shows the pivot pitching moment with and without feedback at sea level and 10,000 ft. At both altitudes the feedback system reduces pivot pitching moment slightly at low speed thereby increasing static margin but at high speeds the opposite is true, with a marked increase in the sea level case. This is a result of a marked reduction in negative hub pitching moment which is not accompanied by a similar reduction in positive normal force.

The net effect on static stability is to provide a slight

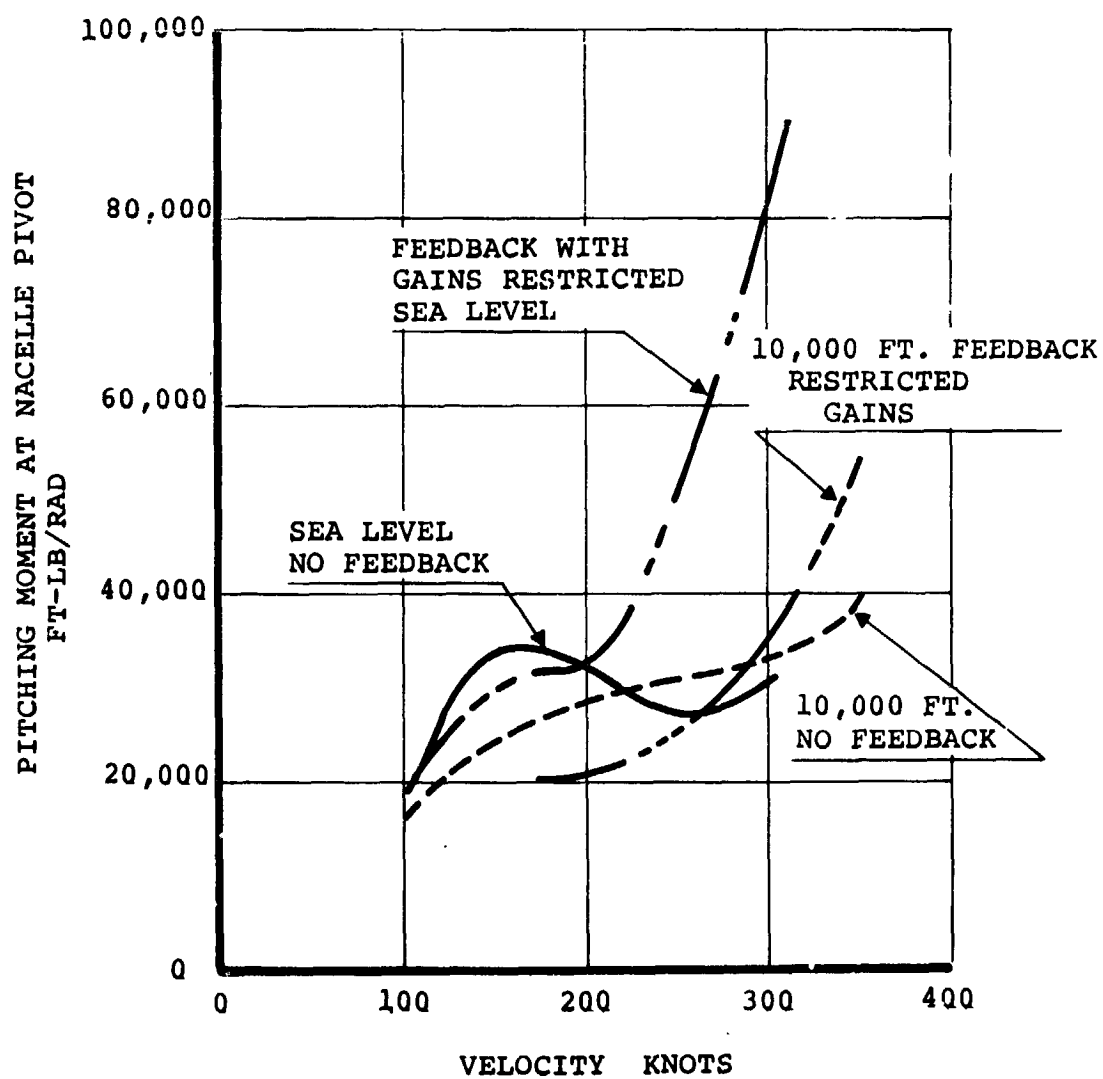


FIGURE 3.8. PITCHING MOMENT ABOUT NACELLE PIVOT WITH AND WITHOUT FEEDBACK

increase at low speed (1.2%  $\bar{c}$  at 150 knots) where improvement is most useful, and to decrease the static margin by approximately 5% at 300 knots when a decrease is acceptable.

In summary, this system, based on a reduction of hub moments criterion, also provides reductions in blade loads and normal side forces, and does not deteriorate the static stability behavior. However, scheduling of gain and azimuth with speed is required and preferably with altitude also.

Since the preceeding analysis was based on static consideration only the systems defined were checked for stability by inspection of their Bode Diagrams. That is the open loop response of the complete system taking account of blade dynamics and wing/pylon/fuselage flexibilities and rigid body freedoms. The diagrams for 150, 250 and 350 knots are shown in Figures 3.9, 3.10 and 3.11. Decibel levels for 350 knots are higher than at lower speeds while the phase response is similar. The levels are for unity gain in the feedback loop. The net decibel levels are obtained by subtracting the gain levels indicated. At 350 knots the phase margin is about the minimum that would be acceptable and a phase shifting network is indicated to improve this margin.

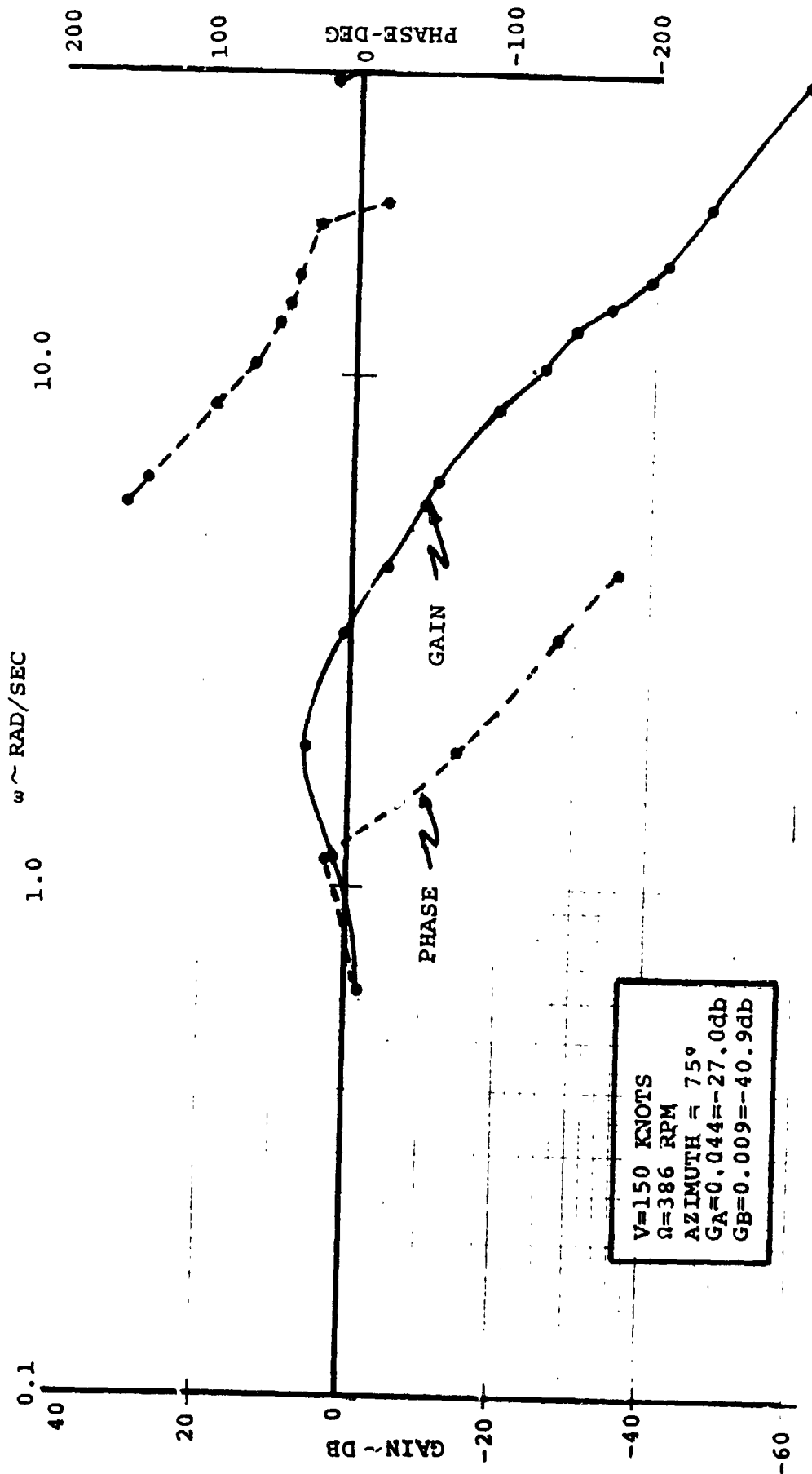


FIGURE 3.9. BODE DIAGRAMS FOR SYSTEM  
DESIGNED TO REDUCE HUB MOMENTS



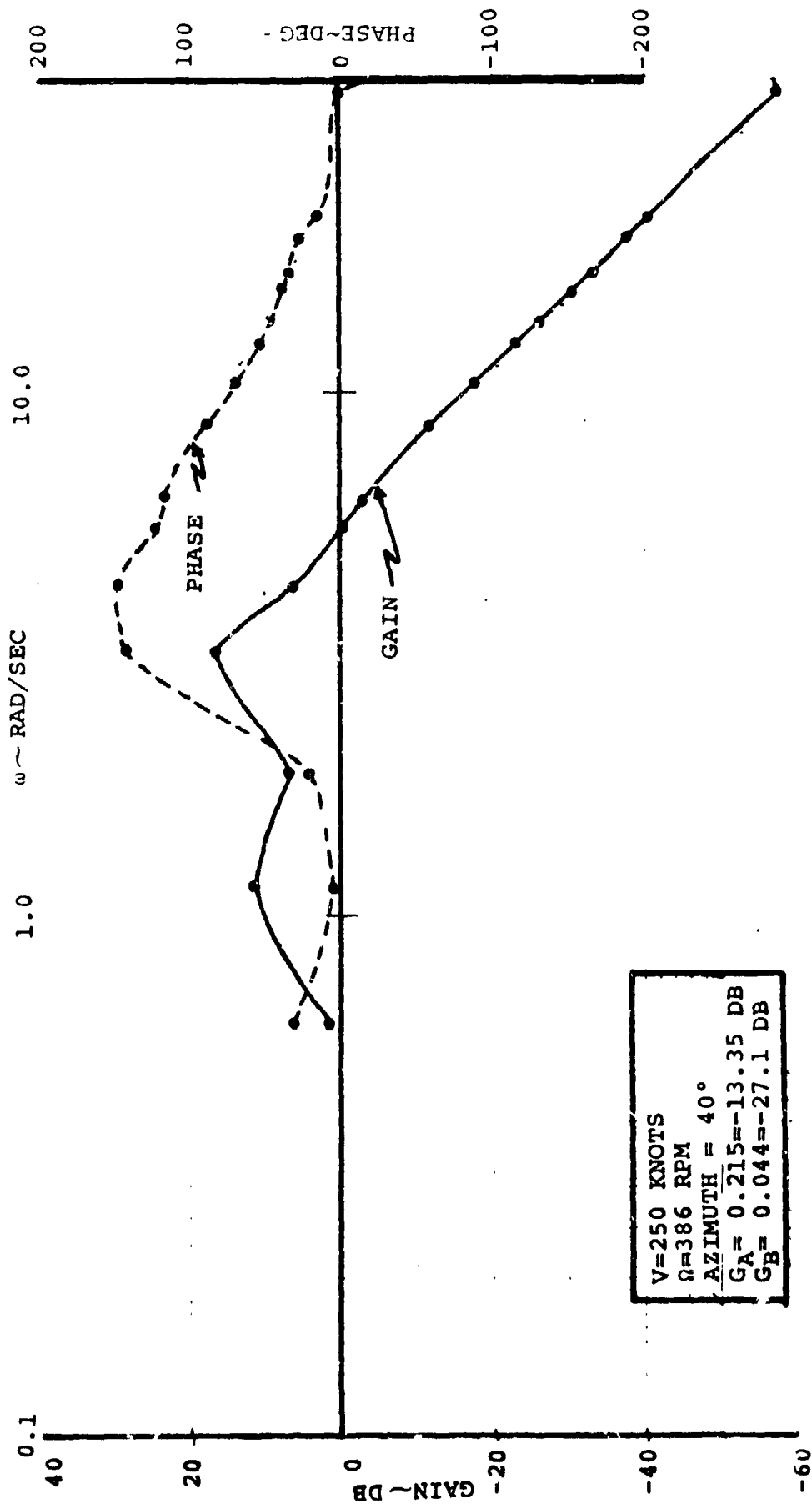


FIGURE 3.10. BODE DIAGRAM FOR SYSTEM  
DESIGNED TO REDUCE HUB MOMENTS

5-09501-7220

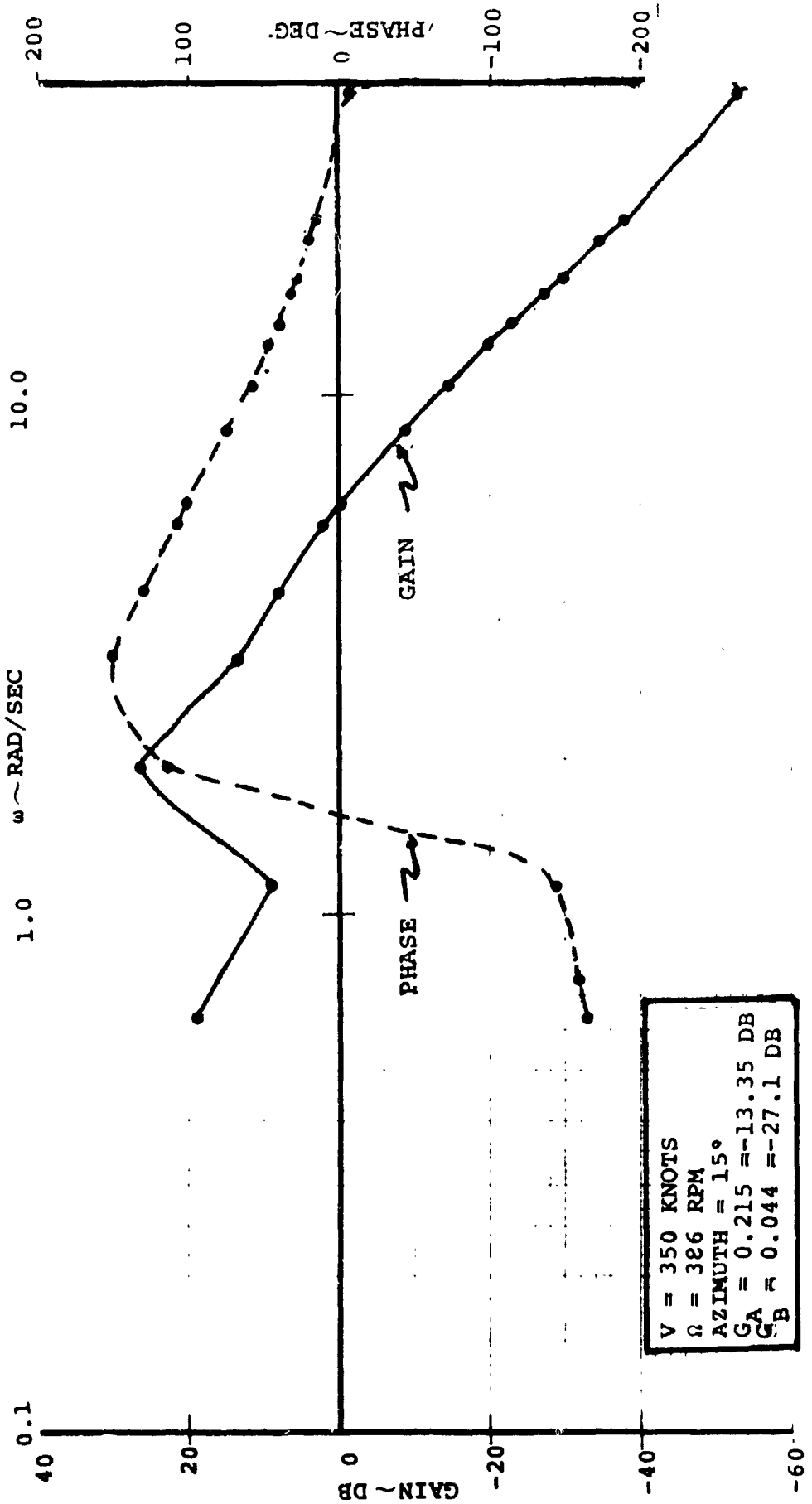


FIGURE 3.11. BODE DIAGRAM FOR SYSTEM DESIGNED TO REDUCE HUB MOMENTS

D222-10060-3

### 3.7 ALTERNATIVE SYSTEM DEFINITIONS

Since objectives additional to minimization of hub moments may be required and since a load alleviation system is required to operate under transient loading conditions as well as static, a more general investigation was initiated. In the preceeding study the system was designed to zero out hub moments due to steady state loading conditions and it was fortuitous that a slight improvement in static margin at low speeds came out of the system. In the present study the behavior of hub forces and moments and nacelle pivot moments are examined to see if a better approach is available. To develop a general picture of the behavior of hub forces and moments and nacelle pivot moments as functions of gain and azimuth, they were evaluated for the complete azimuth range and for a set of gain values ranging from 0 to 1.0 radian of cyclic per radian of shaft angle. Contours of forces and moments were then plotted as functions of gain and azimuth as shown in Figures 3.12 and 3.13 for 250 knots and 100 knots respectively. From these the contours for zero forces and moments and pivot moments were constructed and superimposed in Figures 3.14 and 3.15. Examination of Figures 3.12 through 3.15 permits system parameters to be selected according to different objectives. For example, if minimization of pivot moments was of

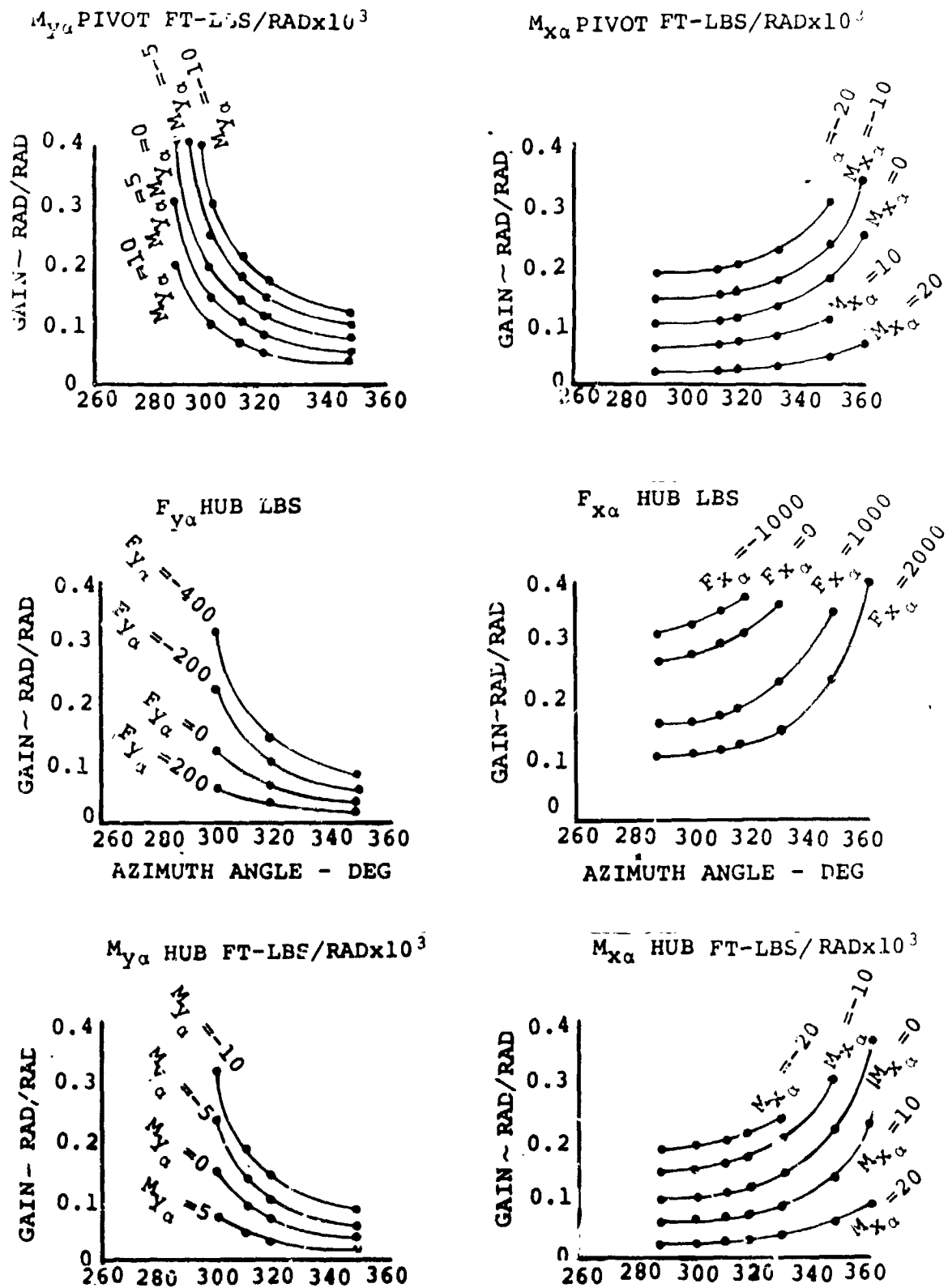


FIGURE 3.12. FORCES AND MOMENTS VS GAIN/AZIMUTH AT 100 KNOTS, 386 RPM AND SEA LEVEL.

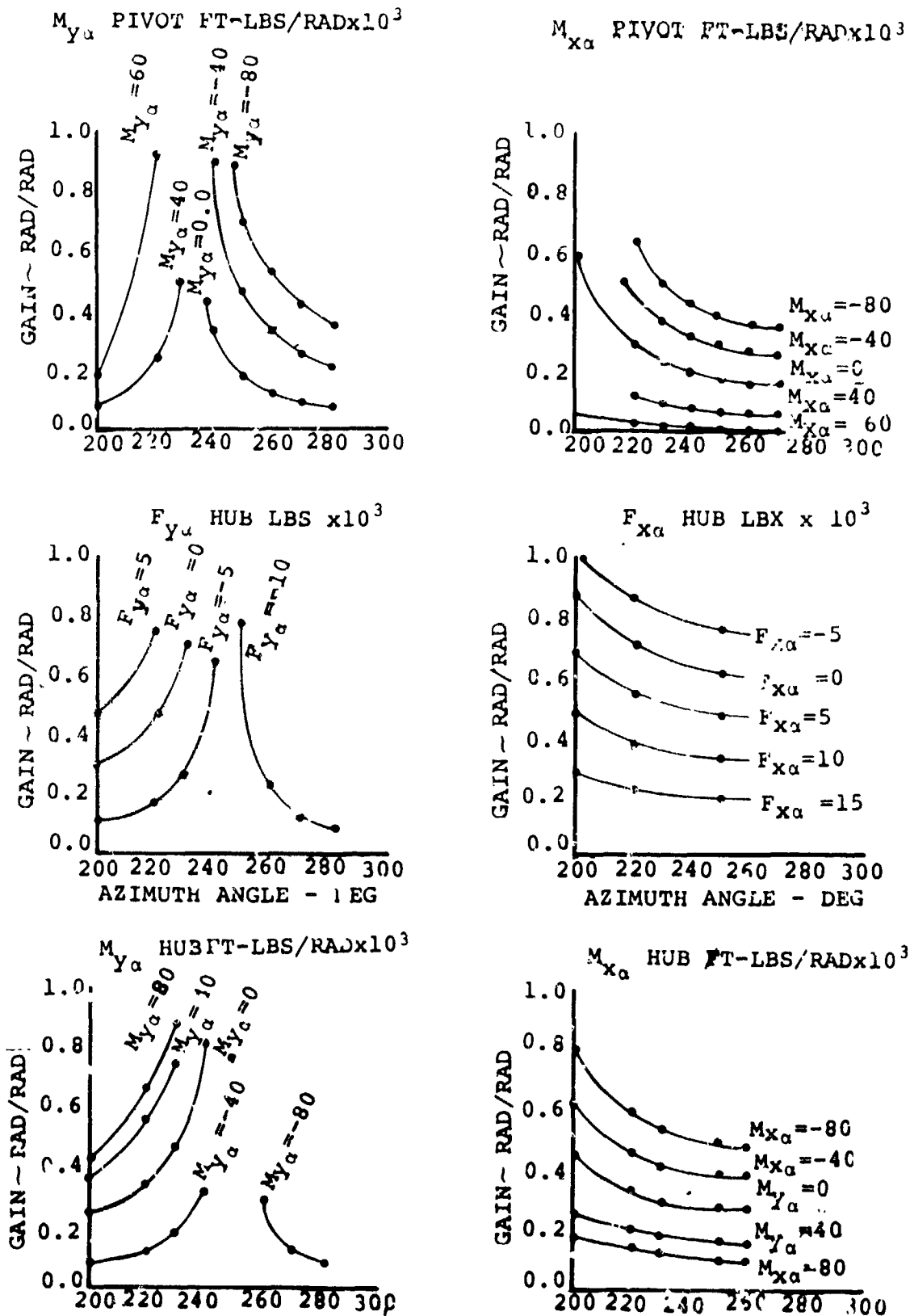


FIGURE 3.13. FORCES AND MOMENTS VS GAIN/AZIMUTH  
AT 250 KNOTS 386 RPM AND SEA LEVEL

$V = 100$  KNOTS  
 $\Omega = 386$  RPM  
 ALTITUDE = SEA LEVEL

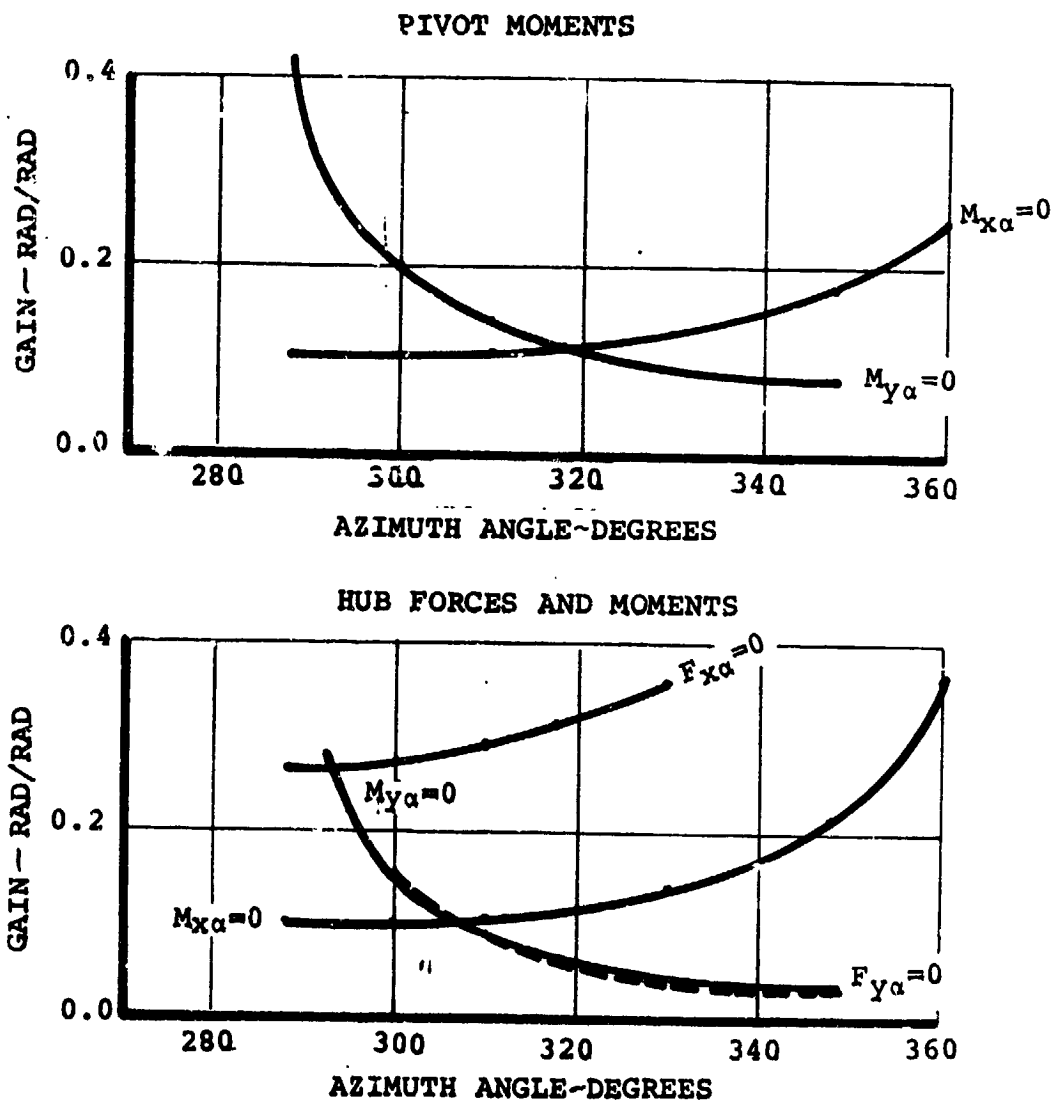


FIGURE 3.14 GAIN/AZIMUTH FOR ZERO FORCES AND MOMENTS AT 100 KNOTS

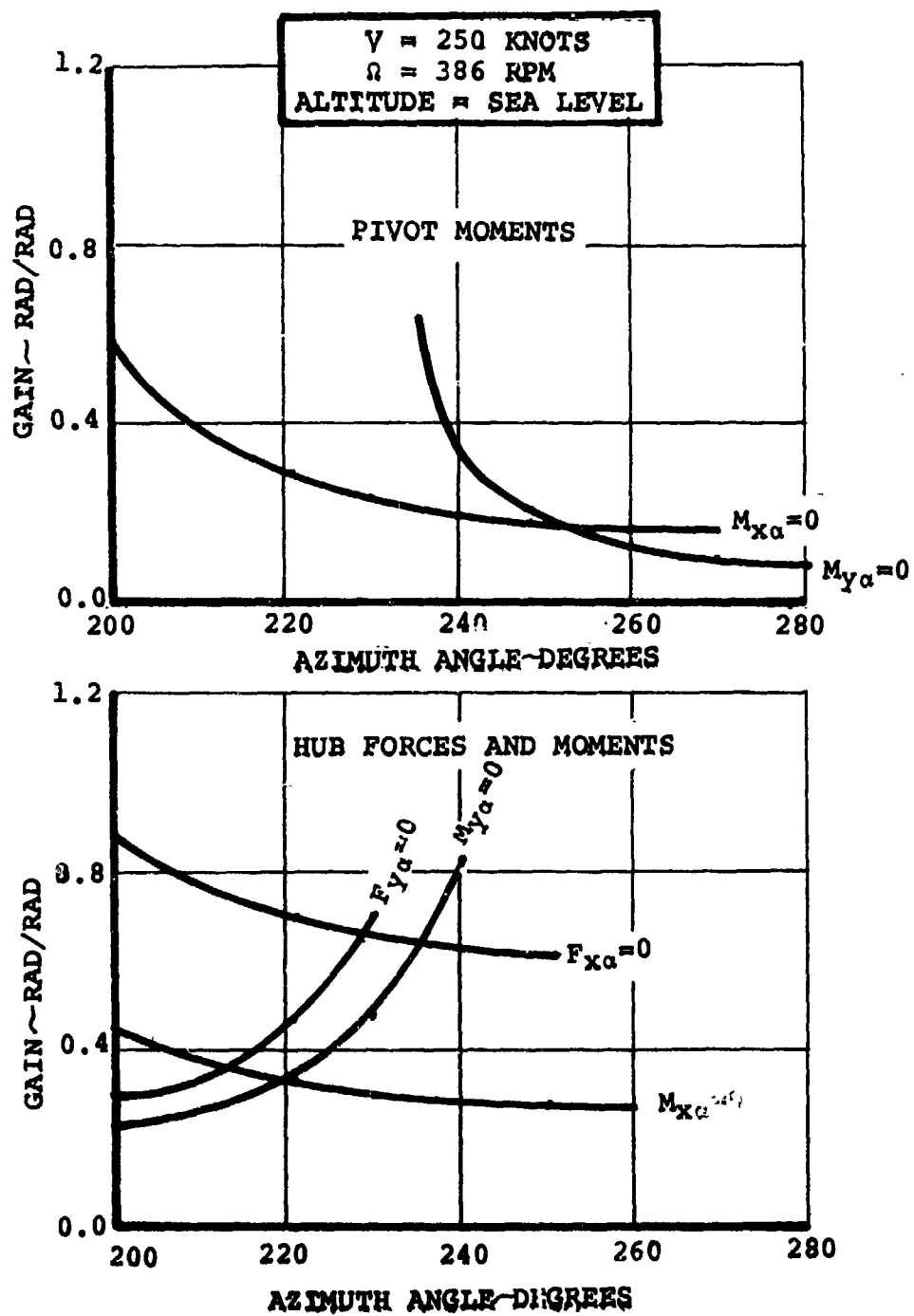


FIGURE 3.15. GAIN/AZIMUTH FOR ZERO FORCES AND MOMENTS  
AT 250 KNOTS

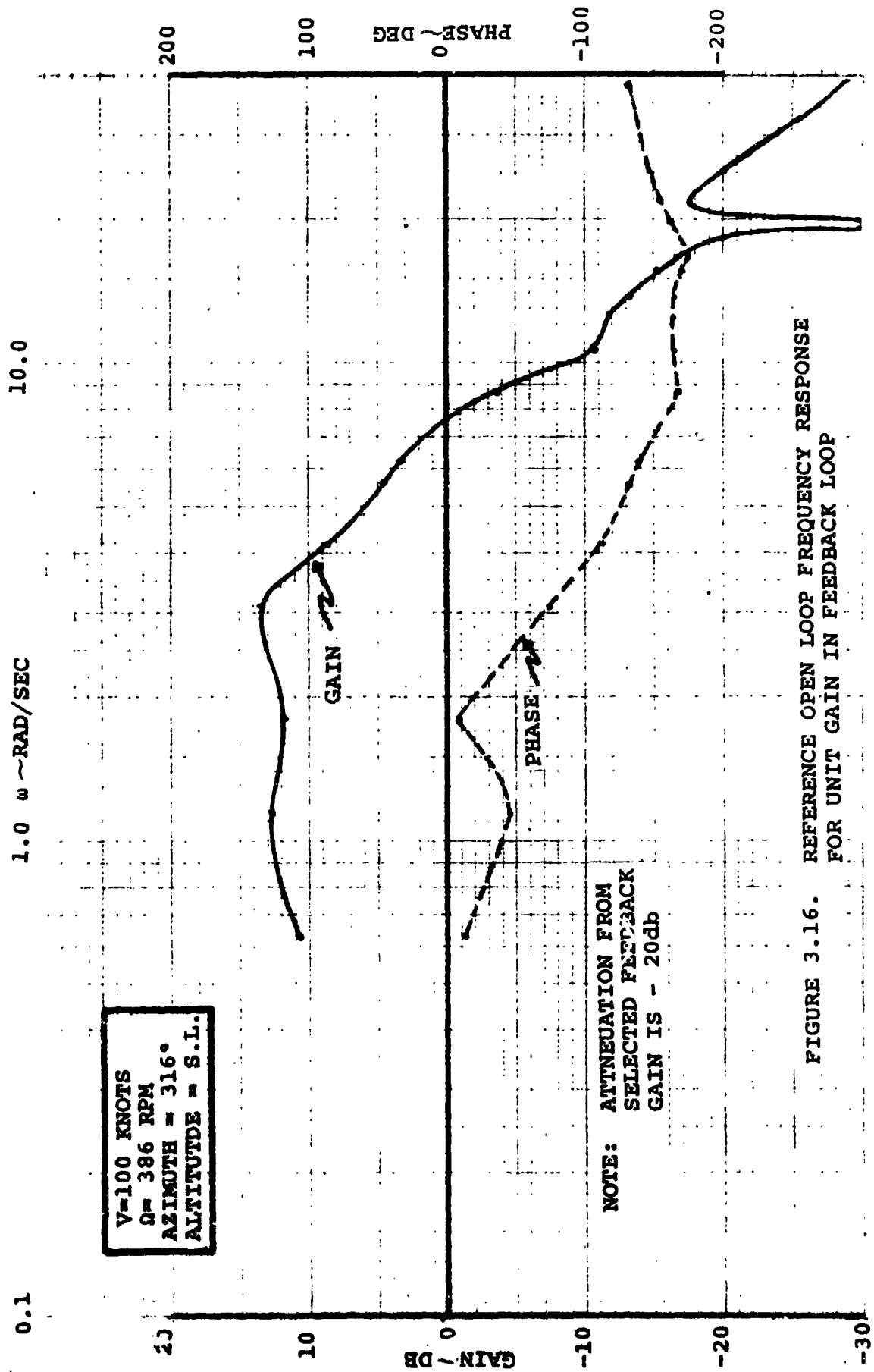


FIGURE 3.16. REFERENCE OPEN LOOP FREQUENCY RESPONSE FOR UNIT GAIN IN FEEDBACK LOOP



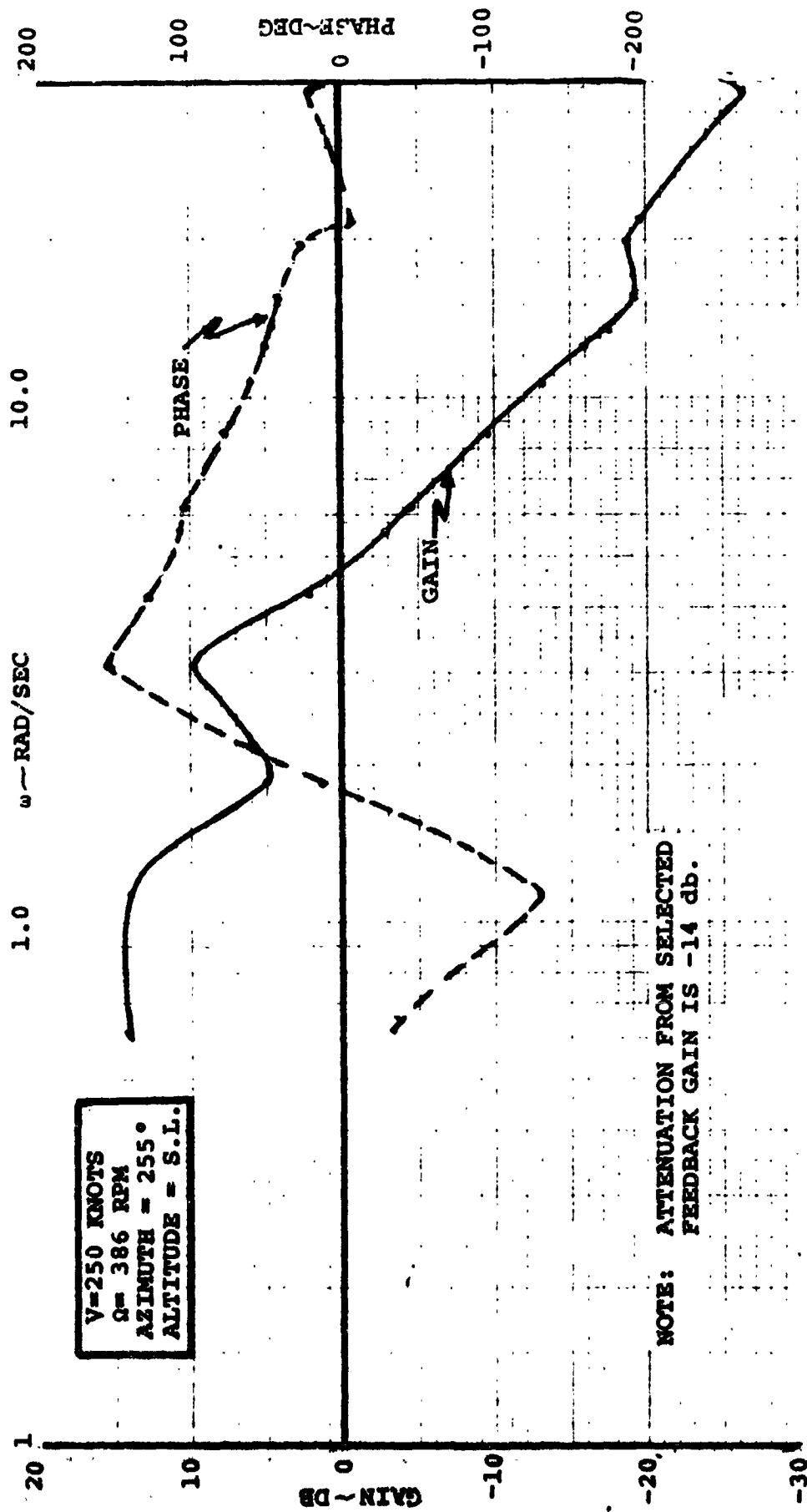


FIGURE 3.17. REFERENCE OPEN LOOP FREQUENCY RESPONSE  
FOR UNIT GAIN IN FEEDBACK LOOP

overriding importance, the system gains would be set to give an azimuth of 255-degrees and a gain of around 0.2 at 250 knots with scheduling to give an azimuth of 316-degrees and gain 0.1 at 100 knots. Bode diagrams for these two conditions are given in Figures 3.16 and 3.17 and it is noted that adequate gain and phase margins exist. An attractive alternative might be to reduce the pitching moment about the pivot to zero, and at the same time minimize hub forces and moments as far as possible. Thus, by selecting an azimuth around 230 degrees and gain approximately 0.65, the pivot pitching moment is still zeroed, but so also are the hub normal and side forces and pitching moment; only the hub yawing moment remains, and it is seen from Figure 3.12 that this azimuth and gain setting will result in a hub yawing moment of approximately -100,000 ft lb/radian compared with one of approximately +100,000 ft-lb/radian when no feedback is present. There is, of course, a net reduction in total hub moment because the pitching moment has been reduced to zero. The same reasoning applies at other speeds. At 100 knots the equivalent selection is a gain setting of 0.26 and azimuth 293-degrees. In this case the total residual hub moment is approximately -30,000 ft lb/radian compared with a value without feedback, obtained by resolving 25,000 ft lb/radian of yawing moment and 10,000 ft lb/radian of pitching moment.

The above two examples do not exhaust the possibilities; for example a net nose down pivot moment might be beneficial and

this could be provided by increasing azimuth while keeping a gain setting which made  $F_{X_0}$  zero.

It is clear that this approach to the selection of feedback system gains and azimuth is a powerful and flexible tool which may be used not only to reduce rotor effects but to actively improve the static stability of the aircraft.

### 3.8 DYNAMIC RESPONSE CONSIDERATIONS

Many of the situations in which a load alleviation system might reasonably be expected to work effectively are dynamic in nature. These include transient maneuvering and gust loading conditions. In such cases the blade loads and hub moments depend on the transient response of the blades, which is governed not only by shaft angle of attack, but by rate and acceleration associated with the rigid body and flexible response of the airframe. Thus, in a dynamic situation the behavior of the whole aircraft must be analyzed with a full accounting of interactions between gust velocities and rotor, pylon, wing and fuselage responses.

The potential importance of transient response may be seen from Table 3.2 in which the frequencies and interactions associated with the components of the Model 222 Tilt Rotor Research Aircraft are listed.

The feedback control system envisioned for static cases has certain fundamental limitations when confronted with the fully coupled dynamic situation. Ashby's "Law of Requisite Variety" states that to control a multivariable system, the number of controls provided must not be less than the number of independent variables. In the static case there are two independent variables, blade flap and blade lag, and a good job of controlling these can be accomplished by the use of the two parameters, feedback gain and azimuth. In the dynamic situation there are many more independent degrees of freedom, all influencing the blade response, to a greater or less degree.

TABLE 3.2. SUMMARY OF FREEDOMS AND INTERACTIONS WITH BLADE FREEDOMS

FREEDOM	FREQUENCY	FORCING FROM GUST	COUPLING TO ROTOR	COUPLING FROM ROTOR
Wing Vertical Bending	3.5 Hz	Direct forcing by wing lift	Acceleration excites ( $\Omega - \omega_L$ ) mode	( $\Omega - \omega_L$ ) response forces wing mode
Wing Chord	5.5 Hz	Small	Yaw excites ( $\Omega - \omega_\beta$ ) mode	Hub side force and yawing moment excites chord bending
Wing Torsion	6.1 Hz	Small	Shaft angle, position, rate and acceleration excites ( $\Omega - \omega_\beta$ )	Hub normal force and pitching moment excites wing twist
Aircraft Normal Acceleration	---	Acceleration directly proportional to wing lift	Normal acceleration excites ( $\Omega - \omega_\beta$ ) mode. Velocity relieves gust velocity.	Hub normal force adds to normal acceleration
Aircraft Short-Period Mode	.04 Hz at 80 knots to 0.66 Hz at 250 knots	Forced by lift and pitching moment $\propto V_{gust}$ and aircraft response	Attitude, rate and acceleration excite ( $\Omega - \omega_\beta$ )	Hub normal force and pitching moment influence short period characteristics

NOTE 1. ( $\Omega - \omega_L$ ) denotes the lower cyclic lead-lag mode  $\sim 0.25$  per rev or 1.6 Hz.

( $\Omega - \omega_\beta$ ) denotes the lower cyclic flap mode  $\sim 0.33$  per rev or 2.1 Hz.

Unless additional feedback loops are provided to give control over at least those variables which strongly influence the rotor behavior, swashplate feedback by itself of the type envisioned in Paragraphs 3.5 and 3.6 will be of limited effectiveness since it provides control only over a small component of the total forces acting on the aircraft. Nevertheless useful reduction in blade load transient may be demonstrated even in the absence of special measures to control aircraft normal acceleration and short period modal response.

#### 3.8.1 Method of Investigation and Results. Cruise.

The aircraft was subject to a relatively long period, five second (1-cosine) gust and the time history of the hub forces and moments were examined with Aq feedback present at different azimuths, and a gain setting sufficiently small that no instabilities were generated. From the variation of forces and moments with azimuth a region was selected for further investigation and the variation of loads with gain determined.

The effect of feedback is evaluated from the transient response of the hub forces and moments. Sample responses are shown in Figures 3.18 and 3.19 for the 250 knot case with an azimuth setting of 150-degrees. Two maximum load points in the time history are observed, an initial loading associated with the peak gust intensity and an overswing loading of opposite sign. In some cases the second peak is more severe than the first.

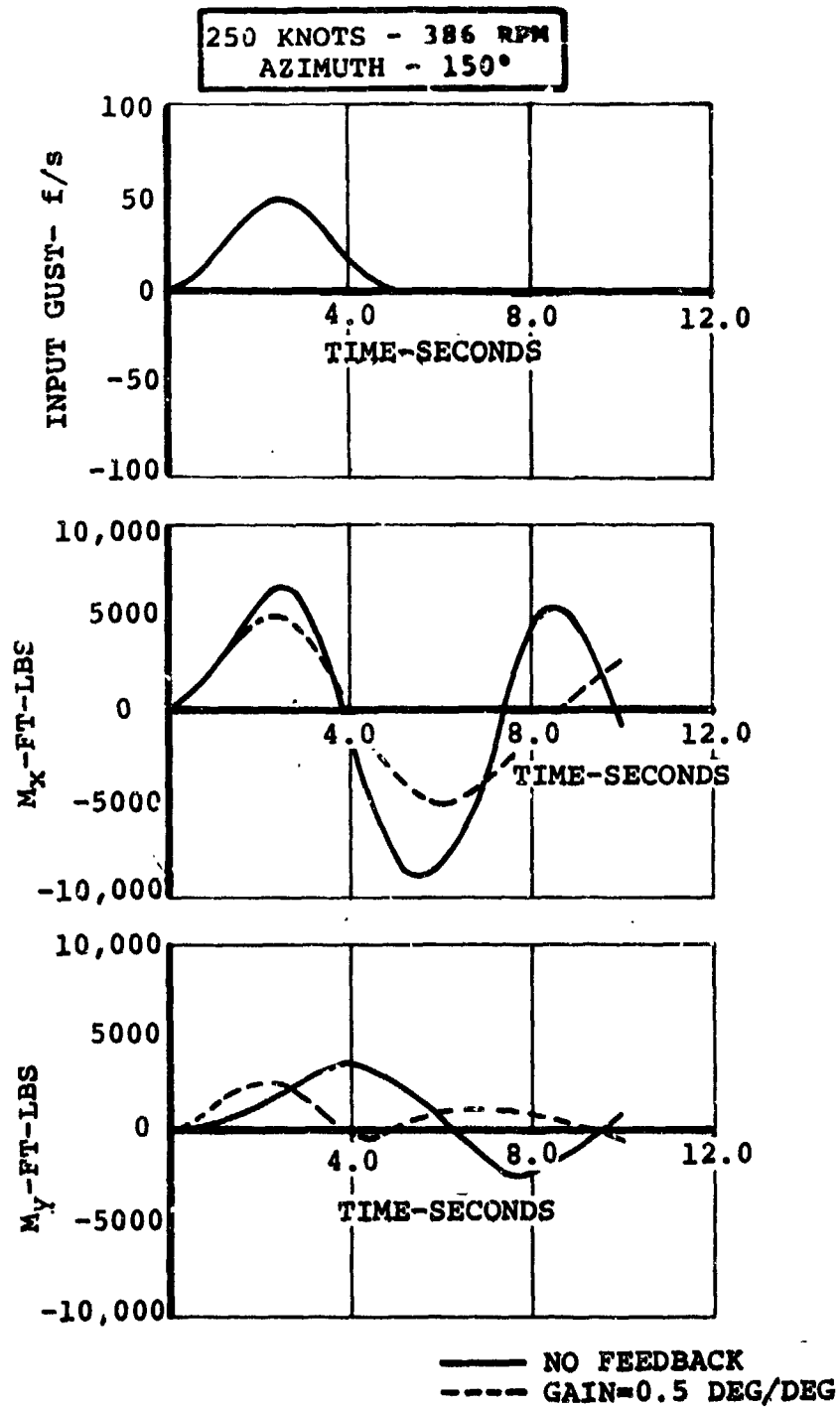


FIGURE 3.18. EFFECT OF FEEDBACK ON THE DYNAMIC RESPONSE OF ROTOR HUB MOMENTS, AT 250 KNOTS, 386 RPM.

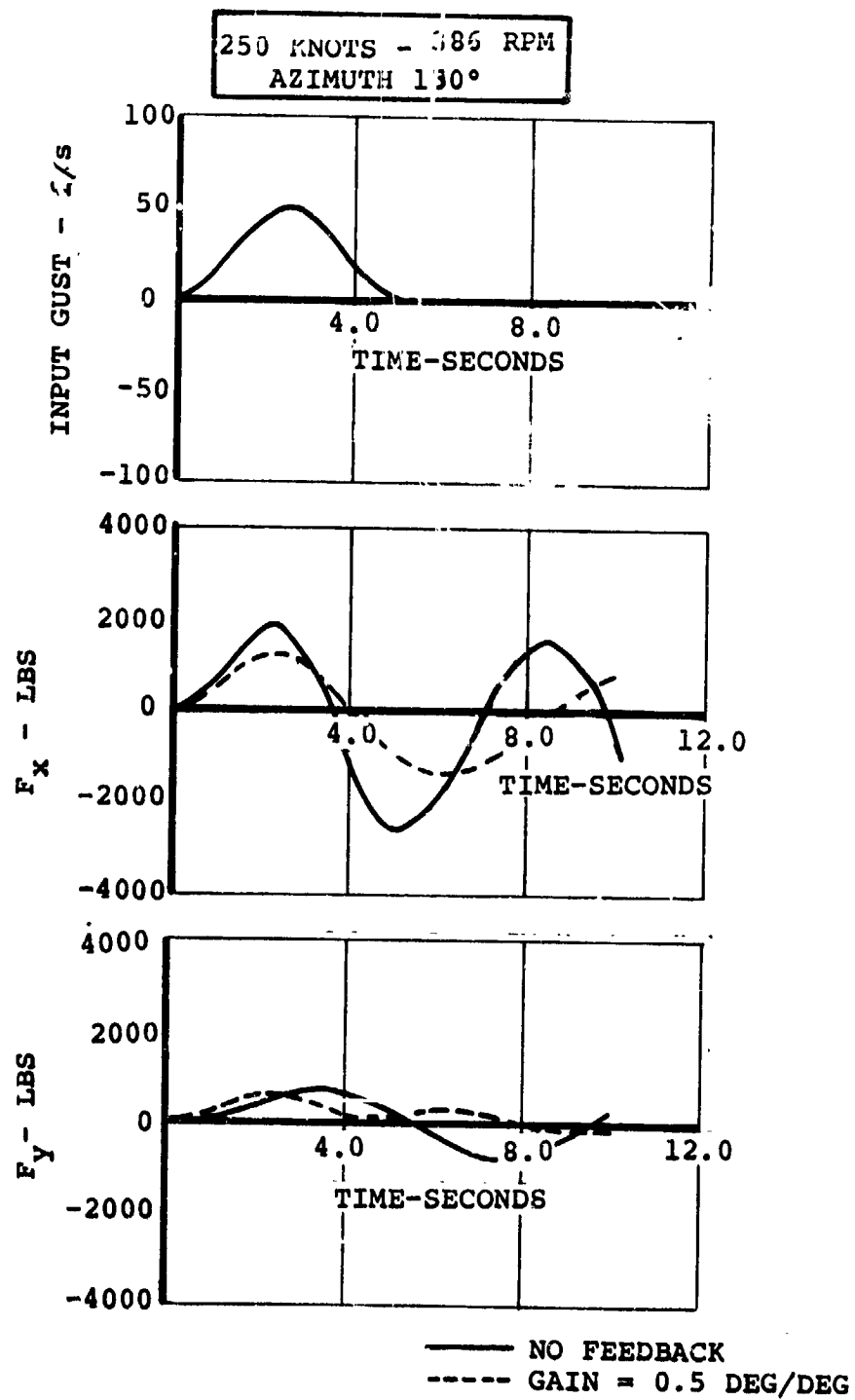


FIGURE 3.19. EFFECT OF FEEDBACK ON THE DYNAMIC RESPONSE OF ROTOR HUB FORCES AT 250 KNOTS, 386 RPM.



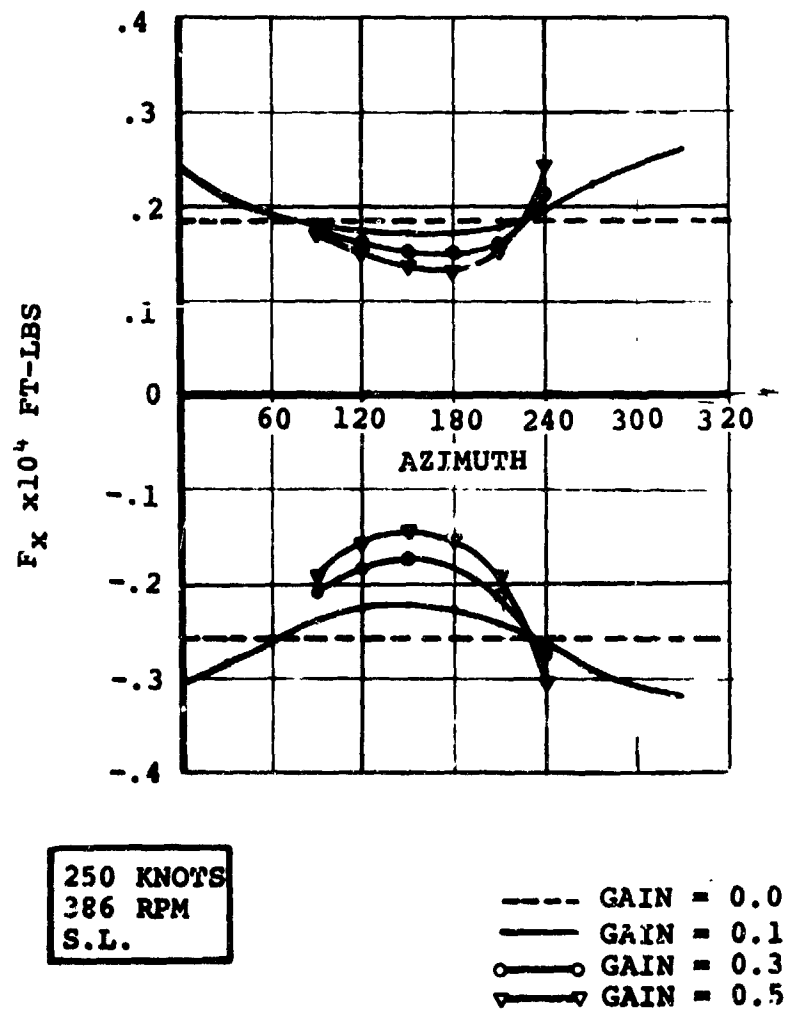
$F_x$  vs GAIN/AZIMUTH

FIGURE 3.20. VARIATION OF PEAK HUB NORMAL FORCE  
WITH GAIN AND AZIMUTH OF FEEDBACK

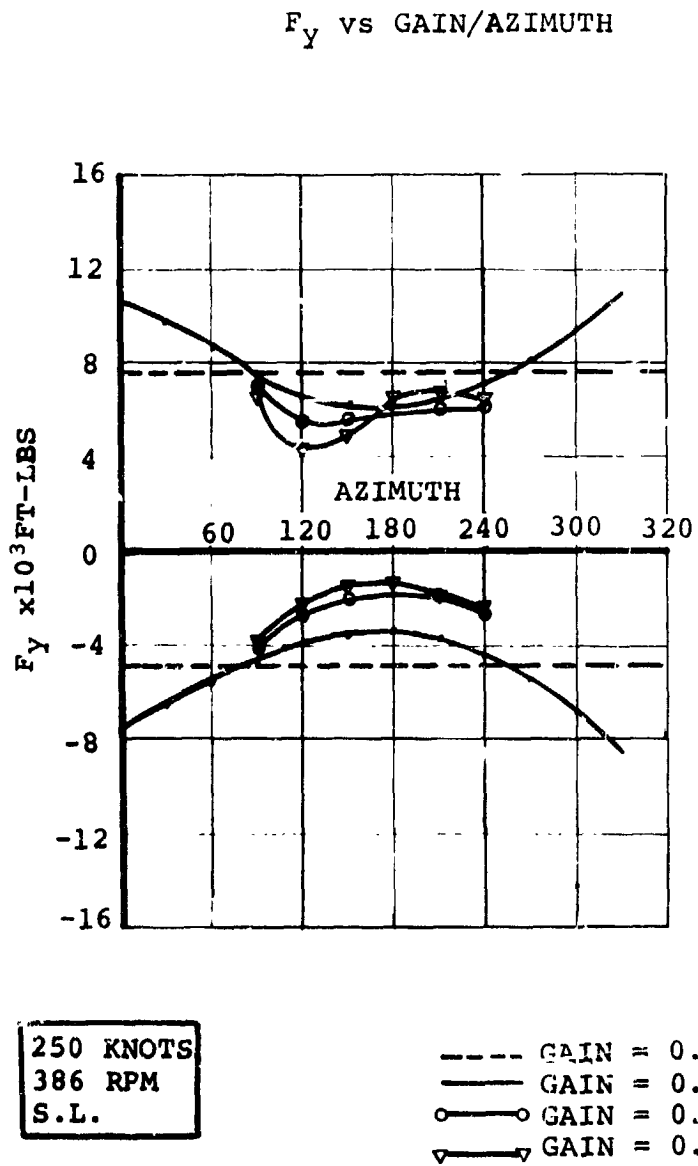


FIGURE 3.21. VARIATION OF PEAK HUE SIDE FORCE WITH GAIN AND AZIMUTH OF FEEDBACK

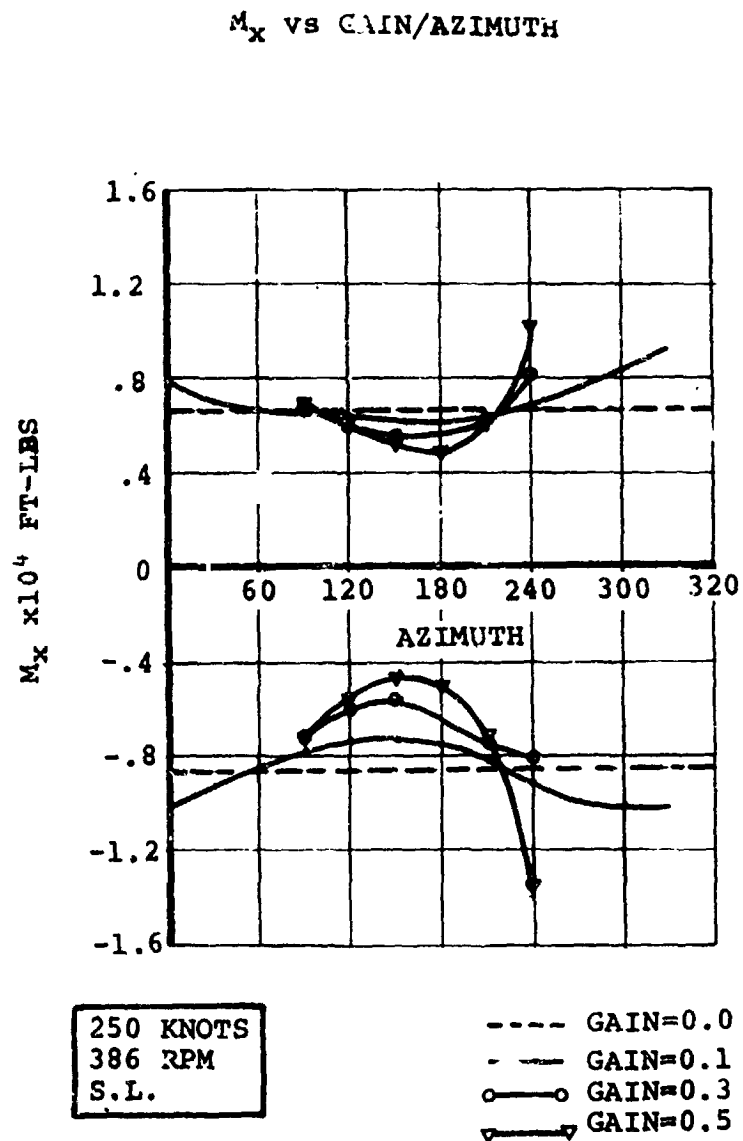


FIGURE 3.22. VARIATION OF PEAK HUB YAWING MOMENT WITH GAIN AND AZIMUTH OF FEEDBACK

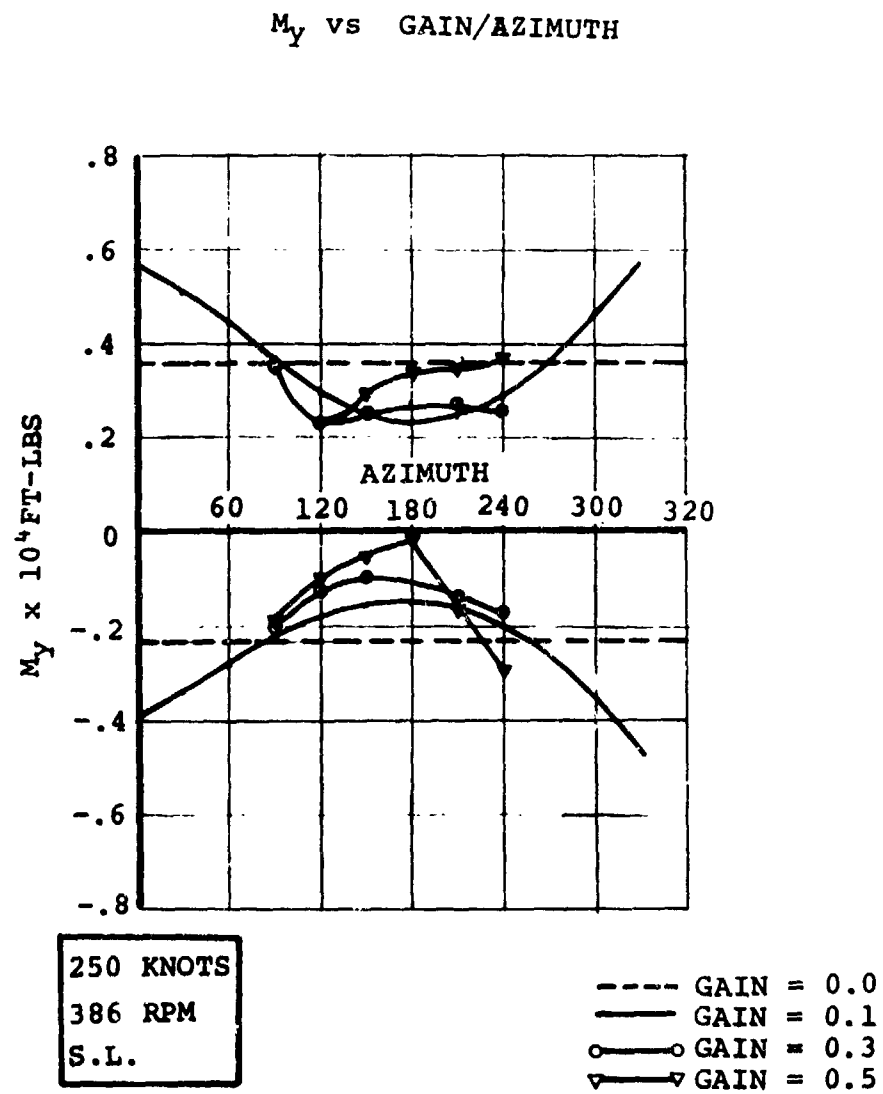


FIGURE 3.23. VARIATION OF PEAK HUB PITCHING MOMENT  
WITH GAIN AND AZIMUTH OF FEEDBACK

The peak loads for a range value of azimuth and gain are plotted in Figures 3.20 through 3.23. It is seen that an optimal value of azimuth occurs at approximately 150-degrees, and both the first and second peak loads reduce with gain. The reduction is approximately linear for low values of gain, but a point of diminishing returns is reached around a gain setting of 0.5 degrees per degree of alpha, and at higher settings instabilities were encountered. The reduction in loadings are as follows:

<u>PEAK NUMBER</u>	<u>ZERO GAIN</u>		<u>GAIN 0.5</u>		<u>REDUCTION FACTOR</u>	
	<u>1</u>	<u>2</u>	<u>1</u>	<u>2</u>	<u>1</u>	<u>2</u>
F <sub>X</sub> Normal Force Lb	1850,	-2600	1300,	-1450	0.7	0.55
F <sub>Y</sub> Side Force Lb	7600,	-5000	5000,	-1500	0.66	0.3
M <sub>X</sub> Yawing Moment Ft-Lb	6600,	-8600	5000,	-4500	0.76	0.525
M <sub>Y</sub> Pitching Moment Ft-Lb	3700,	-2300	3000,	-500.0	0.81	0.22

The same system (i.e., gain 0.5 and azimuth 150-degrees) was evaluated for 350 knots as shown in Figure 3.24 and 3.25 with the following results:

<u>PEAK NUMBER</u>	<u>ZERO GAIN</u>		<u>GAIN 0.5</u>		<u>REDUCTION FACTOR</u>	
	<u>1</u>	<u>2</u>	<u>1</u>	<u>2</u>	<u>1</u>	<u>2</u>
F <sub>X</sub> Normal Force Lb	3400,	-3500	1600,	-600	0.47	0.17
F <sub>Y</sub> Side Force Lb	1300,	-900	600,	---	0.46	----
M <sub>X</sub> Yawing Moment Ft-Lb	5000,	-4500	2500,	-500	0.50	0.11
M <sub>Y</sub> Pitching Moment Ft-Lb	2700,	-1800	1500,	---	0.55	----

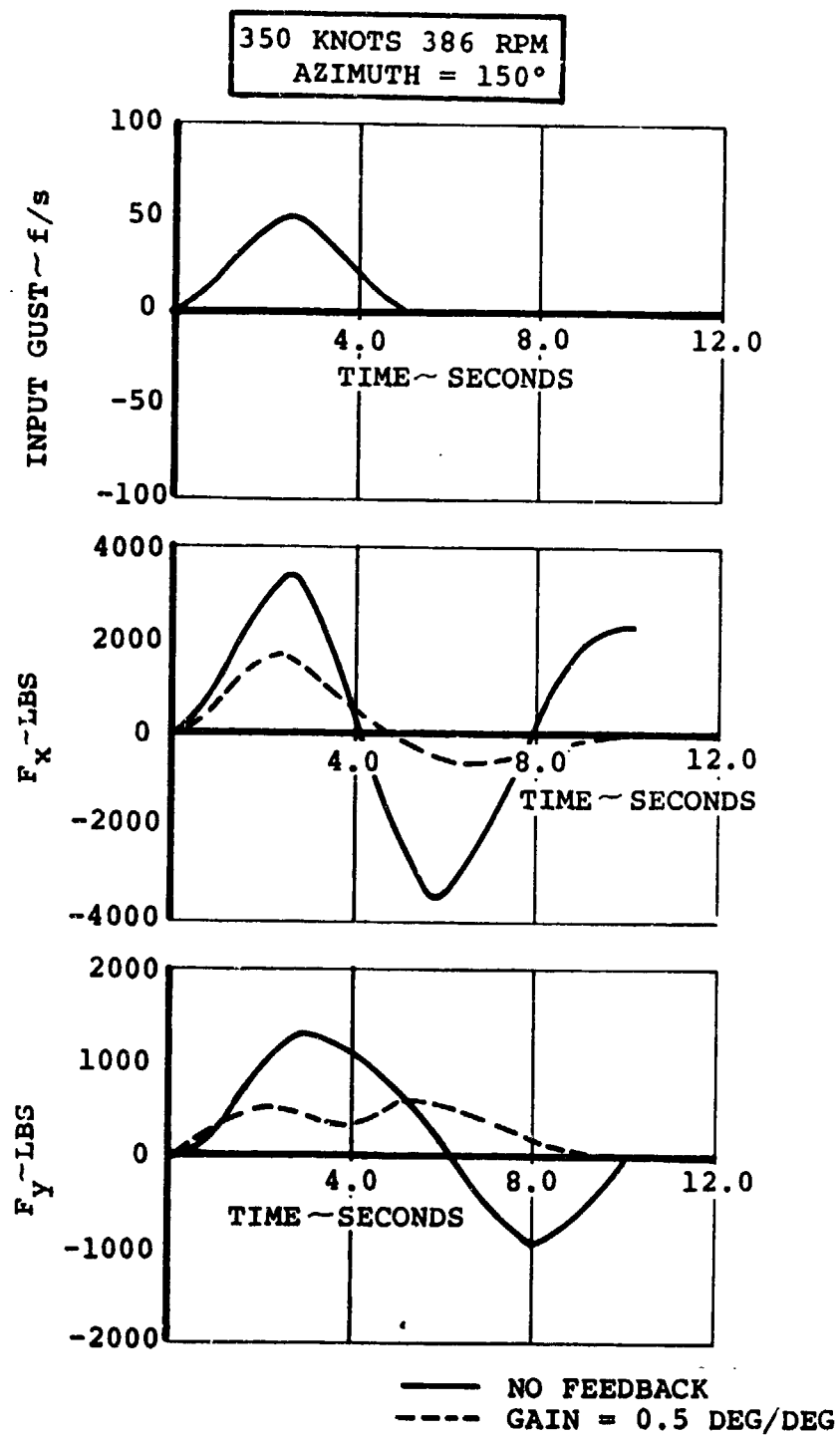


FIGURE 3.24. EFFECT OF FEEDBACK ON THE DYNAMIC RESPONSE OF ROTOR HUB FORCES AT 350 KNOTS, 386 RPM

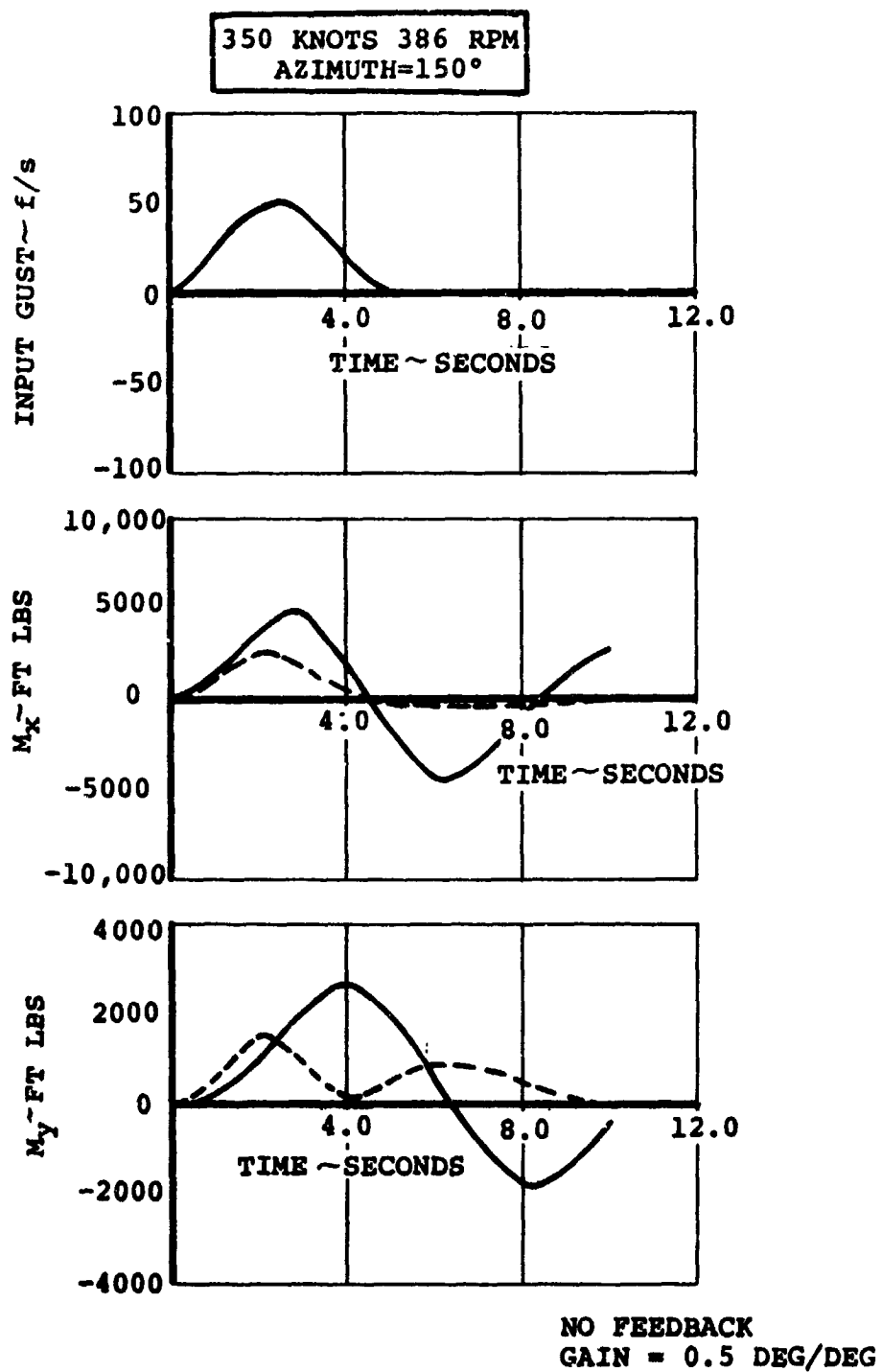


FIGURE 3.25. EFFECT OF FEEDBACK ON THE DYNAMIC RESPONSE OF ROTOR HUB MOMENTS AT 350 KNOTS, 386 RPM

The results presented above indicate that useful reductions in blade load response may be achieved even when swashplate feedback alone is used. However, azimuth settings are significantly different from those determined from purely static considerations although the net gain required is approximately the same.

Attempts to achieve a compromise in azimuth and gain between the static and dynamic cases do not appear to be profitable. As may be seen from Figure 3.15, the azimuth suitable for the dynamic case (150-degrees) is removed from the desirable static value of 216-degrees. Alternatively at the 216-degree value the dynamic system does not produce significant reduction in load. However, the system characteristics may be adjusted with frequency so that such compromises are unnecessary. Since azimuth is a reflection of the relative gain in the  $A_1$  and  $B_1$  channels this affords a method of tailoring azimuth to frequency by the use of different transfer functions for filters in the  $A_1$  and  $B_1$  loops.

### 3.8.2 Results in Transition Velocities

The effect of azimuth and gain were explored for the transition case of 80 knots and 551 RPM. Figures 3.26 through 3.29 show the variation of forces and moments with azimuth and gain. In this flight condition the most beneficial effects occur around 180-degrees with gain 0.015 degrees per degree of angle of attack. The time history of hub forces and moments is shown



in Figures 3.30 and 3.31 for this case. The reductions in loads for this case are of a similar order of magnitude to those in cruise, but it is noted that maximum benefit occurs at a different azimuth and there is a substantial increase in the sensitivity to gain.

It is seen that with an azimuth of 180-degrees and a gain setting of 0.15 degrees per degree that the following reductions are obtained.

PEAK NUMBER	ZERO GAIN		GAIN 0.15		REDUCTION FACTOR	
	1	2	1	2	1	2
F <sub>X</sub> Normal Force Lb	550,	---	400,	---	0.73	----
F <sub>Y</sub> Side Force Lb	22,	58	----	---	0.0	0.0
M <sub>X</sub> Yawing Moment Ft-Lb	10200,	---	9000,	---	0.88	----
M <sub>Y</sub> Pitching Moment Ft-Lb	1400,	-3200	600,	-800	0.43	0.25

It is noted that in the transition case the tendency to over-swing loading is significantly reduced. This is a function of the short period mode frequency and damping, which is of the order of 0.04 Hz and 60% critical without feedback, becoming critically damped at the azimuth and gain selected, as shown in Figures 3.32 and 3.33.

### 3.9 CONCLUSIONS AND DIRECTION FOR DEVELOPMENT

A number of conclusions may be drawn from the preceding studies of load alleviation. The first is that under static conditions, a swashplate feedback system may be designed which will fulfill

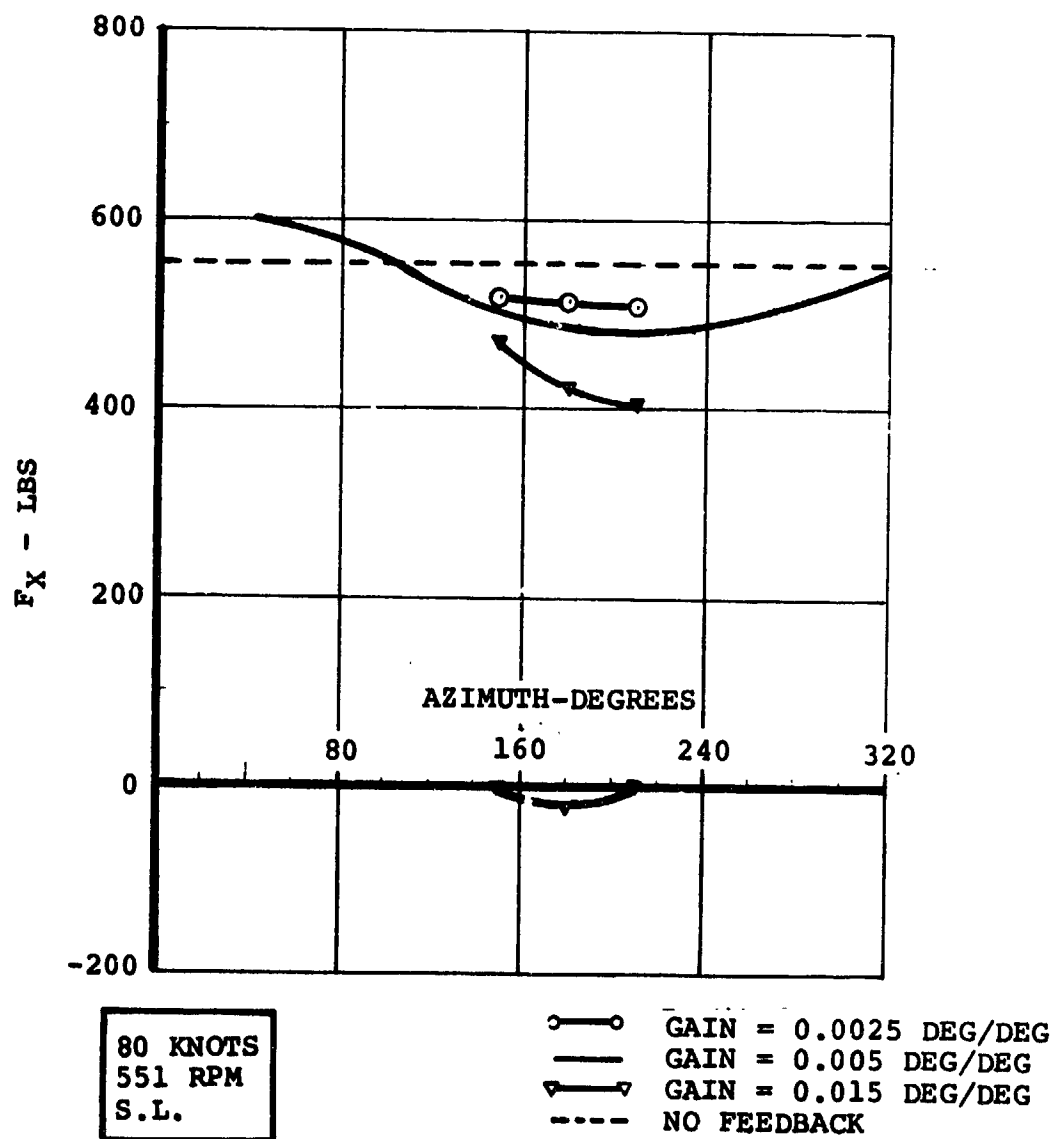
$F_X$  VS GAIN/AZIMUTH

FIGURE 3.26. VARIATION OF HUB NORMAL FORCE WITH AZIMUTH AND FEEDBACK GAIN AT 80 KNOTS AND 551 RPM.

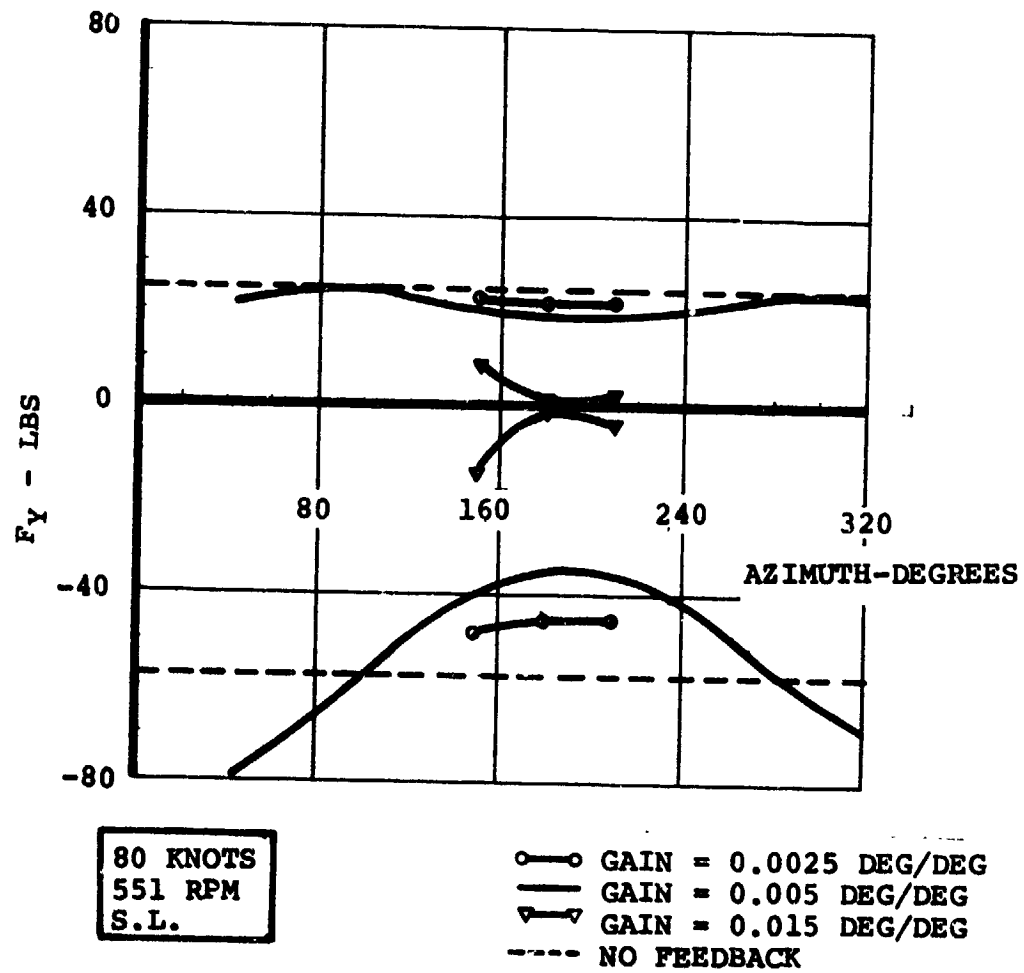
F<sub>y</sub> VS GAIN/AZIMUTH

FIGURE 3.27. VARIATION OF HUB SIDE FORCE, WITH AZIMUTH AND FEEDBACK GAIN AT 80 KNOTS AND 551 RPM.

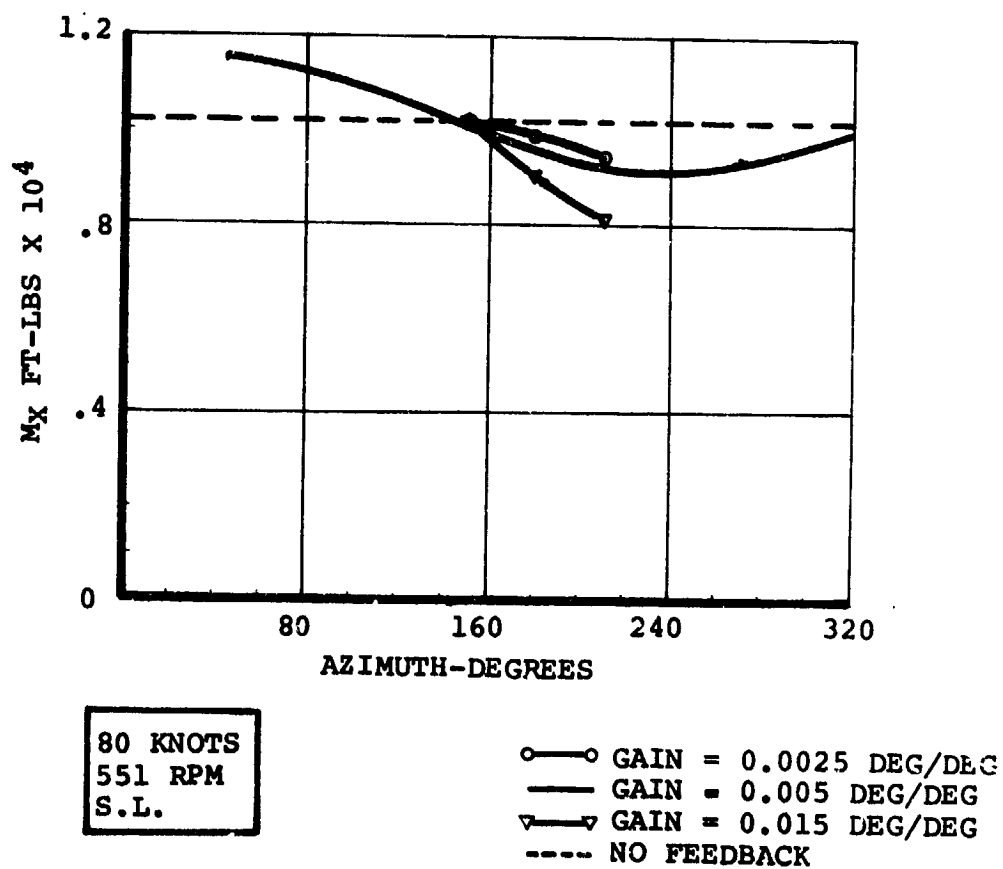
$M_X$  VS GAIN/AZIMUTH

FIGURE 3.28. VARIATION OF HUB YAWING MOMENT WITH AZIMUTH AND FEEDBACK GAIN AT 80 KNOTS AND 551 RPM.

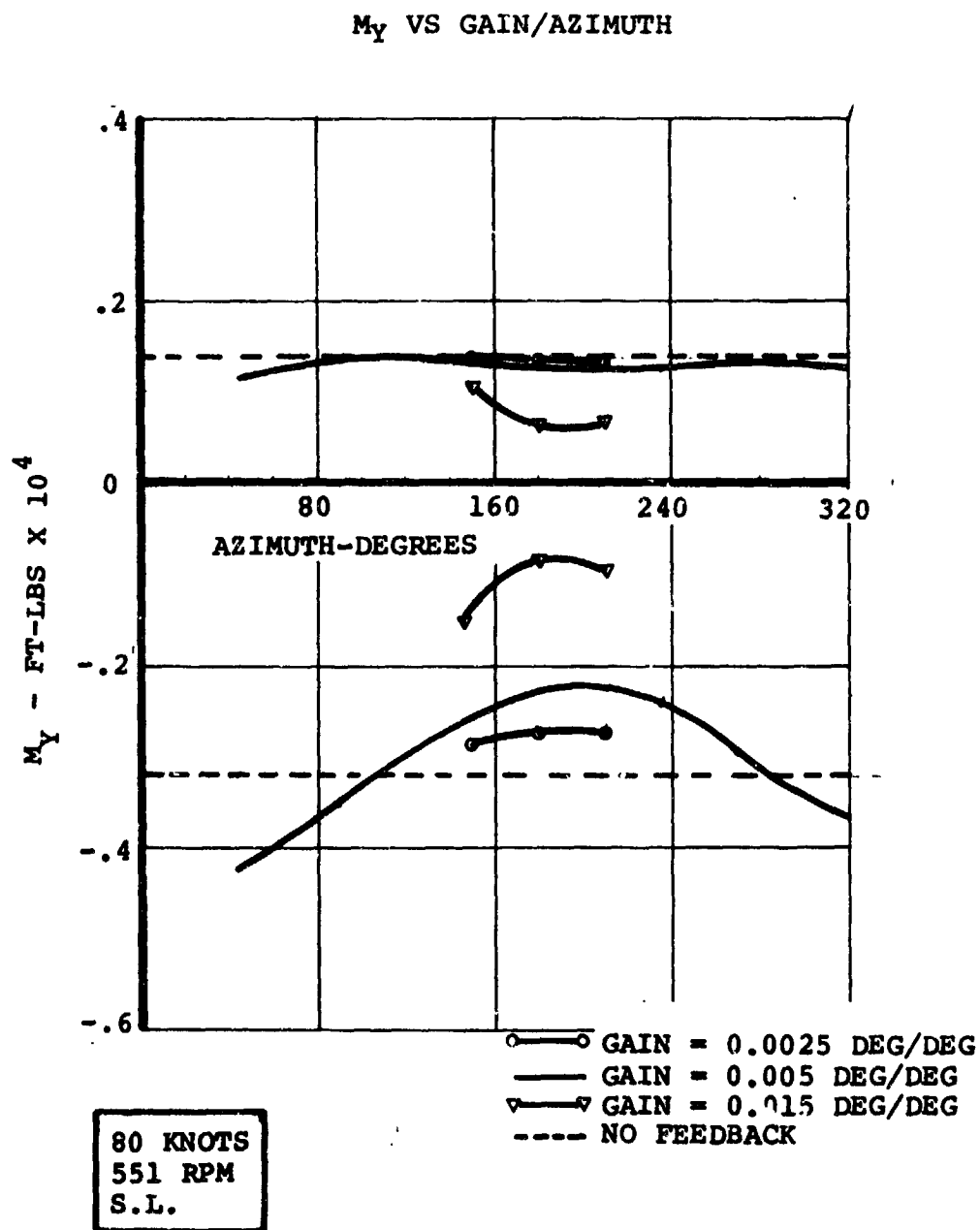


FIGURE 3.29. VARIATION OF HUB PITCHING MOMENT WITH AZIMUTH AND FEEDBACK GAIN AT 80 KNOTS AND 551 RPM.

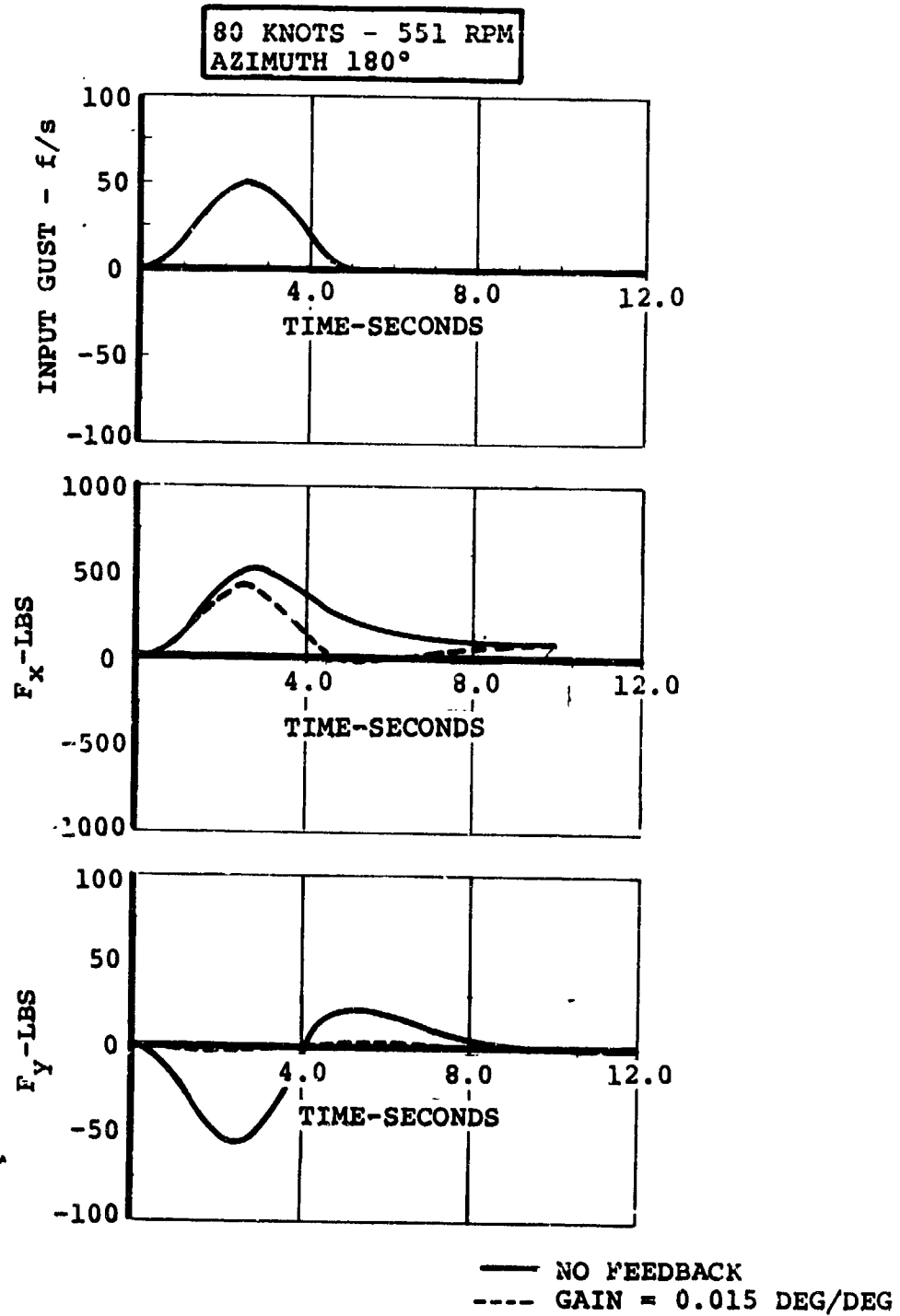


FIGURE 3.30. EFFECT OF FEEDBACK ON THE DYNAMIC RESPONSE OF ROTOR HUB FORCES AT 80 KNOTS AND 551 RPM.

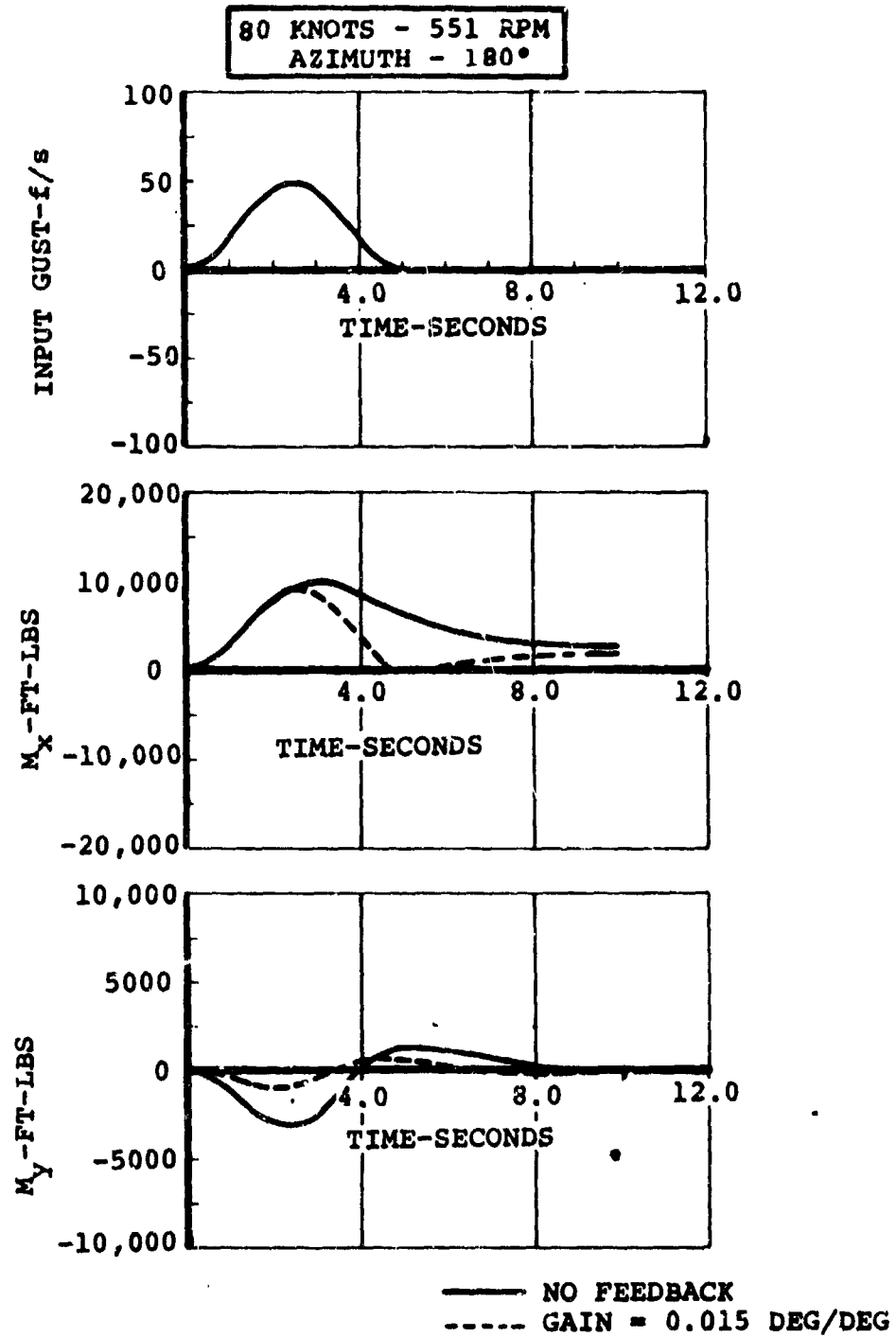


FIGURE 3.31. EFFECT OF FEEDBACK ON THE DYNAMIC RESPONSE OF ROTOR HUB MOMENTS AT 80 KNOTS AND 551 RPM.

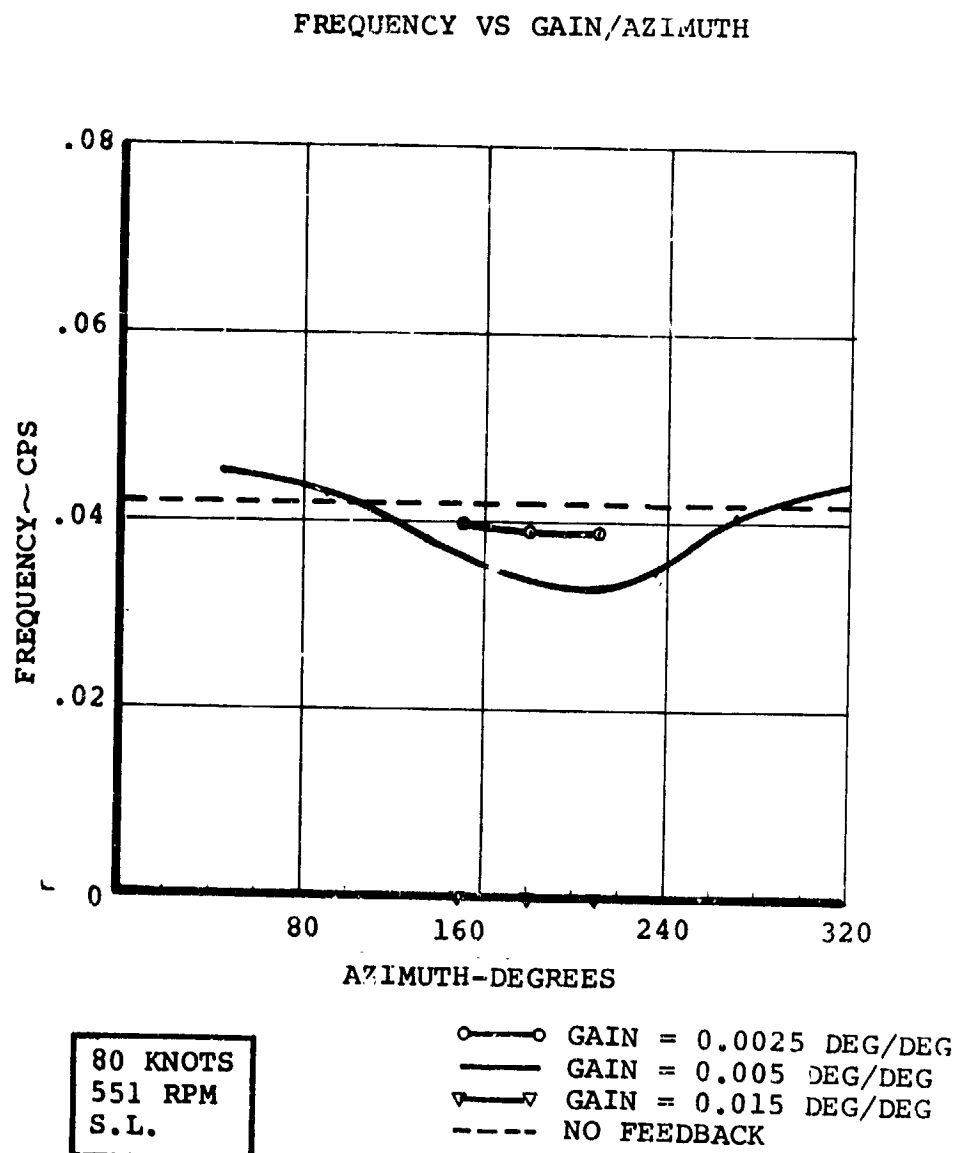
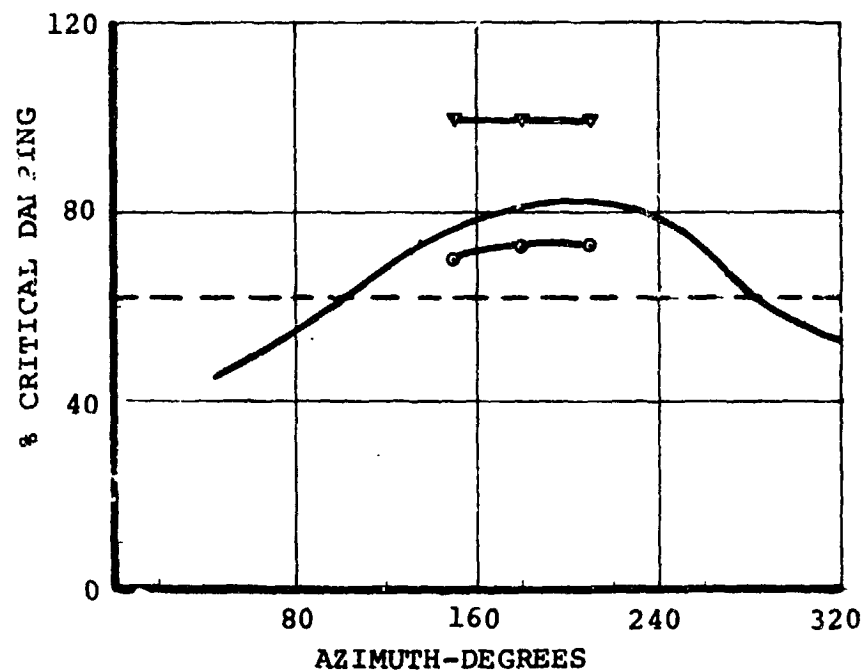


FIGURE 3.32. VARIATION OF SHORT PERIOD MODE FREQUENCY  
 WITH AZIMUTH AND FEEDBACK GAIN.  
 V=80 KNOTS.  $\Omega$ =551 RPM.



## % CRITICAL DAMPING VS GAIN/AZIMUTH



80 KNOTS  
551 RPM  
S.L.

○—○ GAIN = 0.0025 DEG/DEG  
— GAIN = 0.005 DEG/DEG  
▽—▽ GAIN = 0.015 DEG/DEG  
---- NO FEEDBACK

FIGURE 3.33. VARIATION OF SHORT PERIOD MODE DAMPING  
WITH AZIMUTH AND FEEDBACK GAIN.  
V=80 KNOTS.  $\Omega$ =551 RPM.

one or more of a possible set of objectives. For optimal performance scheduling of feedback gain and azimuth as a function of flight condition, (speed and RPM) is necessary. Although the system demonstrated for 250 knots was even more effective at 350 knots, reduced speeds and increased RPM's call for different azimuth settings and reduced gain.

The response characteristics of the blade loads in dynamic situations may also be substantially improved by feedback. Differences in behavior noted between transition and moderately high speed cruise are caused by changes in the short period mode of the aircraft, and in the damping of the blade flapping mode. At 80 knots the short period mode is almost critically damped and its low frequency makes it unresponsive to the gust wave length assumed, with the result that blade loads show little tendency to overswing.

A promising area for additional analytically and experimental study will be the use of spoiler, flap and elevator feedback to modify the basic aircraft response characteristics so that the demands on a swashplate feedback load alleviation system are more nearly constant over the operating range.

The current study was performed for two conditions; the alleviation of loads due to a steady state condition and of those induced by flying through a discrete 5 second period gust. Other gust wavelengths must also be considered in

the design of a useful system, and this raises the question of compatibility from the standpoint of frequency. The nature of the blade load response varies with the type and frequency (period) of the loading condition.

Thus, variation of gain and azimuth with frequency is anticipated as a requirement. This may be accomplished using appropriate transfer functions to shape the signals in the  $A_1$  and  $B_1$  channels. At a given frequency the azimuth of the net feedback signal may be controlled by the relative frequency response in the two channels.

Relative phasing of the  $A_1$  and  $B_1$  signals may also be of value when unsteady loading conditions are encountered. The value of phasing the feedback signals applied to the swashplate is discussed in detail in Section 5. The investigation of such effects including the complimentary use of feedback to the conventional controls is recommended for further analytical and wind tunnel study. The general outline of further investigation and implementation is given in Section 9.

#### 4. DIRECT LIFT FEEDBACK CONTROL

##### 4.1 BACKGROUND AND OBJECTIVES

Alleviation of aircraft normal acceleration response to gusts has long been the objective of many aircraft design teams. With gust alleviation it was hoped to relieve structural loads, improve the ride qualities, lessen pilot fatigue, and/or provide a more stable flying platform. While many early attempts at gust alleviation were disappointing (References 4.1, 4.2, & 4.3) it is thought that in many of these the attempt was being made without a full understanding of all aspects of flight dynamics and control system theory. Advances in avionics and in analytical and simulation techniques would today provide a much higher probability of success. In support of this view, attention is drawn to the striking success of systems with very similar objectives such as the LAMS system which is in operation on the B-52 bomber. This leads to the feeling that it is worthwhile to renew investigations of direct lift control systems using current feedback system technology and spoiler flap technology. The application of direct lift techniques in Tilt Rotor aircraft is particularly interesting for several reasons. One is that these aircraft will spend the greater portion of their time at low altitudes and thus be in turbulent air, and a system which responds to reduce the characteristically high lift curve slope of such aircraft would provide

distinct improvements in ride quality. Another consideration is a high gust response will tend to limit the effectiveness of the swashplate feedback blade load alleviation system. Since blade response is stimulated by linear and angular accelerations of the rotor hub and cyclic pitch control will not be particularly effective in compensating for such inputs, direct lift feedback may improve the effectiveness of the blade load alleviation system in minimizing blade loads. Finally, in a typical tilt rotor design such as the Model 222, provision of a direct lift control system represents a relatively modest increment in design effort and hardware modification. Full span flaps and spoilers are current features; automatic electrical control of the full span flaps and symmetrical spoiler control are seen as relatively minor modifications, along with automatic control of the elevators to compensate for flap induced pitching moment.

Objectives of the gust alleviation system will be:

- 40% to 60% reduction in normal acceleration response to gusts
- no adverse effect on aircraft flying qualities
- simplicity of system design

Evaluation of the gust alleviation system was made in three parts. The first section discusses the approach to alleviating gusts, the math model, and the feedback loops. The second section discusses the results in terms of gain, system stability and gust alleviation. In the third section some

conclusions are drawn about the effectiveness of the system and its practicality for a tilt rotor aircraft.

#### 4.2 GUST ALLEVIATION SYSTEM APPROACH

A tilt rotor aircraft design with full span spoilers and flaps has been used to evaluate a gust alleviation system using direct lift control (DLC). For gusts which tend to increase the load factor, spoilers are deflected to "dump" wing lift and thus negate the effect of the gust. For gusts which decrease load factor, flaps are deflected thus increasing lift and negating the gust response. Both spoiler and flap deflection generate an aircraft pitching moment which could be trimmed by gearing the elevator to both the spoiler and the flaps.

A schematic of the system is shown in Figure 4.1. First order approximations for flap, spoiler, and elevator actuators have been made. In each case  $\tau_{ACT} = .05$  seconds.

To keep the system as simple as possible no filtering has been employed and only a minimum of signal shaping to indicate whether the flap or spoiler should be deflected was used. Aircraft angle of attack was sensed rather than normal acceleration in order to achieve some lead on aircraft response. The time lead is of two forms. First, if angle of attack is sensed at the nose of the aircraft there will be a finite time until the gust reaches the wing. The time lead increment will be of the form

$$\Delta t_1 = \frac{(\text{length from nose to wing leading edge})}{(\text{aircraft velocity})}$$

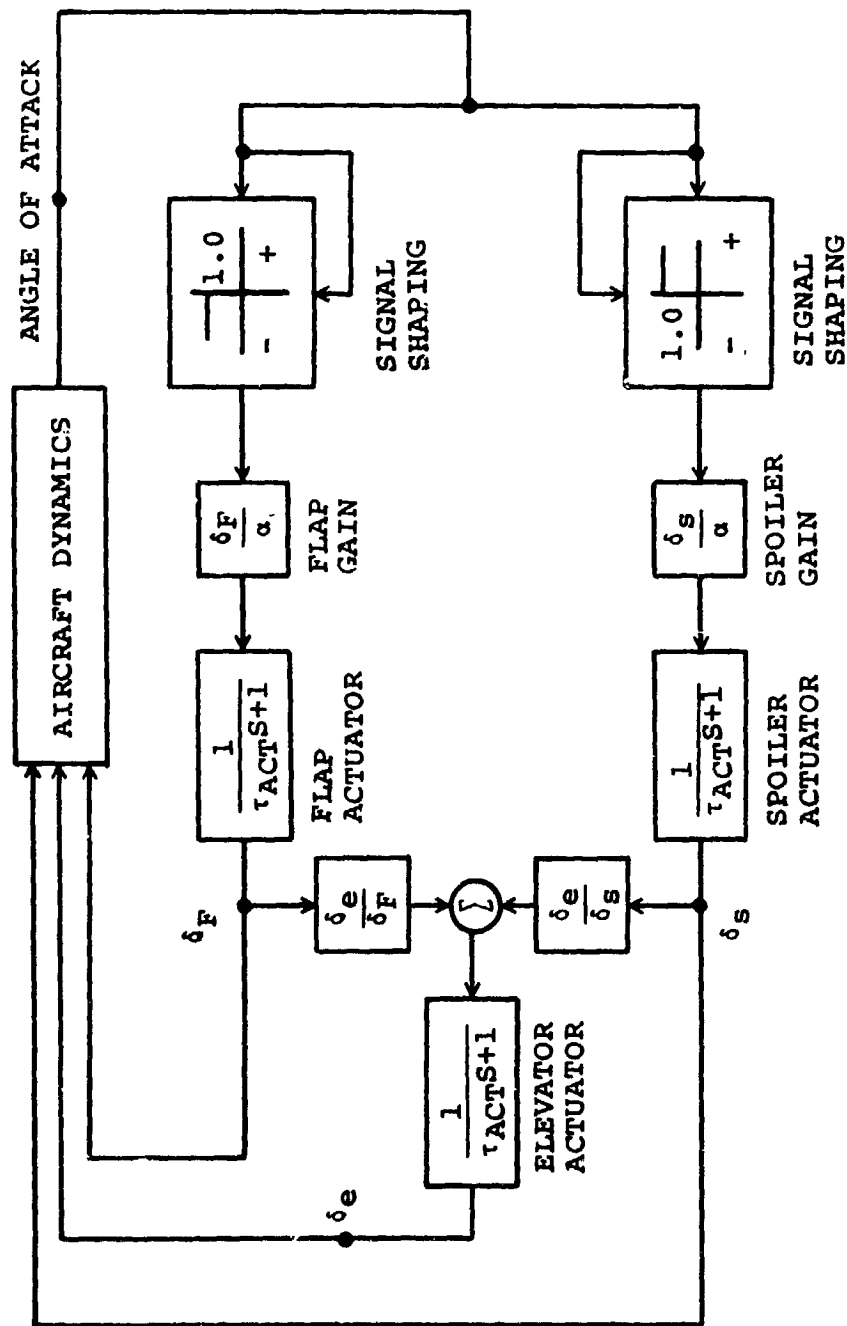


FIGURE 4.1. SCHEMATIC OF DIRECT LIFT CONTROL  
GUST ALLEVIATION SYSTEM

Second, it is known that the growth of wing lift due to angle of attack takes a finite time (call this  $\Delta t_2$ ). Thus, by sensing angle of attack a total time lead of  $(\Delta t_1 + \Delta t_2)$  can be achieved which would be unavailable if  $N_z$  acceleration was sensed. The DLC gust alleviation system was evaluated for a cruise flight velocity of 250 knots and a landing approach flight condition of 100 knots with nacelle incidence of 25-degrees.

#### 4.3 EVALUATION OF DLC GUST ALLEVIATION SYSTEM

The angle of attack system was evaluated at 100 knots and nacelle incidence of 25-degrees and 250 knots and nacelle incidence of 0-degrees. The 100 knot case was to represent a landing approach condition and it was desired that gust alleviation help the pilot hold a precision glideslope. This aspect is especially important in the instrument flight regime when one considers the steep glideslopes (7 to 20 degrees) being proposed for V/STOL aircraft. The 250 knot case represents a cruise flight condition and the purpose of the system will be to improve ride qualities.

Evaluation of the 250 knot cruise condition indicated that with a very simple system a 60% reduction in normal acceleration response to a ramp gust could be achieved with little effect on the short period mode (Figure 4.2). Spoiler gain was  $\delta_s/\alpha = 9.75$  and flap gain was  $\delta_F/\alpha = 4.95$ . Figures 4.3



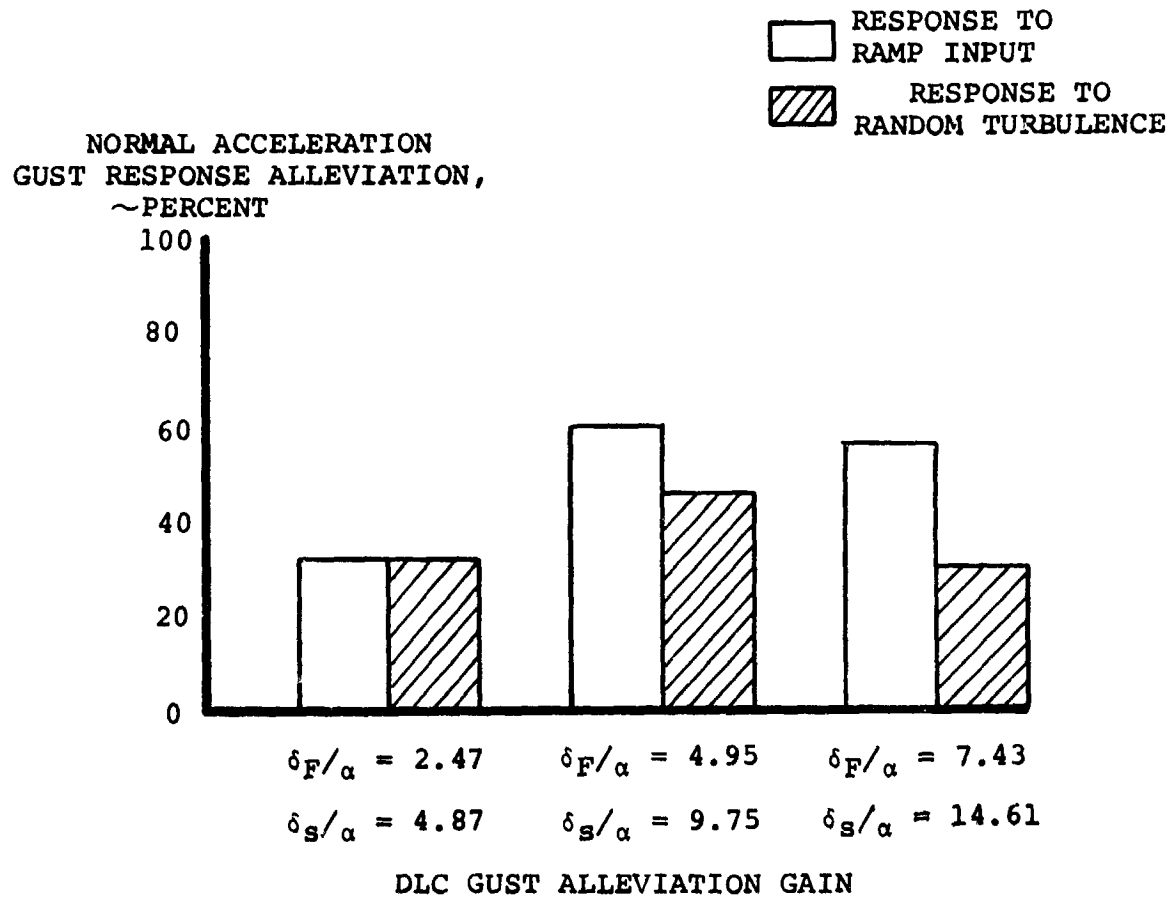


**FIGURE 4.2. EFFECT OF GUST ALLEVIATION SYSTEM GAIN  
ON NORMAL ACCELERATION RESPONSE  
250 KNOTS**

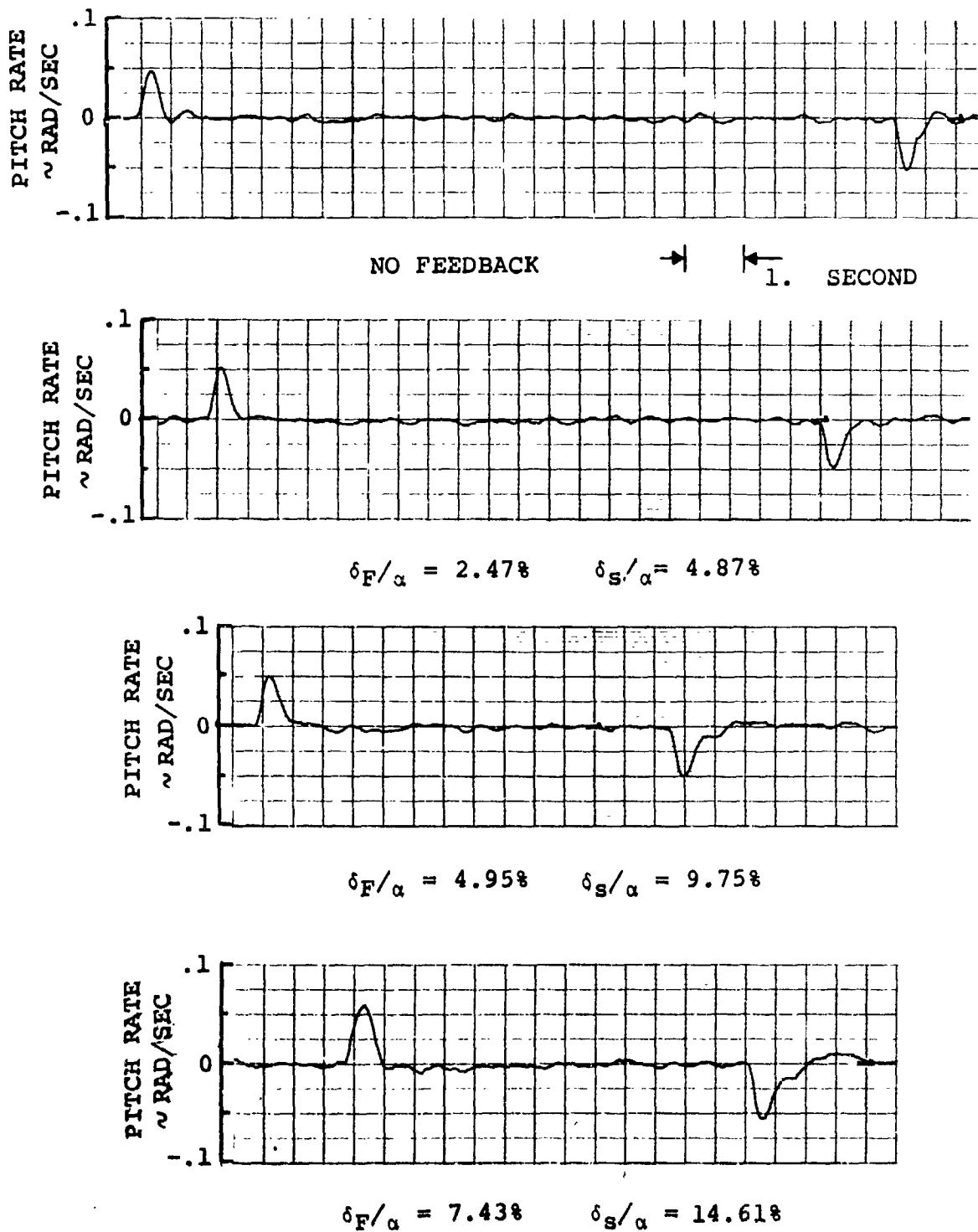


FIGURE 4.3. AIRCRAFT PITCH RATE RESPONSE TO RAMP GUST  
WITH AND WITHOUT DLC GUST ALLEVIATION SYSTEM

and 4.4 show the normal acceleration and pitch rate time history responses for various spoiler and flap gains. In this configuration the pitching moment due to small deflection of spoiler and flap is of such magnitude that elevator was not deemed necessary to trim the moments. The gain level can have a significant effect on aircraft flying qualities. At higher levels of gain the short period mode seems to be adversely affected as seen by the traces of Figures 4.3 and 4.4. A more detailed study of the system dynamics will have to be performed to determine if this problem can be overcome so that further effectiveness can be accomplished. In the second portion of the 250 knot study the aircraft was flown through random turbulence with the system off and the system on (Figures 4.5 to 4.8). The same gain variation as with the ramp gust was applied. At a gain level of  $\delta_F/\alpha = 4.95$  and  $\delta_S/\alpha = 9.75$ , a 45% reduction in normal acceleration gust response was achieved. Although this level of gust alleviation is not as great as for the ramp gust, it is significant and indicates that with further study of possible signal shaping a gust alleviation level of 60% could be reached and possibly more.

At a velocity of 100 knots and a nacelle incidence of 25-degrees, the same DLC gust alleviation system was evaluated. The aircraft was flown through random turbulence and the actual and RMS normal acceleration responses were measured. Aircraft normal acceleration gust response was reduced by 15% in the

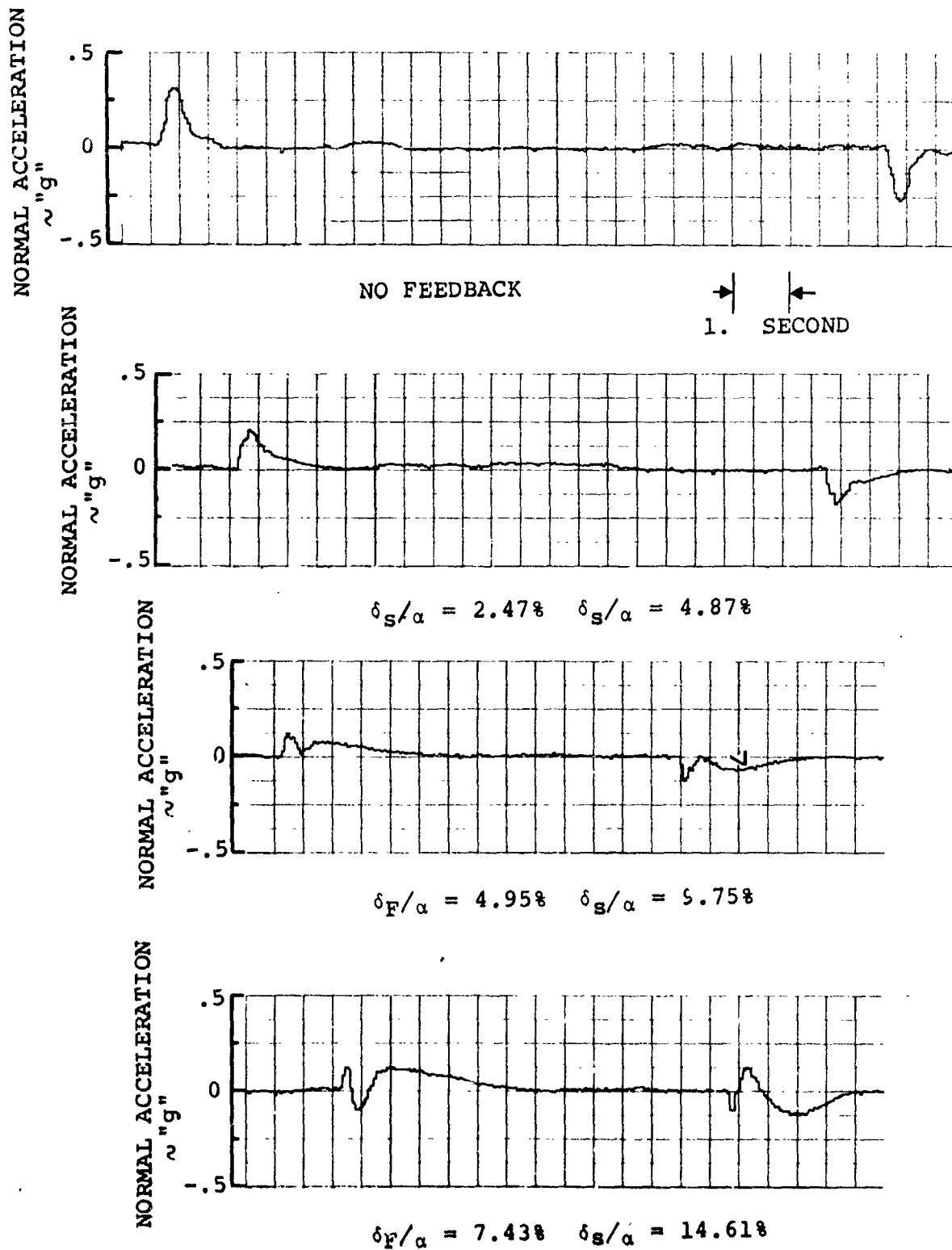


FIGURE 4.4. AIRCRAFT CABIN NORMAL ACCELERATION RESPONSE TO RAMP GUST WITH AND WITHOUT DLC GUST ALLEVIATION SYSTEM

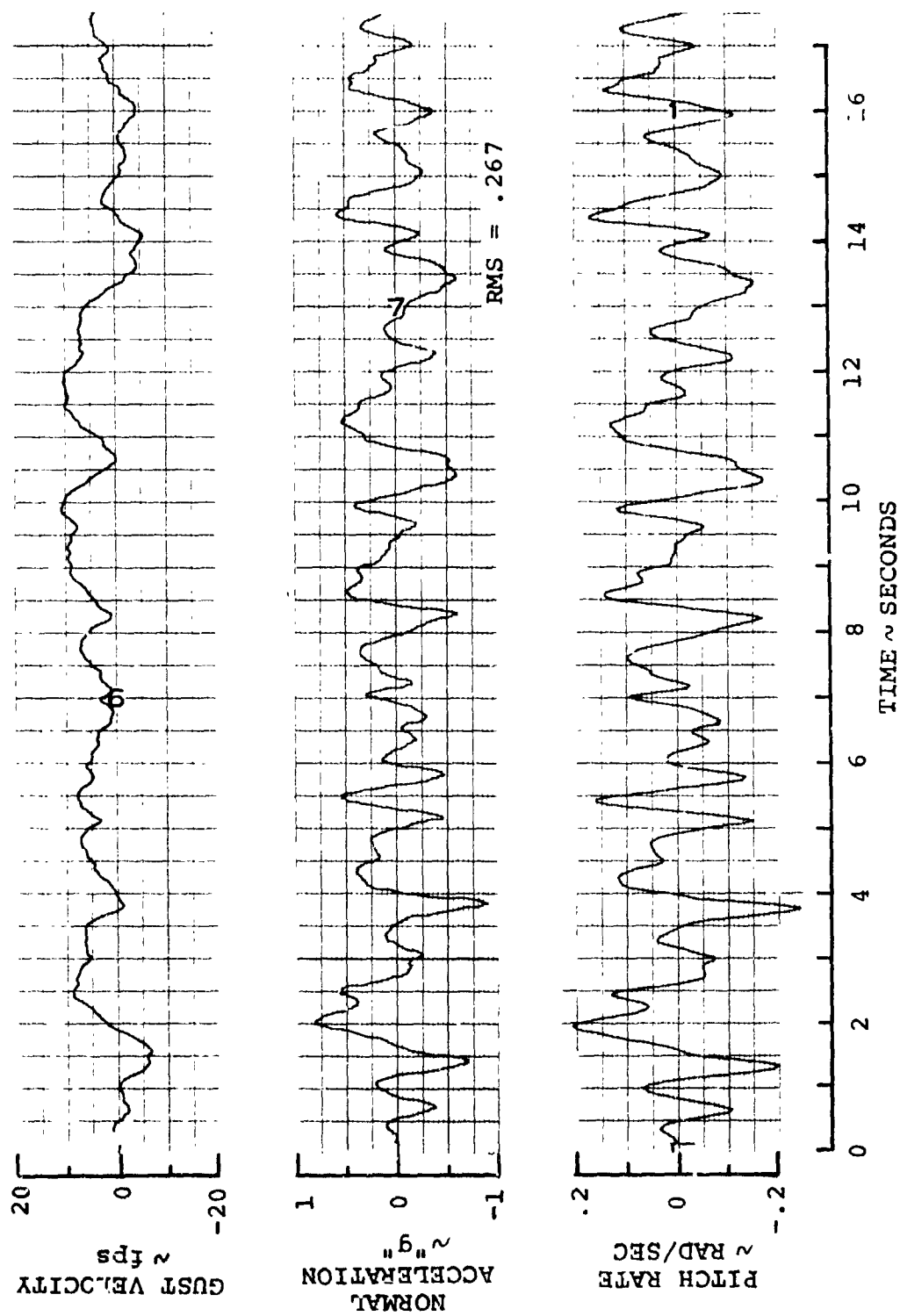


FIGURE 4.5. AIRCRAFT RESPONSE TO RANDOM TURBULENCE  
250 KNOTS NO FEEDBACK

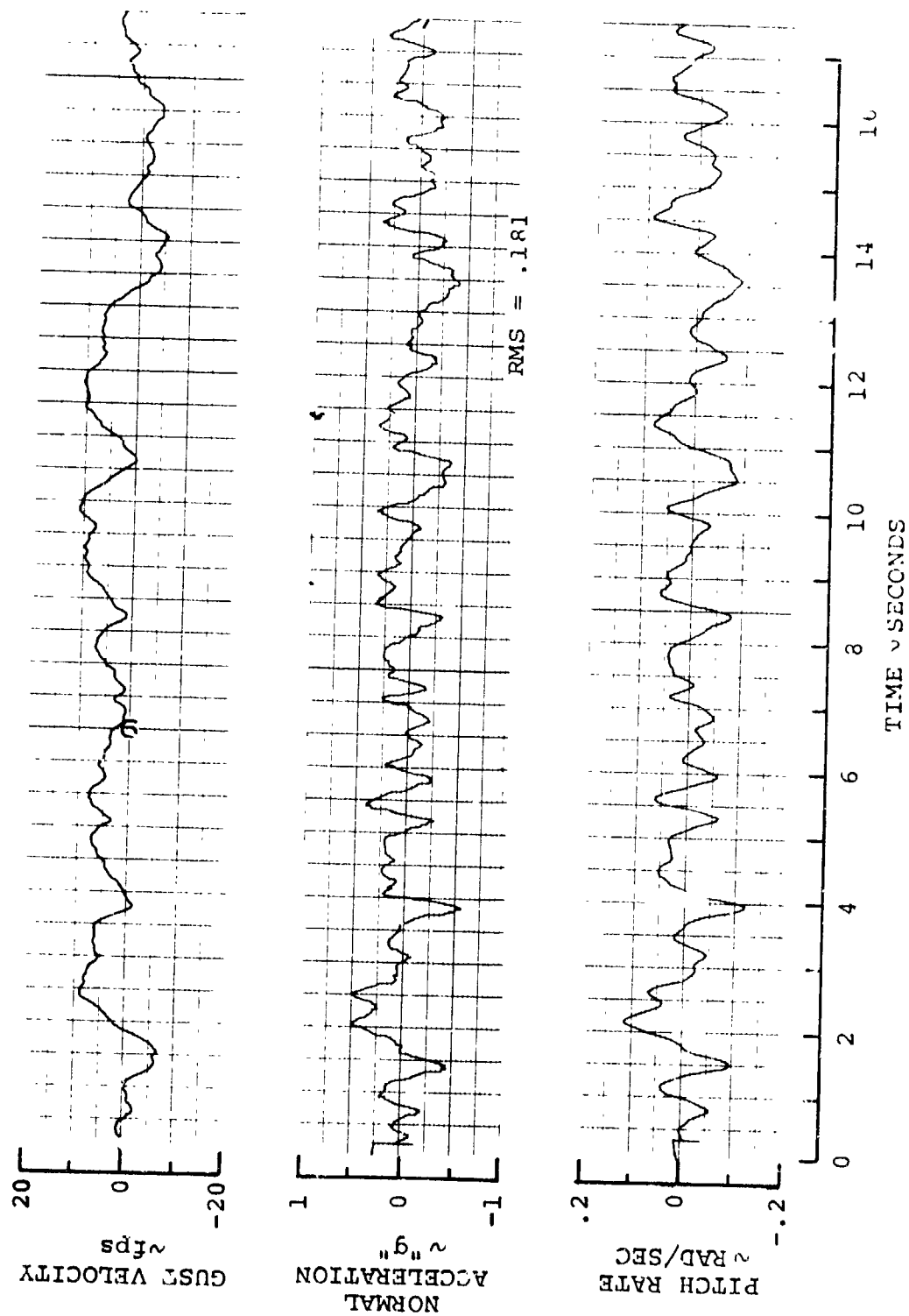


FIGURE 4.6. AIRCRAFT RESPONSE TO RANDOM TURBULENCE  
 250 KNOTS  $\delta_F/\alpha = 2.47$   $\delta_S/\alpha = 4.78$

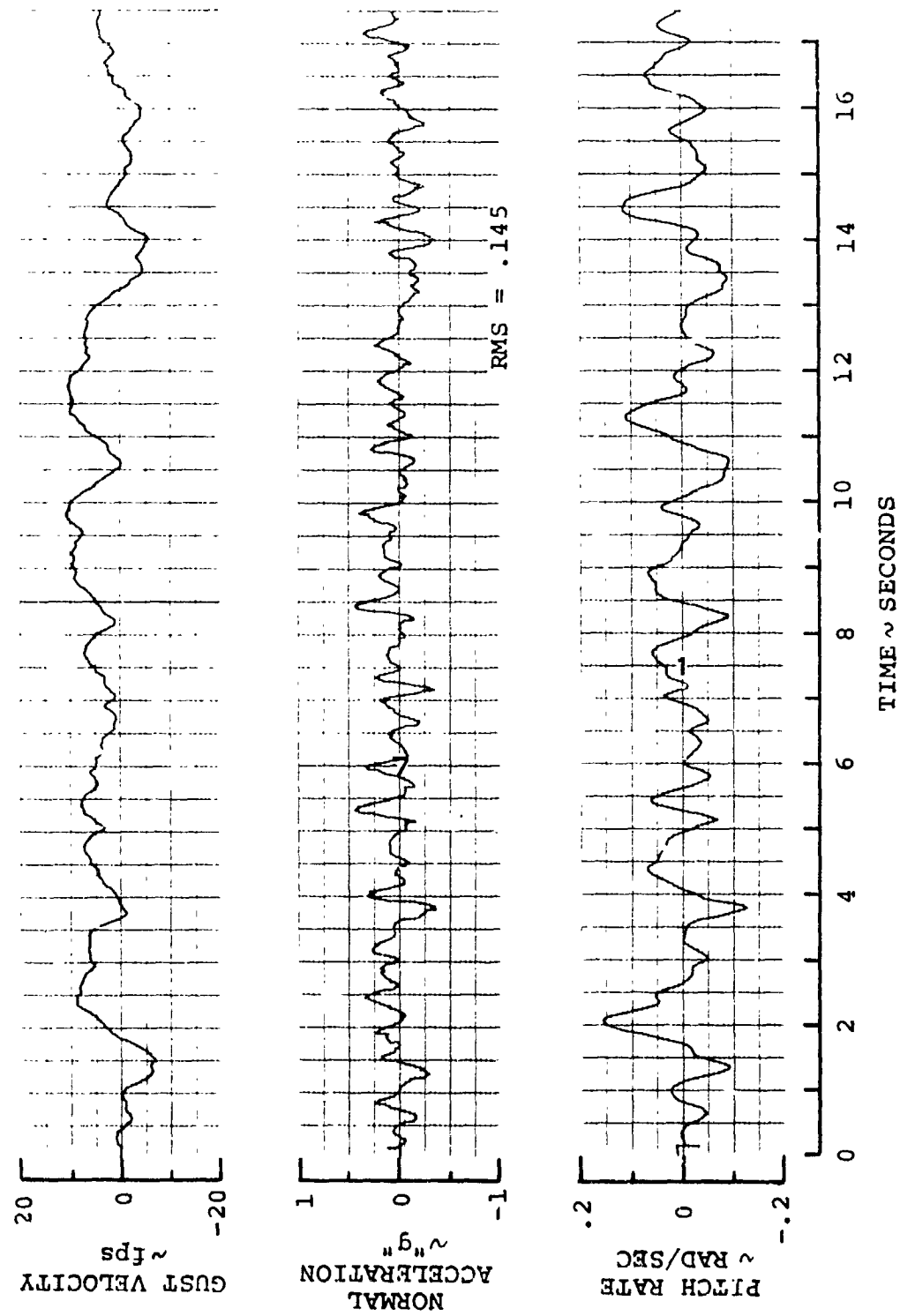


FIGURE 4.7. AIRCRAFT RESPONSE TO RANDOM TURBULENCE  
 250 KNOTS  $\delta_F/\alpha = 4.95$   $\delta_S/\alpha = 9.75$

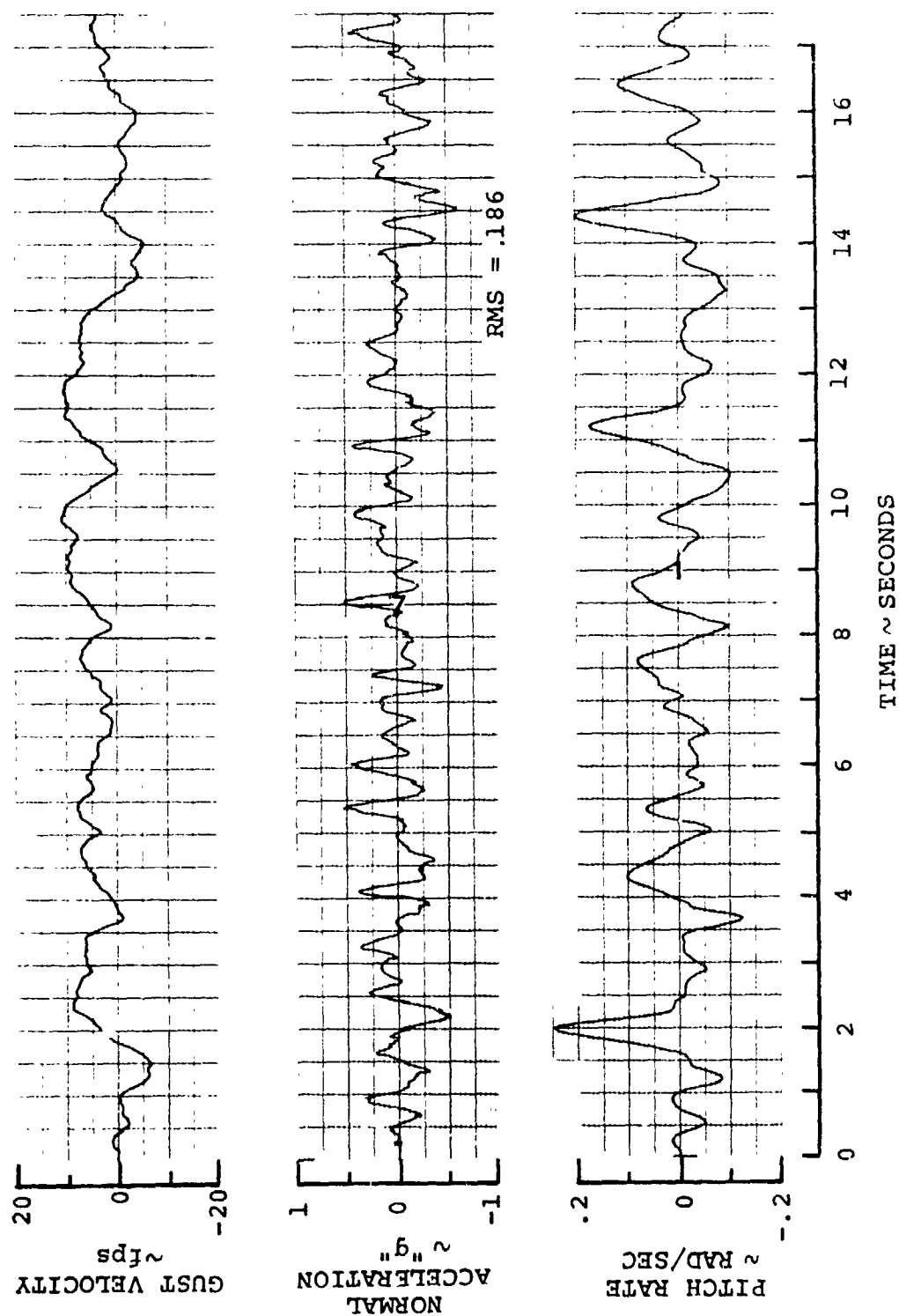


FIGURE 4.8. AIRCRAFT RESPONSE TO RANDOM TURBULENCE  
 250 KNOTS  $\delta_F/\alpha = 7.43$   $\delta_S/\alpha = 14.61$



best configuration. As seen in Figures 4.9 through 4.13 the aircraft dynamic response seems to be more affected than at 250 knots. It is evident that at certain values of gain the phugoid mode is excited in conjunction with the short period mode - resulting in an increase in RMS response level rather than a decrease. At 100 knots the dynamic responses of the aircraft are more complicated because of the rotor shaft angle and the slower response of the aircraft at this velocity. A more detailed design of the DLC gust alleviation system and further analytical studies are required to ensure that other aircraft modal responses are not degraded. Thus, flap and spoiler operation may actually excite the wing bending mode, so that an associated modal suppression system as discussed in Section 6 might be needed to counteract this tendency. This should be the subject of further work.

Throughout the evaluation of this system, particular concern was paid to spoiler and flap deflection rates. At all gain variations the maximum spoiler rate was 120-degrees per second and the maximum flap rate was 80-degrees per second. Minimum design rates for these surfaces for roll control are 110-degrees per second and 50-degrees per second respectively, so that the rates required for gust alleviation represent only modest increases.

DLC gust alleviation using an angle of attack sensor has been shown to be of sufficient merit to warrant further investigation.

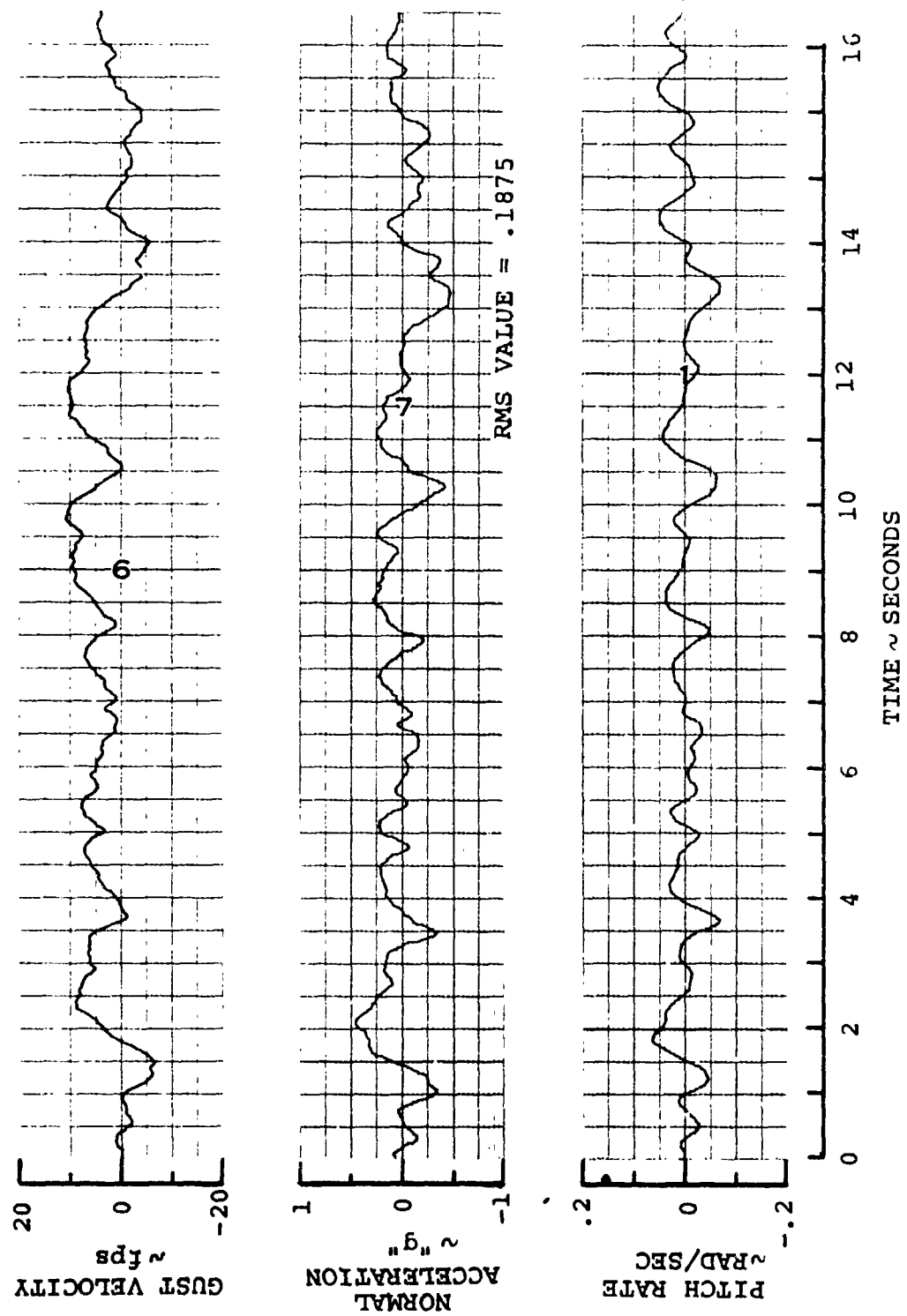


FIGURE 4.9. AIRCRAFT RESPONSE TO RANDOM TURBULENCE  
100 KNOTS NO FEEDBACK

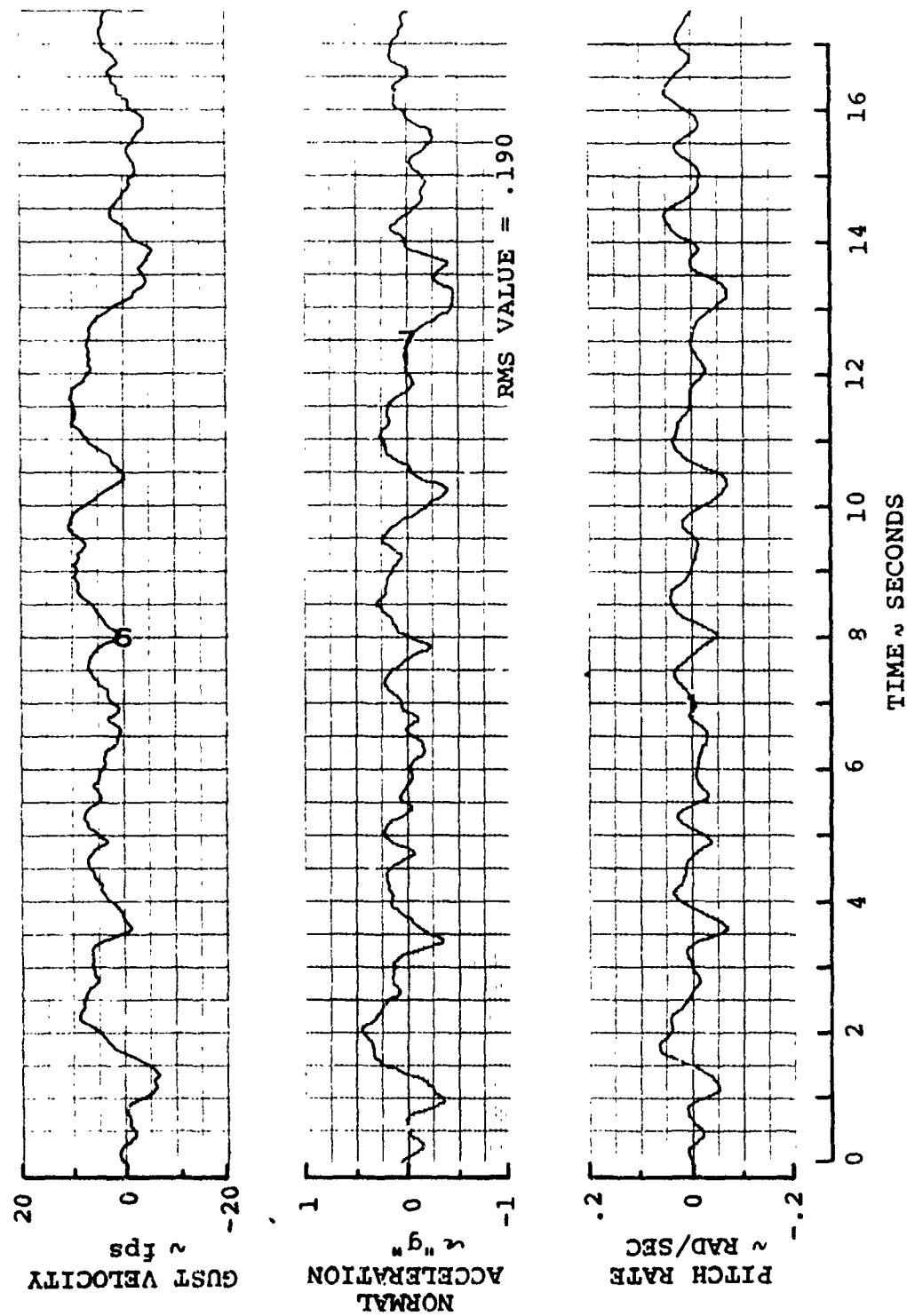


FIGURE 4.10. AIRCRAFT RESPONSE TO RANDOM TURBULENCE  
 100 KNOTS  $-\delta_F/\alpha = 1.24$   $-\delta_S/\alpha = 2.44$

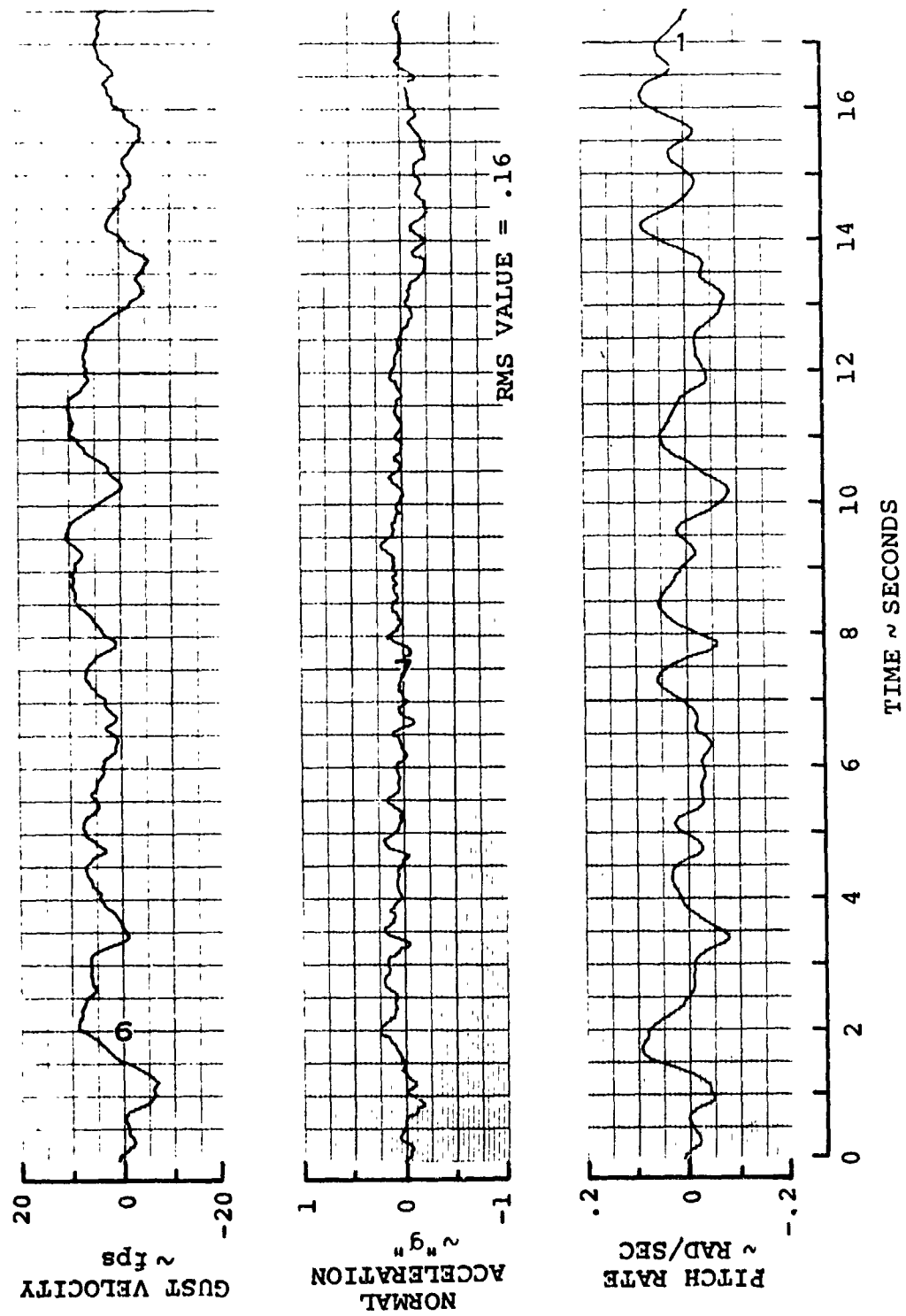


FIGURE 4.11. AIRCRAFT RESPONSE TO RANDOM TURBULENCE  
 100 KNOTS  $\delta_F/\alpha = 2.47$   $\delta_S/\alpha = 4.78$

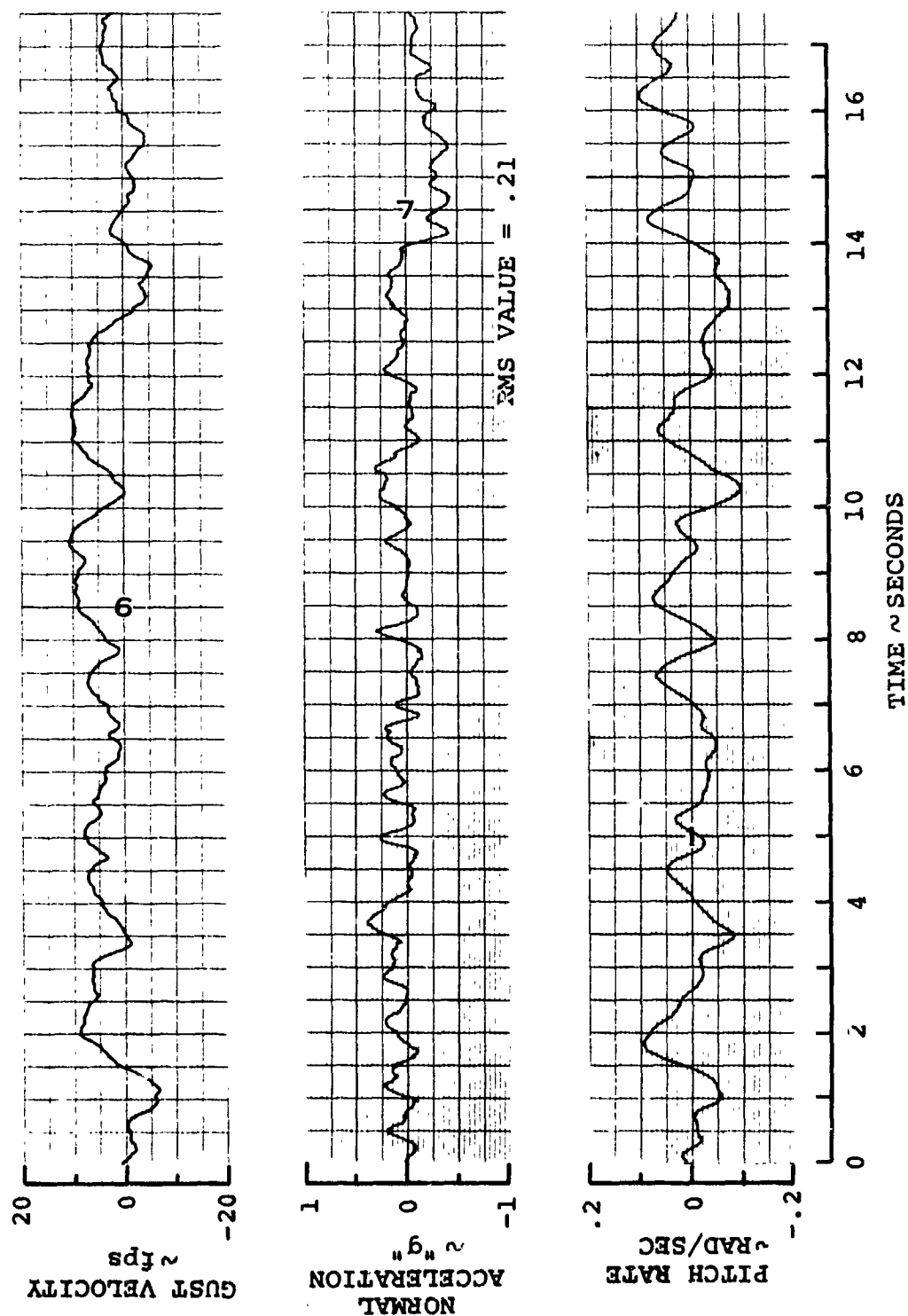


FIGURE 4.12. AIRCRAFT RESPONSE TO RANDOM TURBULENCE  
 100 KNOTS  $\delta_F/\alpha = 4.95$   $\delta_B/\alpha = 9.75$

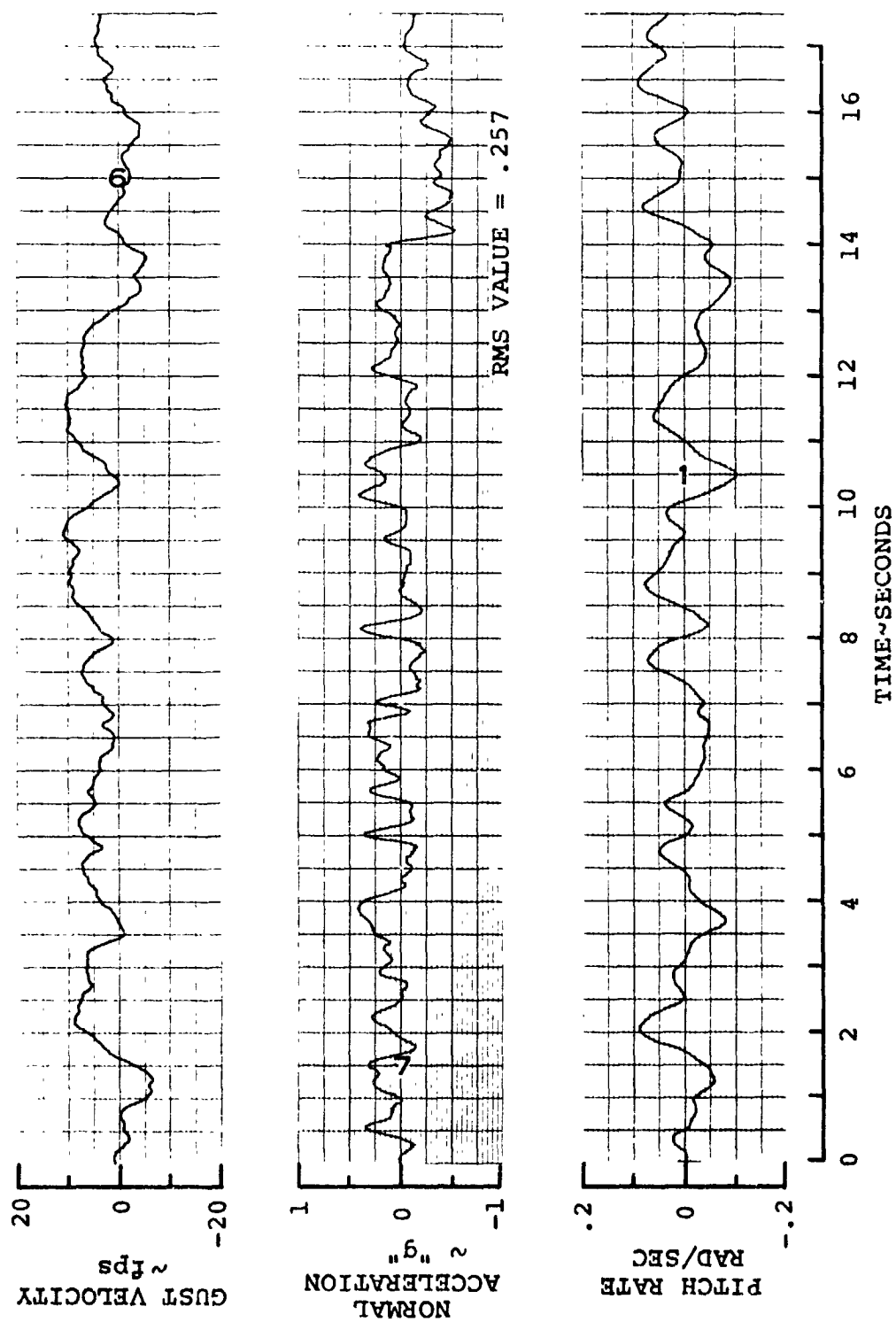


FIGURE 4.13. AIRCRAFT RESPONSE TO RANDOM TURBULENCE  
 100 KNOTS  $\delta_F/\alpha = 7.43$   $\delta_S/\alpha = 14.61$

At 250 knots a 45% alleviation of the normal acceleration response to random turbulence was shown and at 100 knots 15% alleviation was seen.

#### 4.4 CONCLUSIONS

This study has proven the feasibility of DLC gust alleviation in the cruise flight regime and has shown that such a system has promise in the transition, approach and landing regime. In the 250 knot cruise configuration a 45% reduction in the response to random turbulence was noted. At optimum gains the aircraft short period response was not adversely affected. In a 100 knot transition configuration with nacelle incidence of 25-degrees a 15% reduction in normal acceleration response was seen. Some adverse affect on aircraft flying qualities but it is believed that with further study and the use of elevator feedback these problems may be overcome.

Mechanization of the system on a full scale aircraft presents no major problems. Spoiler and flap actuators which can produce rates of 120-degrees per second and 80-degrees per second respectively will be required for the task. Some additional study is required to determine an optimum configuration and location for the angle of attack sensor.

## 5. MODAL SUPPRESSION AND AEROELASTIC STABILITY AUGMENTATION

### 5.1 BACKGROUND AND OBJECTIVES

The concept of using swashplate feedback for modal suppression and stability augmentation in tilt rotor aircraft is attractive for a number of reasons which are listed below.

- O Benefits:
1. Comfort. The mass distribution of a typical tilt rotor aircraft such as the M222 (i.e., large mass concentration at the wing tips) is such that a responsive or lightly damped wing mode may result in an uncomfortable level of cabin vibration at the wing frequency. Cabin accelerations will be of the order of 50% of wing tip accelerations in the fundamental modes at frequencies near the body frequencies of the crew.
  2. Safety. While the aircraft will be built, under current design philosophy, with adequate margins of stability, the presence of a correctly designed modal suppression system would increase margins to the point where loss of wing stiffness due to partial structural failures would not be catastrophic.
  3. Advanced Configurations. Development of successful and reliable modal suppression and aeroelastic stability augmentation systems would open up the path to more advanced design concepts. Currently wing design is constrained by stiffness requirements associated with the stability of wing/pylon/rotor dynamic interactions and this has associated penalties in weight and performance. Reduction of stiffness constraints would permit the use of a thinner wing with no weight penalty.



- O Cost: Since SAS swashplate actuators are already present for the SAS and blade load alleviation system, no major new hardware items are involved; only sensors, which are envisioned as accelerometer and signal conditioning avionics, are required additionally.
- O Effectiveness: Rotor forces applied at the wing tip are highly effective in forcing or damping the modes.

In the immediate future, however, the value of modal suppression systems will lie in improvement in ride qualities in turbulent air, and potential improvement in the fatigue life of the wing and blades. Studies for the SST, and operational equipment for the B-52 have shown that feedback (modal suppression devices) improve the structural gust response and the aircraft ride qualities. Studies for modal suppression of the SST may be reviewed in Boeing Document D3-7600-10 and D3-7600-11.

Longer term applications would address battle damage survival where the loss of wing stiffness due to partial destruction would be compensated for by feedback.

In a new generation of aircraft reliance on feedback might be proposed as the primary source of aeroelastic stability.

## 5.2 RATIONAL OF CURRENT STUDY

The study presented below concentrates on the use of swashplate feedback to augment the damping in the wing vertical bending mode characteristics of the Boeing Vertol M222 Tilt Rotor Aircraft are used for the investigation. This

mode was selected, (rather than the whirl flutter mode for example), because its response has a more direct association with near term applications. Also test data in relation to wing bending mode suppression was to be acquired and the analytical conclusions could be checked against test data.

For a tilt rotor aircraft with a soft in-plane rotor, the wing vertical bending mode has been shown to be important from several aspects:

- O gust response
- O aircraft weight
- O air resonance.

If response in the wing vertical bending mode could be altered or suppressed, improvement in the above categories could be made. Swashplate feedback has been proposed as a means for vertical bending modal suppression. Investigation of this feedback has proceeded in three distinct segments:

- O initial investigations with a simplified system concept
- O introduction of actual hardware characteristics and refined approach to optimization
- O proposed use of a "wobbling" swashplate to obtain maximum effectiveness in suppressing the vertical bending mode.

Initial investigations were primarily exploratory in nature to determine what could be done to improve wing vertical bending response. As shown in Figure 5.1, a perfect feedback loop was envisioned. Filtering, actuator dynamics or sensor dynamics were not been considered. Results were encouraging

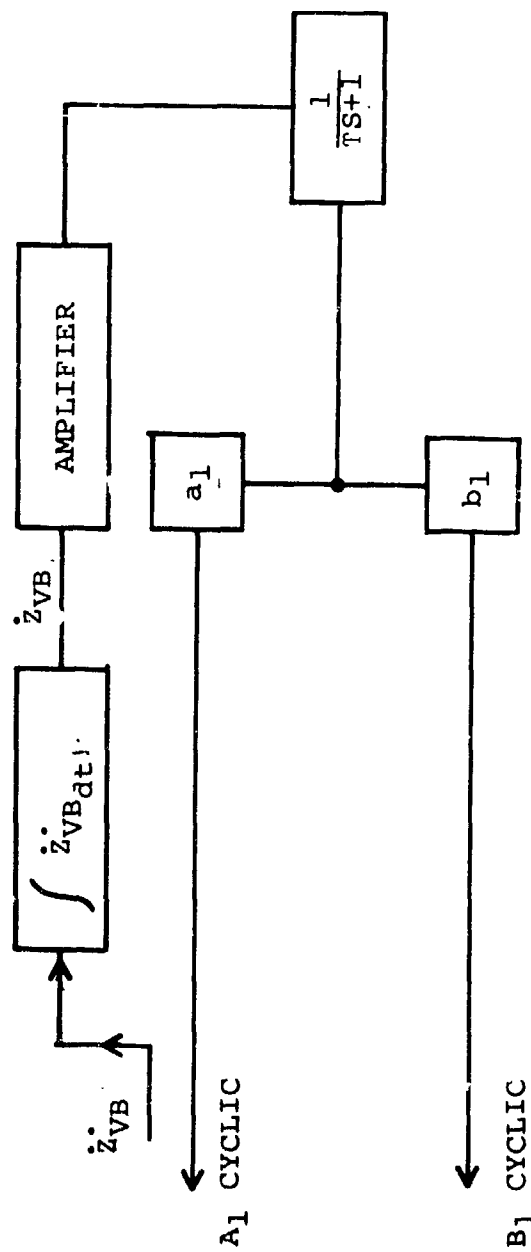


FIGURE 5.1. SCHEMATIC OF SIMPLIFIED AEROELASTIC STABILITY AUGMENTATION SYSTEM.

and lead the research to the second phase of study.

The second phase of the study used the system of Figure 5.2. This was felt to be fully representative of an actual hardware system. Representation of filters, actuators, sensors and phase shifters were made using actual frequency response calibrations.  $A_1$  and  $B_1$  feedback signals were assumed to be in phase. In this system a more refined approach was taken with special consideration to possible trouble spots. If trouble was located, "fixes" were proposed and evaluated. Four different styles of feedback were evaluated:

- O acceleration feedback with bandpass filter and phase shifter
- O acceleration feedback without filter and phase shifter
- O rate feedback
- O position feedback

The above systems were synthesized and analyzed using the combined tools of Bode analysis and root locus plots. The systems were evaluated with all the wing fundamental structural modes present, but not rigid body freedoms, since it was planned to measure the analytical predictions against data generated testing a cantilevered wing/rotor system in the NASA-Ames 40x80-foot wind tunnel.

In a third phase of the study a system using a "wobbling" swashplate and a possible research program is discussed. It is believed that



this style system would make most useful effect of available cyclic pitch. With this viewpoint the advantages and disadvantages of the system are specified.

### 5.3 MATHEMATICAL MODEL FOR MODAL SUPPRESSION STUDIES

A windmilling rotor semi-span cantilevered model was used as the basis for each of the studies. Included in the model were blade flap and lag degrees of freedom represented by coning and cyclic modes of the rotor. Fully coupled wing vertical bending, chord and torsion modes were included. Figures 5.3 and 5.4 define the frequency and damping spectrum for the model with the rotor spinning at 386 RPM. There were slight differences in the math model for the initial studies which reflected the differences between the 1/9 scale model and the 26-foot rotor full scale test.

There is a high degree of confidence that the mathematical model is representative of the physical system desired.

Figures 5.5 through 5.10 show the correlation of the mathematical model analysis with actual test results. Note the high degree of correlation for the wing vertical bending mode. Attempts to excite the other modes were not very successful, as anticipated, which was one of the reasons for selecting the vertical bending mode for study.

The mathematical model of the feedback system provides six degrees of freedom which have the flexibility to represent nearly anything the analyst would desire in the way of transfer functions. A detailed description of the feedback capability

CRUISE CONFIGURATION  
386 RPM  
26-FT ROTOR  
SEMI-SPAN MODEL

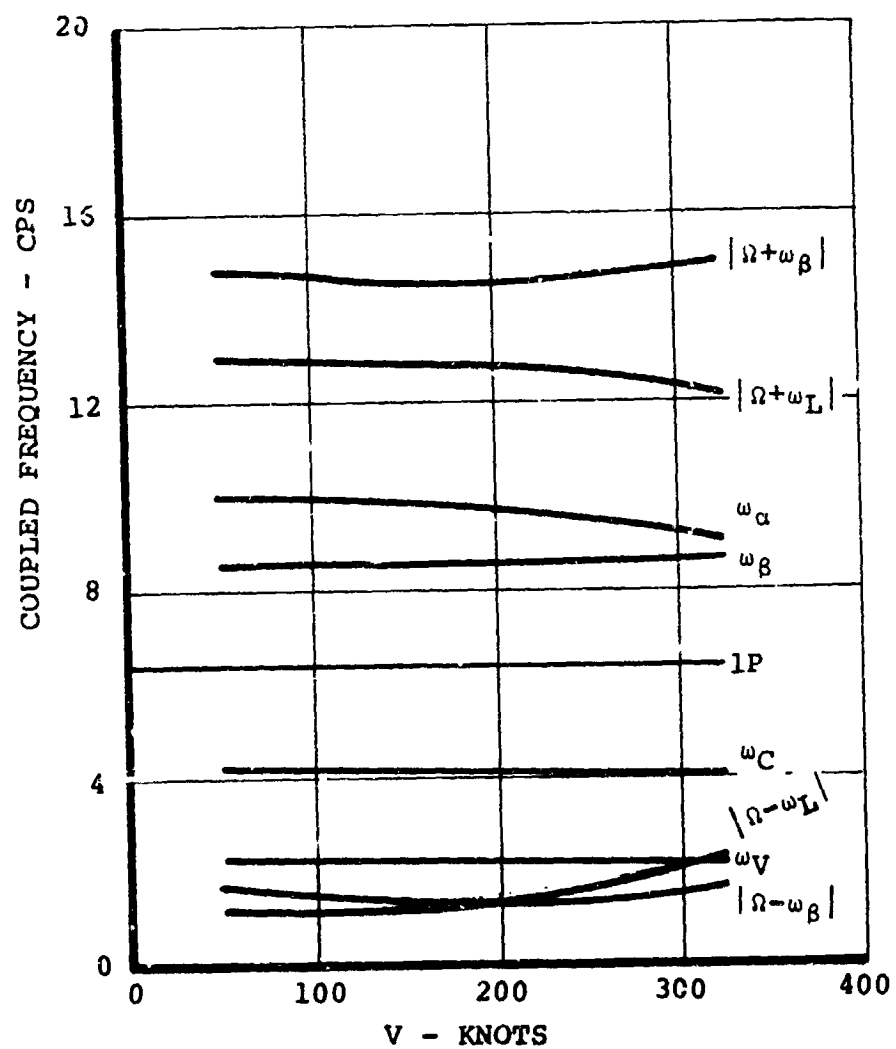


FIGURE 5.3. EFFECT OF VELOCITY ON TILT ROTOR MODAL FREQUENCY

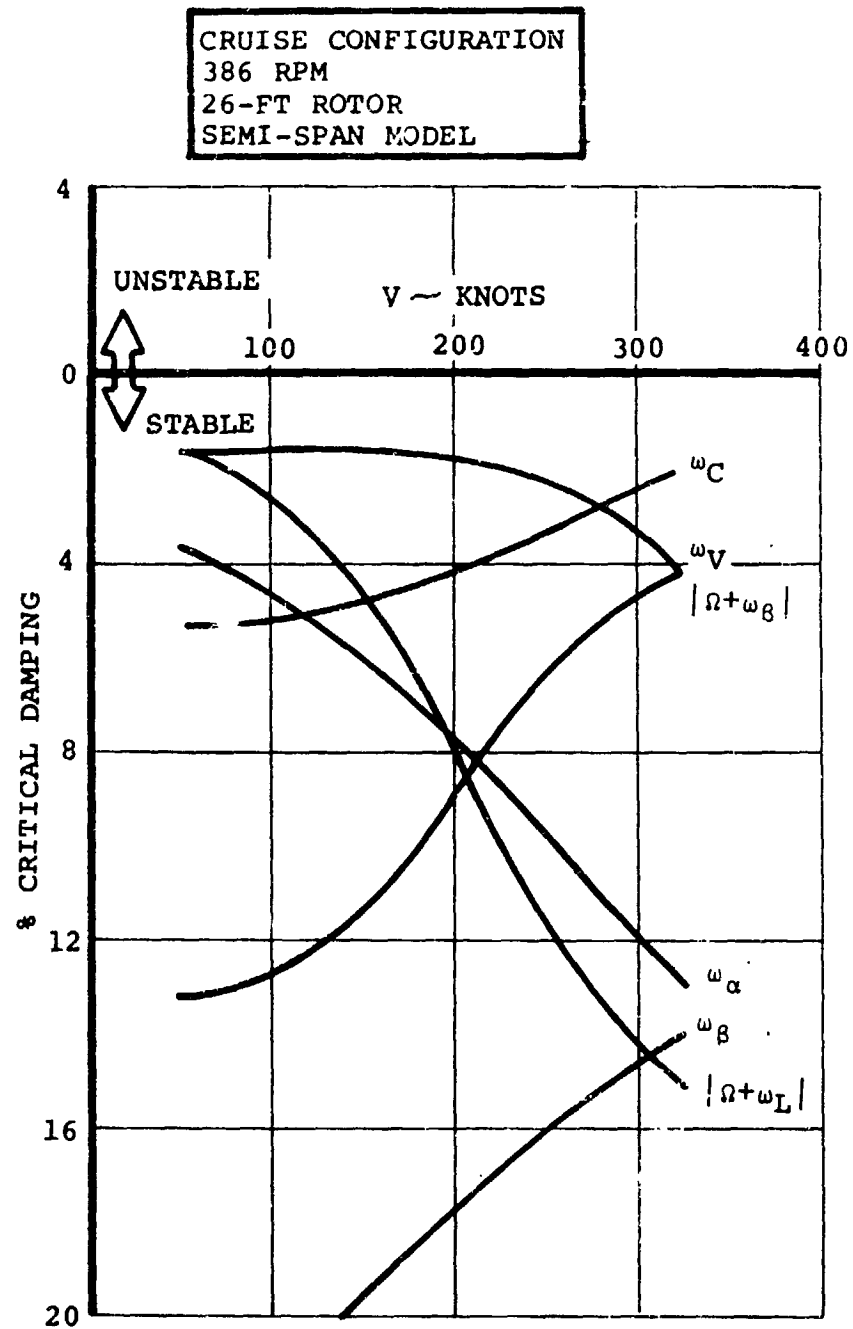


FIGURE 5.4. EFFECT OF VELOCITY ON TILT ROTOR MODAL DAMPING.



NASA AMES 40 X 80 WIND TUNNEL  
TEST 410

100 KNOTS

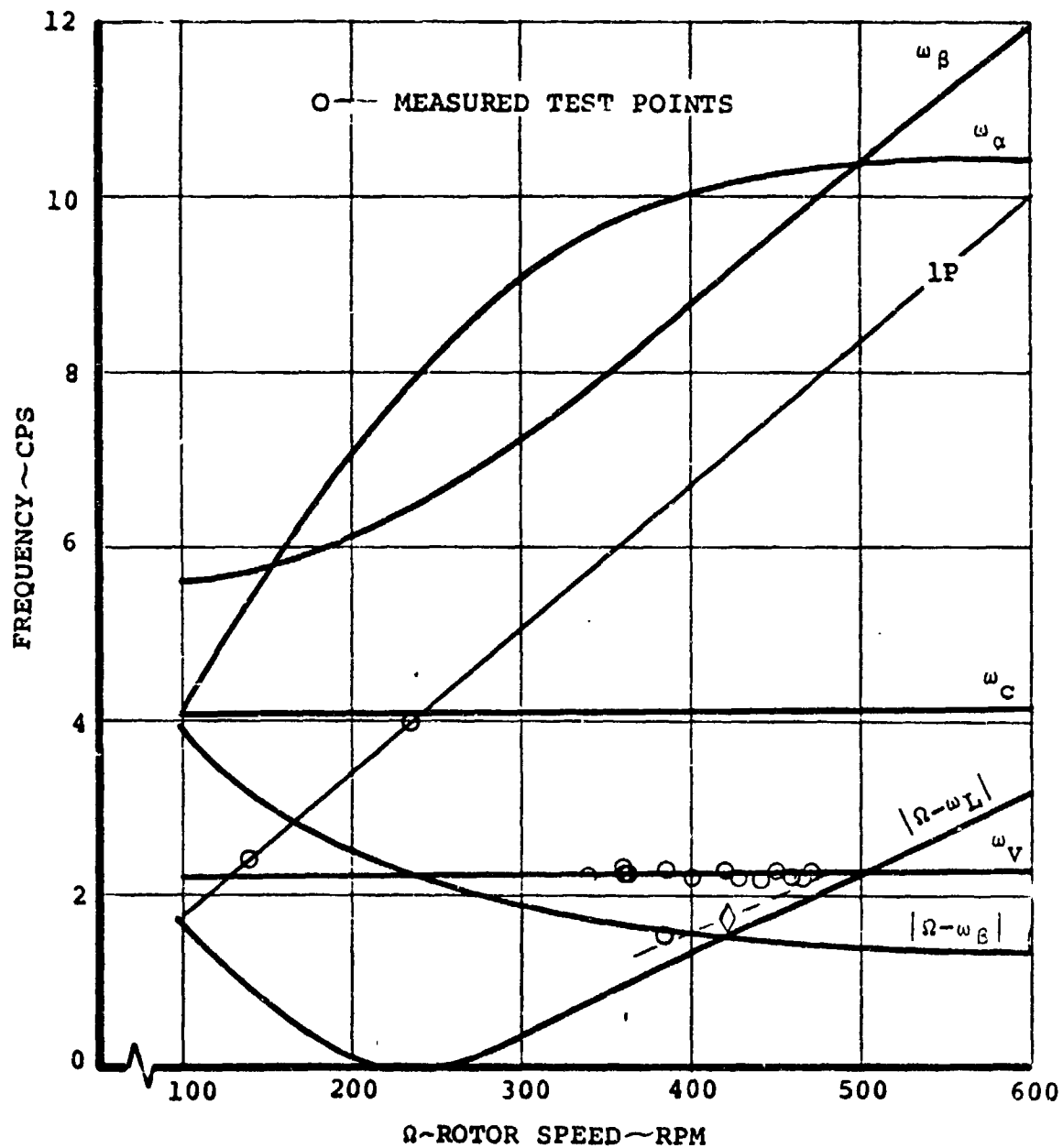


FIGURE 5.5. 26 FT. ROTOR - FULL STIFFNESS WING -  
MODAL FREQUENCIES AT  $V = 100$  KNOTS.

MODEL-222 FULL SCALE ROTOR TEST IN NASA  
AMES 40 X 80 FOOT TUNNEL: FULL STIFF WING

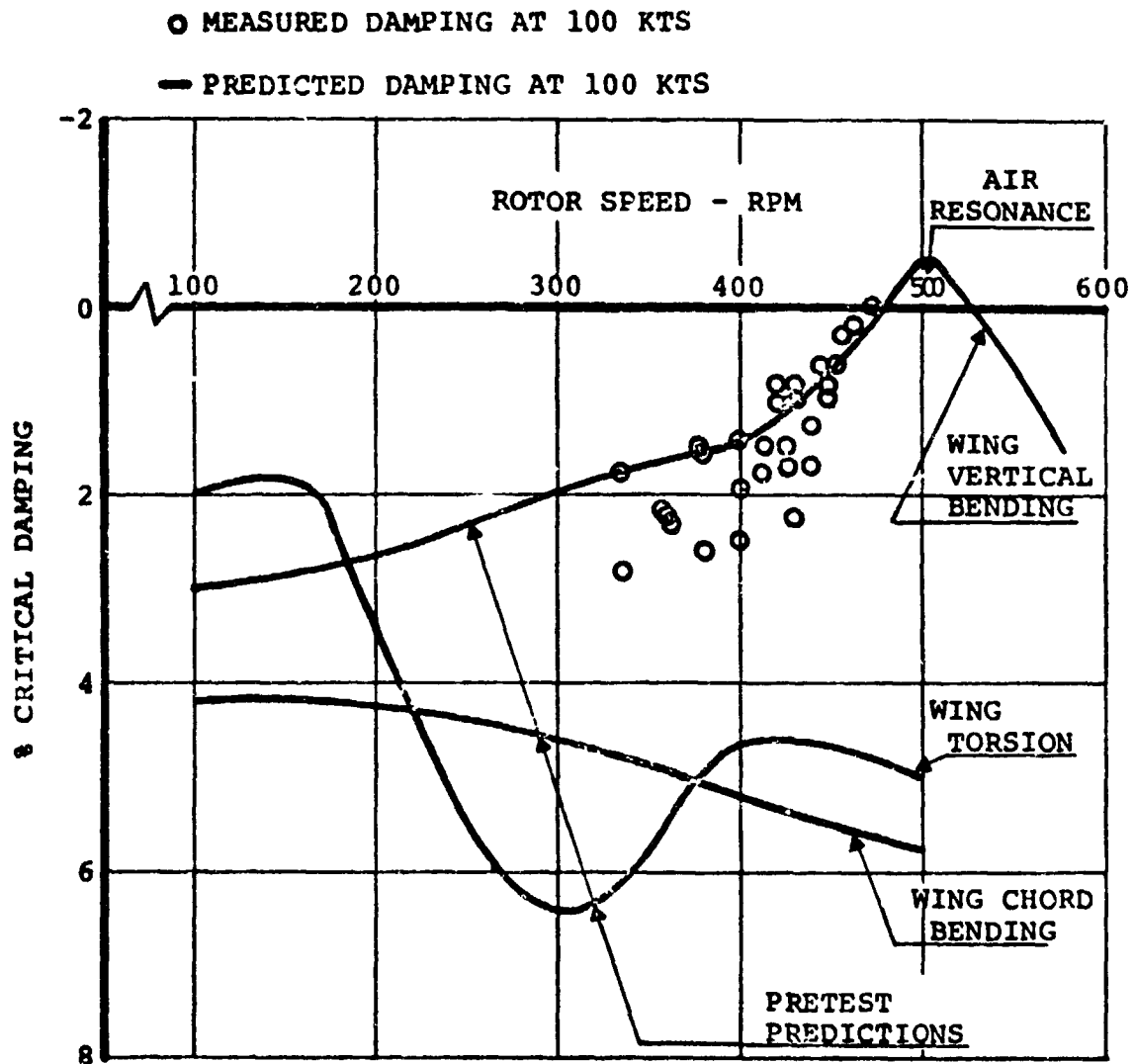


FIGURE 5.6. CORRELATION OF PREDICTED AIR RESONANCE MODE DAMPING AND MEASURED DAMPING OF THIS MODE DURING TEST.  $V = 100$  KNOTS.

NASA AMES 40 X 80 WIND TUNNEL  
TEST 410

150 KNOTS

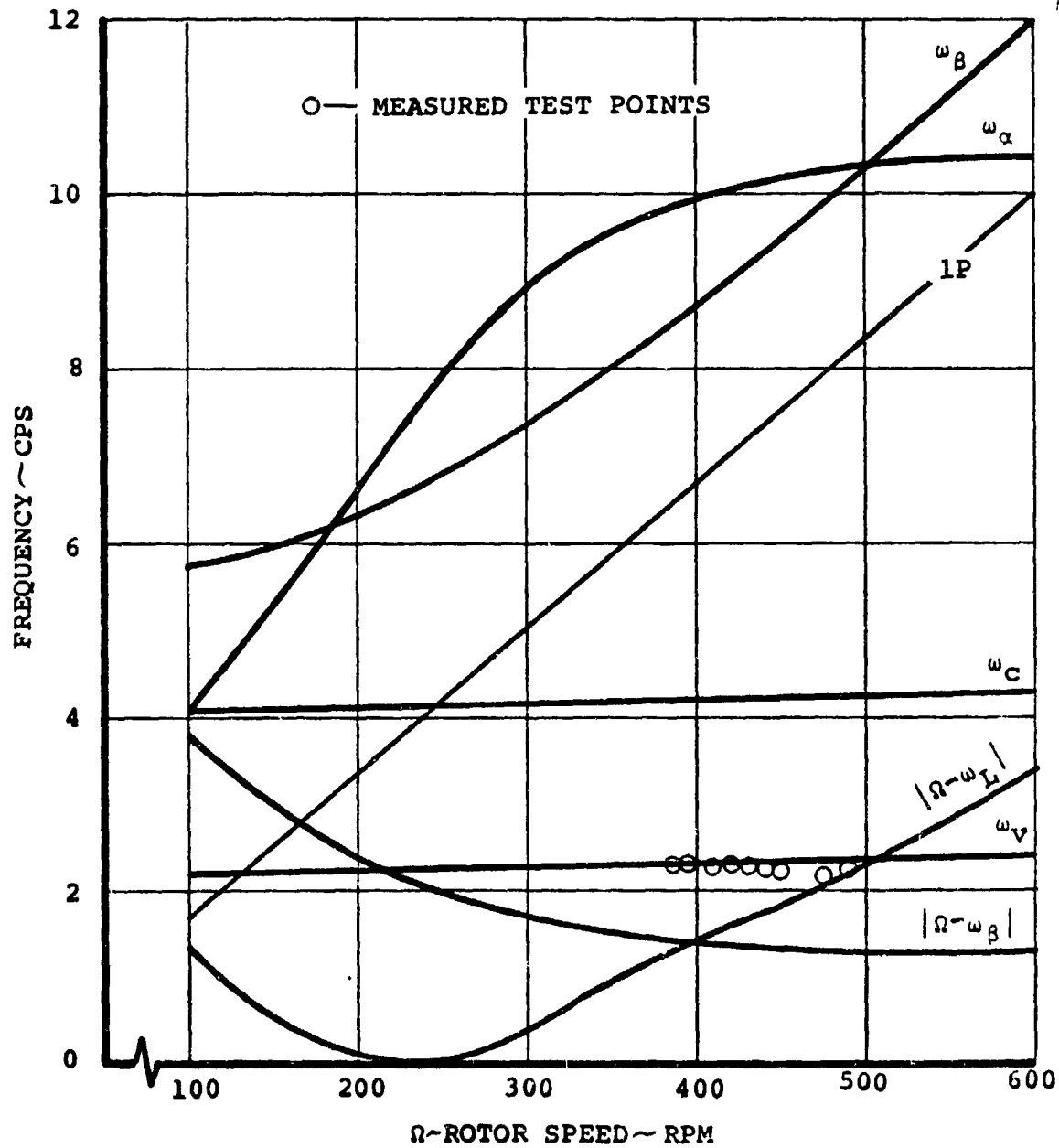


FIGURE 5.7. 26 FT. ROTOR - FULL STIFFNESS WING -  
MODAL FREQUENCIES AT V = 150 KNOTS.

MODEL-222 FULL SCALE ROTOR TEST IN NASA  
AMES 40x80 FOOT TUNNEL: FULL STIFF WING

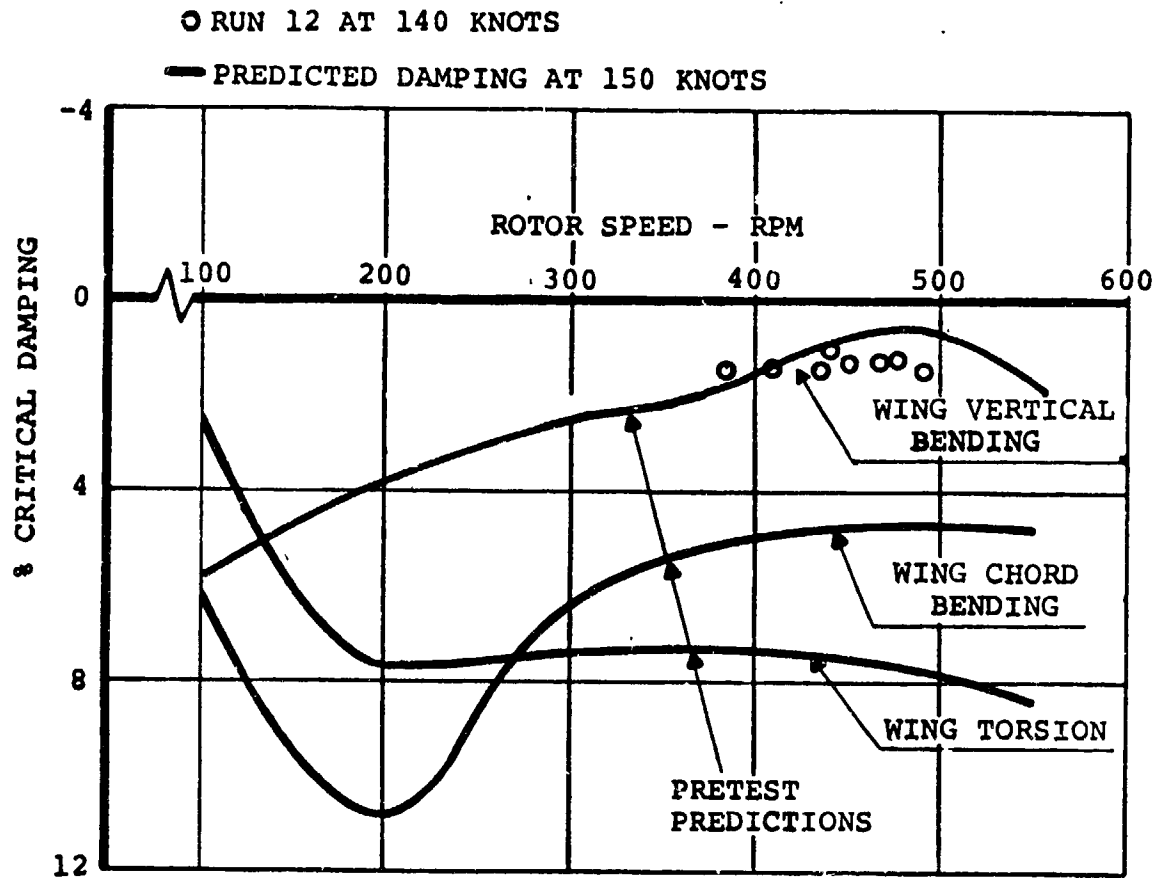


FIGURE 5.8. CORRELATION OF PREDICTED AIR RESONANCE MODE DAMPING AND MEASURED DAMPING OF THIS MODE DURING TEST.  $V = 140$  KNOTS AND  $150$  KNOTS.

NASA AMES 40 X 80 WIND TUNNEL  
TEST 410

200 KNOTS

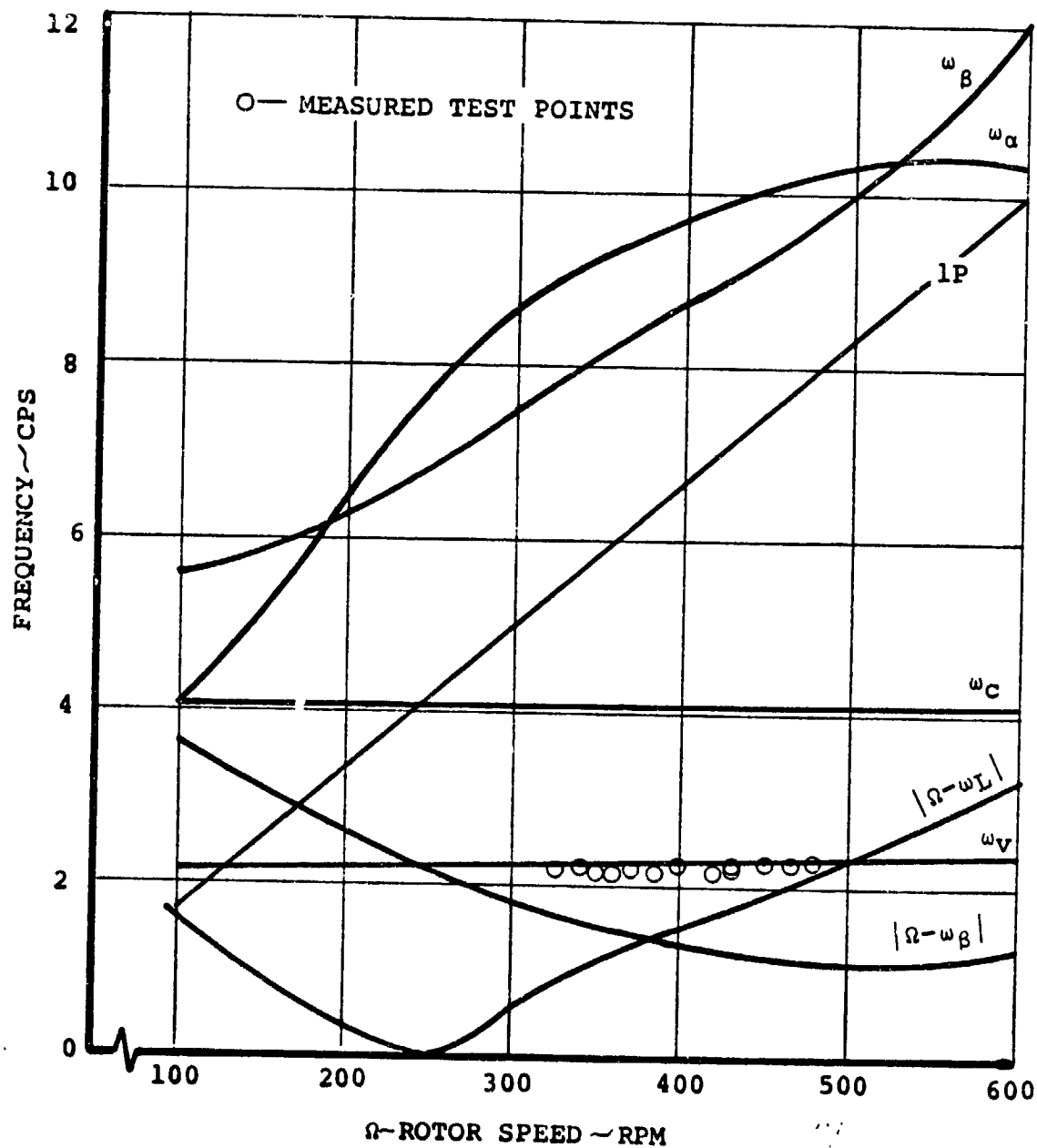


FIGURE 5.9. 26 FT. ROTOR - FULL STIFFNESS WING -  
MODAL FREQUENCIES AT  $V = 200$  KNOTS.

MODEL-222 FULL SCALE ROTOR TEST IN NASA  
AMES 40x80 FOOT TUNNEL: FULL STIFF WING

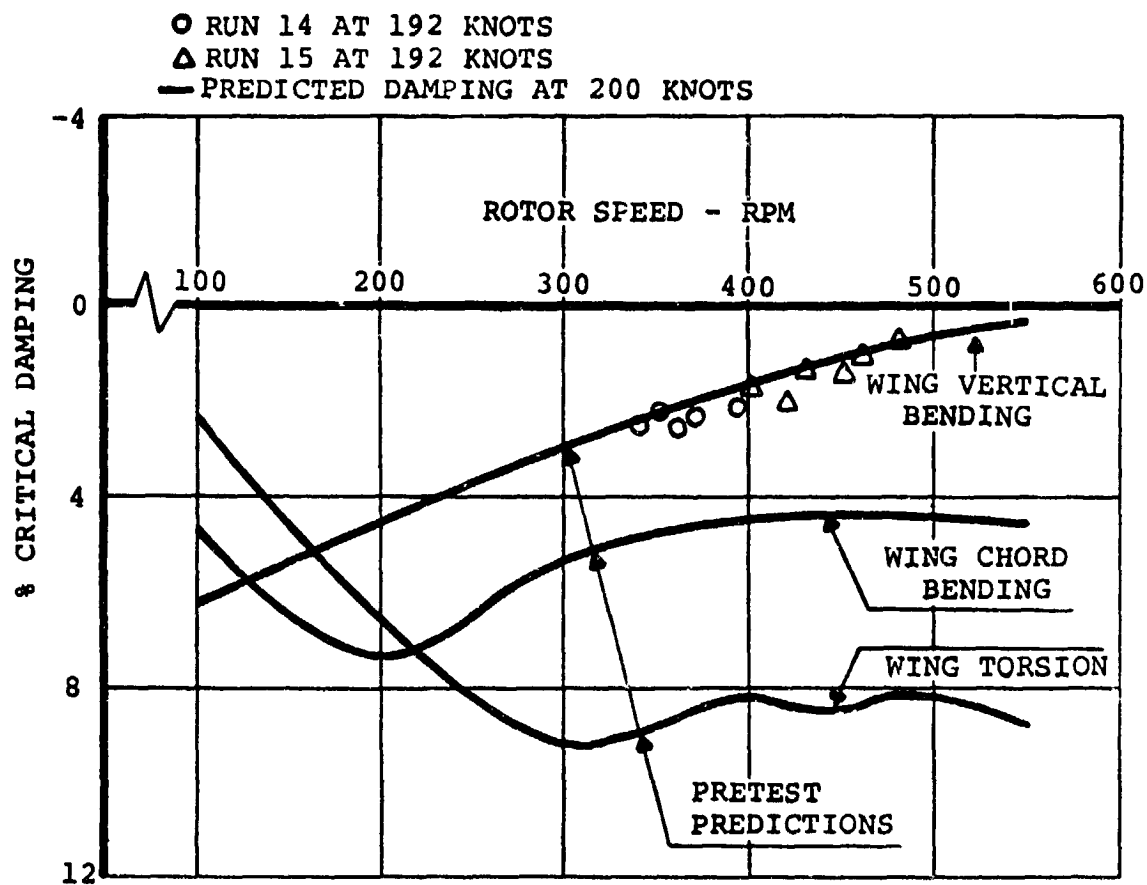


FIGURE 5.10. CORRELATION OF PREDICTED AIR RESONANCE MODE DAMPING AND MEASURED DAMPING OF THIS MODE DURING TEST.  $V = 192$  KNOTS AND 200 KNOTS.

is contained in Boeing Document D210-10435-1, Flying Qualities and Aeroelastic Stability Analysis - C-48 User's Document.

A high degree of confidence also exists in the validity of the feedback modelling as will be illustrated by correlation in Paragraph 5.5.1.

#### 5.4 INITIAL EXPLORATIVE STUDIES

During the initial work to augment the damping in the wing vertical bending mode, four parameters were felt to be important:

- O feedback signal
- O cyclic azimuth position
- O feedback loop gain
- O feedback loop time constant.

To better understand the general problem each one of these parameters was studied in an elementary manner. The effect on the wing vertical bending mode was noted along with the effect on the wing torsion mode. The block diagram of the feedback system is given in Figure 5.1.

Since the purpose of this system was to increase damping in the wing vertical bending mode, the obvious choice for a feedback signal was wing tip velocity. Experience with SAS systems and general background knowledge of feedback control systems indicated that damping may be increased in a mode by feeding back the rate of change of the modal deflection - wing tip vertical velocity. At the time it was felt to be unnecessary to investigate other feedback signals. (More

about this in Section 5.5).

Cyclic azimuth position was the second parameter to be considered. It was felt that there was an optimum orientation of the hub forces and moments which would yield the most damping in the wing vertical bending mode without destabilizing other modes. Orientation of the hub forces and moments was obtained by inputting various amounts of  $A_1$  and  $B_1$  cyclic pitch (Figure 5.11) per unit feedback signal. Thus, by varying the ratio of  $A_1$  to  $B_1$  the force and moment orientation was moved around the azimuth. It was subsequently realized that this procedure also controlled the net phase of the feedback signal. To investigate azimuth variation effect, carpet plots with  $A_1$  and  $B_1$  gain variations were made.

Feedback loop gain was expected to control the level of damping attained. The gain was therefore increased until either the damping no longer increased or some other mode was driven unstable. As discussed below, the torsion mode was driven unstable and thus defined the maximum level of gain.

Feedback loop time constants ( $\tau$ ) of 0., .05 and .1 seconds were investigated to yield some insight into the effect of actual feedback system hardware (actuators, sensors, etc.) on the dynamics of the overall system. These values of  $\tau$  were chosen because experience indicated that control system time constants varied between .05 and .1 seconds.





Several different areas of the flight envelope were explored to evaluate the effect of different velocity and RPM combinations. Major emphasis was placed on the cruise flight conditions (386 RPM; 100, 150 and 200 knots) and some study has been made of corner conditions of the flight envelope. Discussion of the individual conditions follows.

#### 5.4.1 Discussion of Results of Initial Study

Perfect feedback ( $\tau = 0.0$  seconds) was evaluated for the flight conditions of 386 RPM, 100 knots and 386 RPM, 200 knots. Variations in  $A_1$  and  $B_1$  gain were made and the only modes significantly effected were the wing vertical bending and wing torsion modes (Figures 5.12, 5.13, 5.14 and 5.15). Gains are expressed in degrees of cyclic per foot per second. Significant increases in wing vertical bending damping are seen in both conditions. At maximum gain at 100 knots 32% critical damping is achieved; at 200 knots 80% critical damping is achieved. However, at these gains the wing torsion mode is driven unstable in both cases. Figures 5.16 and 5.17 define the gain envelope for stability of both the wing vertical bending and torsion modes. Using this criteria the designer may pick values of gain which give him a satisfactory solution. For instance at 200 knot values of  $a = .4$  and  $b = -.4$  yield a decrease in torsion damping from 1.8% to .9% but a dramatic increase in vertical bending damping from about 1% to 20%. If a further increase in damping is required in the vertical bending mode and it is desired to have no

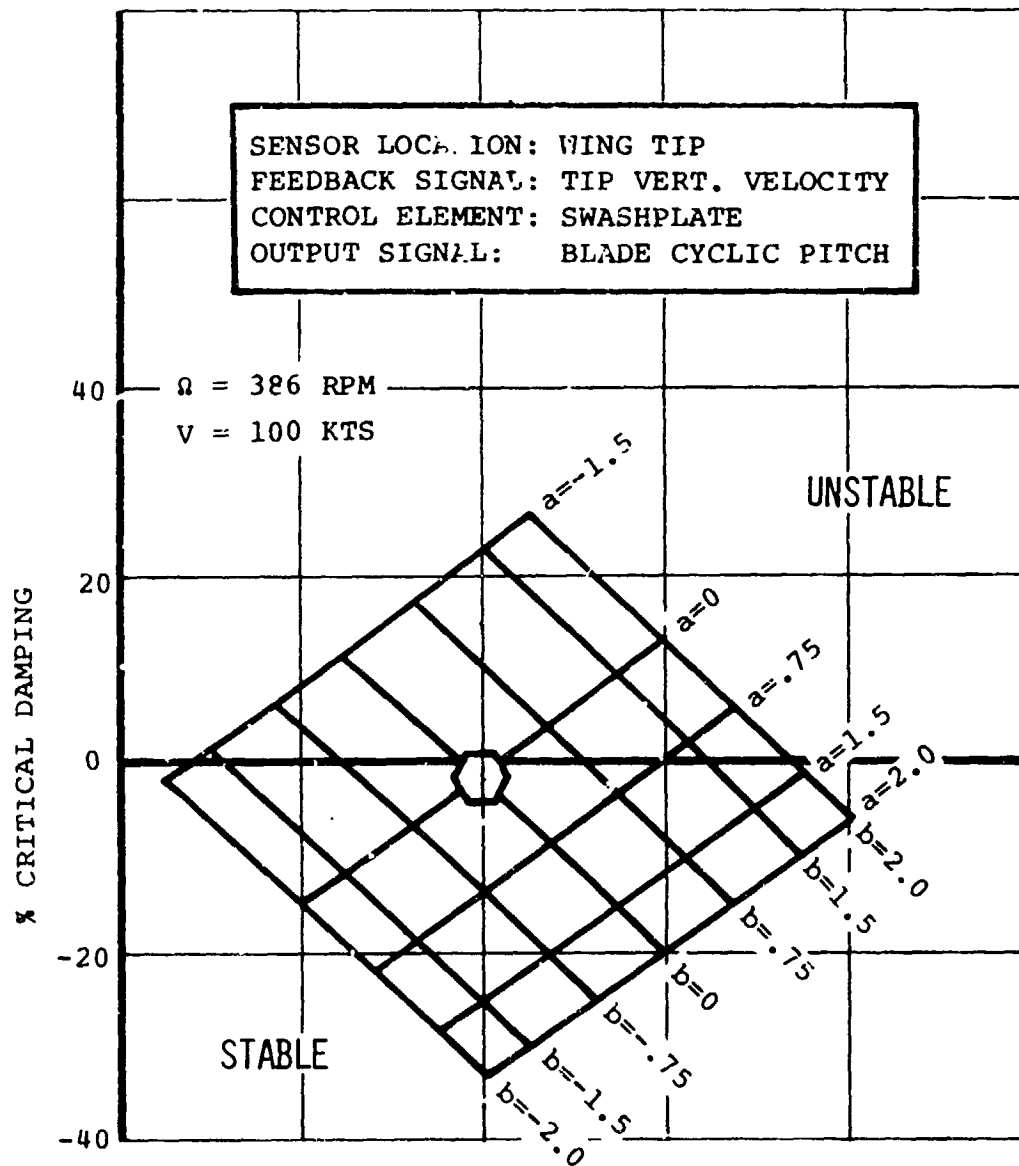


FIGURE 5.12 FEEDBACK EFFECT ON MODAL DAMPING OF  
 WING VERTICAL BENDING MODE

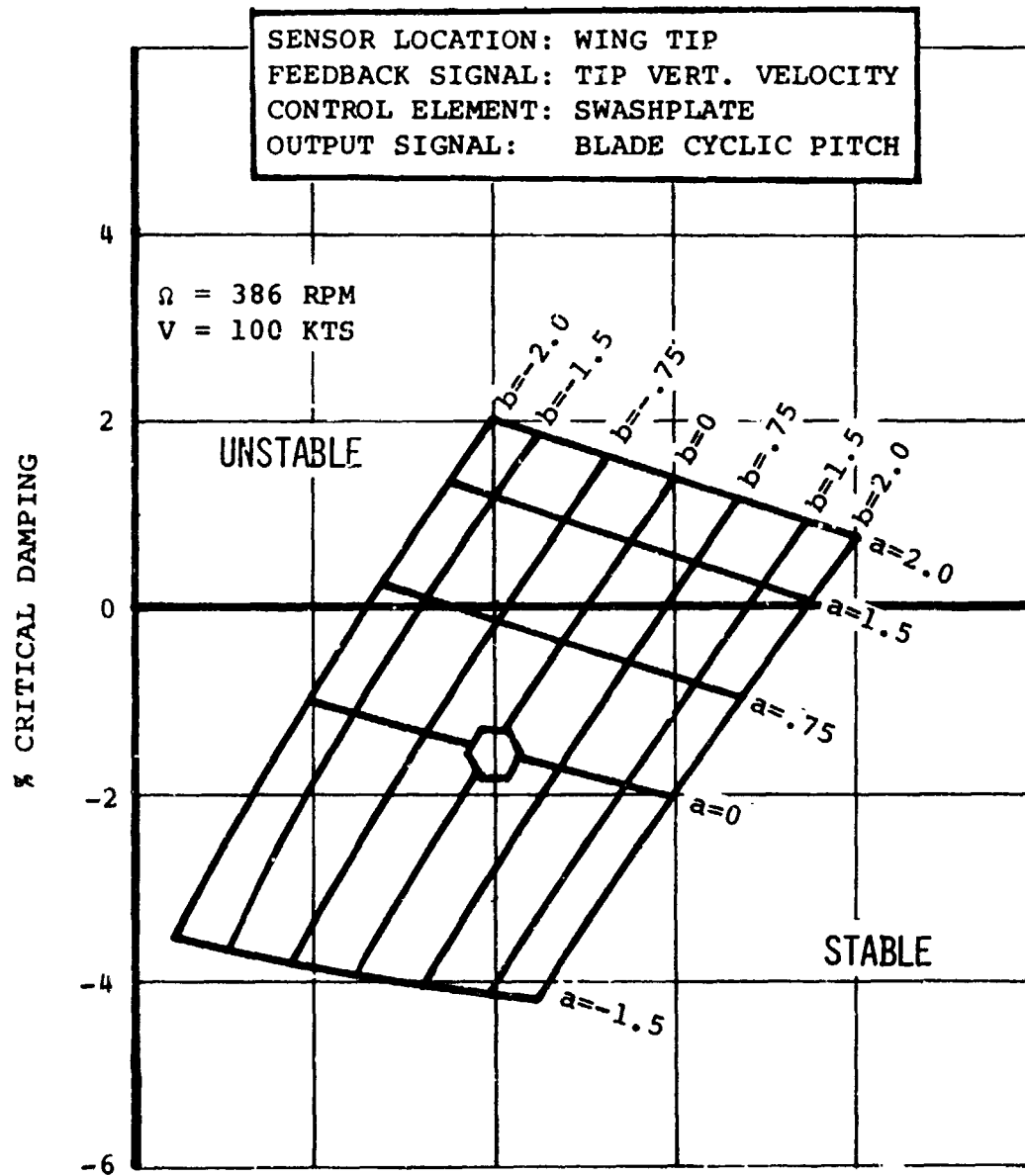


FIGURE 5.13 FEEDBACK EFFECT ON MODAL DAMPING OF  
 WING TORSION MODE

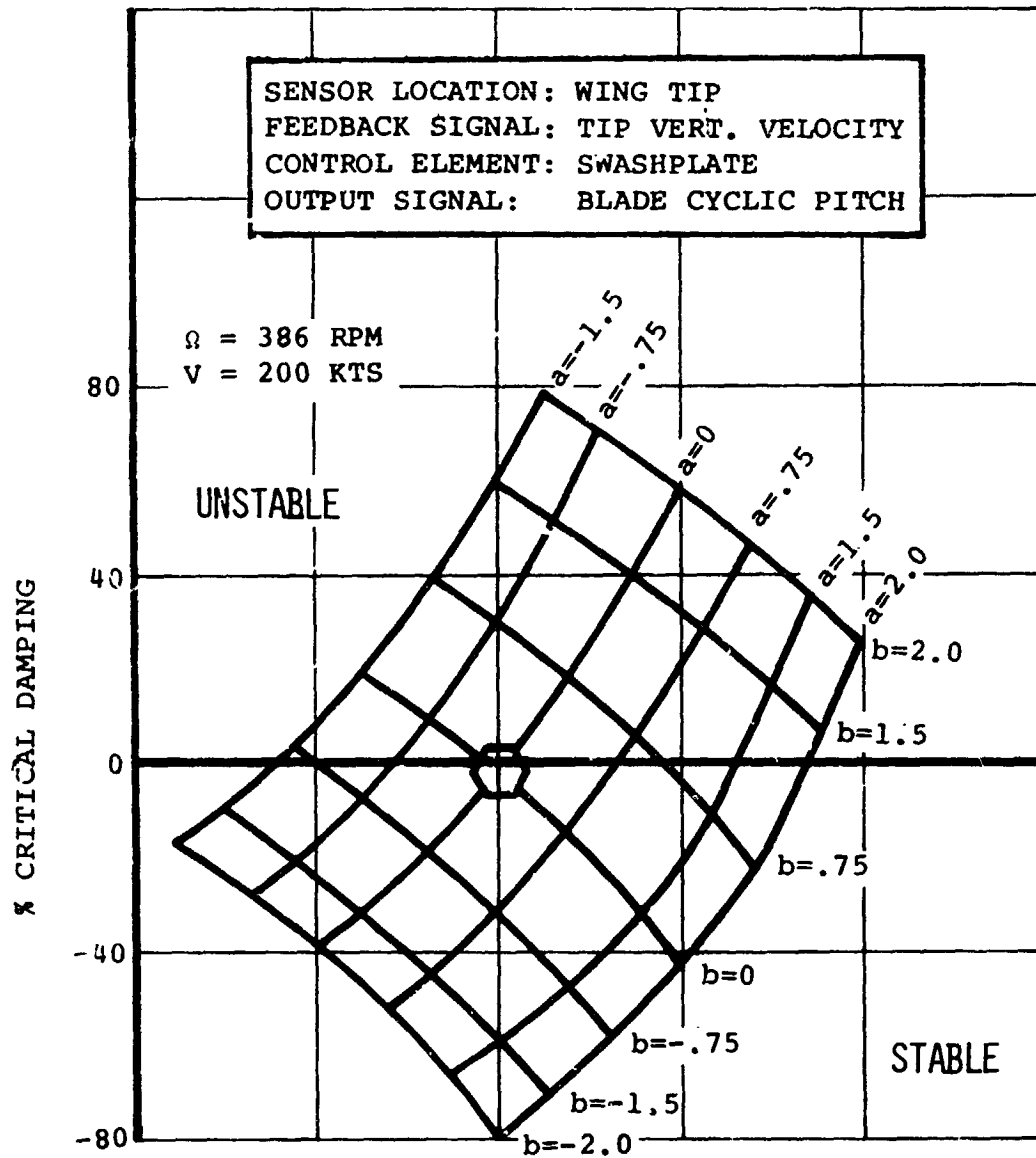


FIGURE 5.14 FEEDBACK EFFECT ON MODAL DAMPING OF  
 WING VERTICAL BENDING MODE

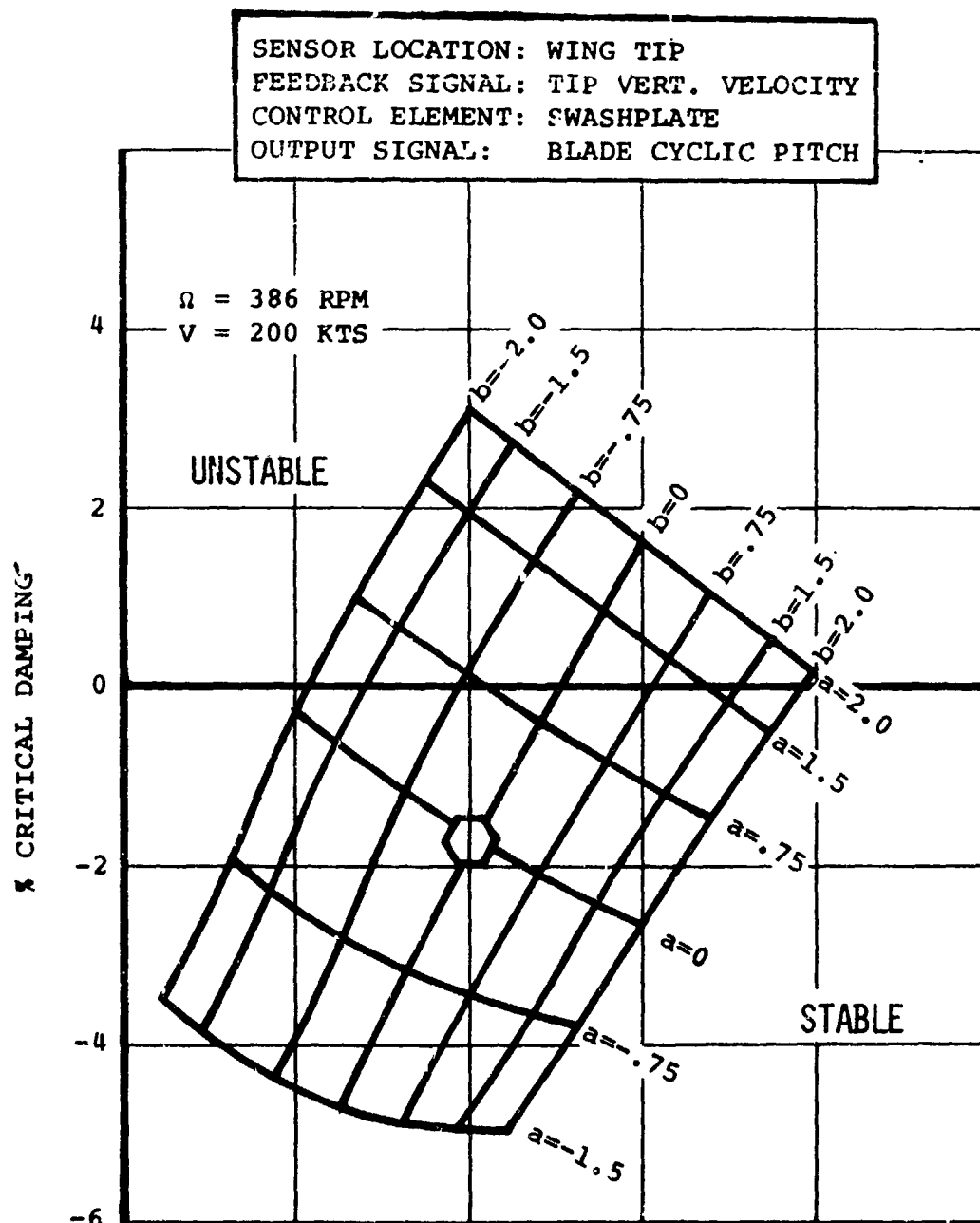


FIGURE 5.15 FEEDBACK EFFECT ON MODAL DAMPING OF  
 WING TORSION MODE

SENSOR LOCATION: WING TIP  
 FEEDBACK SIGNAL: TIP VERT. VELOCITY  
 CONTROL ELEMENT: SWASHPLATE  
 OUTPUT SIGNAL: BLADE CYCLIC PITCH

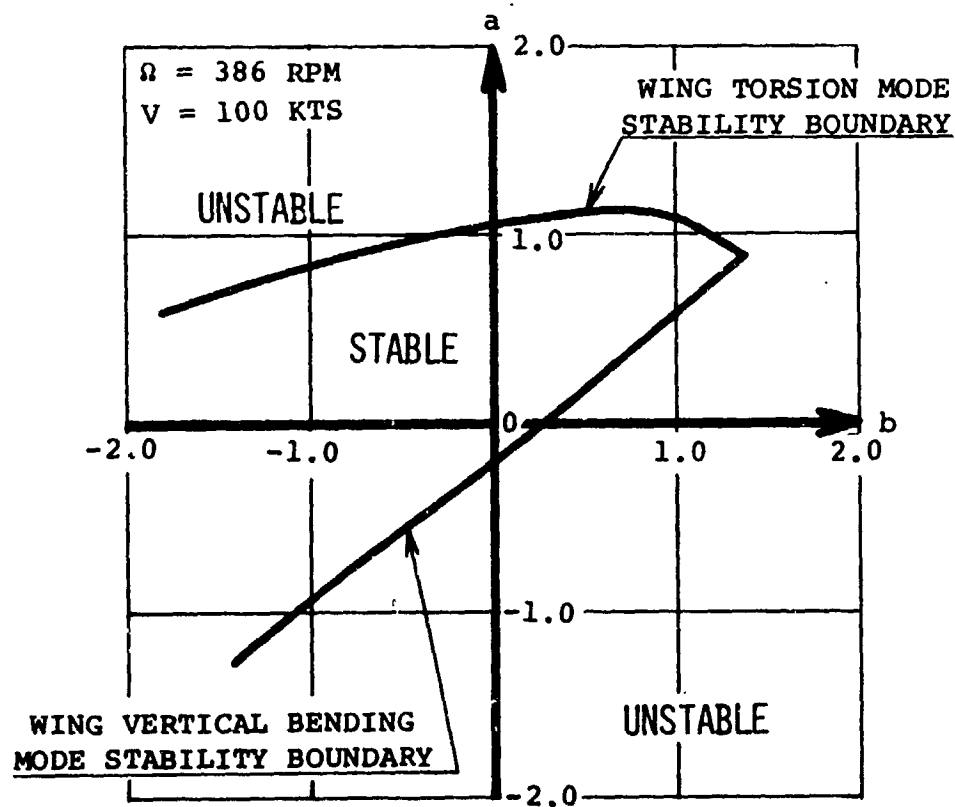


FIGURE 5.16 FEEDBACK EFFECT ON MODAL DAMPING OF  
 STABILITY FOR FEEDBACK COMBINATIONS

SENSOR LOCATION: WING TIP  
 FEEDBACK SIGNAL: TIP VERT. VELOCITY  
 CONTROL ELEMENT: SWASHPLATE  
 OUTPUT SIGNAL: BLADE CYCLIC PITCH

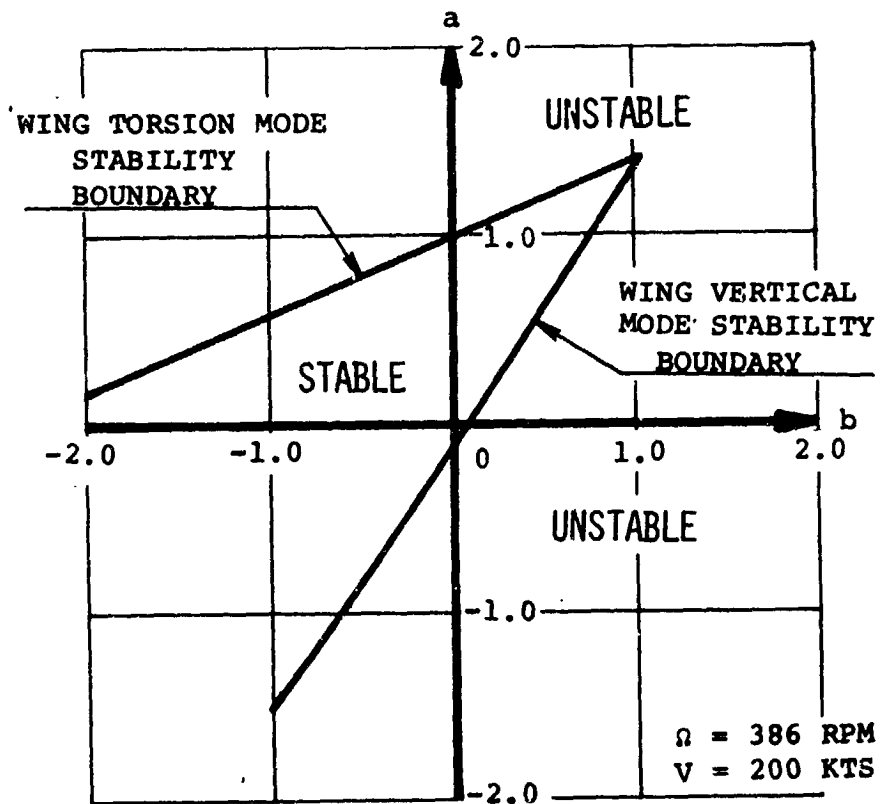


FIGURE 5.17 FEEDBACK EFFECT ON MODAL DAMPING OF STABILITY FOR FEEDBACK COMBINATIONS



effect on the wing torsion mode a more complex analysis must be performed as discussed in Section 5.5.

#### 5.4.2 Ideal System With First Order Time Lag

Control system time constants were evaluated at the flight condition of 386 RPM and 150 knots. Figures 5.18, 5.19, 5.20 and 5.21 show the effect of gain at time constants of .05 and 0.1 seconds on the wing vertical bending and torsion modes. Stability root migration with gain is much the same as with zero time constant; however, as seen in Figures 5.22 and 5.23 the effect of time constant is to reduce effectiveness. The vertical bending mode is more affected by  $\tau$  than the torsion mode. Damping is decreased 11% in the vertical bending mode while there is only a .5% change in the wing torsion mode. Since there is such a large variation in the modal response of interest it behooves the analyst to carefully evaluate the dynamic characteristics of each piece of system hardware and include this information in his math model.

#### 5.4.3 Variations With RPM

Evaluation of the feedback system at 500 RPM and 100 knots was made (Figures 5.24, 5.25, and 5.26). Feedback with zero time constants was investigated for a range of  $A_1$  and  $B_1$  gain.

The results are similar to those at 386 RPM and indicate no drastic changes in system operations with RPM.

An extreme 200 RPM condition was investigated at velocities of 100 and 200 knots (Figures 5.27 through 5.32). The same trends are evident here as at 386 RPM and 500 RPM. The gain

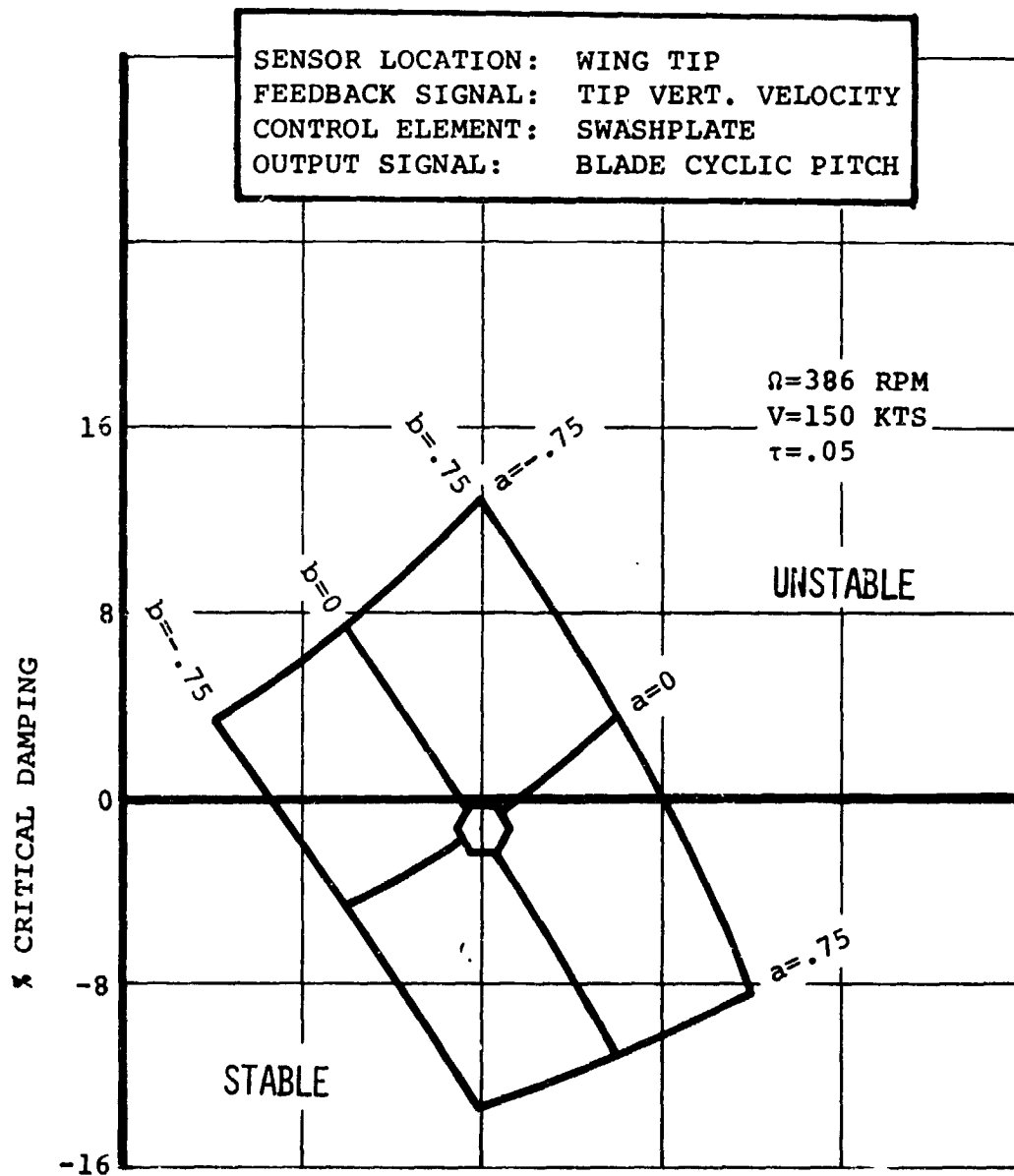


FIGURE 5.18. FEEDBACK EFFECT ON MODAL DAMPING OF WING VERTICAL BENDING MODE WITH TIME CONSTANT

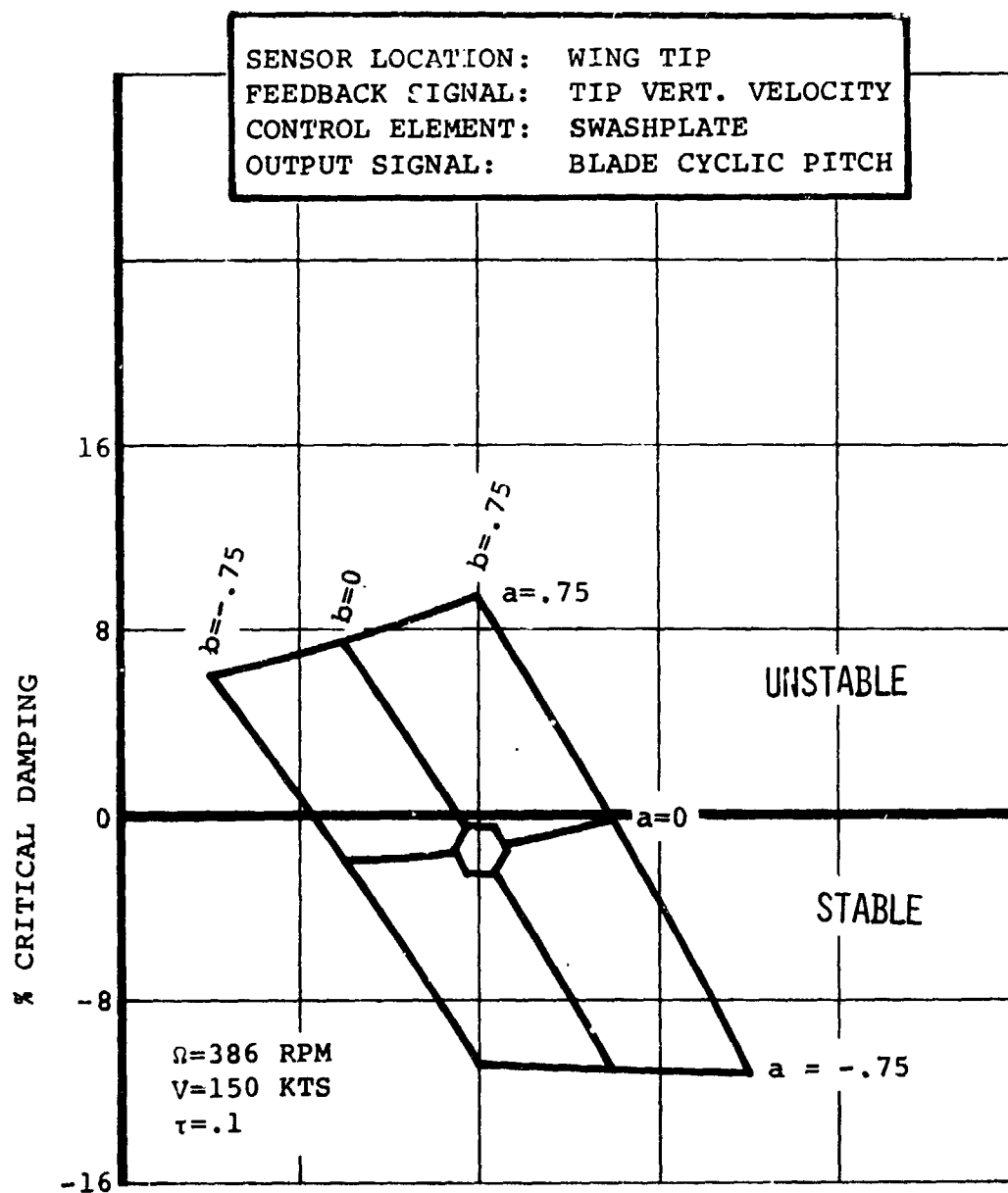


FIGURE 5.19. FEEDBACK EFFECT ON MODAL DAMPING OF WING VERTICAL BENDING MODE WITH TIME CONSTANT

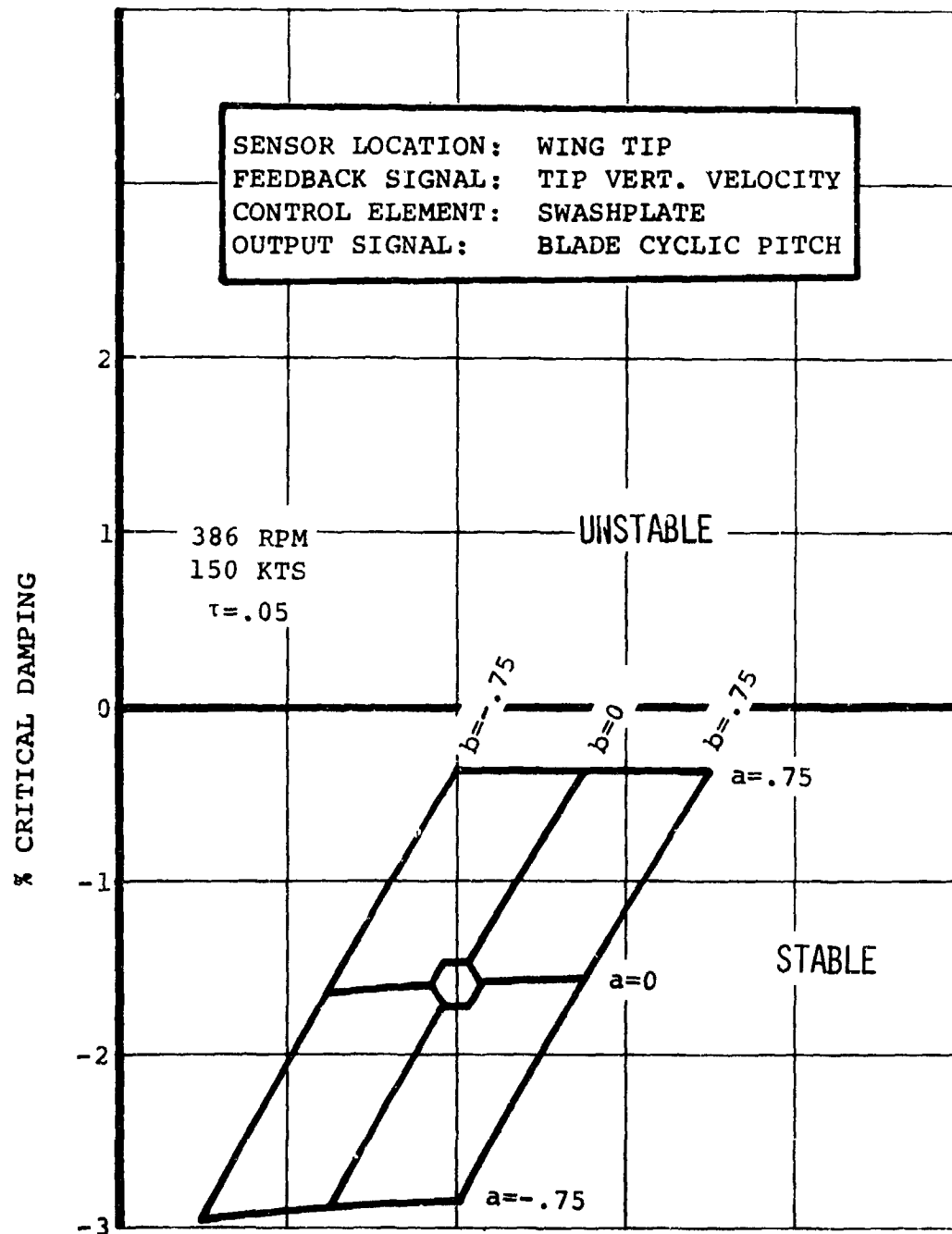


FIGURE 5.20. FEEDBACK EFFECT ON MODAL DAMPING OF WING TORSION MODE WITH TIME CONSTANT

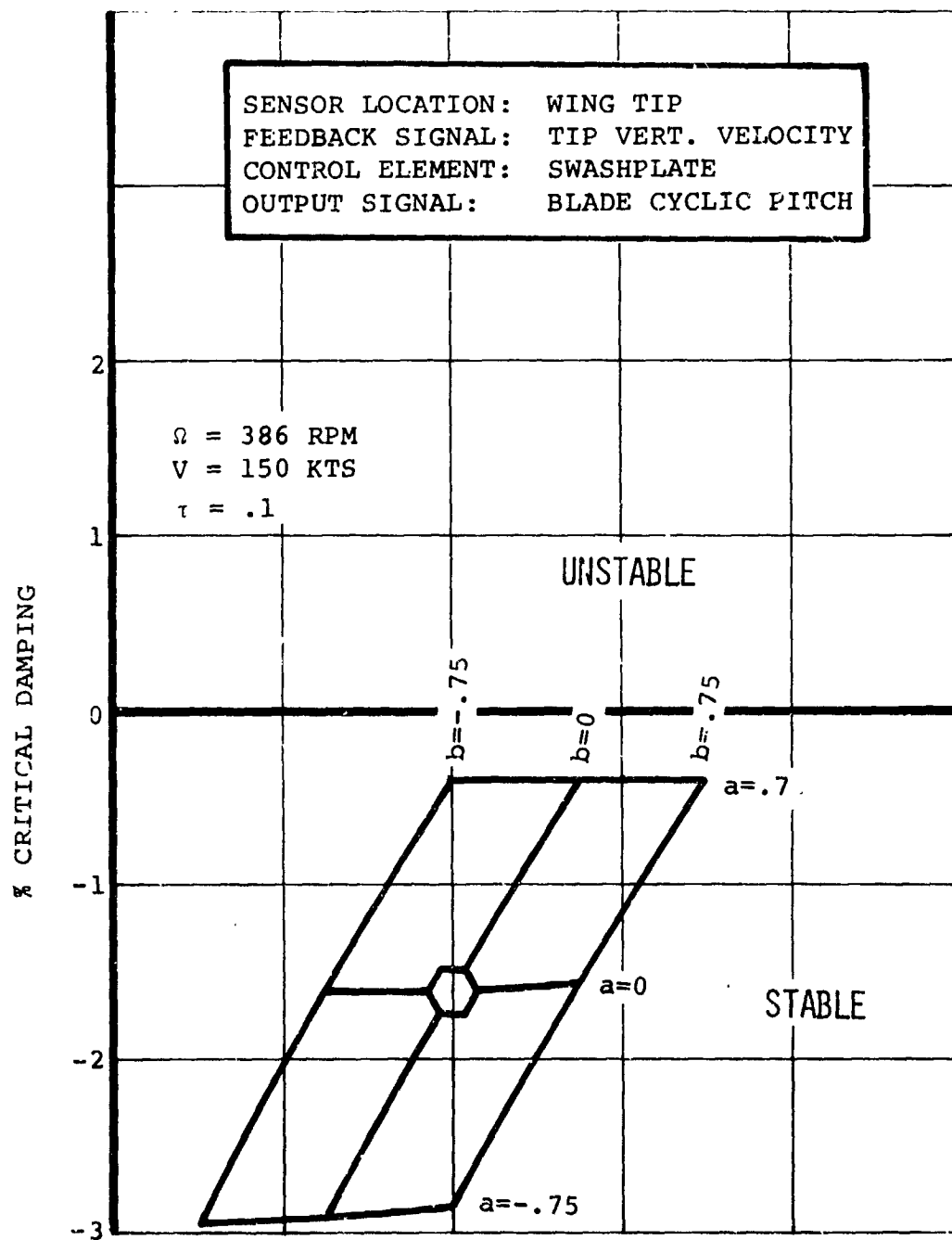


FIGURE 5.21. FEEDBACK EFFECT ON MODAL DAMPING OF WING TORSION MODE WITH TIME CONSTANT

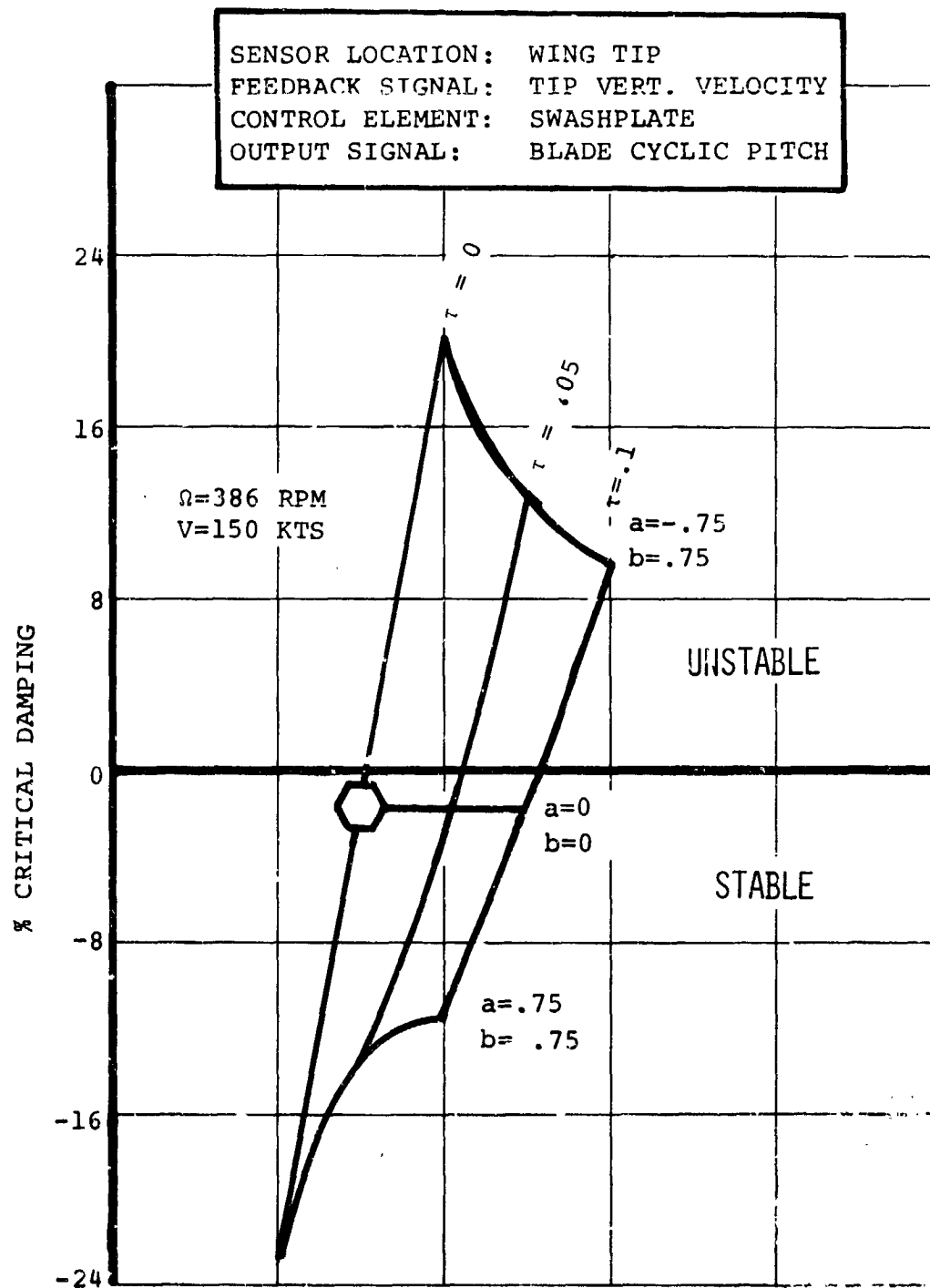


FIGURE 5.22. FEEDBACK EFFECT ON MODAL DAMPING OF WING VERTICAL BENDING MODE WITH TIME CONSTANT

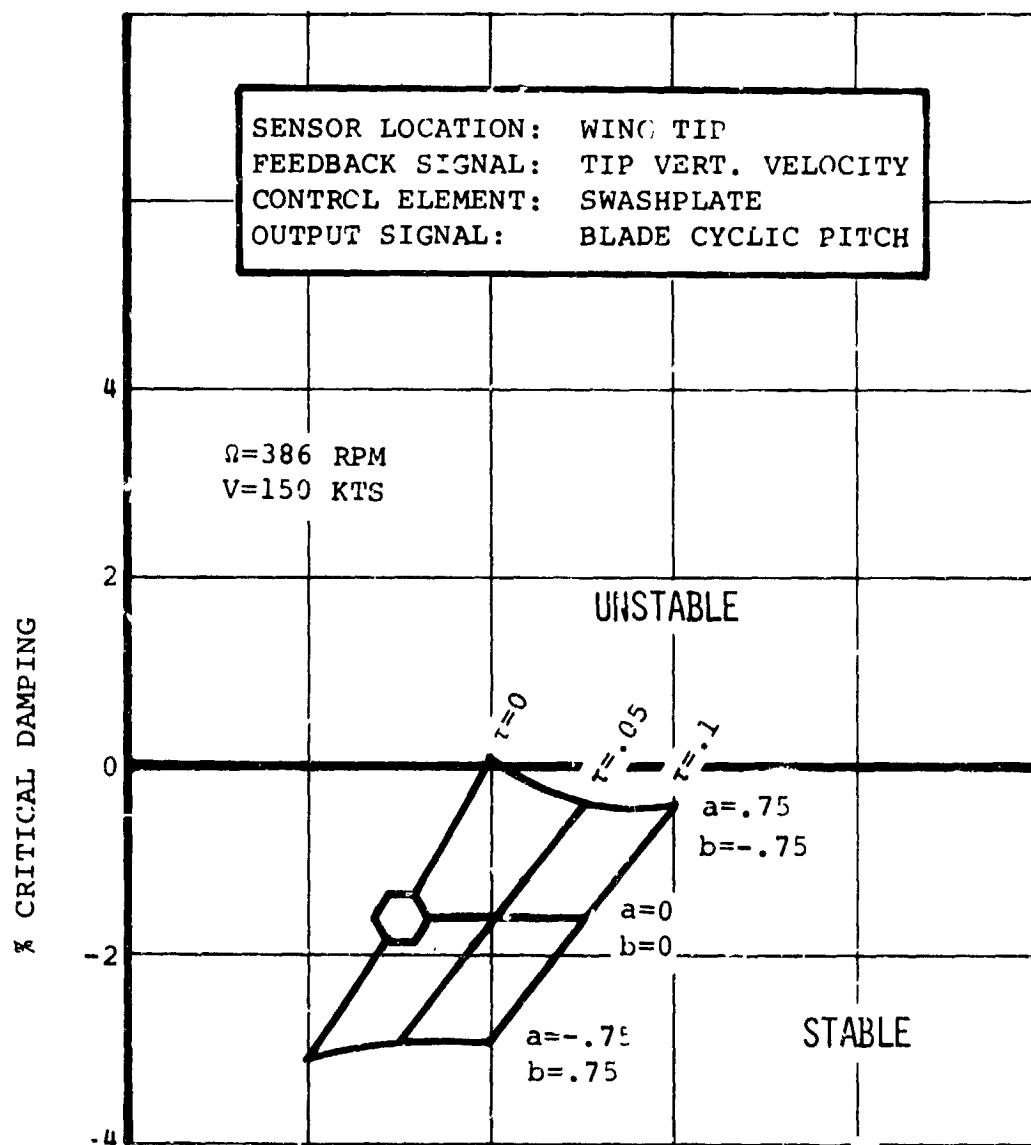


FIGURE 5.23. FEEDBACK EFFECT ON MODAL DAMPING OF  
 WING TORSION MODE WITH TIME CONSTANT

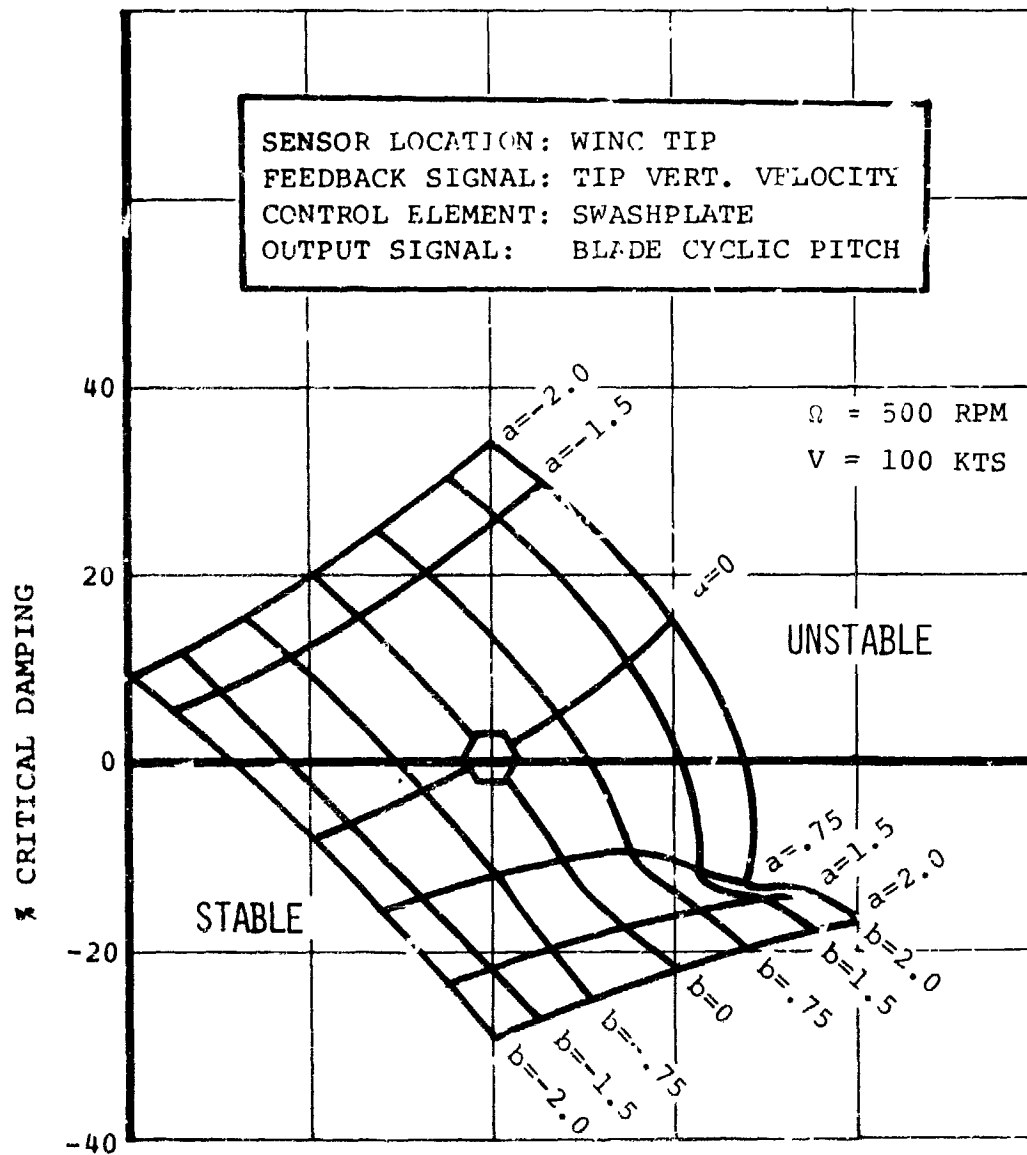


FIGURE 5.24. FEEDBACK EFFECT ON MODAL DAMPING OF  
 WING VERTICAL BENDING MODE



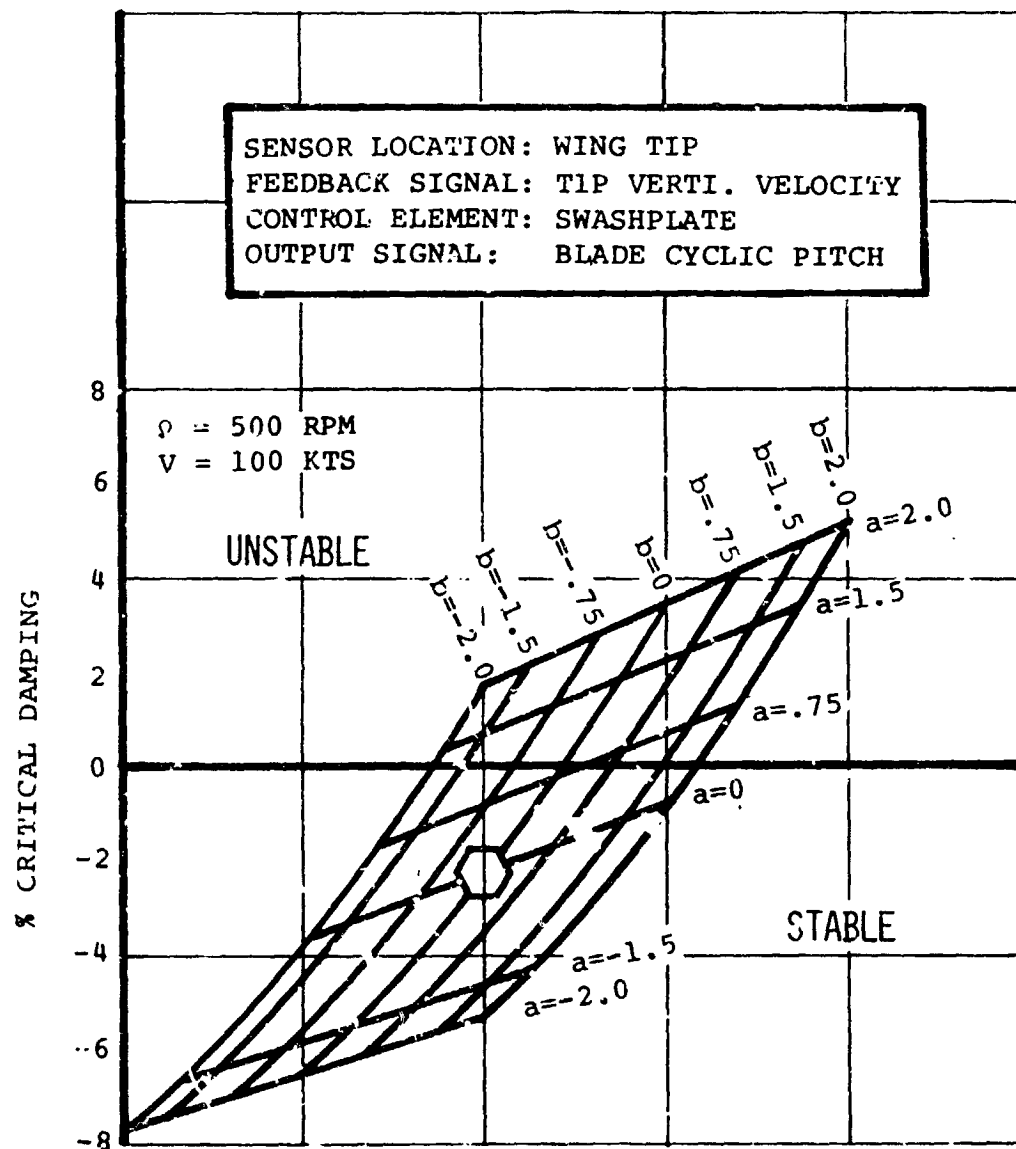


FIGURE 5.25 FEEDBACK EFFECT ON MODAL DAMPING OF WING TORSION MODE

SENSOR LOCATION: WING TIP  
 FEEDBACK SIGNAL: TIP VERT. VELOCITY  
 CONTROL ELEMENT: SWASHPLATE  
 OUTPUT SIGNAL: BLADE CYCLIC PITCH

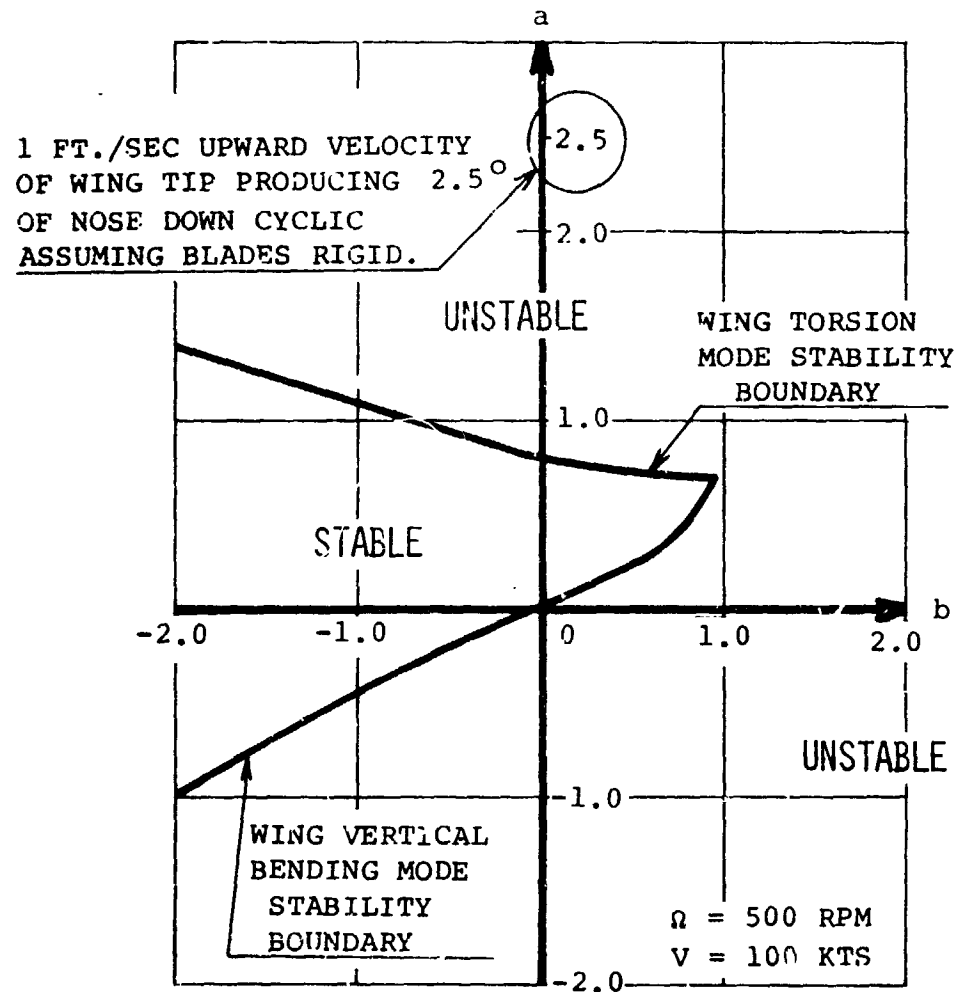


FIGURE 5.26 FEEDBACK EFFECT ON MODAL DAMPING OF STABILITY FOR FEEDBACK COMBINATIONS

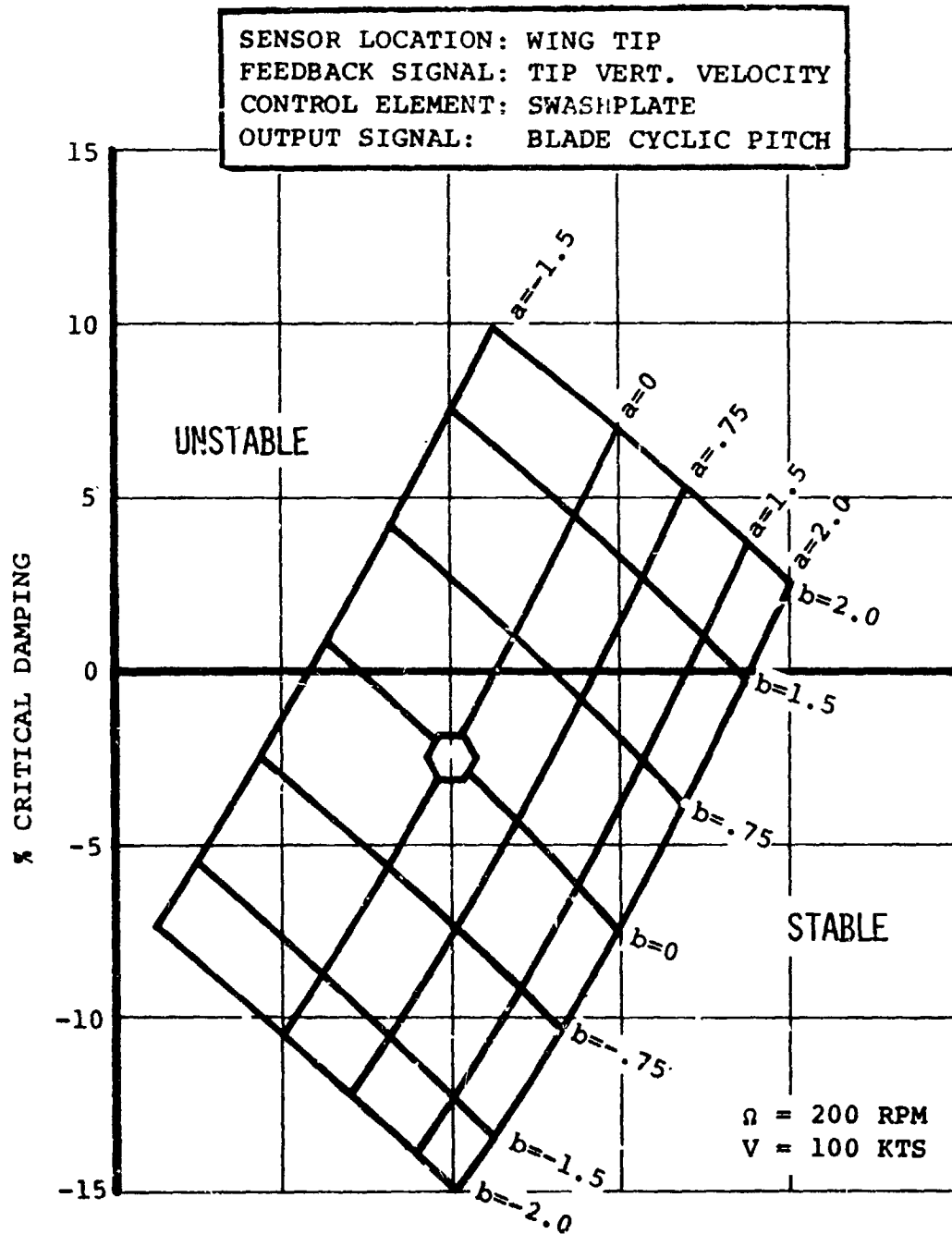


FIGURE 5.27 FEEDBACK EFFECT ON MODAL DAMPING OF  
 WING VERTICAL BENDING

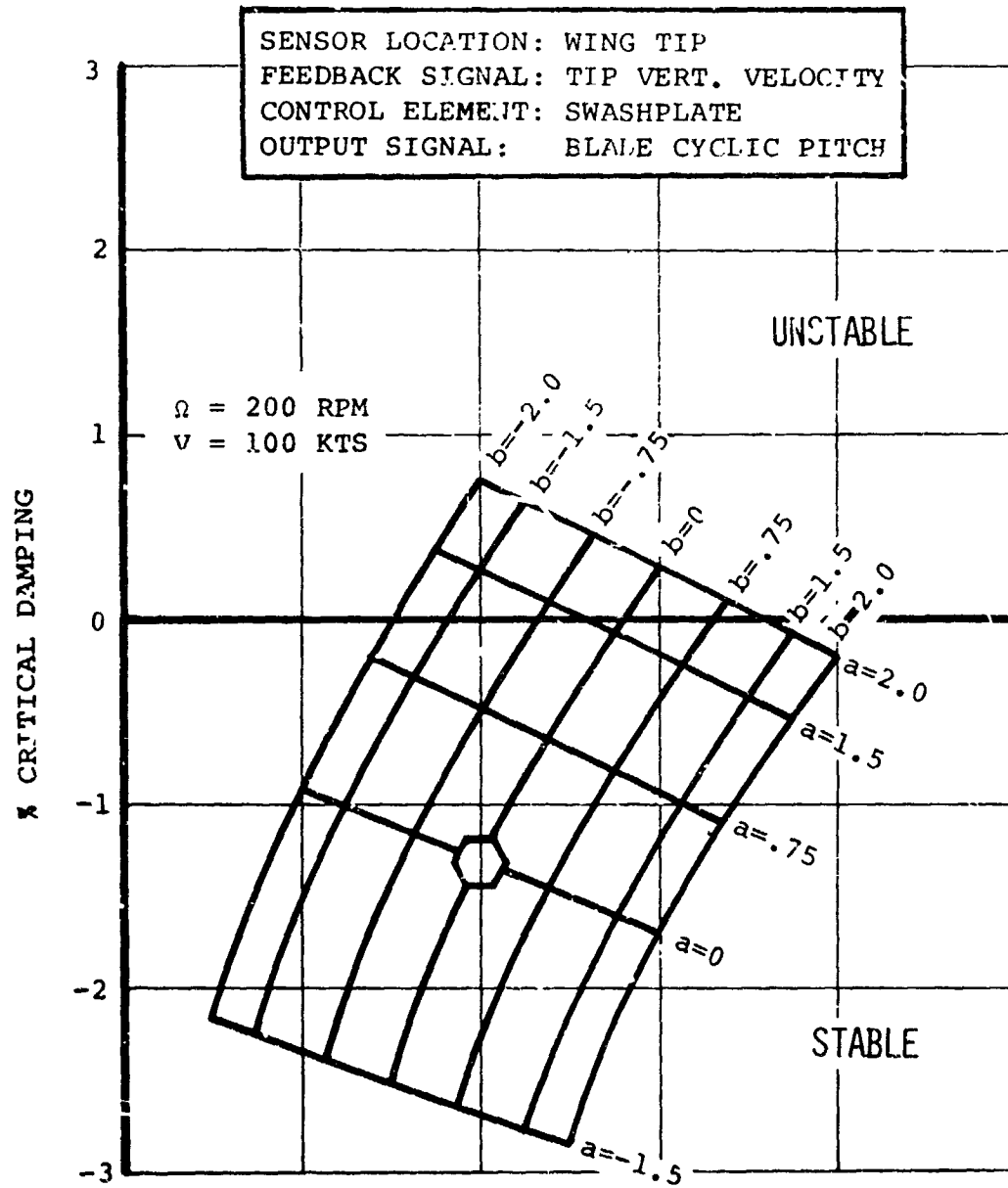


FIGURE 5.28 FEEDBACK EFFECT ON MODAL DAMPING OF WING TORSION MODE

SENSOR LOCATION: WING TIP  
 FEEDBACK SIGNAL: TIP VERT. VELOCITY  
 CONTROL ELEMENT: SWASHPLATE  
 OUTPUT SIGNAL: BLADE CYCLIC PITCH

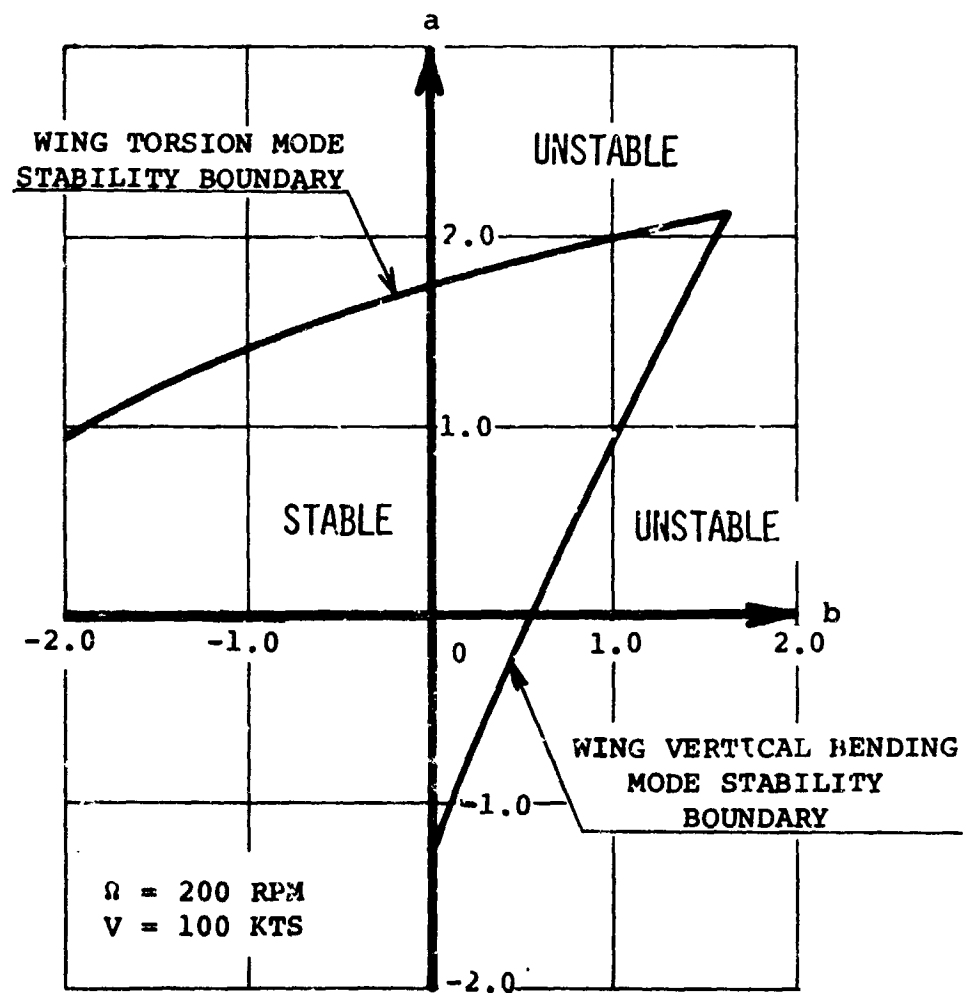


FIGURE 5.29 FEEDBACK EFFECT ON MODAL DAMPING OF AIRCRAFT STABILITY FOR FEEDBACK COMBINATIONS

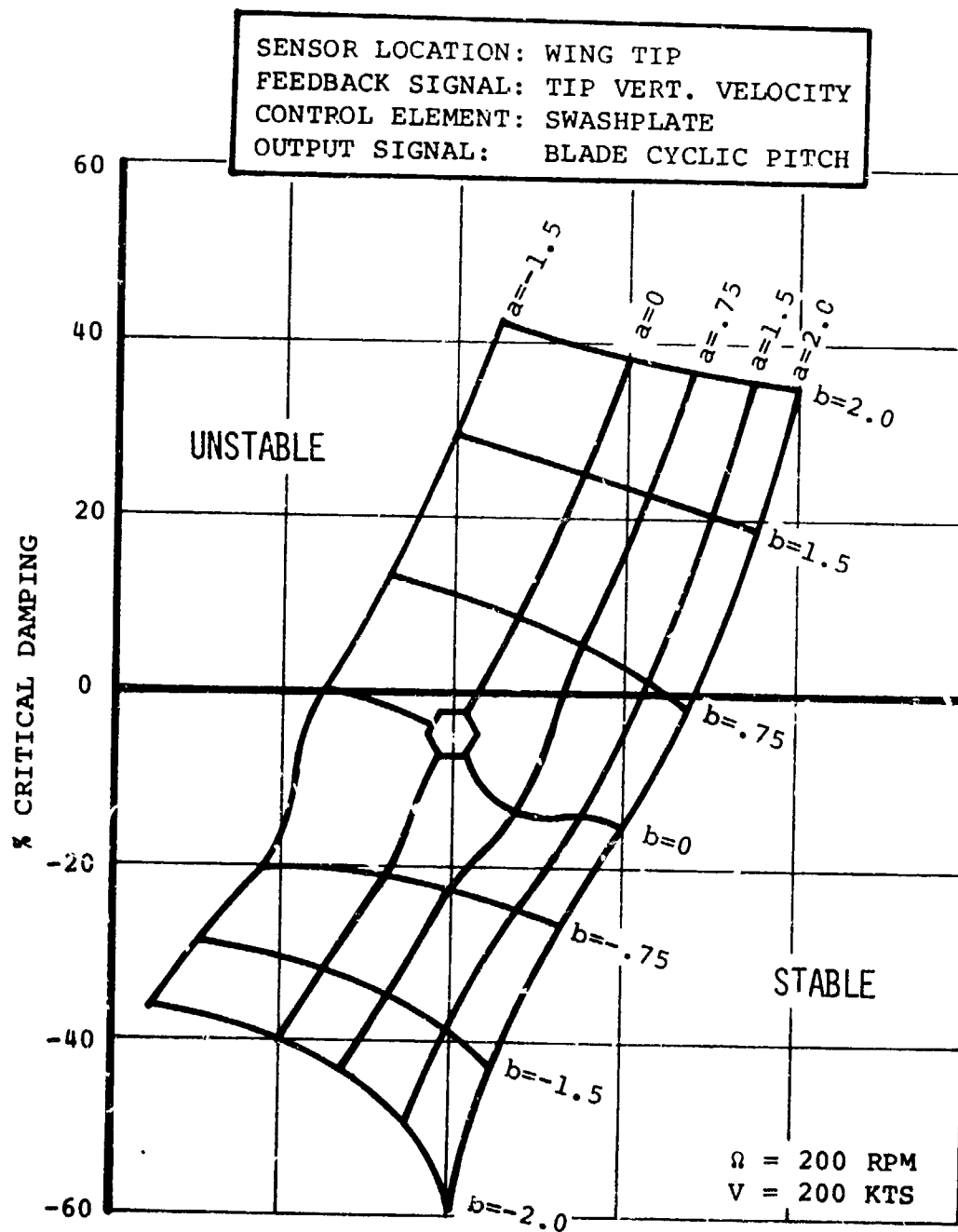


FIGURE 5.30 FEEDBACK EFFECT ON MODAL DAMPING OF  
 WING VERTICAL BENDING

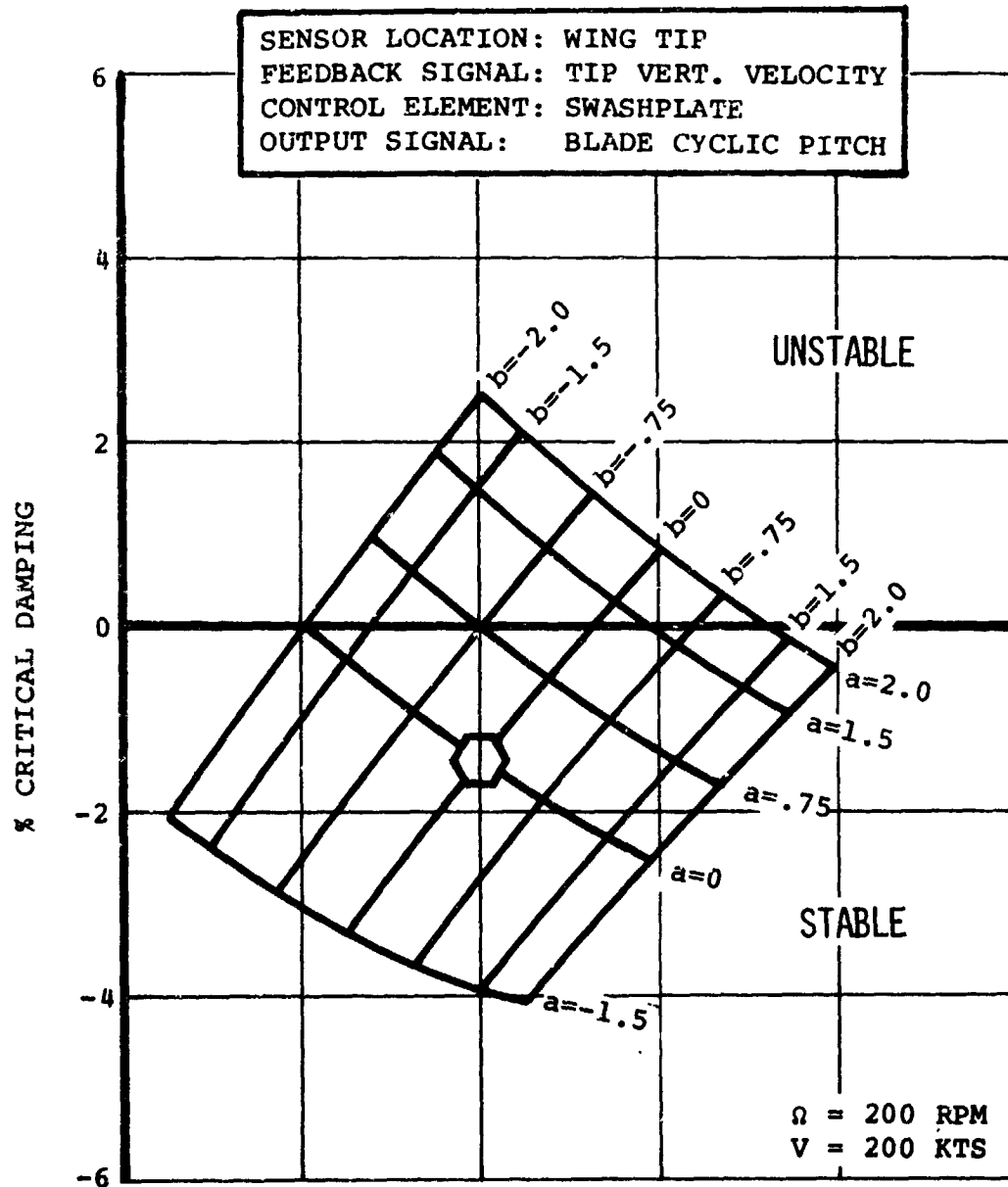


FIGURE 5.31 FEEDBACK EFFECT ON MODAL DAMPING OF  
 WING TORSION MODE

SENSOR LOCATION: WING TIP  
 FEEDBACK SIGNAL: TIP VERT. VELOCITY  
 CONTROL ELEMENT: SWASHPLATE  
 OUTPUT SIGNAL: BLADE CYCLIC PITCH

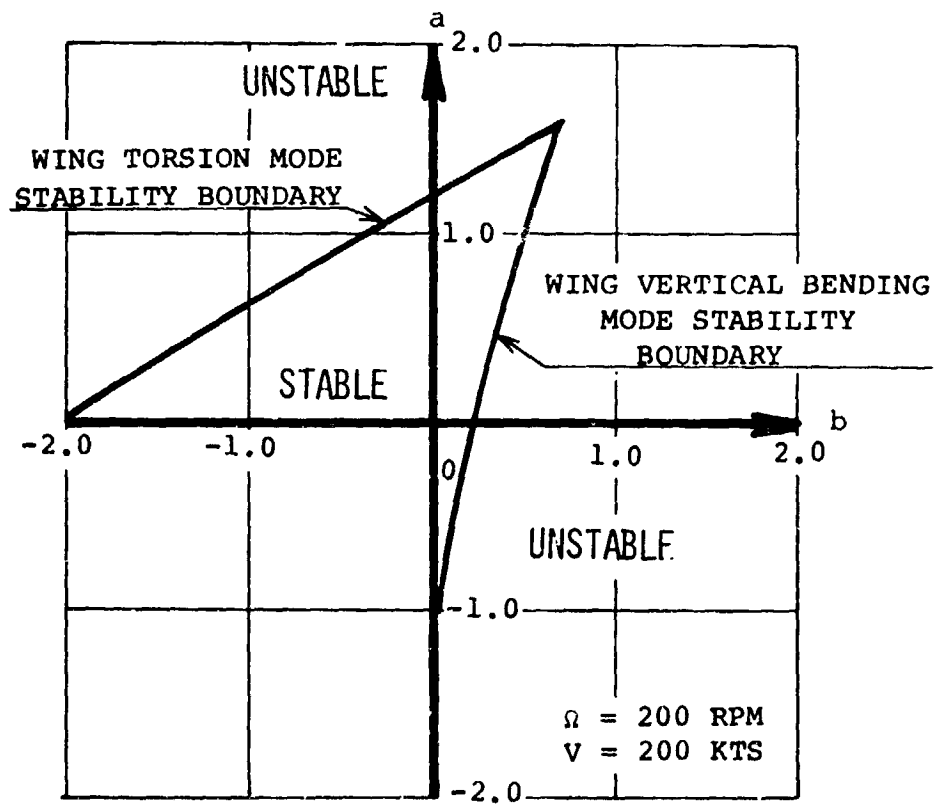


FIGURE 5.32 FEEDBACK EFFECT ON MODAL DAMPING OF AIRCRAFT  
 STABILITY FOR FEEDBACK COMBINATIONS



envelope (Figures 5.29 and 5.32) are a little larger, but exhibit the same general shape. A total gain envelope for the portions of the flight envelope investigated is shown in Figure 5.33. Assuming a time constant of .05 seconds and a desire to maintain a minimum of 1% critical damping in the torsion mode the optimum gain would be  $a = .4$  and  $b = -.75$  yielding a vertical bending mode damping of 11% at 150 knots.

From this exploratory study it was concluded that rate feedback showed great potential for adding damping to the wing vertical bending mode. There were several areas which needed further investigation:

- 0 other feedback signals
- 0 effect of actual hardware dynamics
- 0 instabilities in other modes and corrective action.

The second portion of the study investigated these parameters using a refined optimization approach.

#### 5.5 SYNTHESIS OF AN OPTIMIZED SYSTEM ACCOUNTING FOR HARDWARE COMPONENT DYNAMICS

Using the lessons learned from the initial studies the approach to the feedback system synthesis was refined and a more detailed study was undertaken. Specific additions to the analyses were

- 0 refined approach to cyclic azimuth selection
- 0 inclusion of actual hardware dynamics
- 0 shaping and filtering of feedback signal.

SENSOR LOCATION: WING TIP  
 FEEDBACK SIGNAL: TIP VERTICAL VELOCITY  
 CONTROL ELEMENT: SWASHPLATE  
 OUTPUT SIGNAL: BLADE CYCLIC PITCH

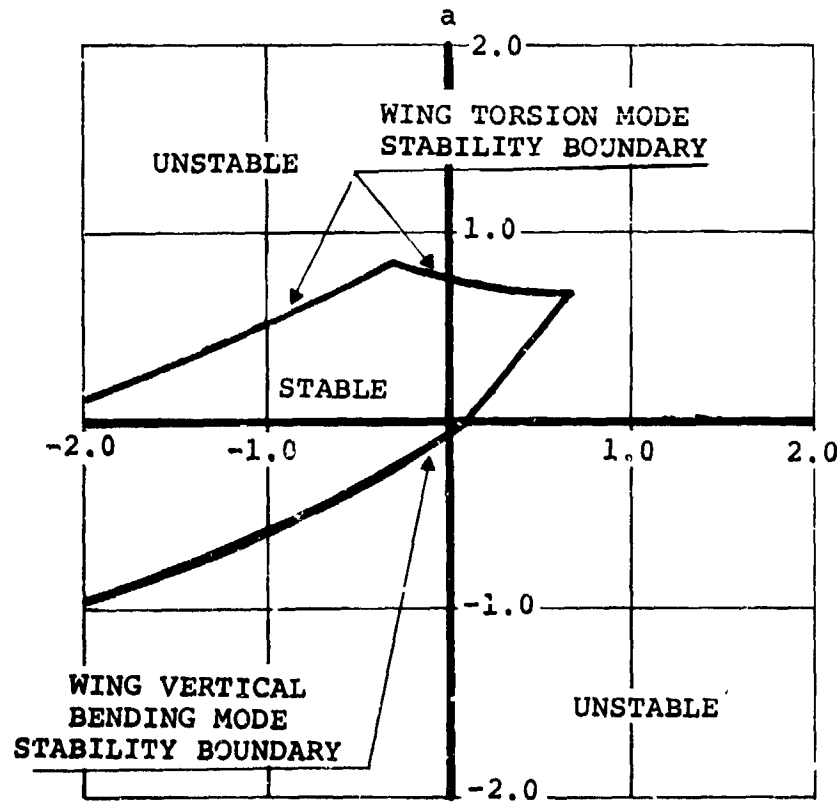


FIGURE 5.33. COMPOSITE FEEDBACK GAIN ENVELOPE FOR VARIOUS FLIGHT CONDITIONS

Instead of selecting the cyclic azimuth position on the basis of the stability roots which reflect the magnitude and phase of the control force, azimuth position was chosen on a magnitude basis only and phase controlled if necessary by phase shaping. Determination of the azimuth which yields maximum response in wing vertical bending was accomplished by calculating the Bode diagrams for a rosette of azimuth positions. Azimuth location which yielded the largest response at the wing vertical bending frequency was chosen as the feedback control setting.

Since system lags have a significant effect on the level of damping achievable, it is clear that inclusion of actual system hardware response characteristics would improve the quality of any conclusions drawn about modal suppression feedback systems. The model therefore used characteristics from the 26-foot rotor set up tested in the 40x80-foot NASA-Ames tunnel. These include:

- actuator dynamics
- sensor transfer functions
- swashplate control rod stiffnesses

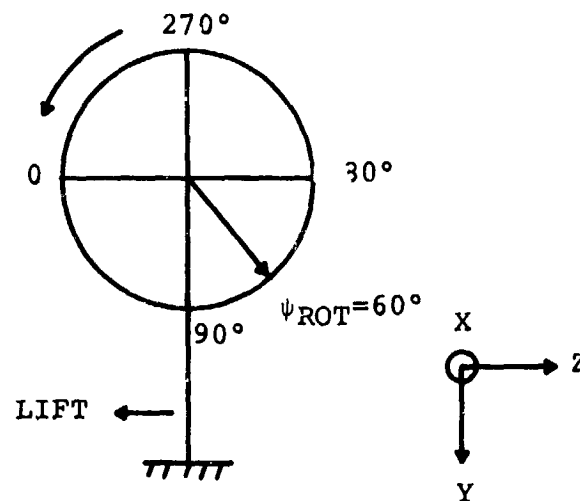
Other pieces of hardware in the feedback loops had frequency characteristics which would not affect operation of the feedback system (i.e., their break frequency was much higher than any other frequency in the system).

The basic feedback sensor was an accelerometer mounted on the nacelle in such a manner as to sense wing tip vertical acceleration. The position selected was nodal in the torsion mode.

Acceleration, rate and position feedback were evaluated by shaping the accelerometer signals to determine if the intuitive choice of rate feedback was correct. Rate and position feedback signals were obtained by integrating the acceleration signal once and twice respectively (see Figure 5.2). The capability for filtering and phase shifting was made available to attenuate modes which might go unstable (e.g., the wing torsion mode) or shift the phase at the vertical bending frequency to get a pure position, rate or acceleration signal.

A rosette of cyclic azimuth positions were run for various flight conditions (rpm and velocity variations) and Bode diagrams plotted. From these the azimuth position ( $\psi_{rot}$ ) was chosen which yielded the largest response in the wing vertical bending mode. It was  $\psi_{rot} = 60$  degrees and is shown in Figure 5.34. Figures 5.35, 5.36, and 5.37 show the Bode plots for the acceleration signal for  $\psi_{rot} = 60$  degrees. The plots for the remaining rpm and velocity conditions may be viewed in Boeing Document D160-10019-1, Pretest Calculation of Open Loop Frequency Response and Stability of High Rate and Low Rate Swashplate Feedback Systems of M222 26-Foot Rotor Test. The plots in this document have had a bandpass filter added to them. The filter is defined in the document.

With the chosen azimuth position several different systems were evaluated. For each system the hardware dynamics were included in the Bode plots and the gain-phase relationships evaluated to determine the need for phase shifting or filtering.



#### MATH MODEL SIGN CONVENTIONS

- $\Delta\theta = A_1 \cos \psi + B_1 \sin \psi$

POSITIVE  $A_1$  YIELDS NOSE DOWN PITCHING MOMENT ( $0^\circ$  to  $180^\circ$ )

POSITIVE  $B_1$  YIELDS NOSE LEFT YAWING MOMENT ( $90^\circ$  to  $270^\circ$ )

- Values of  $\psi_{ROT}$  demanded give magnitudes of  $A_1$  and  $B_1$  cyclic such that the maximum blade angle occurs at the azimuth position shown above.

FIGURE 5.34 MATH MODEL SIGN CONVENTIONS AND VECTOR ORIENTATION  
FOR HI-RATE SYSTEM

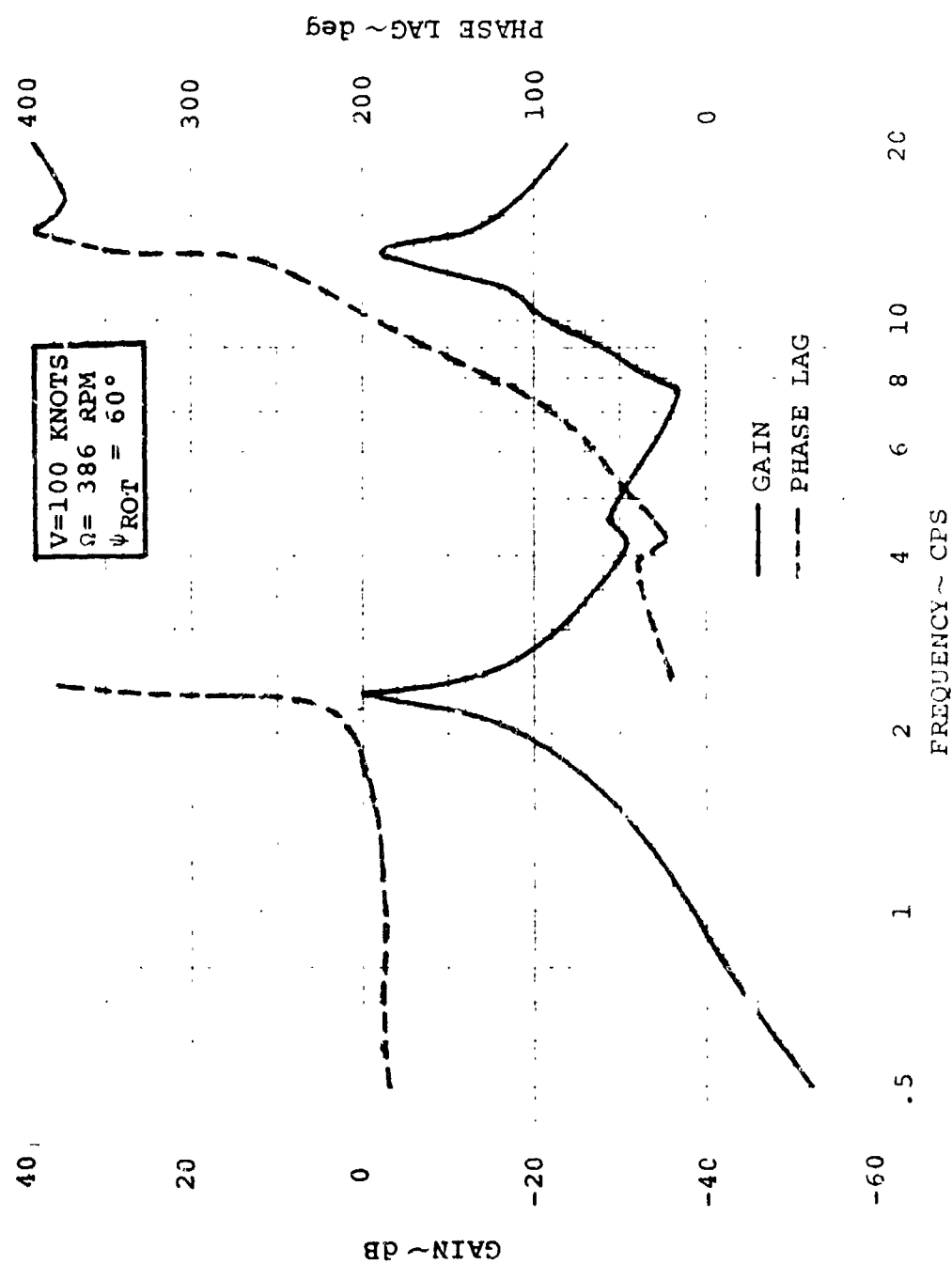


Figure 5.35. Aeroelastic Stability Augmentation System  
 Open Loop Frequency Response - Acceleration  
 Feedback - 100 Knt Cruise

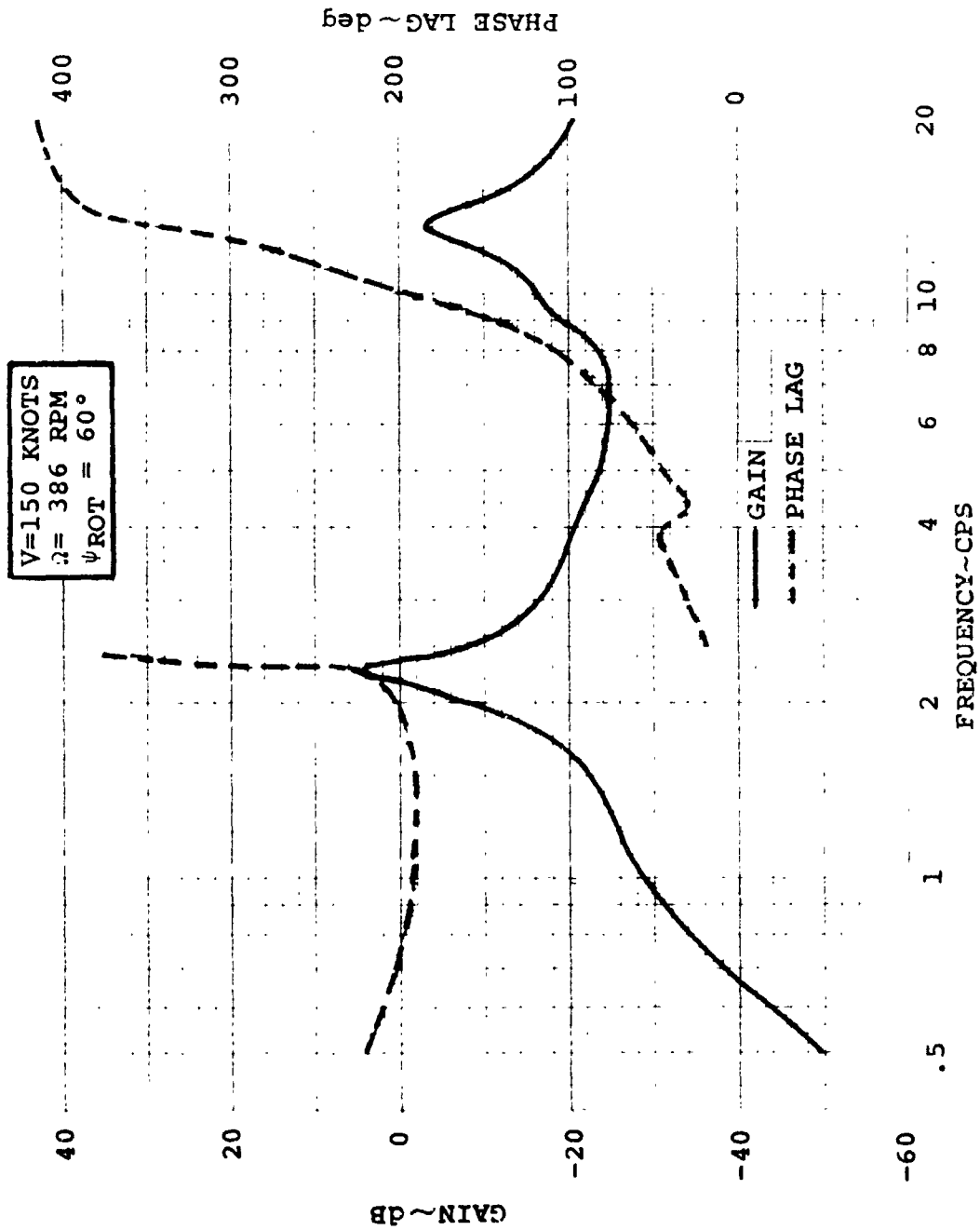


Figure 5.36. Aeroelastic Stability Augmentation System  
Open Loop Frequency Response - Acceleration  
Feedback - 150 Knot Cruise

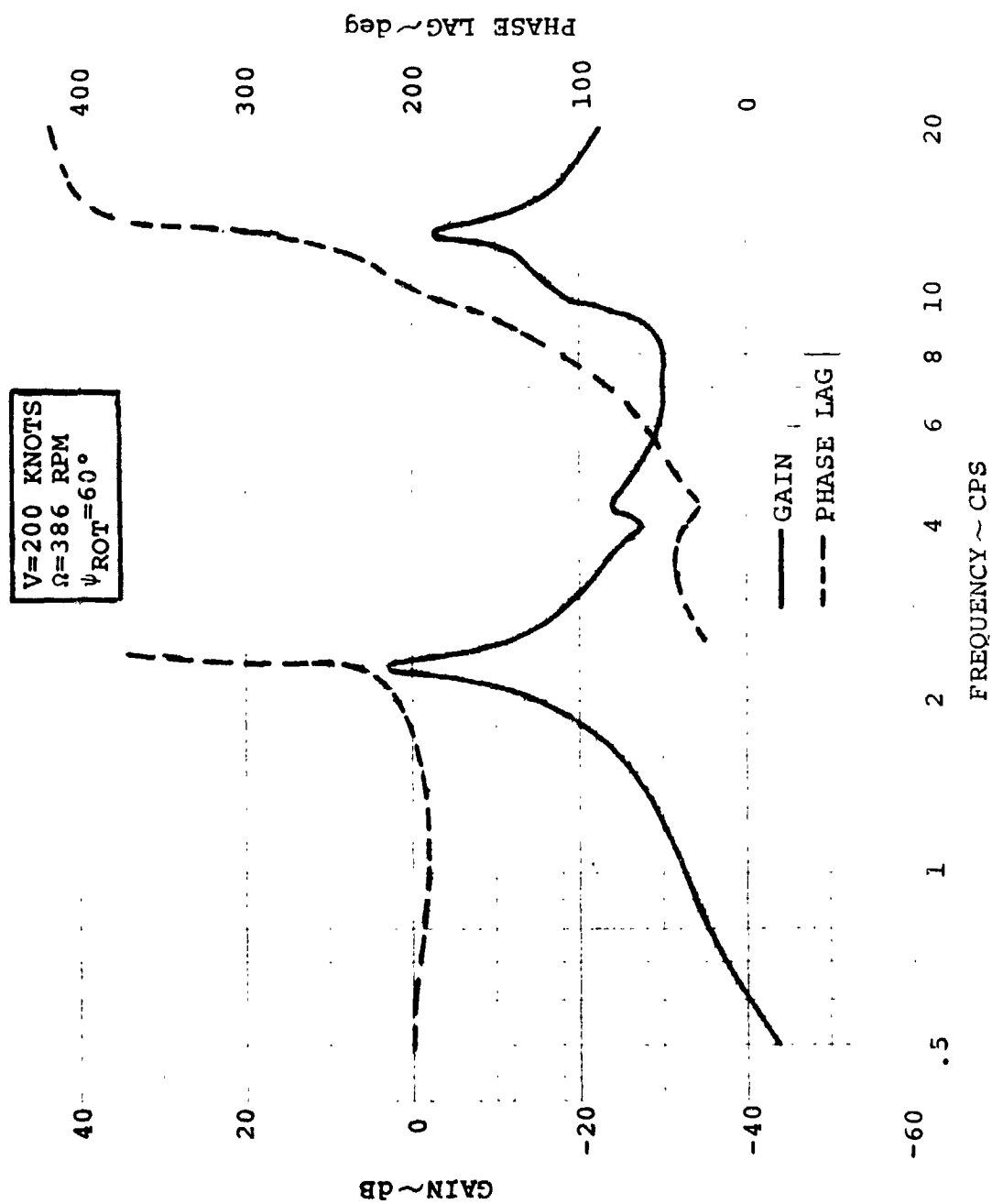


Figure 5.37. Aeroelastic Stability Augmentation System  
Open Loop Frequency Response - Acceleration  
Feedback - 200 Knot Cruise



### 5.5.1 Acceleration Feedback

Acceleration feedback was the first to be evaluated because preliminary model testing had already indicated that useful improvement could be obtained with this system. On the block diagram of Figure 5.2, it is the loop without integrators. Figures 5.35, 5.36, and 5.37 shows the Bode plots for acceleration feedback at 386 RPM and 100 knots, 150 knots, and 200 knots. On a Bode plot instability is indicated when the phase is 180-degrees and the gain is 0 dB or greater; however, if the gain is to be increased the 180-degree crossing should be of concern. In each velocity case there is a 180-degree crossing at approximately 9 cps which for the mathematical model being evaluated is the wing torsion mode - the mode which went unstable in the simplified case. A fourth order narrow bandpass filter was put in the system to eliminate instabilities. Bode plots for the system with the filter are shown in Figures 5.38, 5.39, and 5.40. This takes care of stability at higher and lower frequencies. The phase at 2.2 cps was not satisfactory and was shifted by 90-degrees using a phase shift network and the loop was closed. Stability root variation with gain is shown in Figures 5.41, 5.42, and 5.43. In the best case the wing vertical bending damping was increased from 1.5% to 17%. This system was installed and tested on the 26-foot rotor in the Ames tunnel. Figures 5.44 and 5.45 show excellent correlation for the Bode analysis and the effect of gain on vertical bending damping. This correlation raises the confidence level in the program and leads us to believe that our physical representation of the feedback system is correct.

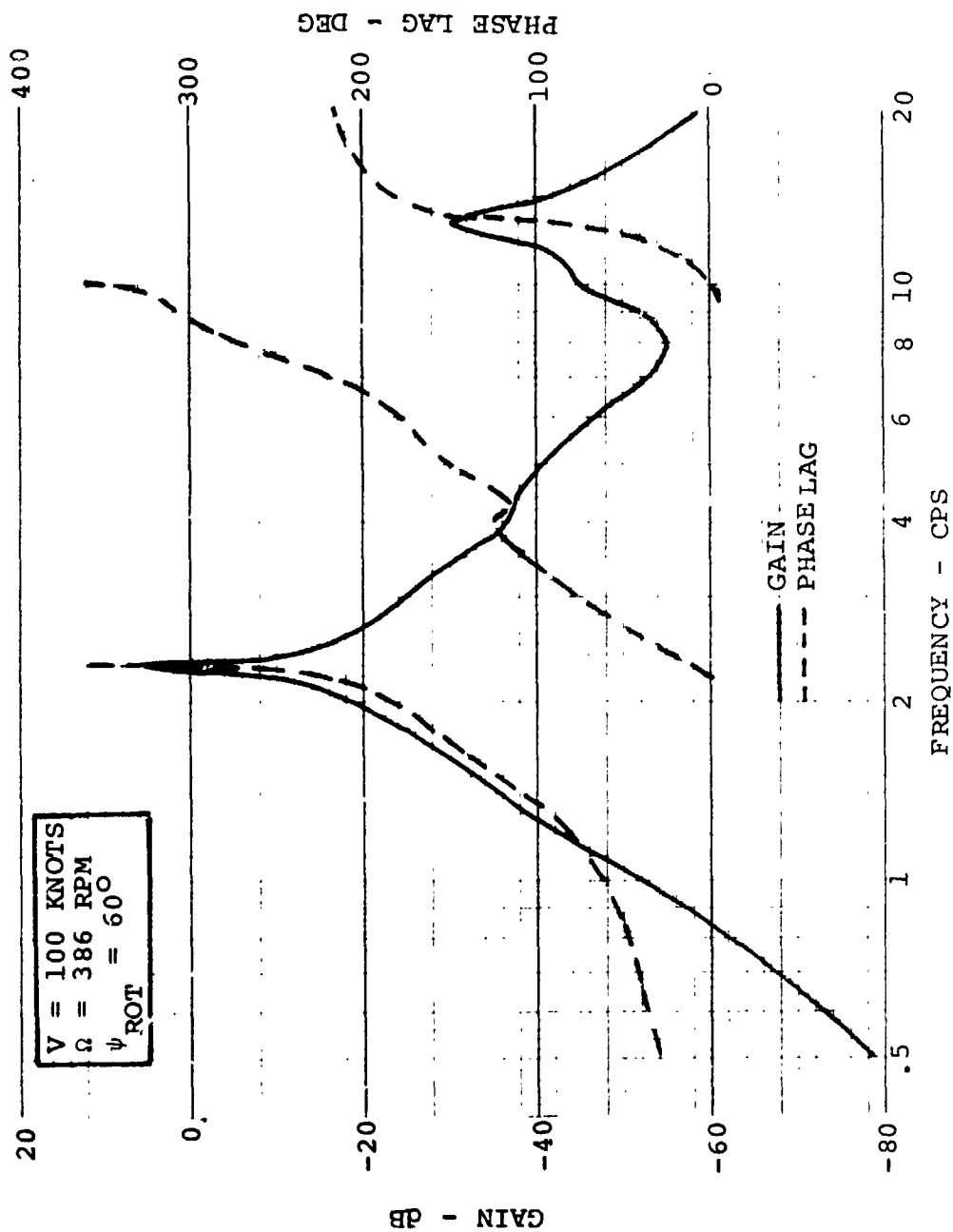


FIGURE 5.38. AEROELASTIC STABILITY AUGMENTATION SYSTEM OPEN LOOP FREQUENCY RESPONSE FILTERED ACCELERATION FEEDBACK - 100 KNOTS.

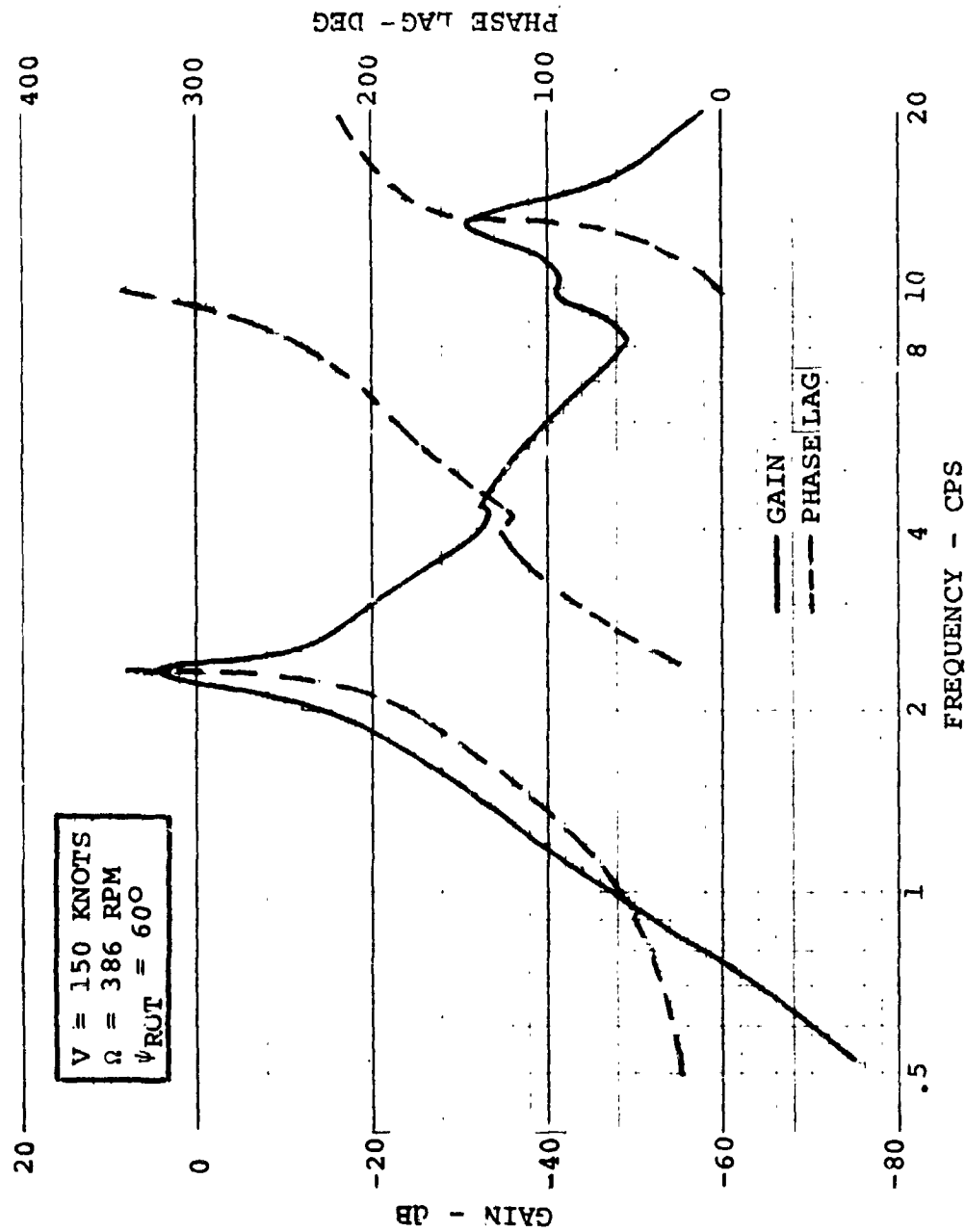


FIGURE 5.39. AEROELASTIC STABILITY AUGMENTATION  
SYSTEM OPEN LOOP FREQUENCY RESPONSE  
FILTERED ACCELERATION FEEDBACK - 150 KNOTS.

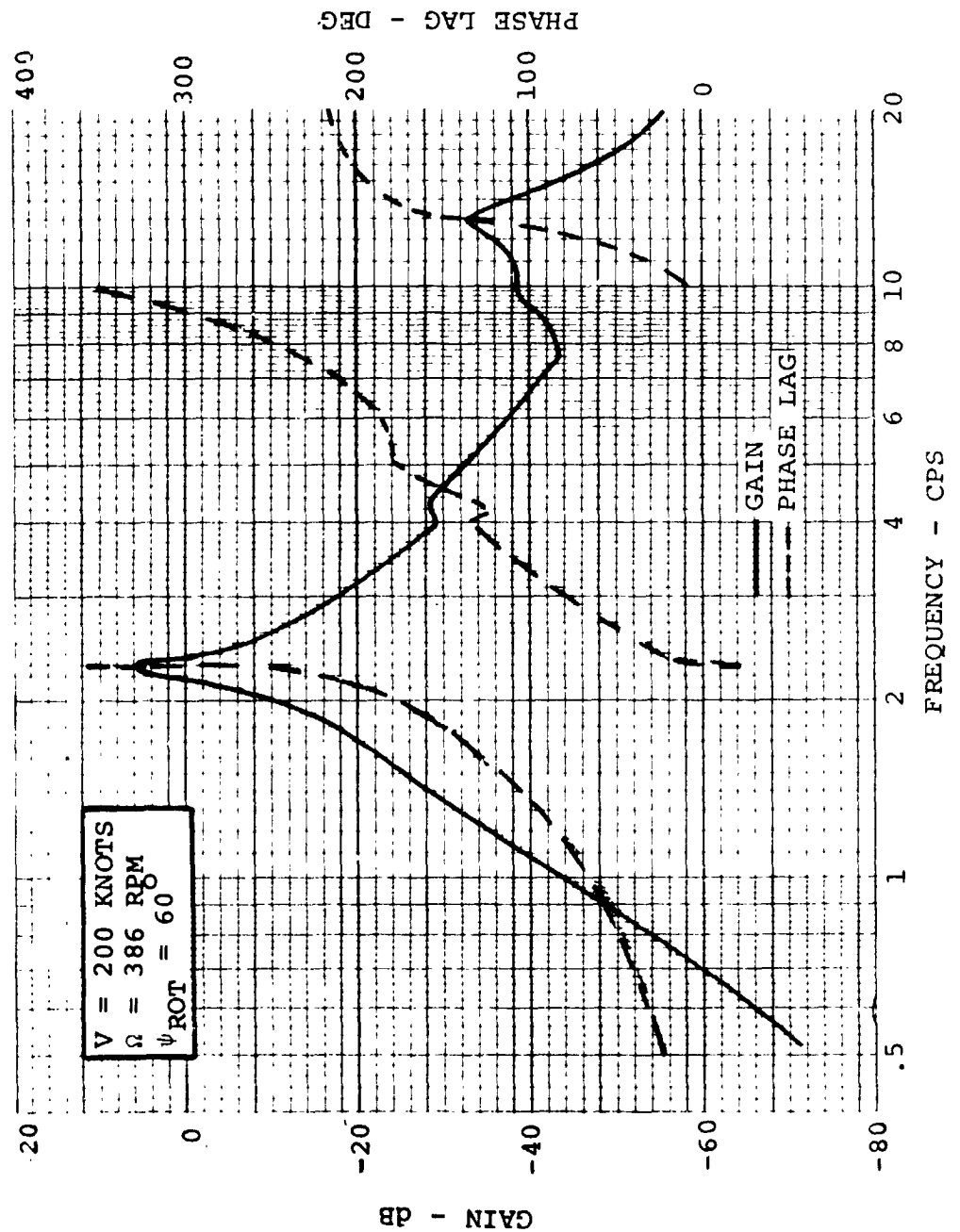


FIGURE 5.40. AEROELASTIC STABILITY AUGMENTATION SYSTEM  
OPEN LOOP FREQUENCY RESPONSE FILTERED  
ACCELERATION FEEDBACK - 200 KNOTS.

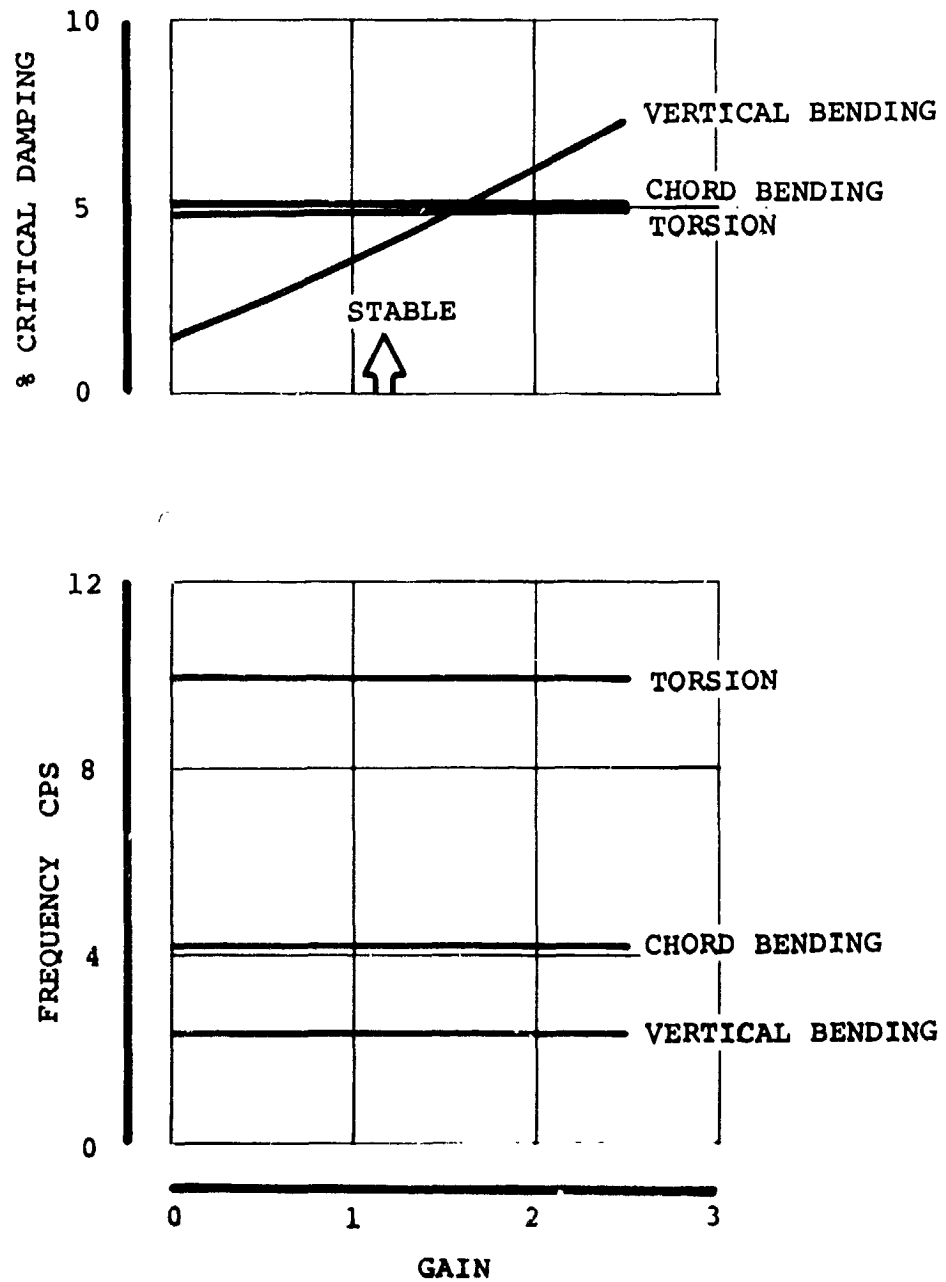


FIGURE 5.41. EFFECT OF GAIN ON MODAL STABILITY ROOTS FOR FILTERED ACCELERATION FEEDBACK - 100 KNOTS

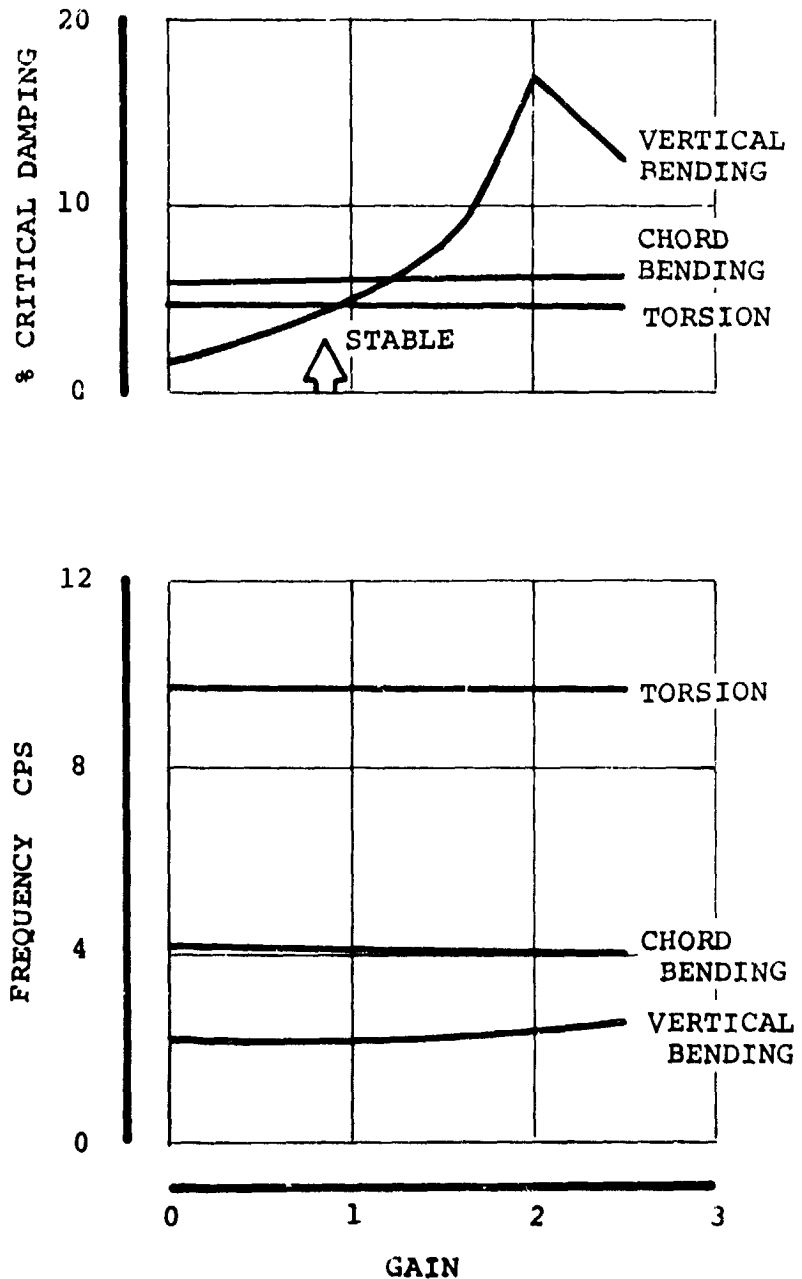


FIGURE 5.42. EFFECT OF GAIN ON MODAL STABILITY ROOTS FOR FILTERED ACCELERATION FEEDBACK - 150 KNOTS

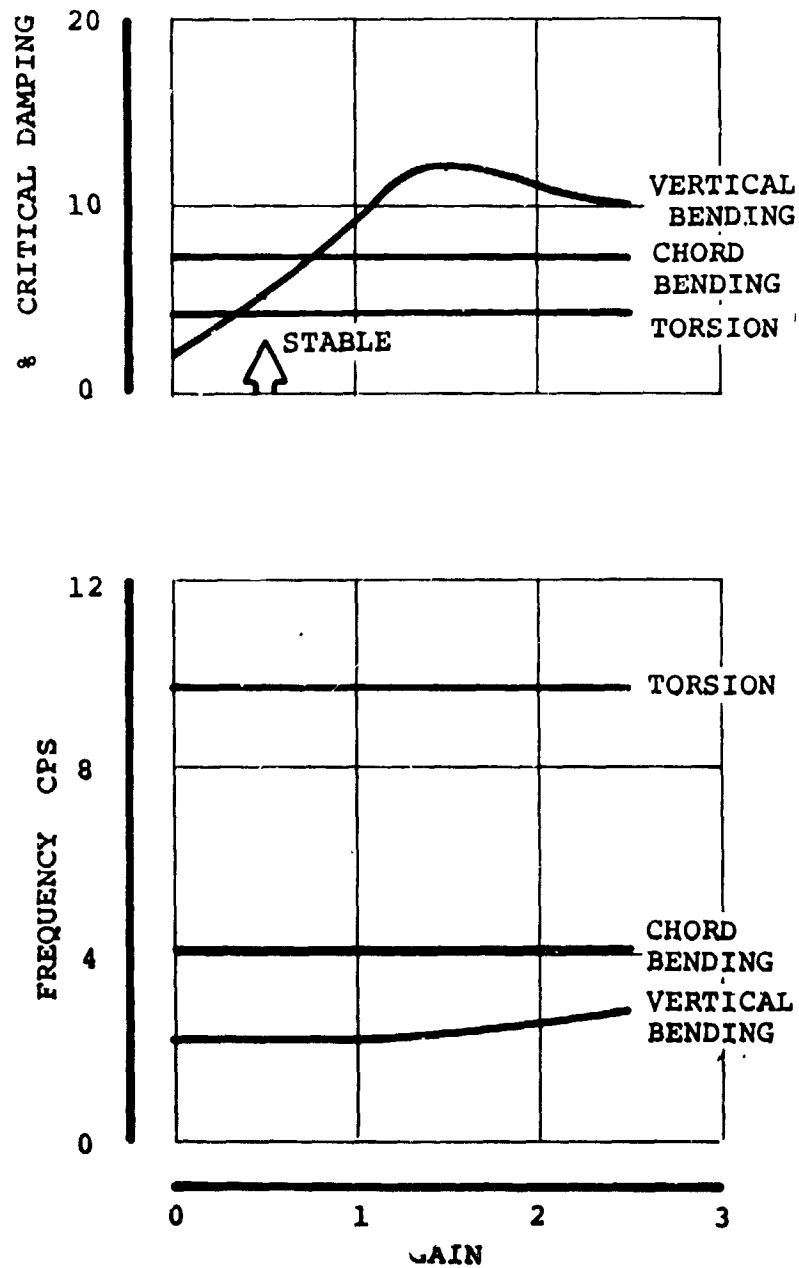


FIGURE 5.43. EFFECT OF GAIN ON MODAL STABILITY ROOTS FOR FILTERED ACCELERATION FEEDBACK - 200 KNOTS

REV. A

Post-test analysis of the system indicated that possibly use of acceleration feedback was not the most efficient method to increase stability, so rate and position feedback were evaluated analytically.

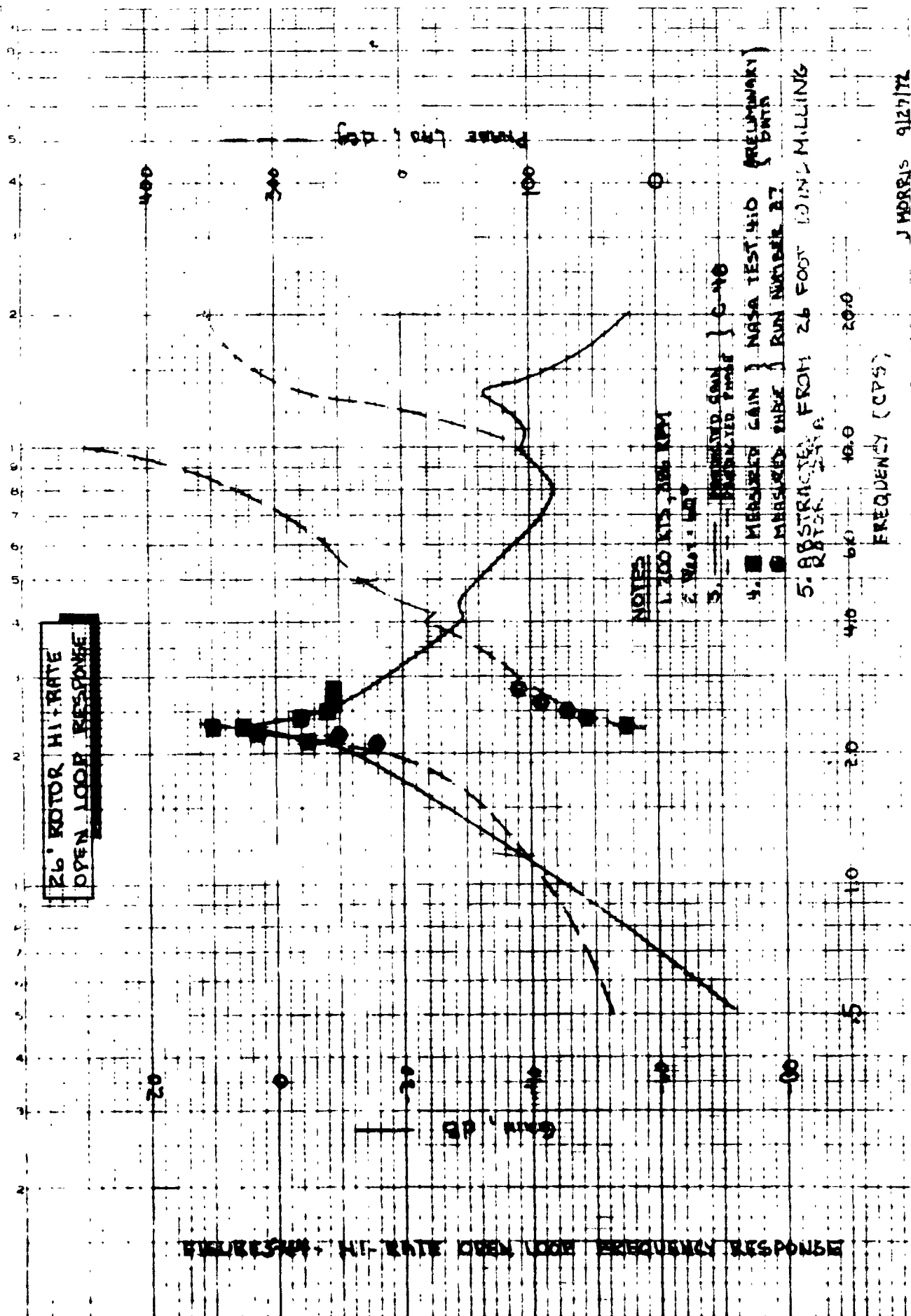
#### 5.5.2 Rate Feedback

The second system evaluated was a rate feedback system. As seen in the Bodes of Figures 5.46, 5.47, and 5.48, the 180-degree crossing occurs when the gain is well down from the vertical bending peak at 2.25 cps. At test 40 dB separate the two. There are no filtering requirements to ensure stability. The only filter required may be on the accelerometer to remove excess noise. This filter will have a high break frequency and will not affect the system response. Stability roots were run for the system and appear on the root loci of Figures 5.49 and 5.50 for 100 and 200 knots. A damping ratio of .33 was achieved at a gain of .762 deg/ft/sec without degrading the other stability roots. It therefore appears that this system can be more effective than the acceleration system and permits simpler signal shaping.

#### 5.5.3 Position or Deflection Feedback

The last feedback system to be evaluated was a position system. With this system it was hoped to raise the frequency of a given mode and thus postpone or eliminate a resonance condition.





TEST 416: NASA AMES 40 X 80 FOOT TUNNEL  
M-222 26' DIAMETER ROTOR TEST  
NASA FULL STIFF WING

192 KTS 386 RPM  
HIGH & LOW RATE LOOPS CLOSED  
LOW RATE  $G_Y = 300$   
 $G_P = 204$

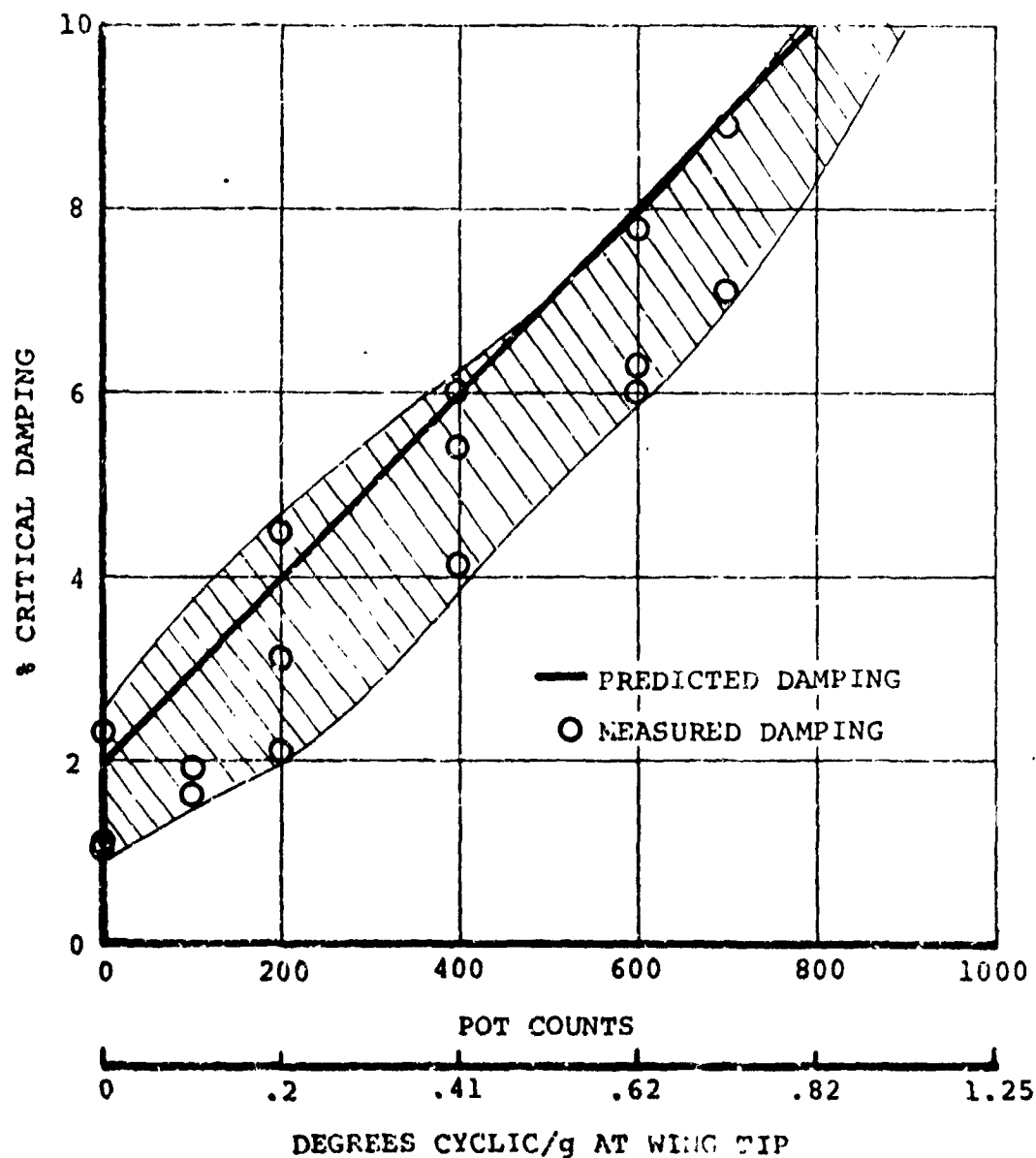


FIGURE 5.45. 26 FOOT ROTOR TEST DATA  
DAMPING VERSUS HIGH RATE SYSTEM GAIN  
AT 192 KNOTS, 386 RPM, WITH LOW RATE  
SYSTEM ACTIVE

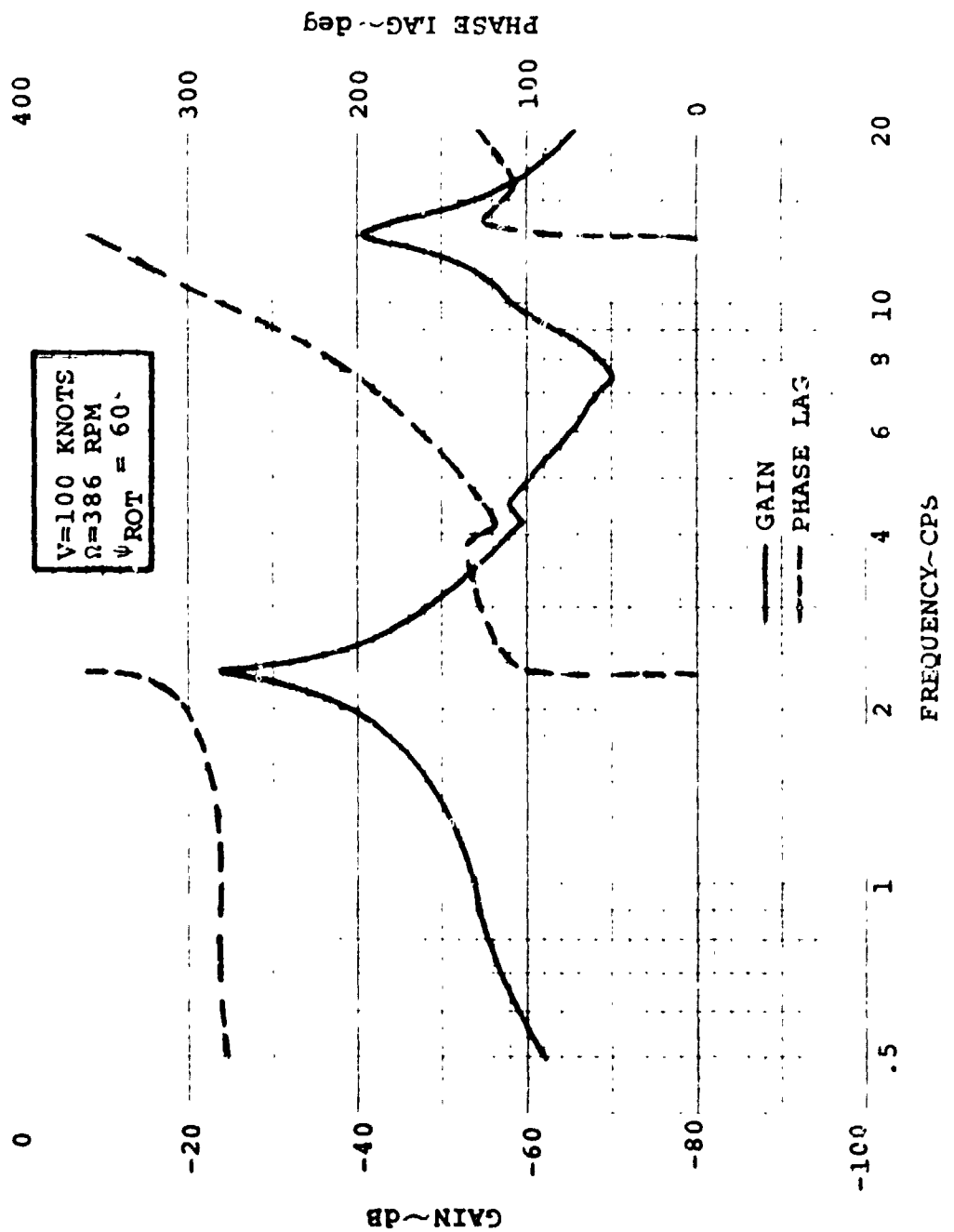


Figure 5.46. Aeroelastic Stability Augmentation System  
Open Loop Frequency Response - Rate Feedback  
- 100 Knots

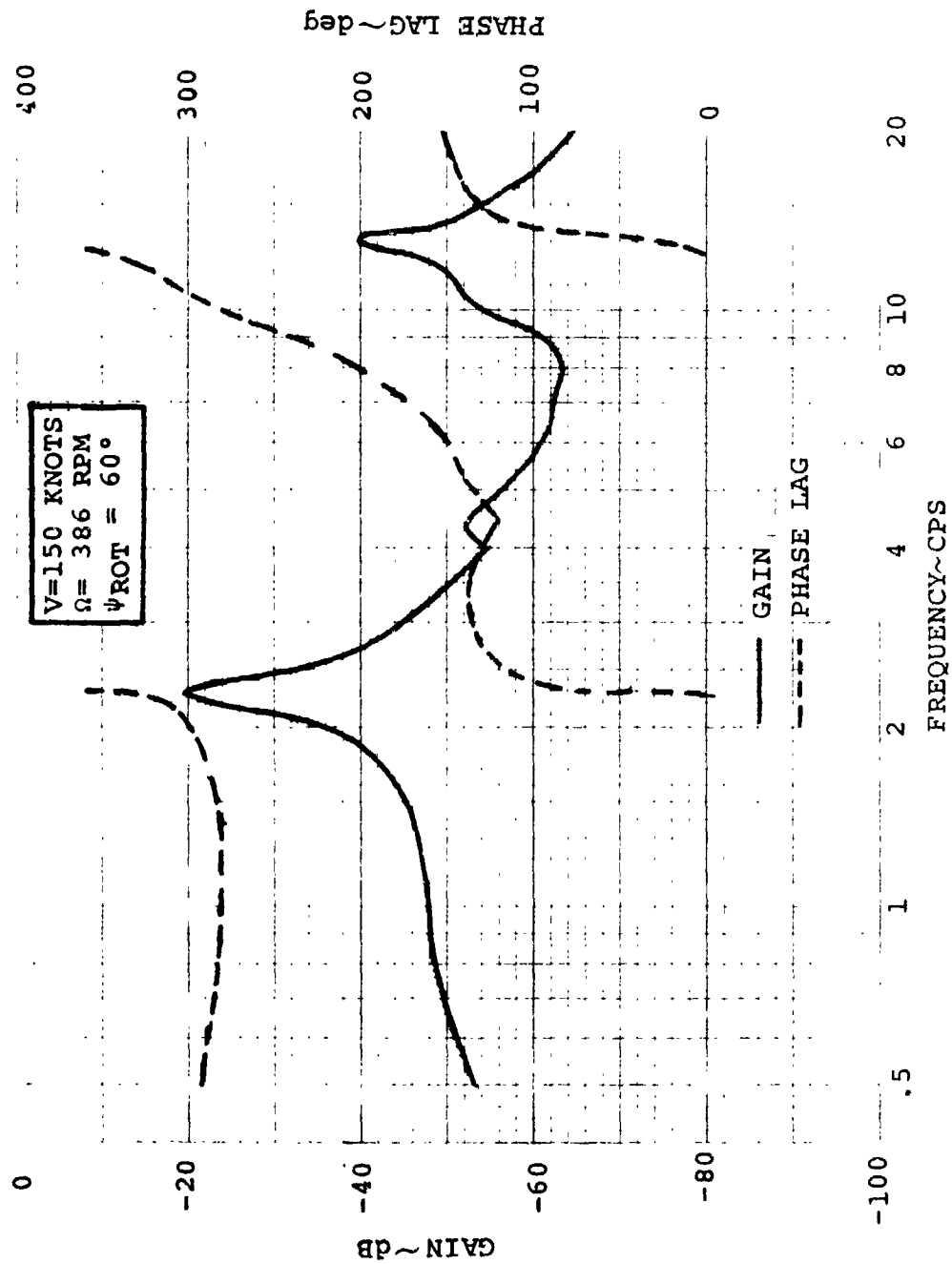


Figure 5.47. Aeroslastic Stability Augmentation System  
 Open Loop Frequency Response -  
 Rate Feedback - 150 Knots

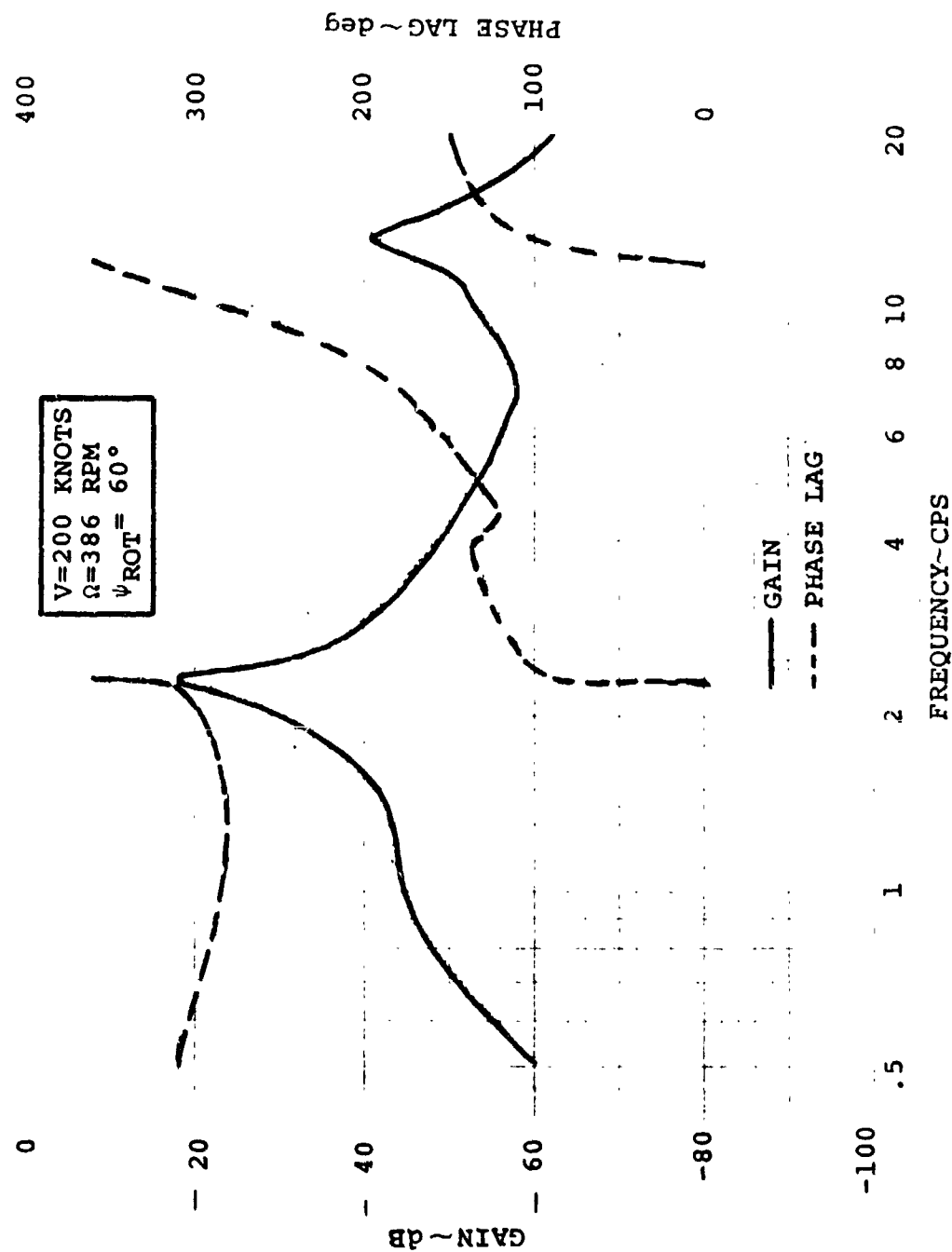


Figure 5.48. Aeroelastic Stability Augmentation System  
Open Loop Frequency Response -  
Rate Feedback - 200 Knots

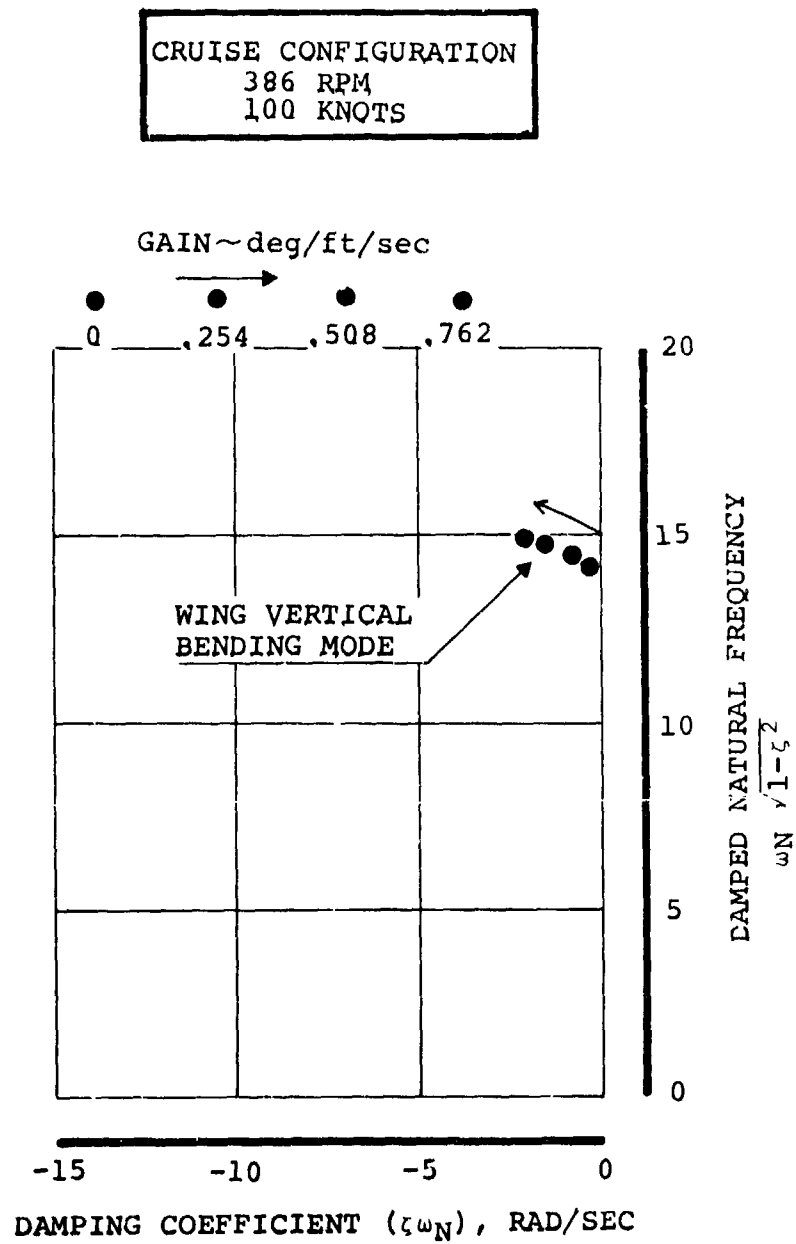


FIGURE 5.49. EFFECT OF RATE FEEDBACK ON WING  
VERTICAL BENDING ROOTS  
100 KNOTS

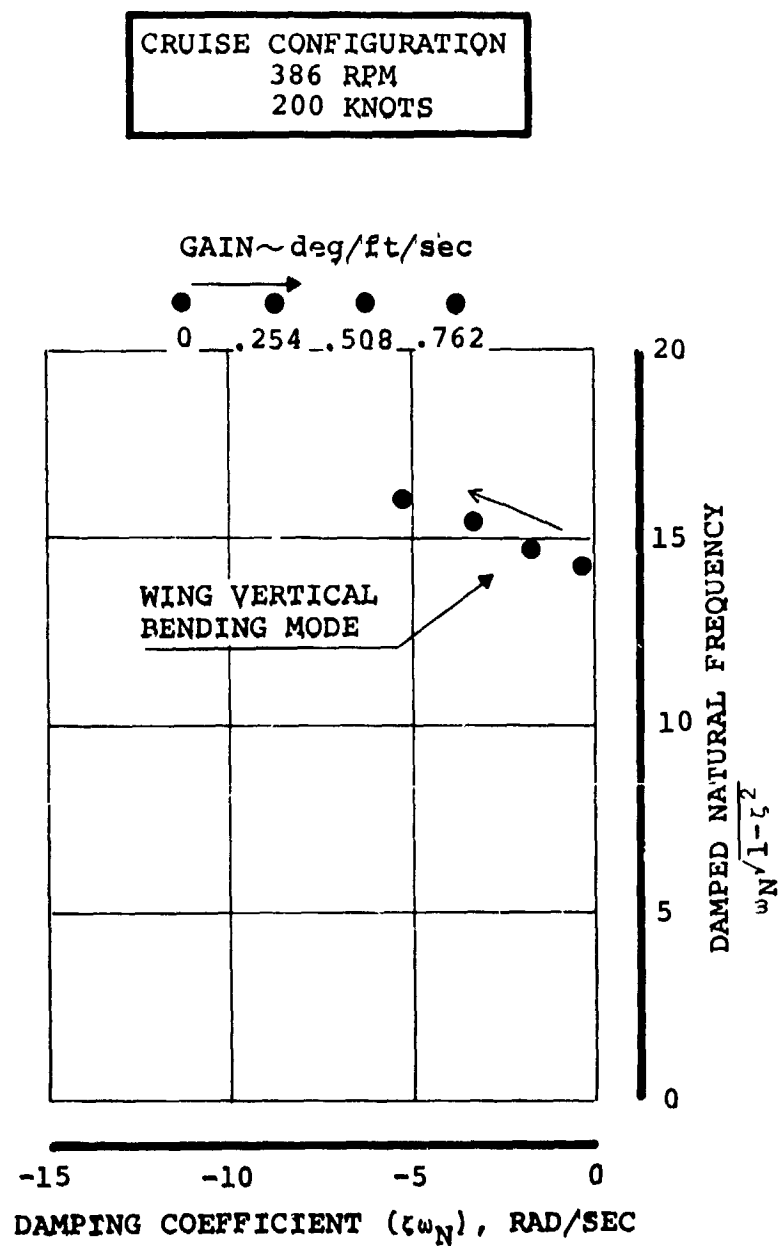


FIGURE 5.50. EFFECT OF RATE FEEDBACK GAIN ON WING VERTICAL BENDING ROOTS 200 KNOTS

Consider the frequency spectrum of Figure 5.3. If the wing vertical bending frequency could be raised to 3 cps without degrading other modes the coalescence of frequencies known as air resonance could be postponed until approximately 400 knots. Then from a dynamics point of view the flight envelope has been widened. Evaluation of the system consisted of examining the Bode plots (Figures 5.51, 5.52, and 5.53) and calculating the stability roots. From the Bode plots there appear to be two 180-degree crossings which may cause trouble. The crossing at 13 cps does not seem to be troublesome because of the dB level being far enough down, however, the crossing at 2.3 cps is a problem and the vertical bending mode will go unstable at higher values of gain. Stability roots were run to see if the system went unstable before a desired level of frequency was reached (Figures 5.54 and 5.55). The root locus shows that high levels of gain are required and that the roots go unstable very quickly.

In summary it is seen that a system based on a rate signal is effective and less troublesome from the point of view of signal shaping than an acceleration based system. The position system could only be expected to be effective very near a stability boundary, so that for purposes of suppression of a basically stable but lowly damped mode, rate feedback should be chosen.



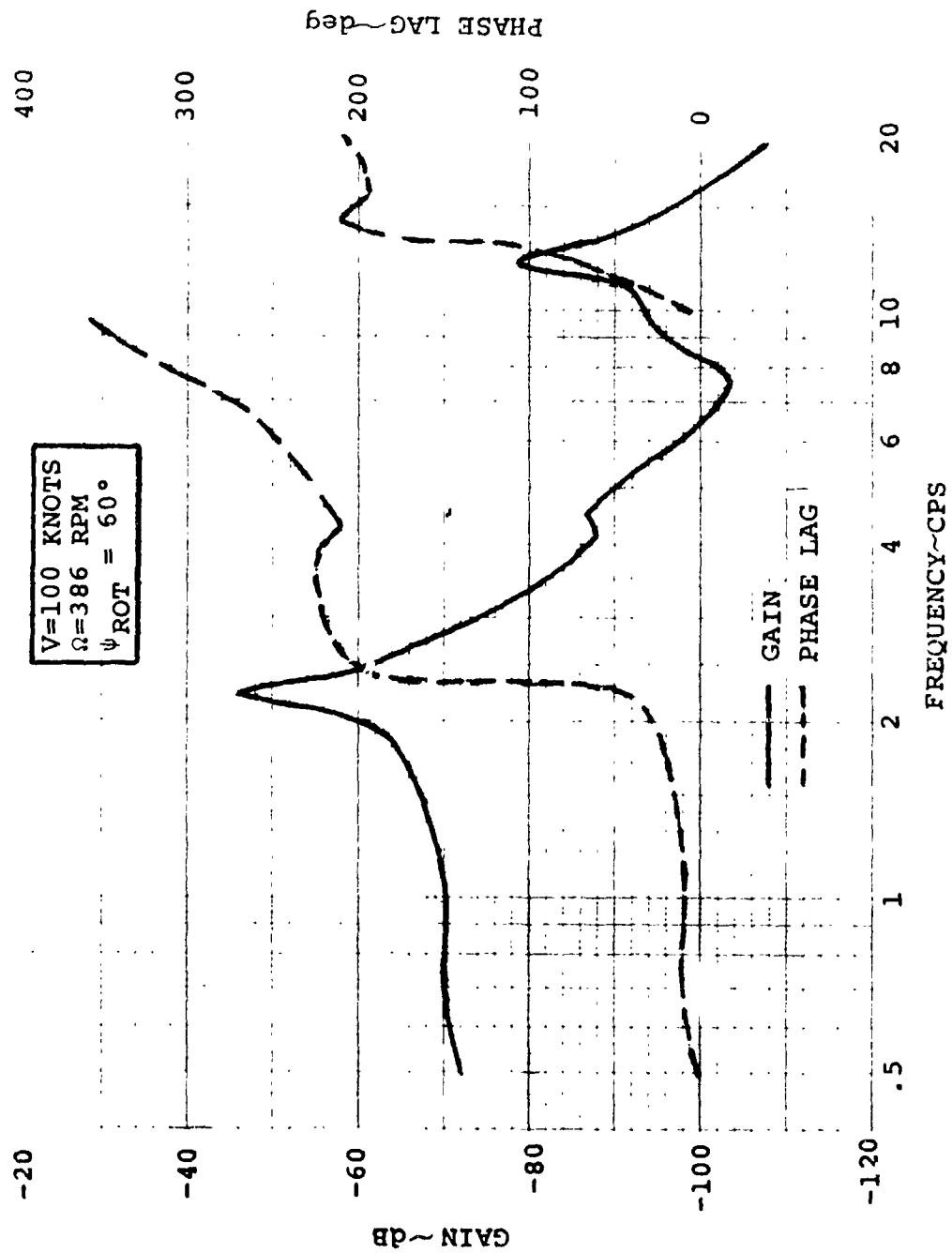


Figure 5.51. Aeroelastic Stability Augmentation System  
 Open Loop Frequency Response -  
 Position Feedback - 100 Knots

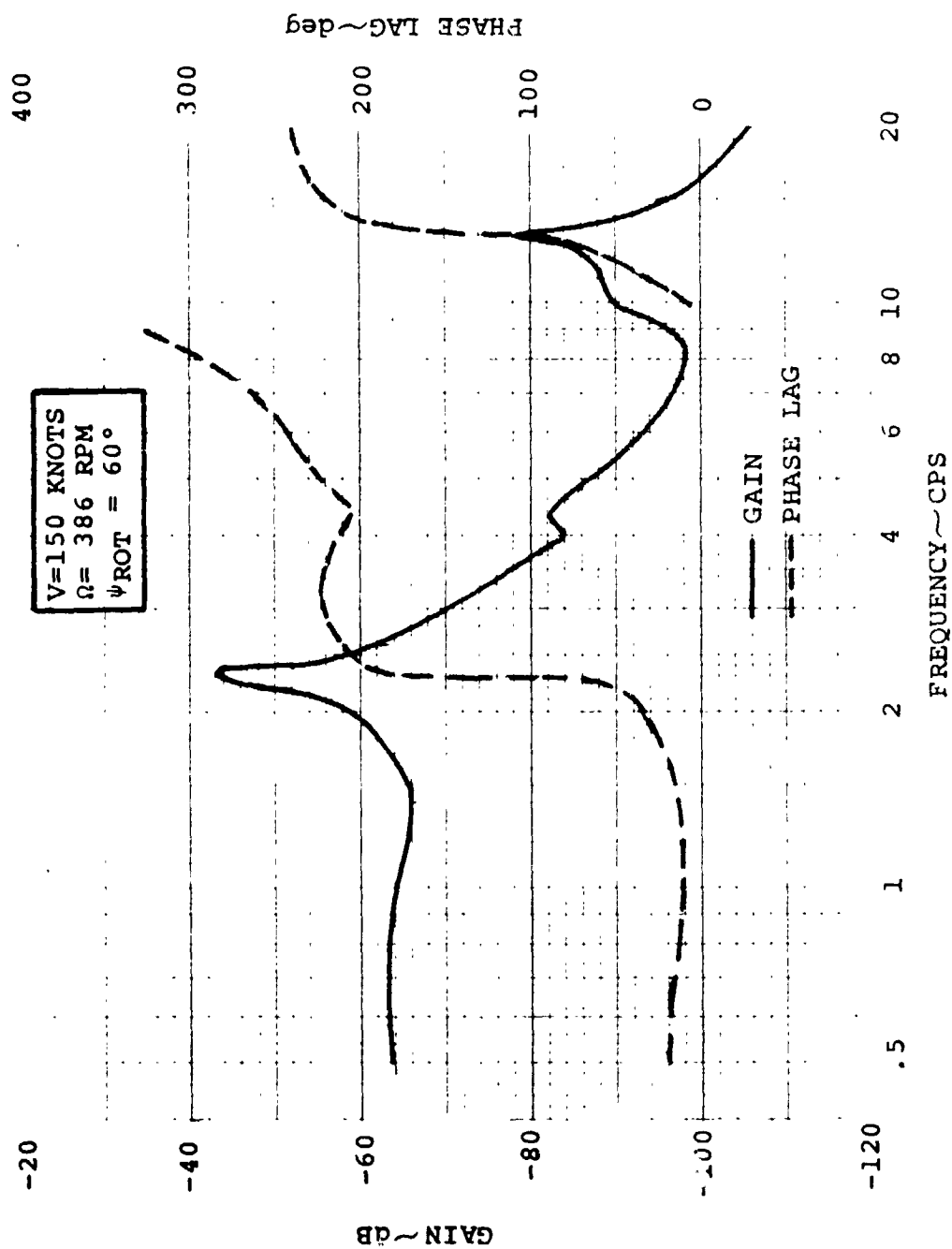


Figure 5.52. Aeroelastic Stability Augmentation System  
Open Loop Frequency Response -  
Position Feedback - 150 Knots

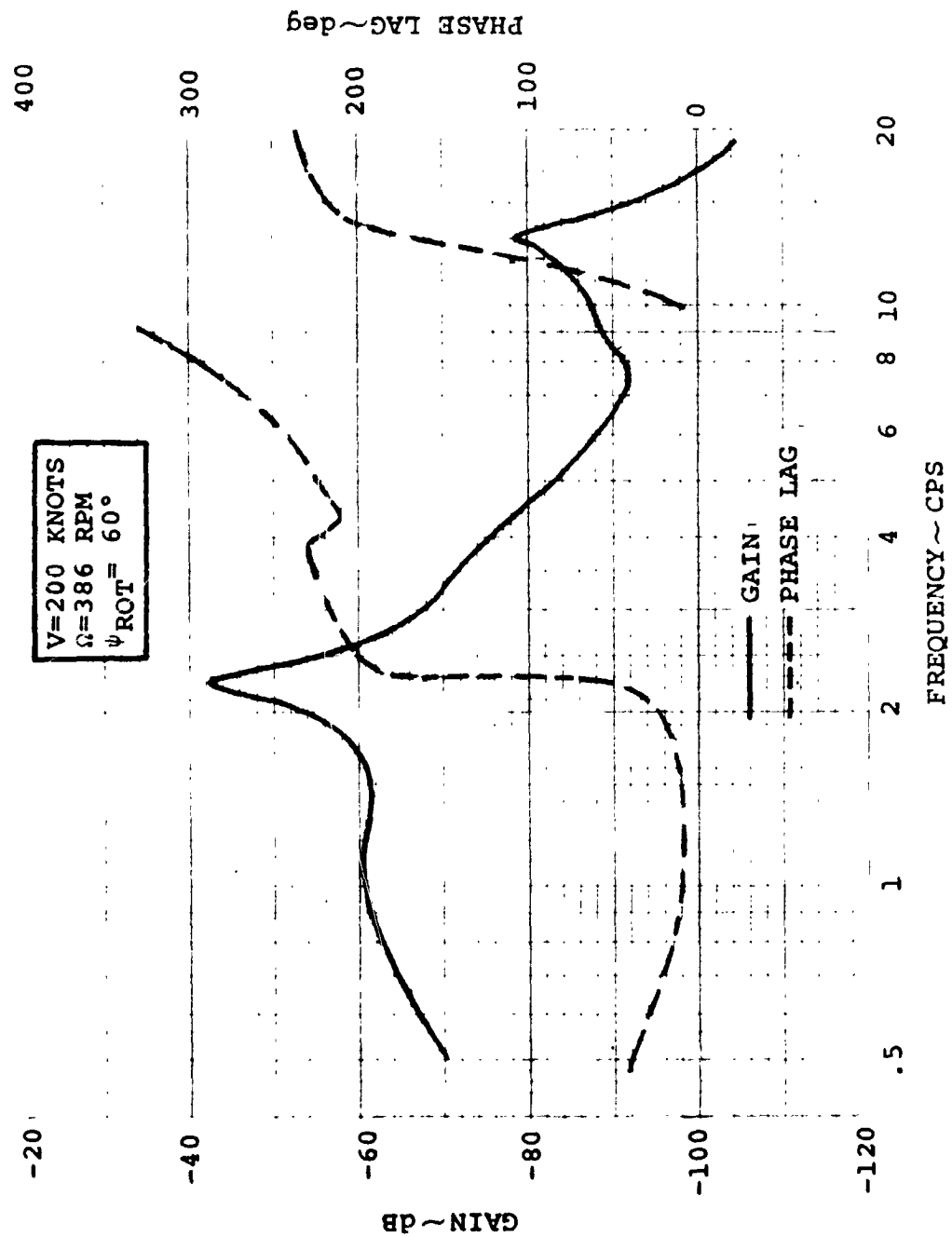


Figure 5.53. Aeroelastic Stability Augmentation System  
Open Loop Frequency Response -  
Position Feedback - 200 Knots

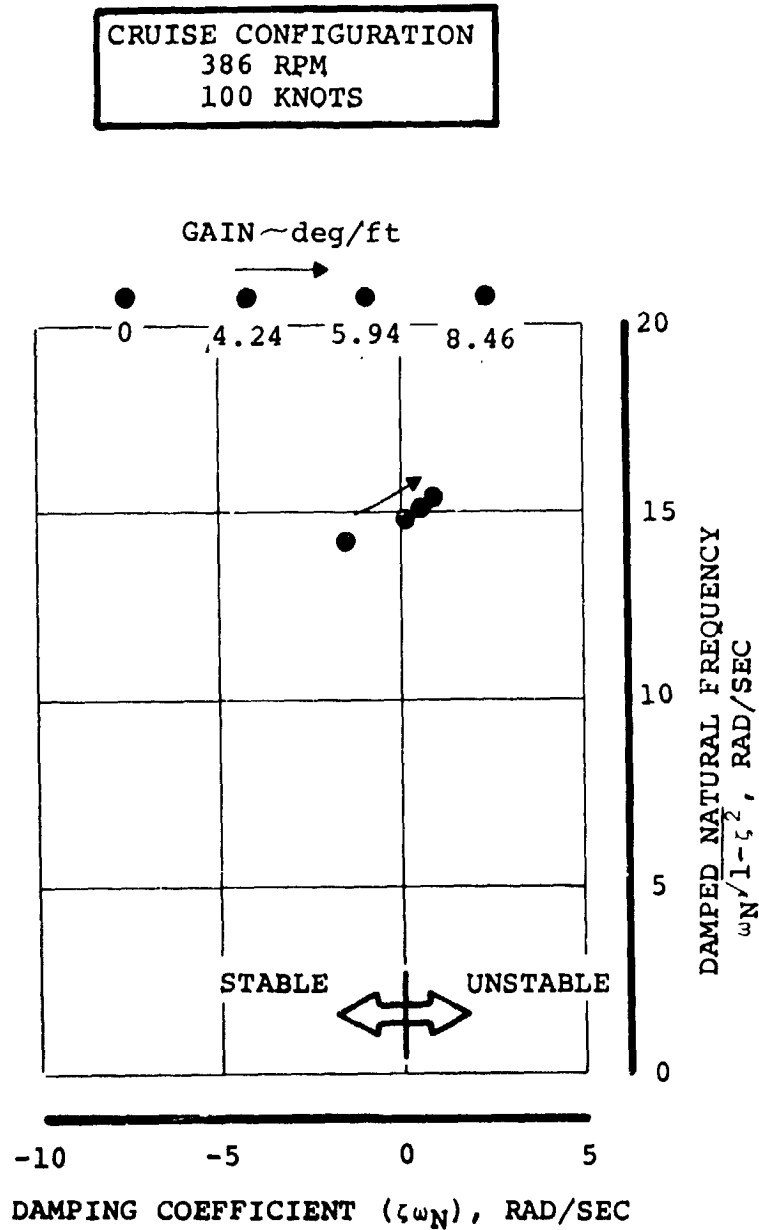


FIGURE 5.54: EFFECT OF GAIN ON VERTICAL BENDING  
STABILITY ROOTS - POSITION FEEDBACK -  
100 knots

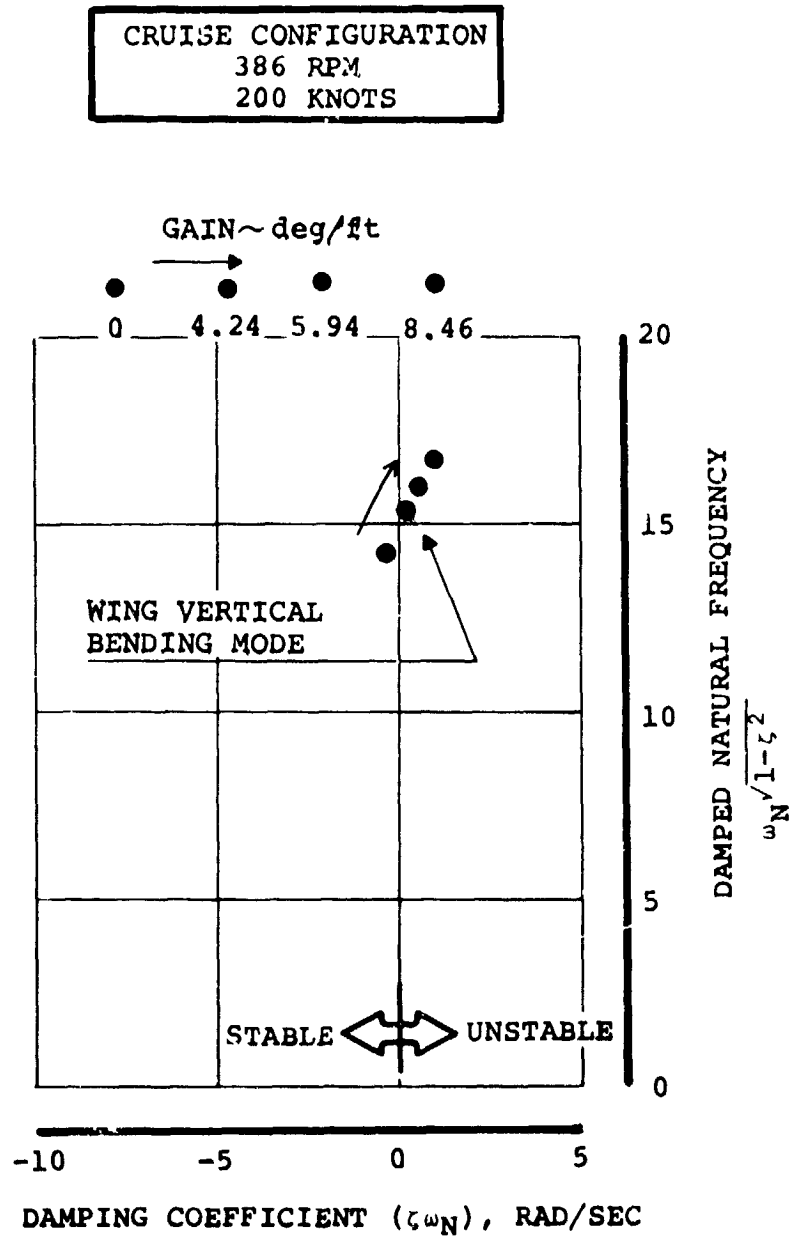


FIGURE 5.55. EFFECT OF GAIN ON VERTICAL BENDING STABILITY  
ROOTS - POSITION FEEDBACK - 200 KNOTS

The important difference between the exploratory analysis (section 5.4) and the more refined analysis of Section 5.5 lies in the fact that in the first approach the azimuth is used to control the system phase relationships, while in the second, force level rather than phase is the criterion for azimuth selection. Hence, in terms of effectiveness of the system per degree of cyclic control authority, the second approach is better; the first system is compromised from the start since some of the authority is being used to control phase instead of generating force.

Following this line of thought it is clear that a still better system may be defined if the available authority is used to generate force only in the direction which is effective. To accomplish this the concept of swashplate "wobble" or phasing between the  $A_1$  and  $B_1$  feedback signals must be introduced.

#### 5.6.1 Phase Swashplate Feedback

Under static conditions the direction of hub force and moment may be controlled completely by selection of the proper ratio  $A_1$  and  $B_1$ . This ratio may be, and frequently is, expressed as a unique axis direction or azimuth about which the swashplate tilts. When dynamic situations are considered it is highly restrictive to continue to think in terms of azimuth since it imposes the constraint of zero phasing between the  $A_1$  and  $B_1$  signals.

The question then arises whether the introduction of relative phasing between the  $A_1$  and  $B_1$  signals can be beneficial in a dynamic system such as those for modal suppression discussed above. To address this question the behavior of the hub forces

resulting from a swashplate oscillation will be discussed more in detail.

It is now known from analysis and test that when the swashplate is given a pitch or yaw oscillation of constant amplitude the resulting oscillatory normal force and side force are phased relative to the swashplate motion and to each other. This means that there is no combination of  $A_1$  and  $B_1$  which can be represented by an azimuth angle which will provide normal force only. Hence, unless special steps are taken some proportion of the authority is dissipated in side force. The special steps involve phasing the  $B_1$  and  $A_1$  feedback signals with respect to each other as derived below.

Stating this in a convenient mathematical form

$$\text{Normal force due to } A_1 \propto A_1 (1 + i \tan \phi_1)$$

$$\text{Side force due to } A_1 \propto A_1 (1 + i \tan \phi_2)$$

Similarly

$$\text{Normal force due to } B_1 \propto B_1 (1 + i \tan \phi_2)$$

$$\text{Side force due to } B_1 \propto B_1 (1 + i \tan \phi_1)$$

Where  $A_1$ ,  $B_1$  are amplitude of pitch and yaw cyclic oscillations

$\phi_1$  is phase of NORMAL FORCE WITH RESPECT TO  $A_1$

$\phi_2$  is phase of SIDE FORCE WITH RESPECT TO  $A_1$

The net side force is given by

$$F_y \propto A_1 (1 + i \tan \phi_2) + B_1 (1 + i \tan \phi_1)$$

$$\text{For } F_y = 0$$

$$\frac{A_1}{B_1} = - \frac{1 + i \tan \phi_1}{1 + i \tan \phi_2} .$$

Hence the condition of  $F_y = 0$  is fulfilled when the relative amplitude

$$\frac{A_1}{B_1} = - \frac{1 + \tan^2 \phi_1}{1 + \tan^2 \phi_2} .$$

And the phase of A relative to B is

$$\begin{aligned} \theta &= \tan^{-1} \frac{\tan \phi_2 - \tan \phi_1}{1 + \tan \phi_1 \tan \phi_2} \\ &= (\phi_2 - \phi_1) \end{aligned}$$

This means that a swashplate motion is identified which does not produce any side force, but generates additional normal force. That is, if normal force and side force produced by a swashplate oscillation have a phase angle  $\theta$  with respect to each other, then imposing this same phase angle on the  $A_1$  and  $B_1$  swashplate motions fed back will effectively reduce the side force to zero. An investigation of the additional effectiveness released by utilizing the swashplate motion to produce only normal force was not possible within the scope of the present contract, but it is clear from the above analysis that determination of this factor is a matter of tedious but elementary manipulation.

In physical terms this means that the feedback system should be designed to produce a wobble in the swashplate rather than a rotation about one unique azimuth axis. In terms of hard-



ware, the only requirement is that independent phase shifting networks be provided for the  $A_1$  and  $B_1$  channels instead of a single device as envisioned in the earlier discussions.

#### 5.6.2 Advantages of Phased or Wobbling Swashplate Control

Immediately identified advantages of phased swashplate control are as follows:

- 0 The fullest use is made of the permitted authority of the system.
- 0 Unwanted side forces are eliminated. In the studies and tests made to date these have not proved to be a problem; however, it is not difficult to envision a situation where side force would stimulate nacelle yaw and possibly introduce new instabilities. Generating only the force specific to the particular mode whose damping is to be increased removes this potential problem.

#### 5.7 CONCLUSIONS

A number of different approaches are possible in designing a swashplate feedback system for modal suppression or damping augmentation. The differences lie in the control of phase and direction of the forces generated by the system. At the simplest level, the best azimuth angle for the swashplate is found with no special account taken of the direction of forces generated. At the second level, the swashplate angle is

selected to produce maximum force level in the direction of the mode, and the phase angle is then controlled electronically. In the most efficient system which eliminates potential side effects and makes optimal use of system authority, the swashplate is given a controlled precession or wobble by introducing a phase angle between the pitch and yaw commands. The difference in cost between the three systems is minimal since only signal conditioning is involved; hence, any practical application of feedback for modal suppression should use the phased swashplate control principle.

6. BLADE TRANSIENT LOADS IN HOVER

6.1 BACKGROUND AND OBJECTIVES

The blade loading discussed in Section 3 arises from skewed flow conditions, and may be alleviated by the application of cyclic pitch in appropriate amounts. In hover, a different type of loading is caused by the rise of cyclic pitch to control the aircraft: this produces coriolis blade loads in the steady state and transient blade response as a result of rapid application of cyclic. There is at present no indication that blade transients generated by cyclic are a problem, as borne out by experience on hingeless rotor helicopters such as the BO-105. Nevertheless, it is of interest to know whether response in the blade modes may be attenuated by the use of feedback control through the swashplate, as an alternative to the more commonly used  $\delta_3$  and  $\alpha_2$  types of mechanical feedback coupling. This type of coupling derives its effectiveness by changing the blade frequency characteristics and would not be admissible for use in a hingeless rotor of optimized design.

The principal restriction of kinematical coupling is that the change in blade angle proportional to blade flap or lag are also in phase with the variable to be modified. Swashplate feedback is not so restricted since rates of blade flap or lag may be sensed and this type of signal, when fed back, is equivalent to the addition of damping. The ability to augment

damping in the blade modes without significantly affecting the frequency characteristics would be an advance in the state-of-the-art which might prove valuable in the future.

To examine the feasibility of such an accomplishment a limited exploratory study was made to determine if feedback would be an efficient method to increase the damping in the lead-lag mode. The study was conducted in two stages:

- o system sensing ideal signal, i.e., blade lead-lag rate
- o system sensing hub in-plane velocity.

Although the investigation did not delve deeply into signal shaping and the optimum configuration, the conclusions drawn are encouraging and indicate that should the requirement arise, a practical system to augment blade damping can be designed using cyclic feedback.

## 6.2 MATHEMATICAL MODEL

The mathematical model used was representative of the symmetrical degrees of freedom of a tilt rotor aircraft in hover. Blade flap and lag modes as well as wing vertical bending, chord, and torsion were included in the model. Representation of the wing elastic modes and the rotor characteristics is similar to the Model 222 tilt rotor aircraft.

Feedback loop characteristics have been represented by transfer functions of control system hardware which have been determined theoretically or by test.

### 6.3 EVALUATION OF SYSTEM SENSING IDEAL SIGNAL

In order to determine a maximum boundary of damping that could be put into the lead-lag mode, the rate of the mode itself was fed back into the cyclic command. It was recognized that this was hardly the basis for a practical system, nevertheless, the results of this study establish criteria for more practical systems. From the block diagram of Figure 6.1, one can see the operation of the system. Blade lead-lag velocity is sensed and filtered through a low-pass filter with a break frequency at 2 cps. The filter was chosen so that signals of higher frequency than  $(\Omega - \omega_L)$  would be attenuated. The filtered cyclic was then fed back through the cyclic actuators in such a manner as to have the maximum cyclic blade angle occur at either 45-degrees or 225-degrees. These two azimuths were chosen to yield a cursory idea of the proper quadrant in which maximum blade angle should occur. Results of the study may be reviewed on Figures 6.2, 6.3, and 6.4. Figure 6.2 indicates that an azimuth of 225-degrees is the proper choice to increase damping in the  $(\Omega - \omega_L)$  mode. Over the gain range investigated, the damping was increased from 2% critical to 13% critical - a significant improvement in terms of structural damping. Root migration with gain is illustrated in Figure 6.3. Note that the path of the roots indicates that pure rate feedback is not being obtained (pure rate feedback is characterized by a root migration that

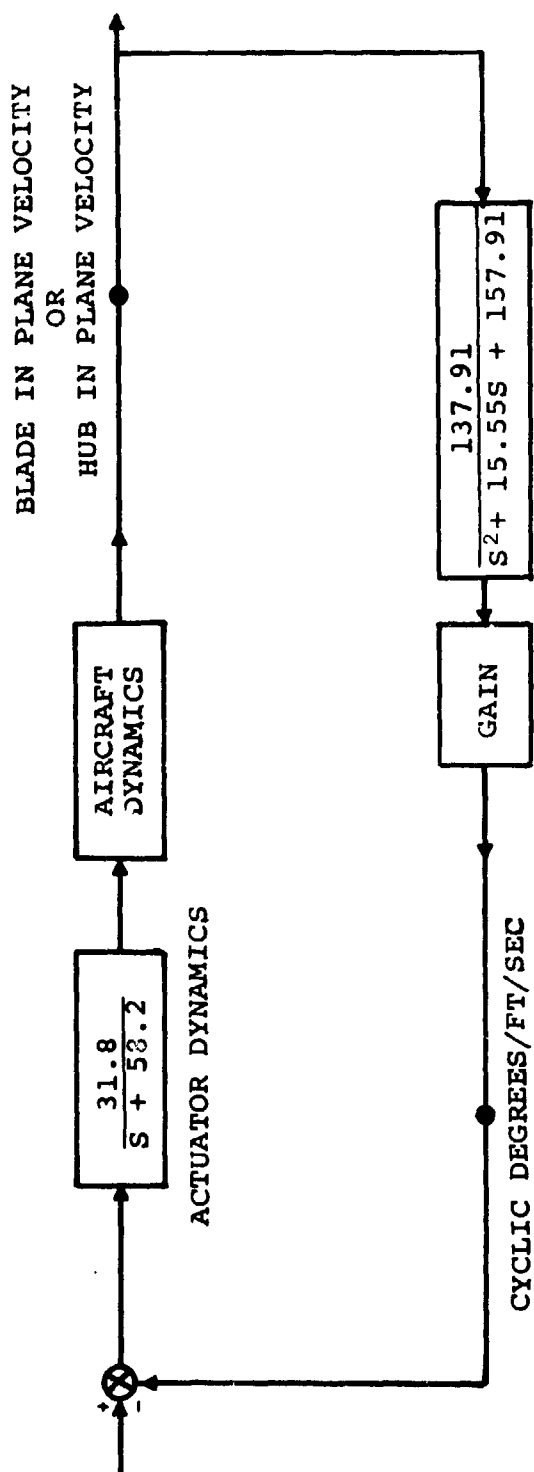


FIGURE 6.1. LEAD-LAG FEEDBACK BLOCK DIAGRAM

SENSOR LOCATION: BLADE TIP  
 FEEDBACK SIGNAL: BLADE LEAD-LAG RATE  
 CONTROL ELEMENT: SWASHPLATE  
 OUTPUT SIGNAL: BLADE CYCLIC PITCH

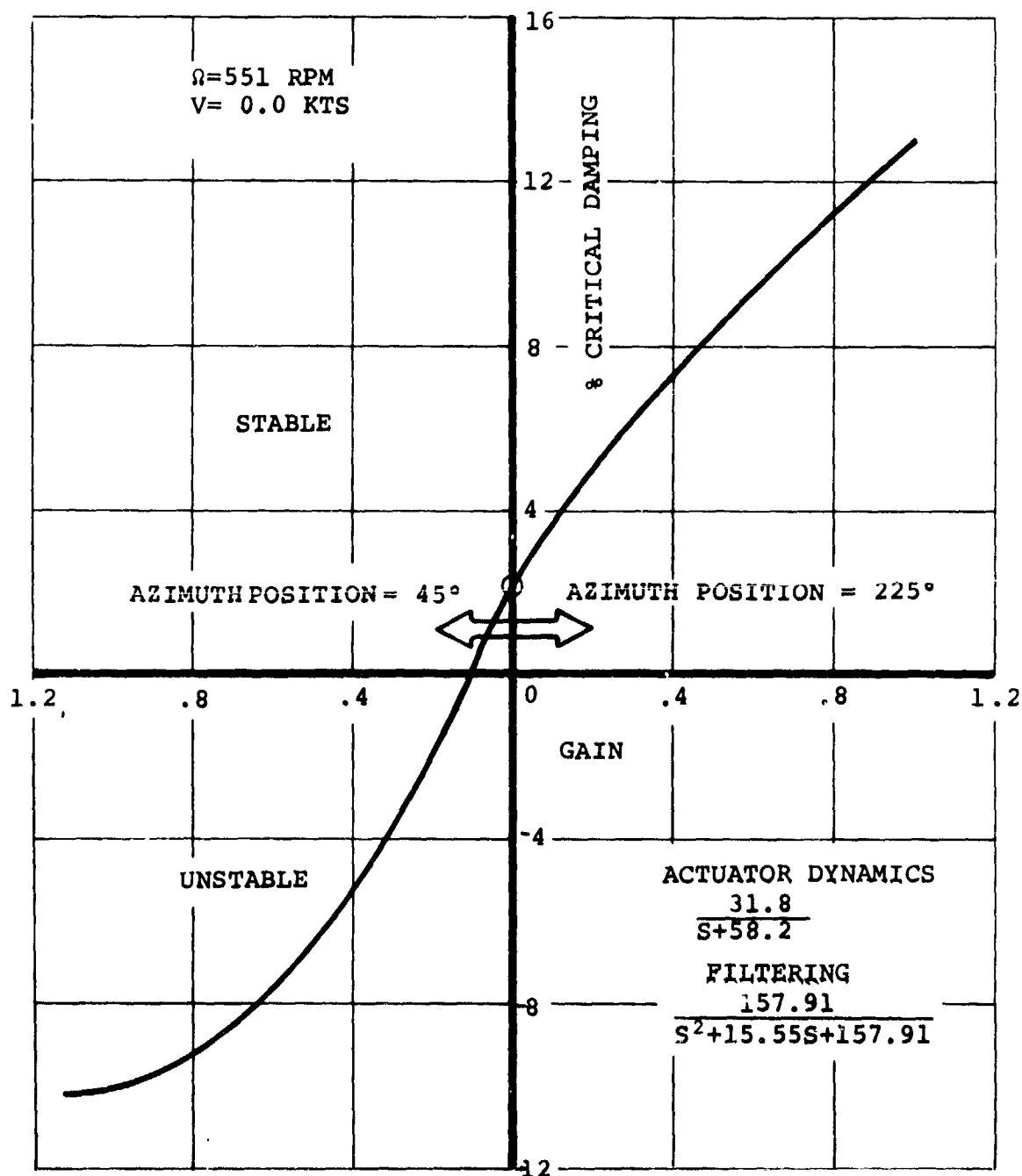


FIGURE 6.2. FEEDBACK EFFECT ON THE LOWER LEAD-LAG MODE

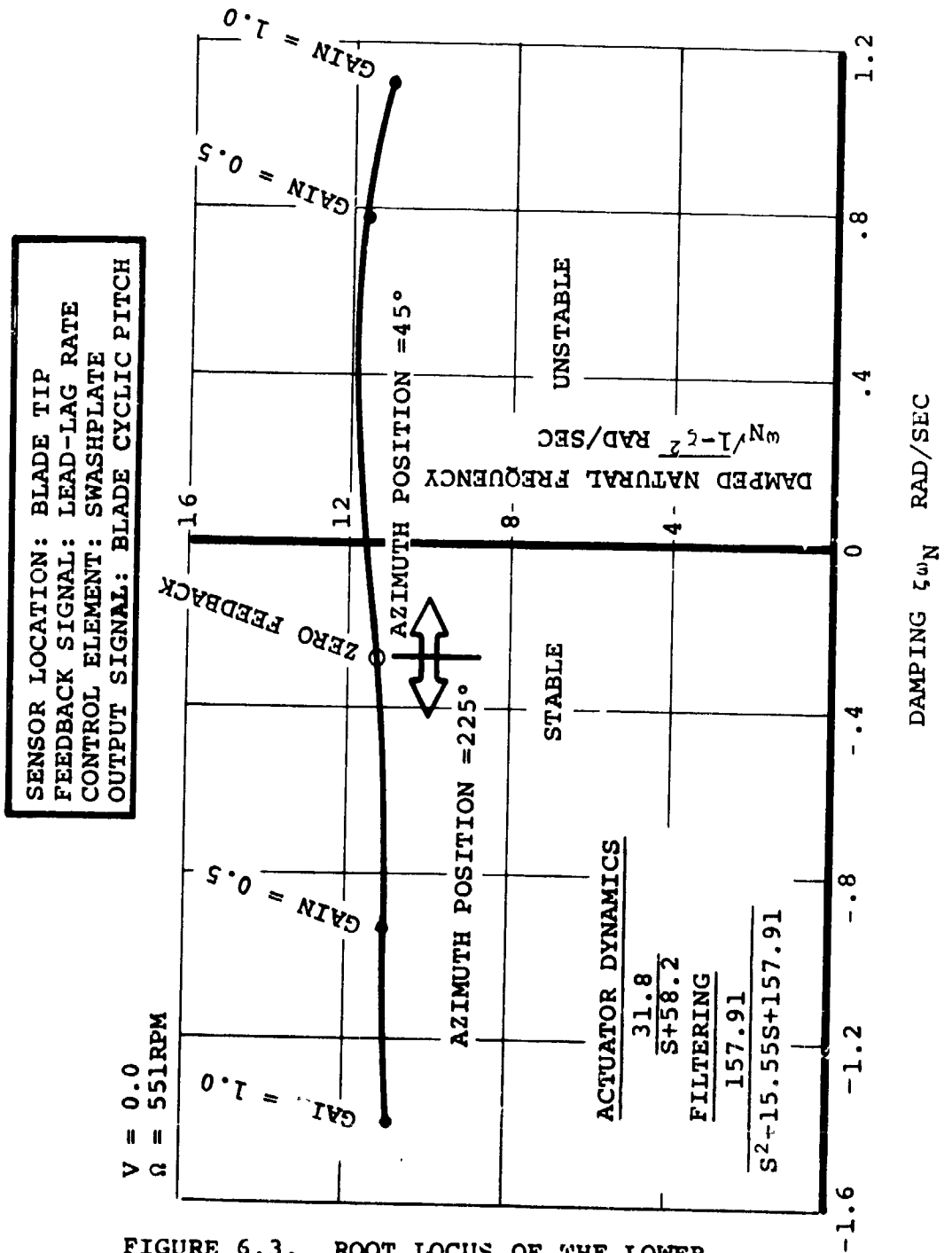


FIGURE 6.3. ROOT LOCUS OF THE LOWER LEAD-LAG MODE



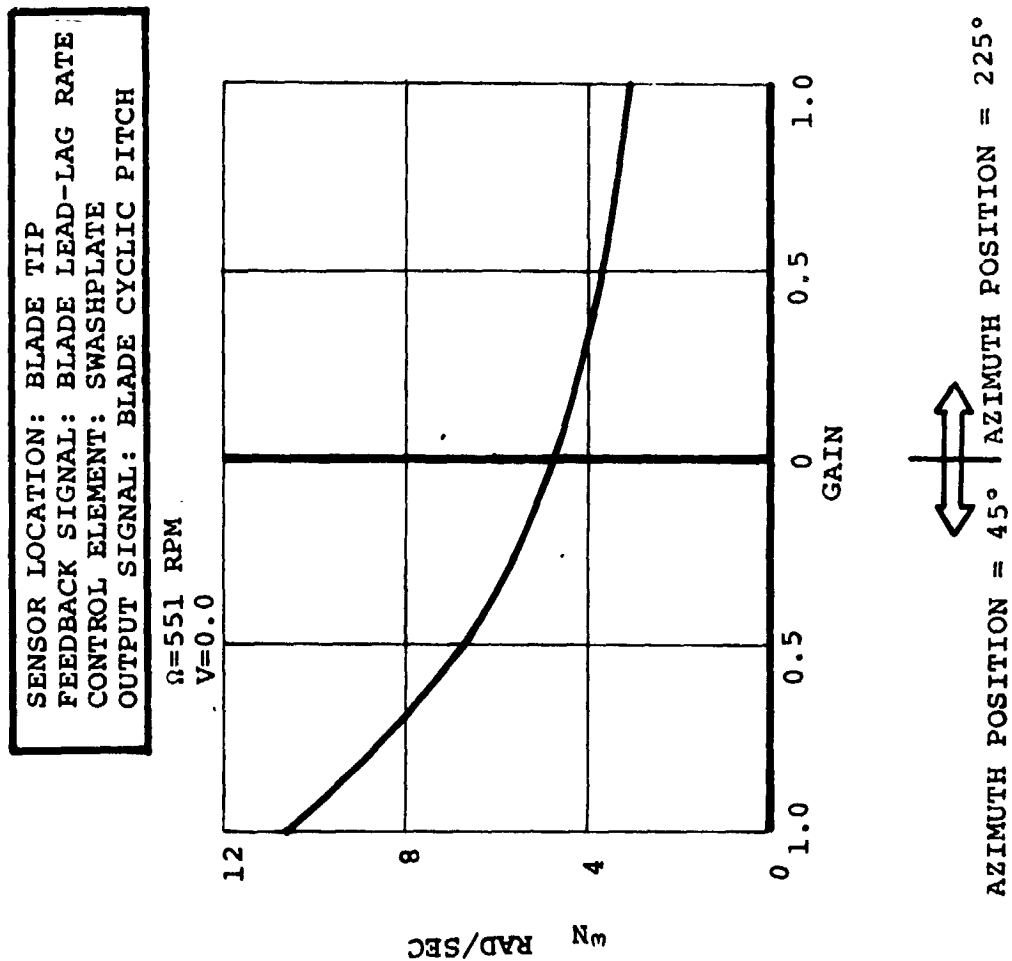


FIGURE 6.4. FEEDBACK EFFECT ON PITCH ATTITUDE

follows an arc with the radius centered at the origin). In fact, there is a phase shift which, if removed, would enable greater values of critical damping to be obtained at lesser values of gain. Degradation of the aircraft characteristics is noted in the root associated with the aircraft pitch degree of freedom. As the gain is increased to the maximum investigated an approximate 30% reduction in the pitch attitude damping coefficient was observed. This is an undesirable by-product which can be eliminated by the proper design of a band-pass filter.

Although the study only entered into limited detail, a significant increase in damping was observed, and it is clear that refinement of azimuth position, phasing and filtering would enable further increases in damping to be obtained.

#### 6.4 EVALUATION OF SYSTEM SENSING HUB IN-PLANE VELOCITY

The study then proceeded to a system using hub in-plane velocity as the feedback signal. Representative actuator and filter transfer functions were used to give some feel for the practical aspects of the problem. Hub in-plane velocity was selected because the  $(\Omega - \omega_L)$  mode of the blade will produce deflections in the plane of the rotor and there is, therefore, some expectation that this signal will produce a similar result when fed back. An accelerometer was mounted

on the hub in a manner to sense hub in-plane acceleration. This signal was integrated to obtain hub in-plane velocity and filtered through a low-pass filter (break frequency at 2 cps) to attenuate the high frequency signals. Four azimuth positions were evaluated: 45-degrees, 124-degrees, 225-degrees, and 304-degrees.

From the evaluation of each of these azimuth positions it was hoped to define the proper quadrant for azimuth position and to obtain a feeling for the optimum gain range. Figures 6.5 through 6.10 delineate the results of the study. For all azimuth positions and gains the system appeared to be very ineffective in augmenting the damping of the  $(\Omega - \omega_L)$  mode.

There was a strong effect on the pitch attitude and a coupled vertical bending mode which can be eliminated by proper filtering. The investigation was suspended at this point. It is believed that with further refinement the design of the feedback loops (with strict attention to the phase relationships) a significant increase in the damping could be obtained.

#### 6.5 CONCLUSIONS

Damping in the lower lead-lag mode  $(\Omega - \omega_L)$  may be increased by the use of feedback as shown by the results for the ideal system studied. Design of system for operational use will entail further study of sensors, signals and feedback loops.

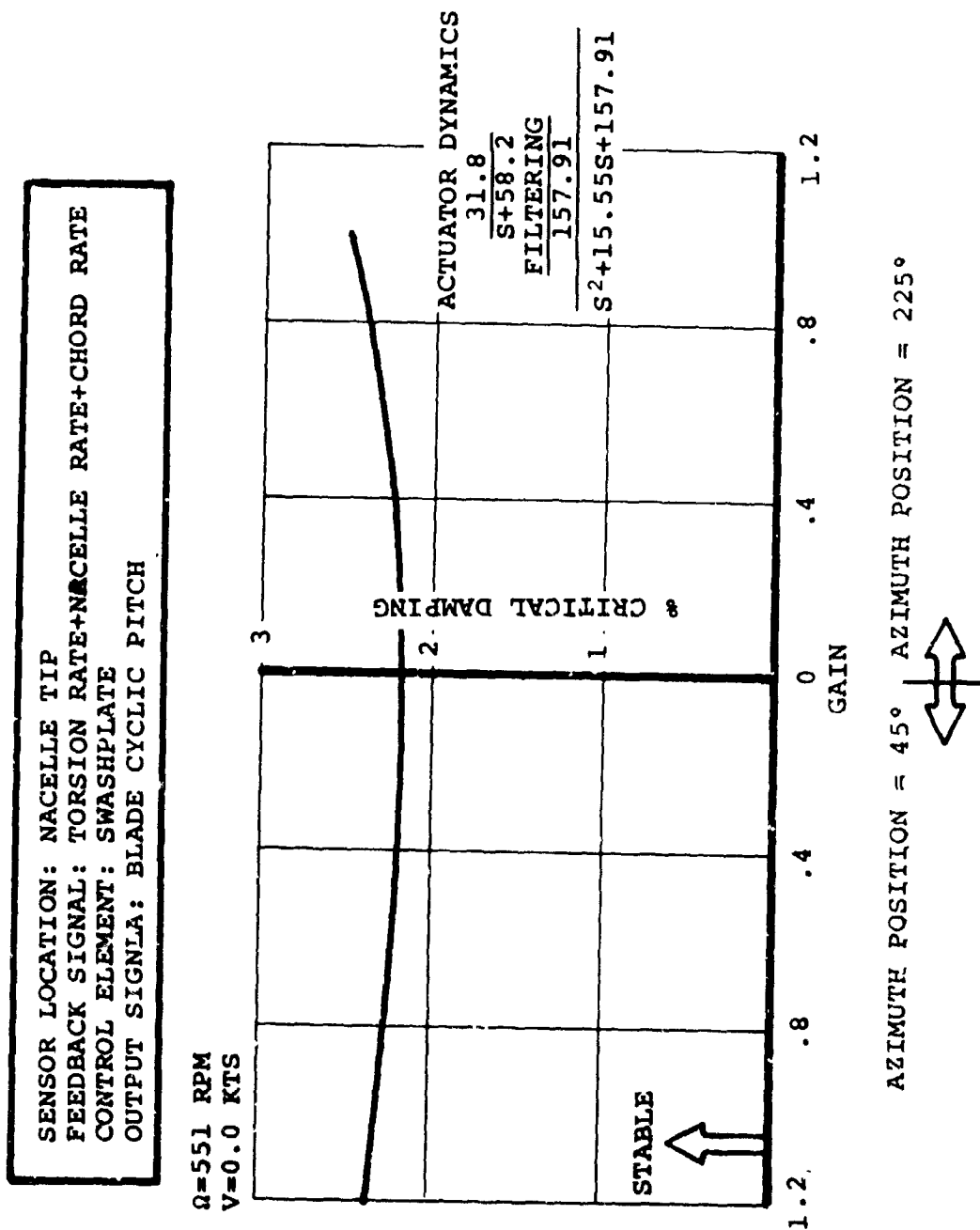
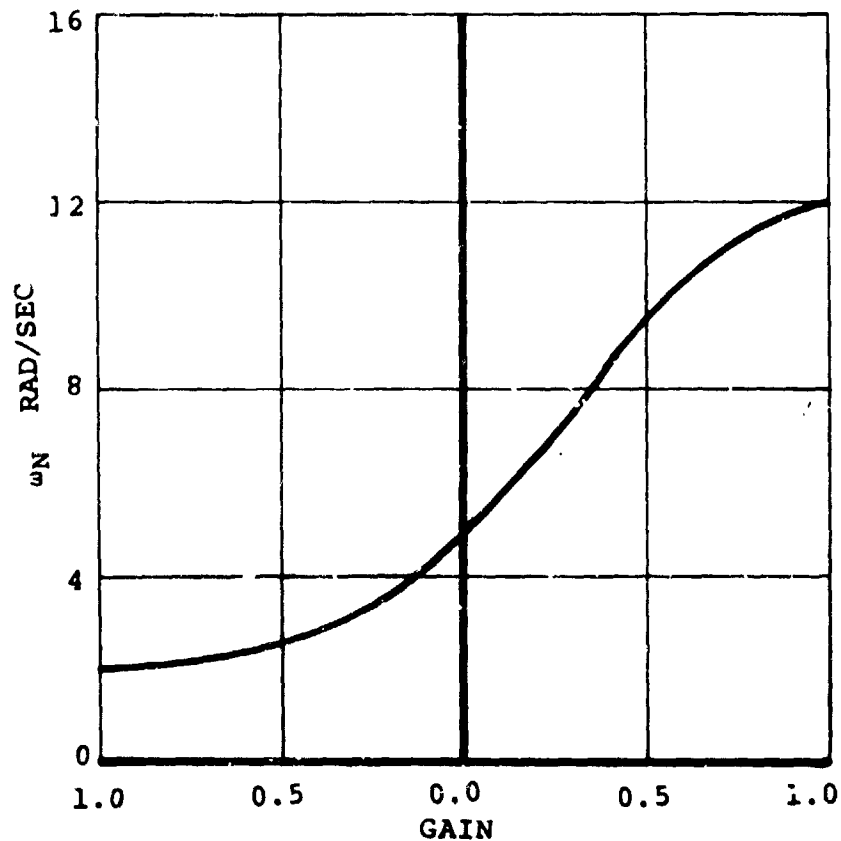


FIGURE 6.5. FEEDBACK EFFECT ON LOWER LEAD-LAG MODE

SENSOR LOCATION: NACELLE TIP  
FEEDBACK SIGNAL: TORSION RATE + CHORD RATE  
+ NACELLE RATE  
CONTROL ELEMENT: SWASHPLATE  
OUTPUT SIGNAL: BLADE CYCLIC PITCH

$\Omega = 551 \text{ RPM}$   
 $V = 0.0$





**FIGURE 6.6 FEEDBACK EFFECT ON PITCH ATTITUDE**

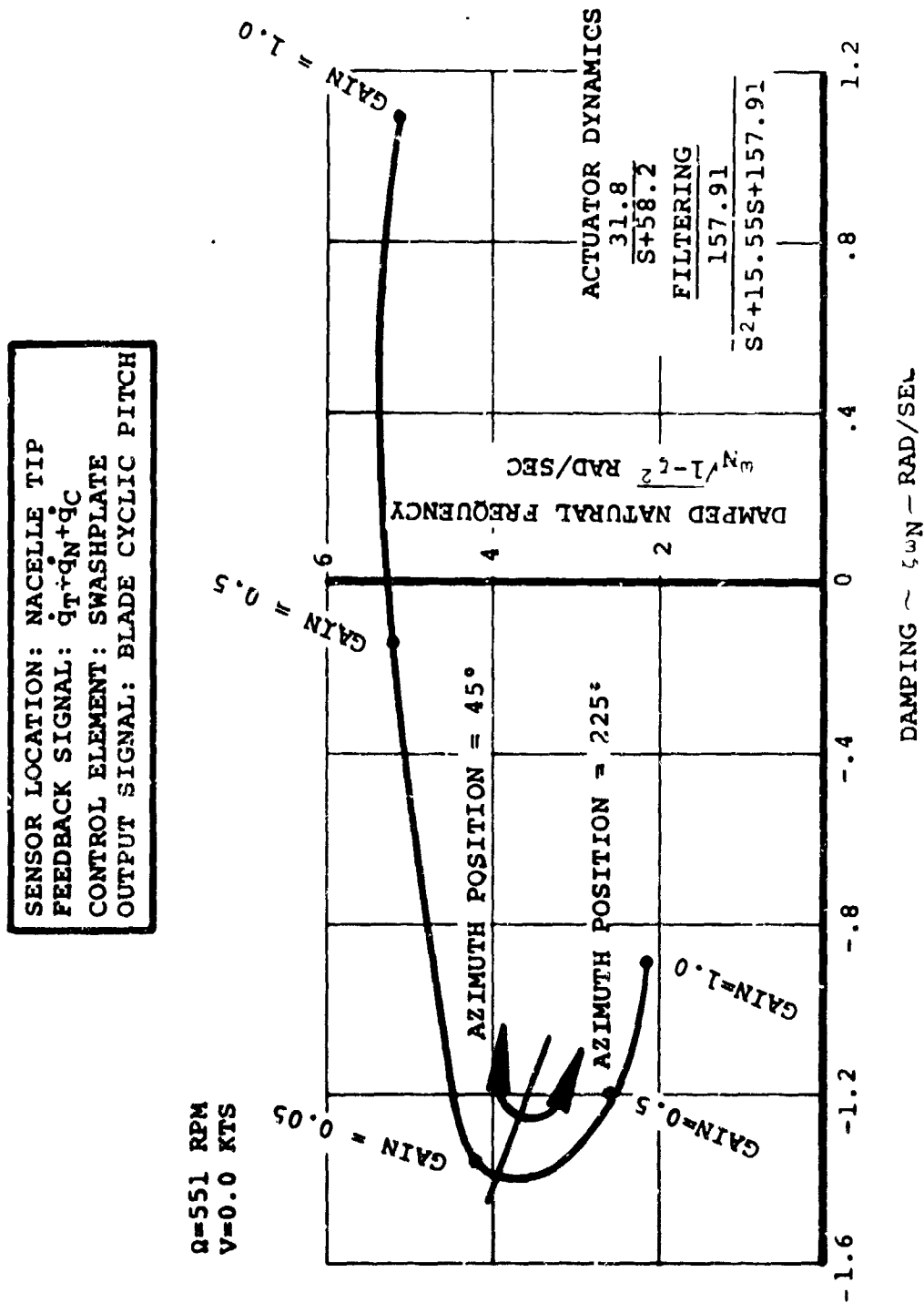


FIGURE 6.7. ROOT LOCUS OF COUPLED VERTICAL BENDING/LEAD-LAG MODE

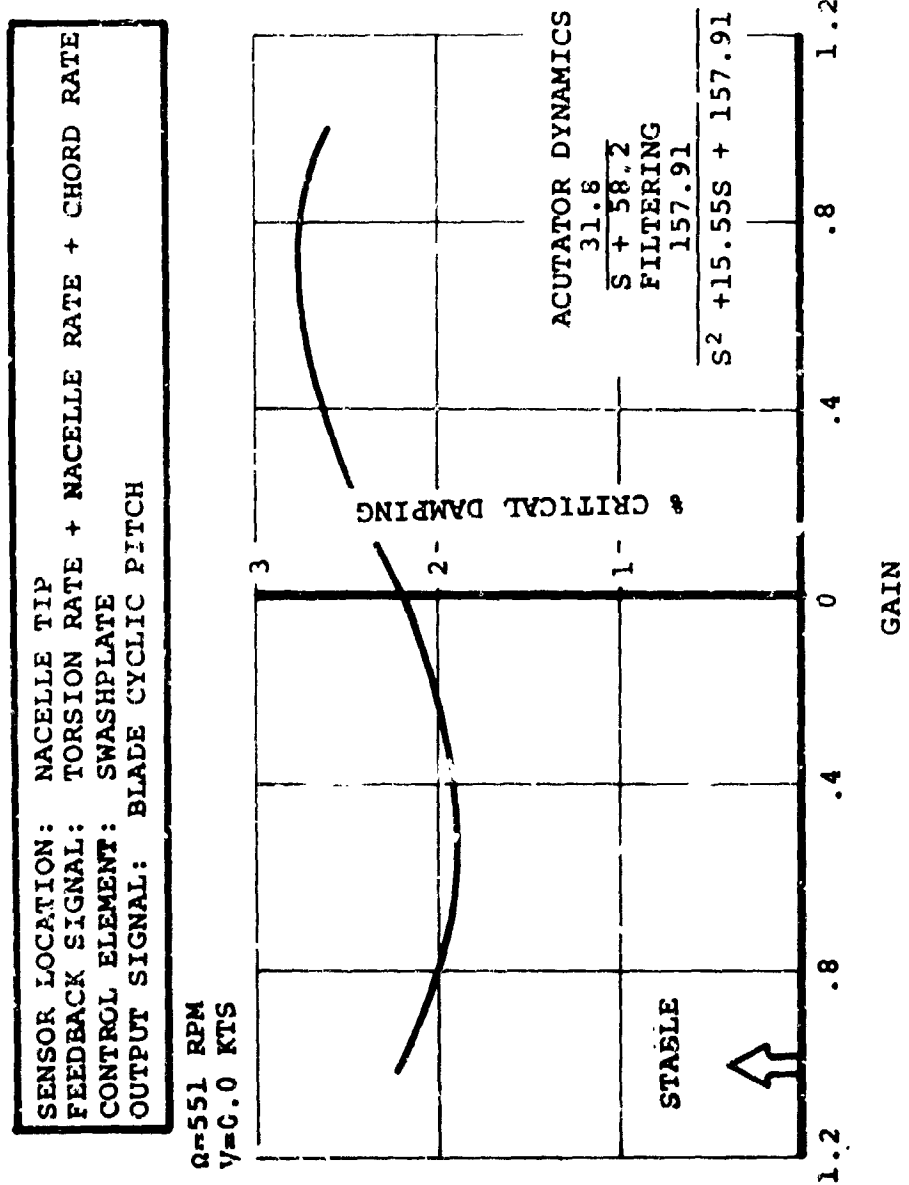
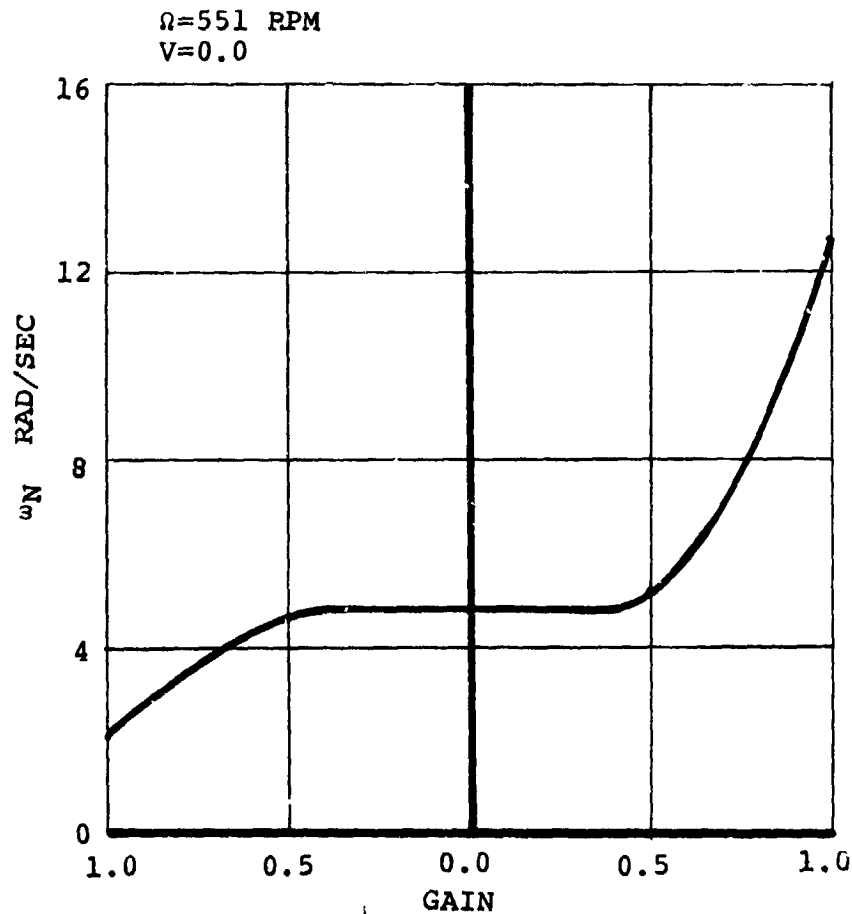


FIGURE 6.8. FEEDBACK EFFECT ON THE LOWER LEAD-LAG MODE

SENSOR LOCATION: NACELLE TIP  
 FEEDBACK SIGNAL: TORSION RATE + CHORD RATE  
 + NACELLE RATE  
 CONTROL ELEMENT: SWASHPLATE  
 OUTPUT SIGNAL: BLADE CYCLIC PITCH



AZIMUTH POSITION =  $124^\circ$  ↔ AZIMUTH POSITION =  $304^\circ$

FIGURE 6.9. FEEDBACK EFFECT ON PITCH ATTITUDE



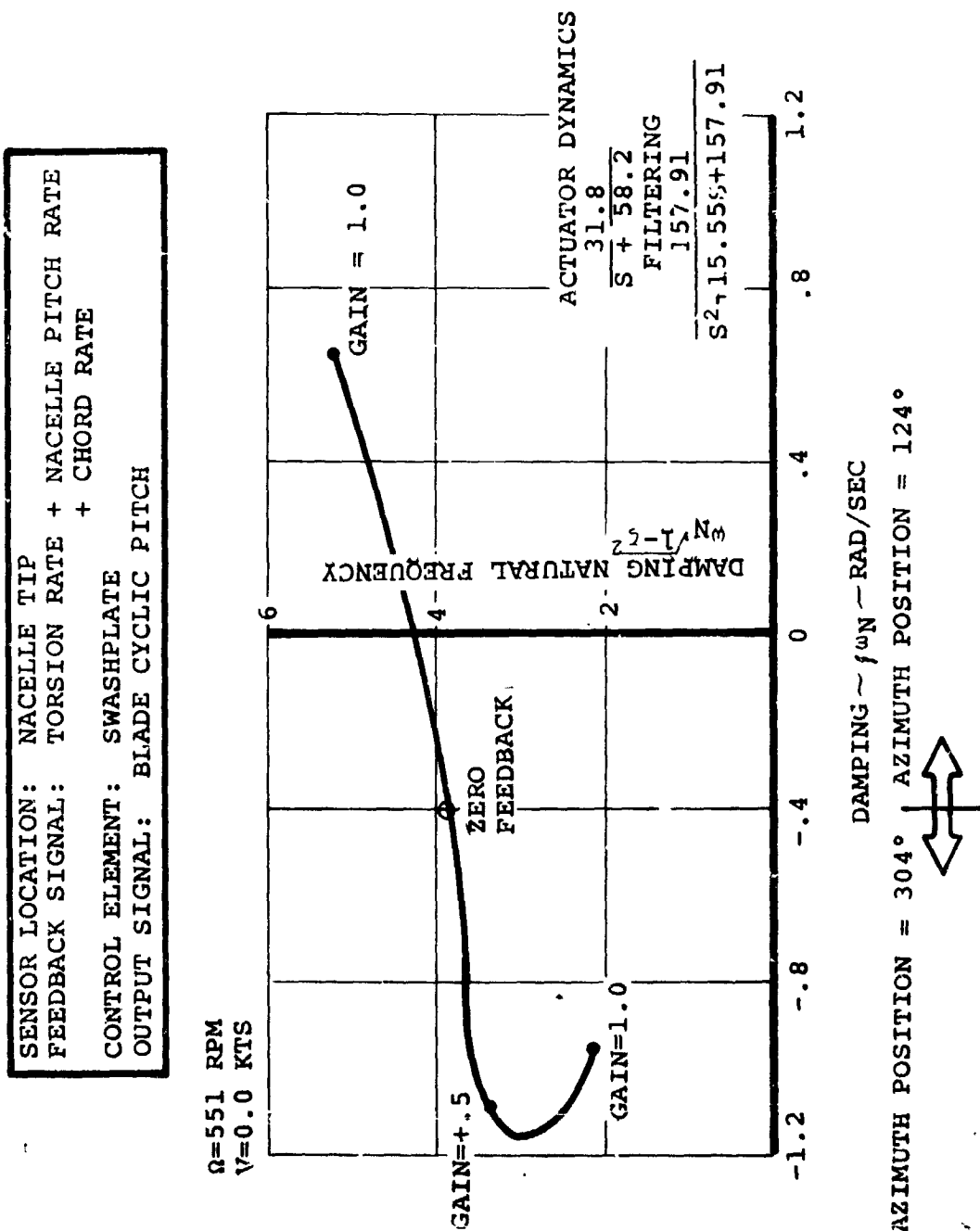


FIGURE 6.10. ROOT LOCUS OF COUPLED VERTICAL BENDING/LEAD-LAG MODE

## 7. THRUST MANAGEMENT AND ROTOR GOVERNING FEEDBACK SYSTEMS

### 7.1 BACKGROUND

Although the study of governing systems was not specifically a part of the work statement of this contract, the study of feedback systems to minimize aircraft response to axial gusts was included in the statement of work. Since the rotor and aircraft response to axial gusts can be completely changed by changes in governing systems, and in fact the governor can itself be the feedback system to minimize gust response, it was necessary to study the governing system as a whole.

This section therefore addresses the problems associated with the design of a thrust management and rotor governing system for a tilt rotor aircraft with large diameter flexible rotors which are lightly loaded in cruise. The power plants are located close to the rotors and cross shafting is provided so that a single power failure can be accommodated.

In a helicopter, rapid response to pilot demand for changes in thrust is of paramount importance to permit accurate height control in hover and near vertical flight. This requirement has resulted in helicopters with direct pilot control of collective pitch, with the governor maintaining rpm by governing fuel flow. In a turboprop airplane, the pilot wants to be able to demand a fixed power, (e.g. max power throughout take-off, or normal rated power throughout climb) and so turboprop

airplanes give the pilot direct control of power (fuel flow) and the governor maintains rpm by governing blade pitch.

A V/STOL aircraft such as a tilt rotor which flies in both helicopter and fixed wing modes needs to meet both of these requirements, so that either both types of governing systems must be installed with some changeover from one to the other as flight mode is varied, or one system must be made to meet satisfactorily the requirement of all regimes of flight.

Use of pilot demand of collective in cruise is considered unacceptable because the extreme sensitivity of power to collective pitch in this regime appears to make it impractical to give the pilot adequate control sensitivity. Installation of two separate systems is undesirable from the point of view of complexity and pilot work load.

Adaptation of the fixed wing airplane system of power demand and collective governing to the helicopter mode can be achieved by making a mechanical demand for collective pitch coincident with the power demand and having the governor perform only a trimming function on the mechanically demanded collective. Such a system is used on the Canadair CL-84, and has received favorable pilot comment. This system has therefore been selected for tilt rotor.

## 7.2 STUDY APPROACH

The study uses three methods of evaluation:

- O inner loop response
- O outer loop response
- O gust response

Inner loop response concerns the RPM response when separated from the aircraft rigid body modes; that is, the aircraft is restrained from moving longitudinally, laterally, vertically and in pitch, roll or yaw. Pertinent structural modes and blade elastic modes remain in the model (See Appendix A for description of math model). Use of this method simplifies the studies and allows the analyst to evaluate the governor only. In the outer loop response all inner loop degrees of freedom are maintained and the aircraft rigid body modes of interest are added to the model. With this technique the analyst knows the governor characteristics from the inner loop response and can concentrate on evaluating the effect on aircraft flying qualities (such as dutch roll response in cruise or vertical response in hover). Gust response evaluation uses the outer loop model and "hits" it with a gust of known magnitude and shape. Time history responses are obtained and effect of the governor on aircraft ride qualities and structural response may be evaluated.

Using these techniques of evaluation three governor configurations were studied:

- O single governor with one sensor (Figure 7.1)
- O dual independent governors (Figure 7.2)
- O single governor with sensors on each rotor (Figure 7.3)

Two modes of operation were considered for each governor. The all operational mode (i.e., all aircraft components operational and performing as designed) and the cross-shaft failure mode (i.e., the cross-shaft connecting the two rotors has been severed and they are free to rotate independently).

The study has been divided into four sections. The first deals with the criteria developed for evaluation of the governor on a tilt rotor aircraft. The second section evaluates the three governor configurations and a final configuration is chosen. Third, the effect of the governor on aircraft flying qualities is evaluated and lastly the aircraft gust response for conditions of no governor, fuel governor and collective pitch governor are analyzed.

### 7.3 DESIGN CRITERIA

Governing accuracy criteria were set up, based on fixed wing propeller airplane experience. The criteria used were:

- O Maximum error of .3% within 3 seconds  
of a disturbance
- O Maximum overshoot of 2% rpm in the transient  
response to a step input

Fulfillment of these goals requires that the RPM variation

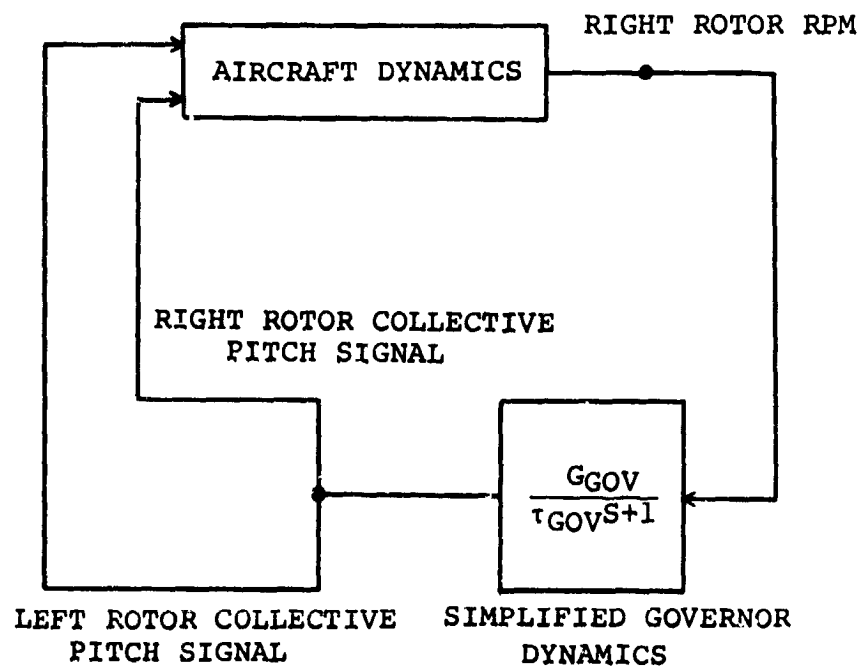


FIGURE 7.1. CANDIDATE GOVERNOR SCHEMATIC  
SINGLE GOVERNOR WITH ONE SENSOR

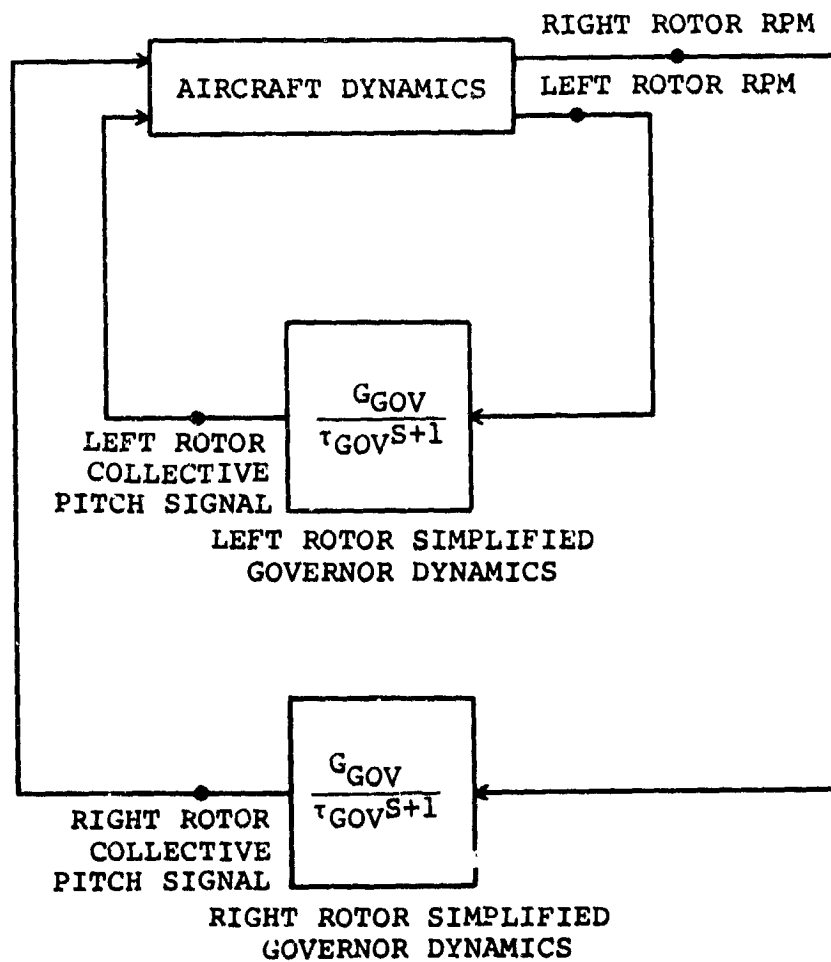


FIGURE 7.2. CANDIDATE GOVERNOR SCHEMATIC  
DUAL INDEPENDENT GOVERNORS

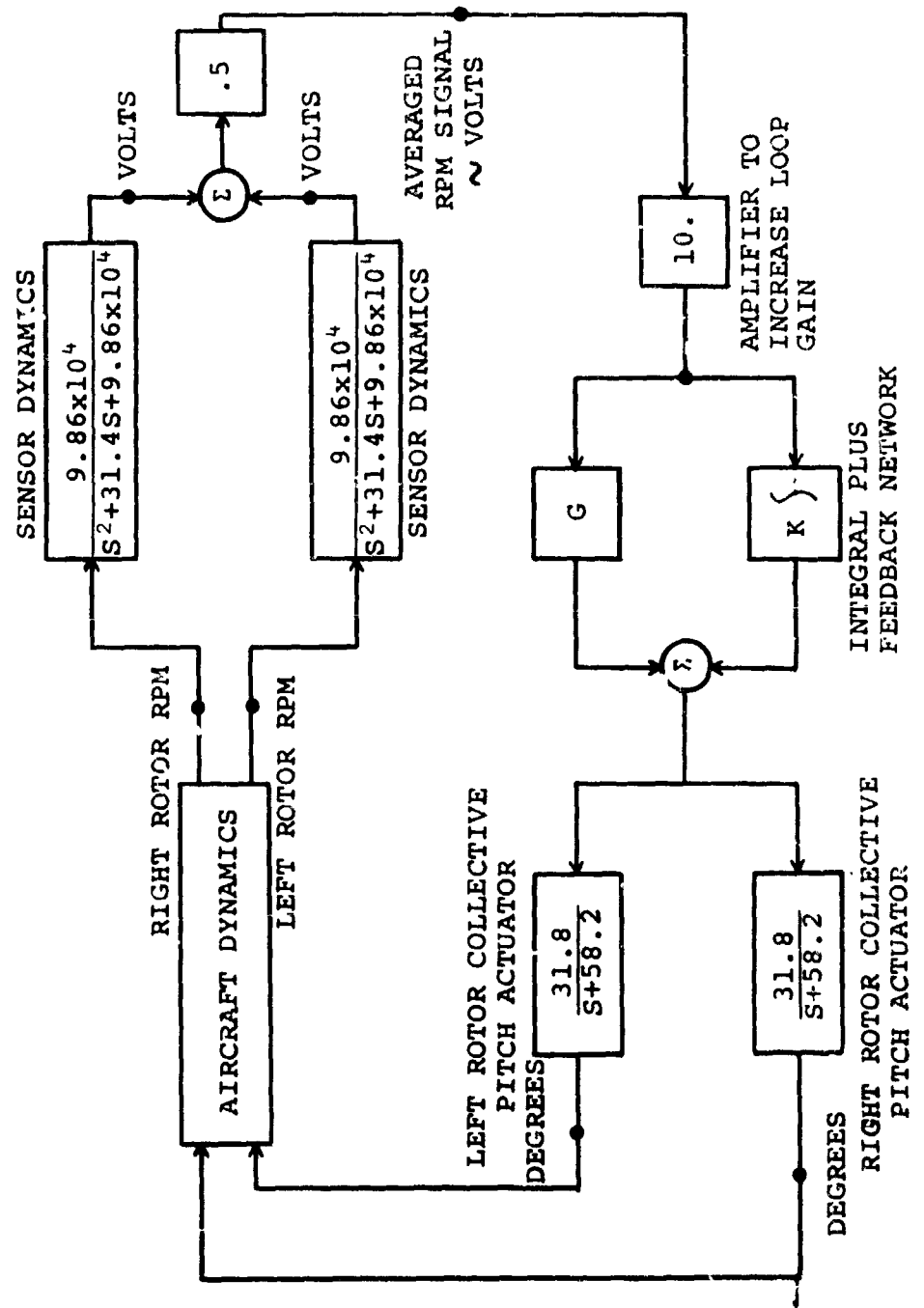


FIGURE 7.3. CANDIDATE GOVERNOR SCHEMATIC  
SINGLE GOVERNOR WITH TWO SENSORS



mode has a frequency of 3.0 radians per second and a damping coefficient of .8. These requirements should be fulfilled in the all-operational mode and the cross-shaft failure mode.

Flying qualities of the aircraft should not be adversely affected; that is, the governor configuration should not affect the rigid body modal response in such a manner that they do not meet the applicable specification requirements. The flying qualities portion of the study will concentrate on evaluating the effect of the governor on:

- O vertical damping in hover
- O roll damping in hover
- O dutch roll damping in cruise
- O phugoid damping in cruise

It is the goal of this study to reduce the axial gust response of the rotor to a near zero level, however, if this is not achievable axial accelerations of .2"g" will be tolerated for a gust velocity of 20 fps. This level of gust response is a result of studies performed for the SST to determine objectionable threshold gust response characteristics in cruise.

#### 7.4 EVALUATION OF COLLECTIVE PITCH GOVERNOR CONFIGURATIONS

Evaluation of the three governor configurations was performed to determine which would best suit the needs of a tilt rotor aircraft. Inner loop studies were made for all configurations

and some limited outer loop studies were made when necessary. The all-operational and cross-shaft failure modes were considered for each configuration.

#### 7.4.1 Single Governor With One Sensor

As shown in Figure 7.1, the single governor with one sensor would sense rotor RPM of either the left or right rotor (in this case the right rotor) and use the error signal to drive collective pitch for governing of both rotors. In the all-operational mode this governing concept is acceptable in that cross-shafting forces the rotors to rotate in unison and rotor RPM is essentially identical. However, if the cross-shaft fails the rotors are spinning independently; therefore, only the side with the sensor is being governed. This effect can be seen from the stability root variation with gain of Figure 7.4. The root associated with the left rotor RPM is not affected by changing governor gain which indicates that this rotor is not being governed. The operation depicted by the root is unacceptable and disqualifies this configuration from further consideration.

#### 7.4.2 Dual Independent Governors

The dual independent governor configuration (Figure 7.2) operates on each rotor separately with no inter-rotor

SINGLE GOVERNOR - 1 SENSOR (RT. ROTOR)  
 HOVER INNER LOOP  
 RPM FEEDBACK  
 $\tau = 0.0$   
 NO CROSS SHAFT

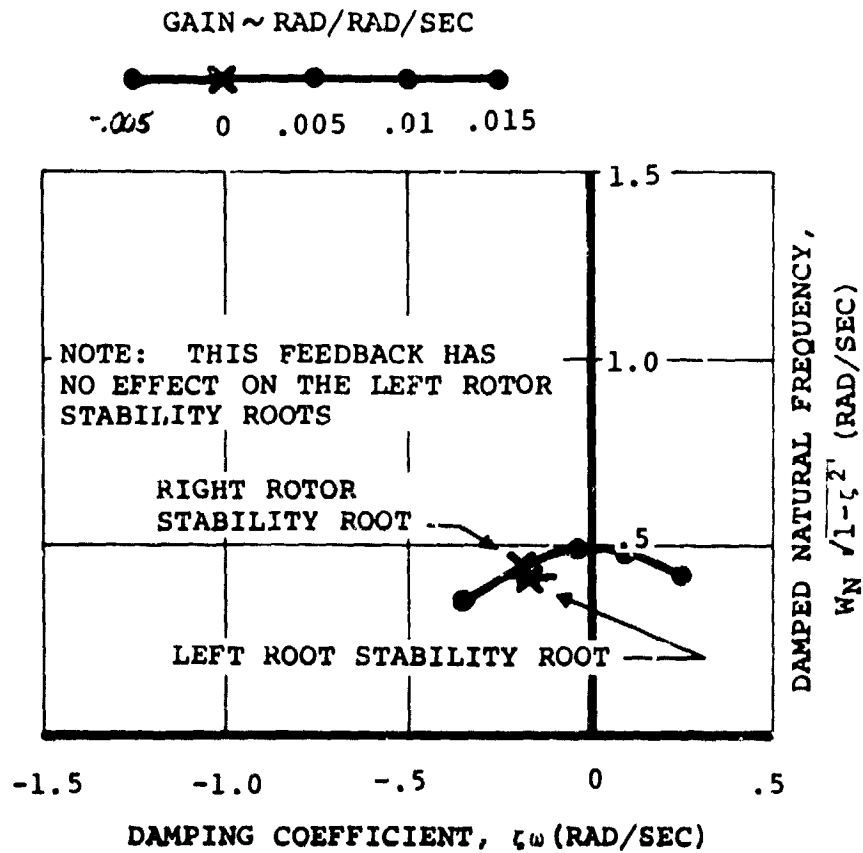


FIGURE 7.4. SINGLE GOVERNOR WITH ONE SENSOR - STABILITY ROOT VARIATION

coupling. Figures 7.5 through 7.9 illustrate that with the cross-shaft out both rotors are governed and the problem seen with the single governor with one sensor does not appear. Note the triangles in Figure 7.5 showing that the presence of the cross-shaft has no effect on the rotor rotation mode root migration. The effects of RPM, integral of RPM and RPM rate feedback were explored for various governor time constants and no problems arose with other modes going unstable.

Although the gains chosen to evaluate this configuration were not of sufficient level to meet the error criteria, the trends are important to note. RPM feedback increases the damping of the rotor rotation mode while keeping the natural frequency constant (for a governor time constant of 0.0). Figure 7.7 illustrates this affect. Notice that the root migration follows an arc of approximately constant radius (constant natural frequency). As the roots follow the arc toward the negative real axis the damping ratio is increased. Also from this figure the destabilizing effect of governor time constant is seen. As time constant is increased the locus of roots is rotated in such a manner that the increase in damping ratio per unit gain is decreased. Integral of RPM feedback (Figure 7.8) increases the damped natural frequency while maintaining

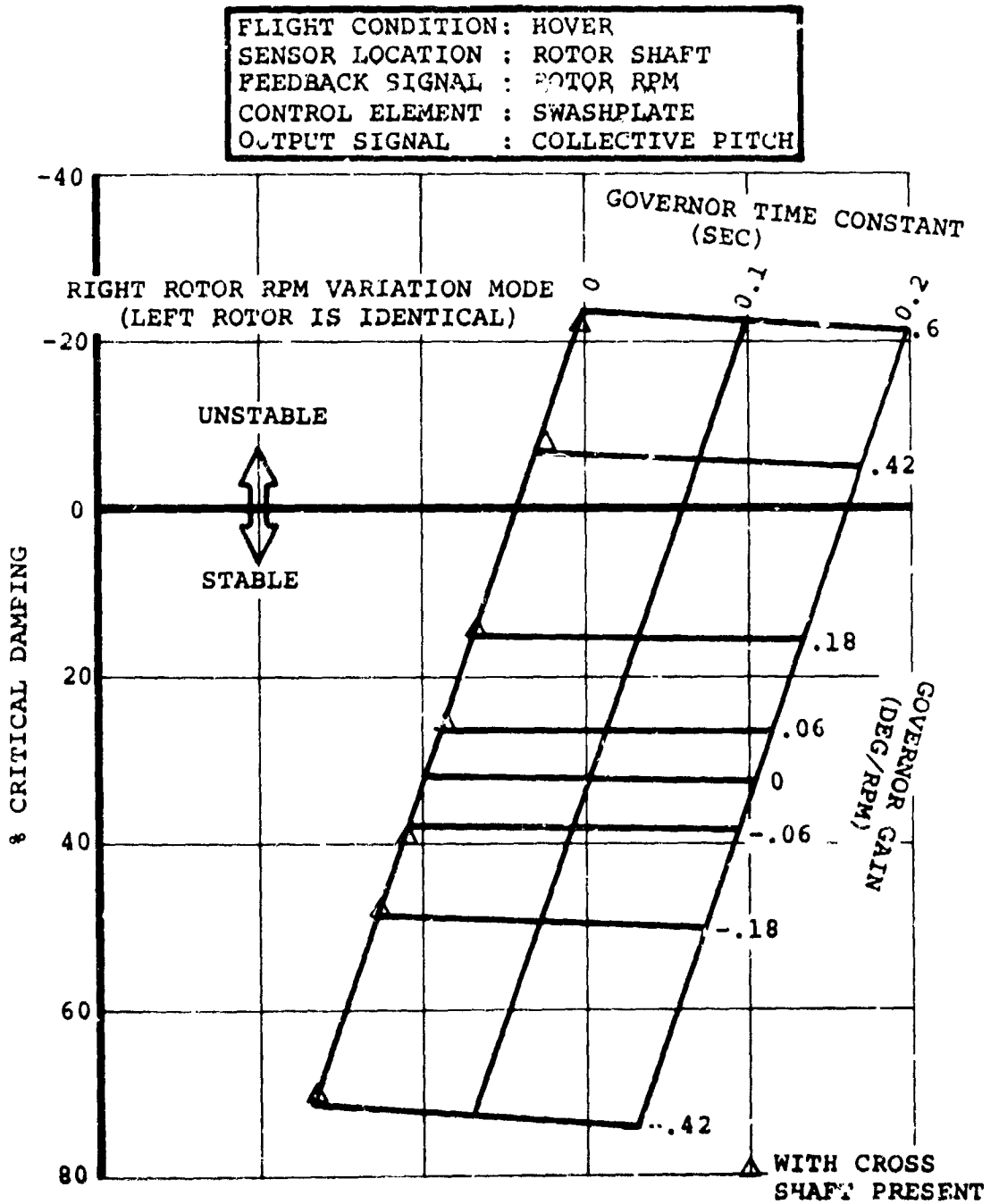


FIGURE 7.5. INNER LOOP STABILITY VARIATION FOR  
 DUAL INDEPENDENT GOVERNORS WITHOUT  
 CROSS SHAFT

FLIGHT CONDITION: HOVER  
 SENSOR LOCATION : ROTOR SHAFT  
 FEEDBACK SIGNAL : INTEGRAL OF RPM  
 CONTROL ELEMENT : SWASHPLATE  
 OUTPUT SIGNAL : COLLECTIVE PITCH

RIGHT ROTOR  
 RPM VARIATION MODE  
 (LEFT ROTOR IS IDENTICAL)

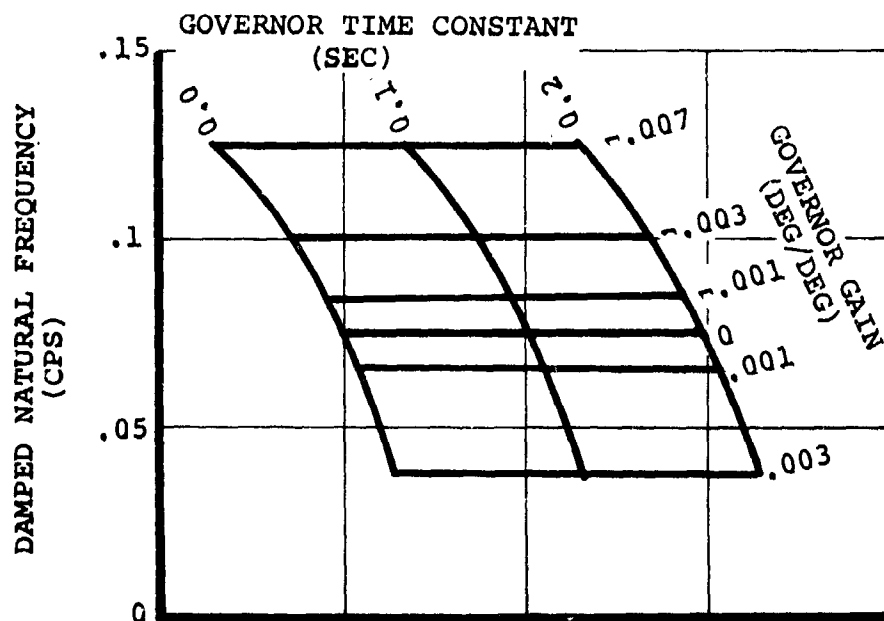


FIGURE 7.6. INNER LOOP STABILITY VARIATION FOR  
 DUAL INDEPENDENT GOVERNORS WITHOUT  
 CROSS SHAFT

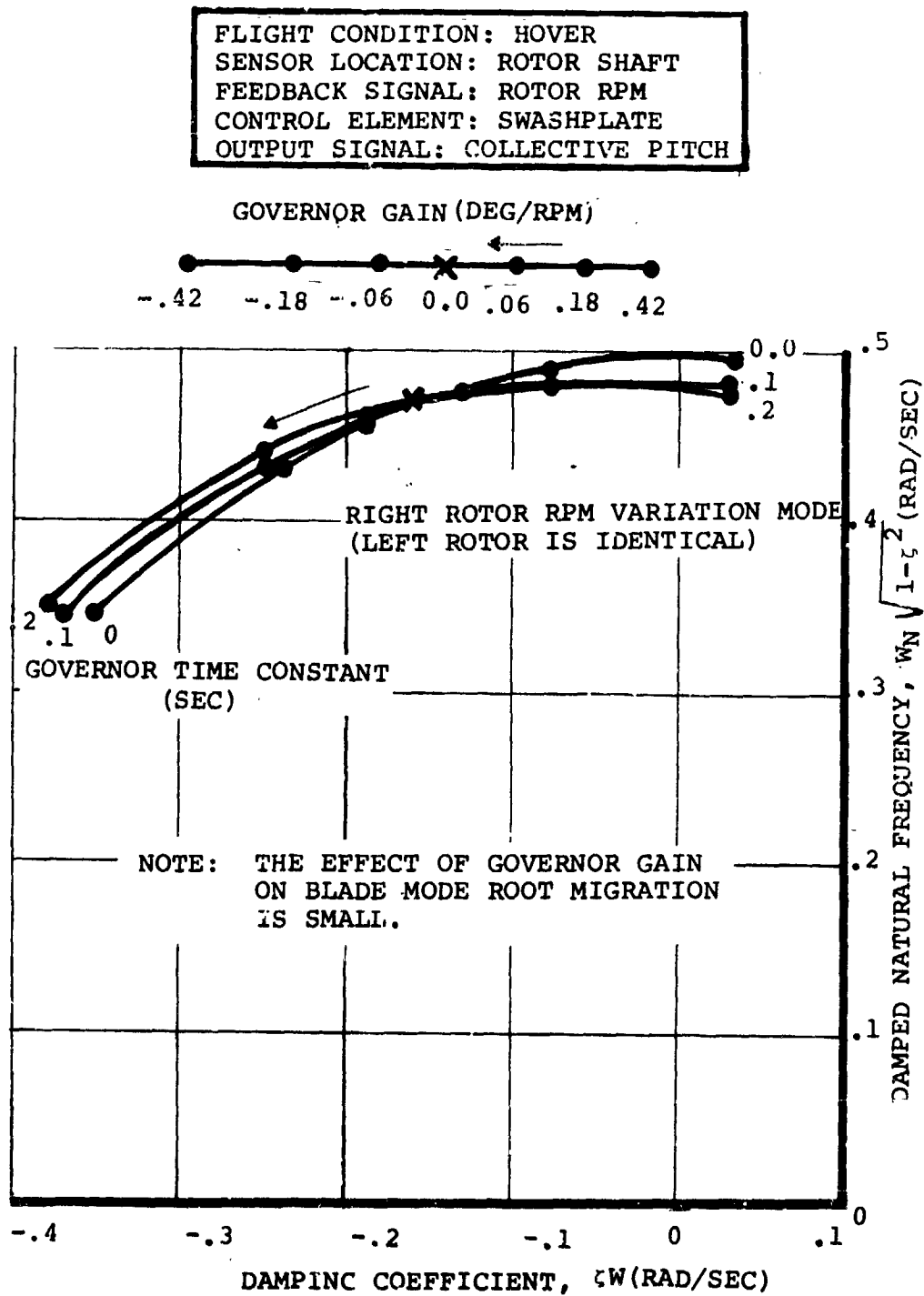


FIGURE 7.7. INNER LOOP STABILITY VARIATION FOR DUAL INDEPENDENT GOVERNORS WITHOUT CROSS SHAFT

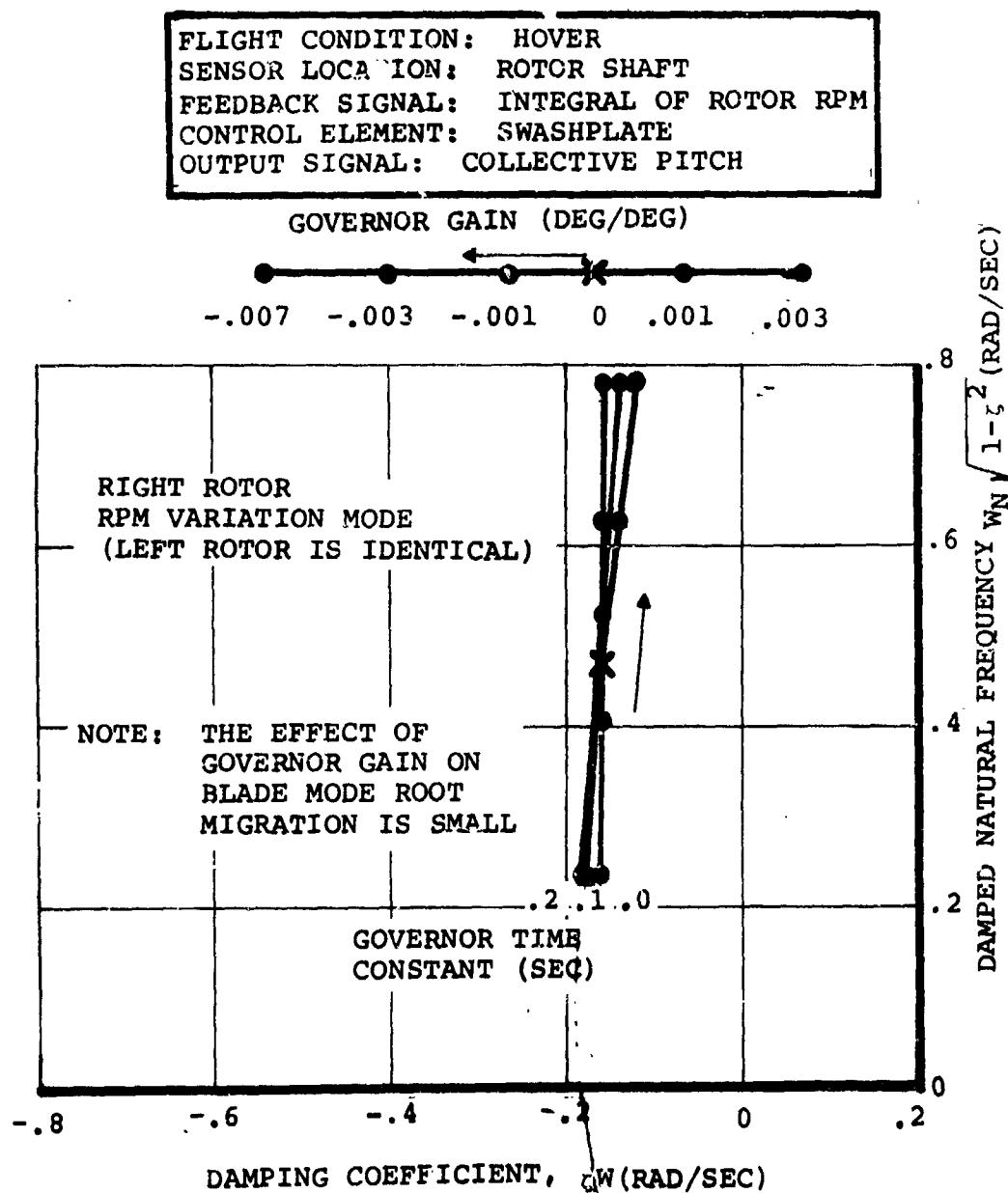


FIGURE 7.8. INNER LOOP STABILITY VARIATION FOR DUAL INDEPENDENT GOVERNORS WITHOUT CROSS SHAFT



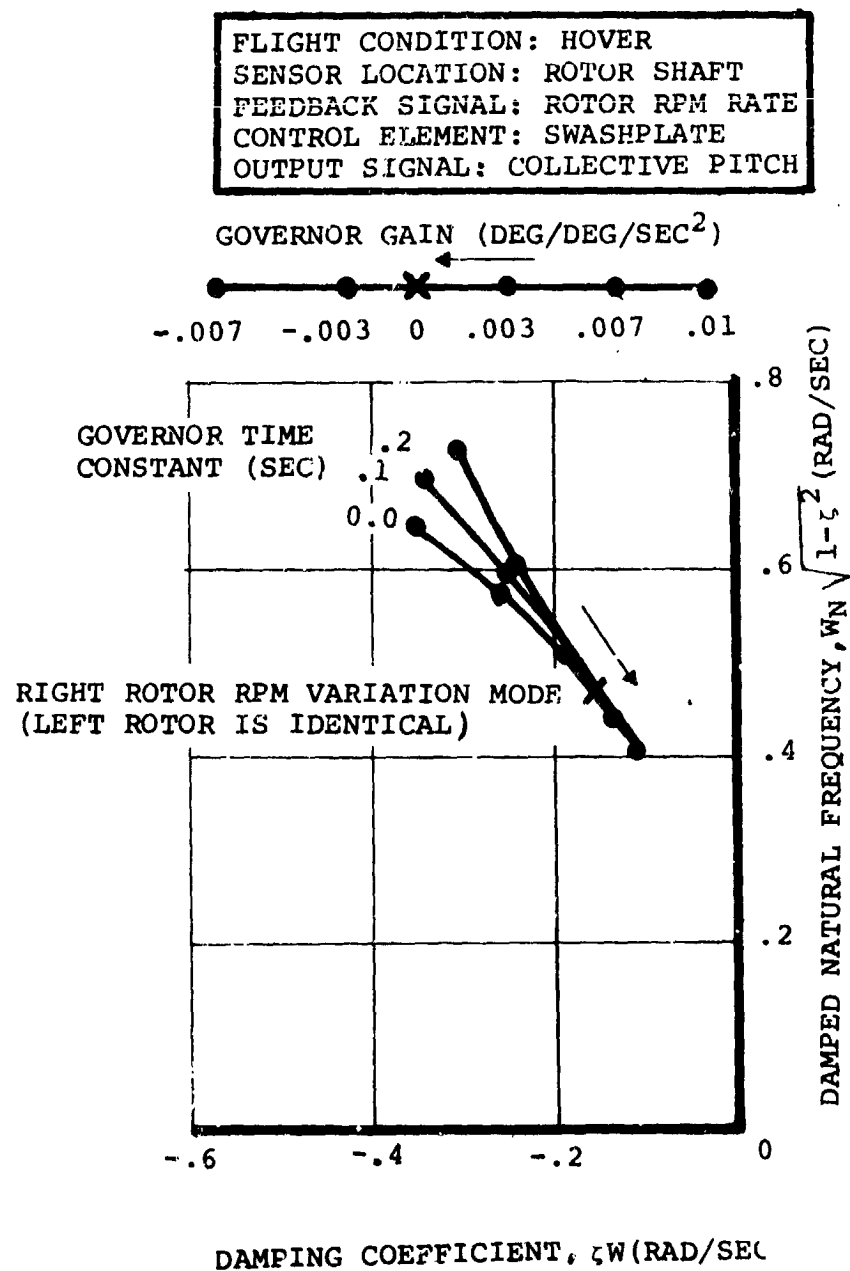


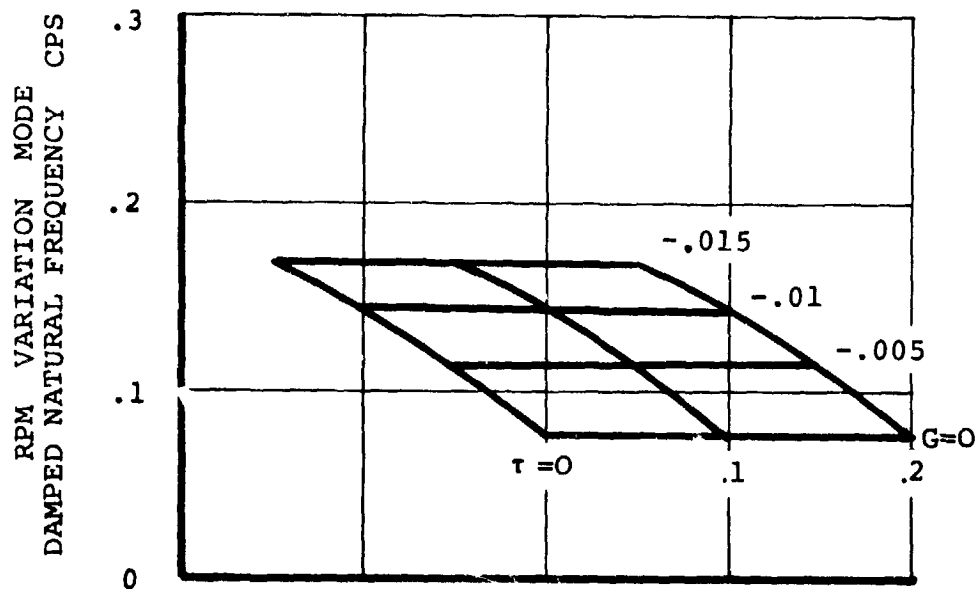
FIGURE 7.9. INNER LOOP STABILITY VARIATION FOR DUAL INDEPENDENT GOVERNORS WITHOUT CROSS SHAFT

a constant level of damping coefficient ( $\zeta\omega_N$ ). Once again the governor time constant is destabilizing in that the locus of roots is driven toward the unstable right half plane for negative feedback. RPM rate feedback (Figure 7.9) decreases the natural frequency and the damping coefficient. As time constant is increased the locus of roots is rotated to be similar to integral of RPM feedback. Analysis of these three graphs indicates that RPM and integral of RPM feedback will be useful in meeting the error criteria. RPM rate feedback is not as desirable for the task at hand.

Results of the inner loop study as discussed above indicated that the dual independent governor configuration could be acceptable to meet the steady state error and transient response criteria for the all-operational and cross-shaft failure mode. However, an earlier flying qualities study (NASA Design Study) indicated that the dual governor configuration could have a deleterious effect on the roll mode in hover and the dutch roll mode in cruise. To confirm this trend the roll and vertical translation degrees of freedom were added to the hover math model and the studies of RPM and integral of RPM were repeated. Figures 7.10 and 7.11 show that adding these degrees of freedom have no effect on the inner loop response (i.e., the inner loop root migration is

DUAL GOVERNOR  
HOVER - OUTER AND INNER LOOP STABILITY  
RPM FEEDBACK  
NO CROSS SHAFT

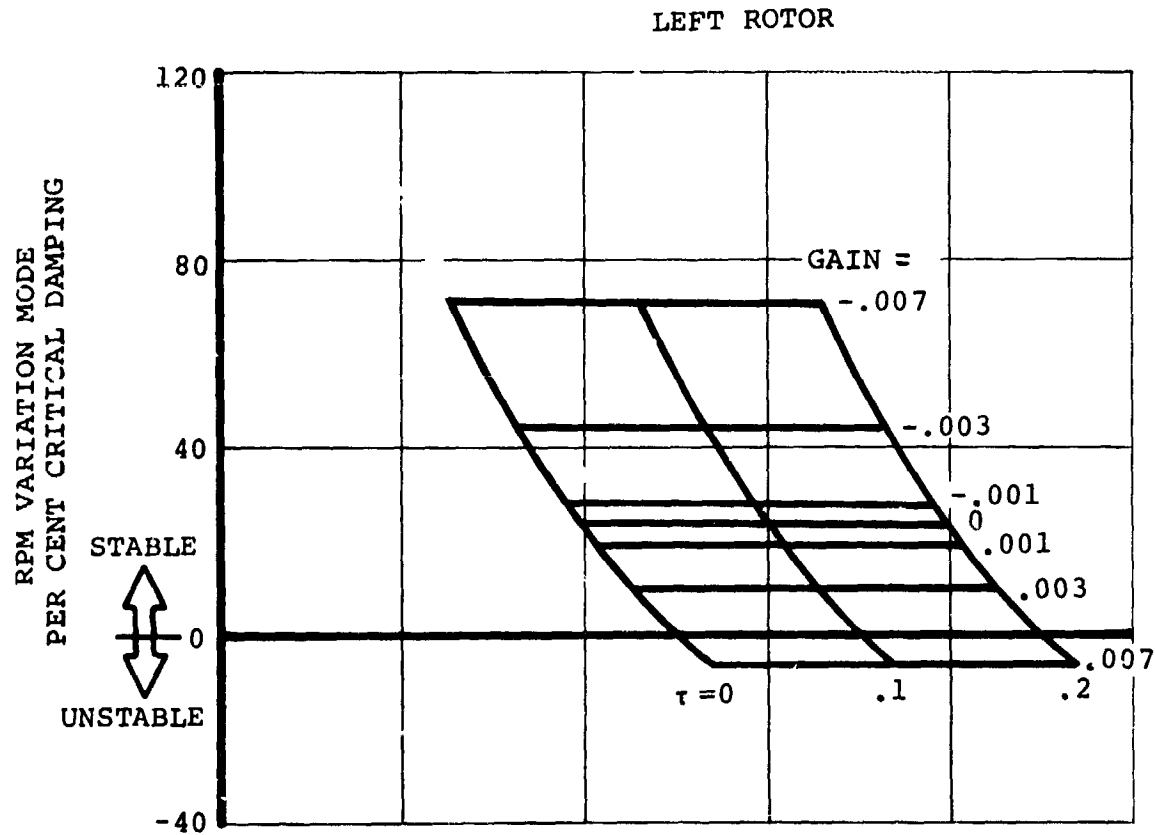
## LEFT ROTOR

NOTES:

1.  $\tau$  IS THE GOVERNOR TIME CONSTANT IN SECONDS
2.  $G$  IS THE GOVERNOR GAIN IN RAD/RAD/SEC

FIGURE 7.10. DUAL INDEPENDENT GOVERNORS - INNER AND OUTER LOOP STABILITY RESPONSE

DUAL GOVERNOR  
HOVER - OUTER AND INNER LOOP STABILITY  
RPM FEEDBACK  
NO CROSS SHAFT



NOTES:

1.  $\tau$  IS THE GOVERNOR TIME CONSTANT IN SECONDS
2. G IS THE GOVERNOR GAIN IN RAD/RAD/SEC

FIGURE 7.11. DUAL INDEPENDENT GOVERNORS - INNER AND OUTER LOOP STABILITY RESPONSE

identical). Figures 7.12 and 7.13 show the rotor rotation and rigid body root migration. Note that in each case both the hover roll and hover vertical translation modes were driven less stable (i.e., the real roots move from the left half plane toward the origin). In cruise the same type of effect would occur for the dutch roll mode and phugoid mode. Although inner loop response for the dual independent governor configuration is acceptable, the effect on the roll and dutch roll modes is not and disqualifies this configuration.

#### 7.4.3 Single Governor With Two Sensors

A schematic of the single governor with two sensors is shown in Figure 7.3. In this configuration the RPM variation of each rotor is sensed, the signals are averaged and collective pitch is fed back as a function of the averaged signal. Since this configuration was felt to be the most likely candidate for an optimum tilt rotor governor system, the feedback loop has been made considerably more complex. Sensor dynamics have been added and are represented as a second order lag with a break frequency of 50 cps. This is a conservative estimate of sensor dynamics in that magnetic tachometers have a "near instantaneous" response. Actuator dynamics are representative of actuators used on Boeing Vertol test hardware. The

DUAL GOVERNOR  
HOVER - OUTER AND INNER LOOP STABILITY  
RPM FEEDBACK  
NO CROSS SHAFT

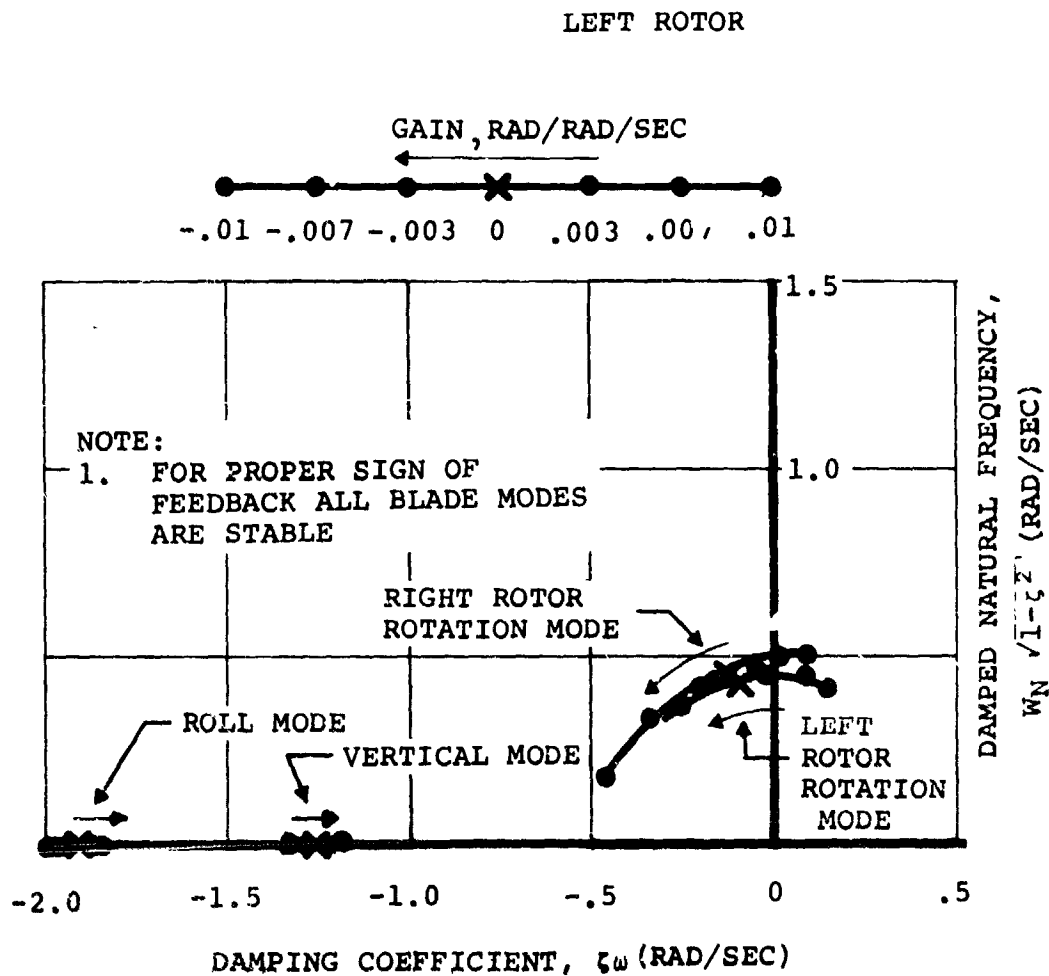


FIGURE 7.12.DUAL INDEPENDENT GOVERNORS - INNER  
AND OUTER LOOP STABILITY RESPONSE

DUAL GOVERNOR  
HOVER - OUTER AND INNER LOOP STABILITY  
RPM FEEDBACK  
NO CROSS SHAFT

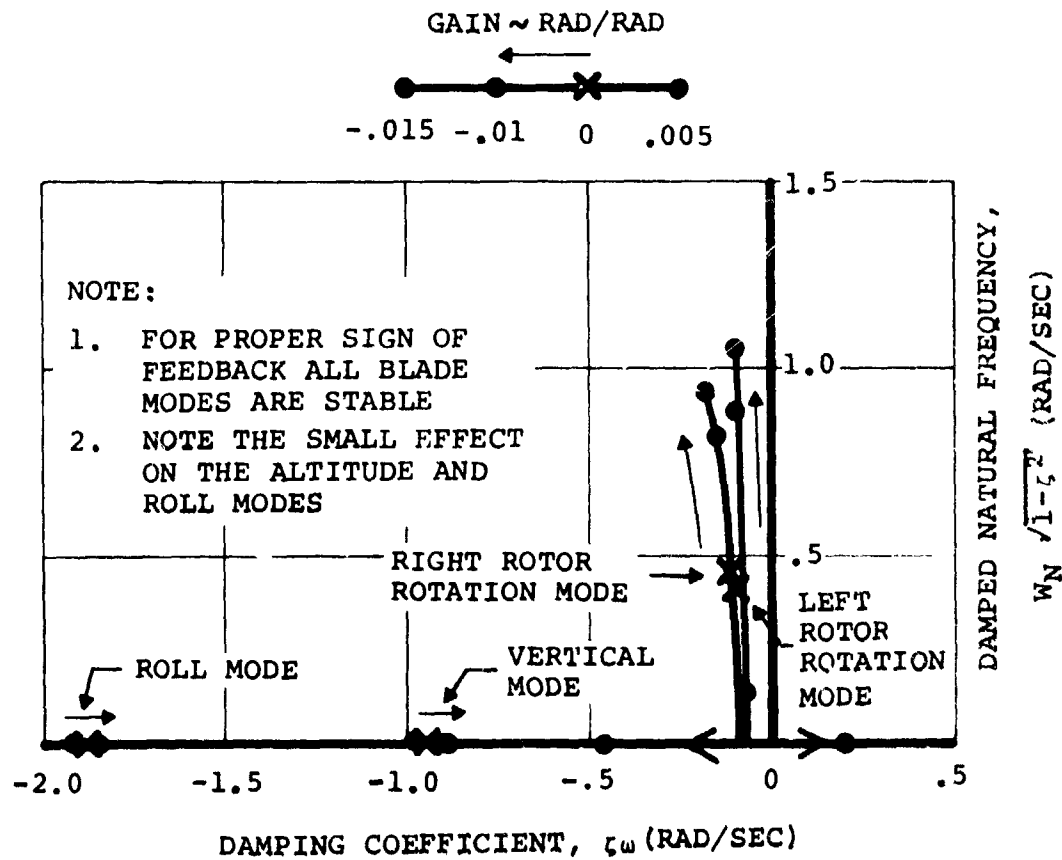


FIGURE 7.13. DUAL INDEPENDENT GOVERNORS - INNER AND OUTER LOOP STABILITY RESPONSE

actuators are represented as first order lags with a time constant of .017 sec. Signal shaping has been added to the system as needed. With the addition of the above hardware to the feedback loop the governor representation is felt to be representative of an actual governor system.

Bode plots (Appendix B) were calculated for RPM feedback in various flight conditions in the all-operational mode and the cross-shaft failure mode to determine the maximum acceptable values of governor gain when designing to a  $30^\circ$  phase margin and a 6 dB gain margin. These plots are especially helpful as working tools in determining if there will be a stability problem. With them the need for filtering and the filter characteristics can be easily identified. The gains are shown in Figure 7.14 as a function of aircraft configuration, velocity and RPM. Maximum gain levels indicated that there would be no stability problem and that the necessary governor gain level would be well within the stability boundaries. For this reason bode plots were not calculated for integral of RPM feedback.

Figures 7.15 through 7.23 show the rotor rotation root migration with gain for:

- RPM and integral of RPM feedback
- cruise and hover modes



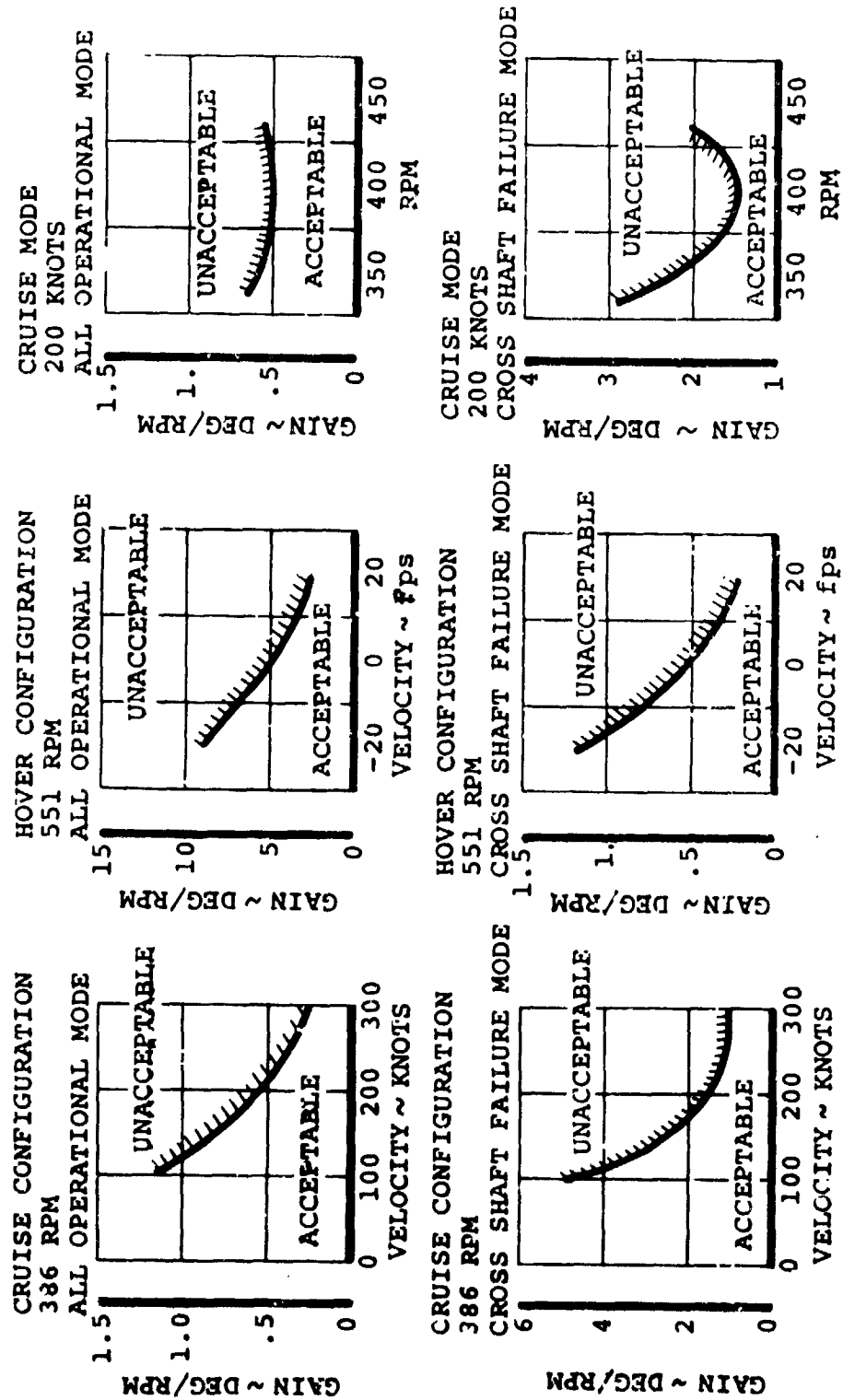


FIGURE 7.14. SINGLE GOVERNOR WITH TWO SENSORS  
GOVERNOR GAIN LIMITS FOR RPM FEEDBACK  
INNER LOOP STABILITY

## O all-operational and cross-shaft failure modes

Note that in each case the governor has no effect on the anti-symmetric rotation mode. Although this is not the most desirable case from a purely RPM governing point of view, it is necessary to keep the hover roll damping and the cruise dutch roll damping from being degraded.

Initially, a straight proportional (RPM) feedback was evaluated (Figures 7.15, 7.16, 7.20 and 7.21). The desired damping ratio (shaping of transient response) could be achieved to meet the error criteria, but the natural frequency was too low in the hover regime (the desired accuracy could not be achieved) and in the cruise configuration the rotor rotation roots were real with one root very small, thus yielding poor transient response. To improve the accuracy in hover and the transient response in cruise, integral of RPM was fed back (Figures 7.17, 7.22 and 7.23). The gain was increased until the desired natural frequency was obtained. In the hover regime and the 100 knot cruise case, it was found necessary to have proportional as well as integral feedback (Figures 7.18 and 7.19) to achieve the desired accuracy and shaping of the transient response. The table below specifies the steady-state integral and proportional gains required to meet the accuracy and transient response goals.

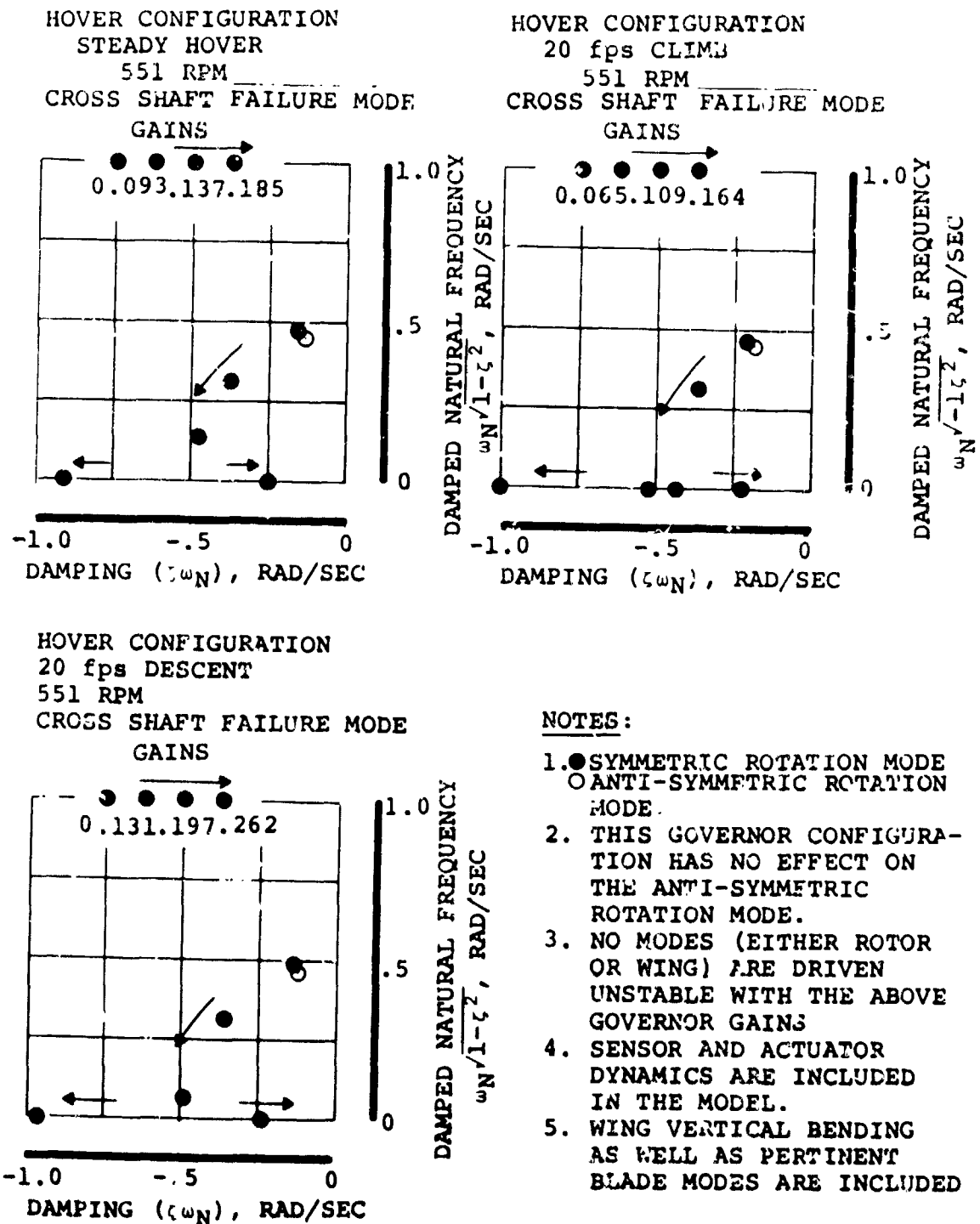
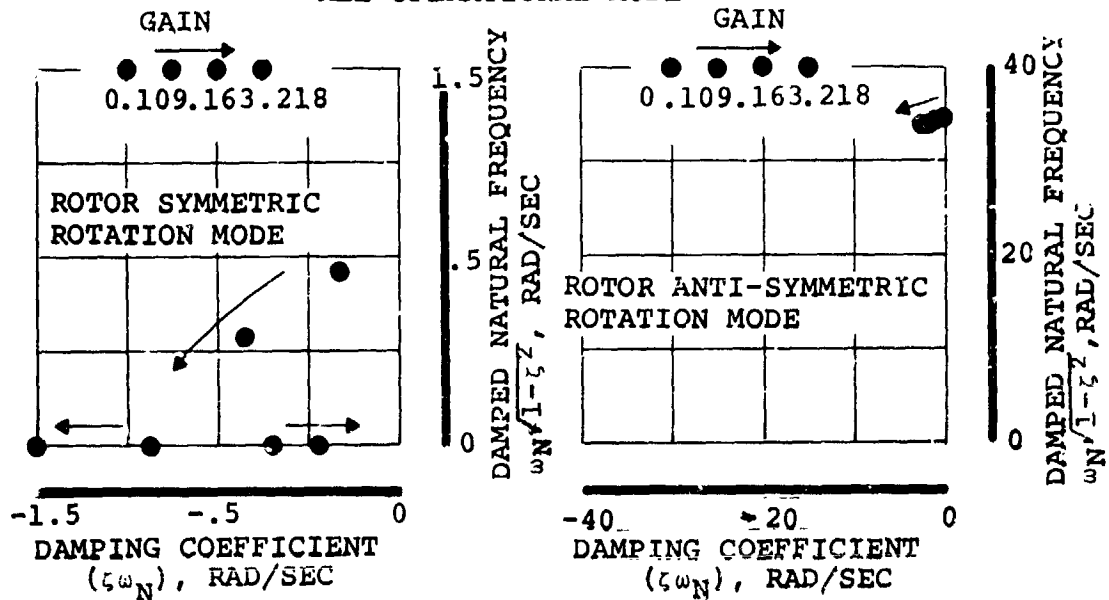


FIGURE 7.15 SINGLE GOVERNOR WITH TWO SENSORS ROTOR ROTATION  
ROOT MIGRATION WITH RPM FEEDBACK

HOVER CONFIGURATION  
STEADY HOVER  
551 RPM  
ALL OPERATIONAL MODE



HOVER CONFIGURATION  
20 fps CLIMB  
551 RPM  
ALL OPERATIONAL MODE

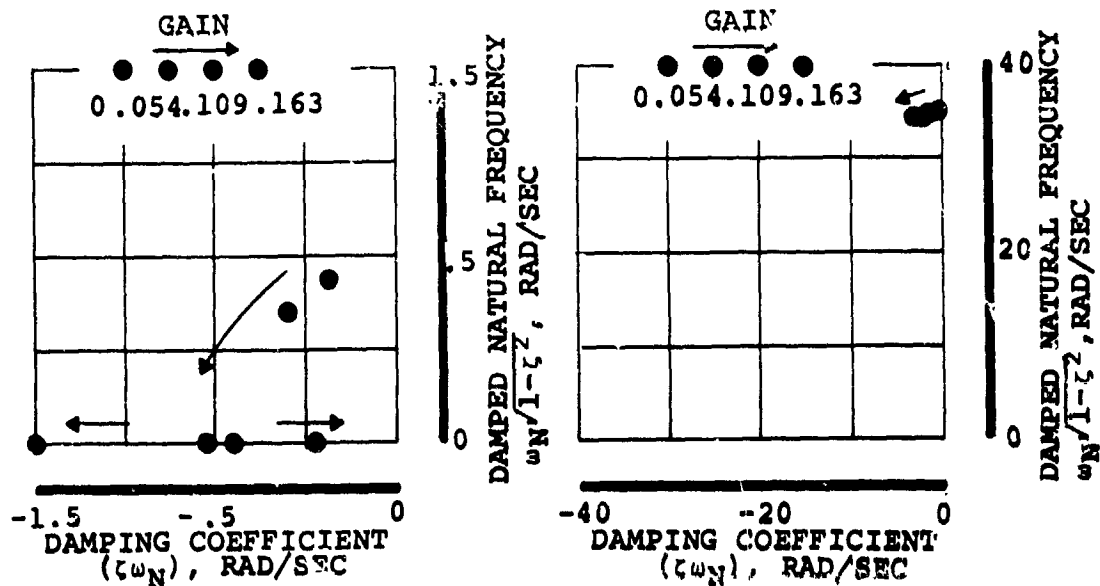
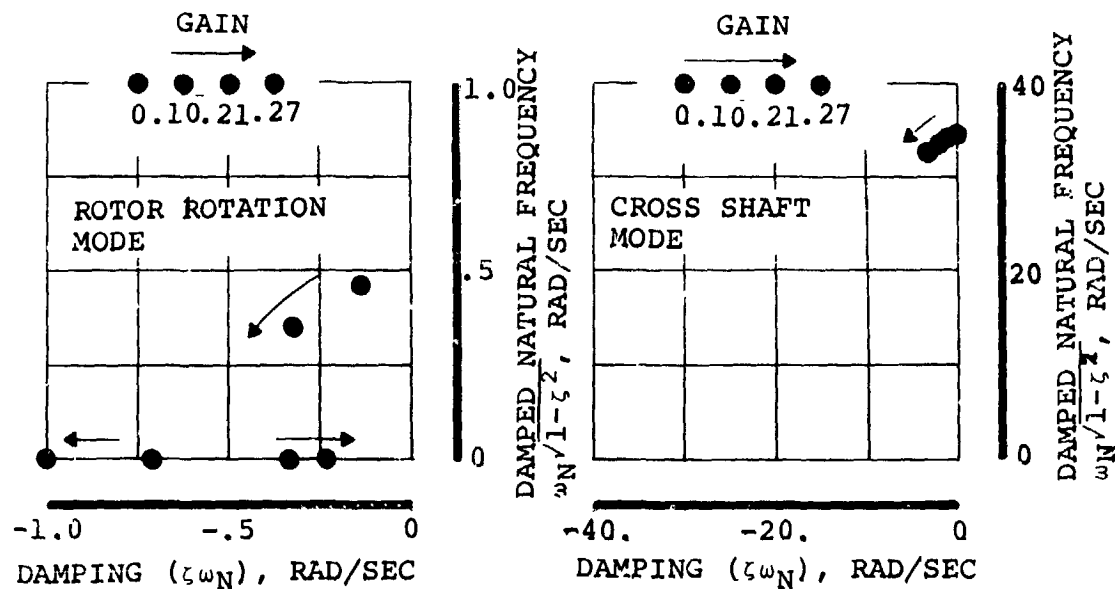


FIGURE 7.16a. SINGLE GOVERNOR WITH TWO SENSORS  
ROTOR ROTATION ROOT MIGRATION  
WITH RPM FEEDBACK

HOVER CONFIGURATION  
20 fps DESCENT  
CROSS SHAFT PRESENT  
551 RPM

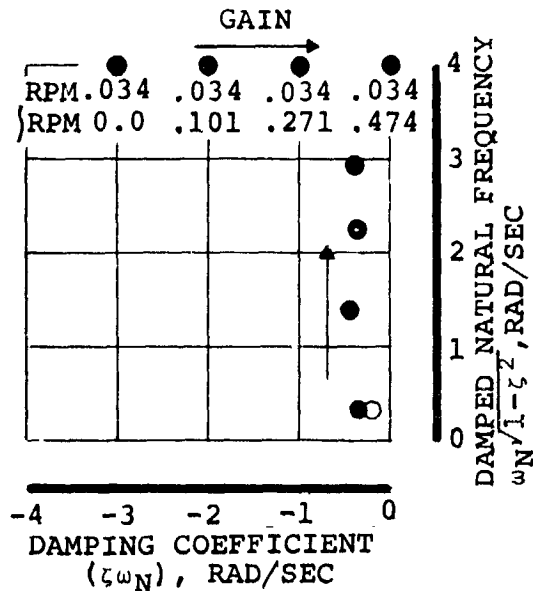


NOTES:

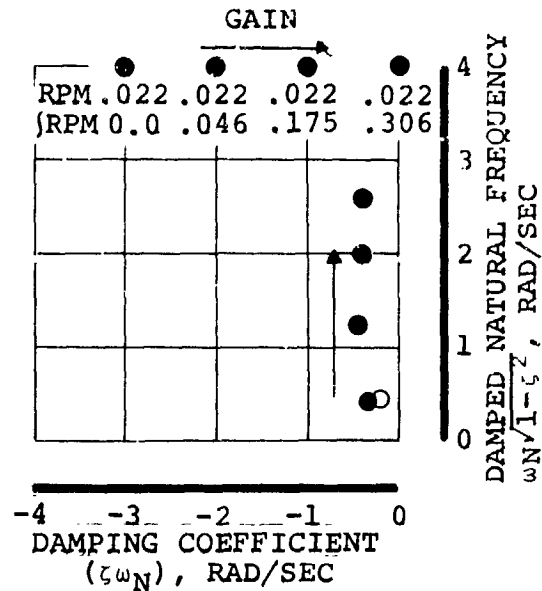
1. This governor configuration has no effect on the cross shaft (anti-symmetric rotor rotation) mode.
2. No modes (either rotor or wing) are driven unstable with the above governor gains.
3. Sensor and actuator dynamics are included in the model.
4. Wing vertical bending as well as pertinent blade modes are included in the model.

FIGURE 7.16b. ROTOR ROTATION ROOT MIGRATION  
WITH RPM FEEDBACK

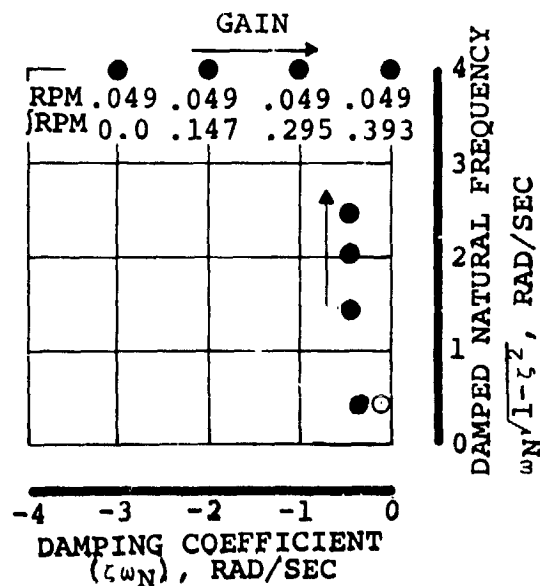
HOVER CCNFIGURATION  
STEADY HOVER  
551 RPM  
CROSS SHAFT FAILURE MODE



HOVER CONFIGURATION  
20 fps CLIMB  
551 RPM  
CROSS SHAFT FAILURE MODE



HOVER CONFIGURATION  
20 fps DESCENT  
551 RPM  
CROSS SHAFT FAILURE MODE

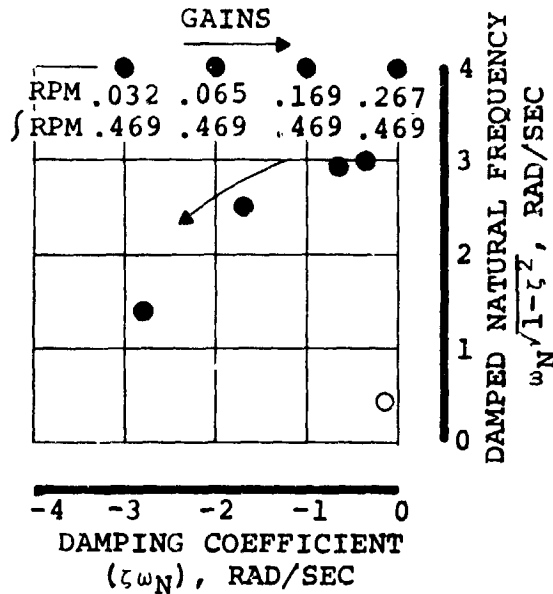


NOTES:

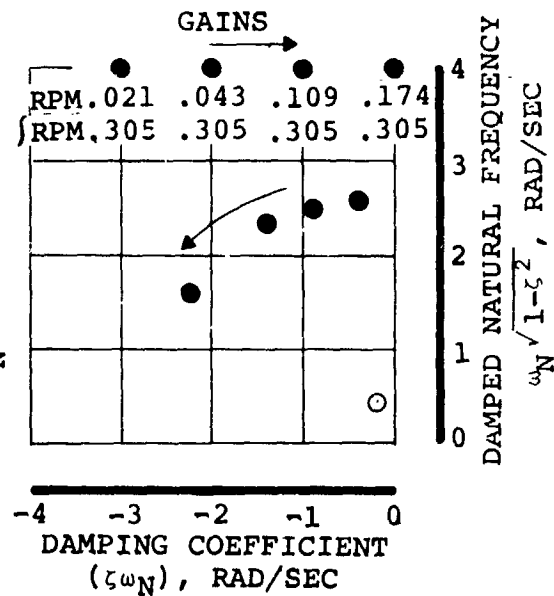
1. ● SYMMETRIC ROTATION MODE  
○ ANTI-SYMMETRIC ROTATION MODE
2. THIS GOVERNOR CONFIGURATION HAS NO EFFECT ON THE ANTI-SYMMETRIC ROTATION MODE.
3. NO MODES ARE DRIVEN UNSTABLE WITH THE ABOVE GOVERNOR GAINS
4. SENSOR AND ACTUATOR DYNAMICS ARE INCLUDED IN THE MODEL.
5. WING VERTICAL BENDING AS WELL AS PERTINENT BLADE MODES ARE INCLUDED.

FIGURE 7.17. SINGLE GOVERNOR WITH TWO SENSORS  
ROTOR ROTATION RCOT MIGRATION WITH  $\int +$  RPM FEEDBACK

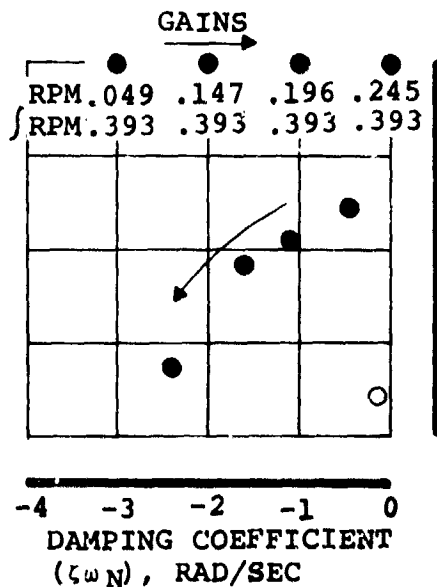
HOVER CONFIGURATION  
STEADY HOVER  
551 RPM  
CROSS SHAFT FAILURE MODE



HOVER CONFIGURATION  
20 fps CLIMB  
551 RPM  
CROSS SHAFT FAILURE MODE



HOVER CONFIGURATION  
20 fps DESCENT  
551 RPM  
CROSS SHAFT FAILURE MODE



#### NOTES:

1. ● SYMMETRIC ROTATION MODE  
○ ANTI-SYMMETRIC MODE
2. THIS GOVERNOR CONFIGURATION HAS NO EFFECT ON THE ANTI-SYMMETRIC ROTATION MODE
3. NO MODES ARE DRIVEN UNSTABLE WITH THE ABOVE GOVERNOR GAINS
4. SENSOR AND ACTUATOR DYNAMICS ARE INCLUDED IN THE MODEL
5. WING VERTICAL BENDING AS WELL AS PERTINENT BLADE MODES ARE INCLUDED

FIGURE 7.18. SINGLE GOVERNOR WITH TWO SENSORS  
ROTOR ROTATION ROOT MIGRATION WITH { + RPM FEEDBACK

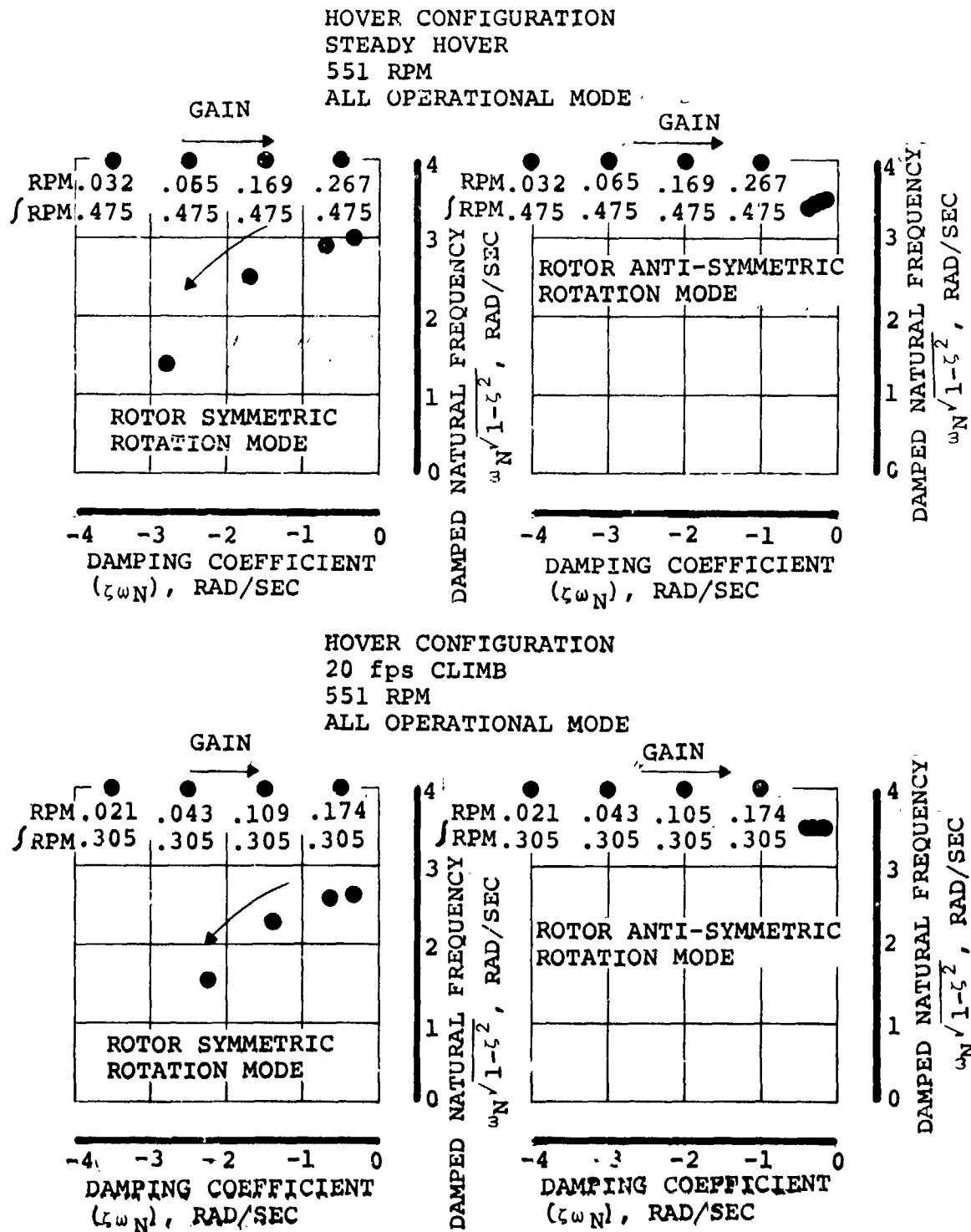
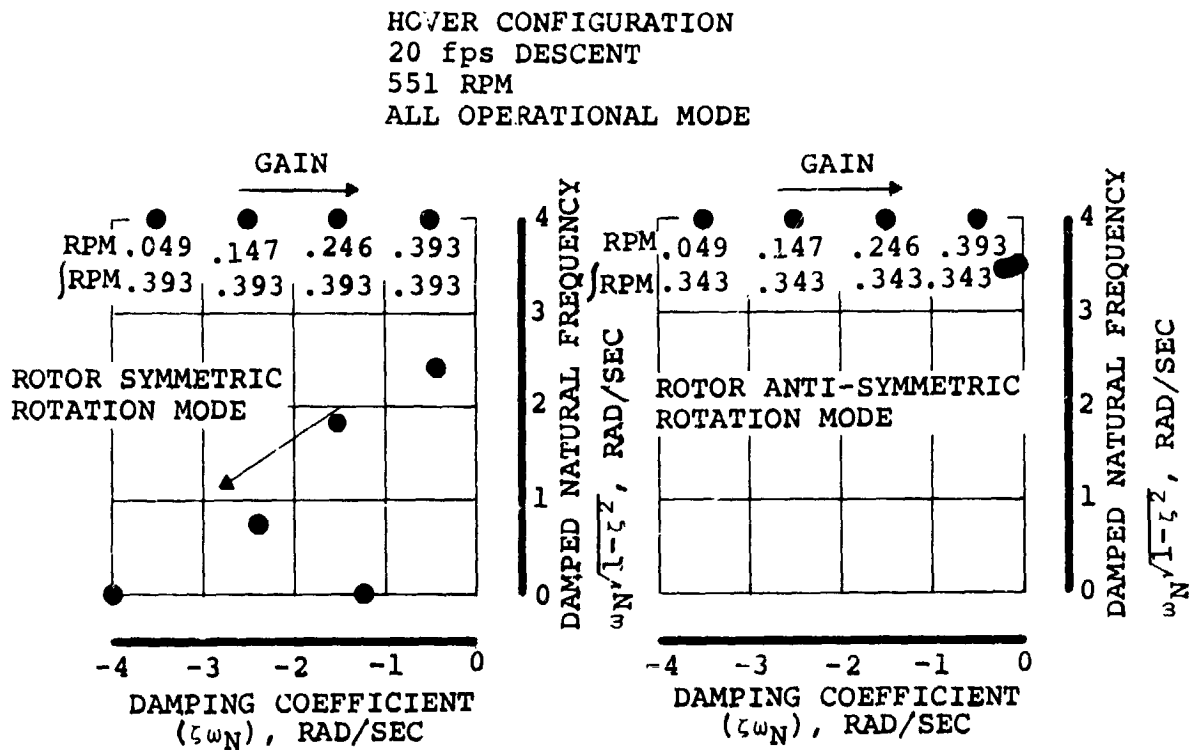


FIGURE 7.19a. SINGLE GOVERNOR WITH TWO SENSORS  
ROTOR ROTATION ROOT MIGRATION WITH  $\int$  RPM FEEDBACK

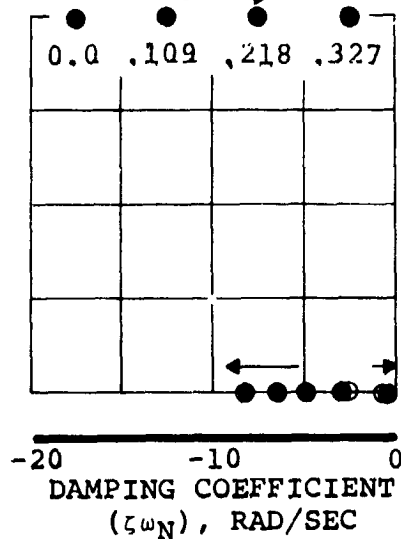


**NOTES:**

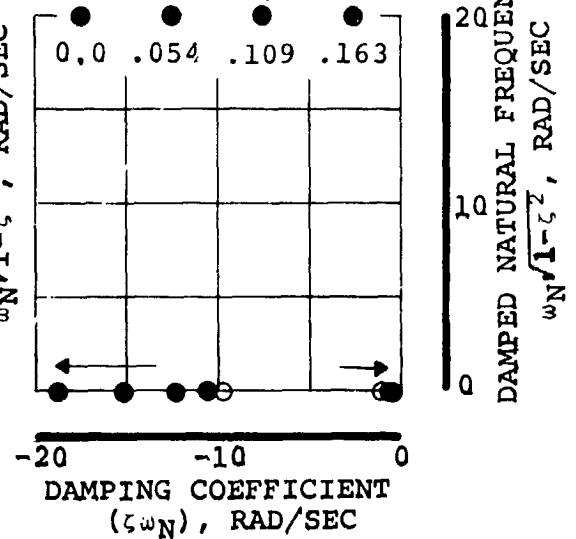
1. THIS GOVERNOR HAS NO EFFECT ON THE CROSS SHAFT (ANTI-SYMMETRIC ROTATION) MODE.
2. NO MODES ARE DRIVEN UNSTABLE WITH THE ABOVE GOVERNOR GAINS
3. SENSOR AND ACTUATOR DYNAMICS ARE INCLUDED IN THE MODEL.

FIGURE 7.19b. SINGLE GOVERNOR WITH TWO SENSORS ROTOR ROTATION  
ROOT MIGRATION WITH  $\int +$  RPM FEEDBACK

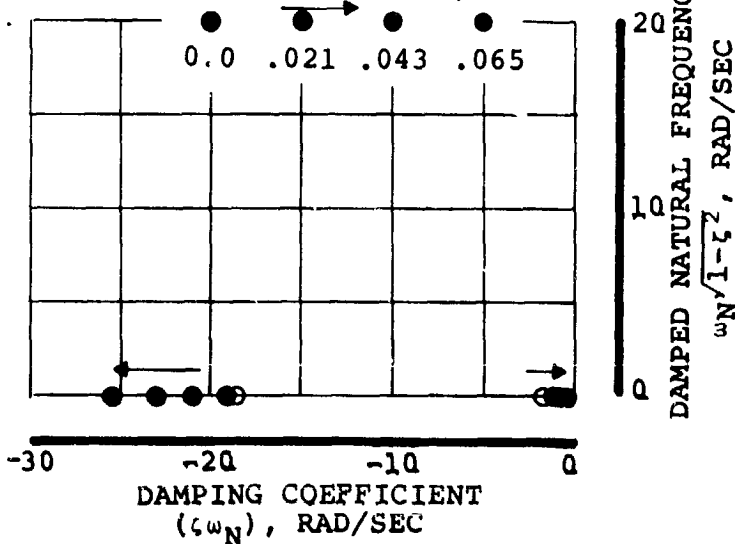
CRUISE CONFIGURATION  
100 KNOTS  
386 RPM  
CROSS SHAFT FAILURE MODE  
GAIN DEG/RPM



CRUISE CONFIGURATION  
200 KNOTS  
386 RPM  
CROSS SHAFT FAILURE MODE  
GAIN ~ DEG/RPM



CRUISE CONFIGURATION  
300 KNOTS  
386 RPM  
CROSS SHAFT FAILURE MODE  
GAIN ~ DEG/RPM

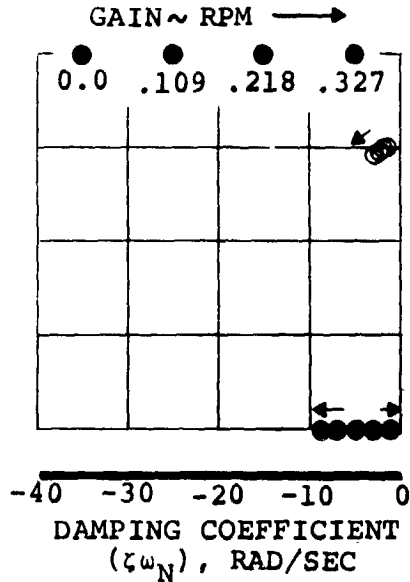


#### NOTES:

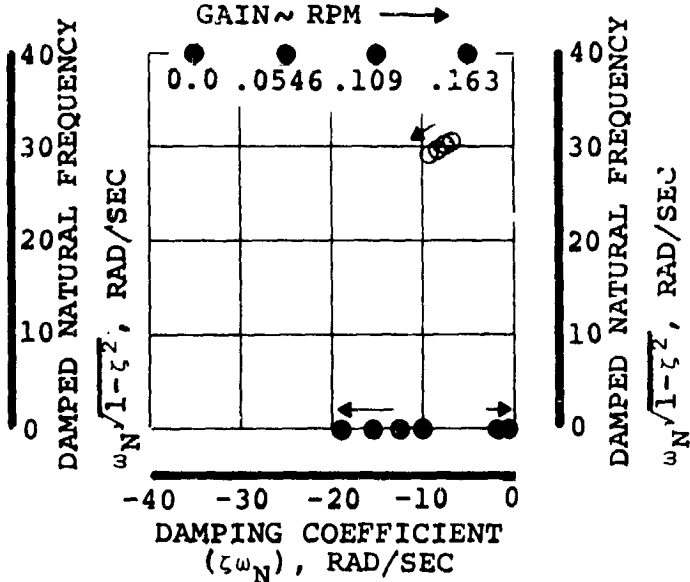
1. ● SYMMETRIC ROTATION MODE  
○ ANTI-SYMMETRIC ROTATION MODE
2. THIS GOVERNOR CONFIGURATION HAS NO EFFECT ON THE ANTI-SYMMETRIC ROTATION MODE
3. NO MODES ARE DRIVEN UNSTABLE WITH THE ABOVE GOVERNOR GAINS
4. SENSOR AND ACTUATOR DYNAMICS ARE INCLUDED IN THE MODEL
5. THE FOLLOWING UNCOUPLED WING MODES ARE INCLUDED IN THE MODEL
  - VERTICAL BENDING
  - CHORD BENDING
  - TORSION

FIGURE 7.20. SINGLE GOVERNOR WITH TWO SENSORS  
ROTOR ROTATION ROOT MIGRATION WITH RPM FEEDBACK

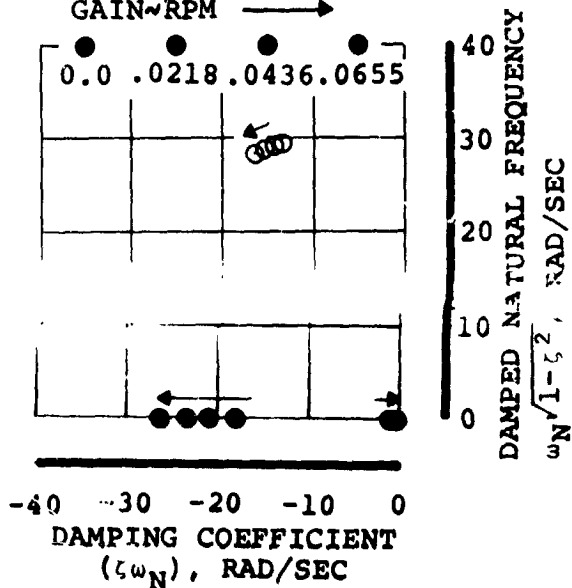
CRUISE CONFIGURATION  
100 KNOTS  
386 RPM  
ALL OPERATIONAL MODE



CRUISE CONFIGURATION  
200 KNOTS  
386 RPM  
ALL OPERATIONAL MODE



CRUISE CONFIGURATION  
300 KNOTS  
386 RPM  
ALL OPERATIONAL MODE  
GAIN ~ RPM →

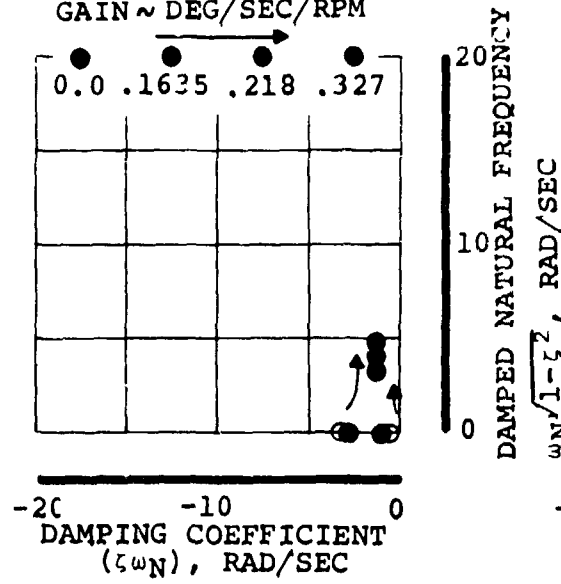


#### NOTES:

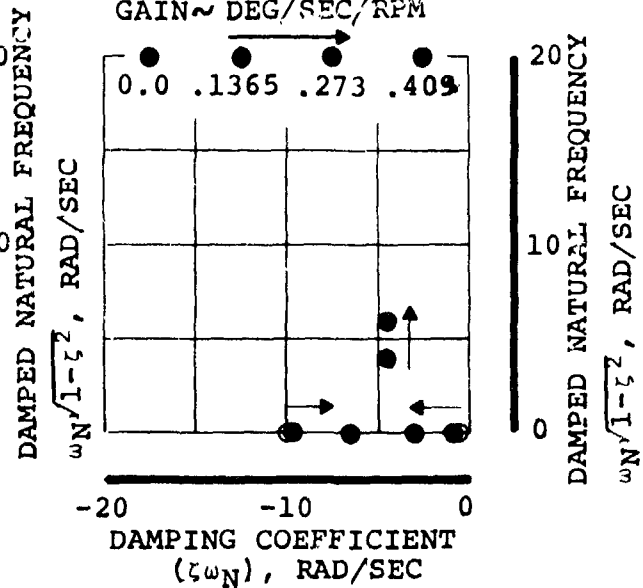
1. ● SYMMETRIC ROTATION MODE  
○ ANTI-SYMMETRIC ROTATION MODE
2. NO MODES ARE DRIVEN UNSTABLE WITH THE ABOVE GOVERNOR GAINS
3. SENSOR AND ACTUATOR DYNAMICS ARE INCLUDED IN THE MODEL
4. THE FOLLOWING UNCOUPLED WING MODES ARE INCLUDED IN THE MODEL
  - VERTICAL BENDING
  - CHORD BENDING
  - TORSION

FIGURE 7.21 SINGLE GOVERNOR WITH TWO SENSORS  
ROTOR ROTATION ROOT MIGRATION WITH RPM FEEDBACK

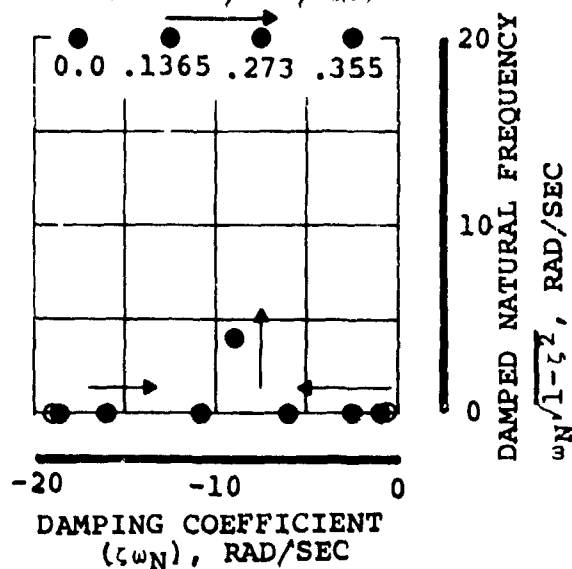
CRUISE CONFIGURATION  
100 KNOTS  
386 RPM  
CROSS SHAFT FAILURE MODE  
GAIN ~ DEG/SEC/RPM



CRUISE CONFIGURATION  
200 KNOTS  
386 RPM  
CROSS SHAFT FAILURE MODE  
GAIN ~ DEG/SEC/RPM



CRUISE CONFIGURATION  
300 KNOTS  
386 RPM  
CROSS SHAFT FAILURE MODE  
GAIN ~ DEG/SEC/RPM

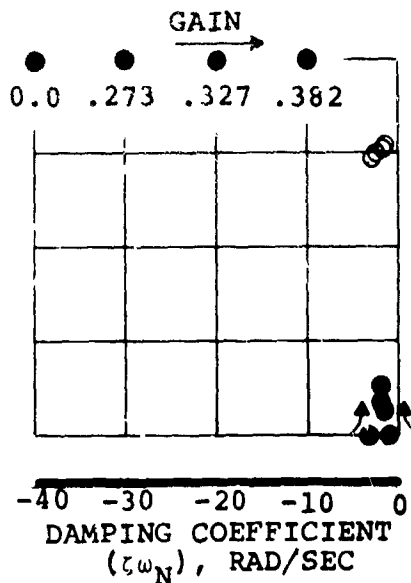


#### NOTES:

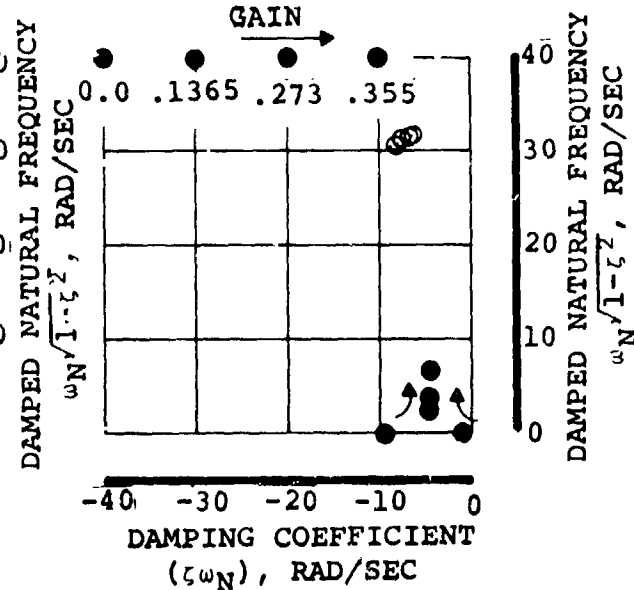
1. ● SYMMETRIC ROTATION MODE  
○ ANTI-SYMMETRIC ROTATION MODE
2. THIS GOVERNOR CONFIGURATION HAS NO EFFECT ON THE ANTI-SYMMETRIC ROTATION MODE
3. NO MODES ARE DRIVEN UNSTABLE WITH THE ABOVE GOVERNOR GAINS
4. SENSOR AND ACTUATOR DYNAMICS ARE INCLUDED IN THE MODEL
5. THE FOLLOWING UNCOUPLED WING MODES ARE INCLUDED IN THE MODEL
  - VERTICAL BENDING
  - CHORD BENDING
  - TORSION

FIGURE 7.22. SINGLE GOVERNOR WITH TWO SENSORS  
ROTOR ROTATION ROOT MIGRATION WITH INTEGRAL FEEDBACK

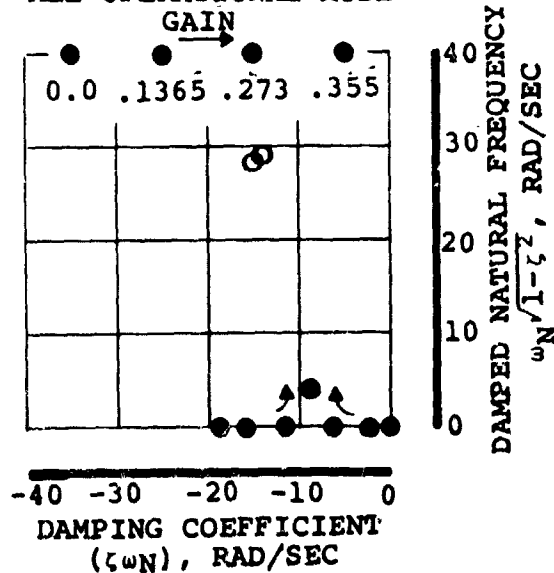
CRUISE CONFIGURATION  
100 KNOTS  
386 RPM  
ALL OPERATIONAL MODE



CRUISE CONFIGURATION  
200 KNOTS  
386 RPM  
ALL OPERATIONAL MODE



CRUISE CONFIGURATION  
300 KNOTS  
386 RPM  
ALL OPERATIONAL MODE



NOTES:

1. ● SYMMETRIC ROTATION MODE  
○ ANTI-SYMMETRIC ROTATION MODE
2. THIS GOVERNOR CONFIGURATION HAS NO EFFECT ON THE ANTI-SYMMETRIC ROTATION MODE
3. NO MODES ARE DRIVEN UNSTABLE WITH THE ABOVE GOVERNOR GAINS
4. SENSOR AND ACTUATOR DYNAMICS ARE INCLUDED IN THE MODEL
5. THE FOLLOWING UNCOUPLED WING MODES ARE INCLUDED IN THE MODEL
  - VERTICAL BENDING
  - CHORD BENDING
  - TORSION

FIGURE 7.23. SINGLE GOVERNOR WITH TWO SENSORS  
ROTOR ROTATION ROOT MIGRATION  
WITH RPM FEEDBACK

Flight Condition	Integral of RPM Feedback Gain (Steady State Gain)	RPM Feedback Gain (Steady State Gain)
Cruise - 100 Kts	.327 deg/sec/RPM	.0164 deg/RPM
Cruise - 200 Kts	.273 deg/sec/RPM	0.0
Cruise - 300 Kts	.355 deg/sec/RPM	0.0
Hover - Steady	.475 deg/sec/RPM	.268 deg/RPM
Hover - 20 fps Climb	.306 deg/sec/RPM	.175 deg/RPM
Hover - 20 fps Descent	.393 deg/sec/RPM	.246 deg/RPM

In the hover regime the range of steady state gains is not so critical with climb or descent airspeed and it would be acceptable to have a constant gain in the hover regime of:

- O .475 deg/sec/RPM
- O .245 deg/RPM (Figure 7.24)

In the cruise regime, the minimum requirements can be satisfied throughout the flight envelope with steady state gains of:

- O .355 deg/sec/RPM
- O .0177 deg/RPM (Figure 7.24)

#### 7.5 EFFECT OF GOVERNOR ON FLYING QUALITIES

In the hover configuration, the governor system may influence the vertical translation and roll modes. Since the chosen governor configuration averages RPM from each rotor, there will be no effect when the aircraft rolls since one rotor will

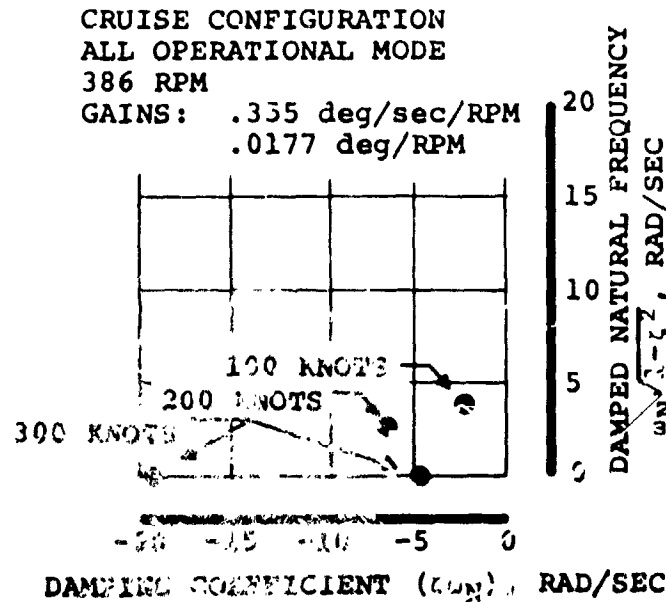
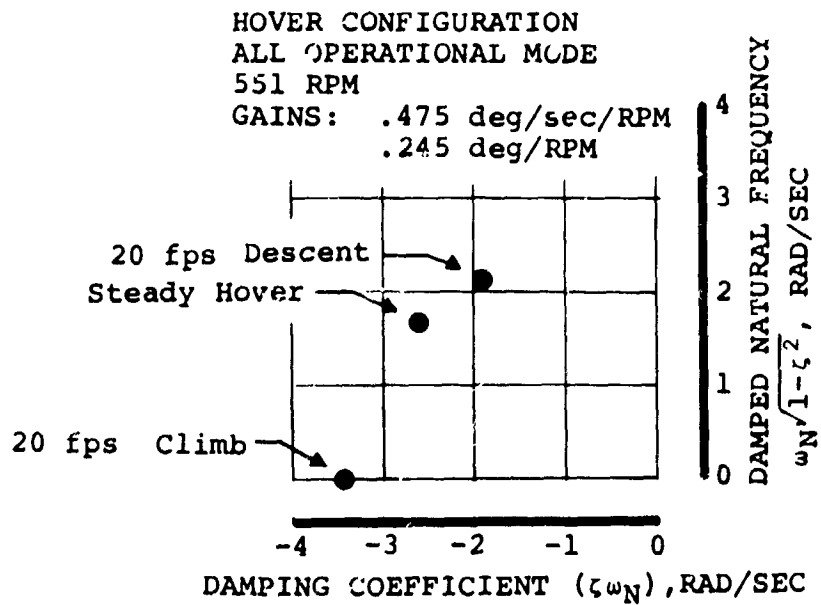


FIGURE 7.24. SINGLE GOVERNOR WITH TWO SENSORS  
ROTOR ROTATION ROOT MIGRATION WITH VELOCITY

tend to increase RPM and the other will tend to decrease RPM. In the vertical mode both rotors tend to move in unison. The governor will tend to maintain constant thrust and thus decrease vertical damping. With no governor the RPM would tend to stay constant for a short period of time (because of rotor inertia effects) and the thrust would increase or decrease - whichever would be in the stable sense - during this interval. Figure 7.25 illustrates the governor effect on the roll and vertical modes in root locus form for a tilt rotor aircraft in the hover configuration. Note that for the vertical mode the root is moved toward the right half plane when the governor is operational which indicates a less stable condition. In fact the vertical damping is reduced by approximately 50%, but as depicted by Figure 7.26 this is still an acceptable damping level.

In the cruise configuration the dutch roll and phugoid modes may be affected. The dutch roll mode will be unaffected by the single governor with two sensors for the same reasons that the roll mode in hover is unaffected (Figure 7.27). The phugoid mode will be adversely affected by the governor because the governor reacts very fast when compared to the phugoid period thus effectively eliminating any prop/rotor effect ( $T_u$  AND  $M_u$ ). For the high wing configuration the rotor effect is stabilizing therefore loss of the prop/rotor effect will destabilize the phugoid (i.e., the aircraft will behave as a jet in this mode). There is an interesting trade-off in the cruise configuration between phugoid damping and aircraft gust



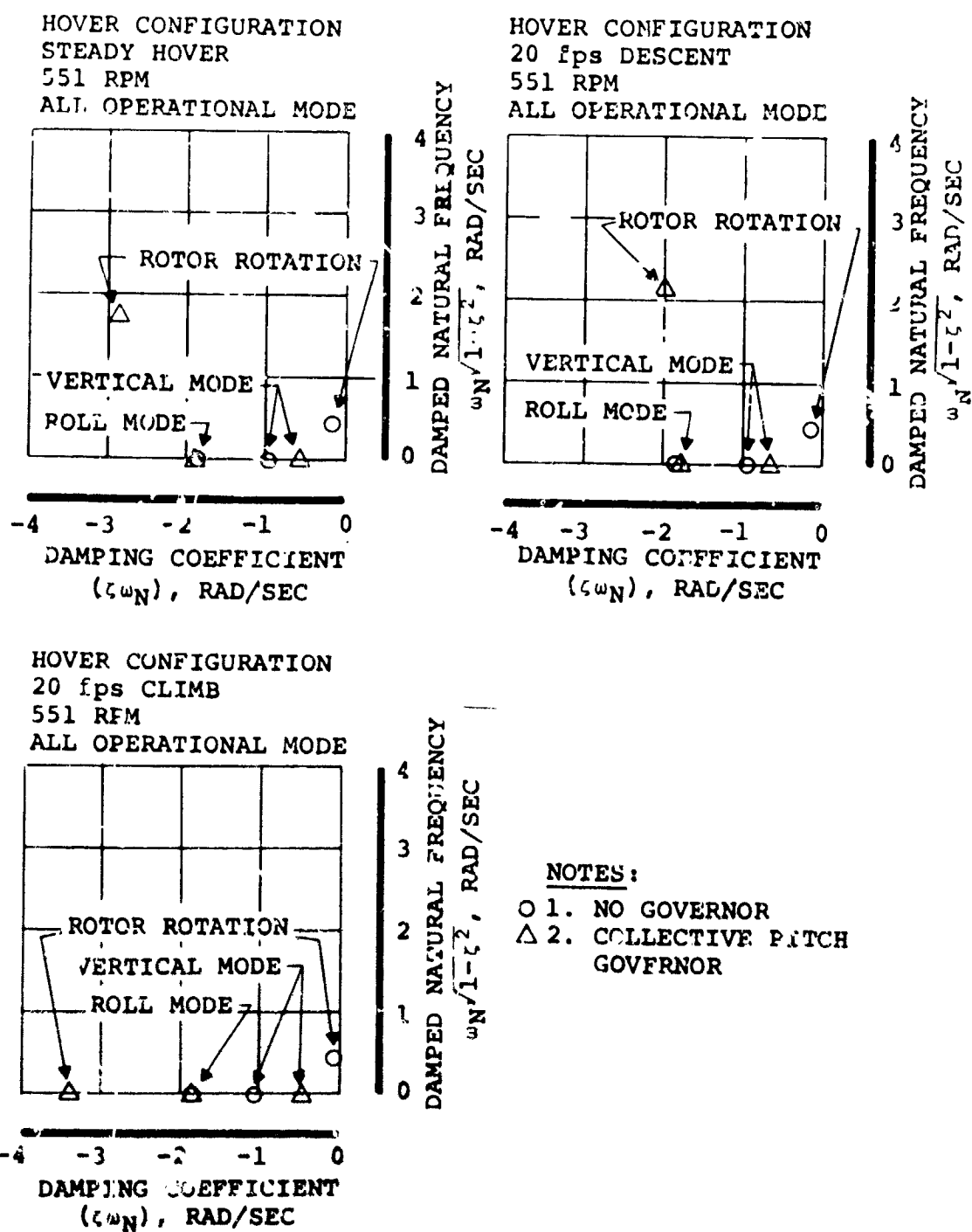


FIGURE 7.25. EFFECT OF GOVERNOR ON HOVER ROLL AND VERTICAL TRANSLATION MODES

VELOCITY DAMPING, PER SEC

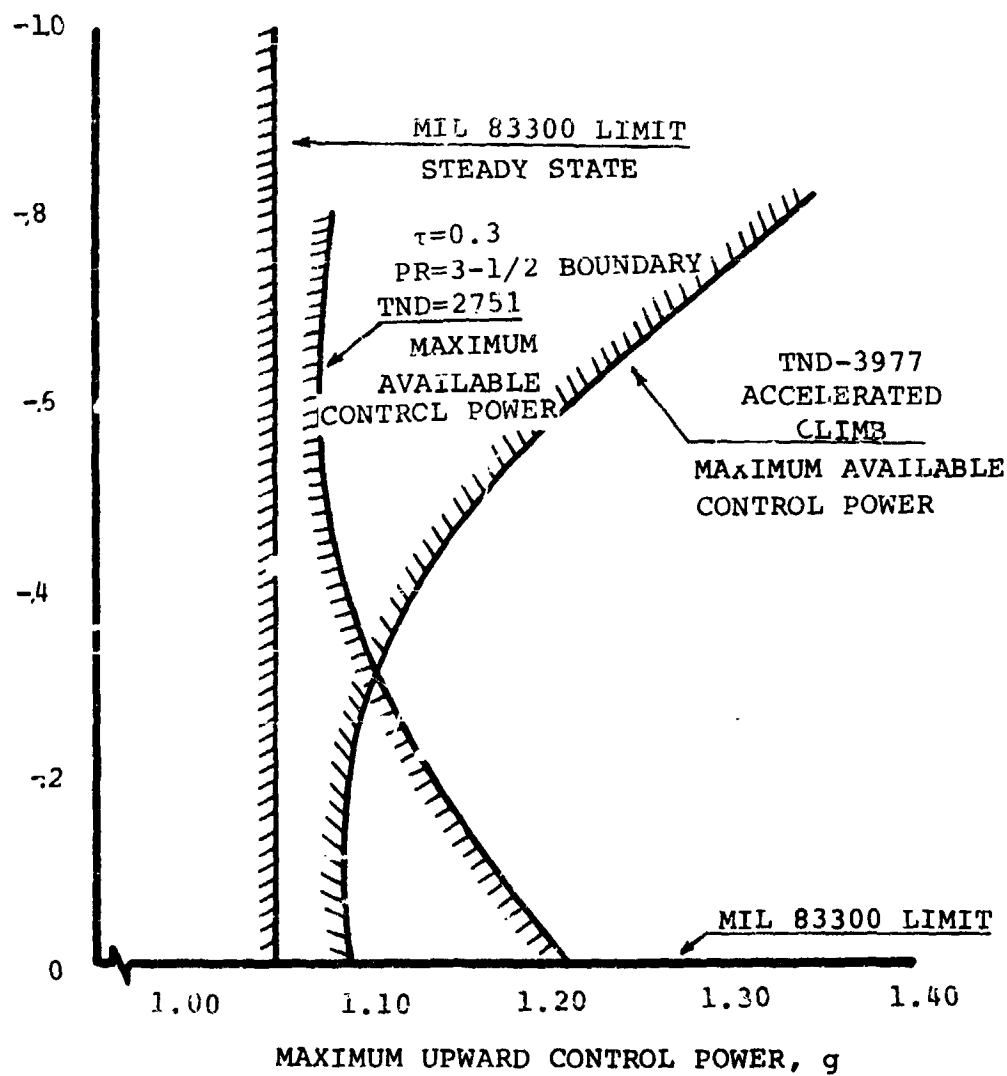


FIGURE 7.26. CRITERIA FOR ACCEPTABLE HOVER CONTROL

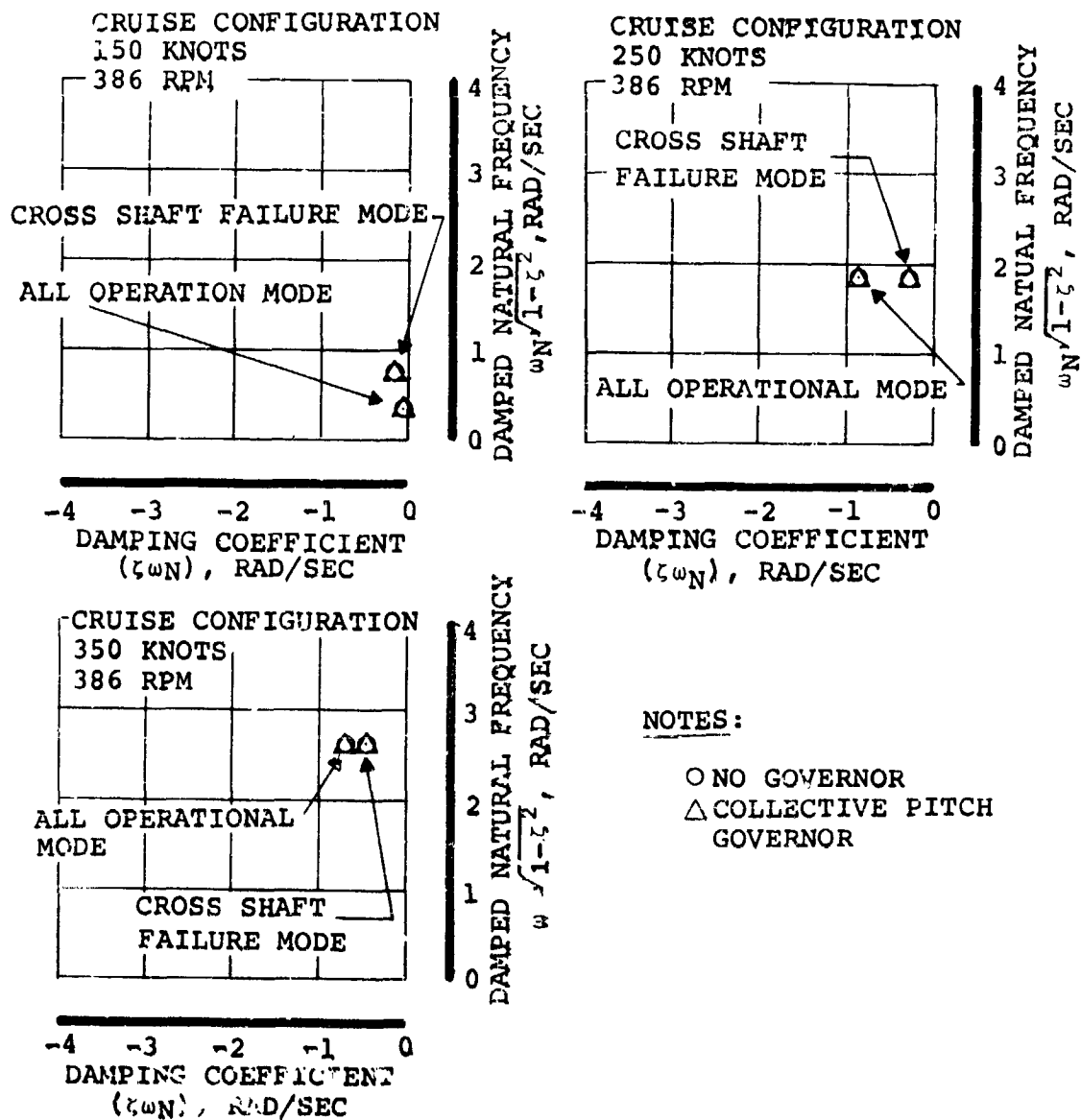


FIGURE 7.27. EFFECT OF GOVERNOR ON DUTCH ROLL MODE

response. For a very "clean" aircraft it may be necessary to have some auxiliary damping from the prop/rotors to meet the MIL Spec 8785B level 1 requirements of a damping ratio of at least .04 in the phugoid mode. One way to obtain this would be to reduce the governor efficiency (and axial gust response relief) to retain some phugoid damping from the rotors.

However, in early tilt rotor configurations one of the most frequently expressed pilot comments concerned the aircraft axial gust response (AFFTC-TR-60-4), therefore it seems for future tilt rotor configurations, aircraft gust response will necessarily be heavily weighed and the trade-off between gust response and phugoid damping cannot be considered lightly.

#### 7.6 GUST RESPONSE

On earlier tilt rotor and tilt wing aircraft, which were designed more from a helicopter viewpoint than fixed-wing, one recurring pilot comment was the poor turbulence response along the longitudinal axis (AFFTC-TR-60-4). Since that time it has become apparent that at least part of the adverse response problem stems from the use of fuel governing rather than collective pitch governing. Figure 7.28 illustrates in a crude manner three different modes of RPM control and the effect of each when hit by an axial gust. There are five parameters to be considered when evaluating axial gust response:

- O gust input
- O RPM
- O fuel flow

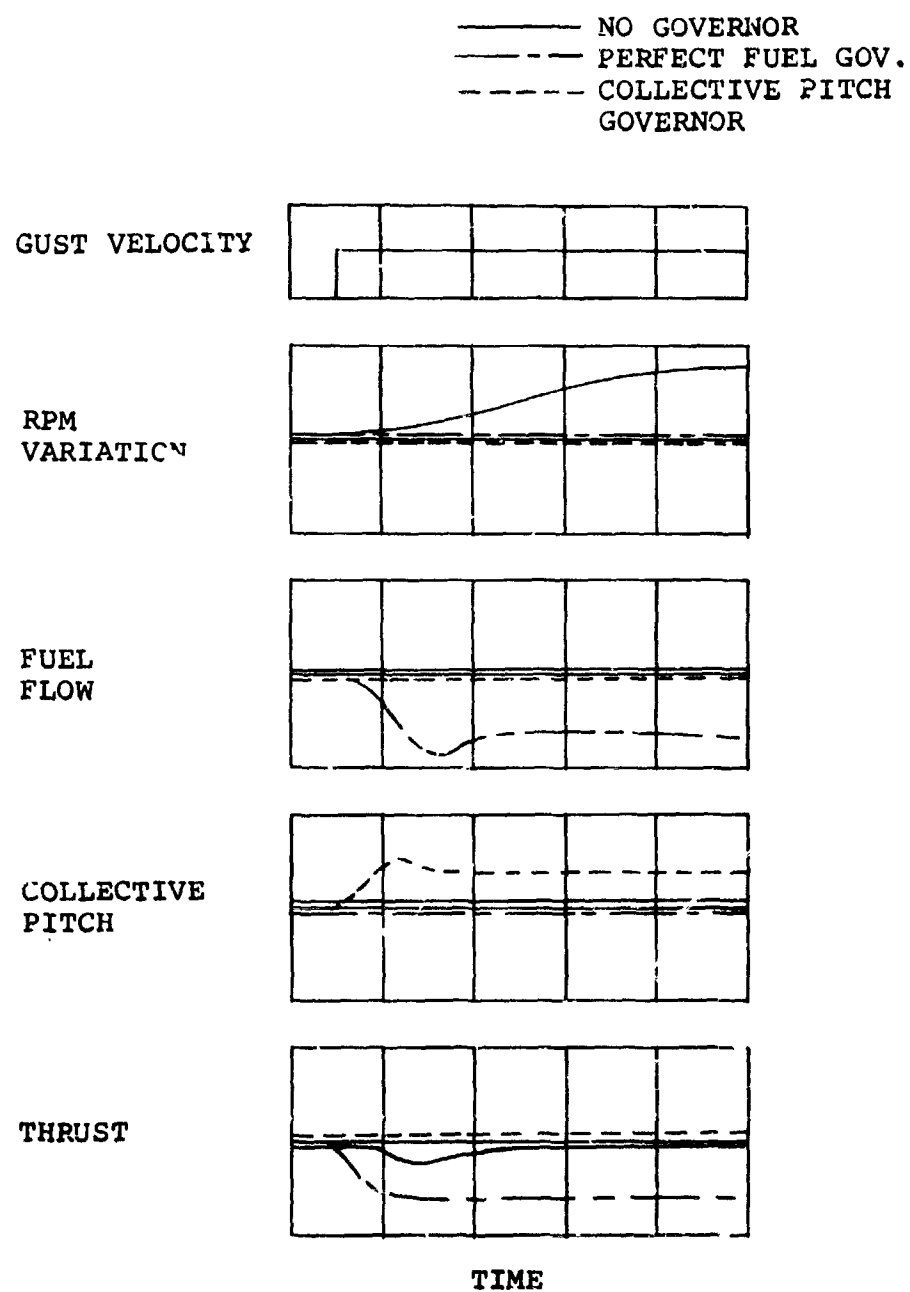


FIGURE 7.28. EFFECT OF GOVERNOR SYSTEM CONFIGURATION ON POWER SYSTEM PARAMETERS

- O collective pitch
- O thrust

Of the three control modes, consider first the case of no RPM governing. When hit by an axial gust, fuel flow and collective pitch stay constant and rotor RPM starts to vary. The result is that in the steady state the thrust does not change substantially from its pre-gust value. For a high inertia rotor there will be some change in thrust as the rotor inertia delays the rpm decay whereas for a small inertia rotor or propeller the RPM will nearly track the gust shape and little thrust variation will be seen. From a gust response point of view, a low rotational inertia rotor having no governor is an acceptable solution; however, without a governor the RPM variations are of such magnitude as to make the system unacceptable. Next consider the perfect fuel governor (i.e., one that keeps RPM absolutely constant by controlling fuel flow). When the rotor is hit by a gust the fuel flow increases or decreases, collective pitch remains constant and RPM is constant resulting in a change in thrust. The change in thrust will result in acceleration along the longitudinal axis which will be detrimental to the ride and handling qualities of the aircraft. The fuel governor then is the converse of the no governor case - RPM control is acceptable but gust response is not. The collective pitch governor varies rotor blade angle to control RPM at constant power setting. When the rotor is hit by a gust, fuel flow remains unchanged and collective

pitch varies in a manner to maintain constant RPM and constant thrust. This configuration governor then solves the aircraft axial gust problem by:

- 0 reducing aircraft gust response
- 0 eliminating the RPM variation

Time history gust responses were run for the three modes of operation discussed above. Collective pitch governor dynamics and gains were employed as defined in paragraph 7.4.3. Perfect fuel governing was evaluated to establish an upper limit gust response for that configuration and to show a comparison with collective pitch style governing. The no governor case allowed the rotor to freely spin on the hub. Response in both hover and cruise configurations was evaluated. RPM variation, cabin acceleration and significant structural responses have been plotted for each case.

Two gust shapes were used in the evaluation: 1-cos and random. The 1-cos shape was used to evaluate the governor response in cruise and hover (i.e., determine if the accuracy and transient response goals were met). Random turbulence was used in the 300 knot cruise case to illustrate the aircraft response with governor operative when encountering turbulent air. The turbulence model was obtained from NASA and is described in Reference 7.2. Results of the gust response study were much as expected except that the adverse acceleration response of the fuel governor in cruise was worse than anticipated. Figures

7.29 through 7.31 show the results.

In the cruise configuration, the collective pitch governor effectively keeps the RPM within the 2% transient error and the .3% steady state error criteria while reducing the longitudinal acceleration response to gusts to a near zero level. Significant structural blade elastic modes show no adverse response. In the worst case (fuel governing) the structural load and blade modal response is well below allowable limits. Comparison of the fuel governor and collective pitch governor traces indicate at a glance the desirability of the collective pitch governor from a gust response viewpoint. Longitudinal acceleration is reduced from a peak value of 9 ft/sec<sup>2</sup> to 2 ft/sec<sup>2</sup> at 100 knots (the worst case for the collective pitch governor) and at 300 knots from 7 ft/sec<sup>2</sup> to less than 1 ft/sec<sup>2</sup>. Thus at cruise velocities the pilot may fly through a 20 fps axial gust with minimum aircraft response. Use of the collective pitch governor should effectively solve the longitudinal acceleration problem noted in AFFTC-TR-60-4. Improvement in the structural gust response is also noted with collective pitch governing. Although even with fuel governor the blade modal response and wing chord bending response is small, the collective pitch governor improves the response on the same order of magnitude as the acceleration response is improved. Figure 7.32 illustrates the aircraft flying through clear air



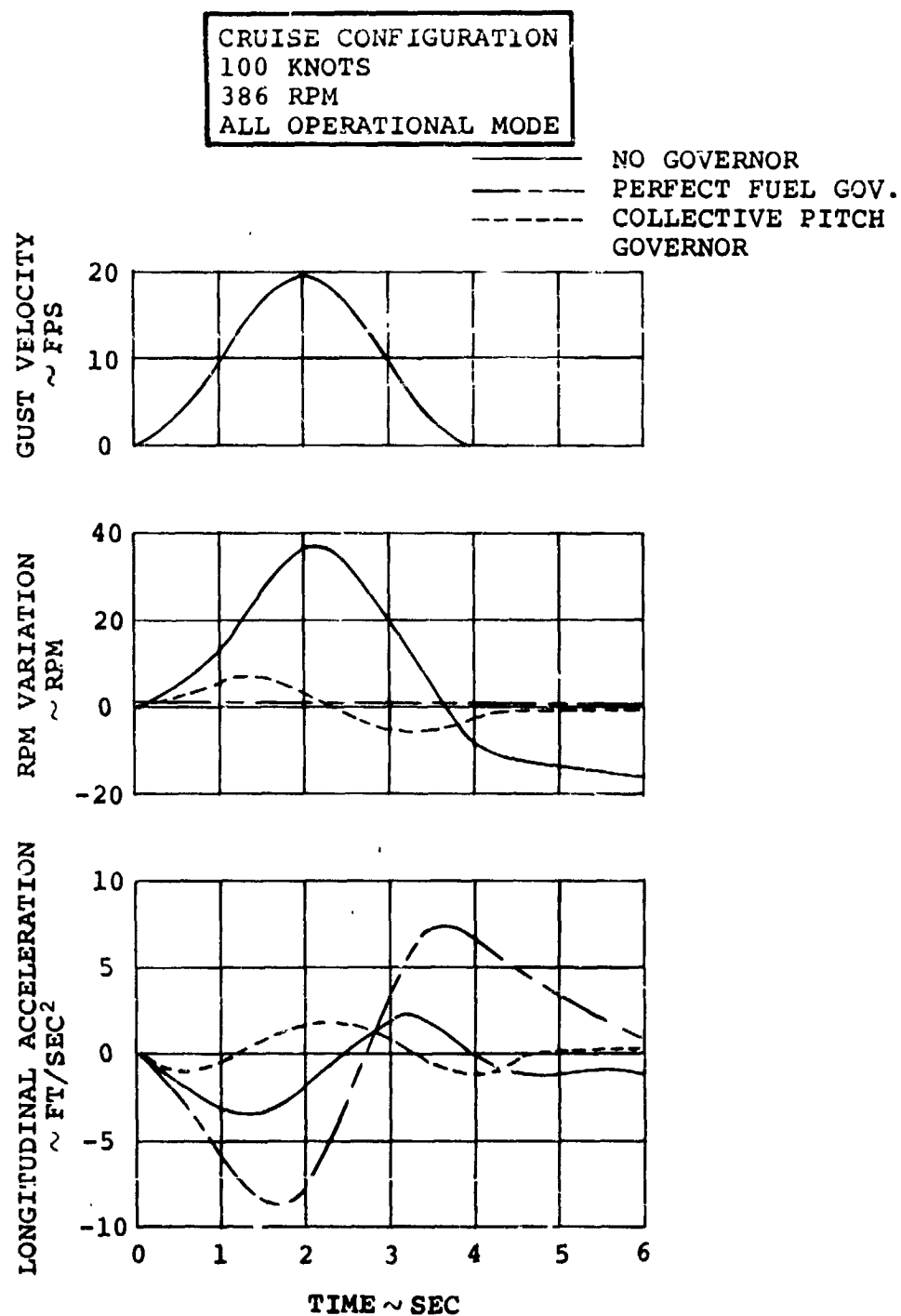


FIGURE 7.29a. AIRCRAFT RESPONSE TO 1-COS AXIAL GUST  
100 KNOT CRUISE

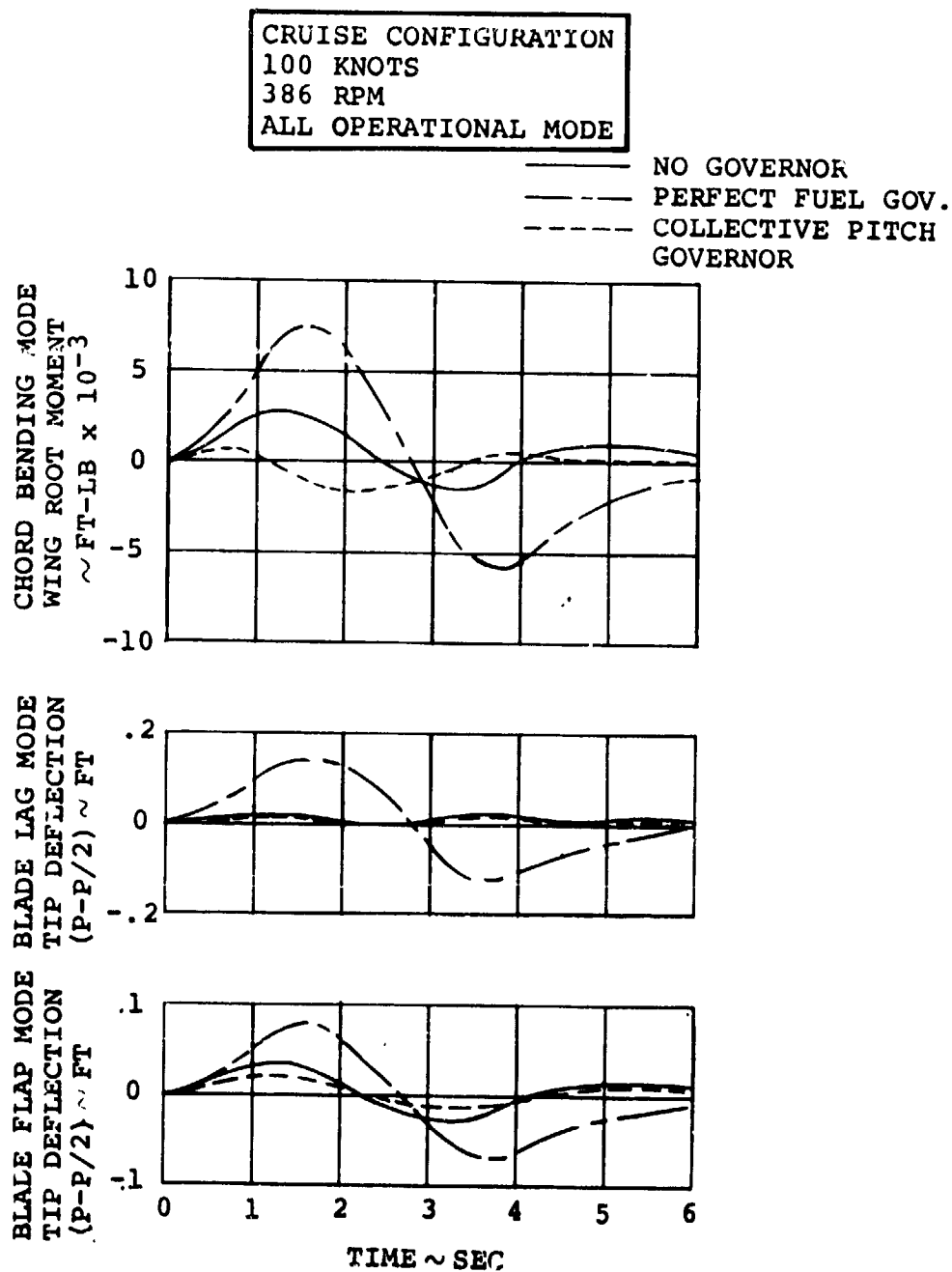


FIGURE 7.29b. AIRCRAFT RESPONSE TO 1-COS AXIAL GUST  
100 KNOT CRUISE

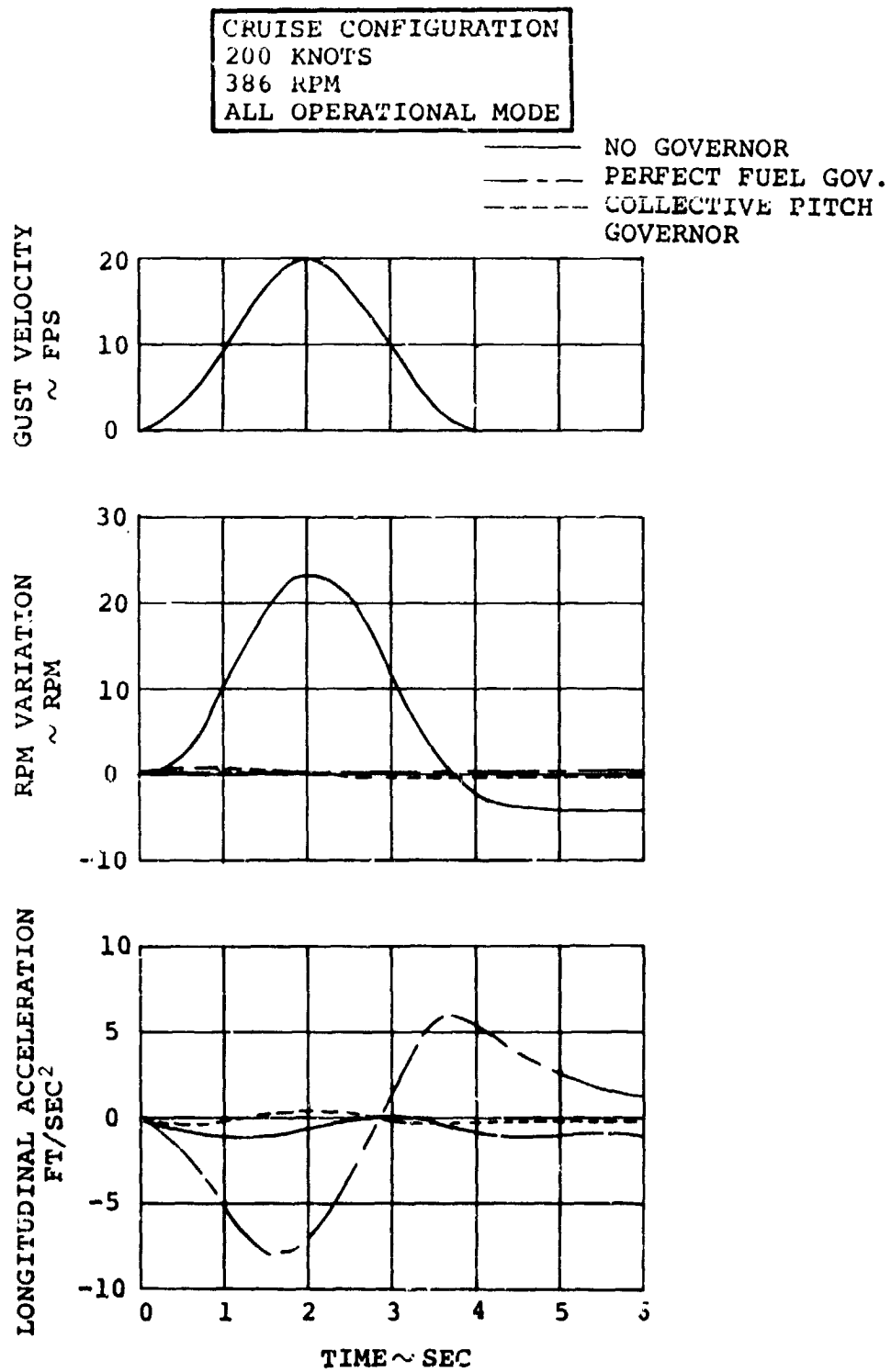


FIGURE 7.30a. AIRCRAFT RESPONSE TO 1-COS AXIAL GUST  
200 KNOT CRUISE

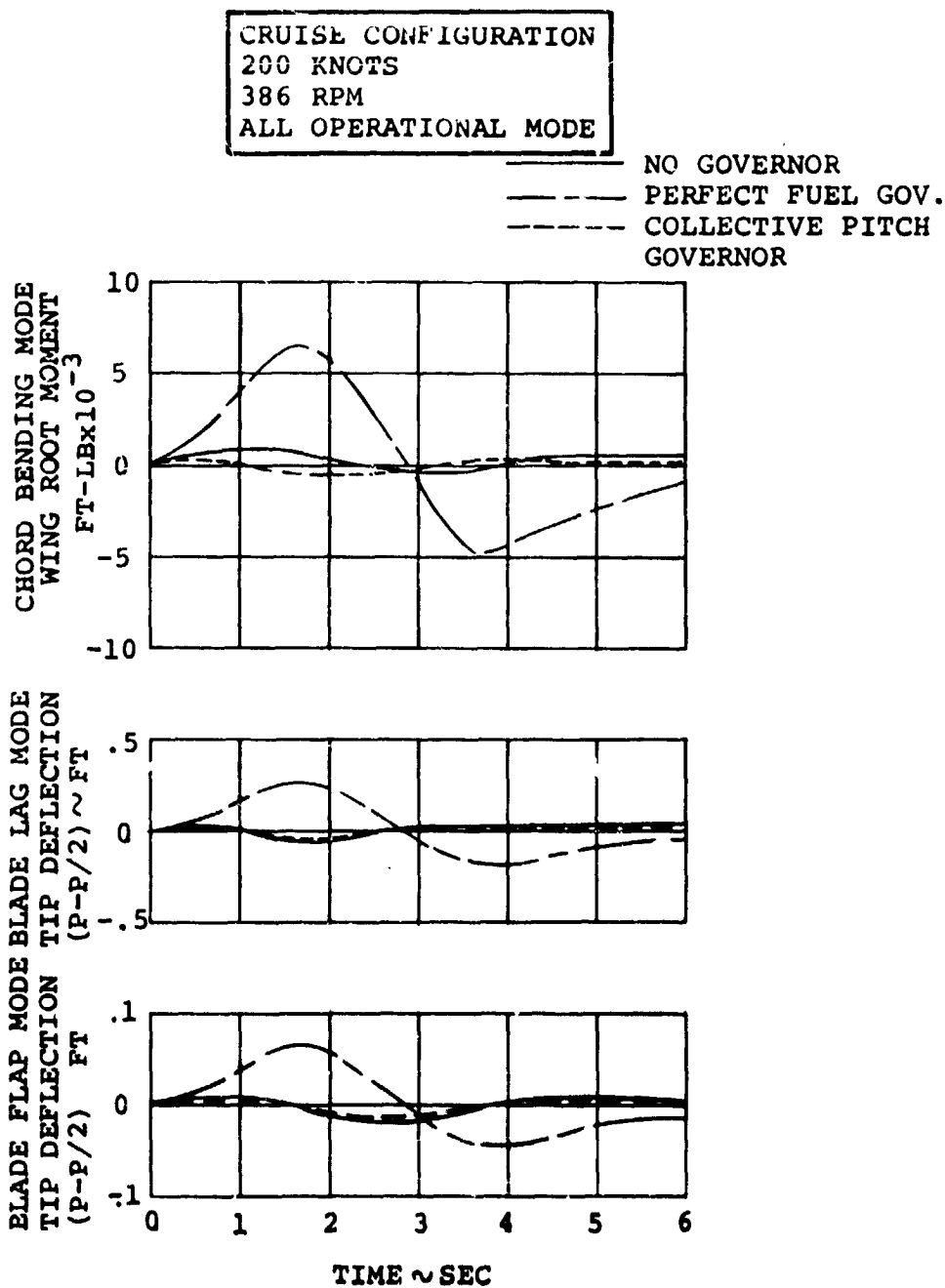


FIGURE 7.30b. AIRCRAFT RESPONSE TO 1-COS AXIAL GUST  
200 KNOT CRUISE

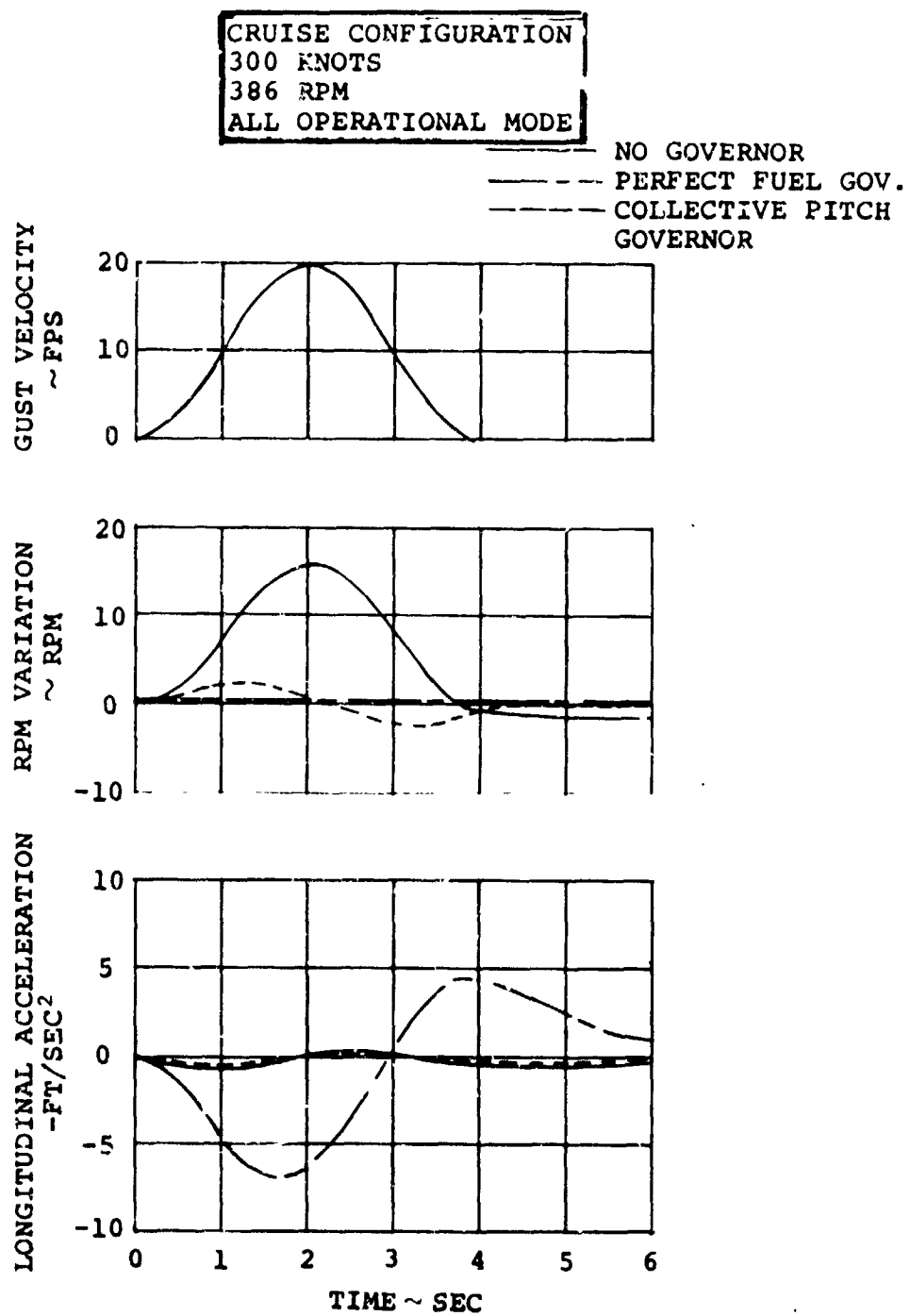


FIGURE 7.31a. AIRCRAFT RESPONSE TO 1-COS AXIAL GUST,  
300 KNOT CRUISE

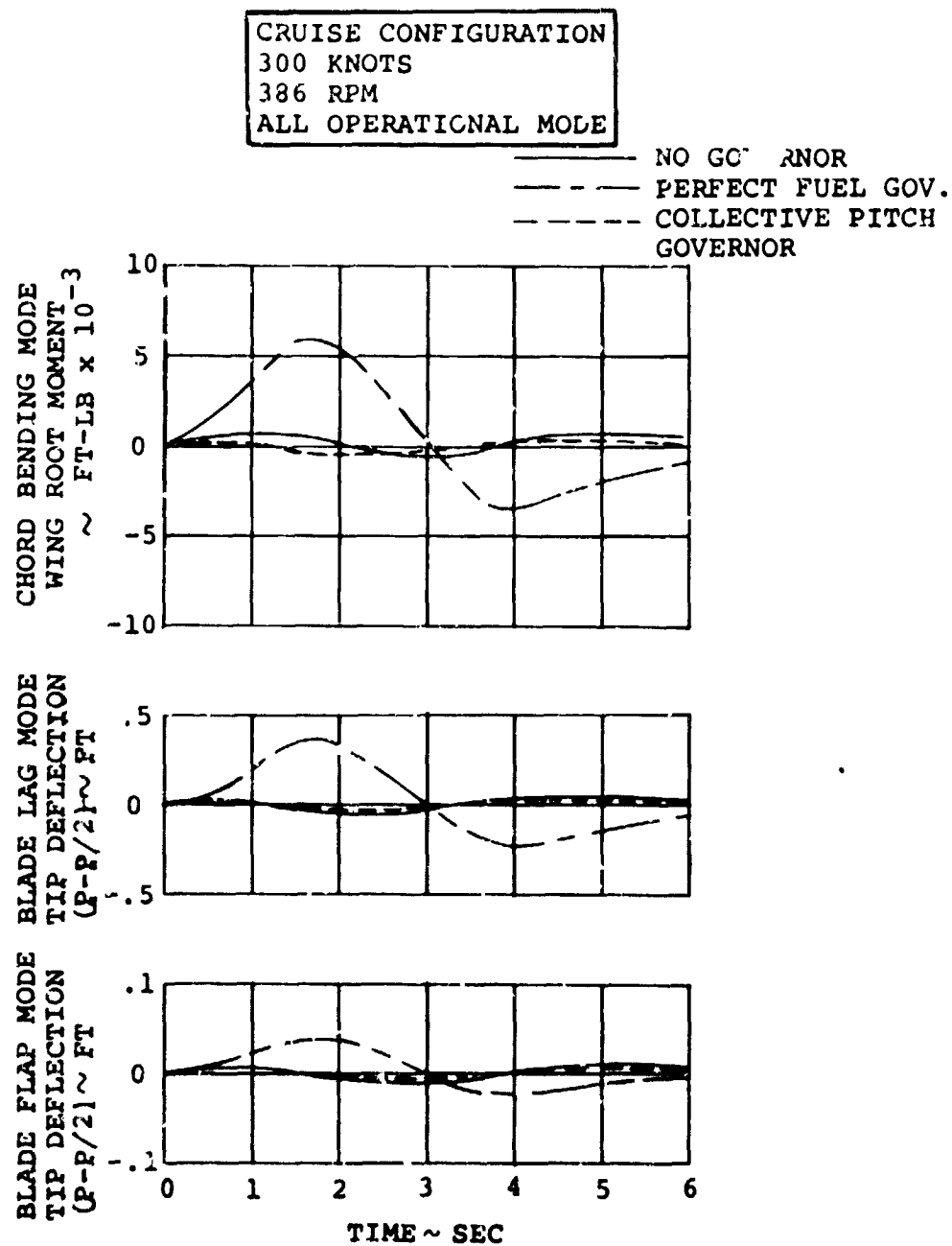


FIGURE 7.31b. AIRCRAFT RESPONSE TO 1-COS AXIAL GUST  
300 KNOT CRUISE

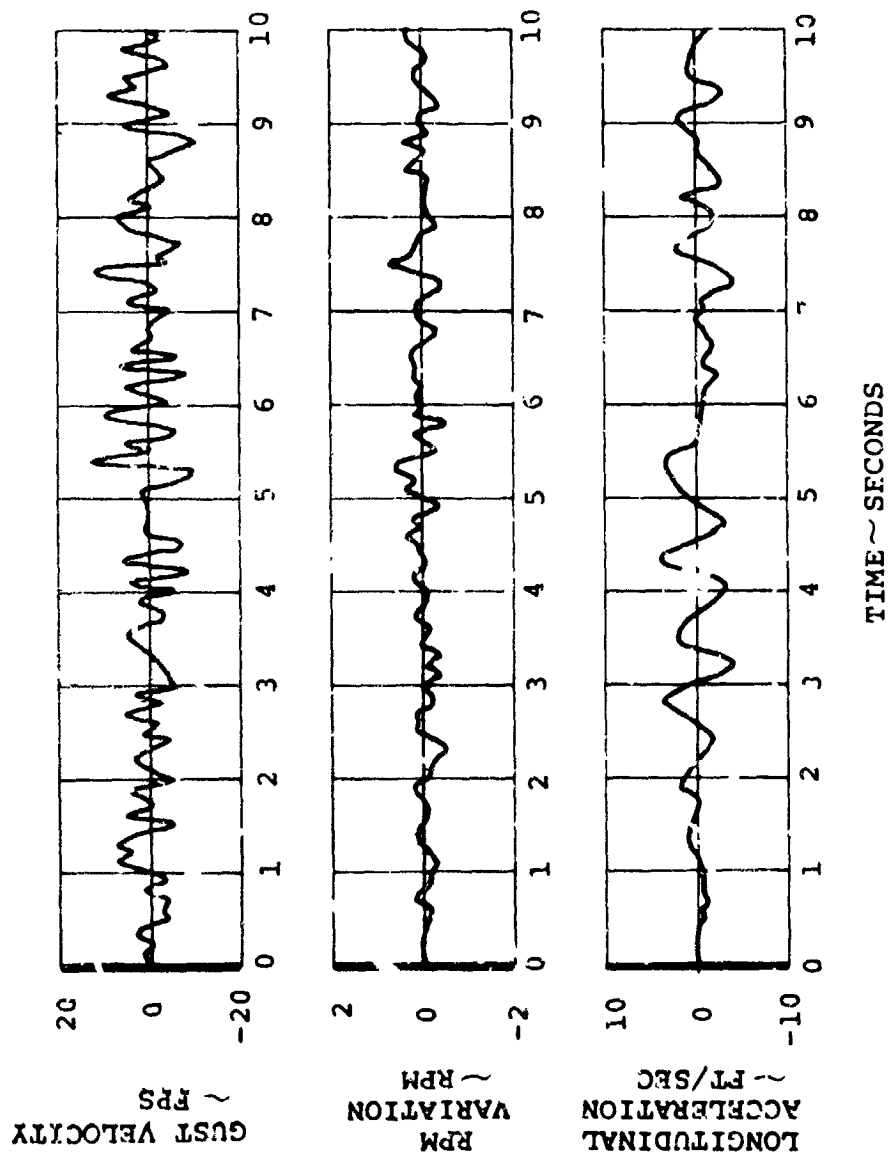


FIGURE 7.32. AIRCRAFT RESPONSE TO AXIAL RANDOM TURBULENCE  
300 KNOTS - COLLECTIVE PITCH GOVERNOR

turbulence at 300 knots with the governor operative. Note that the same desirable characteristics are present as observed with the 1-cos gust. The RPM error is well within the specified bounds and in fact the peak variation is never greater than 1 RPM (.3% error). Longitudinal acceleration is attenuated with maximum acceleration never greater than .125 "g".

In the hover configuration, collective pitch governing improves the aircraft gust response in much the same manner as cruise, even if the improvement in gust response is not as striking. The effect is shown in Figures 7.33 through 7.35. RPM variation is well within the transient and steady state goals, acceleration and structural response is improved. Once again the wing bending moments are well within allowable limits for an aircraft of this type and the blade responses are small enough to be considered insignificant.

One major difference between cruise and hover is the similarity in vertical acceleration for the no governor and fuel governor cases. Because of the slower rotor response (lower natural frequency) than in cruise, the rotor does not respond as quickly and there is a larger vertical acceleration response. Although good gust response is desirable in hover, the RPM hold capability is more important along with the effect on flying qualities as described in paragraph 7.5.

The collective pitch governor has a significant beneficial effect on aircraft gust response in both cruise and hover. In



fact the analysis shows that in cruise the collective pitch governor eliminates one portion of the adverse gust response seen in earlier tilt rotor aircraft.

#### 7.7 CONCLUSIONS

A collective pitch governor which senses the RPM variation of each rotor and feeds back collective pitch proportionally to the averaged signal has been chosen as the configuration which satisfies the requirements of a tilt rotor aircraft. RPM variation has been shown to be within the error criteria for 1-cos and random axial gusts. In the rigid body modes which may be affected there is either no degradation or a small degradation which is not harmful to the flying qualities of the aircraft. The most significant improvement this governor configuration makes on the aircraft is in axial gust response in cruise. The "bucking" or "jerking" of earlier tilt rotor configurations has been eliminated so that the aircraft may now fly in turbulent conditions with a minimum of longitudinal response in cruise.

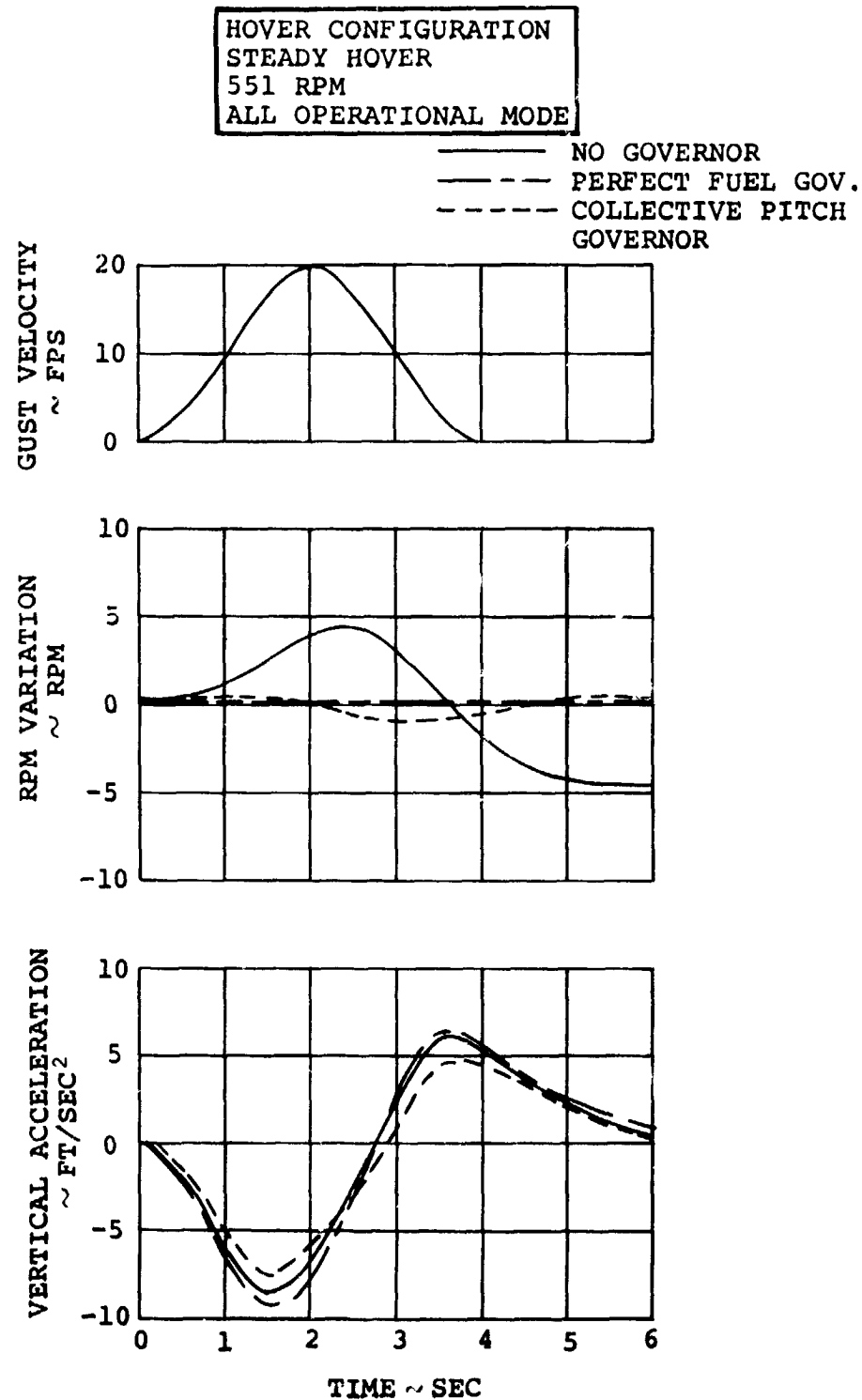


FIGURE 7.33a. AIRCRAFT RESPONSE TO 1-COS AXIAL GUST  
STEADY HOVER

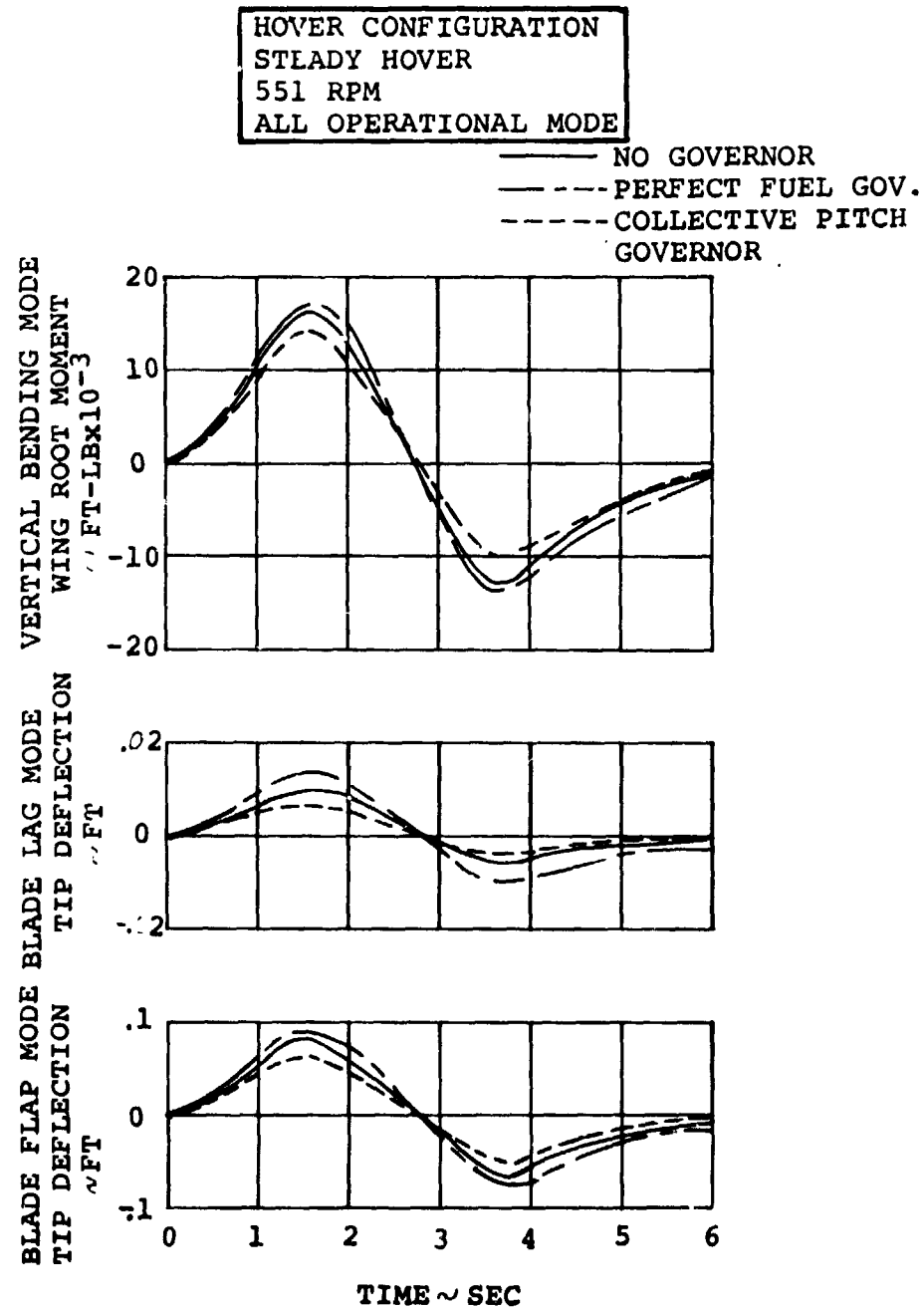


FIGURE 7.33b. AIRCRAFT RESPONSE TO 1-COS AXIAL GUST  
STEADY HOVER

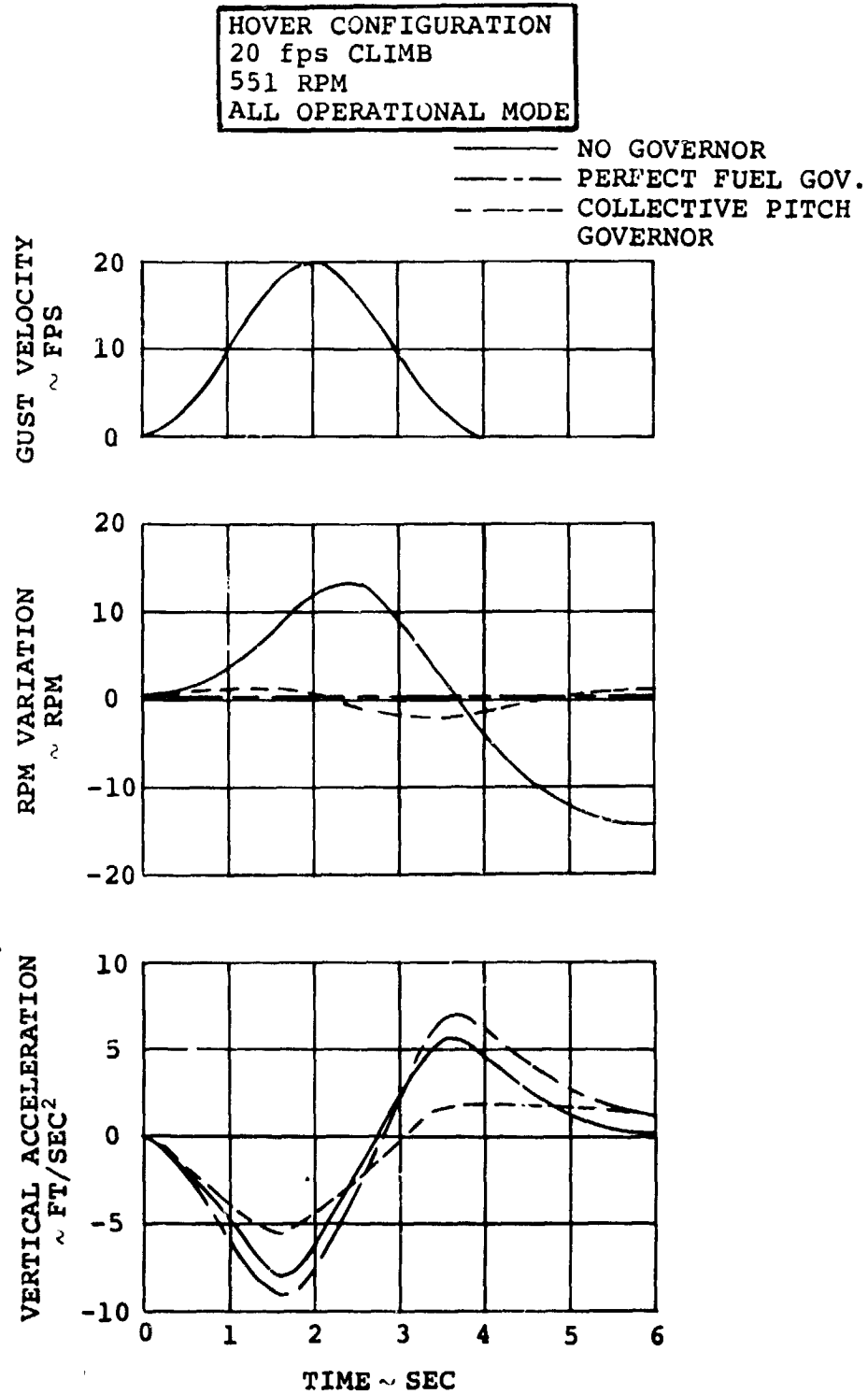


FIGURE 7.34a. AIRCRAFT RESPONSE TO 1-COS AXIAL GUST  
 HOVER - 20 fps CLIMB

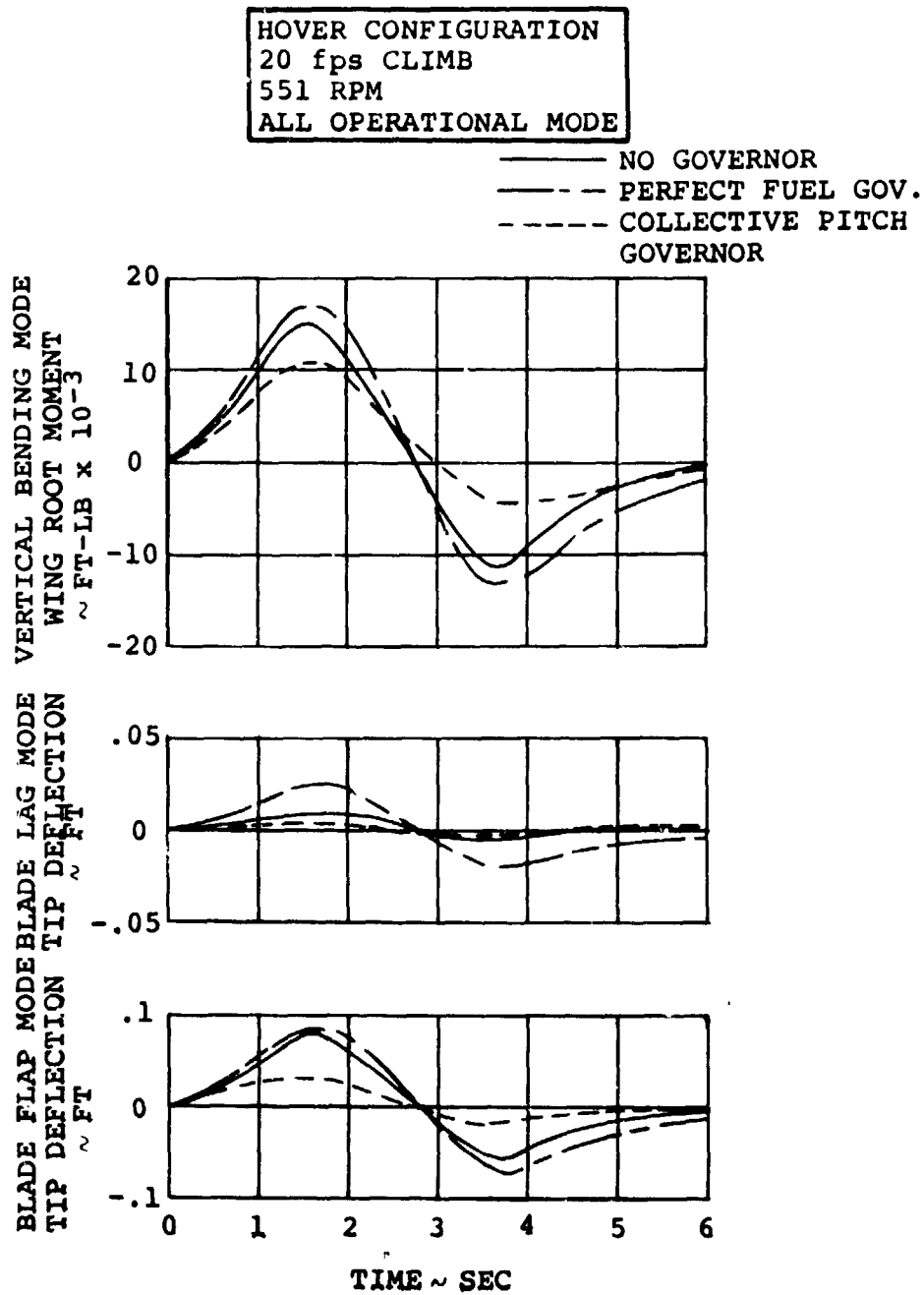


FIGURE 7.34b. AIRCRAFT RESPONSE TO 1-COS AXIAL GUST  
 HOVER - 20 fps CLIMB

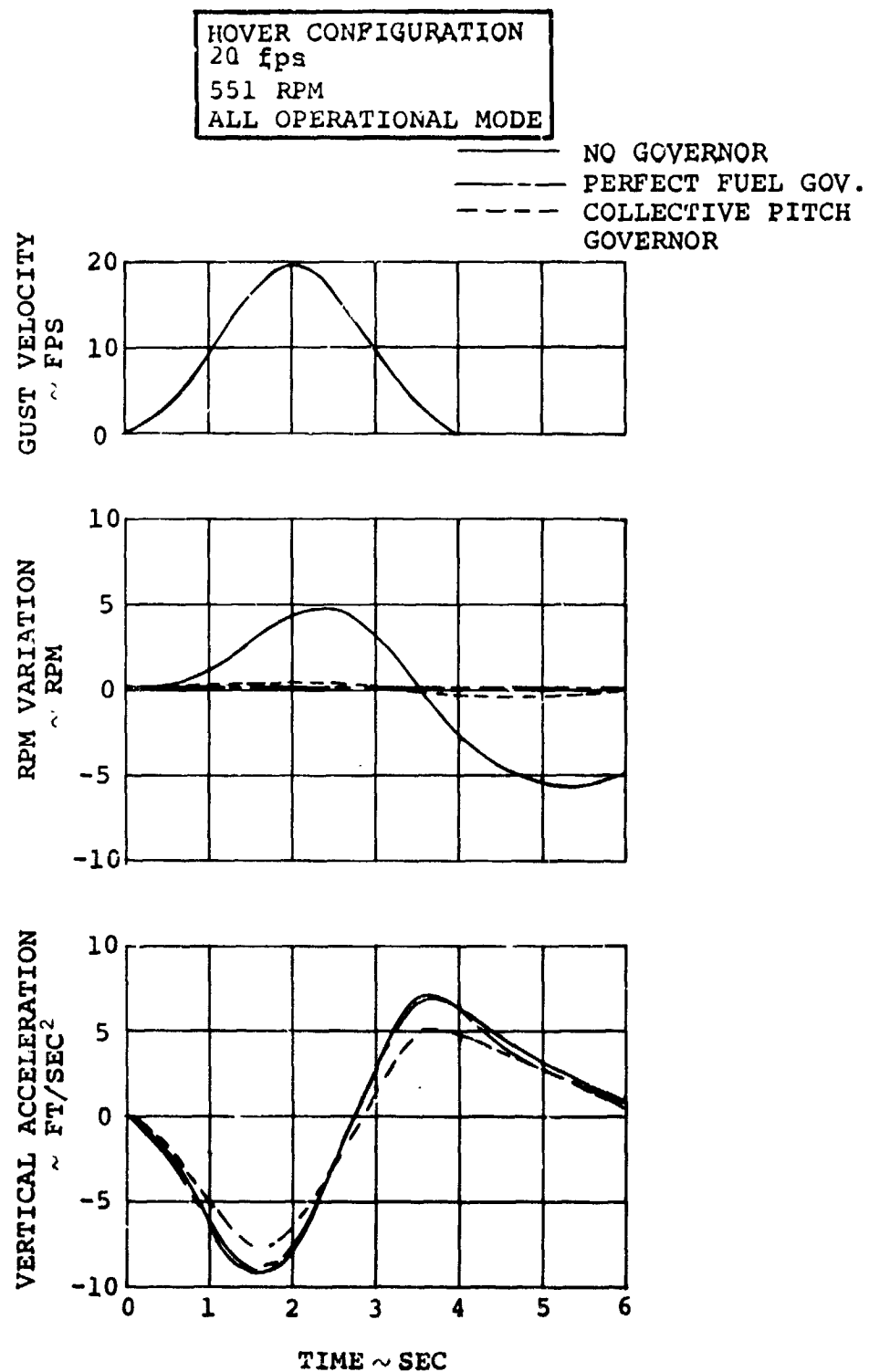


FIGURE 7.35a. AIRCRAFT RESPONSE TO 1-COS AXIAL GUST  
 HOVER - 20 fps DESCENT

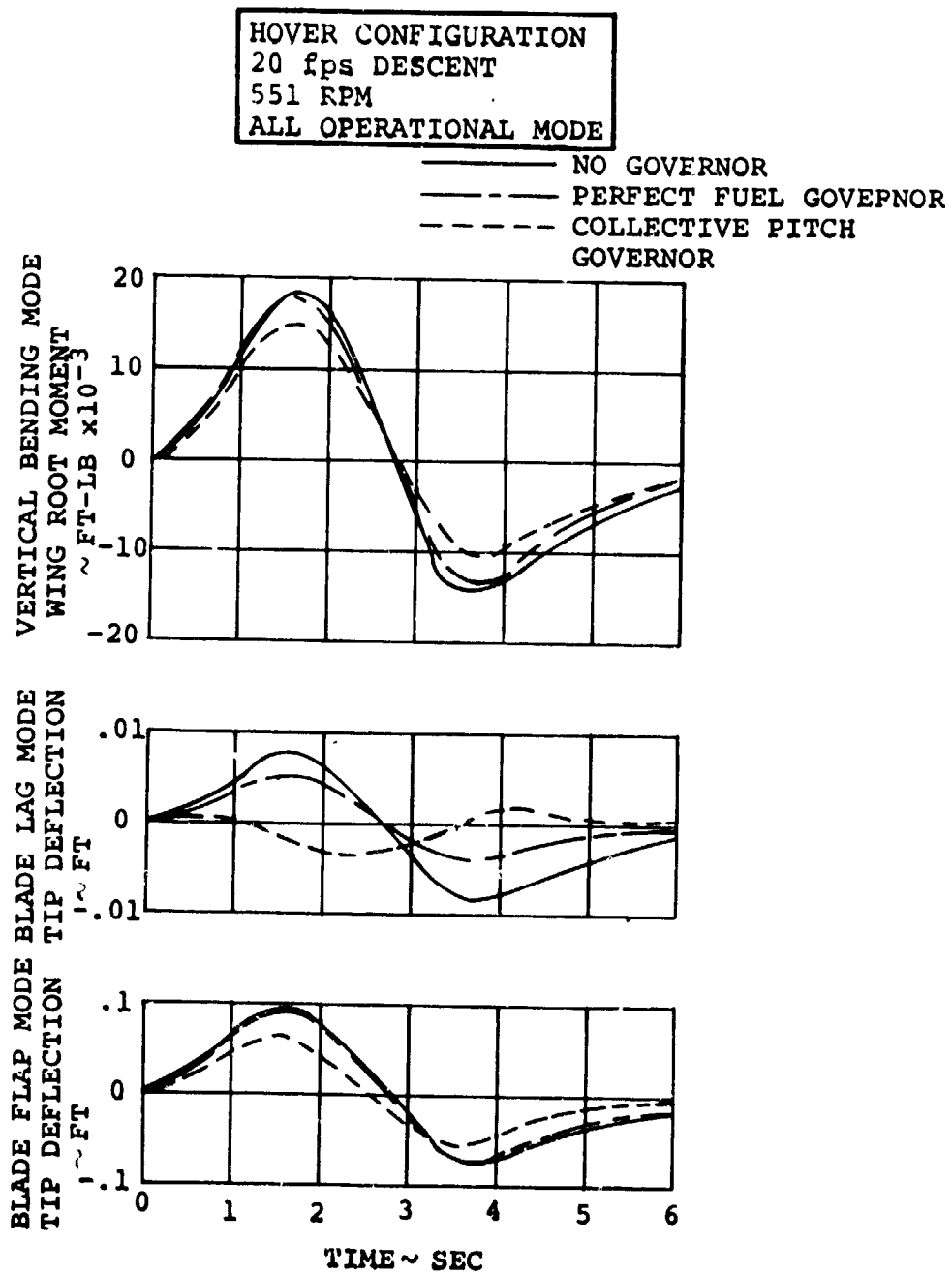


FIGURE 7.35b. AIRCRAFT RESPONSE TO 1-COS AXIAL GUST  
 HOVER - 20 fps DESCENT

8. APPLICATIONS OF SWASHPLATE FEEDBACK SYSTEMS TO FOLDING  
TILT ROTOR CONFIGURATIONS

Applications of swashplate feedback for the folding tilt rotor aircraft fall into two categories:

1. loiter or low speed cruise, and
2. spin up and spin down.

In both of the above categories the level of blade loads is not prohibitive without feedback; however, the loads may be reduced to a lower level for gust alleviation or stability augmentation.

In the loiter or low speed cruise regime the same concepts of load alleviation may be applied as in Paragraphs 3 and 7. The rotor will be fully operational and spinning at design RPM; hence, the configuration will be identical to tilt rotor configurations previously analyzed. An area of concern for this system will be, if and how, to phase out swashplate feedback as the aircraft approaches the folding regime of flight. This problem will not be one of advancing the technology, but rather one of gain scheduling.

Spin up and spin down of the rotor may be a possible cause of high blade loads. To investigate the level of these loads, a scale model test of the folding tilt rotor was undertaken in 1971 using a 1/9 scale semi-span model. The results may be reviewed in Ref. 8.1, Air Force Technical Report AFFDL-TR-71-62, Vol. VII. In summary, various spin up and spin down schedules were tried to investigate the effect on blade loads. In each



case the loads were small. There was not a large variation in loads for the different spin schedules and, in fact, the final schedule was chosen on a basis of drag, not blade loads. It therefore appears that feedback will not be required during spin up and spin down, and it may be convenient to phase it out at some rpm lower than normal cruise.

## 9. CONCLUSIONS AND RECOMMENDATIONS

The analytical studies reported in Sections 2 through 8 confirm that substantial benefits may result from the proper use of feedback using the active controls and also the conventional controls. There is a high level of confidence in the validity of the results based on the correlation with test data performed using the methodology of this report. Examples of this predictive and correlation capability are given in the text and a more extensive coverage of its topic is given in the test report on the full scale test of the Model 222 26-foot diameter rotor in the NASA-Ames 40 X 80-foot tunnel. Hence the broad conclusions and recommendations of the report may be accepted without reservation.

The parametric studies on rotor derivatives show that the low in-plane stiffness rotor enjoys a negative hub pitching moment under normal flight conditions so that the net destabilizing effect of the rotor on static stability is less than that which would exist for a high stiffness blade and this is confirmed by test data. This has beneficial effects on horizontal stabilizer area requirements.

Studies in blade load alleviation and stability augmentation show that various alternative objectives may be met using cyclic feedback. Cases examined included minimization of blade flapping, and minimization of net pitching moment about the aircraft center of gravity. No stability problems were en-

countered although additional shaping was recommended in one case to increase the phase margin. It was found that the requirements of gain and azimuth might be different in dynamic gust response cases compared with steady state alleviation and methods of resolving these requirements are identified and recommended for further study.

The use of feedback through the conventional control systems for direct lift control and alleviation of normal acceleration response in turbulent air was studied and found to be effective in cruise and less effective in transition. The reductions in response demonstrated were 45% in cruise and 15% in transition. These results are extremely encouraging since they were obtained without special effort at optimization, or inclusion of elevator feedback effects to trim the pitching moments due to flap and spoiler application.

Collective pitch governor studies indicated that a governing system which senses the RPM variation of each rotor and feeds back collective pitch proportional to the averaged signal should be chosen as the configuration which satisfies the requirements of a tilt rotor aircraft. RPM variation has been shown to be within the error criteria for  $(1-\cos)$  and random axial gusts. This governor system does not produce any significant degradation in the flying qualities of the aircraft and the response to axial or head on gusts is very substantially attenuated.

Extensive work on modal suppression showed that very substantial increases in damping of selected modes could be accomplished and this result has been fully confirmed by full scale tests in the 40 X 80-foot tunnel. Attempts to introduce additional damping to the blade modes in hover showed some promise, but this topic was not fully developed because it is of somewhat academic interest at the present time.

A general conclusion which emerges from these studies is that the full potential of some systems depends on interaction with an associated system. These relationships are summarized in Table 9.1. Thus, the effectiveness of a blade load alleviation system will be enhanced if aircraft acceleration response to gusts is reduced by direct lift control. Conversely the effectiveness of a direct lift feedback system may be improved when working in conjunction with a high rate swashplate modal suppression system. Thus, there is a strong case for the eventual implementation of all the feedback controls listed, however, priority should be given to the conventional SAS, rotor governing and blade load alleviation systems.

TABLE 9.1. SUMMARY OF FEEDBACK CONTROL SYSTEM RELATIVE APPLICATIONS AND INTERACTIONS

IDEV	SENSORS SIGNALS	BENEFITS	LIMITATIONS	RELATION TO OTHER SYSTEMS
BLADE LOAD ALLEVIATION/ STABILITY AUGMENTATION SYSTEM	AQ OR STRAIN	REDUCTION IN BLADE LOADS AND IMPROVE- MENT IN FLYING QUALITIES.	BLADE LOADS NOT COM- PLETELY CONTROLLED BY CYCLIC FEEDBACK. A/C ACCELERATIONS ALSO FORCE BLADES.	BLADE LOAD CONTROL CAN BE IMPROVED FURTHER BY CON- CURRENT USE OF DIRECT LIFT FEEDBACK.
DIRECT LIFT	AQ OR NORMAL ACCELERATION	ATTENUATES ACCEL- ERATIONS DUE TO GUSTS. IMPROVES HEIGHT CONTROL.	ATTENUATION PROBABLY LIMITED BY WING MODAL RESPONSE, WHICH MAY BE EXCITED BY SYSTEM. MAY REQUIRE ASSIST FROM MODAL ATTENUATION SYSTEM.	WILL HELP BLADE LOAD SYSTEM BY REDUCING ACCELERATION FORCING OF THE BLADES.
ROTOR COLLECTIVE/ COVERING	RPM	CONTROLS RPM AND BLADE RESPONSE TO AXIAL GUSTS. ALSO FORE AND AFT ACC- ELERATION IN CRUISE. DOES NOT DEGRADE A/C LATERAL DIRECTIONAL RESPONSE TO GUSTS.	EFFECTIVENESS NOT SIGNIFI- CANTLY LIMITED IN CRUISE OR HOVER SINCE LONGITUDINAL FORCES ARE PREDOMINANTLY FROM ROTOR. SOME LIMITA- TION IN NORMAL "G" ATTENU- ATION AT HIGH SPEED END OF TRANSITION DUE TO WING LIFT.	NO SIGNIFICANT INTERACTION WITH OTHER SYSTEMS.
MODAL SUPPRESSION SYSTEM	MODAL ACCELER- ATION OR RATE	DAMPING INCREASE IN AEROELASTIC MODES. MAY BE USED TO AUG- MENT EFFECTIVENESS OF DIRECT LIFT "G" CONTROL.	EFFECTIVENESS REDUCED AT HIGH FREQUENCIES DUE TO BLADE TIME CONSTANTS. SENSITIVE TO FLIGHT CONDITION.	PROBABLY HIGH LEVEL OF INTERACTION WITH DIRECT LIFT SYSTEM.
CONVENTIONAL SAS	A/C RATES, SIDE- SLIP AND ANGLE OF ATTACK	PROVIDES ACCEPTABLE SHORT PERIOD, ETC. CHARACTERISTICS.	DOES NOT ATTEMPT TO PRO- VIDE POSITIVE CONTROL OF GUST RESPONSE LOADS, ETC.	RELATIVELY LITTLE DIRECT INTERACTION. USES SAME ACT- UATORS ADDING OR SHARING AUTHORITY.

## 10. HARDWARE CONSIDERATIONS

### 10.1 INTRODUCTION

From the standpoint of hardware implementation the feedback control is subdivided into two major subsystems: the Stability Augmentation System (SAS) which accomplished the functions of rate damping, load alleviation, mode suppression, and turn coordination, and the Governor System which accomplished the function of rotor speed stabilization and collective control quickening in hover. In the SAS system we are primarily concerned with the load alleviation and modal suppression sections of the system. Changes in the currently proposed Model 222 hardware which would be needed to implement the recommendations of this report are discussed in paragraphs 10.4 and 10.5. In each case changes have been suggested which would reflect the minimum cost and modification to the Model 222 flight control system.

### 10.2 STABILITY AUGMENTATION SYSTEM (SAS)

SAS stabilization occurs through differential electrohydraulic actuators (extensible link type) inserted in the primary mechanical flight control system. The actuation points for the SAS are as follows: primary longitudinal control for longitudinal rate damping, longitudinal load alleviation and longitudinal mode suppression; primary lateral control for lateral rate damping; primary directional control for yaw rate damping; lateral cyclic control at each rotor for lateral load alleviation and lateral mode suppression. A typical hardware functional block diagram of the SAS is

shown in Figure 10.1.

#### 10.2.1 Redundancy

The level of redundancy of the SAS is dictated by the required authority, and by the SAS failure requirements.

A fail functional system requires at least triple redundancy regardless of the authority. Fail functional is defined as the capability of the system to continue to perform its function without any degradation after any single failure.

A fail operative system requires at least dual redundancy. Fail operative is defined as the capability of the system to perform its function after any single failure with any or all of the following restrictions: a) Reduction of system authority after failure; b) Tolerable transient at failure; c) Manual shutdown of failed channel to restore system function.

Reduction of failure transient in a fail operative system can be achieved through cross coupling of SAS feedbacks. A hard-over in one channel link is partially compensated by motion of the other link(s) in the opposite direction commanded by the cross feedback. If the required SAS authority is ample enough, then avoidance of an intolerable transient at first failure in a fail operative system may require a level of redundancy above dual. Because the required SAS authority can be significantly different from one control axis to another, different levels of SAS redundancy can be adopted for the various control axes.

## 10.2.2 Hardware

### 10.2.2.1 Sensors

Load Alleviation - There is a variety of sensors which can be used for load alleviation. The strain gage type sense load variations directly; their sensitivity and frequency response are quite adequate. The reliability record of this type of sensors in an aircraft environment, however, is not well established and even with utmost care in installation, the sensor is one order of magnitude less reliable than the rest of the system. At present Boeing-Vertol uses a strain gage type of sensor in its cruise guide indicator to monitor rotor loads. The angle of attack/yaw sensor ( $A(q)$  sensor) type senses load variations indirectly by sensing the resultant effect of loads on aircraft motions. The most commonly used type is the differential pitot-static pressure type used as a sideslip sensor on the CH-46 and CH-47 production aircraft. This device is very reliable and has adequate sensitivity and frequency response. Its range of operation, however, is above 40 knots airspeed, thus making it unusable at hover and low speed operation. Another device developed recently and not yet in production is a differential airspeed sensor based on the generation of vortices by a strut in the airstream at a rate which is proportional to the airspeed past the strut. This is a very sensitive device and operates at airspeeds down to 1 knot. Its frequency response is quite adequate. The device is being tested by the Flight Dynamics Laboratory and should have an established reliability record



in the time frame of interest for the stowed rotor aircraft.

Mode Suppression - The most practical and reliable type of sensor available for mode sensing is an accelerometer. Units are now available off-the-shelf with the required sensitivity and high frequency response. Highly selective filtering must be accomplished in order to discriminate mode frequencies from the normal aircraft vertical accelerations due to gusts and maneuvers. An alternate type of sensor is a sensitive strain gage located on the wing skin. Filtering of the signal output is again necessary to discriminate mode frequencies from normal wing loads due to gusts and maneuvers.

#### 10.2.2.2 Signal Processing

Electrical signal processing does not present any major problem. Use of integrated circuits and micrologic permits such functions as signal amplification, filtering, logic switching and redundancy management to be accomplished without the need for cumbersome and complex circuits. Multiple filters of the Tchebyscheff or Butterworth types can be used for highly selective filtering in the mode suppression feedback. Micro-electronic components available now are highly reliable and relatively inexpensive.

#### 10.2.2.3 Actuators

The actuators required for SAS are high power, fast acting differential actuators. The requirement can best be met by electrohydraulic actuators. Two types have been considered and found to be adequate. One is of the position summing

type (total SAS piston movement and authority is the sum of the piston movement and authority of the individual actuator units); the other is of the force summing type (total SAS force is the sum of the forces of each unit).

### 10.3 GOVERNOR SYSTEMS

Rotor speed governing is achieved by controlling the collective blade pitch angle only; no engine power control is involved in speed governing. The governor actuator is inserted differentially into the collective linkage of the primary controls; thus, a single actuator controls blade pitch on both rotors. Integral control is used in order to achieve the objective of a steady state governing accuracy of 0.3% of rotor speed. The rotor speed demand signal is programmed as a function of nacelle tilt angle. This demand signal is compared to actual rotor speed signal and the difference is used to drive the governor actuator. Provision can be made in the governor to accept control quickening through a washed-out signal from the longitudinal control stick transducer. The functional block diagrams of three separate possible govern system configurations are shown in Figures 10.1, 10.2 and 10.3 and described below. Each of the configurations is redundant in order to comply with the failure safety requirements.

#### 10.3.1 Dual Electromechanical Governor System

Figure 10.2 shows a dual electromechanical system with one channel active and one in synchronized standby. Switching from the active to the standby channel occurs automatically

upon sensing of a failure in the active system. The logic to sense a failure requires a third rotor speed sensor and third feedback to determine by majority voting which of the two channels has failed. Provision is made for manual operation of the governor after failure of both active and standby channels and their subsequent shutdown. Manual operation is possible only if the two failures do not involve either motor or clutch in both channels. In manual operation, the rotor blade pitch is positioned through a beep switch to the angle providing the desired rotor speed. This mode of operation obviously requires a substantial increase in pilot workload and does not provide either accurate or fast rotor speed control.

The system is thus fail functional at first failure; however, safety of manual operation after second failure is not obvious, in light of the required additional pilot workload to operate the governor.

#### 10.3.2 Triple Electrohydraulic Governor System with Model Channel

Figure 10.3 shows a system consisting of three active channels and a model channel. Each channel controls one section of a triple electrohydraulic force summing actuator. Each actuator section has a failure monitor/pressure feedback valve which provides pressure equalization among the three sections in normal operation, and if equalization fails to occur, provides the failure signal to the channel logic.

The three active channels by themselves provide fail functional capability at first failure and the possibility of hardover at second failure. In order to provide a fail functional capability at second failure, a model electrical channel is added which is used only to detect a second failure and to immediately shut down the failed channel. In order to achieve the dual fail functional capability, three independent hydraulic supplies are required, and an electrical supply which has a dual fail functional capability. The failure detection logic associated with the model channel is relatively much more complex than the logic required to detect first failure.

#### 10.3.3 Quadruple Electromechanical Governor System

Figure 10.4 shows a system consisting of four active channels. The actuator is quadruple electromechanical; each channel is velocity summed through mechanical differentials in the actuator. Failure in one channel is detected as a motor runaway condition; if the channel fails dead, there is no need to detect the failure and remove the channel from operation in flight. A fail functional capability is achieved at both first and second failure because any runaway of one motor due to channel failure is compensated by the remaining three or two motors until the failed channel is automatically removed from operation. A quadruple system instead of a triple system is chosen because the simplicity of the failure detection logic in a quadruple system far outweighs the

additional complexity of a fourth motor in the electromechanical actuator. This is not the case in the electrohydraulic actuator system of Figure 10.2 where addition of a fourth section would make the actuator too costly, too heavy and too complex. No hydraulic power supply is needed for this system. The electrical supply must have a dual fail functional capability in order to achieve dual fail functional capability for the entire system.

#### 10.4 MODIFICATIONS OF FLIGHT CONTROLS

##### 10.4.1 Tilt Rotor Modified Flight Control System

A minimal change approach to modifying the proposed Model 222 Flight Control System to include full load alleviation/mode suppression and lift augmentation is shown on the flight controls schematic of Figure 10.5. Four dual extensible link actuators are added as shown. These are essentially the same units now used for roll and yaw SAS for  $A_1$  (lateral) cyclic feedback actuators, and their function is to provide the capability of differential yaw control.

## 10.5 HARDWARE MODIFICATIONS

Assuming that the rate damping capability is present in the aircraft operating through differential actuators in the longitudinal, lateral, and directional axes, addition of the load alleviation, lift gust alleviation and modal suppression functions entails the following hardware changes.

### 10.5.1 Load Alleviation

Two dual extensible link actuators must be added in each of the two nacelles for complete differential cyclic control. The SAS electronics must have the added circuits to process the load alleviation signal from the sensors. Dualized load alleviation sensors comprising the angle of attack sensors and the sideslip sensors must also be added.

### 10.5.2 Lift Gust Alleviation

In order to control the spoilers, the flaps and the elevator individually, three sets of dual extensible links must be added in the control linkages located so as to permit collective operation of the flaps and the spoilers. The required circuitry for signal processing must be added in the dual SAS electronic boxes. Dual  $A(q)$  sensors or dual accelerometers must be mounted to sense lift gusts.

### 10.5.3 Modal Suppression

Modal suppression can be added without addition of any actuators, since the actuators for mode suppression are the same as those used for load alleviation. The SAS electronic boxes must be modified to hold the necessary circuits to process the mode suppression signals. The sensors for mode suppression are dual wing tip accelerometers.

In summary, the addition of the above functions requires doubling of the complexity of the SAS electronics over that of the standard rate damping SAS, addition of four dual extendible link actuators and the mounting of dualized  $A(q)$  sensors, dualized accelerometers, dualized angle of attack sensors and dualized sideslip sensors.

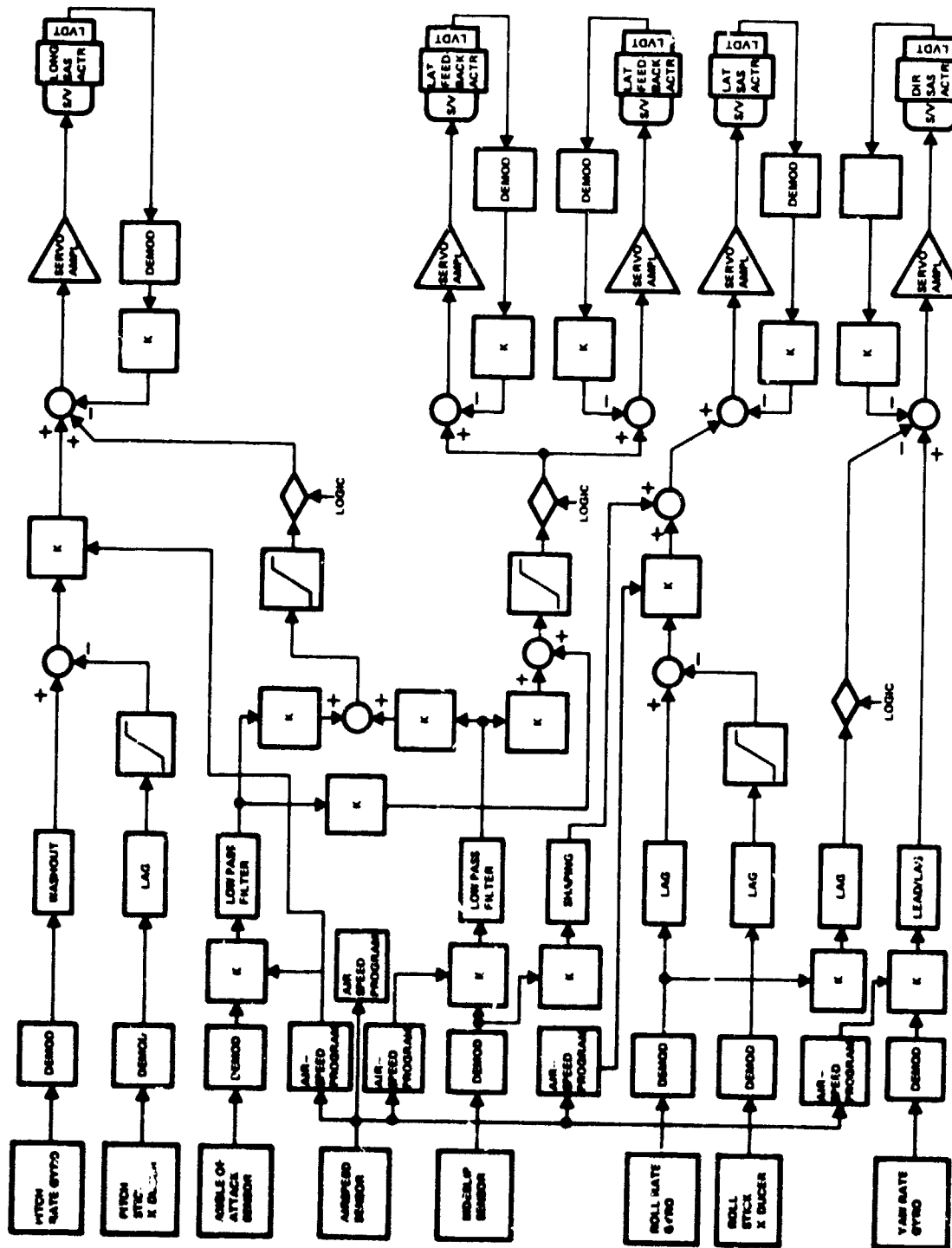


**Figure 10.1** Stability Augmentation System - Functional Block Diagram - One Channel



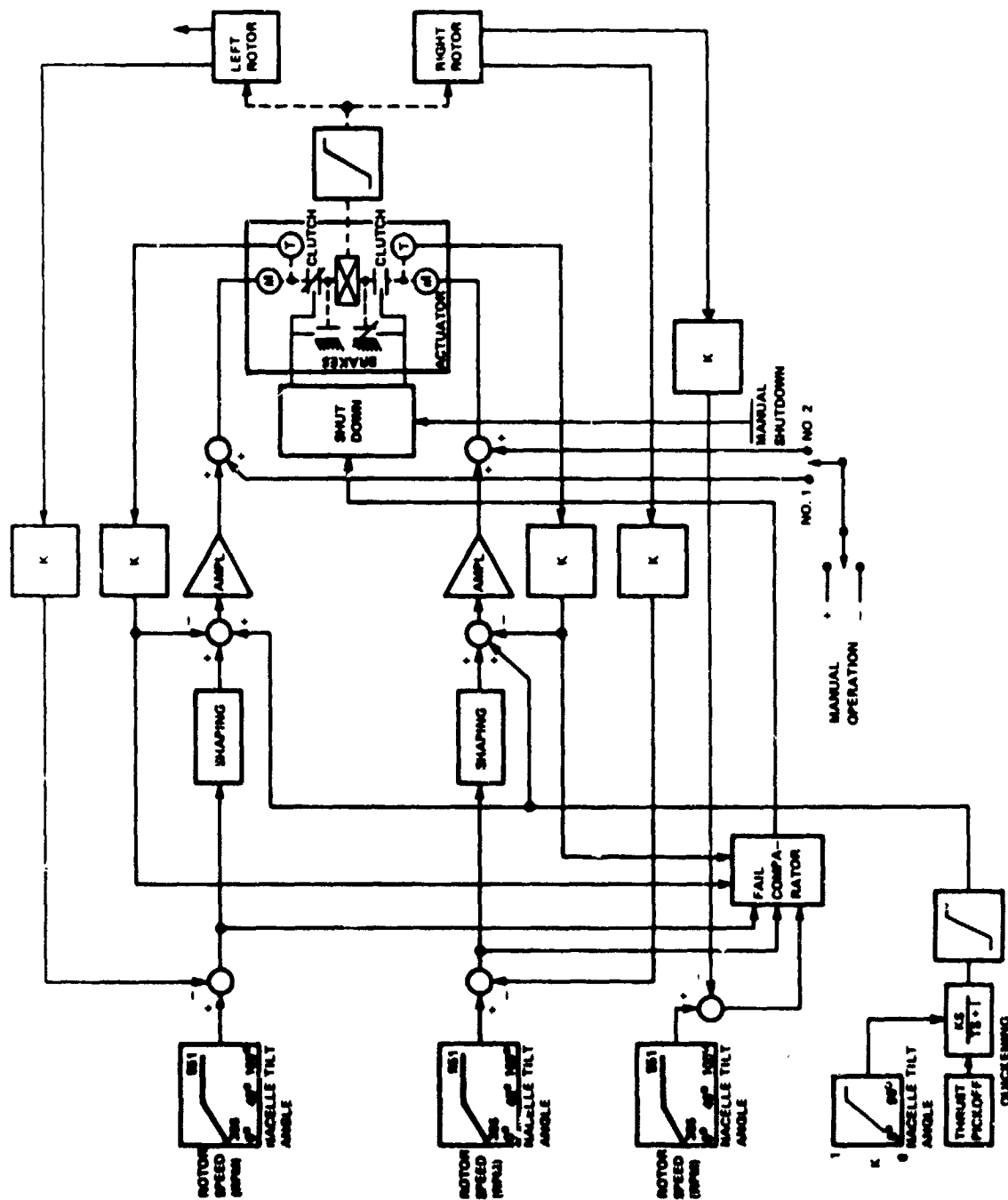


Figure 10.2 Governor - Dual Electro-Mechanical System

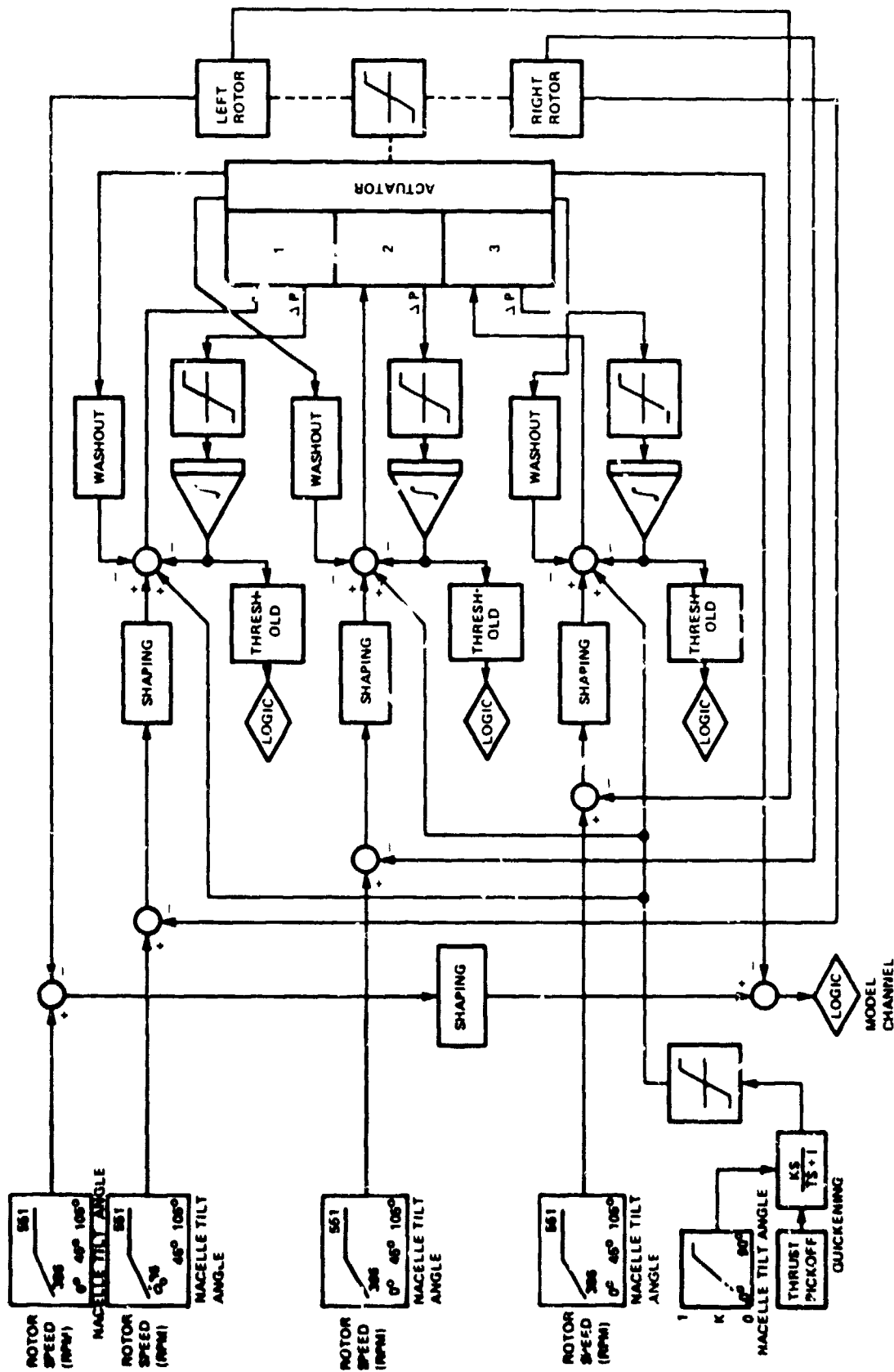
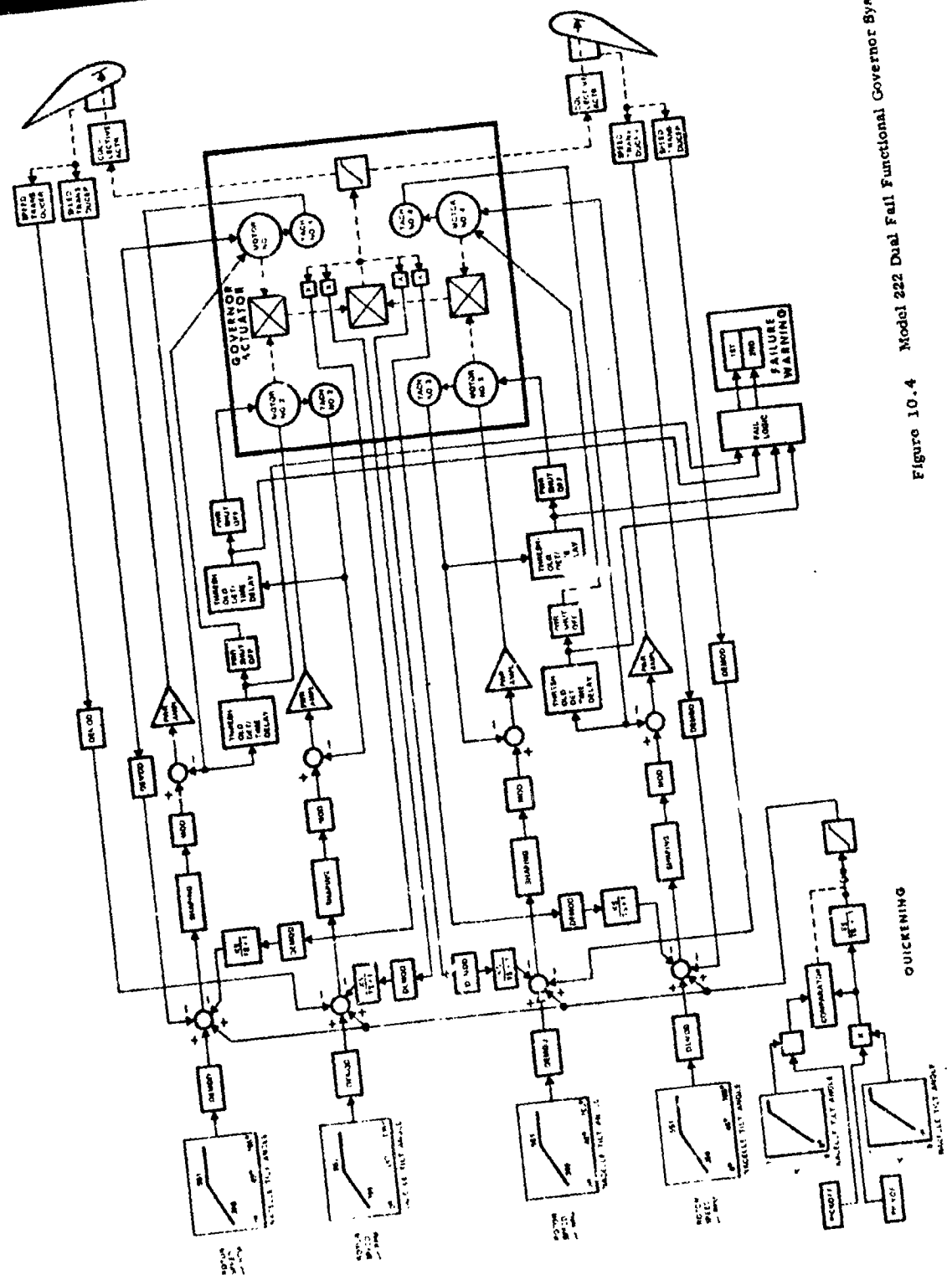


Figure 10.3 Governor - Triple Electro-Hydraulic

REPRODUCIBILITY OF THE ORIGINAL PAGE IS POOR.

D222-10000-3



QUICKENING

Figure 10.4 Model 222 Dual Fail Functional Governor System

D222-10060-3

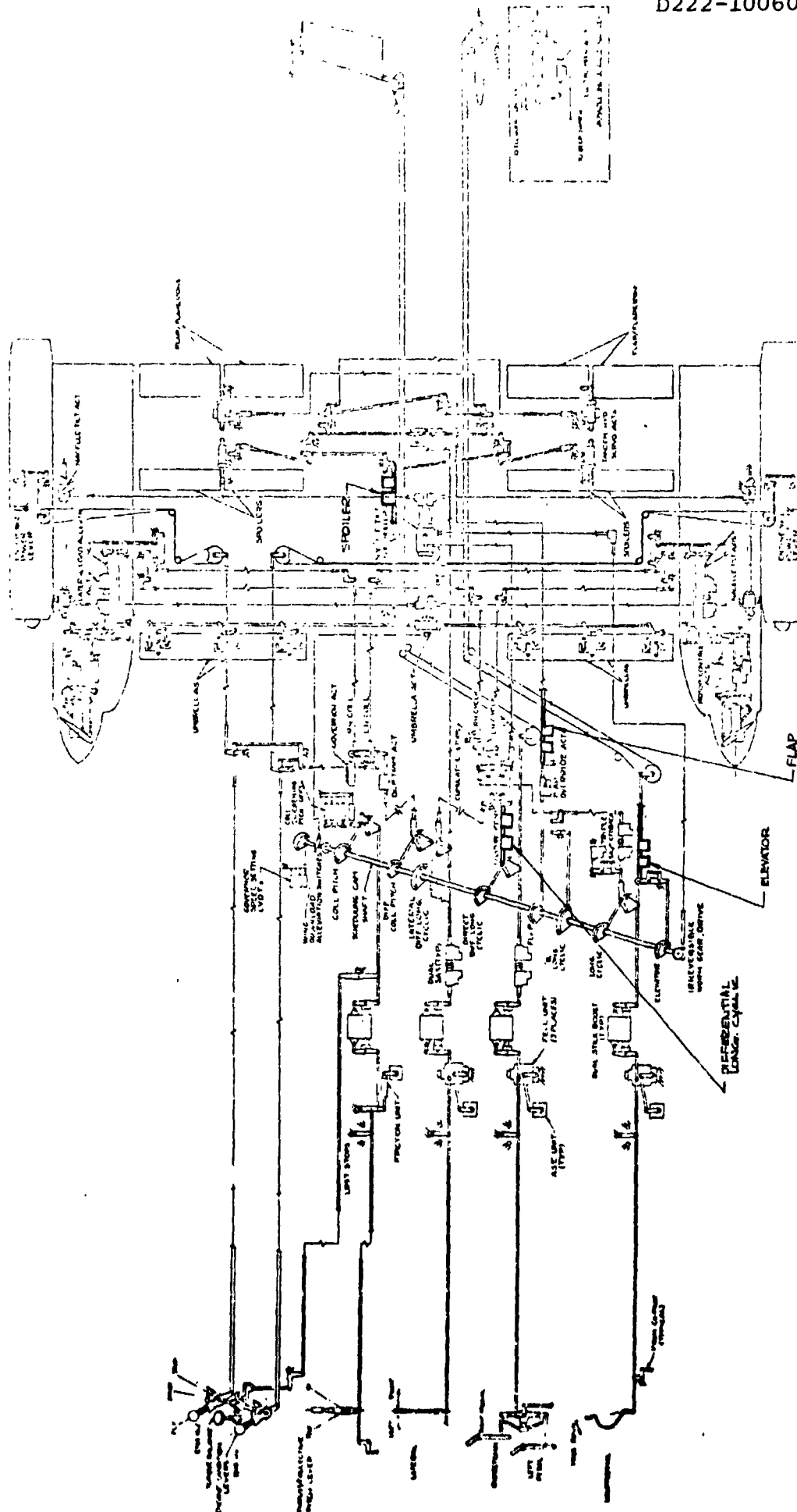


Figure 10.5 Flight Controls - schematic

## 11.0 RECOMMENDED PROGRAMS

The programs of work recommended below fall under three major headings. These are:

- (a) Analytical studies
- (b) Wind tunnel tests
- (c) Full scale flight test implementation

Discussion of (c) is divided into programs for which provision has been made in the Boeing proposal for a tilt rotor research vehicle, and additional programs which would entail modifications to the control system or additional sensing and avionic components.

### 11.1 RECOMMENDED ANALYTICAL STUDIES

A group of recommended analytical studies are set out in Table 11.1. These include investigations directed toward more efficient use of swashplate feedback for load alleviation and modal suppression, the combination of different types of feedback control, and first cut feasibility studies on control configured vehicles and systems where reliance is placed on feedback to maintain aeroelastic stability.

In the course of the current contract, aspects of the load alleviation systems and modal suppression systems emerged which merit additional study. These include the resolution

TABLE 11.1 RECOMMENDED ANALYTICAL STUDIES

System	Objectives	New Aspects	Possible Advantages	Methodology Requirements
1) Free flight blade load alleviation systems and stability augmentation	Control of blade loads in transient maneuvers and gusts	Evaluate use of transfer functions to control azimuth as function of frequency. Also phased $A_1$ and $B_1$ feedback.	More positive achievement of objectives, and removal of conflict between static and dynamic cases	Minor modifications to existing capability (C-48)
2) Aeroelastic stability and modal suppression	Reduction of modal response	Explore use of phased $A_1$ and $B_1$ cyclic and/or tip vanes or flaps for damping	More effective use of available cyclic. Reduction of side effects.	As above
3) Combined direct lift and swash-plate feedback for blade loads alleviation	Explore whether more effective control of blade loads is possible using conventional control feedback along with cyclic feedback	Assessment of combined systems	Reduction of short period mode response and increased effectiveness of blade loads reduction systems	Modifications to existing capability to permit representation of direct lift and swash-plate systems simultaneously
4) Control configured vehicle studies	Explore use of swash-plate feedback to replace horizontal and vertical stabilizers	Partial or complete removal of empennage	Reduction in weight and drag	Minor changes to capability
5) Feedback for primary control of aeroelastic stability	Replace reliance on stiffness by feedback system	Parametric study of stiffness	Thinner and lighter wings	Minor changes

D222-10060-3

of azimuth requirements at different frequencies of loading. In Section 3 it is shown that the feedback azimuth appropriate to static conditions is significantly different to that required for alleviation of a gust. A method of resolving this conflict may be to control azimuth as a function of frequency by the agency of different attenuating filters in the  $A_1$  and  $B_1$  channels.

Another aspect which has emerged from the current study and confirmed by tests is that a dynamic conception of the rotor is required for adequate mathematical modelling. This is particularly apparent in attempts to obtain pure normal force and pitching moment feedback signals. It was found that under oscillatory conditions no azimuth existed about which the swashplate could be rotated to produce normal force without an accompanying component of side force. It had been expected from static experience that such an azimuth could be found, but on reflection it is obvious that under dynamic conditions, the swashplate will require a precession or wobble in order to produce a force or moment vector which may be adjusted to give normal force or pitching moment without an associated side force and yawing moment. Such a precession is generated by providing time phasing between the pitch and yaw cyclic signals

demanded by the control system. The advantages of such an arrangement are twofold:

- (1) All the system authority (which is limited for several reasons) is directed to producing useful output, with a correspondingly more effective system
- (2) Potentially adverse loadings are removed, i.e., the oscillatory side forces generated when only normal force is required

The studies reported in the current volume have not attempted to explore the potential of these concepts. It is proposed that they be the subject of a separate investigation which would include the following topics:

- (a) Phase and relative  $A_1$ ,  $B_1$  gain optimization of a blade load alleviation system over a practical range of static and transient gust and maneuver conditions
- (b) Phase and relative  $A_1$ ,  $B_1$  gain optimization of a modal suppression system under the same conditions
- (c) Integration of both systems with a governing and direct lift feedback system and reevaluation of optimal settings

It is also proposed that this may be confirmed by wind tunnel test demonstration as outlined in Paragraph 11.2. An initial



and fairly inexpensive demonstration of the effectiveness of phased swashplate feedback is proposed using a reactivated 1/9.26 scale model in the Princeton tunnel, and it is hoped that by the time further model work using the 1/4.622 scale model and full scale flight testing, the principles of phased swashplate feedback would be well established, and be demonstrated further.

In the work to date, feedback has not been considered a primary means of ensuring aeroelastic stability, but only as a modal suppression or damping augmentation system. It is now proposed to explore the potential benefits in weight and performance that would accrue from the use of feedback to relax wing stiffness requirements and permit the use of thinner and lighter wing structures.

An additional concept which merits analytical investigation in the near term is the control configured tilt rotor vehicle. It is considered that a stage of development and validation of analytical methodology relating to tilt rotor feedback control systems has been reached, where studies of advanced control configured vehicles may be profitably undertaken. The controls configured tilt rotor system would use rotor forces and moments to provide the stability and control currently envisioned to come from the empennage and empennage controls. Thus,

longitudinal and directional stability and control would be provided by rotor forces and moments only. Lateral directional control and stability would be provided by differential rotor forces and moments including differential collective and aileron and spoiler motions. For example, the yaw damping and stiffness effectiveness of a vertical stabilizer would be replaced by differential collective signals proportional to rate of sideslip and angle of sideslip respectively. The dynamics of the rotor are an integral component of any such system and it is believed that a state-of-the-art has now been demonstrated where meaningful analytical studies may be undertaken. These studies would determine the control ranges required, the feedback system characteristics in terms of gains and authorities and would investigate the effect of the systems on the rotor blade stresses. Required nacelle tilt rates and the effect of these on the nacelle tilting system would be investigated. These would logically precede attempts at tunnel demonstrations and full scale design.

#### 11.2 PROPOSED WIND TUNNEL PROGRAMS

A number of wind tunnel programs are proposed in Table 11.2. These envision tests on the 1/4.622 scale model of the M222 aircraft and further testing of the 1/9.622 scale model discussed earlier to investigate new system concepts.

TABLE 11.2 PROPOSED WIND TUNNEL PROGRAMS

Test	Model	Tunnel	Test Objectives	Special Requirements
1. Blade Load Alleviation Study	1/4.622 Scale	BV or suitable alternative (with gust generator)	Develop and demonstrate load alleviation system. Evaluate transfer function control of azimuth as function of frequency. Also phased A <sub>1</sub> and B <sub>1</sub> feedback.	Monkey pole suspension
2. Rotor Governing and Blade Load Alleviation	1/4.622 Scale	BV or suitable alternative (with gust generator)	Demonstrate satisfactory operation	None
3. Modal Suppression System	1/4.622 Scale	BV or suitable alternative (with gust generator)	Design and demonstrate modal suppression system using rate and deflection signals and phased A <sub>1</sub> and B <sub>1</sub> feedback	Test for compatibility with lift control system
4. Direct Lift Control	1/4.622 Scale	BV or suitable alternative (with gust generator)	Acquire spoiler and flap Modifications to current oscillatory lift, pitching moment and downwash data design lift control system. Demonstrate.	
5. Phased Swashplate Feedback and Azimuth Control As Function of Frequency	1/9.622 Scale	Princeton Tunnel	Explore use differential A <sub>1</sub> and B <sub>1</sub> transfer function and wobbling swashplate concept to reduce blade loads and suppress modal response	Existing model with minor mods to electronics

The tests proposed for the 1/4.622 scale model are in two groups. The first three use currently defined hardware and may be performed with little or no modification to the existing model. The fourth which is intended to demonstrate a direct lift system would require control system modification to permit symmetric actuation of flaps, spoilers and elevators. Reactivation of the 1/9.622 scale model involves minimal hardware modifications since only the electronic processing of feedback signals would need changing.

The 1/9.622 scale model test would investigate the use of the concepts of signal shaping discussed in Section 11.1. The 1/4.622 scale tests would involve demonstration of currently defined systems and also the new concepts of signal shaping discussed and demonstrated in the 1/9.622 scale test. Programs 1, 2 and 3 might profitably be merged into one test while number 4, the direct lift program, might entail a second installment. The first section (Tests 1, 2, 3) probably represents a 2-3 week period of tunnel occupancy and test 4 is probably a similar time span since the swashplate systems settings would be reoptimized during this test.

The 1/9.622 test is a research oriented activity and will, therefore, also require approximately a 2-3 week tunnel occupancy.

### 11.3 PROGRAMS PLANNED AND ADDITIONAL RECOMMENDED PROGRAMS: FULL SCALE FLIGHT TEST

Recommended full scale flight test programs associated with feedback controls are listed in Table 11.3.

#### 11.3.1 BLADE LOAD ALLEVIATION SYSTEM AND STABILITY AUGMENTATION ON THE NASA TILT ROTOR RESEARCH VEHICLE

The NASA Tilt Rotor Research Aircraft is configured to include a load alleviation swashplate feedback system. The system as proposed by Boeing Vertol senses angle of attack and sideslip and processes these signals to give swashplate  $A_1$  and  $B_1$  cyclic responses; the objective is to reduce the blade loads induced by trim changes, gusts and maneuvers and concurrently improve aircraft dynamic stability. The system will be flight tested and optimized. The flight test program of development and testing will be preceded by scaled model testing to demonstrate the system. The model testing is discussed in Section 11.2.

#### 11.3.2 DIRECT LIFT FLIGHT PATH CONTROL AND GUST ALLEVIATION

The rotor swashplate systems discussed are of limited force level and have significant time lags due to rotor response. The alleviation of "g" response to high frequency turbulence requires a more powerful and faster acting system which provides a direct feedback on aircraft lift. It is proposed that the flap and spoiler controls be modified to accept symmetric

TABLE 11.3 RECOMMENDED PROGRAMS ON FULL SCALE AIRCRAFT WITH SUPPORTING MODEL TEST PROGRAMS\*

SYSTEM DESIGNATION	OBJECTIVE	CURRENTLY PLANNED FOR NASA RESEARCH VEHICLE?	GROUND TESTING	FLIGHT TESTING	SUPPORTING MODEL PROGRAMS	AIRCRAFT MODIFICATIONS AND SPEC. HARDWARE
1. LOAD ALLEV. FEEDBACK SYSTEM	REDUCE BLADE LOADS/IM- PROVE A/C STABILITY CHARACTERISTICS	YES	FUNCTION- AL CHECKS. DEMONSTRATE FREQUENCY SYSTEM RESPONSE STABILITY CHECKS	TUNNEL DEMONSTRATION ON SCALED MODEL		HARDWARE INCLUDED IN M222 TILT ROTOF RESEARCH AIRCRAFT PROPOSAL
2. DIRECT LIFT CUST ALLEVIATION	ATTENUATE AG LEVELS IN TURBULENCE. IMPROVE APPROACH HEIGHT CONTROL	NO	FUNCTION- DEVELOP AND AL CHECKS DEMONSTRATE AND PRE- SYSTEM QUENCY RESPONSE STABILITY CHECKS FULL SCALE DATA AC- QUISITION IN 40X80 TUNNEL	1. ACQUIRE TUNNEL DATA ON LIFT VARIATION RESPONSE OF FLAPS, SPOILERS AND ELEVATORS. 2. SCALED MODEL DEMONSTRATION 3. FULL SCALE CONFIRMATION OF FLAP/ SPOILER/ ELEVATOR DATA.		MODIFIED FLAP AND SPOILER SYSTEM. SENSORS AND AVIONICS.
3. MODAL SUPPRESSION SYSTEM USING SWASHPLATE FEEDBACK	AUGMENT DAMPING IN STRUCTURAL MODES	NO	FUNCTION- DEVELOP AND AL & FREQ. DEMONSTRATE RESPONSE IN FLIGHT FULL SCALE DEMONSTRATIONS. IN 40 X 80	1. ADDITIONAL TESTING WITH 1/9 SCALE MODEL, PRINCETON. 2. 1/4 SCALE MODEL DEMONSTRATION		SENSORS AND AVIONICS. EXISTING ACTUATORS PROBABLY O.K.

\* SEE TABLE 11.2 FOR DETAILS OF SCALED MODEL TEST PROGRAMS.

commands from an angle of attack sensor. The system will also command suitable amounts of phased elevator travel to reduce pitching response caused by the gust and flap and spoiler operation.

The effectiveness of such a system would be examined on a scaled model prior to a full scale commitment and as indicated in Table 11.3 model or full scale tests to acquire empirical data on oscillating flap and spoiler lift and downwash is probably advisable prior to final definition of the system.

#### 11.3.3 MODAL SUPPRESSION SYSTEMS BASED ON ROTOR/SWASHPLATE FEEDBACK

A recommended program which is a ready adaptation from the load alleviation system is the modal suppression or aeroelastic stability augmentation system. The system has a substantial number of hardware items in common with the load alleviation/stability augmentation system discussed above. Common swash-plate actuators may be used with different sensors and signal shaping. The ability of such a system to reduce wing response in turbulent air would be explored and damping measurements made. Such a system has been demonstrated in the 40 X 80 tunnel at NASA Ames, and very substantial increases in wing damping shown to be available. The system envisioned here would be more advanced in certain respects than those tested to date.

The chief differences will be in the type of feedback signal used and in the phasing of the pitch and yaw cyclic commands. It is believed that a more efficient use of the available control authority may be brought about by the use of phased  $A_1$ ,  $B_1$  or wobbling swashplate control. The modal suppression system by reducing the wing response will attenuate the associated cabin accelerations due to turbulent air, and will thus supplement the direct lift control system, which is highly effective in counteracting gust force on the overall aircraft, but is not necessarily effective in reducing modal responsiveness.



#### 11.4 PLANNING COSTS AND SCHEDULES

Planning costs and schedules are presented in this section for a program which will evaluate the following systems:

- . Load alleviation feedback
- . Direct lift gust alleviation
- . Modal suppression systems using swashplate feedback

The planned program will include flight tests and will be supported by analytical studies and scaled model wind tunnel tests.

##### 11.4.1 ANALYTICAL STUDIES

Studies will be performed to support the planned program including pretest predictions and safety analyses. In addition, investigations will be made of control configured vehicle surface studies, and feedback for primary control of aeroelastic stability. The planned program does not include the implementation of the results of the additional studies.

##### 11.4.2 DESIGN AND HARDWARE MODIFICATION AND INSTALLATION

The tilt rotor aircraft's flight control system will be modified to incorporate the planned systems (including sensors, actuators and SAS control box circuits). Components will be bench checked and the modified and/or added components will be

installed on the aircraft at offsite Government facilities.

#### 11.4.3 MODEL WIND TUNNEL TESTING

A contractor's tilt rotor model will be refurbished and modified to incorporate the planned systems modifications. Three test programs will then be conducted to determine the following characteristics:

- . Blade load alleviation
- . Rotor governing and blade load alleviation
- . Modal suppression system
- . Direct lift control
- . Phase swashplate feedback

The tests will be conducted at the contractor's wind tunnel and at the Princeton facilities. The gust generator required for one phase of model testing has not been priced in this plan. It was assumed one would be available in the 1977 time frame. Tunnel occupancy will be for 280 hours and the total test period will be seven (7) weeks.

#### 11.4.4 GROUND AIRCRAFT TESTS

The modified control system in the aircraft will be proof loaded. Functional and frequency response stability checks will also be made.

11.4.5 FLIGHT TESTS

The modified control systems will be demonstrated in a four (4) week flight test program after completion of NASA tests on the tilt rotor research aircraft in the 1978 time frame. Testing will be performed by NASA with Boeing Vertol providing supporting personnel. No 40' x 80' wind tunnel testing is included in this estimate.

The planning costs presented are based on projected CY 1977 planning dollars which is intended to represent an average for the period of performance:

	<u>M.H.</u>	<u>COST \$</u>
ANALYTICAL STUDIES & PRETEST PREDICTIONS		
ENGINEERING	8,500	277,525
HARDWARE MODIFICATION		
DESIGN		
ENGINEERING	2,734	89,265
FABRICATION & INSTALLATION		
ENGINEERING LIAISON	560	18,284
DEVELOPMENTAL LABOR	1,644	38,075
PLAN. LIAISON, PROD. SUPPORT & TOOL SERVICES	253	5,976
QUALITY CONTROL	181	4,442
MATERIAL		<u>13,780</u>
	2,638	169,322

D222-10060-3

	<u>M.H.</u>	<u>COST \$</u>
WIND TUNNEL TESTING		
ENGINEERING	12,178	397,612
DEVELOPMENTAL LABOR	7,595	175,900
PLAN, LIAISON, SERVICES	1,110	27,635
QUALITY CONTROL	835	20,490
MATERIAL	<u>          </u>	<u>22,750</u>
	21,778	644,387
GROUND TESTS		
ENGINEERING	640	20,896
FLIGHT TESTS	480	15,672
MANAGEMENT DATA REDUCTION & REPORTS	<u>3,920</u>	<u>127,988</u>
	5,040	164,556
TOTAL RECOMMENDED PROGRAM	40,690	1, 256,290

D222-10060-3

FORM 49101-0, 071

REFERENCES

- 2.1 Alexander, H., Amos, A., Tarzanin, F., Taylor, R., V/STOL Dynamics Rotor-Airframe Technology Volume II, Air Force Report AFFDL-TR-72-40, May 1972.
- 3.1 Fry, B., Feedback Control Tests on a Windmilling 2.81 Foot Diameter Soft-in-Plane Hingeless Tilt-Rotor in the Cruise Mode, Boeing Document D222-10047-1, November 1972.
- 3.2 Magee, J., Wind Tunnel Tests of a Full Scale Hingeless Prop/Rotor Designed for the Boeing Model 222 Tilt Rotor Aircraft, Boeing Document D222-10059-1, March 1973.
- 4.1 Shufflebarger, C.C., Tests of a Gust Alleviating Way in the Gust Tunnel, NACA-TN-802, April 1941.
- 4.2 Donely, P. and Shufflebarger, C.C., Tests of a Gust Alleviating Flap in the Gust Tunnel, NACA-TN-745, January 1940.
- 4.3 Kraft, C., Initial Results of a Flight Investigation of a Gust Alleviation System, NACA-TN-3612, April 1956.
- 5.1 Arnold, J. Supersonic Transport Longitudinal LAMS SAS Conceptual Study, Boeing Document D3-7600-10, May 1969.
- 5.2 Arnold J. and Townsend, J., Supersonic Transport Lateral LAMS SAS Conceptual Study Results, Boeing Document D3-7600-11, May 1969.
- 5.3 Morris, J. and Spittle, R., Flying Qualities and Aeroelastic Stability Analysis - C-43 Users Document, Boeing Document D210-10435-1, April 1972
- 5.4 Alexander, H. R., Morris, J. and Spittle, R., Pretest Calculation of Open Loop Frequency Response and Stability of High Rate and Low Rate Swashplate Feedback Systems of M222 26' Rotor Test, Boeing Document D160-10019-1, October 1972.
- 7.1 Deckert, W. and Ferry, R., Limited Flight Evaluation of the XV-3, Air Force Report AFFTC-TR-60-4, May 1960.
- 7.2 McFarland, R., Wind, NAPS-80 NASA-Ames Program Specification, October 1970.
- 8.1 VanWagensveld, D., et al; Wind Tunnel Tests of the Aerodynamics and Dynamics of Rotor Spin Up, Stopping and Folding on a Semi Span Folding Tilt Rotor Model. Air Force Report AFFDL-TR-71-62, Volume VII, October 1971.

APPENDIX A - DESCRIPTION OF THE MATH MODEL

The math model used to evaluate the various feedback configurations was designed with emphasis on simplicity so that any affects of the feedback could be easily evaluated. At no point, however, was the model stripped of the necessary blade, structural, and rigid body modes so that it was not fully representative of a tilt rotor vehicle with a soft in-plane rotor. In cruise, aerodynamics were tailored to yield flying quality modes which were representative of this style aircraft. In hover the aerodynamics represented a case with all flaps down and all umbrellas fully open (i.e., no fuselage or wing aerodynamics). A normal evaluation case would contain twelve to fifteen degrees of freedom including blade elastic modes, wing vertical bending, wing chord bending, wing torsional bending, any of the six rigid body freedoms, and generalized feedback freedoms. A more complete description of the math model is included in the C-48 User's Document (D210-10435-1).

Physical characteristics of the math model are similar to the Boeing Model M222. Figure A.1, A.2, and A.3 show the rotor geometrical properties and the blade frequency properties from various RPM and collective pitch settings. Figure A.4 delineates the wing uncoupled modal frequencies.

FIGURE A.1 MODEL 222 - ROTOR BLADE PROPERTIES

WEIGHT DISTRIBUTION - LB/IN

x/R	$\Delta W/\Delta X$ , LB/IN
1.0 (TIP)	1.422
.975	1.422
.975	.395
.95	.395
.90	.395
.85	.404
.80	.684
.75	.406
.70	.409
.60	.414
.50	.422
.45	.436
.30	.313
.25	.308
.20	.303
.15	.356
.10	.486
.072	.583
.072	6.4
0 (ROOT)	6.4

TWIST DISTRIBUTION - DEG

x/R	$\theta$ , DEG
1.0 (TIP)	-7.79
.975	-7.79
.9	-5.19
.8	-1.73
.75	0.
.70	1.73
.6	5.19
.5	8.66
.4	12.12
.35	13.85
.3	16.10
.25	18.75
.2	22.20
.15	27.85
.10	33.38
.072	33.38
0 (ROOT)	33.38

BLADE FLAP EI

x/R	$EI_{\beta} \times 10^{-6}$ , LB.IN. <sup>2</sup>
1.0	3.78
.9	3.86
.8	3.84
.7	4.21
.6	4.31
.5	4.92
.45	5.50
.3	7.54
.2	10.50
.15	13.82
.10	27.55
.072	49.16
.072	$1 \times 10^6$
0 (ROOT)	$1 \times 10^6$

BLADE LAG EI

x/R	$EI_{\gamma} \times 10^{-6}$ , LB.IN. <sup>2</sup>
1.0 (TIP)	535.
.9	535.
.8	520.
.7	510.
.6	510.
.5	520.
.45	540.
.3	41.57
.2	35.00
.15	36.76
.10	44.71
.072	50.98
.072	$1 \times 10^6$
0 (ROOT)	$1 \times 10^6$

Radius = 156 Inches

Chord (Constant) = 18.85 Inches



MODEL 222 TILT ROTOR RESEARCH AIRCRAFT

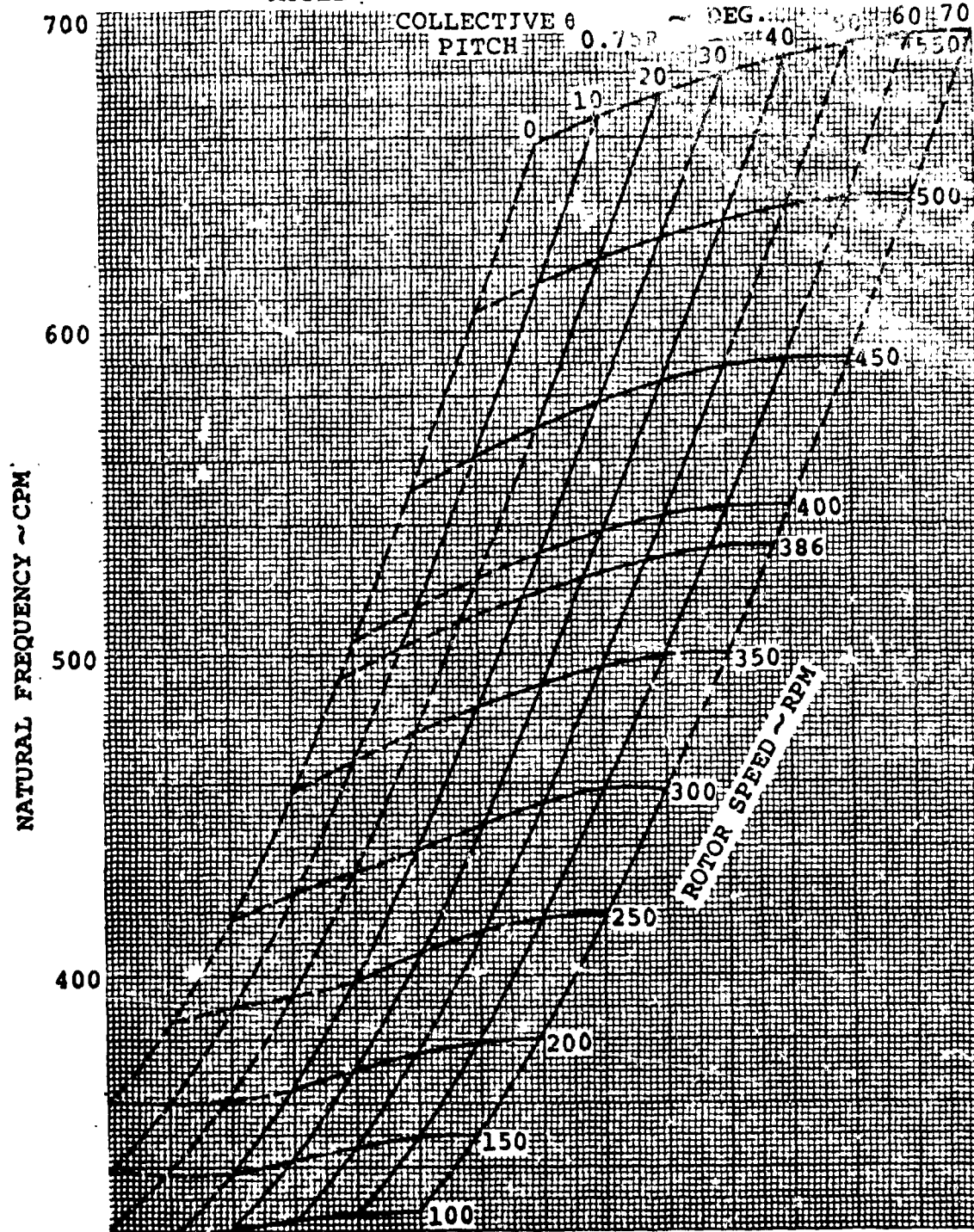


FIGURE A.2 · MODEL 222 ROTOR BLADE VARIATION OF 2ND BENDING NATURAL FREQUENCY WITH ROTOR SPEED AND COLLECTIVE PITCH

## MODEL 222 TILT ROTOR RESEARCH AIRCRAFT

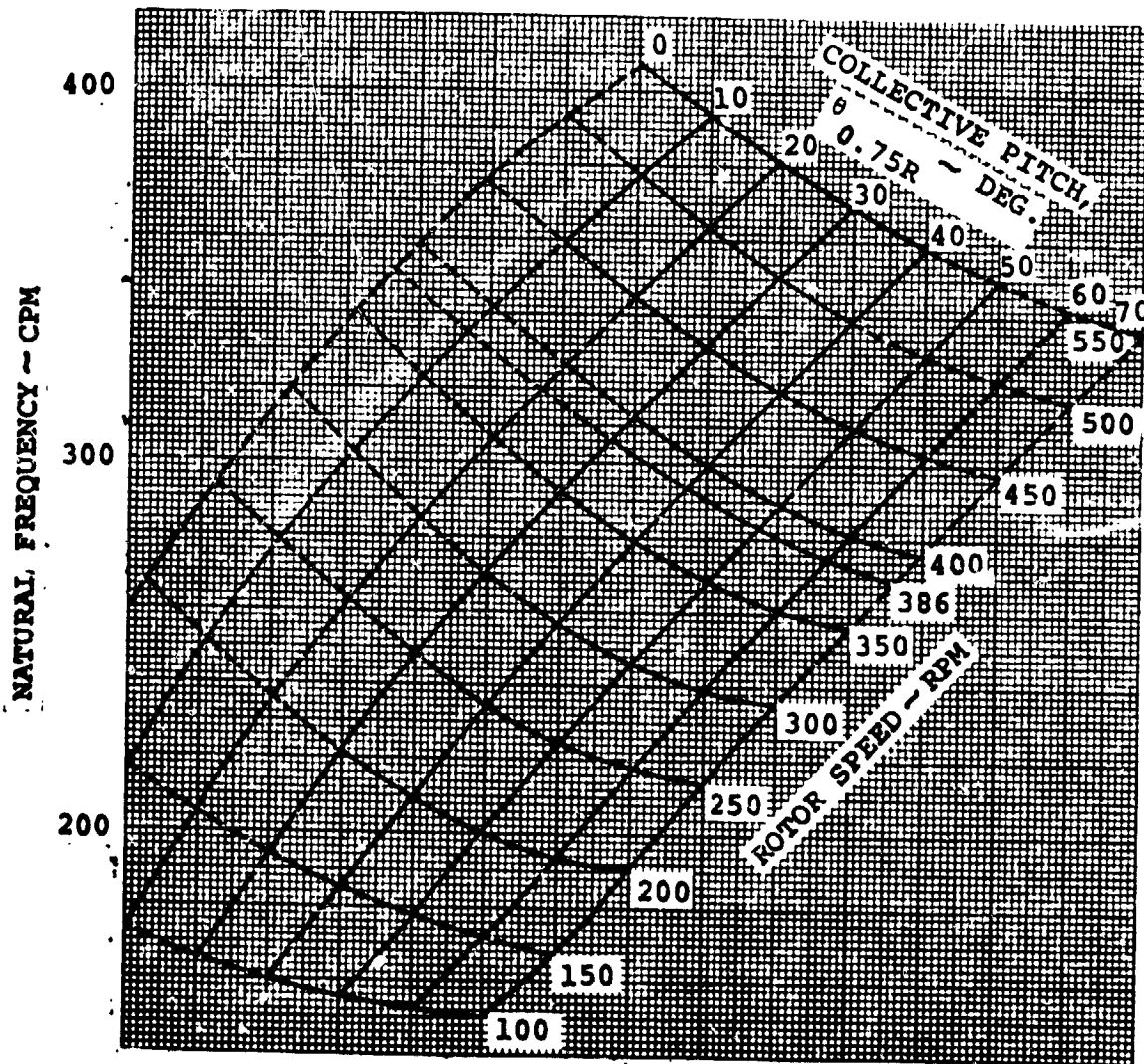


FIGURE A.3 - MODEL 222 ROTOR BLADE VARIATION OF 1ST BENDING NATURAL FREQUENCY WITH ROTOR SPEED AND COLLECTIVE PITCH

## MODEL 222 TILT ROTOR RESEARCH AIRCRAFT

SYMMETRIC MODE	FREQUENCY
VERTICAL BENDING	3.6 CPS
CHORDWISE BENDING	5.4 CPS
TORSION	6.1 CPS
ANTISYMMETRIC MODE	FREQUENCY
VERTICAL BENDING	11.2 CPS
CHORDWISE BENDING	9.1 CPS
TORSION	5.7 CPS

**FIGURE A.4 WING UNCOUPLED FREQUENCIES (BLADES OFF)**  
**CRUISE CONFIGURATION**

APPENDIX B - SINGLE GOVERNOR WITH TWO SENSORS BODE ANALYSIS

Bode analysis was made of the governor feedback loops for RPM feedback in various flight conditions to determine the maximum gains and need (if any) for filtering of high frequency signals. A criteria of 30-degrees phase margin or 6 dB gain margin (whichever is most stringent) was used. These margins are well recognized in the literature (for example, Saucedo and Shiring - Introduction to Continuous and Digital Control Systems) as limits which yield good transient and steady-state response.

The following definitions of gain and phase margin were applied.

- o the gain margin is the reciprocal of the gain at the frequency at which the phase angle reaches 180-degrees
- o the phase margin is the phase angle in degrees which the phase diagram must be shifted in order to obtain 180-degrees phase angle at unity gain.

All governor components in the block diagram of Figure have been represented except the sensor dynamics. Sensor frequency response is essentially "flat out" to 50 cps and spot checks of the Bode diagrams indicated that the sensor dynamics did not influence the maximum gain levels.

Levels of gain specified on the Bode plots correspond to values of G on the block diagram and have units of volts per

volt. They are not to be confused with values of loop gain which have units of degrees per RPM.

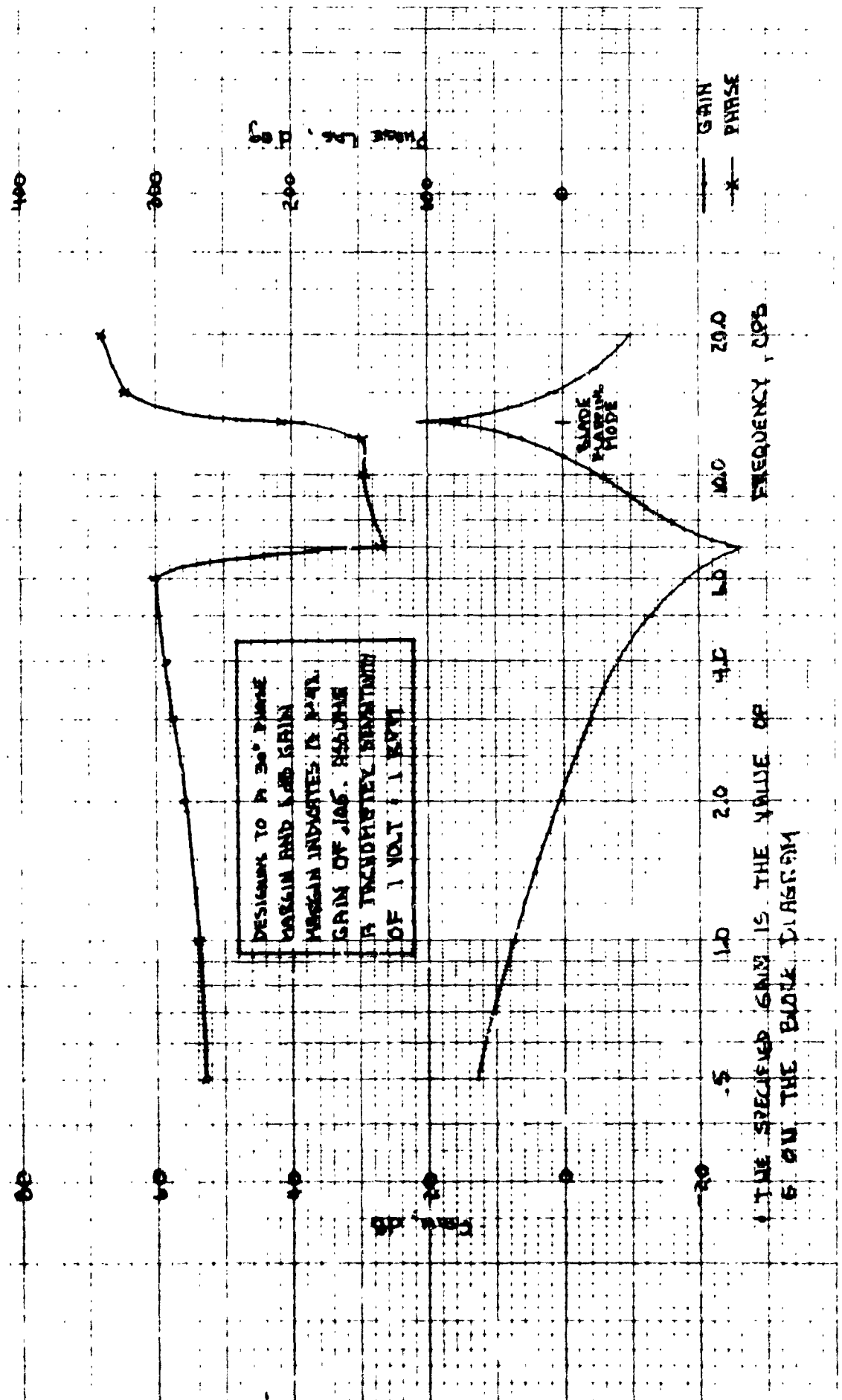
The harmonic response was obtained using an option of the C-48 Flying Qualities and Aeroelastic Stability Program. A description of the program is contained in Boeing Document D210-10435-1.

#### REFERENCES

- B.1 Saucedo, R., and Schiring, E., Introduction to Continuous and Digital Control Systems, The MacMillan Company, New York, 1970.

HOVER  
55% RPM  
NO X-SHAFT

FIGURE 8-1 ROTOR ROTATION FREQUENCY RESPONSE  
WITH ACTUATOR DYNAMICS



THE SPECIFIED GAIN IS THE VALUE OF  
G ON THE BODE DIAGRAM

FIGURE 8-2 ROTOR ROTATION FREQUENCY RESPONSE  
WITH ACTUATOR DYNAMICS

HOVER CONFIGURATION  
CROSS SHAFT PRESENT  
20 FPS CLIMB  
551 RPM

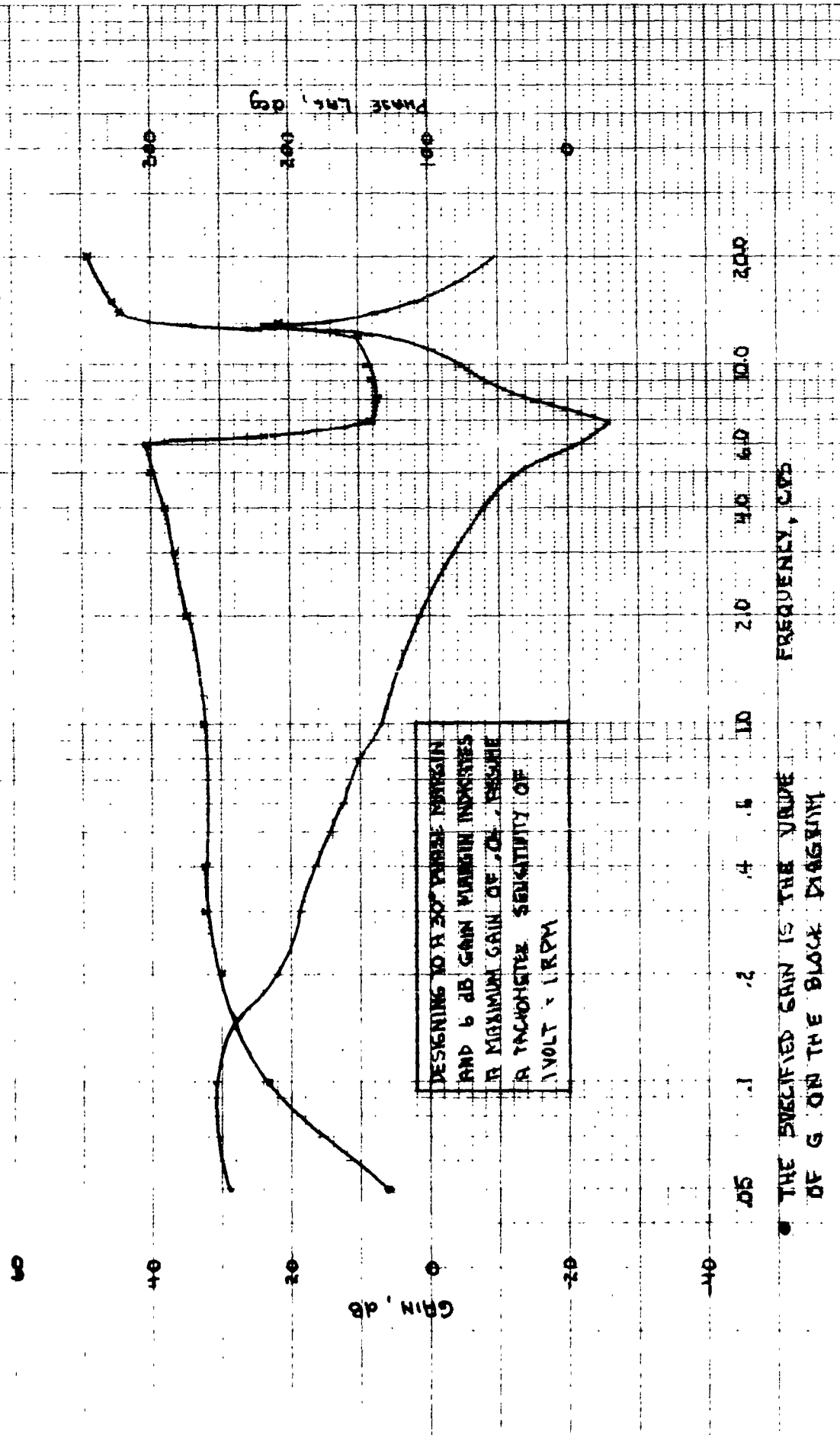
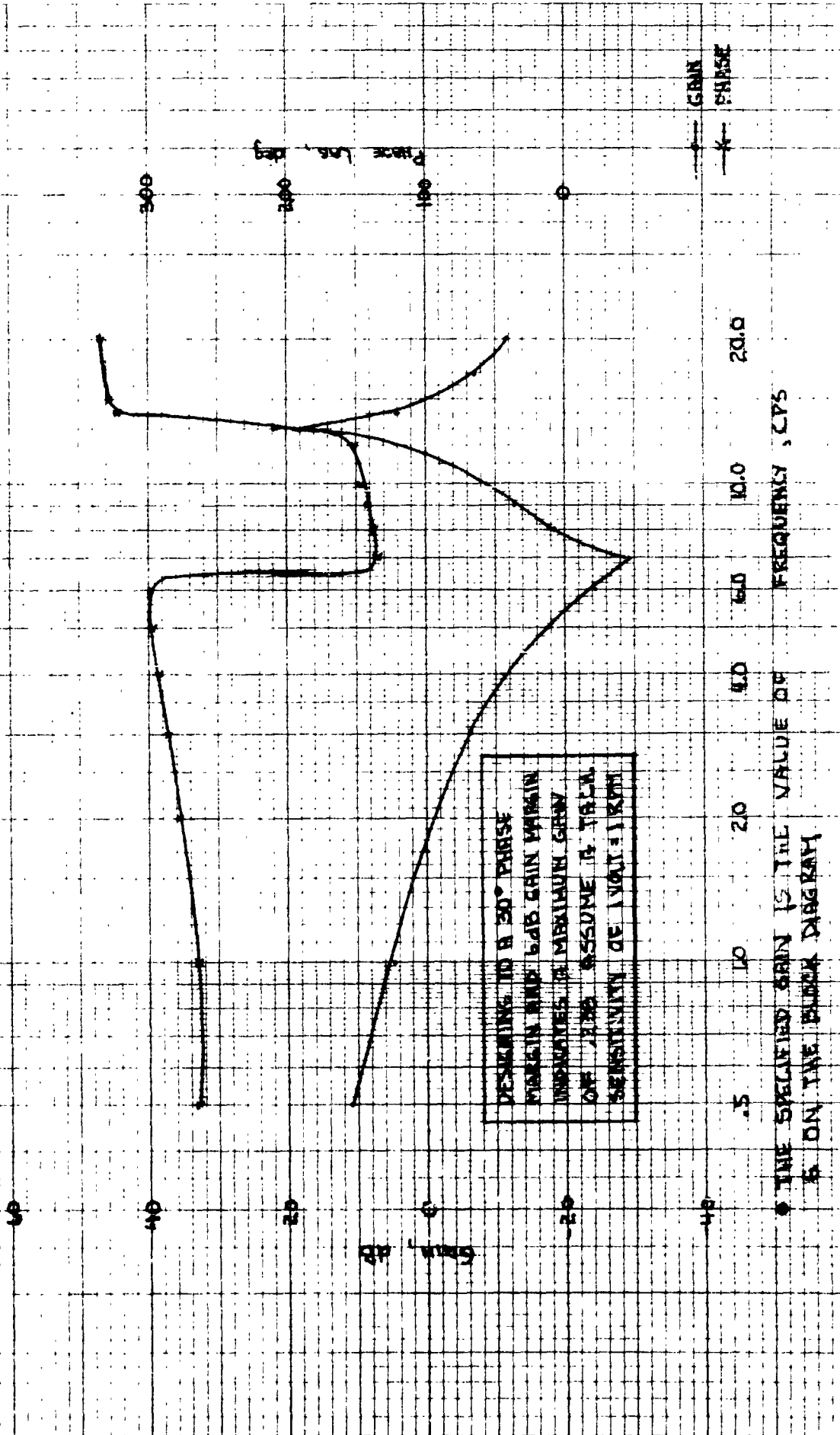


FIGURE 6.3 ROTOR ROTATION FREQUENCY RESPONSE  
WITH ACTUATOR DYNAMICS

MOVER CONFIGURATION  
CROSS SHAFT FLASHT  
20 CPS DESCENT  
551 RPM





STEADY HOVER  
CROSS SHAFT PRESENT  
551 RPM

FIGURE B.4 ROTOR ROTATION FREQUENCY RESPONSE  
WITH ACTUATOR DYNAMICS

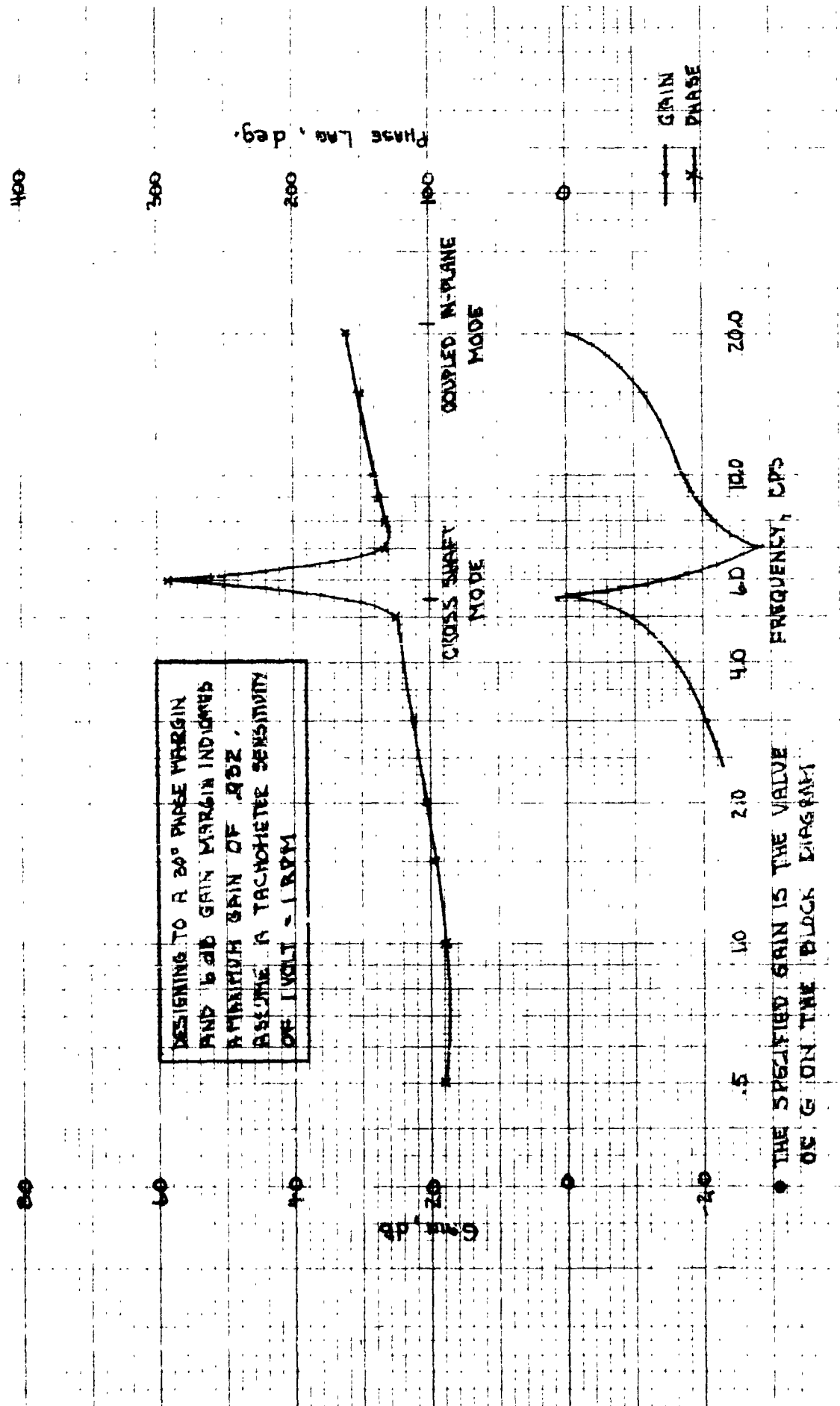


FIGURE 8.5 ROTOR ROTATION FREQUENCY RESPONSE  
WITH ACTUATOR DYNAMICS

HOVER CONFIGURATION  
CROSS SHAFT PRESENT  
20 FPS CLIMB  
551 RPM

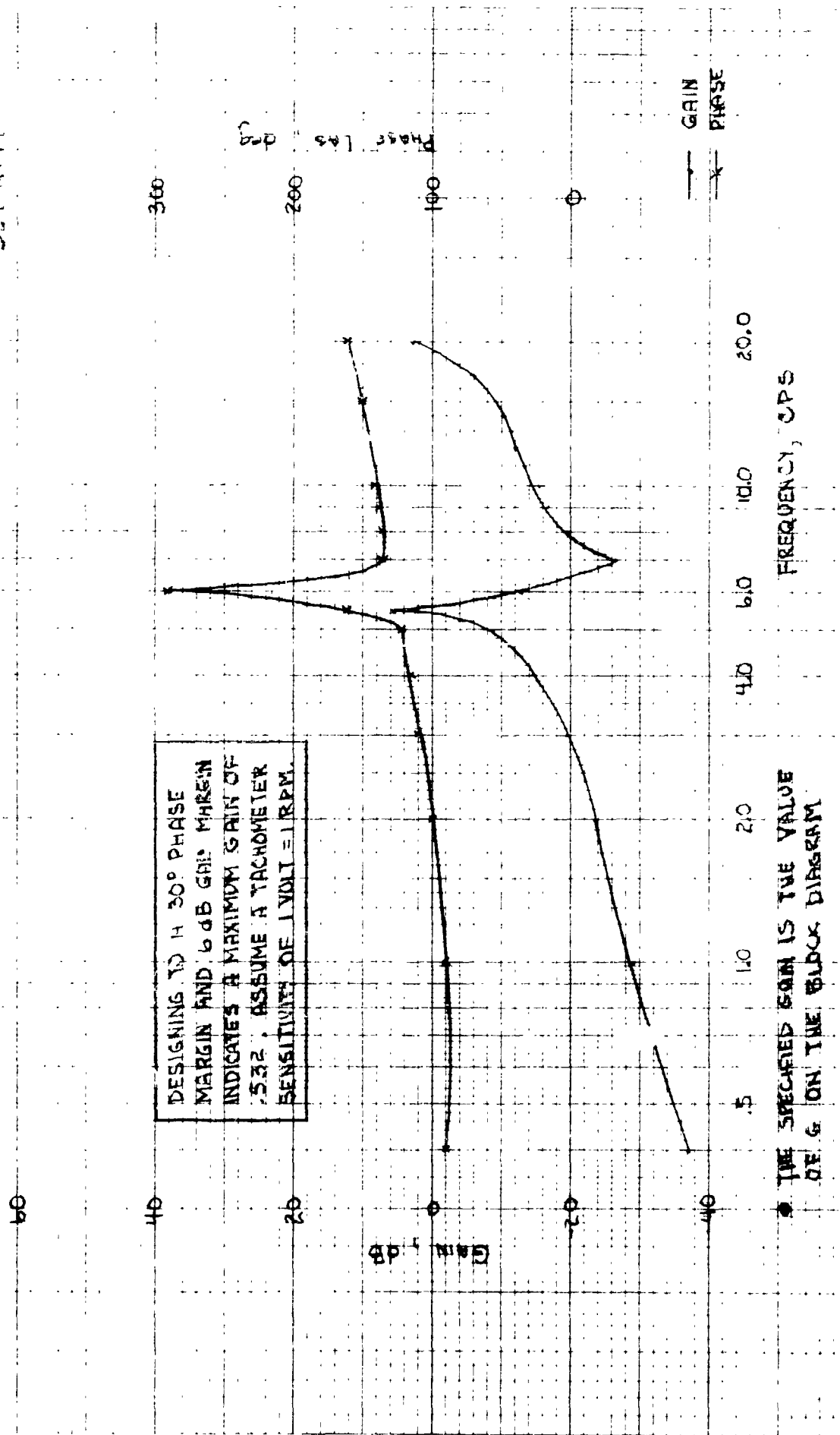
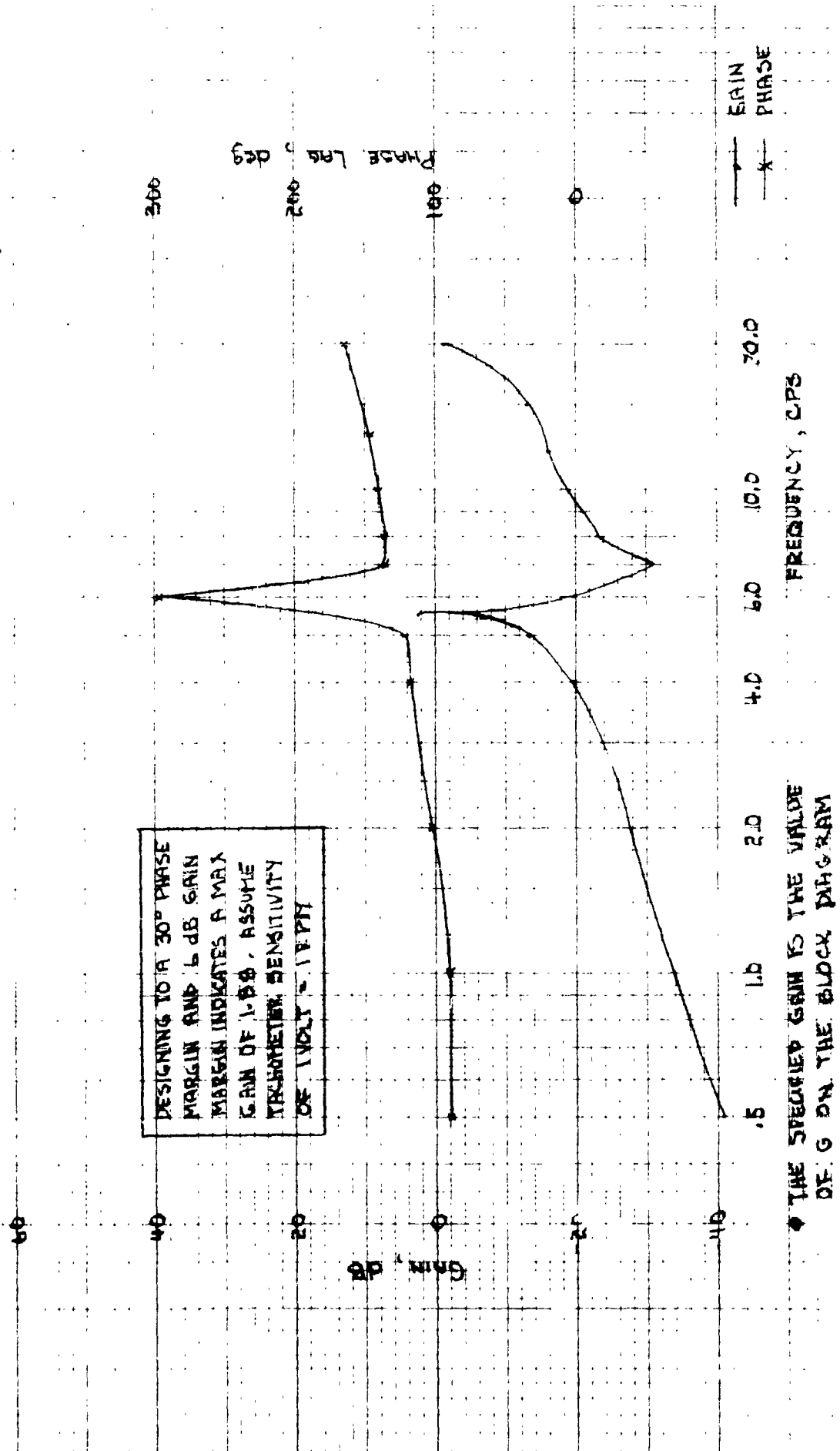


FIGURE B.6 ROTOR ROTATION FREQUENCY RESPONSE  
WITH ACTUATOR DYNAMICS

HOVER CONFIGURATION  
CROSS-CHART PRESENT  
20 FPS DESCENT  
55 RPM



CRUISE CONFIGURATION  
NO CROSS SHAFET  
386 RPM  
100 KNOTS

FIGURE B.7 ROTOR ROTATION FREQUENCY RESPONSE  
WITH ACTUATOR DYNAMICS

DESIGNING TO A 30° PHASE MARGIN  
AND 6 DB GAIN MARGIN INDICATES  
A MAXIMUM GAIN OF 120. ASSUME  
A TACHOMETER SENSITIVITY OF  
1 VOLT / 1 RPM.

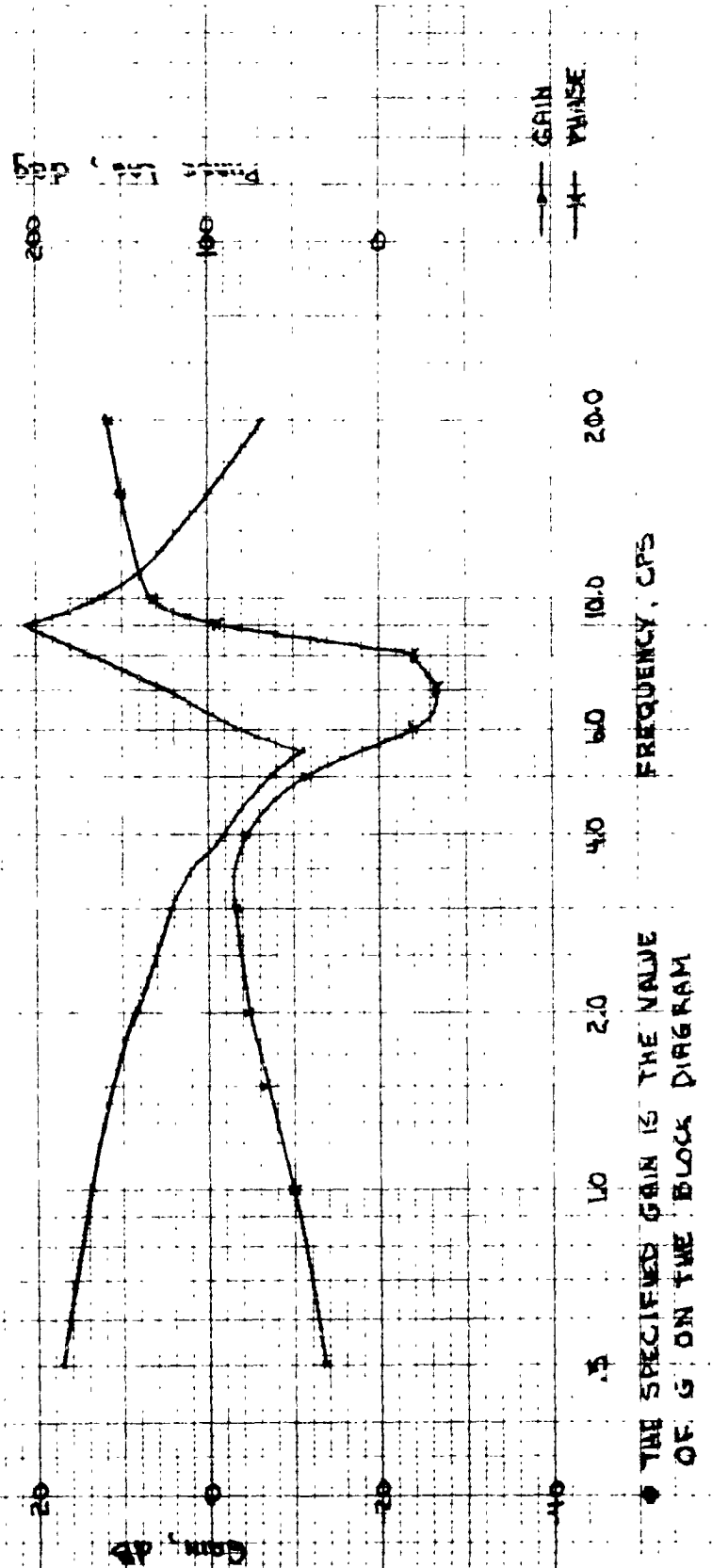


FIGURE B-8 ROTOR POSITION FREQUENCY RESPONSE  
WITH ACTUATOR DYNAMICS

CRUISE  
200 KNOTS  
306 RPM  
NO CROSS SHAFT  
400

DESIGNING TO A 30° PHASE  
MARGIN AND 6 DB GAIN  
MARGIN INDICATES A MAX.  
GAIN OF 304. ASSUME A  
TACHOMETER SENSITIVITY  
OF 1 VOLT = 1 RPM

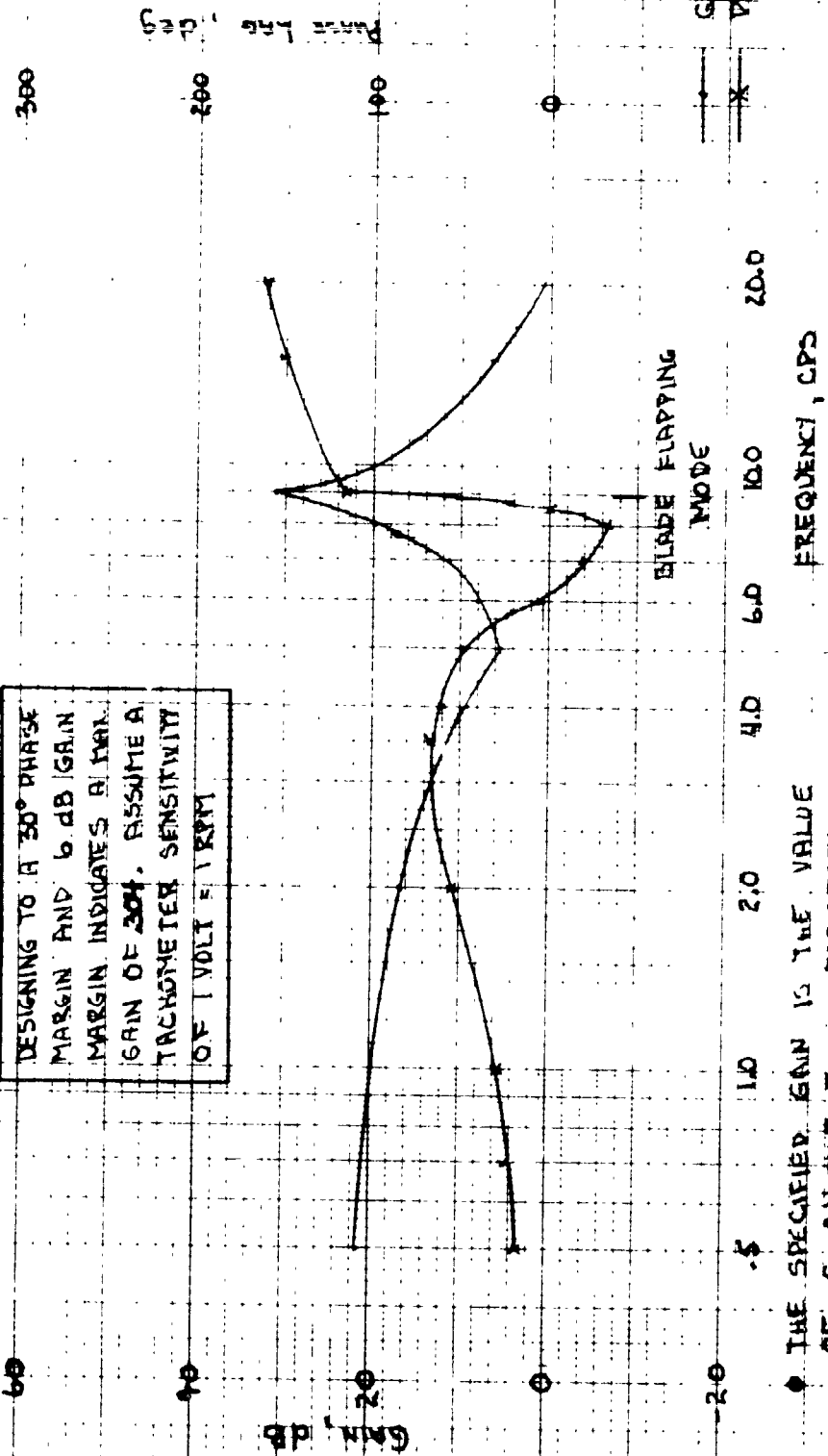


FIGURE B.9 ROTOR ROTATION FREQUENCY RESPONSE  
WITH ACTUATOR DYNAMICS

CRUISE CONFIGURATION  
NO CROSS SHAFT  
386 RPM  
300 KNOTS

DESIGNING TO A 30° PHASE MARGIN  
AND 6dB GAIN MARGIN INDICATES  
A MAXIMUM GAIN OF .224.  
ASSUME A TACHOMETER SENSITIVITY  
OF 1 VOLT/1 RPM

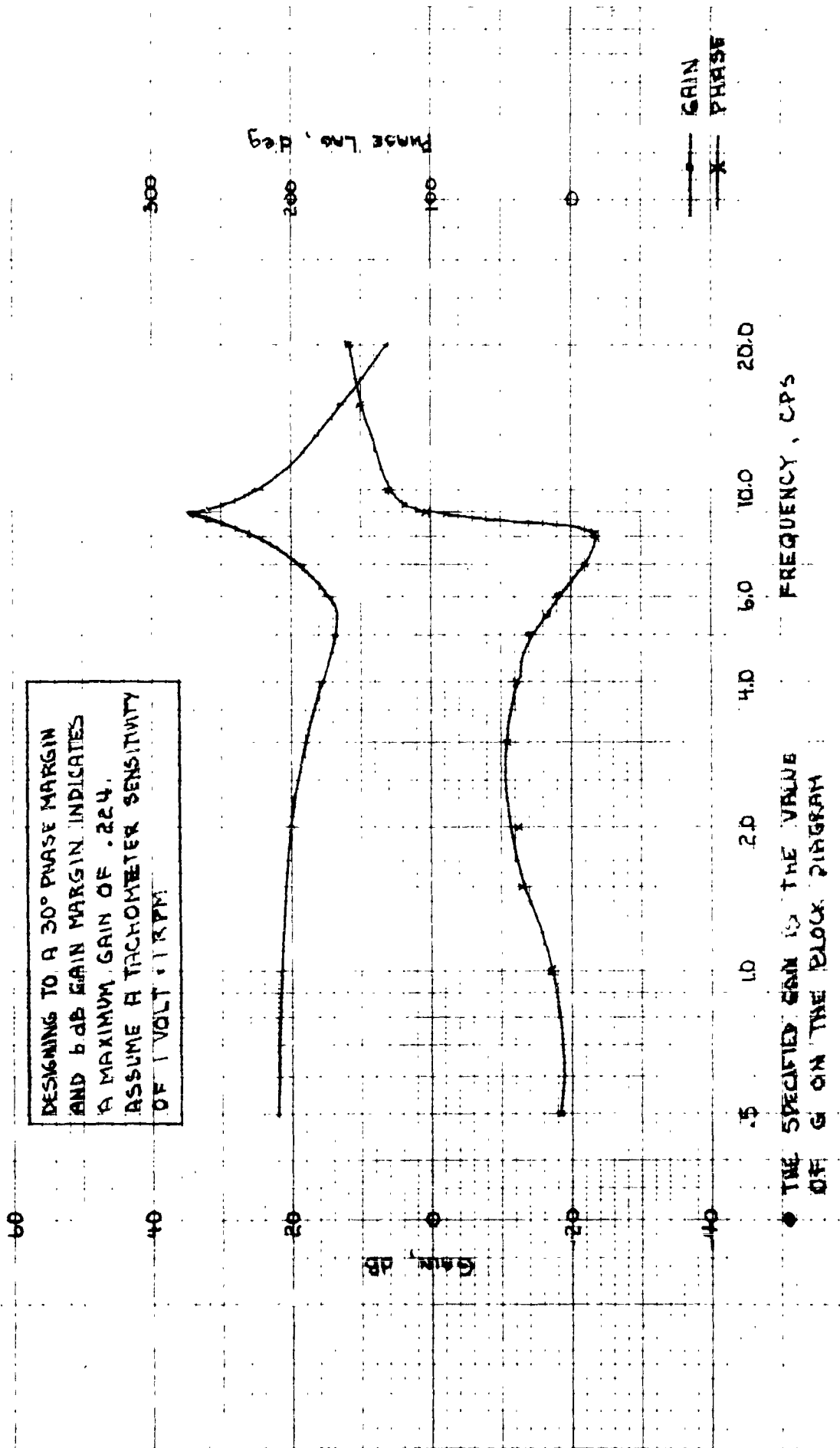
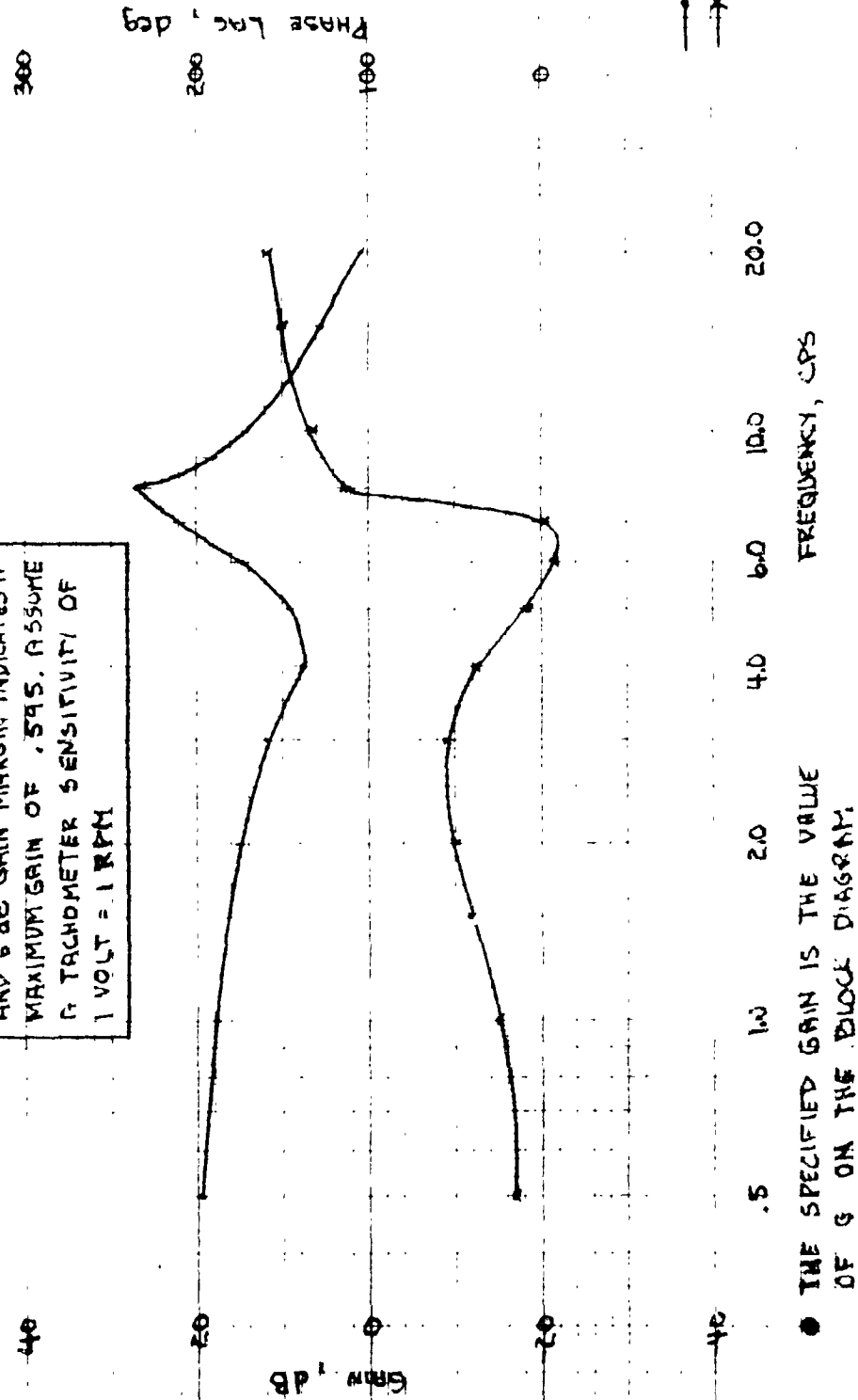


FIGURE B.10 ROTOR ROTATION FREQUENCY RESPONSE  
WITH ACTUATOR VARIATIONS

CRUISE CONFIGURATION  
CROSS SECTION PRESENT  
200 KNOTS  
336 RPM

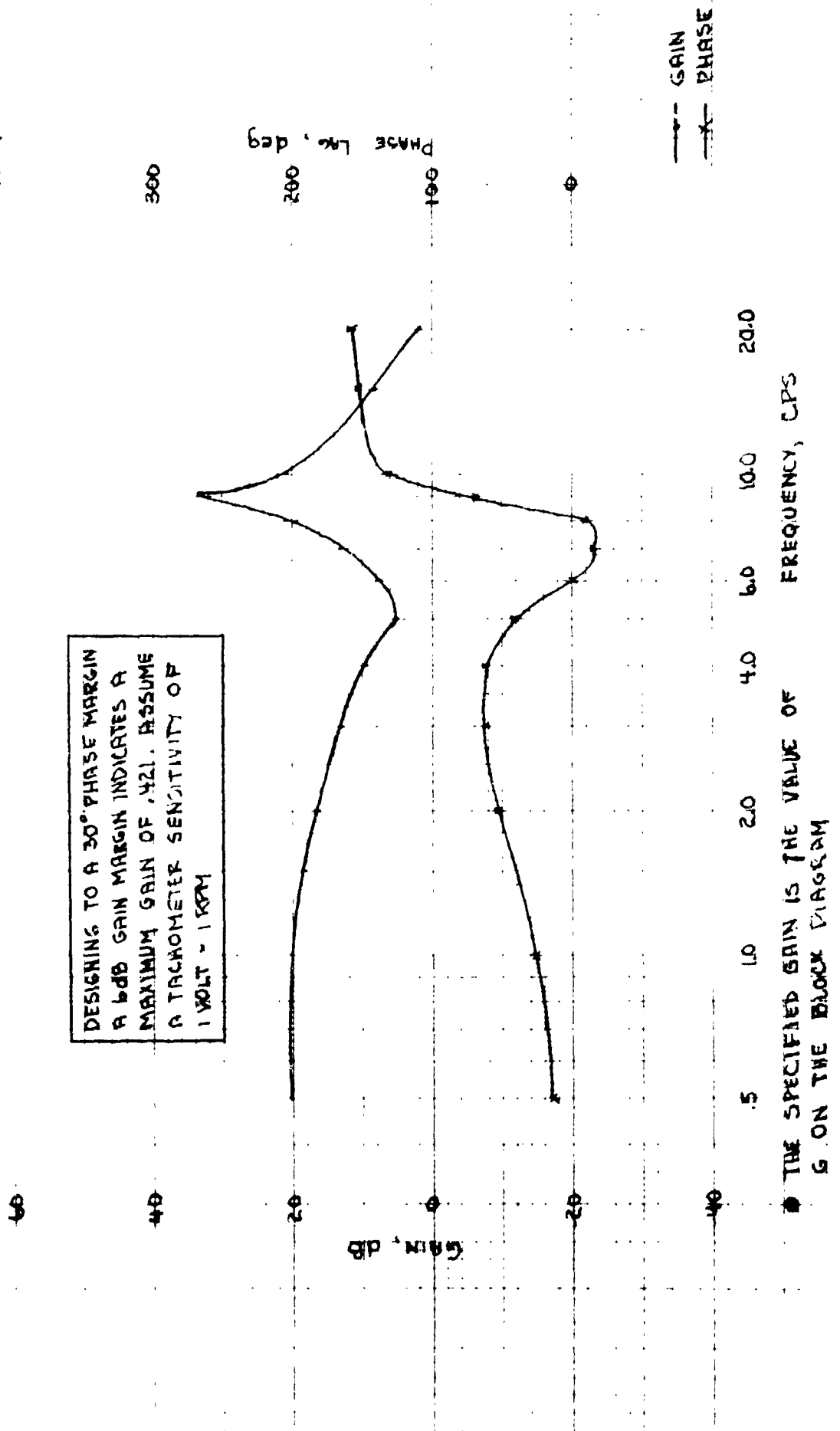
DESIGNING TO A 30° PHASE MARGIN  
AND 6 DB GAIN MARGIN INDICATES A  
MAXIMUM GAIN OF .595. ASSUME  
A TACHOMETER SENSITIVITY OF  
1 VOLT = 1 RPM



● THE SPECIFIED GAIN IS THE VALUE OF G ON THE BLOCK DIAGRAM.

FIGURE B.11 ROTOR ROTATION FREQUENCY RESPONSE  
WITH ACTUATOR DYNAMICS

CRUISE CONFIGURATION  
CROSS SHAFT ABSENT  
200 KNOTS  
436 RPM

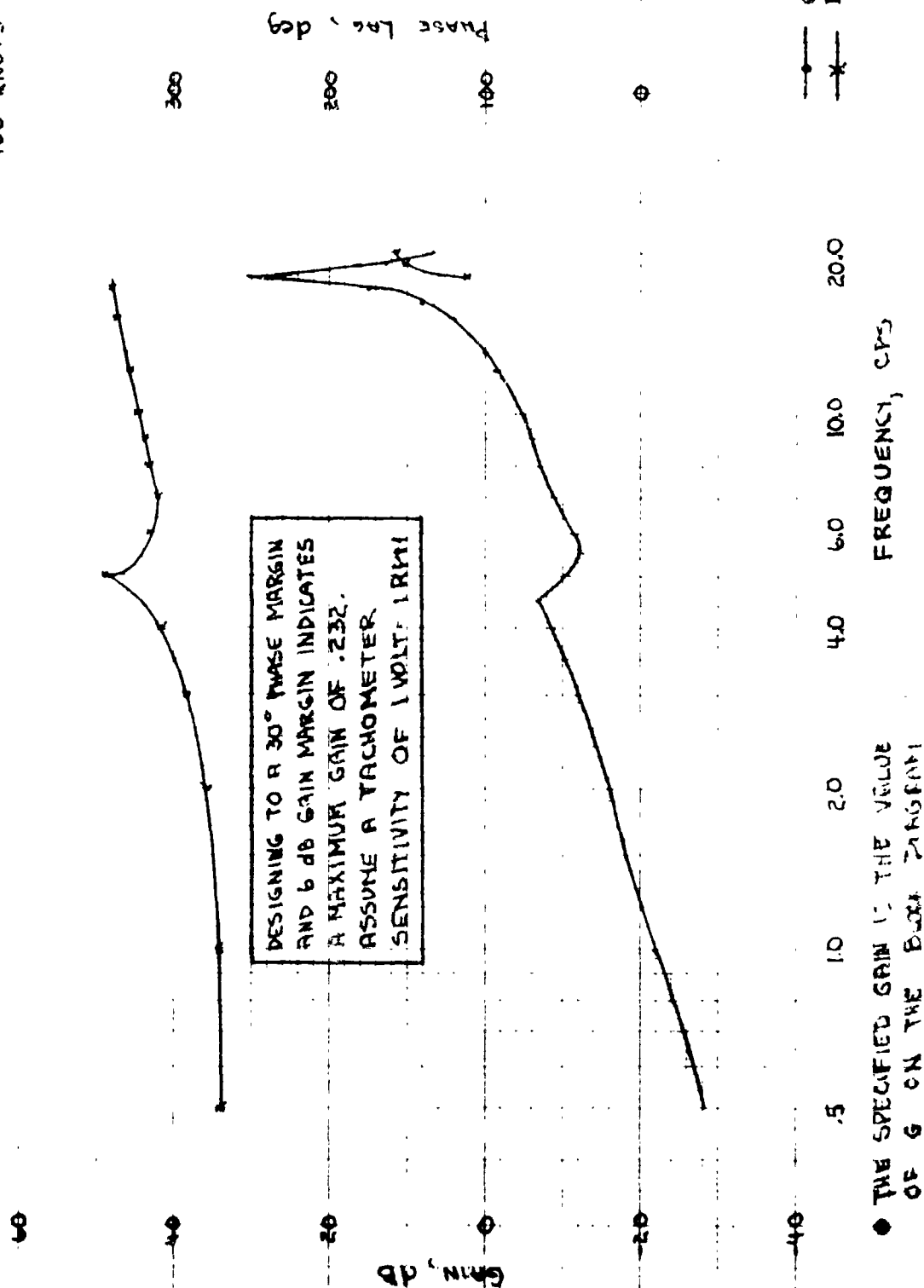


THE SPECIFIED GAIN IS THE VALUE OF  
G ON THE BLOCK DIAGRAM



FIGURE B-12 ROTOR ROTATION FREQUENCY RESPONSE  
WITH ACTUATOR DYNAMICS

CRUISE CONFIGURATION  
DROSS SHAFT PRESENT  
386 RPM  
100 KNOTS



D222-10060-3  
REV. A

FIGURE B-13 ROTOR ROTATION FREQUENCY RESPONSE  
WITH ACTUATOR DYNAMICS

CRUISE  
200 KNOTS  
CROSS SHAFT PRESENT  
386 RPM  
400

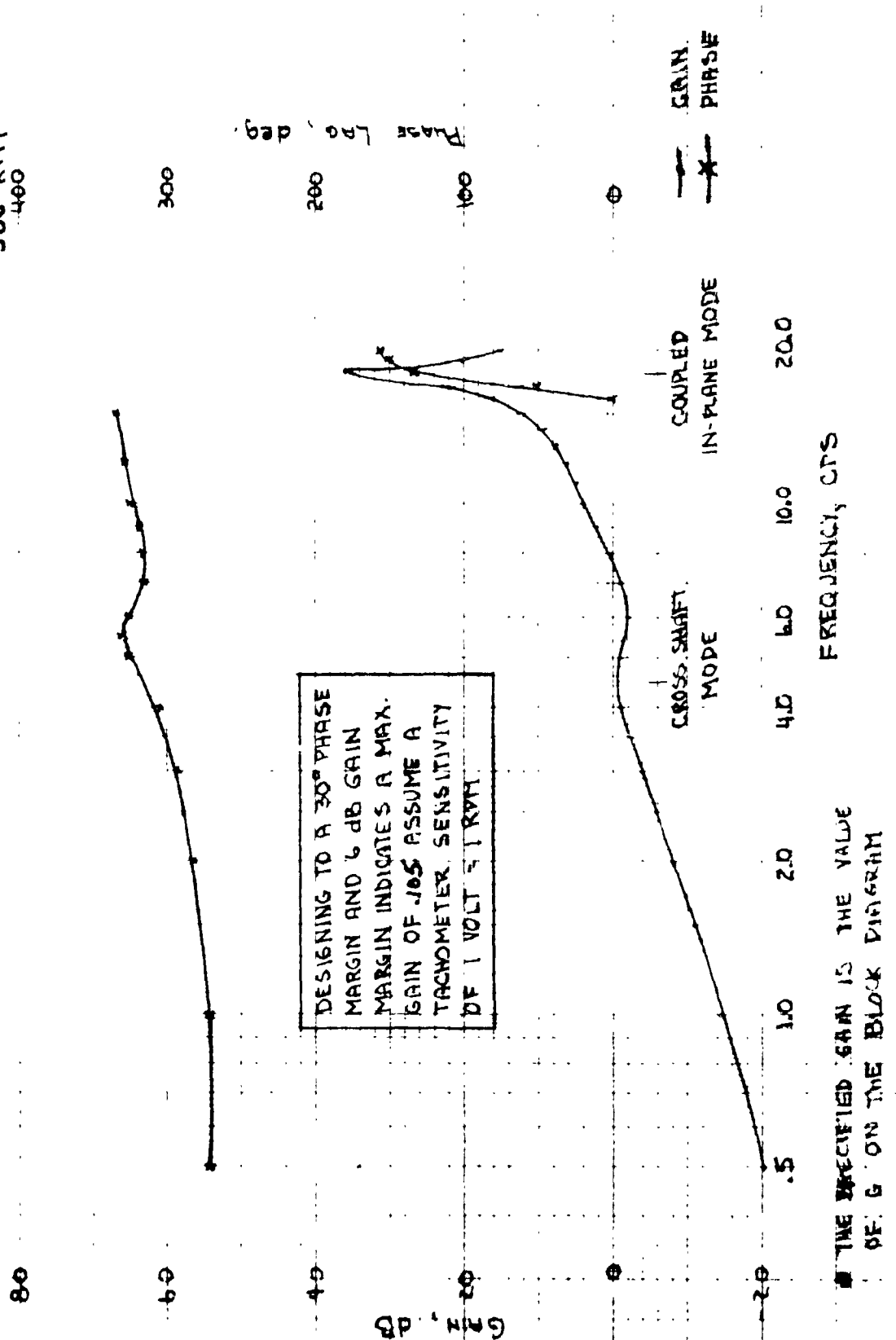


FIGURE B.14 ROTOR ROTATION FREQUENCY RESPONSE  
WITH ACTUATOR DYNAMICS

CRUISE CONFIGURATION  
CROSS SHAFT PRESENT  
386 RPM  
300 KNOTS

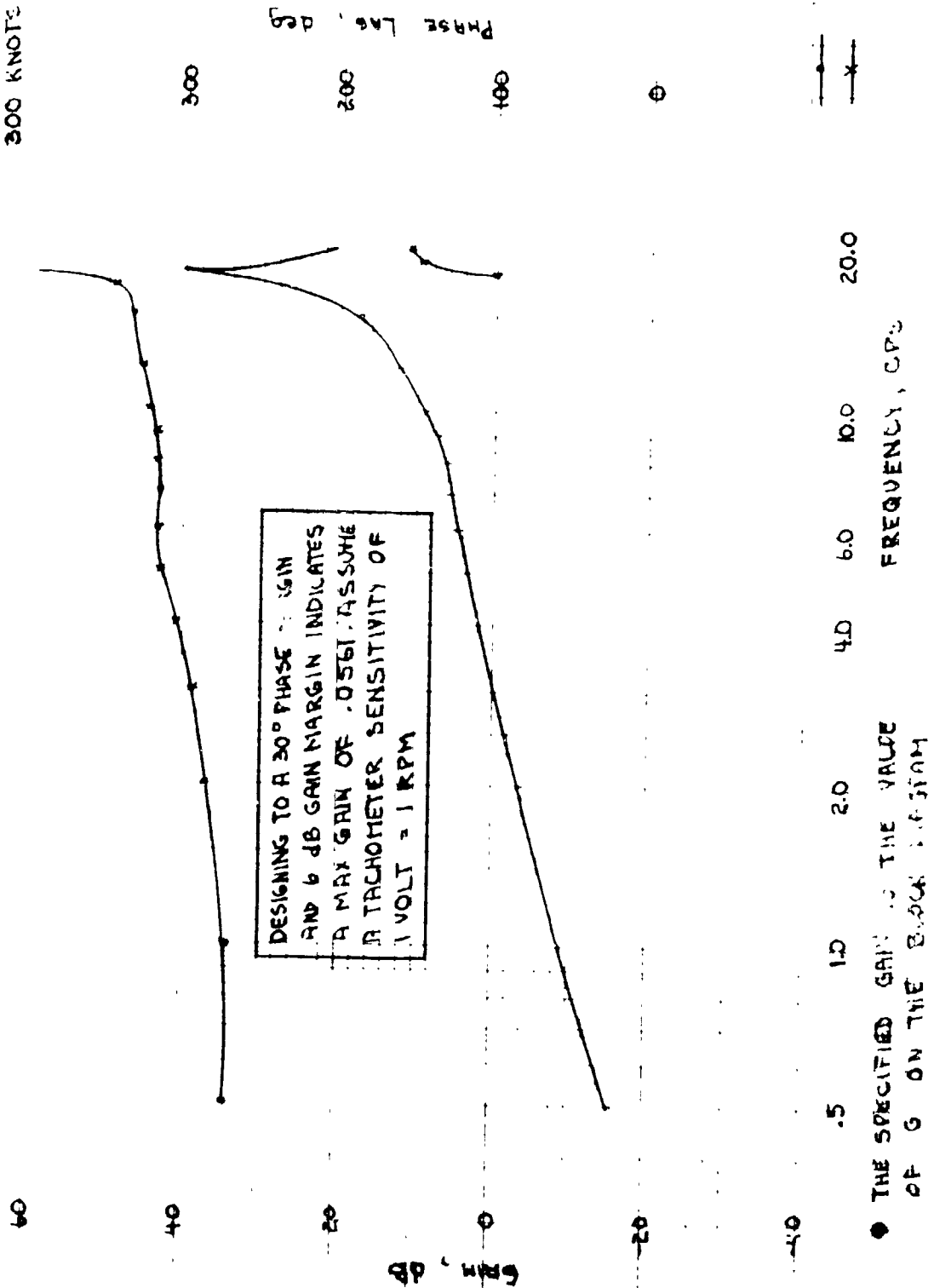


FIGURE B-15 ROTOR ROTATION FREQUENCY RESPONSE  
WITH ACTUATOR DYNAMICS

CRUISE CONFIGURATION  
CROSS SHAFT PRESENT  
200 KTS  
336 RPM

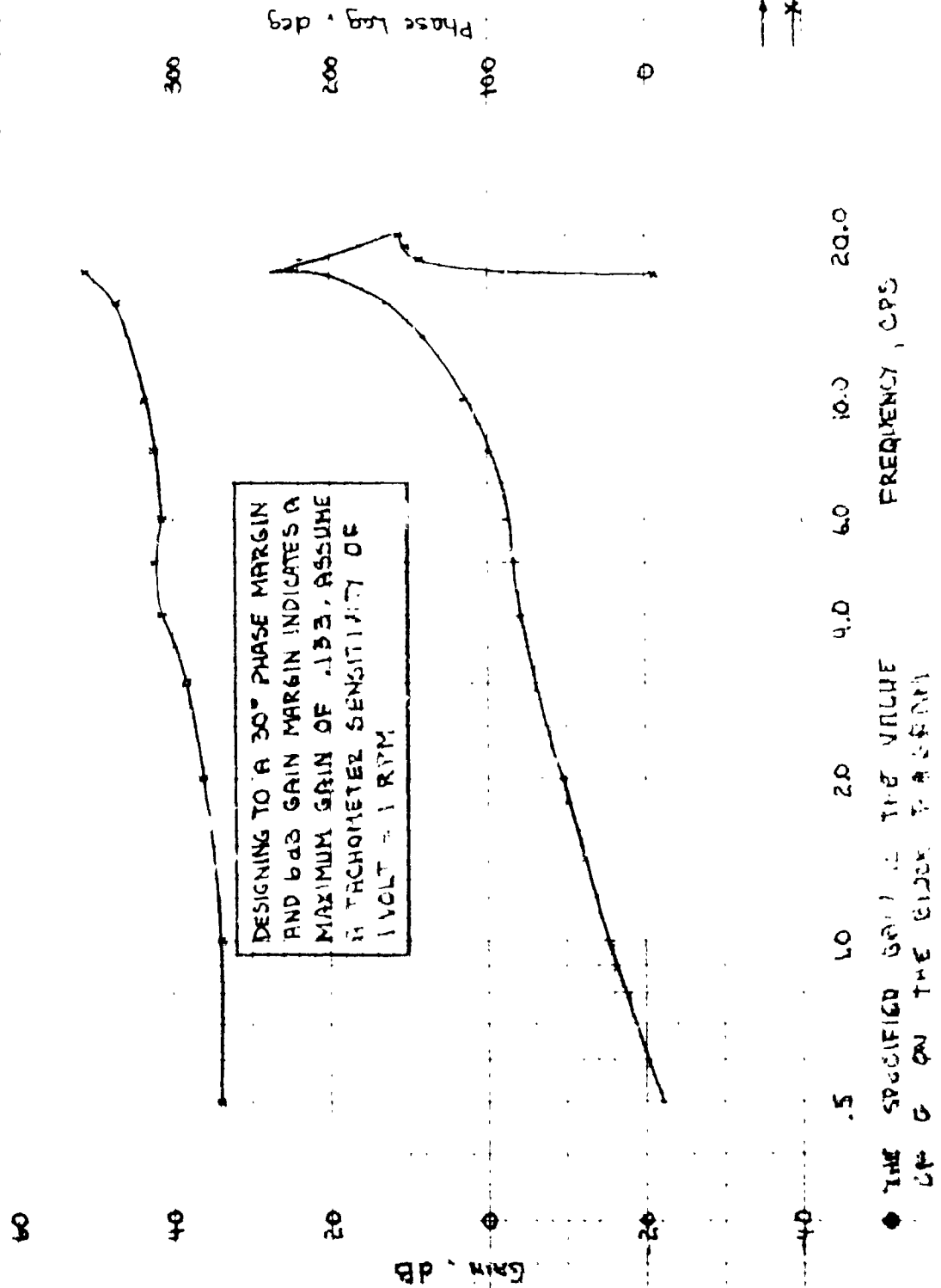
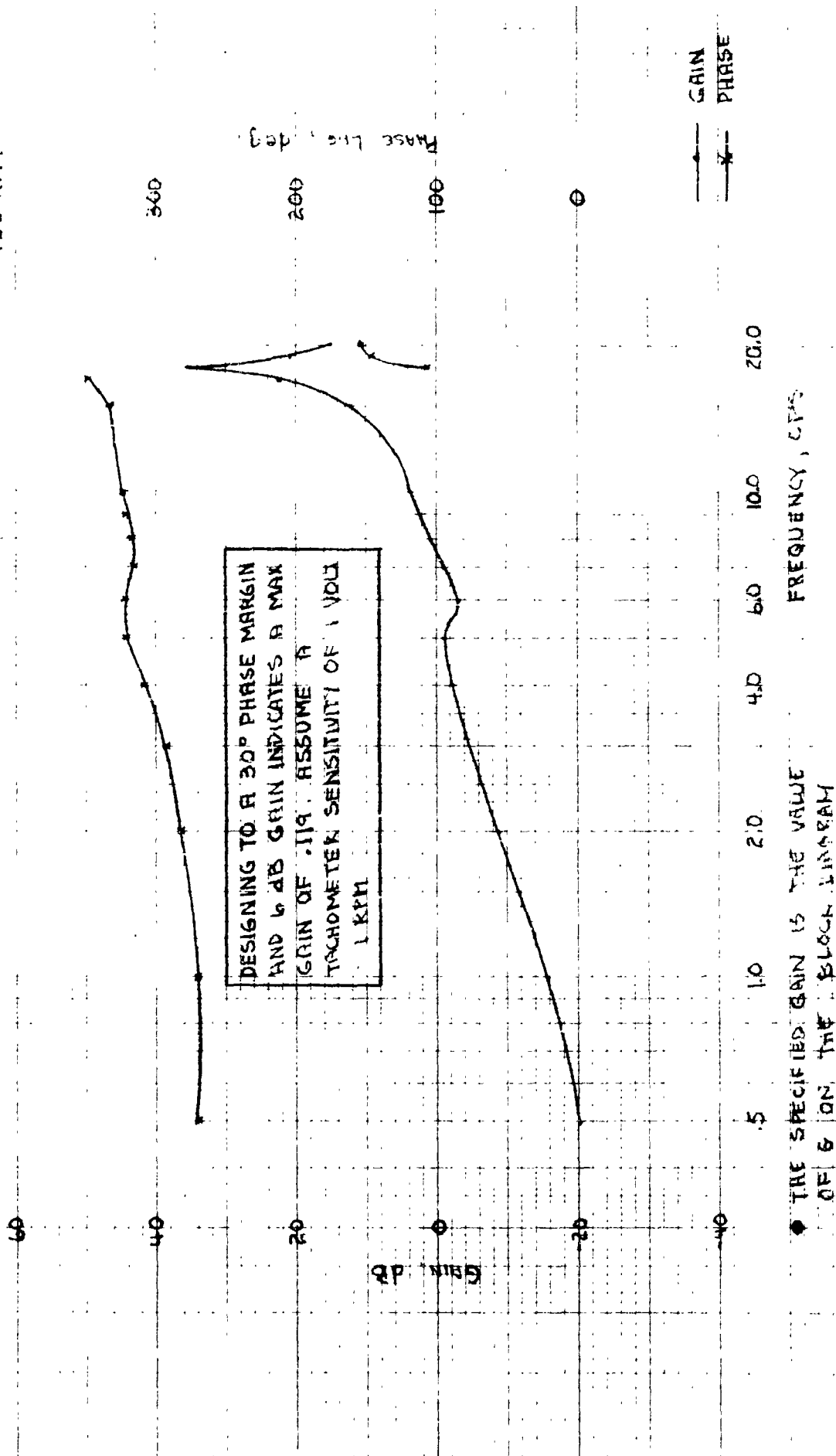


FIGURE B.16 ROTOR ROTATION FREQUENCY RESPONSE  
WITH ACTUATOR DYNAMICS

CRUISE CONFIGURATION  
CROSS SHAFT PRESENT  
200 KTS  
436 RPM



APPENDIX C - "FLY BY WIRE": CONVERSION OF M222 CONTROL SYSTEM  
TO ELECTRICAL SIGNALING

Because the tilt rotor control system requires extensive mixing, gain and shaping changes as a function of flight conditions, it appears to be a good candidate for a fly-by-wire system. While a fly-by-wire study is not proposed at the present time as part of the follow on program, the following paragraphs discuss some aspects which should be given further consideration at a later date.

A block diagram for a possible fly-by-wire control system to do the same job is also given (Figure C-1). This system would use the same cockpit controls, artificial feel units and ASE actuators as the proposed Model 222. Also, the swash-plate actuators, spoiler actuators and flaperon actuators would remain the same. Dual hydraulic power actuators would be added for the rudder and for the governor. Thirteen quadruple-driven actuators would then be added as shown to convert electrical signals to mechanical inputs at the hydraulic power actuators. These could possibly be electro-ram type actuators of the type we now propose to use for the governor system on the Model 222 (or they could be electro-hydraulic).

A summary of the actuator tradeoff is given below. The rest of the tradeoff consists of replacing five ratio changers, eight scheduling cams, fourteen stages of mechanical mixing,

SHADED BOX  
INDICATES SPECIAL  
FBW EQUIPMENT

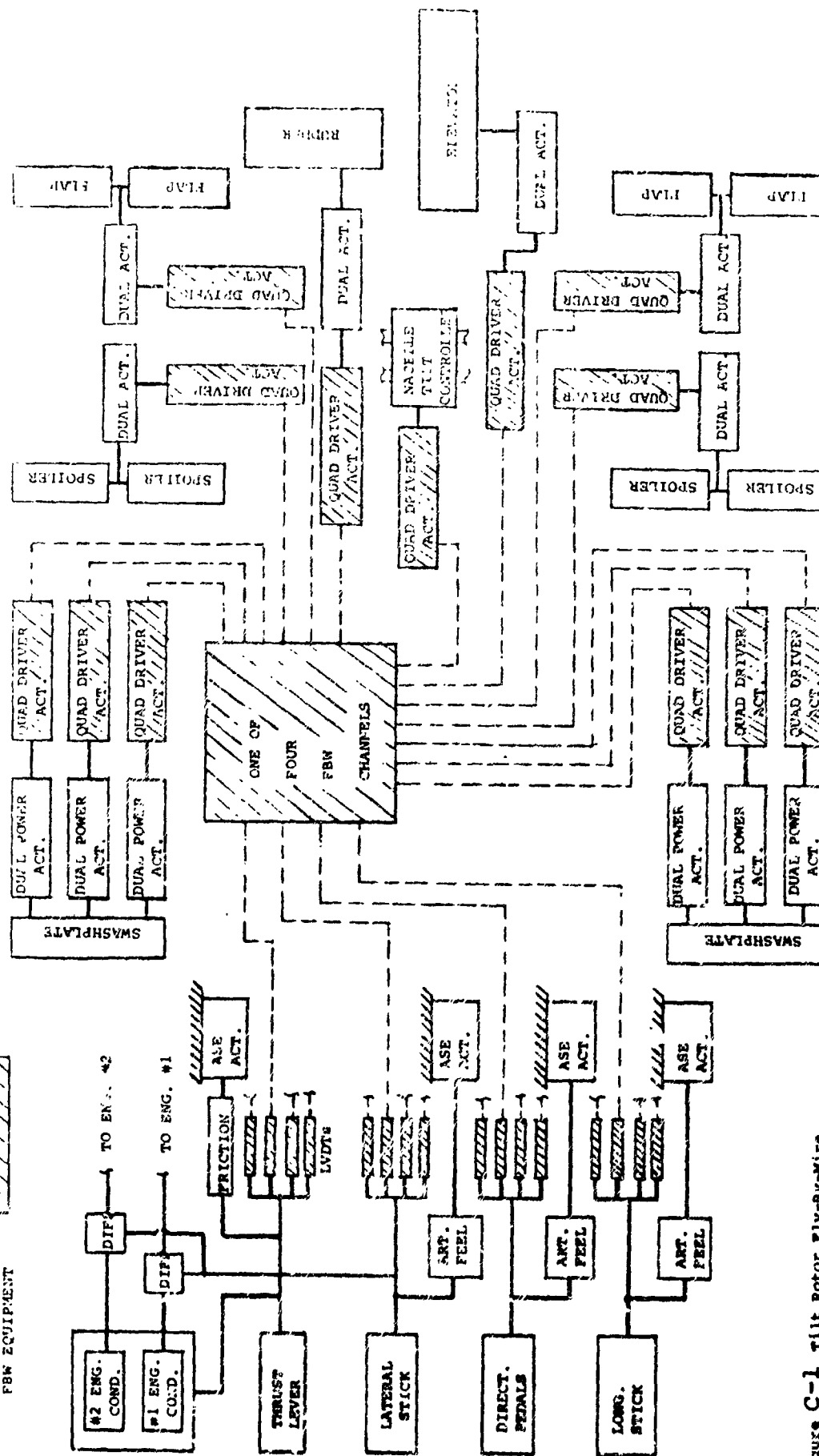


Figure C-1 Tilt Rotor Fly-By-Wire Control System (FBW)

(mechanical differentials), four governor speed settings LVDTs, four collective pitch "quickenings" LVDTs, and 90% of the mechanical routing linkage -- with, sixteen cockpit LVDT pick-offs, four individual channel FBW control boxes and the associated wiring. It is assumed that the sensors required and much of the automatic system electronics would be the same in both systems. The tradeoff in actuators between the tilt rotor FBW control system and mechanical system with full load alleviation/mode suppression capability is:

DELTA ACTUATOR COUNT - remove from mechanical system

- a) 4 dual stick boost actuators
- b) 8 dual extensible link SAS actuators
- c) 1 triple extensible link SAS actuator
- d) 1 quadruple electromechanical governor actuator
- e) 1 electromechanical DCP trim actuator

ADD FOR FBW SYSTEM

- a) 13 quadruple-driven actuators
- b) 2 dual power actuators at rudder and elevator